University of Glasgow

Gao, Xuan (2023) *Adipocyte hyperplasia and hypertrophy in the development of Type 2 Diabetes Mellitus.* PhD thesis.

https://theses.gla.ac.uk/83754/

Adipocyte hyperplasia and hypertrophy in the development of Type 2 Diabetes Mellitus

Xuan Gao

Submitted for degree of Doctor of Philosophy

Institute of Cardiovascular and Medical Sciences

College of Medical, Veterinary and Life Sciences

University of Glasgow

July 2023

Abstract

Increasingly obesity and obesity-induced type 2 diabetes mellitus (T2DM) are becoming significant societal issues affecting health and longevity in today's world. When the human body takes in excess energy it is stored in adipocytes. Adipocytes store the excess energy via the processes of hypertrophy and/or hyperplasia. Storing energy through hypertrophy leads to the formation of large adipocytes, which are considered unhealthy due to their increased propensity to induce insulin resistance and inflammation. Consequently, these large adipocytes increase the risk of developing T2DM. Therefore, understanding how adipocyte hypertrophy and hyperplasia are regulated is essential for investigating the etiology of T2DM.

South Asians are a susceptible population for T2DM and develop the disease at a younger age and lower BMI compared to European Caucasians. Notably, when South Asians migrate to Europe or America, their probability of developing T2DM is two to four times higher than Caucasians with the same BMI. Thus, understanding the causes of South Asians' susceptibility to T2DM is also crucial for comprehending the disease.

This thesis first investigated the relationship between adipocyte hypertrophy and hyperplasia, obesity and T2DM by undertaking a cross-sectional analysis of subcutaneous adipose tissue (SAT) samples obtained through needle biopsy from human cohorts of varying age, ethnicity (South Asian and Caucasian), exercise status and insulin resistance. Adipocytes were isolated from human SAT, and their diameter and gene expression were measured. It was found that adipocyte diameter increased with age and declined with metabolic fitness, changes which were related to changes in expression of genes involved in adipocyte differentiation capacity and adipokine secretion. Long-term exercise mitigated the effect of aging, whereas insulin-resistant individuals exhibited exacerbated age-related effects. Insulin-resistant individuals had a significantly higher proportion of very large adipocytes than age and BMI-matched healthy controls. Interestingly, healthy, young, lean South Asians had adipocyte size distribution and gene expression more akin to older and higher BMI Caucasians. In particular, young South Asians had a proportion of very large adipocytes similar to that seen in insulin-resistant Caucasians.

Based on these findings, this thesis then conducted a longitudinal analysis of adipocytes from the GlasVEGAs study, a study where South Asians and European Caucasians gained 6.4% body weight through overfeeding. The results showed that at baseline, and after weight gain, South Asians had a higher proportion of large and very large adipocytes and a lower proportion of small and medium-sized adipocytes. Compared to Caucasians, South Asian adipocytes exhibited lower expression of genes involved in insulin signalling and lipid oxidation and higher expression of genes involved in lipid storage and inflammation, potentially explaining the increased susceptibility of South Asian to T2DM.

The work in this thesis demonstrated successful stimulation of preadipocyte differentiation in vitro, however possibly due to low sample size, no significant differences were discerned. Gene expression patterns suggested that South Asians may have lower adipogenesis capability than Europeans at baseline and after weight gain, though the effect lacked statistical significance. These findings underscore the importance of considering adipogenesis in future research exploring the link between adipose tissue function and T2DM in South Asians, Europeans, and potentially other populations.

This thesis presented the first exploration of circulating extracellular vesicle (EV) concentration and size in response to acute feeding. A peak in both EV concentration and size was observed two hours post-feeding, returning to fasting levels six hours later. This pattern was consistent across healthy males and females, suggesting that future studies of circulating EV should consider the effects of feeding and that fasted samples may need to be collected as controls. A positive correlation was found between circulating EV size and age in both sexes, indicating the importance of age adjustment in future studies. The EV miRNA profile revealed the MIRLET7 family and MIR125B2 as the highest copy number of miRNA in circulating EV in both fasting and fed states. However, statistical analysis was not possible due to unsuitability of the data for normalisation procedures due to low copy number and lack of complexity of miRNA species. This study successfully established a protocol for collecting, isolating, and measuring EV from blood, and extracting RNA from circulating EV. Future work should include Taqman RT-qPCR to validate the expression of miRNA, thereby validating these initial findings.

The studies included in this thesis have confirmed that aging and South Asian ethnicity can induce adipocyte hypertrophy and potentially reduce hyperplasia, leading to the formation of metabolically unhealthy adipocytes, thereby increasing the risk of T2DM. The research has also explored the possibility of a lower adipogenesis capability in South Asians, and the impact of acute feeding on circulating extracellular vesicle concentration and size, revealing potential implications for future research. Furthermore, it has been demonstrated that long-term exercise can alter adipocyte gene expression, attenuating the adverse impacts of aging and ethnicity. These findings collectively underscore the complex interplay between ethnicity, aging, adipocyte function, and lifestyle factors in T2DM development, highlighting the need for further comprehensive studies.

Table of Contents

List of Tables

List of Figures

Acknowledgement

I would like to express my profound gratitude to my supervisor, Dr Dilys Freeman. Your unending support throughout my PhD journey has been invaluable. Your patience, kindness, fairness, and professionalism have truly shaped my academic life. I hold immense respect and affection for you.

My sincere thanks also go to my supervisor, Prof Jason M.R. Gill. Your professionalism, intelligence, and constructive critiques have consistently inspired me throughout my PhD journey.

I am grateful to the MVLS ISSF Feasibility Award, which funded my mixed meal study and contributed significantly to a chapter in my thesis.

My heartfelt thanks go to Dr James McLaren and Dr Anne Sillars for your collaborative work in GlasVEGAs, MFAT, and the mixed meal study. It was a pleasure working with you both.

I extend my gratitude to Prof Ulf Smith, Dr Birgit Gustafson, and their team for assisting me with adipocyte differentiation in their lab at the University of Gothenburg, Sweden. Your warm hospitality during the cold season was greatly appreciated.

I am thankful to Dr Carlos Salomon and his team for assisting me with EV-related skills at the University of Brisbane, Australia. It was a wonderful experience working with you all.

I express my gratitude to my examiners, Dr Barbara Fielding and Dr Ian Salt, for the time and effort you dedicated to reading my thesis and discussing my work with fairness and kindness. My viva was one of the highlights of my PhD journey, thanks to you. I also thank Prof George Baillie for his excellent organisation and hosting of my viva.

Special thanks to my lab 'mother', Mrs Fiona Jordan, whose humour made our lab a joyous place.

Author's Declaration

I, Xuan Gao, hereby declare that this thesis is entirely my own original work and has not been copied, reproduced, or adapted from any other sources, except where explicitly acknowledged and cited in accordance with academic standards.

I affirm that I have fully complied with all ethical guidelines and requirements related to the research, data collection, and analysis presented within this thesis. Furthermore, I confirm that any assistance received throughout the completion of this thesis has been duly acknowledged and that all necessary permissions have been obtained for the use of copyrighted materials.

I understand that any misrepresentation, plagiarism, or academic dishonesty may lead to severe consequences, including the revocation of the degree awarded based on this thesis.

Definitions/Abbreviations

ANOVA	Analysis of variance
ASAT	Abdominal subcutaneous adipose tissue
BL	Baseline
BMI	Body mass index
BSA	Bovine serum albumin
CD	Collagenase-digestion
cDNA	Complimentary DNA
Ct	Cycle threshold
CVD	Cardiovascular diseases
DMEM	Dulbecco's Modified Eagle's Medium
DMSO	Dimethyl sulfoxide
DPBS	Dulbecco's Phosphate Buffered Saline
DTT	Dithiothreitol
ER	Endoplasmic reticulum
EU	White European origin
EV	Extracellular vesicle(s)
FA-CoA	Fatty-acyl-CoA synthase
FBS	Fetal bovine serum

FFA/ FA	Free fatty acid/ Fatty acid
GlasVEGAs	Glasgow visceral & ectopic fat with weight gain in South Asians
GLM	General linear model
HFD	High fat diet
HIS	Histological analysis
IAA	Iodoacetamide
IBMX	Isobutylmethylxanthine
KRH buffer	Krebs Ringer Hepes buffer
MFAT	Role of alternative pathways of triglyceride synthesis in determining insulin sensitivity in muscle (Muscle and fat)
Mixed meal EV	The effect of a mixed meal on blood-circulating extracellular vesicles
MSC	Mesenchymal stem cell
MWCO	Molecular weight cut-off
NTA	Nanoparticle tracking analysis
ORO	Oil red O
OS	Osmium tetroxide fixation followed by Multisizer counter analysis
P/S	Penicillin-Streptomycin
PCR	Polymerase chain reaction

RT-qPCR	Reverse transcription quantitative PCR
SA	South Asian (Indian, Pakistani, Bangladeshi or Sri Lankan) origin
SD	Standard deviation
SDS	Sodium dodecyl sulfate
SEC	Size exclusion chromatography
SEM	Standard error of the mean
SVF	Stromal vascular fractions
T2DM	Type 2 diabetes mellitus
TG	Triglyceride
WAT	White adipose tissue
WG	Weight gain
WL	Weight loss

Chapter 1 Introduction

1.1 Obesity and type 2 diabetes mellitus (T2DM)

1.1.1 Importance of obesity

Obesity is a major worldwide problem, especially in Western societies, which negatively influences human health (NationalTaskForce, 2000). Body mass index (BMI) is a widely used measurement of adiposity (Gómez-Ambrosi *et al.*, 2011). According to the World Health Organization, BMI between 18.5 and 25 kg/m^2 is defined as normal, and a BMI of at least 25 kg/m^2 is defined as overweight, and BMI over 30 kg/m^2 is defined as obesity (WHO, 2000). According to the World Health Organization (WHO, 2017), in 2017 there were approximately 1.9 billion overweight adults aged 18 years and older, including 650 million who had obesity. The proportion of overweight individuals was 39% of the total adult population (39% of men and 40% of women), and around 13% of adults (11% of men and 15% of women) were obese in 2016 worldwide (WHO, 2017). The prevalence of obesity almost tripled in 2016 compared to 1975 (WHO, 2017). The prevalence of obesity is still rising. It has been estimated that by 2030, 20% of adults will be obese (Kelly *et al.*, 2008).

The obesity epidemic originated in the USA and Europe, with few restrictions on access to or availability of food over the last 50 years. In the USA in 2012, the population with overweight or obesity eclipsed by two-fold the number of people with normal body weight (Ogden *et al.*, 2014). The prevalence of overweight in adults has hovered around 35% from 1960 to 2010 in the USA, and this may be limited by reaching the 'Malthusian' limit in the population. However, the prevalence of obese adults has jumped from 13% to 23% from 1960 to 1994, and reached 32% in 2004, similar to the level of individuals with overweight (Ogden *et al.*, 2014). In 2017-2018, the prevalence of obesity increased to 42% in the USA (NCHS, 2018). In Europe, the prevalence of obesity and overweight varies across different regions. In a longitudinal data report (1992 - 1998 to 1998 - 2005) from populations in five Europeans countries (Italy, the UK, the Netherlands, Germany and Denmark) across different regions in Europe, adult obesity rates have increased from 13 to 17% (von Ruesten *et al.*, 2011). The average rate of obesity reached 23% in Europe in 2017 according to WHO (WHO, 2018).

Aside from the USA and Europe, the increase in the prevalence of obesity can be seen worldwide in line with economic growth. In China, from 1993 to 2009, the prevalence of overweight (BMI 25 - 27.5 kg/m^2) doubled in men (8 - 17%) and increased from 11 - 14% in women. The prevalence of obesity (BMI ≥ 27.5 kg/m^2) almost quadrupled in men (3 - 11%) and doubled in women (5 - 10%) (Liang *et al.*, 2012). In 2015, the average rate of obesity reached 16% in China (Hemmingsson, 2021). Similarly in India, with the increase in obesity rate, it has been estimated that by 2040, the prevalence of overweight and obesity will reach 31% and 10% respectively in men and 27% and 14% in women (Luhar *et al.*, 2020).

Obesity contributes to the increased risk of almost every chronic disease, including diabetes, cardiovascular diseases, cancer, and poor mental health. In the USA, 15% of deaths were attributable to overweight and obesity resulting from poor diet and physical inactivity in 2000 (Mokdad *et al.*, 2004). Ischemic heart disease and stroke are the leading causes of death globally, and obesity is a well-known risk factor for heart disease and ischemic stroke, including their typical antecedents – dyslipidaemia and hypertension (Lozano *et al.*, 2012). Obesity has contributed to 6% of all estimated cancers in the USA in 2007 (Polednak, 2008). Obesity and adiposity are associated with anatomical and functional changes in the human brain. BMI is negatively correlated to brain volume in the elderly (Raji *et al.*, 2010). The risk of Alzheimer's disease is increased in people with overweight in midlife (Anstey *et al.*, 2011). The prevalence of patients getting T2DM is strongly correlated to the prevalence of patients with overweight and obesity. In England, 90% of patients who were diagnosed with T2DM aged 16 - 54 were overweight or obese (27% were overweight and 63% were obese), and only 10% of patients were of healthy weight or underweight in 2009-10 (NationalDiabetesAudit, 2010). The prevalence of obesity/overweight was similar in individuals aged 55 years and over where 84% of T2DM patients were overweight (27%) or obese (48%) and only 16% were of healthy weight or underweight (NationalDiabetesAudit, 2010). Additionally, around 12.4% of individuals with obesity were diagnosed with T2DM in England in 2010 - 2012 (NatCenSocialResearch&UCL, 2014).

Obesity contributes to economic costs and social problems. The total cost of global health services associated with high BMI has been estimated to total US$990 billion annually (WHO, 2019). In the Country / Organisation for Economic Co-operation

and Development (OECD) countries, health services related to obesity cost an average of 3.3% of GDP, with the highest cost in Mexico (5.3%) and Brazil (5%) (OECD, 2019). In the UK, diabetes accounted for approximately 10% of the total NHS budget (~£23.7 billion) in 2011, but this is projected to rise to around 17% (~£39.8 billion) by 2035/36 (NHS, 2012). Obesity and its associated health problems have become a great burden to society.

Therefore, it is of great importance to investigate the pathology and development of obesity in order to decrease the prevalence of obesity and to develop anti-obesity medications and interventions.

1.1.2 Body fat distribution and adipose tissue depots

Obesity is typically defined simply as excess body weight relative to height. However, in recent studies, a more complex definition associated with excess adiposity or body fatness and the distribution of body fat, has been highlighted as better associated with metabolic disease than body size. Body fat distribution is a strong risk factor that predicts obesity-associated health problems such as cardiometabolic disease. Body fat distribution is regulated by a complex series of factors such as sex hormones, use of glucocorticoids, ethnicity, and epigenetic mechanisms (Goossens, 2017a). The distribution of adipose tissue has been assessed for decades using simple measures of skin-fold thickness and waist and hip girths. Such data are expressed in the form of ratios, for example waist/hip ratio (WHR) or the ratio of central to peripheral skin-fold thicknesses (Wells, 2007).

Sex dimorphism in human body composition starts from fetal life and increases primarily during puberty (Wells, 2007). Boys have higher lean mass index (lean mass (kg)/height^2 (m^2)) than girls from birth and the difference in lean mass between the two sexes increases after the first decade of life until the twenties (Fomon *et al.*, 1982, van der Sluis *et al.*, 2002). In terms of fat tissue, fat mass index (fat mass (kg)/height^2 (m^2)) was similar in both sexes at birth and increased dramatically until 1 year of age (Fomon *et al.*, 1982). It then decreased between year 1 to 6 of age in both sexes, after which girls become fatter than boys. The fat mass index in girls increased to a peak at 16-years and then was maintained at around 5 kg/m^2. In boys, fat mass index increases more slowly and reaches a peak

at 10 years of age and is then maintained at around 3 kg/m^2 (Arfai *et al.*, 2002). In adults aged 17 - 65 years, with the same BMI, women (n = 359) had an average of 10.4% ($p < 0.01$) more percent body fat (%fat) compared to men (n = 396) in normal weight, overweight and obese participants (Jackson *et al.*, 2002). A similar study has shown that men (n = 103, aged 21 - 79 years) had 50% more lean mass ($p < 0.001$) and 13% less fat mass ($p < 0.001$) compared to women (n = 131, aged 19 - 63 years) (Ley *et al.*, 1992). Fat composition increases along with aging, and women have a higher fat mass relative to men.

The distribution of body fat is also different between women and men. A study of white and African Americans showed that in adults aged 18 - 64 years, women (n = 1,058) had more abdominal subcutaneous adipose tissue (SAT, $p < 0.0001$) than men (n = 609) across all levels of waist circumference and BMI. In terms of visceral adipose tissue VAT measured with dual-energy-X-ray absorptiometry (DXA), sex differences (higher in women) can be seen in a young age group (18 - 39 years, $p < 0.0001$) but not in older individuals (Camhi *et al.*, 2011). Another similar study using DXA in overweight and obese white, African American and Asian individuals showed that women (n = 215) had more femoral-gluteal SAT ($p < 0.05$) and intermuscular adipose tissue (IMAT, $p < 0.05$) than men (n = 104) (Yim *et al.*, 2008). Females accumulate more fat in the abdominal SAT compartment than males and, at young ages, accumulate more fat in VAT than males in normal, overweight and obese participants. It was shown that in overweight and obese patients, women accumulate more fat in the lower body and in muscle. The differences in body fat composition and distribution between the sexes may be mediated by the sex hormones. As reviewed by Mansor *et al.*, testosterone decreases total and SAT adiposity, abdominal SAT and VAT fat accumulation, and BMI and waist circumference in healthy, but not insulin resistant individuals (Mansour *et al.*, 2017). Whereas estrogen increases accumulation of SAT, loss of estrogen in menopause is associated with increased central fat deposition (Brown and Clegg, 2010).

Glucocorticoids, in addition to their function in the immune system, also regulate energy homeostasis, especially under conditions of stress (Putignano *et al.*, 2004). They stimulate hepatic glucose output and protein and lipid catabolism in muscle and adipose tissue (Putignano *et al.*, 2004). The use of glucocorticoids as a treatment changes body fat distribution and accumulation. Patients on

glucocorticoids (renal transplant patients and other diseases, n = 66) had more deep mediastinal ($p < 0.01$), buccal ($p < 0.001$), and superficial midthigh ($p < 0.05$) fat accumulation compared to healthy participants (n = 42) in both sexes (Horber *et al.*, 1986). Excessive endogenous glucocorticoids can also alter the composition and distribution of body fat. A study has investigated the relationship between the enzyme regulating cortisol production, 11 ß-hydroxysteroid dehydrogenase type 1 (11ßHSD1), glucocorticoid receptor (GRα) and adipose tissue depots in adipose tissue biopsies collected from SAT (abdominal, thigh, gluteal) and VAT (omental) depots in 21 obese women (aged 20 - 44 years, BMI 32.7 ± 1.5 kg/m^2). They found that 11ßHSD1 mRNA levels were highest in abdominal ($p < 0.001$) and omental ($p < 0.001$) depots, while GRα mRNA expression was highest in the omental ($p < 0.001$) depot. Omental 11ßHSD1 mRNA transcription was positively correlated with percentage body fat (%BF, R = 0.46, $p < 0.05$) and omental adipocyte size (R = 0.72, $p < 0.001$), while omental GRα mRNA transcription was negatively associated with %BF (R = -0.51, $p < 0.05$) and omental adipocyte size (R = -0.52, $p < 0.01$) (Michailidou *et al.*, 2007). This suggested that intracellular production of 11ßHSD1 is a predictor of visceral adiposity and adipocyte hypertrophy. Lower GRα mRNA transcription in VAT is associated with obesity. The impact of glucocorticoids on body fat distribution may include the regulation of adipose tissue blood flow, inhibiting cellular proliferation and promoting differentiation of preadipocytes, however, the contribution of each pathway remains unclear.

Ethnicity is a strong predictor of body fat composition and distribution. A cross-sectional study of 852 healthy young adult men (under 30 years) from different ethnicities (Asian, African Americans Hispanic, and non-Hispanic White) assessed body composition among ethnicities (Stults-Kolehmainen *et al.*, 2013). Asians (23.9 ± 3.4 kg/m^2, n = 202) had lower BMI than all other ethnicities, and non-Hispanic Whites (24.7 ± 3.2 kg/m^2, n = 432) had lower BMI than Hispanics (25.7 ± 3.9 kg/m^2, n = 151) and African Americans (26.5 ± 4.7 kg/m^2, n = 67) ($p < 0.0001$). Percent body fat measured by DXA was lower in African Americans (17.0 ± 10.0%) compared to non-Hispanic Whites (17.9 ± 7.2%), Asians (18.9 ± 8.0%) and Hispanics (21.8 ± 8.3%) ($p < 0.0001$). Individuals of Hispanic origin had the highest %BF relative to BMI whereas African Americans had the lowest in healthy young men. However, a similar study in men over 45 years showed that BMI and %BF were

similar among Hispanics, non-Hispanics and African Americans (Carroll *et al.*, 2008). For women, in the same study, even though BMI was similar across the three ethnicities, African Americans had higher %BF (43.9 ± 0.8%, n = 45) than Hispanic (40.9 ± 0.8%, n = 52, *p* < 0.05) and non-Hispanic White (39.7 ± 1.5%, n = 32, *p* < 0.05) women (Carroll *et al.*, 2008).

In young men, Hispanics had the highest regional percentage fat (%fat) compared to men of Asian and non-Hispanic origin, whilst African Americans had the lowest regional %fat in arm, trunk, leg, android and gynoid (Stults-Kolehmainen *et al.*, 2013). However, in older aged men, Hispanics, Whites and African Americans had a similar level of total fat and SAT mass, while African Americans had lower VAT than Hispanics and Whites (Carroll *et al.*, 2008). Additionally, a mixed sex study of participants (aged 30 - 65 years) of Chinese (n = 219), South Asian (SA, n = 207) and European White (EU, n = 201) origin showed that in normal, overweight and obese participants, Chinese had significantly higher VAT mass than EU (*p* < 0.008) measured by DXA, while in obese individuals, SA had more VAT than EU (*p* < 0.001) (Lear *et al.*, 2007). Compared to individuals of White origin, Chinese and SA cohorts had a relatively higher amount of VAT.

In summary, females have a higher percentage fat than males in normal, overweight and obese participants through their lifespan. Glucocorticoids, both exogenous and endogenous, alter body fat composition and distribution. With similar BMI, African Americans have relatively lower %BF at a young age and lower VAT level at older ages compared to Whites, Hispanics and Asians. Chinese and South Asians have a significantly higher level of VAT as a proportion of total body fat than White populations.

1.1.3 Metabolic consequences of obesity

The metabolic complications of obesity, often referred to as the metabolic syndrome, consists of insulin resistance, dyslipidaemia and altered triglyceride TG metabolism. Obesity increases cardiovascular risk through risk factors such as high plasma TG, high low-density lipoprotein (LDL) cholesterol, low high-density lipoprotein (HDL) cholesterol, and insulin resistance. The development of insulin intolerance, insulin resistance and T2DM will be discussed later, and this section will focus on dyslipidaemia and altered TG metabolism related to obesity.

There are five major lipoproteins, chylomicrons, very low-density lipoprotein (VLDL), intermediate-density lipoproteins (IDL), LDL and HDL. Chylomicrons are the largest and are the most lipid-rich lipoproteins and thus have the lowest density. In contrast, HDL is the smallest lipoprotein and contains the least amount of lipid. (Rader, 2008). In healthy individuals, there are three major types of lipids assessed in plasma, including HDL cholesterol, LDL cholesterol and plasma TG. Lipoproteins are large molecular complexes that transport TG and cholesterol in the blood in humans. The structure of lipoproteins includes a hydrophobic neutral lipid core comprised of TG and cholesteryl esters. Surrounding the core is a phospholipid and specialized protein (apolipoprotein) coat. Phospholipids, which are amphipathic, enable the interaction between the lipids caried by the lipoproteins and the aqueous environment of the blood. Apolipoproteins play important roles in the structural integrity of lipoproteins, interactions between lipoproteins and cell surface receptors, lipid transport and a variety of enzymes. Both cholesterol and TG play important roles in the human body: TG is the major mode of energy storage, transport and metabolism, and cholesterol is a key precursor of steroidogenesis and a structural membrane component.

In the exogenous pathway of lipid transport, dietary fat is absorbed by intestinal enterocytes and integrated into chylomicrons, containing apolipoprotein B-48 (APOB48) as its main protein component, which are then transported into lymph and bypass the liver. Once entering the systemic circulation, chylomicrons bind to lipoprotein lipase (LPL) on the luminal surface of capillary endothelium of tissues, mainly muscle and adipose tissue. The TG in chylomicrons is hydrolysed by LPL and free fatty acids (FFA) enter the tissue to be used for energy (in muscle) or storage (in adipose tissue). Then the TG-depleted chylomicron remnant (CMR) is released and captured by the LDL receptor (LDLR) and LDL receptor related protein (LRP) on hepatic cells via binding to apolipoprotein E (APOE). In the endogenous pathway of lipid transport, TG and cholesteryl esters synthesised in the liver, are packaged into VLDL containing apolipoprotein B-100 (APOB100) as the major apolipoprotein component. TG in VLDL is hydrolysed to IDL, and IDL can be captured by liver via binding of APOE to the LDLR or LRP. Alternatively, the TG and phospholipid in IDL can be hydrolysed by hepatic lipase (HL) to form LDL. LDL can be taken up by peripheral cells or by liver via binding of APOB100 to the LDLR (Rader, 2008).

The pathways of HDL metabolism and reverse cholesterol transport are more complex. HDL and its major apolipoprotein, apolipoprotein A-I (APOA1), are both synthesised not only in the liver, but also in the intestine. However, the second major HDL apolipoprotein, apolipoprotein A-II (APOA2), is only synthesised in hepatic cells. Nascent HDL can interact with peripheral cells to remove excess free cholesterol by the interaction with surface protein ATP-binding cassette protein A1 (ABCA1). Some of the facilitated free cholesterol is esterified to cholesteryl ester by lecithin-cholesterol acyltransferase (LCAT) and the nascent HDL forms the larger HDL3. With the further action of LCAT, HDL3 will eventually transform to even larger HDL2 with the addition of more cholesteryl ester. HDL2 carries cholesteryl ester and a free cholesterol back to hepatic cells via an HDL receptor called scavenger receptor BI (SRBI). The cholesteryl esters can also be transferred from HDL2 to APOB containing lipoproteins, such as VLDL and LDL, via the action of cholesteryl ester transfer protein (CETP) and returned to liver by LDLR. The TG and phospholipids in HDL2 can also be hydrolysed by HL or endothelial lipase (EL) remodelling it to HDL3. The cholesterol transported by HDL to the liver pool can be used for bile acid synthesis and is eventually excreted in to the bile and faeces as bile acid or free cholesterol (Rader, 2008).

In obese individuals lipoprotein metabolism is altered resulting in a decrease in plasma HDL, as well as increased plasma VLDL and TG, and is referred to as dyslipidaemia. Within situations of excess energy intake, hypertriglyceridemia may be a major cause of lipid abnormalities because it delays the clearance of TG-rich lipoproteins and formation of LDL. However, a cross-sectional analysis of two national studies, the National Health and Nutrition Examination Survey (NHANES, 1999 - 2010, USA, n = 12,383) and the Study on Nutrition and Cardiovascular Risk (ENRICA, 2008 - 2010, n = 11,765), examined the relationships between BMI, waist circumference (WC) and plasma LDL cholesterol (LDLc) (Laclaustra *et al.*, 2018). In NHANE and ENRICA, the slope of the BMI-LDLc association changed ($p < 0.001$) at BMI 27.1 and 26.5 kg/m^2, respectively, forming an inverted U shape. LDL concentration increased ($p < 0.001$) 2.30 and 2.41 mM per BMI unit below the given point and decreased ($p < 0.001$) 0.37 and 0.38 mM per BMI unit beyond the given point. The WC-LDLc relationship was similar to the BMI-LDLc relationship. This may suggest that in lean individuals, weight loss may

help to lower LDLc for cardiovascular prevention and the diminishing association of BMI-LDLc may indicate metabolic impairment in obese subjects.

Lipolysis of TG-rich lipoproteins may be impaired in obesity due to reduced mRNA expression levels of LPL in adipose tissue. In a study of 38 morbidly obese patients with T2DM (BMI 52.8 ± 7.4 kg/m^2), 10 obese patients (31.7 ± 1.7 kg/m^2) and 12 healthy lean controls (24.5 ± 2.5 kg/m^2), expression of *LPL* in SAT and VAT was examined relative to the control gene *PPIA*. *LPL* expression was highest in lean subjects in both SAT (p = 0.049) and VAT (p < 0.001) compared to obese and morbidly obese subjects. In obese subjects, expression of *LPL* was lower in VAT than in SAT (p < 0.05). This suggests that obesity decreases the expression of *LPL* in VAT to a greater extent than in SAT compared to lean healthy individuals. As a result, increased postprandial lipidemia leads to elevated levels of FFA, which may lead to detachment of LPL from its endothelial surface. A study has shown a significant correlation between postprandial plasma LPL activity and endogenous FFA (r = 0.40, p < 0.05) but not exogenous FFA, supporting that FFA controls endothelial LPL during the physiological condition in humans (Karpe *et al.*, 1992).

HDL metabolism is also strongly affected by obesity because of the increased number of CMR and VLDL, together with impaired lipolysis. The increased TG-rich lipoproteins results in increased CETP activity, which exchanges cholesteryl esters from HDL to TG from VLDL and LDL as reviewed elsewhere (Subramanian and Chait, 2012).

In summary, obesity may lead to an increase of plasma LDL and decrease of HDL, and thus disturbed lipid transportation and metabolism, thus dyslipidaemia. This will cause obesity associated metabolic syndromes.

1.1.4 Obesity, Insulin resistance and T2DM

T2DM is a result of the combination of two leading causes, defective insulin secretion of pancreatic ß-cells and the inability of insulin-sensitive tissues to respond appropriately to insulin (Galicia-Garcia *et al.*, 2020). The secretion and activity of insulin are two essential processes that contribute to glucose homeostasis. Defects in either, or both, of these pathways can lead to impaired

insulin sensitivity and development of T2DM. Benign and metabolic obesity and ectopic fat play important roles in the development of insulin resistance.

1.1.4.1 Insulin synthesis and secretion from pancreatic β-cells

The pancreatic ß-cell is the only cell that can produce and secrete insulin in the human body, and this process is tightly regulated (Cerf, 2013). Immature insulin, also known as pre-proinsulin, is synthesised in the ß-cell, and stored in its cytoplasm. In the maturation process, pre-proinsulin is firstly transferred in the endoplasmic reticulum (ER) to be truncated and conformationally folded to yield proinsulin (Bunney *et al.*, 2017). After that, proinsulin is transported from ER to the Golgi apparatus (GA) entering immature secretory vesicles and stored (Bunney *et al.*, 2017). Mature insulin is produced when proinsulin is cleaved by type I and II endoproteases to form free C peptide and mature insulin in the secretory vesicles (Fu *et al.*, 2013, Halban, 1994).

Once mature insulin is synthesised, insulin is stored in granules until it is released from the ß-cell (Galicia-Garcia *et al.*, 2020). Insulin secretion is mainly stimulated by high plasma glucose concentration (Galicia-Garcia *et al.*, 2020). When plasma glucose concentrations increase, glucose is transported into ß-cells via the glucose transporters 1 and 3 (GLUT1 and GLUT3). It is also thought that low affinity glucokinase (Hexokinase IV) acts as a glucose sensor (*Km* 15 - 20 mM) for the ß-cell (Galicia-Garcia *et al.*, 2020).

Glycolysis is activated as soon as glucose enters the cell which leads to an increased intracellular ratio of ATP/ADP. This then induces the inactivation of ATP-dependent K^+ channels in the plasma membrane. As a result of the membrane depolarization voltage dependent Ca^{2+} channels are activated in the plasma membrane and Ca^{2+} is transported into the ß-cell. The increase in intracellular Ca^{2+} level stimulates the priming and fusion of the insulin-containing secretory vesicles (granules) with the plasma membrane, and results in insulin release (Fu *et al.*, 2013, Boland *et al.*, 2017, Rorsman and Ashcroft, 2018, Seino *et al.*, 2011).

The release of insulin may also be stimulated by other factors including amino acids, fatty acids, and hormones, but these mechanisms contribute to glucose homeostasis only to a modest extent (Boland *et al.*, 2017).

1.1.4.2 Insulin response in healthy individuals

In healthy individuals the major function of insulin is insulin-mediated glucose uptake, and there are three major organs contributing to this mechanism. Skeletal muscle accounts for about 60 - 70% of whole body insulin-mediated glucose uptake via the insulin-dependent transporter glucose transporter type 4 (GLUT4) (Smith, 2002). The liver accounts for about 30% of whole-body insulin-mediated glucose insulin disposal, which is half that of skeletal muscle (Smith, 2002). Adipose tissue accounts for 10% of whole-body insulin-mediated glucose disposal, one sixth that of skeletal muscle (Smith, 2002), and is the third largest organ responsible for glucose disposal.

In the fed state, when circulating insulin and glucose levels increase, the classic insulin signalling pathway starts from insulin binding to the insulin receptor leading to tyrosine autophosphorylation of the receptor β units on the cell membrane. As a result, insulin receptor substrate (IRS) is phosphorylated on tyrosine residues by insulin receptor (IR) and then recruits phosphoinositide 3-kinase (PI3K) to the plasma membrane. After the relocation of PI3K, phosphatidylinositol (4,5)-bisphosphate (PIP2) is phosphorylated by PI3K to generate phosphatidylinositol (3,4,5)-trisphosphate (PIP3). The PIP3 can then activate phosphoinositide-dependent kinase-1 (PDK1), which phosphorylates protein kinase B (PKB, as known as Akt). Once PKB is activated, the downstream pathways of PKB, including glycogen synthesis, gluconeogenesis, glycolysis and lipid synthesis will be activated (Titchenell *et al.*, 2017).

There are four known IRS isoforms, IRS1 and IRS2 have a widely overlapping distribution and IRS1 can be phosphorylated by both the insulin receptor and the insulin-like growth factor 1 (IGF1) receptor to mediate the mitogenic effects of insulin and to stimulate glucose sensing of insulin secretion. IRS1 is the major type in skeletal muscle, while as IRS2 is the major IRS in liver. IRS2 mediates peripheral actions of insulin in adipose tissue and skeletal muscle, as well as the growth of pancreatic β cells (Kido *et al.*, 2001). The functions of IRS3 and IRS4 are less well understood. IRS3 is only found in adipose tissue, β cells and liver, while as IRS4 is only found in thymus, brain and kidney (Withers and White, 2000, Burks and White, 2001).

Glucose uptake by cells is mainly via ATP-independent GLUT. There are at least five subtypes of GLUT that have been identified (GLUT1 - 5). The five subtypes mainly differ in their *Km* for maximal glucose transport and insulin dependency (Table 1-1) (Hunter and Garvey, 1998, Litwack, 2018, Karam, 1997, Wilcox, 2005). This enables the utilisation of glucose in different cell types depending on their specific function. For example, GLUT1 is ubiquitous and is the principal GLUT in brain microvessels. GLUT1 also has high affinity for glucose to enable the transportation of glucose into the cell at low plasma glucose levels to meet the basal needs of the tissues, even at low insulin levels. GLUT4, which is the major GLUT isoform in skeletal myocytes and adipocytes, is highly insulin dependent. In the absence of insulin, 90% of GLUT4 stays in intracellular vesicles (Vargas E, 2020). GLUT4 activation is regulated by PI3K-protein kinase B (PKB, also known as Akt) pathways. PDK1 can be activated by PIP3, and this allows the phosphorylation of PKB by PDK1. Once it has been phosphorylated, PKB phosphorylates the Akt substrate of 160 kDa (AS160), a Rab-GTPase activating protein, inactivating it. The inactivated AS160 leads to activated Rab proteins that stimulate active vesicle formation to translocate GLUT4 storage vesicles (GSV) to allow the translocation of GLUT4 from intracellular vesicles to the plasma membrane, thus GLUT4 is able to transport glucose (Carmichael *et al.*, 2019).

Isoform	Distribution	Glucose affinity	Km (mM)	Characteristics
GLUT1	Brain microvessels Red blood cells Placenta Kidney Ubiquitous	High	1	Basal glucose transporter
GLUT2	Liver Kidney Pancreatic β cells Small intestine	Low	15-20	Insulin-independent
GLUT3	Brain neurons White blood cells Embryos Sperm	High	1.6	Major neuronal glucose transporter. Plasma glucose-independent
GLUT4	Muscle Cells Fat cells Heart	Medium	2.5-5	Sequestered intracellularly and translocate to cell surface in response to insulin
GLUT5	Small intestine Testes	Medium	6	High affinity to fructose, however, GLUT5 is a fructose transporter and does not transport glucose.

Table 1-1 Characteristics of glucose transport proteins (GLUT).

(Hunter and Garvey, 1998, Litwack, 2018, Karam, 1997, Wilcox, 2005)

In addition to regulation of glucose transport by insulin-dependent GLUT, the insulin signalling cascade regulates other critical pathways at the subcellular level, including carbohydrate metabolism, amino acid metabolism and mRNA transcription and translation.

Insulin is involved in carbohydrate metabolism at different levels. It stimulates the transportation of glucose into cells, especially skeletal myocytes and adipocytes via GLUT4 translocation. Insulin stimulates glycogen synthesis in muscle and liver by dephosphorylation of glycogen synthase kinase 3 (GSK3). In addition, insulin supresses glycogen breakdown by dephosphorylation of glycogen phosphorylase (Berg *et al.*, 2002). Insulin also stimulates fatty acid synthesis in adipose tissue and liver leading to formation and storage of TG in adipose tissue and liver.

Lipogenesis refers to the formation of TG, which mainly happens in adipocytes and the liver in healthy individuals. TG synthesis starts from the activation of FFA into acyl-CoA via acyl-CoA synthetase (ACS) to form FA-CoA. The complex FA-CoA and glycerol-3-phosphate (G3P) are acylated into lysophosphatidic acid (LPA) by G3P acyltransferase (GPAT), and then into phosphatidic acid (PA) by acyl-CoA acylglycerol-3-phosphate acyltransferases (AGPAT). PA is then dephosphorylated to diacylglycerols (DAG) by phosphohydrolase (PAP2). DAG can be then catalysed to TG by diacylglycerol acyltransferase (DGAT). (Saponaro *et al.*, 2015b)

FFA used for lipogenesis comes from the diet, peripheral lipolysis, or *de novo* lipogenesis (DNL). DNL mainly happens in the liver and adipocytes after a high-carbohydrate meal, when part of carbohydrate is stored as hepatic glycogen, while the excess is converted to fatty acids and TG (Hellerstein, 1999). Citrate (citric acid), which mainly comes from glycolysis, is the main source of DNL. In the process of DNL, citrate is firstly converted to acetyl CoA by ATP-citrate lyase (ACL), and malonyl-CoA by acetyl-CoA carboxylase (ACC). The malonyl-CoA is then transformed into fatty acids by the multi-enzymatic complex fatty acid synthase (FAS) (Saponaro *et al.*, 2015b). The role of insulin in lipogenesis is mainly promotion of DNL by inhibiting AMPK and therefore suppressing inhibition of ACC by AMPK (Witters *et al.*, 1988).

Lipolysis refers to the hydrolysis of TG, and the release of fatty acids and glycerol into the circulation. TG is hydrolysed by different lipases, including adipose triglyceride lipase (ATGL, mainly in adipocytes), hormone-sensitive lipase (HSL), and monoacylglycerol lipase (MGL). TG is firstly hydrolysed to DAG and one FFA by ATGL. After which, DAG is converted into monoacylglycerol (MAG) with the release of another FFA by MGL, and the MAG is then completely hydrolysed into a third FFA and one molecule of glycerol (Saponaro *et al.*, 2015b). HSL is activated mainly by ß-adrenergic stimulation and inactivated by insulin. A mixed sex study with thirteen subjects (aged 34 ± 3 years, BMI 23.9 ± 0.8 kg/m^2) was carried out where participants received IV placebo (n = 6) or 20% glucose (n = 7), followed by one hour of rest and 20 mins of mental stress. Plasma insulin (placebo versus glucose 5.7 ± 0.9 vs 6.8 ± 1.6 mU/L) and FFA (0.35 ± 0.07 vs 0.46 ± 0.08 mM) concentrations of the two groups were measured (Meijssen *et al.*, 2001). Twenty mins after injection, plasma insulin concentration in the glucose treated group (30.5 ± 4.8 mU/L, *p* < 0.01) increased more sharply than in the placebo group (9.5 ± 1.5 mU/L, *p* < 0.01). Forty mins later, plasma FFA decreased in both groups but were suppressed to a much greater extent in the glucose group (placebo versus glucose 0.27 ± 0.07 mM vs 0.11 ± 0.02 mM, *p* < 0.01). However, ten mins after mental stress, plasma FFA increased by 53% in the placebo group (*p* < 0.01) but remained unchanged in glucose group. This suggests that insulin, especially high insulin levels, suppresses endogenous lipolysis in young and lean participants, and insulin suppression of lipolysis may be stronger than by other hormones.

Insulin can also stimulate protein synthesis in many different tissues directly or indirectly. The effects of insulin promoting protein synthesis involves both transcription of specific mRNA and translation of mRNA into proteins in ribosomes. As reviewed by Hunter and Liu, insulin promotes mRNA transcription of glucokinase, PK, fatty acid synthase and albumin in the liver, pyruvate carboxylase in adipose tissue and amylase in the pancreas (Hunter and Garvey, 1998, Liu and Barrett, 2002). Insulin may also decrease mRNA transcription of liver enzymes, for example carbamoyl phosphate synthetase, a key enzyme in the urea cycle (Reardon and Weber, 1983). Effects of insulin on translation are ubiquitous and are influenced by both insulin and its co-factors.

Thus, in healthy individuals, insulin promotes transportation of glucose into cells to maintain glucose homeostasis, stimulates lipogenesis and protein synthesis, and supresses gluconeogenesis, lipolysis and synthesis of some proteins.

1.1.4.3 Obesity in the development of insulin resistance and T2DM

Obesity leads to insulin resistance and T2DM mainly by decreased insulin stimulated glucose transportation, impaired metabolism in skeletal muscle and adipose tissue, and impaired suppression of glucose output from the liver.

In both adipocytes and skeletal myocytes, insulin-regulated glucose transportation by GLUT4 is disrupted in obese subjects with insulin resistance or T2DM. However, as reviewed by Shepherd and Kahn, in skeletal muscles of obese and T2DM patients, the expression of GLUT4 level was normal (Shepherd and Kahn, 1999). The decreased glucose transportation in skeletal muscle is mainly mediated by impaired translocation, docking or fusion of GLUT4 containing vesicles to the plasma membrane (Shepherd and Kahn, 1999). As mentioned before, GLUT4 translocation and glucose transport function are mainly regulated by insulin and insulin signalling pathways in skeletal muscle and adipocyte. A study has shown that INSR, IRS1, and p85 subunit of PI3K expression were 55, 54, and 64% lower ($p < 0.05$ for all) in abdominus muscle in morbid obesity (n = 8, aged 40 ± 2 years, BMI 52.9 ± 3.6 kg/m^2) compared to lean controls (n = 8, aged 40 ± 2 years, BMI 25.7 ± 0.9 kg/m^2) by immunoblotting (Goodyear *et al.*, 1995).

Downstream regulators of the insulin signalling pathway may also be involved in the impaired glucose transport observed in obese individuals. In a mixed sex study, protein expression of IRS1, IRS2 and PI3K (p85 subunit of PI3K) in abdominal subcutaneous adipocytes was compared in healthy controls (n = 14, aged 44 ± 3 years, BMI 30.0 ± 2.0 kg/m^2), T2DM (n = 12, aged 63 ± 2 years, BMI 29.9 ± 0.9 kg/m^2) and T1DM (n = 8, aged 41 ± 5 years, BMI 27.8 ± 1.2 kg/m^2) (Rondinone *et al.*, 1997). Expression of IRS1 was 70 ± 6% lower in T2DM compared with healthy controls, but did not differ in T1DM adipocytes. In addition, adipocyte expression of IRS1 and PI3K was unchanged in individuals with T2DM and T1DM compared to healthy controls. Both IRS1$^{-/-}$ (n = 9) and IRS2$^{-/-}$ (n = 8) mice showed a disturbed insulin-induced peripheral glucose utilisation compared with WT (n = 11, $p < 0.05$), while decreased endogenous glucose production and hepatic glycogen synthesis

was only significantly lower in IRS2$^{-/-}$ ($p < 0.05$ and $p < 0.05$, respectively) mice (Previs *et al.*, 2000). Similarly, another study showed that only IRS2$^{-/-}$ mice developed disrupted insulin homeostasis because of insulin resistance in liver and skeletal muscle and a lack of ß cell compensation. In mice, even the growth of mice was 'restricted', but no diabetes developed because of an increased insulin secretion (Withers *et al.*, 1998). IRS2 may have a wider and more critical role in insulin signalling in adipocytes, liver, and muscle compared to IRS1. Additionally, another study has examined the insulin dependent PKB signalling pathway in skeletal muscle collected from lean control men (n = 8, aged 52 ± 5 years, BMI 24.3 ± 0.6 kg/m^2), obese men without T2DM (n = 8, aged 45 ± 3 years, BMI 31.7 ± 1.3 kg/m^2) and obese men and women with T2DM (mixed sex, male n = 9 and female n = 3, aged 50 ± 3 years, BMI 34.0 ± 1.3 kg/m^2) (Kim *et al.*, 1999). They found that the insulin stimulated PKB signalling pathway remained unchanged, and that IRS1 and IRS2 protein levels were normal in obese groups compared to the lean controls. However, the increase in PI3K activities associated with IRS1 was significantly lower in diabetes than in lean controls (diabetes, obese vs lean 2.4, 3.7, vs 6.1 -fold change, p value diabetes vs lean < 0.01). Similarly, the increase in IRS2 associated PI3K activities was lower in diabetes than lean controls (diabetes vs lean 1.4 vs 2.2 -fold change, $p < 0.01$). Thus, impaired glucose transportation in obesity may be responsible for the development of insulin resistance and T2DM, and this may be mainly caused by altered levels of PI3K associated with IRS.

In normal conditions, insulin suppresses lipolysis and FFA release from adipocytes as described above. However, there is abundant evidence that plasma FFA levels are increased in obese individuals (Reaven *et al.*, 1988, Boden *et al.*, 1994, Santomauro *et al.*, 1999). In individuals afflicted with impaired glucose regulation and T2DM, the insulin-mediated suppression of lipolysis and FFA release may be compromised (Figure 1-1) (Groop *et al.*, 1989, Saponaro *et al.*, 2015b). The increased FFA, in reverse, disturbs metabolism in other tissues. In muscle, an acute increase of plasma FFA within four hours to a low (516 - 1,207 µM) or high (464 - 1,857 µM) concentration resulted in a significant increase in intramyocellular TG (IMCL-TG) by 9 ± 5% or 33 ± 11% ($p < 0.05$ and < 0.01, respectively) and an increase in insulin resistance demonstrated by a glucose infusion rates test ($p < 0.05$ for all, after 3.5 h) in seven mixed sex lean

participants (aged 26 ± 2 years, BMI 23.3 ± 0.7 kg/m^2) (Boden *et al.*, 2001). The accumulation of IMCL-TG was positively correlated with plasma FFA (r = 0.74, *p* < 0.003). Increased FFA uptake also reduced glucose utilisation via reduced ATP synthesis in skeletal muscle. In the same lean male patients (n = 8, aged 26 ± 1 years, BMI 22.5 ± 0.7 kg/m^2), ATP synthase flux was increased by 60% (*p* = 0.02) at low plasma FFA levels (low, ~36 µM) in response to hyperinsulinemia-euglycemic clamps in gastrocnemius-soleus muscle. In the presence of high lipid infusion (plasma FFA 1,034 µM), the ATP synthase flux was lowered (high vs low 11.0 ± 0.9 vs 14.6 ± 1.2 µM, *p* < 0.05) (Brehm *et al.*, 2006). The perturbation in metabolism, resulting from increased plasma FFA, can potentially exacerbate or even trigger whole-body insulin resistance by impeding the customary compensatory response of increased glycolysis to reduced ATP synthesis, thereby diminishing overall glucose utilization.
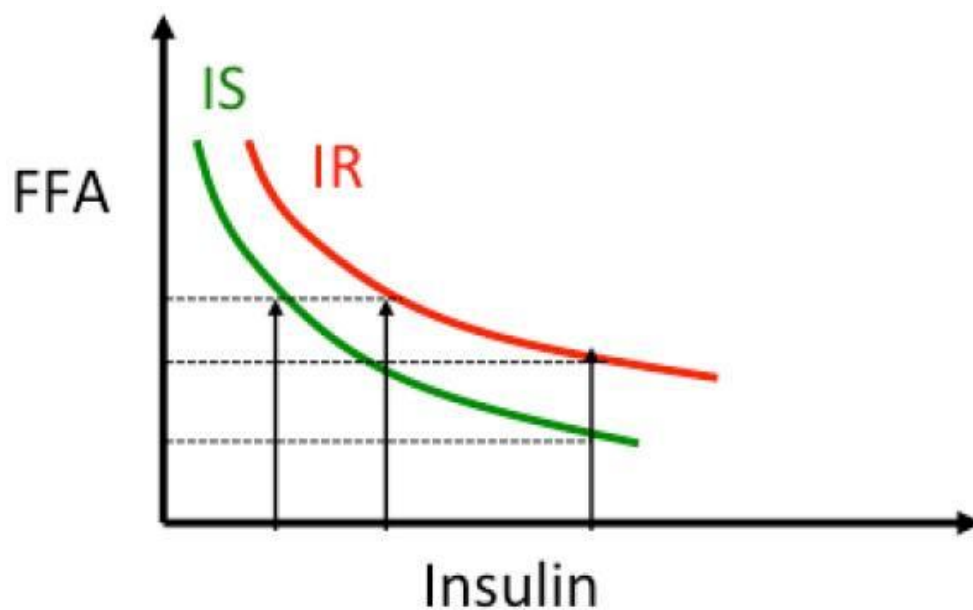
Figure 1-1 Relationship of insulin-stimulated lipolysis in insulin sensitive (IS) and insulin resistant (IR) individuals.

FFA, plasma free fatty acid. Reviewed by (Groop *et al.*, 1989, Saponaro *et al.*, 2015b).

In the liver, excess hepatic glucose production is an essential factor contributing to insulin resistance and disordered whole-body glucose homeostasis in obesity. A study in liver glucose-6 phosphatase (G6Pase) deficient male mice, and enzyme required for endogenous glucose production, showed that G6Pase$^{-/-}$ mice (n was not given) had lower body weight (*p* < 0.01) and %fat (*p* < 0.01) compared to WT mice in response to a high fat/ high sucrose diet (Abdul-Wahed *et al.*, 2014).

Interestingly, when the G6Pase exon 3 was deleted in liver in this knockout mouse model, there was a fast restoration of glucose and a decrease in body weight ($p < 0.05$) and % body fat ($p < 0.01$). Similarly, endogenous glucose production (EGP) was lower ($p < 0.001$) in obese cats than lean cats (n = 12 in each group, same sex distribution), as shown by a triple tracer protocol after an over-night fast and three diets, due to lower glycogenolysis and gluconeogenesis (GNG, $p < 0.03$) (Kley *et al.*, 2009). There was a negative correlation between EGP and BMI ($r^2 = 0.44$, $p < 0.001$), girth ($r^2 = 0.47$, $p < 0.001$) and fasting plasma insulin ($r^2 = 0.34$, $p < 0.003$) in mice. Additionally, non-alcoholic fatty liver disease (NAFLD), which is highly relevant to overweight and obesity, presents a variety of histopathological abnormalities and is associated with insulin resistance and abnormal glucose homeostasis. This may also in turn lead to excessive glucose production from the liver, insulin resistance and T2DM. Obese children with NAFLD (n = 234, aged 15 [4] median [interquartile range, IQR] years) had a much higher BMI (38.1 [8.5] kg/m^2 vs 34.7 [7.1], $p < 0.001$), fasting glucose concentration (15 [11] vs 11 [7] µU/mL, $p < 0.001$) and lower insulin sensitivity index (ISI, 8 [5] vs 12 [7] unit, $p < 0.001$) compared to obese children without NAFLD (n = 337, aged 15 [3] years) (Bedogni *et al.*, 2012). Therefore, excessive glucose production by the liver in obesity may be one of the causes of whole-body insulin resistance.

1.1.5 Adipose tissue expansion theory and the development of T2DM

The major mechanism that contributes to obesity is the expansion of white adipose tissue (WAT), which if it is impaired contributes to the risk of development of insulin resistance and T2DM.

Adiposity may be a better indicator of T2DM than BMI. In a cross-sectional study of adults (n = 3,367, including 2,307 men and 1,060 women) in which 422 (12.53% of total) participants were diagnosed with T2DM it was shown that males (OR 1.68 [1.29, 2.19]) had larger waist-to-hip ratio (> 0.9 for male and > 0.8 for female) (WHR, OR 1.56 [1.18-20.7]), and higher percent body fat (> 20% in male and >28% in female) than females, factors that were strong predictors of T2DM (OR 1.62 [10.1 - 2.68]) (Chen *et al.*, 2020). A longitudinal study with on average 9.2 years follow-up in 3,055 men and 2,957 women (aged 35 - 74 years) who were free of T2DM at baseline showed that both overall and abdominal adiposity were strong

predictors of T2DM (Meisinger *et al.*, 2006). A total of 243 men and 158 women developed T2DM during the follow up, and multivariable-adjusted hazard ratios across quartiles showed that BMI (quartiles, men, 1.0, 1.37, 2.08, and 4.15, women 1.0, 3.77, 4.95, and 10.58), waist circumference (men, 1.0, 1.15, 1.57, and 3.40, women, 1.0, 3.21, 3.98, 10.70) and WHR (men, 1.0, 1.14, 1.80, and 2.84, women, 1.0, 0.82, 2.06, and 3.51) were predictors of T2DM. By joint analysis, the highest risk factor in both sexes was a high BMI combined with high waist circumference and WHR.

However, not all obesity leads to insulin resistance or T2DM eventually. So-called 'benign obesity', or metabolically healthy obesity (MHO), refers to the group of obese individuals that may be free of metabolic risk that is commonly associated with obese subjects. According to the Third National Health and Nutrition Examination Survey, 10% of obese individuals may be MHO based on insulin sensitivity and metabolic syndrome (Eckel *et al.*, 2016). It has been considered that VAT, rather than SAT may contribute mainly to the risk of obesity associated syndromes. However, a mixed sex study of white participants showed that overweight (n = 133, aged 46 ± 1 years), obese with normal insulin sensitivity (benign obese, n = 31, aged 47 ± 2 years) and obese with insulin resistance (obese-IR, n = 96, aged 46 ± 1 years) individuals had higher %fat ($p < 0.001$) and waist circumference ($p < 0.001$) than lean controls (n = 54, aged 45 ± 2 years), however, there was no group difference between benign obese and obese-IR groups. The difference between benign obese and obese-IR group was found in intramyocellular lipids (benign vs IR, women 4.0 ± 0.4 vs 4.6 ± 0.2 AU, $p < 0.001$, men 5.6 ± 1.1 vs 10.5 ± 1.2 AU, $p < 0.001$) and % liver fat (4.3 ± 0.6 vs 9.5 ± 0.8%, $p < 0.001$) in both sexes. Ectopic fat and liver fat, rather than visceral fat, may be more important indicators of the benign obese phenotype. However, MHO may not be a stable condition in the long term. As reviewed, after an up to 10 years follow-up, between one-third to one half of MHO individuals developed unhealthy syndromes (Kramer *et al.*, 2013, Eckel *et al.*, 2018, Hamer *et al.*, 2015).

1.1.6 Epidemiology and risk factors for T2DM

Since the 1980s, when T2DM started increasing with 108 million patients (~2.5% of the population) estimated worldwide, the number of patients has rocketed to 422 million (~5.8% of the population) globally in 2014 (WHO, 2016). The prevalence of

obesity and T2DM is higher than most non-infectious diseases and it has been labelled as an increasing worldwide epidemic. Similar data from the Global Burden of Disease study analysed by Khan *et al*. is shown in Table 1-2 (Khan *et al.*, 2020). The initial increase in T2DM was primarily reported in high-income countries, however since late 2000, increased rates of diabetes have also been observed in low and middle-income countries (WHO, 2016). However, even with better public health care, developed regions, including Western Europe and the USA, still have an overall considerably higher prevalence of T2DM than developing regions like China and India. T2DM is a severe problem globally.

Region	Prevalence (cases per 100,000)
Global	6,059
Europe	8,529
Germany	9,091
France	6,843
Italy	9,938
Spain	8,796
Netherlands	11,344
Switzerland	10,040
Sweden	10,448
Turkey	6,483
Russia	6,865
United Kingdom	8,663
Asia	5,961
China	6,262
India	4,770
Japan	6,737
South Korea	8,835
Saudi Arabia	7,661
Iran	7,000
Australia	5,235
America	7,060
United States	8,911

Table 1-2 Prevalence of T2DM globally in 2017.

Data was originated from the Global Burden of Disease Study and analysed by Khan *et al*. (Khan *et al*., 2020).

In the UK, there were 3.7 million people (~5.6% of the total population) diagnosed with diabetes in 2017 (DiabetesUK, 2017), however, the population of diagnosed diabetes had increased to 3.9 million (~5.9% of the total population) by 2019 (DiabetesUK, 2019). The prevalence is similar to the global prevalence. Within all diabetes, around 90% of patients were T2DM, 8% were T1DM, and 2% were rare types of diabetes (DiabetesUK, 2021). There was an estimated almost 1 million

people with undiagnosed T2DM at the same time (DiabetesUK, 2021). The prevalence of diabetes in Wales (6.31%) and England (~5.88%) was higher than in Scotland (5.49%) and Northern Ireland (5.29%) in 2019 (DiabetesUK, 2019). By estimation, more than 5 million people will have diabetes in the UK by 2025 (DiabetesUK, 2021).

Overweight and obesity contribute to 80 - 85% of the risk of T2DM for individuals (Ng *et al.*, 2014). In addition, a complex combination of genetic (ethnicity and family history), metabolic and environmental factors (age, adiposity), lifestyle (exercise and fitness) and other factors, that interact with one another, contribute to the disease prevalence (Hu *et al.*, 2001, Schellenberg *et al.*, 2013).

Age is an important risk factor for T2DM. The prevalence of impaired fasting glycemia (IFG) and T2DM increase with increasing age. In the USA, around 3.7% of people were diagnosed with diabetes in the 20 - 44 years age group, while this number increased to 13.7% in the 45 - 64 years age group and in the 65 years and above age group, the prevalence increased to 26.9% (Centers for Disease Control and Prevention, 2011). This association between prevalence of T2DM and age can also be found in England, where in men the prevalence of doctor-diagnosed diabetes increased from 0.8% aged 16 - 24 years to 15.7% aged 65 - 74 years, and in women increased from 0.9% aged 16 - 24 years to 10.6% aged 75 years and over (Craig and Mindell, 2008). A similar trend was also found in Japan and Taiwan (Nakano and Ito, 2007, Chen *et al.*, 2006). The reason for the increase in T2DM risk with increased age will be further investigated in this thesis.

Globally, the incidence and prevalence of T2DM varies widely depending on ethnicity. Black populations and Asians have higher incidence rates of T2DM compared to white populations in the United States (Karter *et al.*, 2013), and in the UK (Sattar and Gill, 2015, McKeigue *et al.*, 1991, Haines *et al.*, 2007). The higher prevalence of diabetes in England and Wales compared to the rest of UK, is partially related to the higher percentage of minority ethnicities in England and Wales (14%) than Scotland (4%) and Northern Ireland (1.8%). In the UK, Blacks, South Asians, and Chinese are at a higher risk of developing diabetes. According to a recent analysis of UK Biobank data, the prevalence of T2DM at BMI 30 kg/m^2 in Whites (n = 471,174, mixed sex), was equivalent in the following ethnic groups at lower BMI: Blacks 26.0 kg/m^2 (n = 7,949, mixed sex), Chinese men 26.0 kg/m^2

(n = 569), Chinese women 24 kg/m^2 (n = 965), and South Asians 22 kg/m^2 (n = 9,631, mixed sex) (Ntuk *et al.*, 2014). Similarly, for an equal prevalence of T2DM at waist circumference of 88 cm in White women, waist circumference in the following ethnic groups in women: Black women 79 cm, Chinese women 74 cm and South Asian women 70 cm; and in White men 102 cm equated to: Black men 88 cm, Chinese men 88cm, and South Asian men 79 cm gave equivalent prevalence. In addition, according to the analysis of UK primary care data, South Asians (n = 7,252, mixed sex) and Blacks (n = 4,115, mixed sex) were diagnosed with diabetes at around ten years younger (46 ± 12 and 48 ± 12 years) compared to Whites (n = 79,270, 58 ± 12 years, mixed sex), and similarly, at a lower BMI compared to Whites (Paul *et al.*, 2017). Therefore, in the UK, compared to Whites and even other ethnic minorities, South Asians develop diabetes at younger age, lower BMI and smaller waist circumference.

Exercise is an important intervention to lower the risk of T2DM. Former elite athletes (male, n = 392, aged 73 ± 6 years) had a significantly lower risk of T2DM (OR 0.72 [95% confident interval (CI), 0.53, 0.98]) and impaired glucose tolerance (OR 0.58 [0.38, 0.87]) compared to controls (male, n = 207, aged 72 ± 6 years) in later life (Laine *et al.*, 2014). However, it has been shown that IMCL is higher in athletes compared to lean individuals at similar BMI. In a mixed sex study of subjects aged 25 - 50 years, the IMCL in lean exercise-trained individuals (men, n = 8, BMI 25.3 ± 0.8 kg/m^2, women, n = 1, BMI 24.3 kg/m^2) was higher (2.36 ± 0.37 vs 1.40 ± 0.28% area as lipid, $p < 0.01$) than seven sedentary lean subjects (men, n = 4, BMI 25.2 ± 0.9 kg/m^2, women, n = 5, BMI 21.8 ± 0.9 kg/m^2) by quantitative image analysis of Oil red O stained vastus lateralis tissue. A similar difference was found between T2DM subjects (men, n = 4, BMI 30.9 ± 1.2 kg/m^2, women, n = 4, BMI 37.8 ± 1.1 kg/m^2) and lean (3.04 ± 0.39 vs 1.40 ± 0.28%, $p < 0.01$), but not between obese (men, n = 7, BMI 33.9 ± 1.0 kg/m^2, women, n = 4, BMI 33.8 ± 1.1 kg/m^2) and lean participants (Goodpaster *et al.*, 2001). On the contrary, the correlation between insulin sensitivity by hyperinsulinemic euglycemic clamp and IMCL was only significant in T2DM, obese and lean participants (r = -0.57, $p < 0.05$), but became insignificant whenexercise-trained subjects was added (Goodpaster *et al.*, 2001). Another study has also shown that even with the increased IMCL area density due to an increase in number of lipid droplets, six-month endurance training increased VO2 max ($p < 0.0001$), %fat oxidation ($p = 0.018$), short-chain

beta-hydroxacyl-CoA dehydrogenase (SCHAD, p = 0.003) and citrate synthase (p = 0.042) in five lean men (aged 24 ± 4 years, %fat 17.5 ± 7.7%, BMI was not given) and seven lean women participants (aged 22 ± 1 years, %fat 25.9 ± 4.2%) (Tarnopolsky *et al.*, 2007). Exercise increased the IMCL in athletes to obese or T2DM level, but the increased IMCL did not increased the risk of T2DM or cardiovascular risk in athletes. This is termed the athlete's paradox. This may be caused by increased total mitochondrial area in skeletal muscle (Tarnopolsky *et al.*, 2007), or as reviewed, differences in diet-induced and exercise-induced accumulation of TG in skeletal muscle (van Loon and Goodpaster, 2006). A more nuanced analysis is required to resolve the paradox and will be further investigated in this thesis.

1.1.7 Plasma extracellular vesicles (EV) in obesity and T2DM

EVs are nanosized spherical vesicles which are membrane-bound, and are released from almost all live cells. EVs transport cargos of nucleic acids, proteins and lipids from donor cells for intercellular communication (Zaborowski *et al.*, 2015).

1.1.7.1 Size and components of EV

EVs are categorized by their size (diameter) and how they are produced by cells. Exosomes have a diameter of 20 - 150 nm, microvesicles (MVs) of 100 – 1,000 nm, and apoptotic bodies of 50 – 5,000 nm (Doyle and Wang, 2019). Both exosomes and MVs are produced by healthy living cells. Exosomes are formed intracellularly by inward budding of the membrane of early endosomes and mature into multivesicular bodies (MVBs) (Borges *et al.*, 2013, Doyle and Wang, 2019). They are then either degraded by lysosomes with the MVB or released into the extracellular space when the MVB fuse with the plasma membrane of the cell. In contrast, MV are formed by direct outward budding, or pinching, of the plasma membrane from the donor cells (Borges *et al.*, 2013, Doyle and Wang, 2019). Apoptotic bodies, which are also formed by a separation of the plasma membranes, are released from apoptotic cells as a result of increased hydrostatic pressure after cell contraction (Wickman *et al.*, 2012). Common ways to isolate EV from serum in labs include one, or a combination of, cushion ultracentrifugation (CUC), ultracentrifugation (UC), polymer-based precipitation using Exoquick plus, size exclusion chromatography (SEC) using qEV columns or iodixanol density

centrifugation (DG). The mean and mode sizes of the vesicles from each method are show shown in Table 1-3 (Brennan *et al.*, 2020). With all the EV isolation methods that are used popularly, there is an overlapping isolation of the three subtypes of EVs, and it is difficult to distinguish one from another by size. Therefore 'biological markers' of each subtype of EV, in addition to size, are widely used in recent studies to identify subsets of EV.

Isolation Technique	Modal size (nm)	Median size (nm)
Unprocessed serum	52.4 ± 0.7	58.8 ± 0.4
ExoQuick	—	
ExoQuick plus	57.0 ± 0.7	64.2 ± 3.0
qEV1	64.9 ± 0.7	73.4 ± 2.3
qEV2	56.2 ± 0.9	58.6 ± 1.1
UC	73.2 ± 4.2	92.9 ± 2.4
CUC-UC	93.2 ± 6.6	115.2 ± 3.7
DG-UC	109.0 ± 5.8	130.7 ± 5.9
CUC-DG-UC	104.2 ± 1.3	127.6 ± 3.2
qEV1-DG-UC	118.5 ± 5.5	152.9 ± 6.6

Table 1-3 Size of particles by different EV isolation methods from human serum.

Size was determined by nanoparticle tracking analysis (NTA). Cushion ultracentrifugation (CUC), ultracentrifugation (UC), polymer-based precipitation using Exoquick plus, size exclusion chromatography (SEC) using qEV columns or iodixanol density centrifugation (DG). (Brennan *et al.*, 2020)

The formation of exosomes and the transportation of MVB rely on the endosomal sorting complexes required for transport (ESCRT) pathways. The proteins involved in the ESCRT pathway are generally thought to be present in all or most exosomes regardless of the type of cell from which they originated (Babst *et al.*, 2002, Wollert and Hurley, 2010). Therefore, these proteins are generally recognised as exosome marker proteins. However, there are also exosomes released via ESCRT-independent pathways. When expression of key ESCRT proteins (Hrs, Tsg10, Vps22, Vps24, and nSMase2) were disrupted by siRNA in Hep-2 cells, immunofluorescence (IF) confocal microscopy was still able to detect the production of MVB (Stuffers *et al.*, 2009). Similarly, in ESCRT-depleted Epstein-Barr virus-transformed human B-cells, CD63 positive exosomes were identified (Buschow *et al.*, 2010). The tetraspanin family of proteins, including CD63, CD9 and CD81, are commonly found in exosomes and are often enriched in EVs compared to the cell lysate (Witwer *et al.*, 2013, Sinha *et al.*, 2014). The tetraspanin proteins were initially thought to be biomarkers that could distinguish exosomes from MVs, however, these proteins

have been also identified in MVs and apoptotic bodies (Tauro *et al.*, 2013, Sinha *et al.*, 2014). Tetraspanin proteins were found at 100-fold higher concentrations in MVs than in cell lysates (Escola *et al.*, 1998). Because of the different routes of formation, the presence of cytosolic and plasma membranes in MVs, and the proteins specifically identified in organelles, including mitochondria, Golgi apparatus, nucleus, and endoplasmic reticulum, might be depleted in MVs (Christianson *et al.*, 2013). However, unlike exosomes and MVs, apoptotic bodies contain proteins both from intracellular organelles and plasma membranes of cells (Borges *et al.*, 2013). However, the proteomic profiles of apoptotic bodies and cell lysates are quite similar, whereas there are big differences in protein concentration and content observed in proteomics profiles of exosomes and cell lysates (Doyle and Wang, 2019). Therefore, a combination of size, cell source, and protein content should be used for the identification of subtypes of EV. There is a requirement for identification of new markers to distinguish MVs from exosomes. In the current thesis, the term EVs, rather than the specific name of a subtype, will be preferentially used where the specific subtype is not clear.

The majority of nucleotides contained in EVs are RNAs, predominately RNAs that are shorter than 200 nucleotides (nt) (Zaborowski *et al.*, 2015, Huang *et al.*, 2013, Eirin *et al.*, 2014). In mouse hypothalamic neuronal (GT1-7) cell culture medium isolated EVs, sequencing of the total RNA found within the EV showed that small RNA, including siRNA, tRNA, and miRNA, etc., made up around 15% of total RNA, with retroviral RNA repeat regions (51%), rRNA (0.5%) and mRNA (33%) making up the rest (Bellingham *et al.*, 2012). In EV isolated from human plasma (n = 12, aged 31 - 62 years, sex not given), small RNA sequencing showed that the RNA contents of EV included mRNA (26%), miRNA (19%), miscellaneous RNA (14%), small nuclear RNA (10%), tRNA (9%), rRNA (1%) and others (Chettimada *et al.*, 2020). These data show that the RNA components in EVs mainly consist of mRNA, miRNA and small RNA. This is different to whole live mammalian cells, where rRNA (80%) and tRNA (15%) are dominant. A variety of RNA types have been identified from EV, however whether they are tissue specific and/or EV subtype specific remains unclear. To what extent EV-RNAs are full length and/or fragments of cellular RNA, including transcripts, remains unclear. DNA, which was thought not to be present in EV, has been isolated from human glioblastoma cell culture medium isolated EV (Guescini *et al.*, 2009), primary human glioblastoma cell culture medium isolated EV (Balaj

et al., 2011) and human plasma EV from patients with pancreatic cancer (Kahlert *et al.*, 2014). The size of EV-DNA ranges from 100 - 2,500 bp and it is double stranded. However, the evidence for the presence of DNA in EV is limited mainly to culture cell lines and patients with cancer. The function of EV DNA cargo remains unknown.

1.1.7.2 Plasma EV in obesity and T2DM

Obesity and T2DM affect whole-body metabolism but their influence on EV release and content has not been extensively investigated and very little evidence is available. In a cross-sectional study, plasma EV concentration was found to be higher in overweight (n = 7) and obese patients (n = 20) compared to lean controls (n = 21). Both MV and exosome fractions differed. 'MVs' (overweight vs lean, $p < 0.05$, obese vs lean, $p < 0.005$) and 'exosomes' (overweight vs lean, $p < 0.001$, obese vs lean, $p < 0.05$) (Amosse *et al.*, 2018). Systematic depletion of plasma EVs significantly decreased (halved) macrophage migration inhibitory factor (MIF) in lean (n = 19, 'MVs', $p < 0.005$, 'exosomes', $p < 0.005$), overweight (n = 19, 'MVs', $p < 0.05$, 'exosomes', $p < 0.005$), and obese (n = 19, 'MVs', $p < 0.0001$, 'exosomes', $p < 0.0001$) individuals to a similar extent, but not other soluble factors[1] (Amosse *et al.*, 2018). As highlighted in the literature, soluble factors have a significant role in cell engineering, and their reduction has been observed in obesity and T2DM patients (Krebs *et al.*, 2007). While these factors are typically secreted and present in plasma, the potential role of EVs in providing an additional layer of regulation, possibly by sequestering and transporting these factors, could present a novel avenue for further research.

A study where HepG2 cells (human hepatic cancer cell line) were treated with plasma EVs isolated from female participants (obese, n = 4, aged 34 ± 3 years, BMI 34.3 [1.70] kg/m^2, normal control, n = 4, aged 35 ± 3 years, BMI 23.9 [1.70] kg/m^2) showed that intracellular TG concentrations doubled in cells treated with EV from obese participants ($p < 0.005$) when compared with nontreated cells (N), and were higher ($p = 0.018$) when compared to control EV treated cells (Afrisham *et al.*, 2020). Similarly, GSK3β protein was decreased in cells exposed to obese EV

---

[1] A soluble factor is a bioactive molecule, such as a hormone, growth factor, or cytokine, that is capable of dissolving in bodily fluids. These factors play essential roles in cellular communication, influencing processes like cell growth, differentiation, and immune responses.

compared to non-treated cells (p = 0.002) and cells exposed to control EV (p < 0.002). Glycogen was decreased significantly by one half in cells exposed to obese EV compared to cells exposed to control EV (p = 0.018) (Afrisham *et al.*, 2020). This suggests that plasma EVs in obesity may mediate increased TG accumulation and decreased glycogen synthesis in hepatic cells *in vitro*.

Obesity and T2DM may increase the secretion of plasma EVs, with altered content, which may in turn, have a further influence on other tissues to mediate metabolism that decreases insulin sensitivity. However, the mechanism remains unclear due to lack of evidence.

1.2 The biology of adipose tissue and insulin resistance

Adipose tissue is the largest lipid storage and endocrine organ (Kershaw and Flier, 2004, Scherer, 2006, Wang and Hai, 2015). The involvement of adipose tissue in the regulation of metabolism in healthy and insulin resistant subjects will be discussed in this section.

1.2.1 Types of adipose tissue

1.2.1.1 White adipose tissue

White adipose tissue (WAT) contains white adipocytes each with a large unilocular lipid droplet. WAT is the largest organ of lipid storage and the largest endocrine organ in the human body, and accounts for 3 - 70% of total body weight (Wronska and Kmiec, 2012, Wang and Hai, 2015). Apart from the traditional roles of energy storage and release of FFA when energy is required, white adipose tissue has an endocrine function, including the secretion of adipokines, inflammatory factors, and hormones such as leptin, adiponectin, resistin, and estrogens. WAT plays an important role in the regulation of glucose homeostasis, insulin sensitivity and the inflammatory response.

1.2.1.2 Brown adipose tissue

Brown adipose tissue (BAT) is a thermoregulation organ widely distributed in the infant human and is located in the interscapular, subscapular, axillary, intercostal, perirenal and periaortic regions (Cannon and Nedergaard, 2004).

However, these depots rapidly decrease during development and in adult humans it is only found in small amounts distributed in the supraclavicular, paravertebral, mediastinal, para-aortic and suprarenal regions (Nedergaard *et al.*, 2007). Unlike white adipocytes, brown adipocytes are multilocular lipid storage cells with a significant number of mitochondria (Sell *et al.*, 2004). The brown colour of brown adipocytes comes from the high density of mitochondria. Uncoupling protein 1 (UCP1), which is the distinguishing feature of brown adipocytes, resides in the inner membrane of the mitochondrion. It uncouples electron transport from adenosine triphosphate (ATP) production in the respiratory chain and leads to the generation of heat (Nicholls and Locke, 1984).

There are significant differences in the amount and anatomical distribution of BAT between animals. In rodents, BAT is abundantly located in the interscapular region throughout life, whereas in human the majority of BAT disappears from interscapular region in adults, with only a small portion found in perirenal and axillary depots with decreased *UCP* expression compared to children (Lean *et al.*, 1986). In adult humans, BAT showed no increased in oxygen consumption or interscapular temperature after adrenaline infusion (Astrup *et al.*, 1984). However, in a study cross-sectional mixed sex study (n = 2,934, aged 36 ± 14 years), PET-CT was used to detect BAT from all the potential BAT depots (Lee *et al.*, 2010). BAT was detected in 250 (8.5%) of the participants and was mostly located in the supraclavicular fossae (60.4%) and posterior cervical areas (58.1%). Compared to BAT negative individuals (n = 2,684), BAT positive individuals were more likely to be female (27% vs 43%, *p* < 0.001), younger (36 ± 1 vs 52 ± 1 years old, *p* < 0.001), leaner (20.1 ± 0.1 vs 24.9 ± 0.1 kg/m^2, *p* < 0.01) and have lower fasting glucose concentrations (4.9 ± 0.1 vs 5.5 ± 0.1 mM, *p* < 0.01). Using multi-variate analysis, sex, age (negatively) and BMI (negatively) were independently associated with the presence of BAT, but the association with fasting glucose level lost significance.

In summary, BAT may play an important role in energy homeostasis and temperature sensitivity, however, in adult humans, it only exists in a minority of people in a limited amount.

1.2.1.3 Beige adipose tissue

Beige adipose tissue has been recently identified within WAT and results from the same adipocyte precursors as WAT but has a phenotype intermediate between a white and a brown adipocyte (Kaisanlahti and Glumoff, 2019). The expression of UCP and morphological changes are the key characteristics of beige adipose tissue. The process of WAT developing into beige adipose tissue is called WAT browning.

The mechanisms of WAT browning are complex. Cold exposure is the oldest and most studied physiological stimulus for WAT browning. At low ambient temperature (4°C), as well as in response to ß-adrenoceptor agonist, the expression of UCP increased in BAT in rats, and the expression of UCP was lower in obese fa/fa rats compared to lean controls. The number of BAT and density of mitochondrial cristae increased at low temperature (Cousin *et al.*, 1992).

Exercise is a stimulus known to induce WAT browning. Irisin is an exercise adipokine, which is cleaved from fibronectin type III domain-containing protein 5 (FNDC5), expressed on the surface of white adipocytes and skeletal myocytes. FNDC5, at a concentration of 20 nM, promoted a seven-fold change ($p < 0.05$) in UCP1 in *in vitro* differentiated adipocytes., Ten days after injection of irisin, expression of UCP1 was increased by thirteen-fold ($p < 0.05$) in the subcutaneous adipose tissue depot in WT BALB/C mice (n = 7) (Boström *et al.*, 2012). Other stimulants of adipocyte beiging, include the inflammatory factors interleukin 6 (IL-6) (Abdullahi *et al.*, 2017), and interleukin 4 (IL-4) (Nguyen *et al.*, 2011), thiazolidinediones (TZDs) (Petrovic *et al.*, 2010), have been shown to promote UCP1 expression in WAT of rodents or *in vitro* by activating peroxisome proliferator-activated receptor gamma (PPARγ) coactivator 1 alpha (PGC1A). The browning of WAT increases whole-body metabolic rate in obese mice (n = 6, $p < 0.01$) (Cui *et al.*, 2015). Impaired insulin signalling may dysregulate AMPK activity, contributing to the metabolic dysfunction observed in conditions like obesity and T2DM. The AMPK pathway regulates adipocyte energy balance. AMPK phosphorylates and regulates a variety of proteins that are associated with nutrient metabolism, suppressing anabolic ATP-consuming pathways whilst stimulating catabolic ATP-generating pathways. In AMPKα1/AMPKα2 knockout (AKO) mice, a phenotype of impaired cold tolerance, impaired integrity and biogenesis of WAT mitochondrial was observed. These AKO mice showed increased

adiposity and impaired glucose intolerance and insulin resistance (Wu *et al.*, 2018). This suggests that adipocyte AMPK is involved in thermogenesis and regulation of insulin sensitivity, and may be involved in adipocyte browning. However, the mechanism of WAT browning, as well as its consequences, remains unclear.

1.2.2 White adipose tissue composition and distribution

1.2.2.1 Composition of white adipose tissue

Adipose tissue is composed of different cell types within a collagenous extracellular matrix. Both adipocytes (the major cell type) and the cells comprising the stromal vascular fraction (SVF) are seeded in this connective tissue (Sbarbati *et al.*, 2010). Adipose SVF cells include multipotent stem cells (mesenchymal stem cells, MSC), preadipocytes, fibroblasts, pericytes and endothelial cells of blood and lymphatic vessels, macrophages and other infiltrating immune cells (Ouchi *et al.*, 2011). MSCs are able to differentiate into not only cells of mesodermal lineage, for example adipocytes, but also into cells of non-mesodermal lineage, including neurons, hepatocytes and others (Yarak and Okamoto, 2010). On the other hand, preadipocytes are stem cells that are already committed to become adipocytes and account for 15 - 50% of the number of cells in adipose tissue. Pre-adipocytes play a critical role in the proliferative potential of the adipose tissue depot (Walker *et al.*, 2008, Wronska and Kmiec, 2012). White adipocytes, the primary cell type in WAT, are large spherical cells filled with a single large lipid droplet that takes up almost entire volume (over 90%) of the cytoplasm and stores energy in the form of TG (Ohsaki *et al.*, 2009). The cell size of white adipocytes varies according to the cellular lipid content and normally ranges from 30-130 μm (Wronska and Kmiec, 2012).

1.2.2.2 Distribution of white adipose tissue

In humans, WAT is mainly contained in two depots: subcutaneous adipose tissue (SAT) and visceral adipose tissue (VAT). SAT is located beneath the skin, whereas VAT is located withing the abdominal cavity, lining internal organs (Mittal, 2019). During development, the WAT depot increases significantly in childhood (Staiano and Katzmarzyk, 2012). Distribution of WAT also changes with menopausal status. SAT volume is higher in pre-menopausal women, while VAT volume is higher and

the ratio between abdominal SAT/VAT is lower in post-menopausal women (Mittal, 2019). In addition to age and sex, ethnicity also affects the distribution of WAT.

The distribution of SAT and VAT is significantly different in different ethnicities. A cross-sectional mixed sex study has shown using CT scanning that SA (n = 300, aged 69 ± 6 years, BMI 26 ± 4 kg/m^2) had a higher volume of VAT than Whites (n = 349, aged 70 ± 6 years, BMI 28 ± 4 kg/m^2), whereas African Caribbean (AC, n = 78, aged 71 ± 6 years, BMI 28 ± 4 kg/m^2) had a lower volume (VAT area SA vs Whites vs AC 248 ± 70 vs 227 ± 60 vs 192 ± 67 cm^2, p < 0.0002). Abdominal SAT was higher in SA compared with Whites and AC (SAT area SA vs Whites vs AC 243 ± 50 vs 209 ± 50 vs 213 ± 45 cm^2, p < 0.0001) (Eastwood et $al.$, 2013). Similarly, SA (n = 207, aged 45 ± 8 years, BMI 27.8 ± 4.9 kg/m^2), Chinese (n = 219, aged 45 ± 8 years, BMI 25.7 ± 3.6 kg/m^2), and Aboriginal (n = 195, aged 45 ± 8 years, BMI 28.8 ± 5.1 kg/m^2) people had a higher VAT area (p value vs White, < 0.001, < 0.001 and < 0.01, respectively) than Whites (n = 201, aged 50 ± 9 years, BMI 27.7 ± 5.1 kg/m^2) of the same sex. Abdominal SAT was higher in SA and individuals of Aboriginal origin than in Whites (p vs Whites < 0.001 for both) (Lear et $al.$, 2007). Moreover, both abdominal SAT (including superficial SAT and deep SAT, SSAT and DSAT) and VAT volumes were shown to be higher in SA (n = 81, aged 26 ± 5 years, BMI 24.5 ± 4.9 kg/m^2) than Malays (n = 82, aged 28 ± 5 years, BMI 24.9 ± 3.5 kg/m^2) and Chinese (n = 101, aged 28 ± 6 years, BMI 23.5 ± 2.9 kg/m^2) men (Chinese vs Malays vs SA, volume [cm^3] of SSAT, 1.2 ± 0.4 vs 1.3 ± 0.5 vs 1.4 ± 0.4, p < 0.001, DSAT, 0.7 ± 0.5 vs 1.2 ± 0.9 vs 1.3 ± 0.9, p < 0.001, and VAT 1.0 ± 0.7 vs 1.1 ± 0.7 vs 1.2 ± 0.7, p = 0.003) (Khoo et $al.$, 2014). Thus, SA have more VAT and SAT compared to other ethnic groups with similar age and BMI of the same sex.

1.2.3 Function of white adipose tissue

1.2.3.1 Metabolic function of white adipose tissue

The major metabolic functions of WAT i.e., storage and release of energy and regulation of glucose homeostasis and insulin sensitivity is fulfilled by white adipocytes, and this will be introduced later in 1.2.4.2. In addition, WAT also stores cholesterol and is involved in the metabolism of steroid hormones and expresses sex steroid, glucocorticoid, and estrogen receptors (ESR) (Mohamed-Ali

et al., 1998). This may in turn regulate the development and metabolism of WAT. The function of glucocorticoids has been explained in 1.1.2.

Adipose tissue produces two enzymes that are involved in sex steroid metabolism, 17ß-hydroxysteroid oxidoreductase (HSD17B) and cytochrome-p450-dependent aromatase (CYP19), and they are both expressed in adipocytes and the SVF (Labrie *et al.*, 1991, Crandall *et al.*, 1998). HSD17B can convert estrone (E1) and androstenedione to estradiol (E2) and testosterone respectively, producing the higher binding affinity form for their receptor in each case. Aromatase can also convert androgen precursors in to E2. Testosterone levels inversely correlate with adipose tissue expansion; lower levels are associated with increased adiposity. This hormone may modulate adipose tissue distribution and function, influencing lipid storage, adipokine secretion, and the propensity towards visceral fat deposition. E2, as a form of estrogen, also contributes to body fat distribution and insulin sensitivity. In healthy postmenopausal women (n = 101, aged 57 ± 4 years, BMI 27.9 ± 4.8 kg/m^2), circulating E2 is positively associated with % body fat (r = 0.56, *p* < 0.0001), area of SAT (r = 0.57, *p* < 0.0001) and area of VAT (r = 0.57, *p* < 0.0001), as well as VLDL-C (r = 0.30, *p* < 0.05), VLDL-TG (r = 0.31, *p* < 0.05) and HDL-TG (r = 0.24, *p* < 0.05), but negatively with HDL-C (r = -0.23, *p* < 0.05), adiponectin (r = -0.20, *p* < 0.05) and insulin sensitivity (r = -0.36, *p* < 0.001). The significance of correlations between E2 and metabolic risk factors disappeared when they were adjusted by % body fat, but not SAT area (Marchand *et al.*, 2018). Estrogen can also regulate adiposity through estrogen receptors (ESR). In both male and female ESR1 knock down mice (n ≥ 5, aged 270 - 360 days), WAT increased significantly in epididymal (*p* < 0.001), perirenal (*p* < 0.05) and inguinal (*p* < 0.05) fat pads, showing a role for ESR1 in decreasing adiposity (Heine *et al.*, 2000). ESR1 and ESR2 are also located in the hypothalamus, an area that regulates energy homeostasis (Simerly *et al.*, 1990, Wilkinson *et al.*, 2002). This may suggest that ESR is also involved in energy regulation and appetite control.

1.2.3.2 Tissue stress and inflammation of white adipose tissue

Inflammation is an organism's multi-level response to protect itself from harmful stimuli and begin the healing process, and most inflammation is resolved quickly. However, when the initial stimuli are not eliminated quickly and less harmful acute inflammation is ongoing, it becomes chronic inflammation, which can be

more harmful over a period of time. Obesity and T2DM are associated with a chronic inflammatory response, with a two-fold or higher increase in plasma concentration of cytokines such as tumour necrosis factor (TNF), IL-6, etc. (Wellen and Hotamisligil, 2003, Park *et al.*, 2014).

A key change in the characteristics of WAT in obese individuals is the infiltration of macrophages. These macrophages are an important driver of inflammation in WAT. A biomarker of macrophages (F4/80) was significantly positively correlated to the size and mass of WAT from perigonadal, perirenal, mesenteric and SAT (r^2, 0.39 - 0.90, $p < 0.01$ for all) in C57BL/6J mice (n = 24). A similar correlation was found in humans (n = 14, BMI 19.4 - 60.1 kg/m^2) with the specific macrophage antigen CD68 correlating with BMI ($r^2 = 0.43$, $p < 0.01$) and adipocyte area ($r^2 = 0.86$, $p < 0.001$) (Weisberg *et al.*, 2003). In young and non-obese T2DM subjects (n = 10, aged 20 – 30 years, BMI 18.5 - 24.9 kg/m^2), while expression of IL-6, TNFα, and IL-10, was similar to BMI- and age-matched healthy participants (n = 20), monocyte chemoattractant protein 1 (MCP1) was higher in T2DM ($p < 0.01$). After an intervention of ten-days bed rest, TNFα ($p = 0.02$) and MCP1 ($p < 0.01$) were higher in T2DM compared with controls (Højbjerre *et al.*, 2011). This suggested that inflammation is mild in young and non-obese participants, however, physical inactivity might worsen the inflammatory response. The inflammatory response also in turn contributes to insulin resistance both in animals and in humans (Petrick *et al.*, 2020, Wu and Ballantyne, 2020, Zhu *et al.*, 2021). WAT may also be involved in the development of endoplasmic reticulum (ER) stress. ER stress resulting from obesity is associated with inflammation via the activation of the c-Jun N-terminal kinase (JNK) pathways. Markers of ER stress, including the phosphorylation of eukaryotic translation initiation factor 2-alpha kinase 3 (EIF3AK) and eukaryotic initiation factor 2 (EIF2), were higher ($p < 0.05$ for both) in WAT and hepatic tissue of Wistar rats (n = 5) with high fat diet (HFD) compared to chow diet (n = 5). However expression of ER stress markers in rats (n = 5) with HFD after 8 weeks exercise training were the same as in those on chow diet. Additionally, similar differences were found in inflammatory factors inhibitor of kappa B kinase β (IKKB) and nuclear factor kB (NFKB) between the rat groups (da Luz *et al.*, 2011). Inflammation in obesity and T2DM, however, can be decreased by exercise. In a cross-sectional analysis of women (n = 27,158, aged 55 ± 7 years, BMI 25.9 ± 5.0 kg/m^2), lower level of physical activity and higher BMI were independently

adversely associated ($p < 0.001$ for all) with nearly all lipids (LDL-CL, HDL-DL, total plasma cholesterol, APOA and APOB) and inflammatory factors (C-reactive proteins CRP, and fibrinogen) (Mora *et al.*, 2006). This may contribute to benign obesity, free of cardiovascular disease and T2DM.

1.2.3.3 Endocrine function of white adipose tissue

The endocrine function of adipose tissue relies on white adipocytes secreting a variety of hormones, growth factors, enzymes, cytokines, complement factors and matrix proteins. Adipose tissue also expresses numerous receptors for most of these factors (Table 1-4) (Coelho *et al.*, 2013, Matsuzawa, 2006, Costa and Duarte, 2006).

Factor (protein)	Gene Name	Function
Leptin	*LEP*	Regulation of appetite and energy expenditure by signalling to the brain for body fat storage. Numerous physiological functions including inflammation.
Adiponectin	*ADIPOQ*	Abundant plasma adipokine. Regulation of glucose and lipid metabolism by stimulating fatty acid oxidation, decreasing plasma TG and improving glucose metabolism by improving insulin sensitivity.
Resistin	*ADSF*	Mediates insulin resistance and T2DM by resisting insulin action. Involved in inflammation.
TNFα	*TNF*	Pro-inflammatory cytokine. A multifunctional cytokine that is involved in cell survival, proliferation, differentiation, and apoptosis.
IL-6	*IL-6*	Mediates the acute inflammatory response, including fever. Stimulates acute phase protein synthesis such as C-reactive protein (CRP).
IGF1	*IGF1*	Stimulates systemic body growth.

Table 1-4 Factors that are secreted by WAT into plasma.

ADSF, adipose tissue-specific secretory factor. *IGF1*, insulin-like growth factor 1. (Coelho *et al.*, 2013, Matsuzawa, 2006, Costa and Duarte, 2006).

Leptin is expressed mainly by WAT adipocytes, but also has been detected in placenta, skeletal muscle, gastric and mammary epithelium and brain (Coelho *et al.*, 2013). Leptin induces weight loss in both lean and obese humans represented by a decreased fat mass. In a longitudinal study, mixed sex and ethnicity (Whites,

Blacks, Hispanic and others) participants were divided according to whether they were lean (BMI 20 - 27.5 kg/m^2) or obese (BMI 27.6 - 36.0 kg/m^2) (Heymsfield *et al.*, 1999). All participants (n = 127, aged 39 ± 10 years, BMI 27.9 ± 4.0 kg/m^2) were firstly divided into five groups (age and BMI matched) and treated (abdominal subcutaneous injection) with placebo or leptin at 0.01, 0.03, 0.10, and 0.30 mg/kg per day for four weeks, after which, obese patients (n = 60, aged 41 ± 8 years, BMI 30.7 ± 6.6 kg/m^2) kept for the same treatment for a further twenty weeks (Heymsfield *et al.*, 1999). They found that all the participants who received leptin treatment showed a significant decrease in body weight at four weeks ($p < 0.02$) and in obese individuals after 24 weeks ($p < 0.01$). The decrease was leptin dose dependent. Specifically, the decrease in fat mass was significant in all cohorts at 4 weeks ($p = 0.002$) and in obese participants after 24 weeks ($p = 0.004$), but there was no change in fat-free mass. Circulating leptin was associated with insulin resistance. In Northern Indian women who either had metabolic syndrome (n = 186, aged 28 ± 6 years, BMI 27.2 ± 5.0 kg/m^2) or were metabolically healthy (n = 204, aged 27 ± 7 years, BMI 22.1 ± 4.1 kg/m^2), plasma leptin concentrations (13.4 ± 9.0 vs 8.2 ± 6.3 ng/mL, $p < 0.001$) and HOMA-IR (2.68 ± 2.05 vs 1.72 ± 1.20, $p < 0.001$) were higher in those who had metabolic syndrome than in those who were healthy (Gupta *et al.*, 2010). In the women with metabolic syndrome circulating leptin was positively correlated to insulin resistance (r = 0.11, $p = 0.032$). However, a negative correlation between circulating leptin and insulin resistance has been observed in healthy men (r = -0.57, $p < 0.0001$, n = 50, aged 34 ± 1 years, BMI 27.9 ± 0.9 kg/m^2 and in men with T2DM (n = 12, aged 48 ± 2 years, BMI 30.2 ± 2.6 kg/m^2) but not in women (Kennedy *et al.*, 1997). Many studies have confirmed that circulating leptin is positively correlated with insulin resistance (Osegbe *et al.*, 2016, Ugur-Altun and Altun, 2007, Bidulescu *et al.*, 2020), and positively correlated to risk factors indicative of insulin resistance such as fasting glucose level (Bungau *et al.*, 2020, Ugur-Altun and Altun, 2007), and % body fat (Considine *et al.*, 1996, Frederich *et al.*, 1995, Lu *et al.*, 1998) in both human and animal studies. Therefore, leptin in WAT is associated with a decrease in adipose tissue, however, high circulating leptin levels are associated with obesity and insulin resistance.

Adiponectin, the most abundant plasma adipokine, plays an important role in the regulation of fat distribution, glucose metabolism, lipid metabolism and insulin

sensitivity. In a cross-sectional mixed sex study, plasma adiponectin concentrations (women vs men, 7,609.2 [4,385.8, 11,806.6] vs 5,373.4 [3,451.5, 8,331.2] μg/mL, $p < 0.0001$), age (44 ± 13 vs 47 ± 15 years, $p = 0.004$), BMI (27.1 ± 6.0 vs 23.7 ± 4.2 kg/m^2, $p < 0.0001$), waist circumference (89.2 ± 17.2 vs 86.4 ± 12.3 cm, $p = 0.008$), and % bodyfat (34.8 ± 12.6 vs 17.6 ± 13.6%, $p < 0.0001$) were higher in African American women (n = 398) than men (n = 275). Circulating adiponectin was negatively correlated with BMI (women and men, r = -0.29, $p < 0.0001$ and r = -0.27, $p < 0.0001$, respectively) and waist circumference (r = -0.17, $p < 0.0001$ and r = -0.19, $p < 0.0001$, respectively), and positively correlated with %fat in women (r = -0.12, $p = 0.017$) (Meilleur et $al.$, 2010). Plasma adiponectin was positively correlated with circulating cholesterol (r = 0.13, $p = 0.001$) and HDL (r = 0.20, $p < 0.0001$), whereas there was a negative correlation with circulating TG (r = -0.11, $p = 0.002$) (Meilleur et $al.$, 2010). Similar correlations were found between plasma adiponectin and BMI ($p = 0.004$), waist circumference ($p = 0.006$), HDL-C ($p = 0.017$) and plasma TG ($p = 0.031$) in 284 individuals (men, n = 189, aged 53 ± 9 years, women, n = 125, aged 52 ± 9 years) free of metabolic syndrome (Ntzouvani et $al.$, 2016). In addition, plasma adiponectin was positively correlated with circulating insulin ($p = 0.011$) (Ntzouvani et $al.$, 2016). A multi-variate analysis in a Japanese cohort (n = 4,591, mixed sex), indicated that plasma adiponectin was negatively associated with T2DM (n = 217, 4.7% of total). OR from the lowest to the highest adiponectin quartile were 0.79 [0.55, 1.12], 0.60 [0.41, 0.88], and 0.40 [0.25, 0.64], after adjustment for age, sex, family history, smoking, alcohol drinking, physical activity and BMI (Yamamoto et $al.$, 2014). A similar association between adiponectin and T2DM risk was found in Kazakh participants (n = 1,628) (Ding et $al.$, 2015). Thus, circulating adiponectin is inversely associated with adiposity, abdominal adipose tissue accumulation and risk of T2DM.

Resistin is positively associated with insulin resistance and a pro-inflammatory response. Plasma resistin was positively correlated with HOMA-IR ($p = 0.02$), circulating TNFα, CRP and IL-6 in participants with impaired fasting glucose (IFG, fasting glucose between 5.6 - 6.3 mM, n = 20, aged 45 ± 9 years, BMI 31.6 ± 3.3 kg/m^2) and T2DM (n = 15, aged 51 ± 13 years, BMI 29.9 ± 5.5 kg/m^2) patients, but not in healthy controls (n = 29, aged 45 ± 10 years, BMI 29.8 ± 5.1 kg/m^2) (Siddiqui et $al.$, 2020). This correlation between plasma resistin and insulin resistance was

confirmed (r = 0.21, *p* = 0.003) in a meta-analysis of fifteen studies in patients with T2DM and obesity (Su *et al.*, 2019). In a cross-sectional mixed sex study of healthy participants (n = 92), fasting serum insulin concentration was positively correlated (r = 0.10, *p* < 0.0001) with BMI (Frystyk *et al.*, 1995). This correlation was significantly higher (*p* < 0.05 for both) in moderate (n = 33, aged 50 ± 1 years [mean ± SEM], BMI 27.2 ± 0.2 kg/m^2) and severe obesity (n = 28, aged 50 ± 1 years, BMI 33.0 ± 0.6 kg/m^2) than in controls (n = 31, aged 49 ± 1 years, BMI 22.2 ± 0.3 kg/m^2) (Frystyk *et al.*, 1995). Similarly, plasma IGF-1 concentration was higher (moderate vs severe vs healthy, 690 ± 90 vs 810 ± 90 vs 470 ± 50 ng/L, *p* < 0.05) in moderate and severe obesity than in health. In contrast, plasma GH concentration was lower in the obese groups than in the control group (Frystyk *et al.*, 1995). In randomly selected women (n = 296) aged 40 - 65 years, plasma IGF1 concentrations were not significantly associated with BMI and nor were they associated with metabolic syndrome after adjustment for BMI (Hada *et al.*, 2019). In 4,241 participants (aged 24 - 110 years, mixed sex), the correlation between plasma IGF-1 and BMI was measured in different age quartiles. The correlation was negative in Q1 (24 - 58 years, r = -0.10, *p* = 0.0008), insignificant in Q2 (59 - 66 years) and Q3 (67 - 86 years), and positive in Q4 (87 - 110 years, r = 0.14, *p* < 0.0001). Thus, the relationship between IGF1 and BMI differs by age. In young individuals it is negatively associated with BMI, but in middle aged or older individuals, the relationship becomes insignificant or positive, and this may be caused by decreased IGFBP1.

1.2.3.4 Function of white adipose tissue in each depot

SAT and VAT have different associations with insulin resistance. It has been widely reported that VAT is associated with an increased risk of IR, T2DM and overall mortality, whereas SAT expansion improves insulin sensitivity and is associated with a decreased T2DM relative risk (Mittal, 2019, Costa and Duarte, 2006). In a cross-sectional study of a large population (n = 3,093, women, aged 52 ± 10 years, BMI 26.9 ± 5.6 kg/m^2, men, aged 49 ± 11 years, BMI 28.2 ± 4.3 kg/m^2) without T2DM, risk factors for T2DM, including HOMA-IR, BMI, age, as well as ASAT and VAT thickness area (by CT) were measured and analysed in logistic regression models (Preis *et al.*, 2010). The OR for insulin resistance (HOMA-IR) per standard deviation of AT thickness/area was higher in VAT (3.5 [3.1 - 3.9], *p* < 0.0001) than in ASAT (2.5 [2.2 - 2.7], *p* < 0.0001). VAT more strongly correlated with HOMA-IR than ASAT

(p < 0.0001 for ASAT vs VAT comparison). In addition, VAT also had a strong interaction with BMI and plasma fasting glucose (p = 0.0004), proinsulin (p = 0.003) and HOMA-IR (p = 0.003) (Preis *et al.*, 2010). Similarly, a cross-sectional mixed-sex study of 107 Chinese (women, aged 60 ± 9 years, BMI 24.1 ± 3.6 kg/m^2, men, aged 64 ± 9 years, BMI 25.1 ± 3.2 kg/m^2) showed that VAT and ASAT thickness (by CT) were positively (r = 0.38 and 0.36, p < 0.05) correlated with HOMA-IR. However, in multi-variate analysis when the association between VAT and ASAT with HOMA-IR was analysed together with age, sex, waist circumference and BMI, only the association between VAT and HOMA-IR remained independent (p = 0.003) (Liu *et al.*, 2018). Similar results were shown in Japanese men (n = 294, aged 40 - 49 years) without T2DM (Ahuja *et al.*, 2015), however in young blacks (mixed sex, n = 76, aged 18 - 19 years), ASAT had a stronger association with insulin resistance than VAT (De Lucia Rolfe *et al.*, 2015).

As the metabolically more active WAT, VAT is also correlated with concentrations of some plasma sex steroid concentrations associated with inflammation. In a study of 229 men (aged 54 ± 1 years, BMI 30.6 ± 1.2 kg/m^2), VAT was strongly positively associated with plasma E2 (r = 0.38, p < 0.001), and negatively with plasma bioavailable testosterone /E2 ratio (r = -0.42, p < 0.001), however ASAT was not correlated with either (Gautier *et al.*, 2013). Plasma IL-6 was positively correlated (r = 0.19, p = 0.007) with circulating E2, and negatively with bioavailable testosterone (r = -0.19, p = 0.006) and bioavailable testosterone/E2 ratio (r = -0.30, p < 0.001). VAT is also more strongly correlated with inflammation than SAT. In a cross-sectional mixed study of 1250 healthy participants (52% women, aged 60 ± 9 years, BMI 28.3 ± 5.1 kg/m^2), both ASAT and VAT area (by CT) were correlated similarly with plasma inflammatory markers including CRP, fibrinogen, intercellular adhesion molecule 1 (ICAM1), IL-6, and P-selectin (multivariable model r^2 between 0.06 - 0.28 in ASAT and 0.07 - 0.29 in VAT). However, VAT was more strongly correlated with circulating urinary isoprostanes (multivariable model r^2 VAT vs SAT, 0.10 vs 0.07, p = 0.002) and MCP1 (0.08 vs 0.07, p = 0.04) than ASAT (Pou Karla *et al.*, 2007).

In summary, VAT contributes more to IR and this may relate to the sex steroid and inflammatory response.

1.2.3.5 Adipose tissue function in individuals with insulin resistance, different ethnicities and athletes

WAT plays a significant systemic role in the regulation of whole-body energy homeostasis, insulin sensitivity, and inflammatory response. Therefore, alterations in WAT during the development of T2DM can subsequently result in significant shifts in these crucial physiological and biological processes.

Chronic inflammatory response may be the major change in WAT in T2DM. In a cross-sectional mixed sex study that compared patients with nine years duration of T2DM (n = 581, aged 53 [49, 58] years, BMI 30.0 [26.7, 33.9] kg/m^2) with healthy controls (n = 572, aged 52 [48, 57] years, BMI 26.1 [23.7, 28.9] kg/m^2), risk factors for T2DM were measured in plasma. Plasma IL-6 was independently associated with T2DM (HR 1.6 [1.0, 2.7]) when adjusted for BMI, WHR, fasting glucose and fasting insulin level (Duncan *et al.*, 2003). Similarly, pro-inflammatory markers including circulating IL-6 (T2DM vs health, 239 [31, 1,018] vs 8 [0, 21] pg/mL, *p* < 0.0001), MCP-1 (65.3 [43.4, 134.2] vs 40.0 [24.8, 54.4] pg/mL, *p* = 0.0002), p-selectin (11,967 [9,626, 16,135] vs 9,080 [6,318, 12,792] pg/mL, *p* = 0.03), and TNFα (161.7 [98.6, 197.5] vs 86.3 [68.9, 121.5] pg/mL, *p* = 0.012) were significantly higher in T2DM (n = 25, aged 60 ± 3 years, BMI not given) compared with healthy controls (n = 23, aged 55 ± 4 years, BMI not given) (Randeria *et al.*, 2019). A nested case-control study comparing T2DM (mixed sex, n = 192, aged 56 ± 7 years, BMI 30.7 ± 4.8 kg/m^2) and healthy controls (mixed sex, n = 384, aged 56 ± 7 years, BMI 26.7 ± 3.5 kg/m^2) from 27,548 patients examined inflammation in T2DM. Plasma IL-6 and TNFα were higher in T2DM (*p* < 0.0001 and *p* = 0.0094, respectively), but IL-1β was not different. However, a combination of IL-6 and IL-1β (OR, 3.31 [1.14, 9.87]), rather than higher IL-6, independently predicted the risk of T2DM (Spranger *et al.*, 2003). Therefore, T2DM is strongly associated with inflammation, and TNFα and IL-6 (or together with IL-1β) may be key players in T2DM-mediated inflammation. However, even though WAT produced pro-inflammatory factors that are widely involved in T2DM associated inflammation, the exact role of WAT is still unclear.

As discussed before, VAT is more highly associated with the risk of T2DM, and SA have a relatively higher level of VAT compared with other ethnicities (Yi *et al.*, 2022). Therefore, the higher risk of SA developing T2DM at a lower BMI and a

younger age may be related to VAT mass or VAT metabolism. In a cross-sectional mixed sex study (aged 40 - 84 years) of African Americans (n = 1,893, BMI 30.2 ± 0.1 kg/m^2 [mean ± SEM]), Chinese (n = 803, BMI 24.0 ± 0.2 kg/m^2), Latinos (n = 1,496, BMI 29.4 ± 0.1 kg/m^2), SA (n = 803, BMI 25.8 ± 0.2 kg/m^2), and Whites (n = 2,622, BMI 27.8 ± 0.1 kg/m^2), SA had more VAT than other ethnicities ($p < 0.05$). Plasma adiponectin was lower in SA and resistin was higher ($p < 0.001$) in SA compared with other ethnicities apart from Chinese, with and without adjusting for body composition (Shah *et al.*, 2016a). Exercise, on the other hand, though it has been shown to attenuate the risk of T2DM, increased IMCL (1.1.2) and decreased inflammation (1.2.3.2), may also change the function of WAT. Japanese female athletes (n = 174, aged 20 ± 1 years, BMI 21.6 ± 1.9 kg/m^2) had lower % body fat ($p < 0.001$), less trunk fat mass ($p = 0.036$) and more lean mass ($p < 0.001$) than healthy controls (n = 311, aged 21 ± 1 years, BMI 20.4 ± 2.2 kg/m^2). Plasma leptin ($p < 0.001$) and TNF ($p = 0.01$) were lower in athletes than healthy controls.

1.2.4 Biology of white adipose tissue adipocytes

1.2.4.1 Pre-adipocytes and adipogenesis

MSC and preadipocytes are the two main types of stem cell that are found in WAT (1.2.2.1), and both are involved in the development of adipocytes. Adipocyte differentiation (adipogenesis) is a complex and programmed process in which multipotent stem cells are transformed into mature adipocytes (Rosen and Spiegelman, 2000). During the early development of the embryo, a single fertilized egg is developed into nearly two hundred types of cells to make up multiple developmental lineages and finally a multicellular organism. One of these lineages is mesenchymal stem cells (MSC). The MSC is a spindle-shaped multipotent stem cell, which can be isolated from bone marrow, adipose tissue or other tissue sources (Keating, 2006). As a multipotent stem cell type, the MSC has the potential to differentiate into a variety of cells including bone, cartilage, tendon, ligament, marrow stroma, adipocytes, dermis, muscle and connective tissue (Caplan, 1991). The differentiation of adipocytes consists of two steps. The multipotent MSC is first committed to form a preadipocyte and loses its multipotent ability to differentiate into other lineages (Cornelius *et al.*, 1994). In the next step, the preadipocyte is differentiated into a mature adipocyte which represents the terminal differentiation stage (Ntambi and Young-Cheul, 2000).

Preadipocytes start to generate adipocytes during late embryonic development, and the majority of adipogenesis occurs shortly after birth (Burdi *et al.*, 1985). The preadipocyte and MSC are morphologically indistinguishable.

Physical stimuli, such as low extracellular matrix (ECM) stiffness (Teboul *et al.*, 1995), confluency and round shape (Kuri-Harcuch and Green, 1978, Green and Meuth, 1974) and potential unknown factors, can stimulate MSC to start transforming into committed white preadipocytes (Cristancho and Lazar, 2011). There are two pathways associated with preadipocyte commitment: the Wingless-INT (WNT) signalling pathway and the transforming growth factor-beta (TGFß) superfamily signalling pathway. WNTs are secreted proteins that act as extracellular regulators of preadipocyte commitment and in almost every aspect of embryonic development (Clevers, 2006). The WNT ligands inhibit adipogenesis mainly via the transcription factor ß-catenin (Prestwich and MacDougald, 2007). WNT ligands bind to frizzled receptors and LDL receptor-related protein (LRP) co-receptors, which stimulate the hypophosphorylation of cytoplasmic ß-catenin (Prestwich and MacDougald, 2007). ß-catenin is then translocated into the nucleus where it binds to and activates members of the transcription protein family T-cell factor/lymphoid-enhancing factor (TCF/LEF) and activates downstream targets to inhibit preadipocyte commitment. A study has shown that enforced expression of WNT10A and WNT10B stabilized ß-catenin, suppressed adipogenesis and stimulated osteoblastogenesis in ST2 cells and 3T3T1 preadipocytes to a similar extent, and that WNT6 had a similar but weaker effect (Cawthorn *et al.*, 2012a). Additionally, knockdown of WNT6 stimulated adipogenesis to a greater extent than knockdown of WNT10A and WNT10B, whereas knockdown of ß-catenin completely stopped the inhibition of adipogenesis (Cawthorn *et al.*, 2012a). TGFß, however, regulates adipogenesis by the SMAD signalling pathway. TGFß ligands, such as TGF1, myostatin and growth differentiation factor 11 (GDF11), bind to membrane receptors that phosphorylate plasma SMAD2/3. Activated SMAD2/3 binds and activates the transcriptional factor SMAD4 and stimulates expression of genes that inhibit the expression of *PPARG* and the CCAAT enhancer binding proteins (CEBP) family thus inhibiting adipogenesis. Deleting *TGFB1* in bone marrow MSC of mice led to a significant increase in the expression of *PPARG* and the mature adipocyte marker fatty acid binding protein 4 (FABP4), and suppressed osteoblastogenesis (Abou-Ezzi *et al.*, 2019).

Upon maturation the adipocyte acquires the ability to uptake lipids, form lipid droplets, regulate lipogenesis and lipolysis, respond to insulin and secrete adipokines. The terminal differentiation phase of adipogenesis involves transcriptional regulation of genes which has not been extensively studied. However, it is well known that the positive feedback loop of the transcriptional factors CEBPA and PPARG is the stimulus for the appearance of markers of terminal differentiation. *In vitro* stimulation of embryonic stem (ES) cells from WT mice or PPARG$^{-/-}$ mice showed that *PPARG* was critical to adipogenesis, and that differentiation of ES cells into adipocytes was *PPARG* gene dose-dependent (Rosen *et al.*, 1999). These experiments showed that *PPARG* is the critical transcription factor in adipogenesis.

In some individuals there appears to be a limited ability to produce mature adipocytes from pre-adipocytes (hyperplasic adipocyte expansion) and instead excess fatty acids are stored in existing mature adipocytes leading to an increase in their size (hypertrophic expansion) and development of insulin resistance and T2DM (Cuthbertson *et al.*, 2017, Ibrahim, 2010). When individuals become obese, their excess calorific intake is stored in the form of TG within the adipocytes of white adipose tissue (WAT). If there is insufficient capacity in mature adipocytes, new adipocytes are formed from pre-adipocytes in order to increase storage capacity (Arner and Spalding, 2010). A cross-sectional study of adults (women, n = 40, aged 44 ± 13 years, BMI 25.6 ± 4.5 kg/m^2, men, n = 40, aged 39 ± 10 years, BMI 22.2 ± 2.7 kg/m^2) showed that the size of omental adipocytes was significantly smaller (54.6 ± 4.4 vs 59.6 ± 5.1 µm, $p < 0.01$) than subcutaneous adipocytes (Meena *et al.*, 2014b). However, omental adipocyte size was more strongly associated with measures of adiposity (BMI, waist circumference, and % body fat), HOMA-IR and plasma cholesterol and triglyceride. These correlations were stronger in females than in males (Meena *et al.*, 2014b). Adipocytes of a larger size exhibited increased metabolic activity and secreted a higher quantity of adipokines, including leptin and adiponectin (Skurk *et al.*, 2007). In healthy and moderately obese individuals (n = 49, aged 52 ± 9 years, BMI 30.0 ± 2.7 kg/m^2), ASAT was collected by needle biopsy, and adipocyte size measured (McLaughlin *et al.*, 2010b). Adipocytes were categorized into two groups by size distribution: small (< 60 µm), the tail of a sum of 2 exponentials, and large (60 - 200 µm), the hump of a Gaussian curve. In insulin resistant participants, the proportion of small

ASAT adipocytes was positively correlated with the mRNA expression of pro-inflammatory genes such as, *CD14* (r = 0.54, *p* = 0.003), *CD45* (r = 0.48, *p* = 0.01), *IL-6* (r = 0.42, *p* = 0.028), and *MCP1* (r = 0.54, *p* = 0.003), but not in large cells. The expression of genes associated with inflammation was also correlated with HOMA-IR (McLaughlin *et al.*, 2010b). This may suggest that the maturing of smaller adipocytes into larger size may be disturbed in obese patients, which may subsequently contribute to inflammation and insulin resistance.

1.2.4.2 Insulin signalling pathways in white adipocytes

The classic insulin signalling pathways have been explained before (1.1.4.2). This section will mainly focus on the regulation of the insulin signalling pathway in adipocytes and the consequences of disturbed insulin signalling in adipocytes.

Insulin regulates adipocyte metabolism via interaction with and activation of the insulin receptor. INSR activity maintains adipose tissue mass. Adipocyte-specific *INSR* knockout (AIRKO) mice (n = 11) compared to than WT mice (n = 13) have reduced insulin sensitivity throughout life (*p* < 0.001) and are glucose intolerant (*p* < 0.001) after 16 weeks of age. However, AIRKO mice were protected from high fat diet-induced weight gain with a 90% lower fat mass in major adipose depots than wild type mice. However, hepatic steatosis in AIRKO mice was double (*p* < 0.0001) that in WT mice (Friesen *et al.*, 2016). Thus, a lack of insulin action in adipocytes may cause ectopic fat accumulation. Another study has shown that in AIRKO mice (n = 15) plasma leptin was around three-fold higher in AIRKO mice than in WT mice with at same body weight and there was no correlation between plasma leptin and body weight which was present in WT mice (n = 45, r = 0.73, *p* < 0.05), (Blüher *et al.*, 2002). Interestingly, adipocyte size in AIRKO mice was bimodal with populations of large and small cells, with lower expression level of *SREBF1, CEBPA,* and fatty acid synthase (*FAS*) in small cells compared to adipocytes in controls (Blüher *et al.*, 2002). The insulin signalling pathway also plays an important role in adipocyte differentiation. Expression of *CEBPA* and *PPARG* was severely decreased in embryonic fibroblast cells from *IRS1^{-/-}* and *IRS2^{-/-}* mice both at the protein and mRNA level, which led to an inability of the cells to differentiate into adipocytes (Miki *et al.*, 2001). The offspring of maternal diet-induced C57BL/6J mice showed that, although they had the same body composition and glucose tolerance as in 8-weeks old male offspring from control

mothers, they had decreased INSR, p85 subunits of PI3K and PKB (n = 6 in both groups), with the greatest decrease difference in IRS1 (Fernandez-Twinn *et al.*, 2014). Insulin signalling pathways may be involved in the maternal obesity induced adipocyte insulin resistance in later life.

1.2.4.3 Lipogenesis and lipolysis in white adipocytes

The mechanism of lipogenesis and lipolysis has been explained previously (1.1.4.2).

In adipocytes, proteins involved in lipid droplet formation and function play an important role in lipid metabolism. Perilipin 2 (gene name *PLIN2)* is a member of the family of perilipin lipid droplet coating proteins, which is widely expressed. Perilipin 2 is essential for the formation of lipid droplets both in adipocytes (Li *et al.*, 2018) and in skeletal muscle (Bosma *et al.*, 2012). In adipocytes, perilipin 2 increases lipolysis. During adipogenesis in 3T3L1 cells and mouse embryonic fibroblasts (MEF), expression of *PLIN2* mRNA decreased whereas protein levels did not. *PLIN2* knockdown in MEF differentiated adipocytes showed an attenuation of lipolysis (Takahashi *et al.*, 2016). Whole body deletion of *PLIN2* protected mice from developing obesity and insulin resistance in response to Western diet, and suppressed the *SREBF1* and *SREBF2* genes involved in *de novo* lipogenesis in the liver (Libby *et al.*, 2016). Cell death inducing DFFA Like effector A (CIDEA), is a protein that colocalizes around lipid droplet with perilipin, and is another regulator of lipolysis (Puri *et al.*, 2008b). *CIDEA* is highly expressed in white adipocytes and negatively regulates lipolysis and promotes triglyceride accumulation, as well as the size of lipid droplets (Wolins *et al.*, 2006, Puri *et al.*, 2007). The expression of CIDEA was positively correlated to insulin sensitivity in obese human subjects (n = 13, $p < 0.001$) (Puri *et al.*, 2007).

1.2.4.4 White adipocyte function in individuals with insulin resistance and in different ethnicities

Obesity and T2DM is associated with disturbed adipocyte function that is mediated by adipocyte size. In a cross-sectional study of 43 male participants, biopsies of ASAT and VAT were compared from lean, obese and T2DM groups. In VAT, the size of CD45 leukocytes and M1 macrophages (one way ANOVA, $p = 0.010$) were significantly larger in obese (O) and T2DM compared to lean (L), and the size of

adipocytes was significantly positively correlated (r = 0.65, *p* < 0.001) with HOMA-IR. However, in SAT, despite adipocyte hypertrophy in O compared to L (O vs L, *p* < 0.001), there was no significant difference in the size of immune cells between groups, and no significant correlation was found between adipocyte size and HOMA-IR.

Adipocyte size is larger in SA compared with Whites and is correlated with adipocyte function. In young, lean men, ASAT adipocyte area was significantly larger (3,491 ± 1,393 vs 1,648 ± 864 µm^2, *p* = 0.0001) in SA (n = 29, aged 27 ± 3 years, BMI 24 ± 4 kg/m^2) compared with Whites (n = 18, aged 27 ± 3 years, BMI 23 ± 3 kg/m^2) (Chandalia *et al.*, 2007). The size of adipocytes was negatively correlated with glucose disposal rate (r = -0.57, *p* = 0.0008) and circulating adiponectin concentration (r = -0.71, *p* < 0.0001) in both groups. Similarly, in a cross-sectional study of young male SA (n = 15, aged 26 ± 3 years, BMI 26.7 ± 5.3 kg/m^2) and Whites (n = 20, aged 27 ± 8 years, BMI 26.6 ± 2.5 kg/m^2), SA had a significantly higher ratio of small (< 20 µm) and very large (≥ 90 µm) ASAT adipocytes (and a lower ratio of medium (20 - 43 µm) adipocytes (Balakrishnan *et al.*, 2012) than Whites. In both SA and Whites, the ratio of a total of medium, large (43 - 90 µm) and very large adipocytes, was positively correlated with insulin resistance (r = 0.69, *p* < 0.01).

In summary, adipocyte hypertrophy plays an important role in the development of T2DM, larger adipocytes predict higher risk of T2DM, however, even though VAT adipocytes are smaller than SAT, they contribute to insulin resistance more than SAT in obesity. SA have larger adipocytes than Whites and this contributes to the higher risk of T2DM.

1.3 Extracellular vesicles (EVs) released from white adipose tissue and adipocytes

As mentioned before, there are no specific markers for adipose tissue derived EV, therefore, in the current review, adipose tissue derived EVs refers to EVs either containing markers of adipocytes (adiponectin, FABP4, etc.), or EVs derived from *in vitro* culture adipose tissue.

1.3.1 Function of white adipose tissue derived EVs

Adipose tissue derived EVs may play an important role in the paracrine cross talk between adipocyte and macrophages. EV produced by SAT and VAT, as well as EVs derived from Simpson Golabi Behmei Syndrome (SGBS)-adipocytes, were able to stimulate the differentiation of primary monocytes into macrophages. These macrophages had a similar cytokine secretion profile to macrophages found in human adipose tissue (Kranendonk *et al.*, 2014b). In addition, EV produced by VAT were more effective than EVs produced by SAT at stimulating monocyte differentiation. The same applied to adiponectin-positive EVs, rather than adiponectin-negative EV (Kranendonk *et al.*, 2014b). Differentiated macrophages were mixed with *in vitro* cultured adipose tissue and the conditioned medium was collected. When human adipocytes were exposed to the medium, insulin signalling was inhibited as assessed by decreased PKB phosphorylation (Kranendonk *et al.*, 2014b). When palmitic acid was added to 3T3-L1 differentiated adipocytes thereby triggering a stress response, EVs derived from the adipocytes could act as chemo-attractants for monocytes and primary macrophages (Eguchi *et al.*, 2015). Mice injected with murine adipose tissue-derived EVs exhibited increased plasma levels of TNFα and IL-6. These cytokines were secreted by macrophages, which had differentiated from peripheral blood monocytes under the influence of the adipose tissue derived EVs (Deng *et al.*, 2009). When plasma EVs containing high retinol binding protein 4 (RBP4) from ob/ob mice were injected into WT mice, the WT mice developed insulin resistance (Deng *et al.*, 2009). Therefore, EVs derived from adipose tissue may mediate communication with immune cells and may contribute to whole body insulin resistance.

The effect of EV produced by SAT and VAT on insulin signalling was examined in a hepatocyte cell line (HepG2), as well as in myotubes differentiated from a myoblast cell line (C2C12) (Kranendonk *et al.*, 2014c). After exposure to SAT and VAT-derived EVs, hepatic cells showed a negative correlation between PKB signalling and *G6P* gene expression (Kranendonk *et al.*, 2014c). EV produced by VAT of obese individuals were taken up by HepG2 cells and hepatic stellate cell lines (Koeck *et al.*, 2014). Consequently, these cells showed dysfunctional regulation of extracellular matrix and dysregulation of TGFß signalling pathways (Koeck *et al.*, 2014). This mechanism was proposed to link liver fibrosis with obesity and NAFLD *in vivo*.

The presence of adipocytes within the tumour microenvironment may be involved in tumour progression. Obesity is a risk factor for melanoma and its malignant progression. In a study of human EVs derived from SAT that had been isolated from plasma, there was a positive correlation between EV count and donor BMI (Lazar *et al.*, 2016). When SAT derived EVs from overweight and obese donors were applied to melanoma cells at equivalent concentration, the migration of melanoma cells was higher than that in the presence of the equivalent concentration of EVs from lean donors, in a dose-dependent manner (Lazar *et al.*, 2016). This was thought to be mediated by fatty acid oxidation as inhibition by etomoxir reversed the effect (Lazar *et al.*, 2016). Additionally, EVs derived from mature 3T3-F442A adipocytes contained abundant proteins involved in fatty acid oxidation (Lazar *et al.*, 2016).

1.3.2 Adipose tissue EV and whole-body metabolic status

Circulating EV levels are associated with the risk of T2DM, NAFLD, and other metabolic syndromes, however, it is unclear to what extent adipose tissue EVs are involved. Plasma EVs which contain CD9 and adiponectin are thought to originate from adipose tissue, and they have been isolated from patients with aortic aneurysm (Kranendonk *et al.*, 2014c). However, due to the lack of specific markers for adipose tissue EV, it is difficult to be specific about the tissue origin of plasma EV. For example, proteomic profiling of purified EVs from human plasma showed the existence of PPARγ, however, as PPARγ is also expressed in vascular endothelial cells and immune cells, it cannot specifically identify adipose tissue EVs (Looze *et al.*, 2009). Similarly even though adiponectin is uniquely expressed in adipocytes, only a minor proportion of EVs secreted from 3T3-L1 adipocytes contain adiponectin (DeClercq *et al.*, 2015) and therefore it is also not a reliable marker of plasma adipocyte derived EVs. These data suggest that when interpreting studies on plasma EVs, extreme caution is required.

The number of *ex vivo* VAT-EVs, but not SAT-EVs per gram of fat, was correlated with insulin resistance (but not BMI or plasma CRP levels) in patients (n = 11) with aortic aneurysm, from whom the ASAT was collected (Kranendonk *et al.*, 2014b). Similarly, the number of SAT-EVs from 16 individuals was negatively correlated with waist circumference, presence of metabolic disorders, and the number of EV

derived from VAT was positively correlated with plasma liver enzymes (Kranendonk *et al.*, 2014c).

Plasma EVs that were positive for perilipin A from *ob/ob* mice, could activate monocytes in blood and adipose tissue of WT mice (Eguchi *et al.*, 2015). EVs containing perilipin A were higher in mice with HFD-induced obesity and in humans with metabolic disorders than their respective controls (Eguchi *et al.*, 2016). In humans, concentration of these EVs could be reduced by a three-month low-calorie diet. One year after gastric bypass surgery, FABP4 positive EVs were isolated from plasma of the patients and miRNA profiling was performed (Hubal *et al.*, 2017). Changes in miRNA profile were shown to be associated with insulin signalling pathways by Ingenuity Pathway Analysis (IPA), and the degree of change was correlated with HOMA-IR and plasma concentrations of branched chain amino acids.

In patients with vascular disease (n = 1,012), plasma EVs were isolated, which contained cystatin C, a protein marker of kidney function, and CD14 (Kranendonk *et al.*, 2014a). There was a positive correlation between the numbers of cystatin C^+ EVs and plasma CRP and negative correlation with HDL-C. In addition, plasma HDL-C was positively correlated with the concentration of $CD14^+$ EVs. Cystatin C^+ EVs predicted the presence of metabolic disorders (OR, 1.57 [1.19, 2.17]), but not obesity and IR. In contrast, $CD14^+$ EV inversely predicted the hazard of T2DM (HR, 0.84 [0.75, 0.94]) over a 6.5-year follow-up (Kranendonk *et al.*, 2014a). However, there was no evidence in these studies that the EV risk markers were derived from adipose tissue.

1.3.3 EVs from adipose tissue MSC (ADSC)

1.3.3.1 ADSC-EVs in vascular disease

A study showed that there was no difference in EV number and size between SAT derived ADSC-EVS and VAT derived-ADSC-EVs in obese and healthy weight individuals (Togliatto *et al.*, 2016). The content of VEGF and MMP2 (markers of EV angiogenic potential) was lower in SAT-EVs and VAT-EVs in obese compared with EVs derived from same tissue in normal weight individuals. Additionally, the content of MIR126, but not MIR130A (both pro-angiogenic miRNAs) was decreased

in ADSC-EVs from obese individuals (Togliatto *et al.*, 2016). This suggests that ADSC-EVs, either from SAT or VAT, may disturb the pro-angiogenic potential *in vitro*. ADSC-EVs was stimulated by platelet-derived growth factor (PDGF) with increased angiogenic responses in protein composition (Lopatina *et al.*, 2014). ADSC-EVs have also been shown to promote migration and tube formation by human umbilical vein endothelial cells (Kang *et al.*, 2016). MIR31 in these EVs were thought to be the active agent via HIF1 inhibition.

1.3.3.2 ADSC-EVs and neurodegenerative disease

ADSC shows potential in the treatment of neurodegenerative disorders, for example, amyotrophic lateral sclerosis. Murine ADSC-EVs protected motor neurone-like NSC-34 cells from oxidative damage and increased their viability (Bonafede *et al.*, 2016). Similarly, human ADSC-EVs protected neurones from being damaged by glutamate (Wei *et al.*, 2016). ADSC-EVs prevented apoptosis in mice neuronal cells *in vitro* and increased remyelination in cerebellar slices demyelinated using lysophosphatidyl choline (Farinazzo *et al.*, 2015). Others have shown that ADSC-EVs containing neprilysin, a major ß-amyloid peptide degrading enzyme, could deliver this protein to a neuroblastoma cell line and reduce the secretion of and intracellular levels of ß-amyloid peptide (Katsuda *et al.*, 2013). Thus, this might be a potential therapeutic mechanism for such EVs in Alzheimer's disease.

1.4 Aims and hypotheses

Age, adiposity, central adiposity, cardiovascular fitness and ethnicity all are linked to insulin resistance and T2DM and the effects are overlapping. Currently, it is not clear to what extent adiposity, age, ethnicity, and cardiovascular fitness contribute independently to adipocyte function and morphology. In addition, the role of EVs derived from WAT in the regulation of whole-body insulin resistance and the communication between adipocytes and other cells is poorly understood.

The current study aims to investigate the morphology and function of adipocytes in risk factor groups for age, adiposity, central adiposity, cardiovascular fitness and ethnicity, and to characterise the content and concentration of circulating EVs that may be derived from WAT.

The study hypothesized that:

1. Aging, adiposity, central adiposity and physical inactivity increase the risk of T2DM, whereas endurance exercise decreases it;

2. SA have larger adipocytes than Whites, and the expression of genes associated with insulin resistance, lipolysis, inflammation and tissue stress are higher in SA than Whites;

3. Similar levels of weight gain will adversely affect adipocyte morphology and function to a greater extent in SA than Whites;

4. Circulating adipose tissue derived-EVs contain proteins and miRNAs that are involved in the regulation of whole-body glucose homeostasis and are associated with BMI, HOMA-IR and age.

Chapter 2   Methods

2.1 Subjects

Three independent human patient/volunteer studies contributed to this thesis: the Glasgow Visceral & Ectopic fat with weight Gain in South Asians study (GlasVEGAs, University of Glasgow Ethical Approval project number 200140035) the role of alternative pathways of triglyceride synthesis in determining insulin sensitivity in muscle study (MFAT, West of Scotland Research Ethics WOSREC REC 4 Ref 16/WS/0002, R&D reference GN15DI528) and the effect of a mixed meal on blood-circulating extracellular vesicles study (Mixed meal, project number University of Glasgow Ethical Approval 200170080). All participants gave informed consent, and all studies were carried out according to the Declaration of Helsinki.

Demographic data including age, body weight, body height and waist circumference were collected and/or measured during recruitment. Body weight index (BMI) was calculated by body weight (in kg) divided by the squared body height (in metres). Waist circumference was taken with the participant in a relaxed standing position, with feet together and arms crossed over the chest, at the end of expiration of a breath. The circumference was taken by a tape ruler at the narrowest point between the inferior border of the tenth rib and the iliac crest, by Dr James McLaren and Dr Anne Sillars.

2.1.1 GlasVEGAs study

GlasVEGAs was a longitudinal study to determine the differences in changes of adipose tissue function and metabolism in response to weight gain (WG) and weight loss (WL) between European and South Asian ethnicities (Figure 2-1). Recruitment was carried out from 28/07/2015 to 21/04/2017 by Dr James McLaren. Participants (male, aged 19 – 30 years, and BMI < 25 kg/m^2) were recruited from the white European population (EU, n = 20, self-reported both parents of white European origin) or the South Asian population (SA, n = 13, self-reported both parents of Indian, Pakistani, Bangladeshi or Sri Lankan origin). Exclusion criteria included: diabetes (physician diagnosed or HbA1c ≥ 6.5% on screening); history of cardiovascular disease and regular participation in vigorous physical activity; current smoking, taking drugs or supplements thought to affect

carbohydrate or lipid metabolism, or other significant illness that would prevent full participation in the study.

Abdominal subcutaneous adipose tissue (ASAT) biopsies were collected from each participant, when they were fasted, by Dr James McLaren at baseline (BL) as described below (2.4.1). Participants were then provided with high energy snacks (premium ice cream, chocolate bars, potato chips, cheese, dried fruit and sugary drinks) and asked to eat until they felt more full than usual in order to gain 7% weight (minimum of 5% over baseline weight) over approximately six weeks. ASAT was collected again after a minimum of 5% weight gain (WG).

The weight loss phase aimed to achieve 7 - 15% (minimum of 5%) weight loss from the peak weight gain. It was implemented by issuing an alternate day low calorie diet or online Weight Watcher diet (www.weightwatchers.co.uk) (Hoddy *et al*., 2014, Johnston *et al*., 2014). The alternative low-calorie diet required each participant to eat *ad libitum* the first day and then intake ~600 Kcal (~25%) of daily energy requirement on the next day. ASAT biopsies were collected again after a minimum of 5% weight loss (Figure 2-1). The progress of weight loss lasted for about 12 weeks.
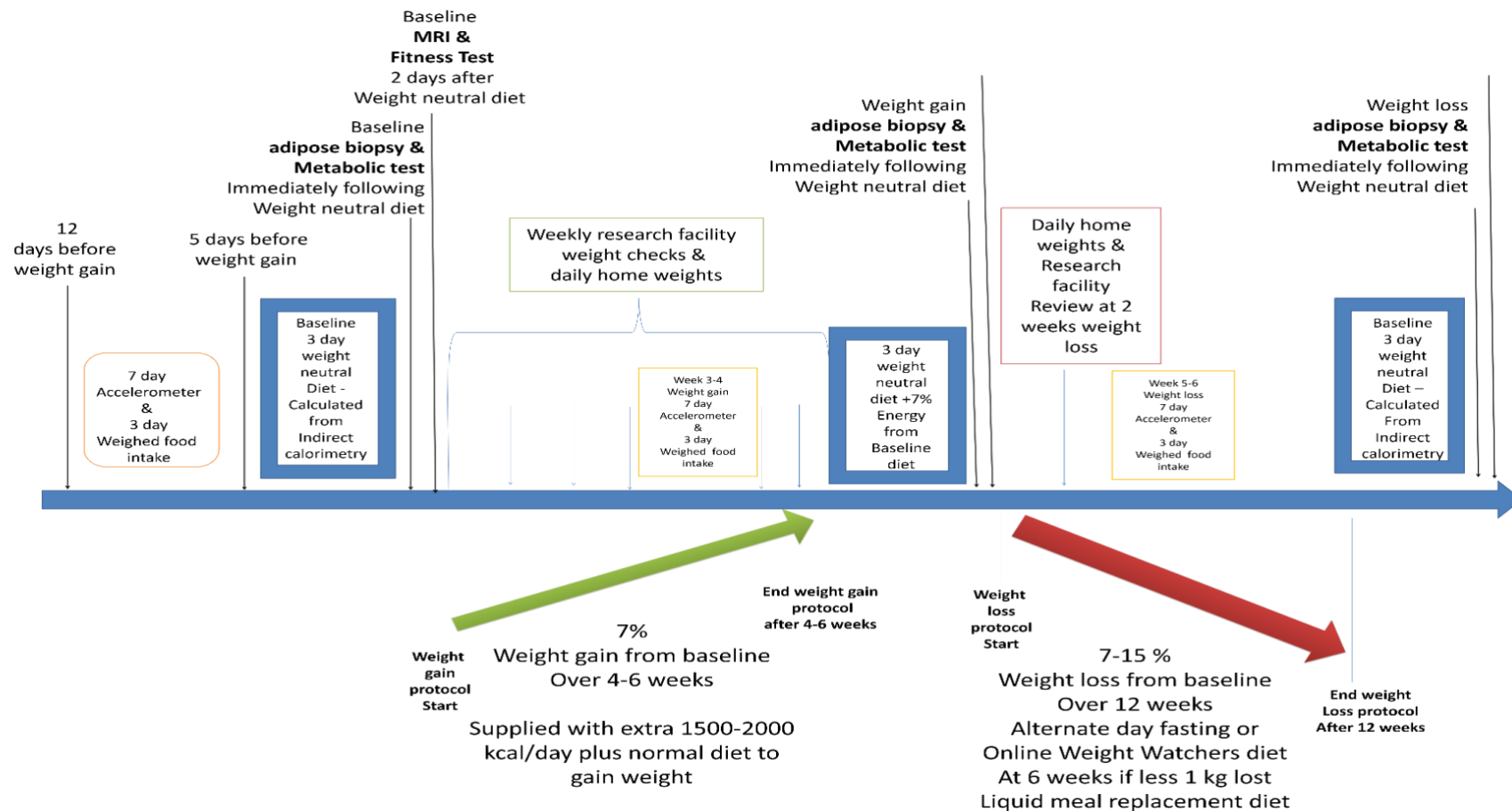
Figure 2-1 Overview of GlasVEGAs study protocol.

Participants were asked to gain 7% of body weight (WG) compared to baseline (BL) by extra food intake of high calorie diet over approximately six weeks. After which, they were asked to lose 7 - 15% of body weight (WL) by each alternate day on a low calorie diet or online Weight Watcher diet. MRI scanning, fitness test, ASAT biopsy and blood collection from each participant was carried out at BL, after WG and WL. The protocol was carried out and this figure was prepared by Dr James McLaren.

2.1.2 MFAT study

Male participants (aged 30 – 60 years) were recruited into a cross sectional study. Three groups were recruited according to the following criteria:

i. Older healthy Europeans (OHEU, n = 19), BMI 18 - 27 kg/m^2, who did not engage in regular vigorous physical activity, HbA1c < 6% (< 43.8 mmol/mol).

ii. Older European patients with impaired glucose response (OIGREU, n = 17), with HbA1c = 6.0 – 6.4% (43.8 – 47.4 mmol/mol), impaired fasting glucose (IFG) or impaired glucose tolerance (IGT), or type 2 diabetes controlled by lifestyle only.

iii. Older endurance trained European athletes (OETEU, n = 20), BMI 18 - 27 kg/m^2, undertaking more than 5 hours per week of vigorous endurance-based exercise training ≥ 2 years, HbA1c < 6% (< 43.8 mmol/mol).

Exclusion criteria included female sex, aged < 30 or > 60 years of age, and a history of cardiovascular disease or other serious chronic health conditions. The patients were recruited and ASAT was collected (2.4.1) by Dr Anne Sillars. Dr Anne Sillars carried out quantitation of gene expression in MFAT adipocytes. Adipocyte sizing was carried by Dr Anne Sillars and the author.

2.1.3 Mixed meal EV study

Staff and postgraduate students at the University of Glasgow (n = 14) were recruited for this study. Exclusion criteria included metabolic disease (such as type 2 diabetes, cardiovascular disease, thyroid disease) and aged < 18 years.

Blood (~10 mL, after at least 10 hours fasting) was collected from each participant (2.7.1) using a cannula inserted into the antecubital fossa by Dr Anne Sillars. Participants were then provided with a standard mixed test meal (containing ~800 Kcal, 30% fat, 47% carbohydrate and 17% protein), which reflects the typical west coast of Scotland diet (Burton *et al.*, 2008). Thereafter further 10mL samples were collected via the intravenous cannula at 0.5, 1, 2, 4 and 6 hours as shown in Figure 2-2. The tube and specific method of blood collection are described in 2.7.1.
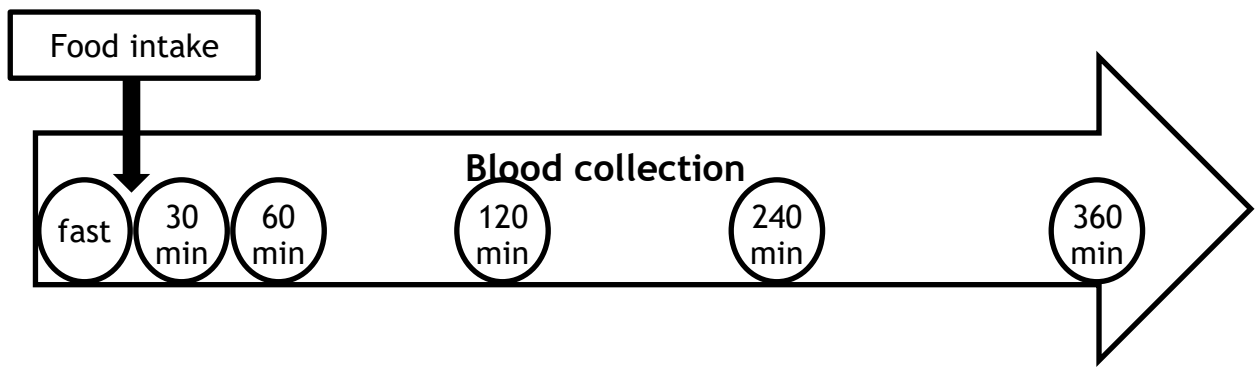
Figure 2-2 Process of blood collection in the mixed meal EV study.

Approximately 10 mL blood was collected from each participant using a cannula inserted into the antecubital fossa by Dr Anne Sillars. Participants then consumed a standard meal containing ~800 kCal (30% fat, 47% carbohydrate and 17% protein). After this 10 mL blood samples were collected from the cannula at 0.5, 1, 2, 4, and 6 hours. Blood was collected into a 4.5 mL citrate tube, a 4 mL EDTA tube and a 2 mL sodium fluoride/ potassium oxalate tube.

2.2 Assessment of resting energy expenditure and cardiovascular fitness

Resting metabolic rate (RMR) was measured fasted (with no ingestion of caffeine over the proceeding 12 hours) in the morning of the test day using a ventilated hood and Quark Cardio-pulmonary exercise testing (CPET) metabolic cart (COSMED, Rome, Italy) (American Thoracic Society, 2003). The test was carried out at laboratory environmental conditions, which were controlled at 24°C, and external stimuli was minimised. Prior to the test, participants were asked to rest for 30 mins. These measurements were carried out by Dr James McLaren and Dr Anne Sillars for the GlasVEGAs and MFAT studies respectively.

Maximal exercise was undertaken on a walking treadmill at a continuous speed of 5.5 km/h under the supervision of technician John Wilson (Kaminsky *et al.*, 2015). Heart rate was monitored during the test. After 6 mins of warm-up, the gradient of the treadmill was increased by 3% inclination every two mins until 24% when participants reached their maximal physical effort which was maintained for two mins. The expired air from each participant was collected when the participant was getting close to the maximal physical effort. Expired air was collected into Douglas bags and was processed in two stages. Firstly, an exact volume of 500 ml air in the Douglas bags was examined by a gas analyser (Servomex 4000 series, Servomex group Ltd, East Sussex, UK) and percentage fraction of expired oxygen and carbon dioxide were measured. Secondly, the remaining air in the Douglas

bag was extracted by vacuum at constant flow rate through a dry gas meter and thermometer (Harvard apparatus ltd, Kent, UK) which measured volume and temperature of expired air.

VO$_2$ max was confirmed after achieving a minimum two of three possible criteria (Howley *et al.*, 1995), including respiratory exchange ratio (RER) ≥ 1.15, heart rate ≥ 90% age predicted maximum and plateau of VO$_2$. VO$_2$ max per body weight was adopted in the current study. VO$_2$ max results were collected and processed by Dr James McLaren and Dr Anne Sillars for their respective studies.

2.3 Body Composition Measurement via Magnetic Resonance Imaging (MRI)

Body composition measurement utilised both MRI and Magnetic Resonance Spectroscopy (MRS). The protocol was pioneered by the university MRI team, which allowed for a comprehensive analysis of body fat and lean mass composition. The results of this innovative approach had been meticulously examined and interpreted by Dr James McLaren and Dr Anne Sillars for their respective studies.

2.3.1 Magnetic Resonance Protocol

Body composition measurement was conducted at the University of Glasgow, BHF Glasgow Cardiovascular Centre, utilising a Siemens 3.0-Tesla magnetic resonance scanner (Magnetom, Siemens). The protocol involved both MRI and MRS with a dedicated transmit/receive coil positioned on the participants' anterior abdominal wall for MRS measurements. The protocol was executed by MR radiographers Rosie Woodward (RW) and colleagues, with Dr James McLaren and Dr Anne Sillars providing on-site medical cover for their respective studies.

The MR protocol for the GlasVEGAs study was designed in collaboration with MR physicists John Foster and Christie McComb at the University of Glasgow, and AMRA physicists ODL, PT, and FW. The acquired MR images were transferred to Linköping, Sweden, for analysis by the AMRA physicist team, who calculated the volumes of lean tissue and fat compartments using fat-referenced MRI. The results were then electronically transferred back to Dr James McLaren, and the research team at the University of Glasgow.

2.3.2 Whole Body Fat and Lean Tissue Analysis

Participants underwent a dual echo 50-minute Dixon-VIBE protocol scan, providing water and fat separated volumetric data. The body composition analysis included total lean tissue, total fat, abdominal SAT and VAT. The MRI limitations meant that the arms were not included in the analysis, and only the posterior abdominal component of SSAT and DSAT could be analysed due to MRI quality. In this thesis, total fat (no arm) was used to describe whole body fat, and total lean (no arm) was used to describe whole body lean tissue.

Fat-referenced MRI software was used to analyse body composition, recognising pure adipose tissue as a value of one voxel (image volume element), while lean tissue has a value of 0. The software can distinguish between fat and lean tissue and calculate their respective volumes.

2.4 Adipocyte isolation and pre-adipocyte proliferation

Adipose tissue used in this study was collected from the GlasVEGAs subjects recruited by Dr James McLaren (2.1.1) and MFAT subjects recruited by Dr Anne Sillars (2.1.2) as indicated above. The tissue collection and isolation follows a standard protocol from Prof Ulf Smith and colleagues (Björntorp *et al.*, 1978).

2.4.1 Abdominal subcutaneous adipose tissue (ASAT) collection

The biopsy site was cleaned with chlorohexidine, followed by injection of a small amount (~2.5 mL) of local anaesthetic (1% lidocaine) under the skin. Liposuction was performed to take a small amount (0.1 to 1 g) of abdominal subcutaneous adipose tissue (ASAT) with a fourteen-gauge biopsy needle and a 50 mL syringe. The ASAT was collected in pre-warmed (37°C) 15 mL Hank's medium 199 (Gibco, 22350029), and the weight of tissue was recorded.

2.4.2 Adipocyte and stromal cell isolation

Freshly made adipose tissue digestion buffer (8 mL, Table 2-1) was pre-warmed (37°C) and then sterilised by 0.20 μm filtration before use. The ASAT biopsy was cut into 25 - 30 mg pieces with autoclaved scissors and transferred into prepared digestion buffer. Tissue was shaken in a water bath (Grant, OLS200) for 50 min at

37°C, 110 rotations/min, and then filtered through a nylon mesh 250 μm filter (Pierce, Thermo Fisher Scientific, 87791) to remove undigested material.

Reagent	Final concentration
Hank's medium 199	X 1
HyClone bovine serum albumin (BSA, Thermo Fisher Scientific, SH30574.02)	4%
Collagenase A (Roche Diagnostics, 11088793001)	0.20 U/mL

Table 2-1 Adipose tissue digestion buffer.

The suspension was allowed to stand for 5 min, and then the floating adipocyte layer (approx. 50 - 100 μL) was collected from the surface with a pipette using a wide bore tip. An aliquot (5 μL) of adipocyte suspension was used for adipocyte sizing (2.4.4), the remaining adipocytes were flash frozen in liquid nitrogen, and stored in a -80°C freezer.

The infranatant containing stromal cells was centrifuged at 300 x g for 10 min at room temperature, washed with 5 ml stromal cell culture medium (Table 2-2), and centrifuged at 300 x g for 10 min at room temperature. The pellet was suspended in 5 mL stromal cell culture medium and transferred into 25 cm^2 tissue culture flasks[2] and transferred to a 37°C 5% CO_2 incubator. After 48 h, the medium containing non-adherent cells was removed leaving the adherent pre-adipocytes in stromal cell culture medium (Table 2-2).

Reagent	Final Concentration
DMEM (Sigma-Aldrich, D5671)	1x
Fetal bovine serum (Sigma-Aldrich, F9665)	10%
Penicillin-Streptomycin (P/S, Sigma-Aldrich, P0781)	100 U/mL
L-Glutamine (Sigma-Aldrich, G7513)	2 mM

Table 2-2 Stromal cell culture medium.

2.4.3 Adipose tissue stromal cell proliferation

Pre-adipocytes were cultured in 25 cm^2 flasks (passage 0), in a 37°C 5% CO_2 incubator, and fed with 5 mL stromal cell culture medium every 3 to 4 days until

---

[2] Certain of our samples were initially cultured in 12.5 cm^2 flasks with 1.5 mL stromal cell culture medium or 75 cm^2 flask with 12 mL stromal cell culture medium. This was optimized to 25 cm^2 flasks with 5 mL culture medium as explained in detail in Chapter 5

80% confluent (usually between 2 and 6 weeks). Once confluence was reached the culture medium was removed and the flask washed twice with 1X Dulbecco's phosphate-buffered saline (1X DPBS, Thermo Fisher Scientific, 14190094) at 37°C, before adding 2.5 mL 0.25% trypsin (Sigma-Aldrich T4049) and incubating in a 37°C 5% CO_2 incubator for four minutes. The flask was then tapped gently to detach the cells, and a volume of stromal cell culture medium twice that of trypsin used was added and mixed. The cell suspension was then centrifuged at 200 x g for 5 min at room temperature. The supernatant was removed, and the stromal cell pellet was resuspended and transferred into 75 cm^2 flasks (passage 1) and cultured until 80% confluent as described above.

Once the pre-adipocytes became 80% confluent in the 75 cm^2 flask, they were detached from the flask with 4 mL trypsin as described above. The cells were counted manually using a haemocytometer (Camlab UK) according to the manufacturer's protocol. The stromal cells were resuspended in freezing medium (DMEM, 20% FBS, 10% dimethyl sulfoxide [DMSO, DLM-10RG-PK], 100 U/mL penicillin-streptomycin, and 2 mM L-Glutamine) at a maximum cell concentration of 500,000 cells/mL. Cells were added in 1mL aliquots into cryo-vials (Greiner Bio-one) and immediately transferred into a Mr Frosty Cryo 1°C freezing container (Thermo Fisher Scientific) overnight at -80°C, and then transferred to liquid nitrogen for longer term storage.

2.4.4 Assessment of adipocyte diameter

Adipocyte diameter was measured on freshly isolated cells. Briefly, 2.5 µL adipocyte suspension was added into 5 µL Krebs Ringer HEPES (KRH) buffer (NaCl 120 mM, $CaCl_2$ 2 mM, KCl 5 mM, $MgCl_2$ 1 mM, $NaHCO_3$ 25 mM, D-glucose 1.1 mM, HEPES 5.5 mM) on a glass slide. Digital pictures (6 - 10 captures) were captured in Image-Pro Plus 4.0 using a 10x lens on a BX50 microscope using Image-Pro Plus Vs 4.0 software (Isakson *et al.*, 2009).

2.4.4.1 Manual measurement of adipocyte size

Intracellular diameters of 100 cells were measured for each sample in Adobe Photoshop Vs7.0 in pixels. Diameter in pixels was converted to micrometers (100 pixels = 78 µm) using the digital image of a stage micrometre at the same

magnification. Adipocyte size was measured in GlasVEGAs by two independent obervers; either Dr James McLaren or Dr Anne Sillars and the author.

2.4.4.2 Automated measurement of adipocyte size

Digital pictures (6 - 10 captures, Figure 2-3) were captured using a 10x lens on a BX50 microscope (Olympus) by Image-Pro Plus 4.0 (Isakson *et al.*, 2009). Then the diameter of adipocytes was measured automatically using ImageJ 1.52a (Wayne Rasband, NIH, USA). Briefly, for the automated measurement a conversion factor between pixels and micrometres was measured by a granular ruler as 80.89 pixels = 100 μm. Pictures were converted to default black and white using an adjusted threshold to allow maximum number of adipocytes to be measured. Intracellular diameter was exported as Feret's diameter[3]. Results from the first 150 cells accessed from each participant was used for the data analysis.
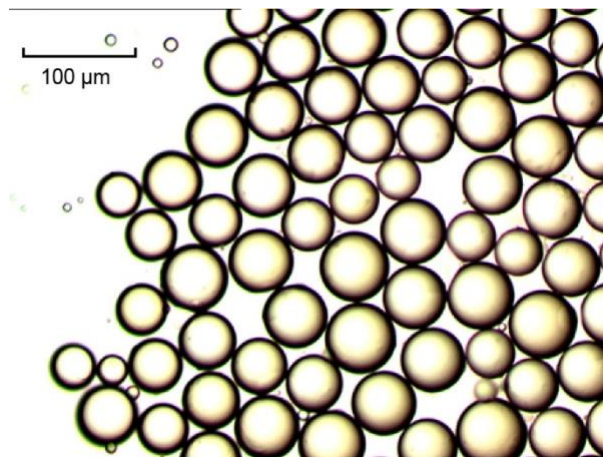
Figure 2-3 Captured image of isolated adipocytes taken under 10x magnification.

2.4.4.3 Adipocyte volume calculation

An adipocyte was assumed to be a sphere and the volume was calculated from the diameter using the formula:

$$Volume = \frac{4}{3}\pi(\frac{1}{2}diameter)^3$$

---

[3] The longest distance between any two points along the selection boundary, also known as maximum calliper. Adipocytes are considered to be circular in KRH buffer, therefore, Feret's diameter was regarded as diameter in this thesis.

2.5 Pre-adipocyte differentiation

2.5.1 Pre-adipocyte defrosting and expansion

Pre-adipocytes that had been frozen in liquid nitrogen (or a -80°C freezer) (2.4.3) were used for differentiation. The cells were defrosted in a 37°C water bath for 2 min before adding to 5 mL of differentiation culture medium (Table 2-3), and then centrifuged at 350 x g for 3 min at room temperature. The supernatant was removed, and the cell pellet was resuspended in 18 mL differentiation culture medium and transferred into a 150 cm^2 flask (passage 2) and incubated in a 37°C 5% CO_2 incubator, until 90% confluent. They were then split into two 150 cm^2 flasks (passage 3) as described previously (2.4.3) and cultured until 90% confluent.

Reagent	Final Concentration
DMEM (Sigma-Aldrich, D6249)	1x
Fetal bovine serum (Gibco, 10270)	10%
P/S (Sigma-Aldrich, P0781)	100 U/mL
L-Glutamine (Sigma-Aldrich, G7513)	2 mM

Table 2-3 Pre-adipocyte differentiation culture medium.

2.5.2 Pre-adipocyte differentiation *in vitro*

Once the pre-adipocytes had reached 90% confluence at passage 3, they were harvested and 1mL of 75,000 cells/mL in differentiation culture medium was added to each of 12 wells in 12-well plates. Plates were incubated for three days in a 37°C 5% CO_2 incubator until confluence was reached.

Pre-adipocytes from six wells were harvested immediately after three days incubation to act as undifferentiated controls. Two wells were used for oil red O (ORO) staining of cellular lipid accumulation (2.5.3), two wells were used for RNA isolation (2.5.4) and mRNA expression quantitation, and two wells were used for cell lysis (2.5.5) to measure protein expression by western blotting.

The remaining wells were harvested after 14 days differentiation. Pre-adipocytes were induced to differentiate by incubation for three days with 1 mL/well differentiation medium (DMEM [Sigma-Aldrich, D6249], 3% FBS [Gibco, 10270], 850 nM insulin [Sigma-Aldrich, I9278], 0.5 mM isobutylmethylxanthine [IBMX, Sigma-Aldrich, I7018], 10 µM dexamethasone [Sigma-Aldrich, D4902], 10 µM pioglitazone

[Cayman Chemical, 71745], 2 mM L-glutamine and 100 U/mL P/S). On the fourth day, the medium was changed to 1 mL/well differentiation maintenance medium (DMEM [Sigma-Aldrich, D6249], 10% FBS [Gibco, 10270], 850 nM insulin, 1 μM dexamethasone,1 μM pioglitazone, 2 mM L-glutamine, and 100 U/mL P/S). The differentiation maintenance medium was changed every three days until day 14. The total time taken for differentiation (including induction and maintenance) was 14 days. The differentiated cells were then harvested after 14 days differentiation for assessment of cellular lipid accumulation, mRNA expression and protein expression as described for undifferentiated controls.

2.5.3 Quantitation of cellular lipid accumulation by Oil red O staining

Medium was removed and cells were washed twice with 1x DPBS. The cells were fixed with 800 μL 4% formaldehyde for 20 min at room temperature, and then washed once with 1x DPBS, followed by two washes with distilled water. Water was then removed, without allowing the cells to dry out completely and the plate was sealed in plastic bags and kept at -20°C until stained.

On the day of staining, the plate was defrosted and allowed to completely dry out. Freshly prepared ORO solution (1 mL, 6:4 Oil Red O [Sigma-Aldrich, O1391]: Millli Q water) was added to each well, and incubated for 60 min at room temperature, and then washed gently with water and drained. Isopropanol (1mL) was then added to each well and incubated for 6 min at room temperature to solubilise the intracellular ORO. Two aliquots per well of 200 μL isopropanol containing the solubilised ORO was transferred to a flat 96-well plate (Corning, 9018), and the absorbance at λ510 nm was read and exported. The ratio of ORO absorbance after differentiation (day 14) relative to the undifferentiated control (day 0) cells was calculated using the exported absorbance read.

2.5.4 RNA extraction from cultured primary pre-adipocytes

Total RNA was extracted from undifferentiated control (day 0) and differentiated (day 14) pre-adipocytes (2.5.2) using Trizol reagent (Thermo Fisher Scientific, 15596026) according to the manufacturer's instructions. Trizol (1 mL) was added to each well (of a 6 well plate) and the isolated RNA was dissolved in 20 μL nuclease-free water (QIAGEN, 129115).

2.5.5 Cell lysis of pre-adipocytes for protein quantitation

Total protein was extracted from undifferentiated control (day 0) and differentiated (day 14) pre-adipocytes (2.5.2) using lysis buffer (Table 2-4) (Gustafson and Smith, 2006). Briefly, the cells were washed with ice cold 1x DPBS twice and completely dried out. Lysis buffer (50 μL; Table 2-4) was added to each well and incubated for 15 secs. The well was then scraped to solubilise cellular material and the resulting suspension collected. The suspension was then centrifuged at 20,000 x g for 10 min at 4°C to remove cellular debris, and the supernatant was stored at -80°C for future use.

Reagent	Final Concentration
Tris-HCl (pH 7.4)	25 mM
NaCl	25 mM
IGEPAL CA-630 (Sigma-Aldrich, I8896)	1%
NaF	10 mM
Protease inhibitor solution (1 tablet in 10 ml water, SIGMAFAST Protease Inhibitor tablets, S8820)	10%

Table 2-4 Cell lysis buffer for differentiation.

IGEPAL CA-630: nonionic, non-denaturing detergent suitable for solubilization, isolation and purification of membrane protein complexes.

2.6 mRNA quantitation by Taqman RT-qPCR

2.6.1 RNA extraction

2.6.1.1 RNA extraction from abdominal subcutaneous adipocytes

Total RNA was extracted from 50 – 100 mg abdominal subcutaneous adipocytes isolated from ASAT (2.4.2) using the RNeasy Lipid Tissue Mini Kit (QIAGEN, 74804) according to the manufacturer's instructions. The RNA was dissolved in 30 μL nuclease-free water (QIAGEN, 129115).

2.6.1.2 RNA extraction from pre-adipocytes

As described before (2.5.4), total RNA was extracted from undifferentiated control (day 0) and differentiated (day 14) pre-adipocytes (1.4.1) using Trizol reagent (Thermo Fisher Scientific, 15596026) according to the manufacturer's instructions. Trizol (1 mL) was added to each well (of a 6 well plate) and the isolated RNA was dissolved in 20 μL nuclease-free water (QIAGEN, 129115).

2.6.1.3 RNA extraction from extracellular vesicles (EV)

Total RNA was extracted from EV sample (~300 µL, 2.7.4) using a miRNeasy Mini Kit (QIAGEN, 217004) following the manufacturer's instructions. The RNA was dissolved in 12 µL nuclease-free water (QIAGEN, 129115).

2.6.2 Quantifying RNA yield and removing DNA contamination

The integrity and purification of isolated RNA was confirmed using a NanoDrop 1000 (Thermo Fisher Scientific). The optical density as 260/280 nm ratio (1.8 - 2.0 acceptable purity) and the concentration of RNA was recorded.

2.6.2.1 Removal of DNA contamination

DNase treatment was applied to all RNA samples to remove any DNA contamination in the samples. A DNA-free kit (Thermo Fisher Scientific, AM1906) was used according to the manufacturer's instructions. The purified RNA was stored at -80°C for future use.

2.6.3 Synthesis of complementary DNA

Single stranded complimentary DNA (cDNA) used for qPCR was reverse transcribed from purified RNA using a high-capacity cDNA reverse transcription kit (Thermo Fisher Scientific, 4368813) according to the manufacturer's instructions. The cDNA was stored at -20°C.

2.6.4 Pre-amplification of cDNA

The quantity of specific cDNA targets was pre-amplified using TaqMan® PreAmp master mix (2x) (Thermo Fisher Scientific, 4384266). Briefly, Tris-EDTA (TE), pH 8.0 buffer (Thermo Fisher Scientific, AM9849) was mixed 1:1 with the TaqMan® Gene Expression assay for the selected target genes (each target TaqMan® Gene Expression Assay mix contributes an equal amount) to make a pooled assay mix. Pre-amplification Reaction Mix was made up as shown in Table 2-5 to allow amplification of the number of cDNA samples being preamplified. Pre-amplification (10 cycles) was carried out in a StepOnePlus Real-Time PCR system (Thermo Fisher Scientific) using the following cycling programme: 95°C for 10 min, then 10 x of 95°C for 15 secs and 60°C for 4 min. After pre-amplification, each

sample was 1:5 diluted in TE, pH 8.0 buffer and stored at -20°C. The uniformity of pre-amplification was checked and the results are shown in Chapter 4.

Reagent	Final concentration
TaqMan PreAmp master mix (2X)	1x
Pooled TaqMan® Gene Expression Assay (20X)	1x
cDNA	1-5 ng/µL
Nuclease-free water	N/A

Table 2-5 Pre-amplification reaction mix (50 µL) per cDNA sample.

2.6.5 RT-qPCR

The pre-amplified cDNA for specific target genes was quantitated using Taqman® real time PCR on a StepOnePlus Real-Time PCR system. The target Taqman® Gene Expression Assays were purchased from ThermoFisher Scientific as listed Table 2-6. Briefly, a RT-PCR reaction mix was made up for each target gene: 1.25 µL target Taqman® Gene Expression Assay, 12.5 µL TaqMan universal PCR master mix (Thermo Fisher Scientific, 4304437), and 5 µL nuclease-free water. Diluted pre-amplified cDNA, 6.25 µL, (2.6.4) was mixed with each PCR reaction mix in duplicate in a MicroAmp fast optical 96-well reaction plate (ThermoFisher Scientific), and underwent PCR according to the following programme: 50°C for 2 min, 95°C for 10 min, then 40 x of 95°C for 15 secs and 60°C for 1 min.

The fluorescence threshold for the FAM-NFQ reporter in each target assay was optimised as 0.2 ΔRn following the manufacturer's recommendation. For the Vic-Tamra reporter, the threshold was optimised individually, in this case, it was 0.12 ΔRn for *ACTB*. No fluorescent signals were analysed for gene expression earlier than C_T=15, as signals between cycle 3 and cycle 15 were considered to be background fluorescence according to the manufacturer's recommendation. Cycle threshold (Ct) value was determined by the StepOnePlus v2.3 software. *PPIA* was used as endogenous control for delta Ct and delta delta Ct analysis (Neville *et al.*, 2011). All the TaqMan® Gene expression assays used for RT-qPCR to examine the genes in the current study are summarized in

Gene symbol	Assay ID	Reporter
ACTB	Hs00605340_m1	Vic-Tamra
ADIPOQ	Hs00605917_m1	FAM-NFQ
APOE	Hs00171168_m1	FAM-NFQ
BSCL2	Hs00949220_m1	FAM-NFQ
CASP1	Hs00354836_m1	FAM-NFQ
CDKN1B	Hs00153277_m1	FAM-NFQ
CIDEA	Hs00154455_m1	FAM-NFQ
CYP19A1	Hs00903411_m1	FAM-NFQ
DLK1	Hs00171584_m1	FAM-NFQ
EPAS1	Hs01026149_m1	FAM-NFQ
ESR1	Hs01046816_m1	FAM-NFQ
FABP4	Hs01086177_m1	FAM-NFQ
GHR	Hs00174872_m1	FAM-NFQ
HIF1A	Hs00153153_m1	FAM-NFQ
HOXC13	Hs00600868_m1	FAM-NFQ
INSR	Hs00961554_m1	FAM-NFQ
KLF14	Hs00370951_s1	FAM-NFQ
LDLR	Hs00181192_m1	FAM-NFQ
LEP	Hs00174877_m1	FAM-NFQ
LPL	Hs00173425_m1	FAM-NFQ
NR1H4	Hs01026590_m1	FAM-NFQ
PIK3R1	Hs00933163_m1	FAM-NFQ
PLIN2	Hs00605340_m1	FAM-NFQ
PPARG	Hs01115513_m1	FAM-NFQ
PPIA	Hs99999904_m1	FAM-NFQ
SIRT1	Hs01009006_m1	FAM-NFQ
SREBF1	Hs01088691_m1	FAM-NFQ
TCF7L2	Hs01009044_m1	FAM-NFQ
TGFB1	Hs00998133_m1	FAM-NFQ
TLR2	Hs00610101_m1	FAM-NFQ
TNF	Hs00174128_m1	FAM-NFQ

Table 2-6 TaqMan® Gene Expression Assays used for RT-qPCR.

Reference genes and genes of interest (GOI). Hs – *Homo sapiens*; '_m' indicates an essay whose probe spans an exon junction and will not detect genomic DNA; '_s' indicates an assay whose probes are designed within a single exon, and will, by definition, detect genomic DNA. The '_s' probe was only selected when there was no '_m' available at the time when experiments were carried out.

2.7 Extracellular vesicles

Extracellular vesicles (EV) were isolated from human plasma. Blood was collected from the participants of the mixed meal EV study (2.1.3) at each time point via intravenous cannula.

2.7.1 Blood collection and plasma isolation

Around 10 mL of blood was collected into sodium fluoride/ potassium oxalate (2mL) (Greiner Bio-one, 454061), sodium citrate 3.8% 4.5 mL (Greiner Bio-one, 454389), and K$_2$EDTA blood tubes (4 ml) (Greiner Bio-one, 454209).

Plasma was collected by centrifugation (2,000 x g for 15 min at 4°C [oxalate tube] or room temperature [K$_2$EDTA tube]) within 30 min and stored at -80°C in 1 mL aliquots.

Platelet-free plasma was collected from citrate tubes centrifuged at 2,000 x g for 15 min at room temperature followed by two centrifugations of the plasma each at 2,500 x g for 15 min at room temperature.

2.7.2 Size exclusion chromatography (SEC)

Plasma (2.7.1) was defrosted and a 500 µL aliquot of each sample was centrifuged at 2,000 x g for 30 min at 4°C. The supernatant was collected and centrifuged at 12,000 x g for 45 min at 4°C. The supernatant was then collected ready for SEC.

2.7.2.1 Size Exclusion Chromatography

Disposable 10 mL polypropylene columns (Thermo Fisher Scientific, 29924) were prepared according to the manufacturer's instruction. Sepharose CL-2B slurry [bead diameter, 60 - 200 nm] (14mL; Sigma-Aldrich CL2B300) was transferred into a prepared 20 mL column (with a porous disc at the bottom) and left at 4°C for 48 h to pack. A second porous disc was positioned on top of the sepharose and pushed down to just above the gel (~10 mL). The stock liquid was flushed through, and the gel washed with 10 mL 1X DPBS prior to use.

Prepared plasma (~500 µL, 2.7.1) was loaded onto the topmost porous disc, and after all the plasma had passed through the disc, 3 - 5 mL of 1x DPBS was loaded onto the column to keep it flowing. Eluate was collected in 25 x 500 µL sequential fractions once the plasma was loaded. All fractions were assessed to determine nanoparticle concentration using nanoparticle tracking analysis (2.7.3) and protein content using a Bradford assay (Bio-Rad DC). Desired fractions enriched with nanoparticles were concentrated (2.7.4) for further study.

Each column was used twice for one participant. First the EDTA sample was processed and second the citrate sample was processed. Columns were washed between each sample run, three times with 10 mL 1x DPBS followed by 10 - 14 mL 0.5 M NaOH until the pH of the eluate reached 14. The column was then reset to pH 7 by flushing with 10 - 15 mL 1x DPBS until the pH of the eluate reached 7.

2.7.3 Nanoparticle tracking analysis (NTA)

NTA was used to analyse particle size distribution and concentration in the pooled fractions. Pooled SEC fractions from EDTA plasma were analysed using a Nanosight NS 500 (Nanosight Ltd, Amesbury, UK) equipped with autosampler and NanoSight NTA v3 software in the Exosome Biology Laboratory (EBL, University of Queensland, Australia). Other pooled fractions (collected in EDTA and citrate, 2.7.1) were analysed using a Nanosight NS 500 and NanoSight NTA v3 software in the Institute of Cardiovascular and Medical Sciences (ICAMS, University of Glasgow, UK). NTA was run according to the manufacturer's instructions. Samples were diluted to a concentration in which there were 50 - 100 particles in each frame (Salomon *et al.*, 2014a, Salomon *et al.*, 2014b).

2.7.4 Concentration of EV fractions

The fractions that were pooled for EV enrichment were concentrated using an Amicon ultra-15 centrifugal filter unit (ultracel-100K, Sigma-Aldrich, UFC910096). Briefly, desired fractions were pooled and loaded into the filter unit, and centrifuged at 4,000 x g for 5 min at 4°C. The eluate (~250 μL) was collected from the receptacle (column) using a glass Pasteur pipette. It was then made up to the original volume of plasma loaded onto the SEC column (2.7.2). EV samples were stored at -80°C.

Each filter unit was used twice for each participant's EDTA and citrate plasma samples. The filter units were washed between each sample using three centrifugations at 4,000 x g for 15 min at 4°C with 15 mL 1x DPBS, 15 mL 0.1 M NaOH, and 15 mL 1x DPBS respectively.

2.7.5 Micro RNA sequencing

miRNA was extracted from 200 μL concentrated EV samples (2.7.4) using exoRNeasy Plasma Kits (Qiagen 217004, UK) and quality control of isolated RNA was performed on the Agilent Bioanalyser using small sample pico chips.

In collaboration with Glasgow Polyomics, miRNA sequencing was undertaken on the NextSeq platform by Julie Galbraith. miRNA libraries were prepared using a small RNAseq QIAgen kit and quality control was assessed on the Agilent Bioanalyser. Samples were run using a single end, 75 bp read length achieving at least 10 million reads per sample on the Nextseq platform. miRNA sequencing analysis was performed only for the male participants (n = 7) using the samples collected at baseline and 120 mins postprandial.

A MultiQC report for the quality of miRNA sequencing was generated by Graham Hamilton. The miRNA sequencing experiment was supervised by Dr Martin McBride.

2.8 Statistics

Statistics were performed using Minitab Vs 19 (Minitab Ltd) and figures were drawn using GraphPad Prism Vs 9.1.1 Normal distribution for all the parameters was checked using the Ryan-Joiner test. Non-normally distributed data were log or square root transformed to achieve normal distribution. Data that failed to be transformed was analysed as non-parametric data.

2.8.1 Univariate analysis

Analysis of inter-observer agreement between the two independent observers for adipocyte sizing was performed by Bland-Altman Plot. Results were displayed as mean and standard deviation (SD) for parametric data, and as median [95% confident intervals] for non-parametric data. Two group comparisons of cross-sectional parameters were made using two-sample t-test for normally distributed data or Mann-Whitney U-test for non-parametric data. When there were more than two groups, comparisons were made using one-way ANOVA with *post hoc* Tukey's for individual group comparison, and Kruskal Wallis analysis combined with *post hoc* Dunn test for non-parametric data. For longitudinal comparisons, differences

between time points was examined using paired t-test for two group comparison or repeated measures ANOVA using a general Linear Model for more than two groups. Significance level was p less than 0.05. Pearson correlation was performed to check the linear relationship between two normally distributed parameters and the result was expressed using R^2 and p value ($p < 0.05$ was considered significant). For non-parametric parameters Spearman rank correlation was carried out.

2.8.2 Multivariate analysis

General linear model (GLM) ANOVA was performed to analyse the impact of confounders on non-paired group comparisons. For analysis of the effects of confounders on repeated measures comparisons a mixed effects model ANOVA was used. Interactions between factors and covariates were considered only when $p < 0.1$. For main effects significance was considered as $p < 0.05$.

Chapter 3 The influence of insulin resistance, BMI and cardiovascular fitness on adipocyte size distribution and expression of genes involved in adipocyte function

3.1 Introduction

The increased prevalence of type 2 diabetes mellitus (T2DM) is related to the contemporary human behaviours of feeding (high fat diet) and low physical activity (sedentary lifestyle), which result in an increased accumulation of adipose tissue compared to lean mass (skeletal muscle) (Guilherme *et al.*, 2008). It has been widely accepted that the risk of T2DM is associated with overweight/obesity and adiposity (BMI, waist circumference, etc.), age, family history, ethnicity, and sedentary lifestyle (physical activity, sedentary time, etc.) (Bellou *et al.*, 2018). These factors may contribute to the two pathological steps towards developing to T2DM. Firstly, decreased/impaired insulin response in skeletal muscle, as is observed in obesity, is a primary condition for T2DM. In insulin resistant individuals who have not yet developed T2DM, increased insulin secreted from pancreatic β-cells maintains blood glucose levels. This may progress to the second pathological step when there is a failure of pancreatic β-cells, a failure of insulin production and development of overt T2DM (Guilherme *et al.*, 2008).

Although both total adiposity and adipose tissue distribution are important to insulin resistance, the size of adipocytes may also directly influence adipocyte function and their contribution to insulin resistance. When there is excess energy, adipose tissue expands by increasing the number of adipocytes (hyperplasia) and/or increasing the average volume of adipocytes (hypertrophy) (Salans *et al.*, 1973, Spalding *et al.*, 2008). Insulin sensitivity can be improved by weight loss, and this may be a result of decreased adipocyte size and central adiposity (McLaughlin *et al.*, 2019). In a study of 280 Pima Indians, subcutaneous abdominal adipocyte diameter was 11% and 19% larger in impaired glucose tolerance (IGT) and T2DM than in normal glucose tolerance (NGT) ($p < 0.0001$), and insulin sensitivity was negatively correlated with subcutaneous abdominal adipocyte diameter (r = -0.53, $p < 0.0001$) (Weyer *et al.*, 2000).

Adipocyte morphology and function are critical for the development of insulin resistance and T2DM. Age, adiposity, central adiposity, cardiovascular fitness and ethnicity all are linked to insulin resistance and the effects are overlapping. Total body fatness and aerobic fitness are frequently used in association with each other, and these two physiological parameters are strongly inter-related (Goran *et al.*, 2000). Both fatness and aerobic fitness have been shown to be risk factors for health outcomes, but it is not clear if these effects are related to one another or independently associated with risk factors, i.e. T2DM (Goran *et al.*, 2000). It has been argued that aerobic fitness might be the predominant risk factor, however, the biological and physiological basis of this hypothesis remains unclear (Blair *et al.*, 1996, Farrell *et al.*, 1998, Lee *et al.*, 1998). Currently, it is not clear to what extent adiposity, age, ethnicity, and cardiovascular fitness contribute independently to adipocyte function and morphology.

The size of adipocytes and adiposity changes in humans along with aging. A study showed that in mice, adipocyte diameter, %fat and fat mass increased from young to middle age and decreased with age (Miller *et al.*, 2017). However, there was a lack of direct evidence on the changes in adipocyte size in humans. According to a systematic review of age-related changes in total fat distribution, the changes of %fat and fat mass in Whites, Hispanic, Asians, and Black humans peaked at middle age (late 30s to 70 years old) and then decreased, similarly with mice (Kuk *et al.*, 2009). Therefore, it could be supposed that changes in the size of adipocytes might be similar in humans and mice. Growth hormone is negatively correlated with adipocyte size. In men with abdominal obesity, the use of growth hormone decreased the size of subcutaneous abdominal adipocytes and the total volume of abdominal SAT (Bredella *et al.*, 2017). Decreased adipogenesis in aging may be evidence of age-associated changes in adipocyte morphology, which may lead to increased adipocyte size. A study has shown that the increased secretion of cell senescence markers from adipocyte precursor cells (MSC isolated from ASAT), including TGFB1 protein and p53, were positively correlated with abdominal subcutaneous adipocyte size. The secretion of these markers reduced adipogenesis (reduced expression of *PPARG2* and *ADIPOQ* mRNA) in non-senescent human MSC differentiation *in vitro* (Gustafson *et al.*, 2019a). Similarly, *in vitro* stimulation of adipocyte differentiation showed that both the rate of replication (slope: old vs young 1.31 ± 0.09 vs 1.71 ± 0.09 $\times 10^{-3}$, $p = 0.005$) and differentiation

of preadipocytes (ORO absorbance 0.21 ± 0.02 vs 0.29 ± 0.03, p < 0.05) decreased in old participants (n = 12, aged 71 ± 2 years, BMI 26.2 ± 0.7 kg/m^2) to a greater extent than in young (n = 15, aged 27 ± 1 years, BMI 23.6 ± 0.7 kg/m^2) (Caso et $al.$, 2013). The rate of adipogenesis and adipocyte apoptosis also determines the rate of adipocyte turnover in $vivo$, and this also contributes to the development of adipocyte morphology. A study has shown that adipocyte turnover rate was negatively correlated with adipocyte hypertrophy and positively correlated with adipocyte hyperplasia (Arner et $al.$, 2010c). The changes of adipocyte morphology in adult life may be regulated by the decreased adipogenesis and increased apoptosis along with aging.

Regional fat distribution also changes during aging, and this may relate to altered lipid metabolism in adipocytes. In males > 50 years old and post-menopausal women, there was significantly increased accumulation of intra-abdominal visceral fat volume and decreased leg subcutaneous fat. Relative ASAT was decreased in men as well (Kotani et $al.$, 1994). A longitudinal study has recorded changes in body composition in the elderly over 10 years, finding that with increased total fat mass, there was a decrease in SAT (Hughes et $al.$, 2004). Age-related loss of trunk and leg fat was documented in Japanese people more than fifty years old, and the ratio between trunk and leg fat mass was correlated with WHR (Ito et $al.$, 2001). These data suggest that aging may contribute to the progressive inability of the body to develop SAT to store fat, especially in lower body depots. This may cause the accumulation of fat in VAT and central adiposity. A longitudinal study showed that waist circumference increased approximately 0.7 cm annually from 38 to 66 years old (Noppa et $al.$, 1980). The increase in waist circumference along with age has been widely recorded in both longitudinal (Carmelli et $al.$, 1991, Zamboni et $al.$, 2003) and cross-sectional studies (Teh et $al.$, 1996, Ito et $al.$, 2001) and has been reviewed elsewhere (Shimokata et $al.$, 1989a, Shimokata et $al.$, 1989b, Kuk et $al.$, 2009).

Insulin binding and glucose incorporation into abdominal subcutaneous adipocytes, as well as glucose transport in isolated abdominal subcutaneous adipocytes, were found to decrease in elderly relative to young subjects in $vitro$, with the in $vitro$ glucose transport rate showing a positive correlation with the in $vivo$ glucose disposal rate (Lonnroth and Smith, 1986, Fink et $al.$, 1983). These data indicated that aging was associated with insulin resistance in subcutaneous adipocytes.

However, the basal lipolysis was the same in isolated abdominal subcutaneous adipocytes from elderly and young individuals. When alpha 1 receptorswere stimulated with either isoprenaline or norepinephrine, lipolysis was significantly decreased in adipocytes from elderly individuals only, however the decrease in lipolysis through α2-adrencceptors showed no age difference. It was also observed that the inhibition of agonist-induced lipolysis might be a consequence of decreased activation of PKA and/or the hormone-sensitive lipase complex (Lonnqvist *et al.*, 1990). Interestingly, α2-adrenoreceptor induced lipolysis was negatively correlated, whereas noradrenaline induced lipolysis was positively correlated, with size of abdominal subcutaneous adipocytes in non-obese individuals (Arner *et al.*, 1987). Aging in obese individuals is correlated with an increased lipolytic effect of catecholamines and this may lead to hypertrophy of adipocytes and disturbed ability to store fat in SAT, and subsequently, changes in regional fat redistribution. Secretion of cytokines from adipose tissue, including TNFα, IL-6 and leptin increased during aging, but adiponectin was decreased (Morin *et al.*, 1997, Starr *et al.*, 2009, Coimbra *et al.*, 2014). TNFα treated human adipocytes differentiated from MSC isolated from ASAT, showed an increase in lipolysis through extracellular signal-related kinase (ERK) and increased intracellular cAMP (Zhang *et al.*, 2002).

In the context of obesity, the failure of adipose tissue to store fatty acids effectively is not solely due to the 'overflow' of fatty acids, or lipolysis. It is crucial to consider the role of lipoprotein lipase (LPL) in this process. LPL is responsible for the hydrolysis of triglycerides in lipoproteins, which supply fatty acids to be stored in adipose tissue. However, in obesity, the activity of LPL is often reduced, which impairs the ability of adipose tissue to hydrolyse the triglycerides in lipoproteins effectively. As a result, the supply of fatty acids for storage is limited (Karpe *et al.*, 2011). This perspective challenges the prevailing view in the literature and underscores the need for a more nuanced understanding of the mechanisms driving the storage of fatty acids in adipose tissue.

Physical exercise improves body fitness and resting fat oxidation, and this helps individuals to lose weight and is negatively correlated with mortality (Celis-Morales *et al.*, 2017, Barwell *et al.*, 2009). A study demonstrated that circulating adiponectin was negatively associated with obesity, circulating glucose, lipid levels (total cholesterol, LDL, and TG), and insulin sensitivity in healthy, impaired

glucose tolerant and T2DM individuals. Four weeks exercise resulted in increased circulating adiponectin levels in all groups which suggested, short term physical training may improve insulin resistance and metabolic syndrome (Blüher *et al.*, 2006). However, another study found that short term (1 week) exercise improved insulin sensitivity and circulating adiponectin at the same time, which suggested that increased insulin sensitivity in response to exercise may be independent of increased adiponectinemia (Yatagai *et al.*, 2003). Even though another study demonstrated that short-term (12 weeks) exercise improved physical fitness and peripheral insulin sensitivity in obese patients, the size of abdominal subcutaneous adipocytes and expression of genes involved in lipid metabolism in adipocytes did not change at the mRNA level (*HSL, TNF, IL6, ADIPOA, and LEP*) or at the protein level (mitochondrial oxidative phosphorylation proteins) (Stinkens *et al.*, 2018). In addition, short term exercise stimulated lipolytic response was lower in old compared to young individuals. During 60 mins of submaximal exercise (50% of VO_2 max) lipolysis was lower in elderly individuals than young, as the appearance of circulating FFA was lower in the elderly (Sial *et al.*, 1996). Additionally, physical exercise may correlate with adipogenesis. Three months of physical training increased gene expression of *PPARG* and PPARG coactivator 1 alpha (*PPARGC1A*), and a *PPARGC1A* (rs17650401) polymorphism was correlated with exercise-induced weight loss efficiency (Mazur *et al.*, 2020). However, six-month exercise and diet control stimulated weight loss, but did not change lipolysis or the activity of lipoprotein lipase in abdominal and greater gluteal subcutaneous adipocytes *in vitro* (Berman *et al.*, 2004). Long term exercise, on the contrary, impacted on adipocyte size, adipose tissue distribution and metabolism. Abdominal subcutaneous adipocyte size, adipocyte lipoprotein lipase (LPL) activity, and fat mass were lower in physically active females than sedentary females of normal body weight (Mauriège *et al.*, 1997). However, in obese men, endurance exercise did not change the size of abdominal subcutaneous adipocytes nor the adipocyte expression of genes (*TNF, IL1B, MCP1, HSL, SREBF1, PPARG* and *CIDEA*) (Van Pelt *et al.*, 2017). Thus, exercise, may regulate the function of subcutaneous adipocytes mainly by regulating total fat mass and the size of adipocytes *per se*.

South Asians, an ethnic group with a high risk of Type 2 Diabetes Mellitus (T2DM), exhibit significant differences in adipocyte size, regional adiposity, and even exercise response, when compared to the European White ethnicity which has a

lower incidence of T2DM. Abdominal subcutaneous adipocyte size was larger in South Asians compared to Europeans of similar age and BMI (Chandalia *et al.*, 2007, Anand *et al.*, 2011). Specifically, with similar numbers of adipocytes assessed, South Asians had higher ratios of small/large subcutaneous (small adipocytes, diameter < 20 μm, large, diameter between 44-90 μm) adipocytes (both from periumbilical and gluteofemoral areas), and had more very large adipocytes (> 90 μm) than Whites (Balakrishnan *et al.*, 2012). The size of adipocytes predicted insulin resistance in both South Asian and Whites (Chandalia *et al.*, 2007, Balakrishnan *et al.*, 2012). With similar age and BMI, South Asians had higher %fat, ASAT and lower body fat in some studies (Chandalia *et al.*, 2007, Anand *et al.*, 2011), but not in others (Balakrishnan *et al.*, 2012). However, in the later study, lower body fat was correlated to severity of insulin resistance only in South Asians and not in Whites (Balakrishnan *et al.*, 2012). Moreover, South Asians had more fat accumulation in visceral depots and liver and larger waist circumference (Jenum *et al.*, 2019, Rees *et al.*, 2011, Bodicoat *et al.*, 2014, Anand *et al.*, 2011). In addition, South Asians had higher levels of leptin in adults and infants than Whites after adjustment for age and BMI (Patel *et al.*, 2007, West *et al.*, 2013, Mente *et al.*, 2010). However, lower levels of adiponectin in South Asians compared to Whites was only found in some studies (Mente *et al.*, 2010, Anand *et al.*, 2011, Sulistyoningrum *et al.*, 2013, Martin *et al.*, 2008, Shah *et al.*, 2016b, Ferris *et al.*, 2005), and not in others (Patel *et al.*, 2007). Furthermore, differences in adiposity may not fully explain the differences in higher T2DM risk in South Asians than Whites. When adjusted for age, BMI, fat mass and physical activity, South Asians had lower insulin sensitivity, VO_2 max and decreased fat oxidation during submaximal exercise at the same relative exercise intensity (Hall *et al.*, 2010) than Whites. This suggested that decreased fitness, oxidative capacity and capacity for fat oxidation at the whole-body level may also contribute to the higher risk of T2DM in South Asians.

Aging is associated with adipocyte hypertrophy and central adiposity via decreased insulin sensitivity, altered lipolysis, and fatty acid response. Age, adiposity, central adiposity, cardiovascular fitness and ethnicity all are linked to insulin resistance and their effects are overlapping. They can contribute to altered insulin sensitivity independently or together. Therefore, the current study aimed to measure the size of abdominal subcutaneous adipocytes and measure the

adipocyte expression of genes that are associated with adipocyte differentiation (i.e., *PPARG*), markers of adipocyte lipid uptake and storage (i.e., *LPL* and *SREBF1*), insulin signalling and adipokine production (i.e., *ADIPOQ, INSR*, and *LEP*) and tissue stress response/ inflammation (i.e., *TNF*) (Table 1.1), to systematically understand the impact of BMI, insulin resistance and cardiovascular fitness on the function of adipocytes.

The aim of this chapter was to study the impact of risk factors for T2DM at the level of adipocyte size and gene expression in cohorts with different levels of insulin resistance, and we hypothesized that:

1. Age, adiposity, central adiposity and severity of insulin resistance are positively associated with adipocyte size due to lower hyperplastic expansion and higher hypertrophic expansion. Adipocyte expression of genes associated with differentiation (*PPARG*), lipid uptake and storage (i.e., *LPL* and *SREBF1*), and insulin signalling and adipokine production (i.e., *ADIPOQ, INSR*, and *LEP*) will be negatively associated with age, adiposity, central adiposity and severity of insulin resistance, whereas genes associated with tissue stress and inflammation will be positively associated.

2. Cardiovascular fitness will be negatively associated with adipocyte size due to higher hyperplastic expansion and lower hypertrophic expansion. Adipocyte expression of genes associated with differentiation (*PPARG*), lipid uptake and storage (i.e., *LPL* and *SREBF1*), and insulin signalling and adipokine production (i.e., *ADIPOQ, INSR*, and *LEP*) will be positively associated with cardiovascular fitness, whereas genes associated with tissue stress and inflammation will be negatively associated with cardiovascular fitness.

3. Young and lean South Asians will have a similar adipocyte size and function to older and fatter Whites Europeans.

Gene symbol	Protein name	Function
ADIPOQ	Adiponectin	*ADIPOQ* is expressed in adipose tissue exclusively. The encoded protein circulates in the plasma and is involved inmetabolic and hormonal processes.
CDKN1B	Cyclin Dependent Kinase Inhibitor 1B	Endogenous control for pre-amplification of cDNA.
INSR	Insulin receptor	Binding of insulin or other ligands to this receptor activates the insulin signalling pathway, which regulates glucose uptake and release, as well as the synthesis and storage of carbohydrates, lipids, and protein.
LEP	Leptin	Protein secreted by white adipocytes into the circulation which plays a major role in the regulation of energy homeostasis.
LPL	Lipoprotein Lipase	*LPL* functions as a homodimer and has the dual functions of a triglyceride hydrolase and as aligand/bridging factor for receptor-mediated lipoprotein uptake.
PPARG	Peroxisome Proliferator Activated Receptor Gamma	A regulator of adipocyte differentiation, switches on and maintains adipocyte terminal differentiation.
PPIA	Peptidylprolyl Isomerase A	Endogenous control for adipocyte gene expression.
SREBF1	Sterol Regulatory Element Binding Transcription Factor 1	A transcription factor that regulates genes involved in the promoter of the low-density lipoprotein receptor gene and other genes involved in sterol biosynthesis; marker of lipogenesis.
TNF	Tumour Necrosis Factor α	This cytokine is involved in the regulation of a wide spectrum of biological processes including cell proliferation, differentiation, apoptosis, lipid metabolism, and coagulation. It can cause inflammation.

Table 3-1 Function of genes examined in adipocytes in MFAT study.

3.2 Methods

3.2.1 Subjects

Five subgroups of participants from two studies (the Glasgow Visceral and Ectopic fat with weight Gain in South Asians [GlasVEGAs] and the Muscle Fat study [MFAT]) were involved in the current study as listed below. All participants in this chapter were White Europeans, apart from the uoung Healthy South Asian (YHSA) group. Demographic data were collected and/or measured during recruitment including age, body weight, body height and waist circumference. Body mass index (BMI) was calculated by body weight (in kg) divided by the squared body height (in metres). Waist circumference was measured with the participant in a relaxed standing position, with feet together and arms crossed over the chest, at the end of expiration of a breath. The circumference was taken by a tape ruler at the narrowest point between the inferior border of the tenth rib and the iliac crest, identified by Dr James McLaren or Dr Anne Sillars.

GlasVEGAs was a longitudinal study to explore the relationship between adiposity and insulin resistance in South Asians. Young males (age 18-45 and BMI < 27 kg/m^2, weight stable (± 2 kg) for more than six months) of white European origin (YHEU, n = 18, self-reported both parents of white European origin) or South Asian origin (YHSA, n = 13, self-reported both parents of Indian, Pakistani, Bangladeshi or Sri Lankan origin) were recruited from January 2015 to April 2017 by Dr James McLaren. Exclusion criteria included: diabetes (physician diagnosed or HbA1c ≥ 6.5% on screening), history of cardiovascular disease, regular participation in vigorous physical activity, current smoking, taking drugs or supplements thought to affect carbohydrate or lipid metabolism and other significant illness that would prevent full participation in the study.

MFAT was a cross-sectional study to identify the role played by the two alternative pathways of intracellular triacylglycerol (TG) synthesis in muscle in the aetiology of muscle insulin resistance (IR) in individuals at risk of developing or with newly diagnosed T2DM. Male participants (age 30 – 60 years and of white European origin) were recruited into this study by Dr Anne Sillars. Three groups were recruited according to the following criteria:

i. Older healthy European males (OHEU, n = 18), BMI 18 - 27 kg/m², who did not engage in regular vigorous physical activity, HbA1c < 6% (< 43.8 mmol/mol).

ii. Older European males with impaired glucose regulation (OIGREU, n = 17), with HbA1c = 6.0 – 6.4% (43.8 – 47.4 mmol/mol), impaired fasting glucose (IFG) or impaired glucose tolerance (IGT), or type 2 diabetes controlled by lifestyle only.

iii. Older endurance-trained Europeans (OETEU, n = 20), BMI 18 - 27 kg/m², undertaking more than 5 hours per week of vigorous endurance-based exercise training ≥ 2 years, HbA1c < 6% (< 43.8 mmol/mol).

Exclusion criteria included female sex, age less than 30 or greater than 60 years of age, and a history of cardiovascular disease or other serious chronic health conditions.

3.2.2 Assessment of resting energy expenditure and cardiovascular fitness

Resting metabolic rate (RMR) was measured fasted (with no ingestion of caffeine over the proceeding 12 hours) in the morning of the test day using a ventilated hood and Quark Cardio-pulmonary exercise testing (CPET) metabolic cart (COSMED, Rome, Italy) (American Thoracic Society, 2003). The test was carried out under controlled laboratory environmental conditions, which were ambient temperature 24°C and external stimuli were minimised. Prior to the test, participants were asked to rest for 30 mins. These measurements were carried out by Dr James McLaren and Dr Anne Sillars for the GlasVEGAs and MFAT studies respectively.

Maximal exercise was undertaken on a walking treadmill at a continuous speed of 5.5 km/h under the supervision of a technician, John Wilson(Kaminsky *et al.*, 2015). Heart rate was monitored during the test. After 6 mins of warm-up, the gradient of the treadmill was increased by 3% inclination every two mins until 24% when participants reached their maximal physical effort which was maintained for two mins. The expired air from each participant was collected when the participant was getting close to the maximal physical effort. Expired air was

collected into Douglas bags and was processed in two stages. Firstly, an exact volume of 500 ml air in the Douglas bags was examined by a gas analyser (Servomex 4000 series, Servomex group Ltd, East Sussex, UK) and percentage fraction of expired oxygen and carbon dioxide were measured. Secondly, the remaining air in the Douglas bag was extracted by vacuum at constant flow rate trough a dry gas meter and thermometer (Harvard Apparatus Ltd, Kent, UK) which measured volume and temperature of expired air.

VO_2 max was confirmed after achieving a minimum two of three possible criteria (Howley *et al.*, 1995): respiratory exchange ratio (RER) ≥ 1.15, heart rate ≥ 90% age predicted maximum and plateau of VO_2. VO_2 max per body weight was adopted in the current study. VO_2 max results were collected and processed by Dr James McLaren and Dr Anne Sillars for their respective studies.

3.2.3 Plasma measures

Fasting blood was collected by venepuncture and aspirated into blood sample tubes containing EDTA, lithium heparin, serum and sodium fluoride/potassium oxalate as anticoagulants. All samples were processed and stored at -80°C by Dr James McLaren and Dr Anne Sillars for their respective studies. Serum glucose and insulin level were analysed in one batch at the end of each study by Roche/Hitachi cobas systems (Roche Diagnostics GmbH, Mannheim, Germany). HOMA-IR was calculated by glucose concentration multiplied by insulin concentration then divided by 22.5 using fasting values (Matthews *et al.*, 1985).

3.2.4 Abdominal SAT collection and adipocyte isolation

An abdominal subcutaneous adipose tissue (ASAT) biopsy was collected from each participant by Dr James McLaren and Dr Anne Sillars in their respective studies. The methods for adipose tissue biopsy and adipocyte isolation have been described in more detail in Chapter 2 and were based on a standard protocol from Prof Fredrik Karpe and his group (Marinou *et al.*, 2014). Briefly, a small amount of adipose tissue (around 0.35 g) was collected using a needle biopsy. ASAT was cut into 25 - 30 mg pieces with autoclaved scissors and transferred into filtered digestion buffer (filtered through 0.2 μm filter to sterilise, used at 37°C, Table 2-1). The tissue was shaken in a water bath (Grant, OLS200) for 50 min at 37°C,

110 rotations/min, and then filtered through a Pierce nylon mesh 250 μm filter (Thermo Fisher Scientific, 87791) to remove undigested material.

The suspension was allowed to stand for 5 min, and the floating adipocyte layer (approx. 50 - 100 μL) was collected from the surface with a pipette using a wide bore tip. An aliquot (5 μL) of adipocyte suspension was used for adipocyte sizing.

3.2.5 Assessment of adipocyte size

3.2.5.1 Assessment of adipocyte diameter

Adipocyte diameter was measured on freshly isolated adipocytes by the author. Briefly, 2.5 μL adipocyte suspension was added to 5 μL Krebs Ringer HEPES (KRH) buffer (2.4.4) on a glass slide. Digital pictures (6 - 10 captures, Figure 2-3) were captured using a 10x lens on a BX50 microscope by Image-Pro Plus 4.0 (Isakson *et al.*, 2009). Then the diameter of adipocytes was measured automatically using ImageJ 1.52a (Wayne Rasband, NIH, USA). For the automated measurement a pixels to micrometre conversion factor was derived using a granular ruler: 80.89 pixels = 100 μm. Pictures were converted to default black and white using an adjusted threshold to allow maximum number of adipocytes to be measured. Intracellular diameter was exported as Feret's diameter[4]. After which, results from the first 150 cells accessed from each participant was used for the data analysis.

3.2.5.2 Adipocyte volume

An adipocyte was assumed to be a sphere and the volume was calculated from the diameter using the formula:

$$Volume = \frac{4}{3}\pi(\frac{1}{2}diameter)^3$$

As volume of adipocyte was linearly correlated with adipocyte diameter, association of anthropometric and metabolic parameters with adipocyte size was examined using adipocyte diameter but not volume. The total adipocyte volume

---

[4] The longest distance between any two points along the selection boundary, also known as maximum calliper. Adipocytes are considered to be circular in KRH buffer, therefore, Feret's diameter was regarded as diameter in this thesis.

is the cumulative sum of the volumes of all adipocytes within each diameter category.

3.2.6 RT-qPCR

ASAT was collected following the protocol aforementioned (3.2.4). Around 100mg adipocytes were isolated, and RNA was extracted from the adipocytes. After RNA purification using DNase treatment, single stranded complimentary DNA (cDNA) used for qPCR was reverse transcribed from purified RNA. The cDNA was pre-amplified and then diluted 1:5 in TE pH 8.0 buffer and used for RT-qPCR.

Pre-amplified cDNA for specific target genes was quantitated using Taqman® real time PCR on a StepOnePlus Real-Time PCR system. The target Taqman® Gene Expression Assays were purchased from ThermoFisher Scientific as listed in Table 3-2. Briefly, a RT-PCR reaction mix was made up for each target gene: 1.25 µL target Taqman® Gene Expression Assay, 12.5 µL TaqMan universal PCR master mix (Thermo Fisher Scientific, 4304437), and 5 µL nuclease-free water. Diluted pre-amplified cDNA, 6.25 µL, was mixed with each PCR reaction mix in duplicate in a MicroAmp fast optical 96-well reaction plate (ThermoFisher Scientific), and underwent PCR according to the following programme: 50°C for 2 min, 95°C for 10 min, then 40 x of 95°C for 15 secs and 60°C for 1 min.

Gene symbol	Assay ID	Reporter
ADIPOQ	Hs00605917_m1	FAM-NFQ
CDKN1B	Hs00153277_m1	FAM-NFQ
INSR	Hs00961554_m1	FAM-NFQ
LEP	Hs00174877_m1	FAM-NFQ
LPL	Hs00173425_m1	FAM-NFQ
PPARG	Hs01115513_m1	FAM-NFQ
PPIA	Hs99999904_m1	FAM-NFQ
SREBF1	Hs01088691_m1	FAM-NFQ
TNF	Hs00174128_m1	FAM-NFQ

Table 3-2 TaqMan® Gene Expression Assays used for RT-qPCR.

Reference genes and genes of interest. Hs – Homo sapiens; '_m' indicates an essay whose probe spans an exon junction and will not detect genomic DNA.

3.2.7 Statistics

Statistics were performed using Minitab version 19 (Minitab Ltd) and figures were drawn using GraphPad Prism Vs 9.1.1 Normal distribution for all the parameters

was tested using the Ryan-Joiner test. Non-normally distributed data were log or square root transformed to achieve normal distribution as required. Results were displayed as mean ± standard deviation (SD) for parametric data.

Two group comparisons of cross-sectional parameters were made using two-sample t-test for normally distributed data. ANOVA one-way analysis was adopted for the comparison across the five groups, followed by *post hoc* analysis using Tukey's test.

Chi-squared test was adopted to determine the difference between the expected frequencies and the observed frequencies of four (size of adipocyte) vs five (groups) categories of the contingency table. Group differences of each subgroup of adipocytes was examined using ANOVA one-way analysis, followed by *post hoc* analysis using Tukey's test.

Uni-variate analysis used Pearson's correlations and results were shown as coefficient value (r) and *p* value. Multi-variate analysis was performed using a general linear model (GLM), the strength of the confounders to predict the respondence gene was shown as R^2 of coefficient. Significance level was $p < 0.05$.

3.3 Results

3.3.1 Metabolic and anthropometric parameters, associated with adipocyte function, in the study group cohorts

Metabolic and anthropometric parameters by group are shown in Figure 3-1, Figure 3-2 and Figure 3-3. HOMA-IR, age, RMR and VO_2 max values were spread across the equally range. However, BMI, waist, fasting glucose and fasting TG were clustered lower in OETEU, YHSA, YHEU and OHEU, andhigher in OIGREU.

There were significant differences across the five study groups in HOMA-IR, age, BMI, waist, RMR, VO_2 max, fasting plasma glucose and fasting plasma TG (Table 3-3). The OETEU and YHSA groups had similar mean HOMA-IR, BMI and fasting glucose to YHEU and OHEU, whereas OIGREU had significantly higher levels of these parameters than the other groups. YHEU had the lowest fasting TG, while OIGREU had the highest.

YHSA and YHEU were the youngest among the five groups, while OIGREU was the oldest. YHSA and YHEU had the smallest waist circumference, whereas OIGREU had the largest waist circumference among the five groups.

RMR was lower in OETEU, YHSA and YHEU than in OIGREU, and OHEU were not different from either group. However, OETEU and YHEU had the highest VO_2 max, YHSA was intermediate, whilst OHEU and OIGREU had the lowest VO_2 max.

108
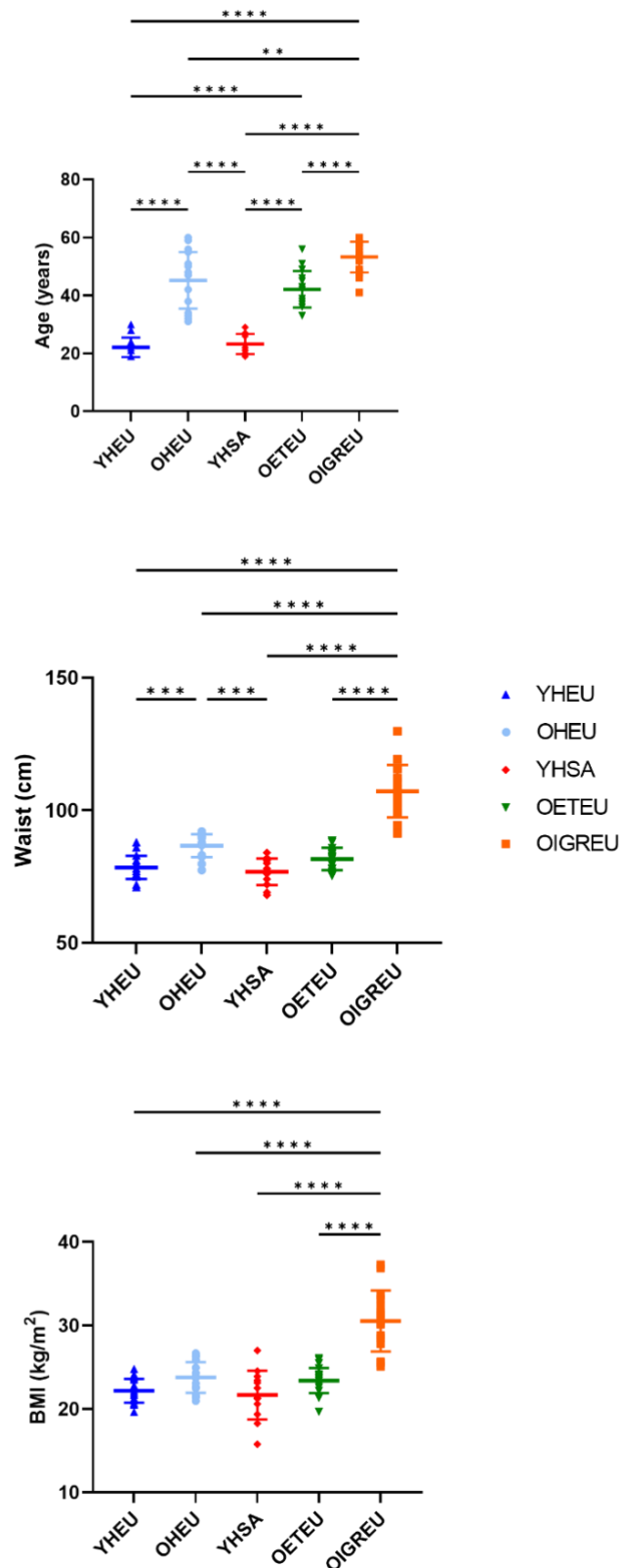
Figure 3-1 Scatter plot of anthropometric parameters.

Participants: Young Healthy European (YHEU), older Healthy European (OHEU), Young Healthy South Asian (YHSA), Older Endurance trained European athletes (OETEU), and Older Europeans with impaired glucose regulation (OIGREU) (n = 18, 18, 13, 20 and 17, respectively). Differences across groups were analysed using one-way ANOVA. Results of *post hoc* analysis using Tukey's test is shown with line and asterisk. **, $p < 0.01$; ***, $p < 0.001$; ****, $p < 0.0001$.

Figure 3-2 Scatter plot of blood metabolic parameters.

Participants: Young Healthy European (YHEU), older Healthy European (OHEU), Young Healthy South Asian (YHSA), Older Endurance trained European athletes (OETEU), and Older Europeans with impaired glucose regulation (OIGREU) (n = 18, 18, 13, 20 and 17, respectively). HOMA-IR, homeostatic model assessment of insulin resistance. Glucose, plasma glucose. TG, plasma triglyceride. Differences across groups were analysed using one-way ANOVA. Results of *post hoc* analysis using Tukey's test is shown with line and asterisk. *, $p < 0.05$; **, $p < 0.01$; ***, $p < 0.001$; ****, $p < 0.0001$. Statistical analysis for fasting insulin was applied using Kruskal Wallis test, and *post hoc* analysis was examined using Dunn's test.

Figure 3-3 Scatter plot of fitness measures.

Participants: Young Healthy European (YHEU), older Healthy European (OHEU), Young Healthy South Asian (YHSA), Older Endurance trained European athletes (OETEU), and Older Europeans with impaired glucose regulation (OIGREU) (n = 18, 18, 13, 20 and 17, respectively). RMR, resting metabolic rate. Differences across groups were analysed using one-way ANOVA. Results of *post hoc* analysis using Tukey's test is shown with line and asterisk. *, $p < 0.05$; **, $p < 0.01$; ***, $p < 0.001$; ****, $p < 0.0001$.

	YHEU (n = 18)	OHEU (n = 18)	YHSA (n = 13)	OETEU (n = 20)	OIGREU (n = 17)	YHEU vs OHEU	YHEU vs YHSA	OHEU vs OETEU	OHEU vs OIGREU
Age (years)	22 ± 3	45 ± 10	23 ± 3	42 ± 6	53 ± 5	< 0.0001	0.37	0.24	0.0063
BMI (kg/m^2)	22.2 ± 1.4	23.8 ± 1.9	21.7 ± 2.9	23.4 ± 1.5	30.5 ± 3.7	0.0069	0.52	0.52	< 0.0001
Waist (cm)	78.4 ± 4.4	86.6 ± 4.3	76.8 ± 5.0	81.6 ± 4.2	107.2 ± 9.9	< 0.0001	0.33	0.0009	< 0.0001
HOMA-IR$^\$$	1.4 ± 1.1	1.4 ± 0.4	1.3 ± 0.8	1.0 ± 0.5	5.8 ± 6.2	0.95	0.81	0.067	0.0063
Fasting glucose (mmol/L)	5.0 ± 0.8	5.2 ± 0.5	4.7 ± 0.4	5.0 ± 0.4	8.1 ± 1.7	0.33	0.24	0.10	< 0.0001
Fasting Insulin (µU/mL) $^{\$\$}$	5.1 [3.3, 6.0]	5.7 [4.5, 6.6]	4.1 [3.4, 9.3]	4.1 [3.3, 5.0]	10.7 [9.1, 14.1]	0.80	0.88	0.21	0.011
Fasting TG (mmol/L)	0.8 ± 0.3	1.7 ± 0.8	1.1 ± 0.6	1.1 ± 0.5	2.4 ± 1.7	< 0.0001	0.087	0.0094	0.12
RMR (kcal/kg/day)	22.0 ± 2.2	20.6 ± 1.9	22.3 ± 3.3	22.5 ± 1.7	19.7 ± 2.3	0.052	0.74	0.002	0.22
VO$_2$ max (ml/kg/min)	51.7 ± 6.1	35.8 ± 5.7	44.0 ± 3.1	54.7 ± 5.2	31.2 ± 5.9	< 0.0001	0.0003	< 0.0001	0.033

Table 3-3 Anthropometric characteristics of all participants.

Participants: Young Healthy European (YHEU), Older Healthy European (OHEU), Young Healthy South Asian (YHSA), Older Endurance trained European athletes (OETEU), and Older Europeans with impaired glucose regulation (OIGREU). Results are shown as mean ± SD for parametric data, and median [95% confidence interval] for non-parametric data. Differences between two groups were analysed using t-test. $, statistical analysis was adopted using log transformed data. $$, statistical analysis was applied using Mann-Whitney U test. HOMA-IR, homeostatic model assessment of insulin resistance. Glucose, plasma glucose. TG, plasma triglyceride. RMR, resting metabolic rate.

3.3.2 Adipocyte size in the study groups

3.3.2.1 Differences in adipocyte size distribution between groups of different age, ethnicity, fitness and glucose response

Adipocyte size distribution is shown in Figure 3-4 to Figure 3-7. YHEU adipocytes showed one peak of size 65 μm in the medium adipocyte range. OETEU, YHSA and OHEU showed a single peak of 85 μm across the medium and large adipocyte ranges. OIGREU had two peaks of 35 μm and 105 μm in the small and large adipocyte ranges, respectively.

Adipocyte diameter was different across the five groups ($p < 0.0001$, Table 3-4). Adipocyte diameter was smallest in YHEU and largest in OIGREU. Adipocyte diameter was similar in OETEU, YHSA and OHEU. There was also no significant difference in adipocyte diameter between OHEU and OIGREU (Figure 3-6, Figure 3-7).

The observed distribution was different from the expected distribution between the four adipocyte size subgroups and five participants groups ($p < 0.0001$, Table 3-4). OETEU ($3.4 \pm 3.6\%$) had the smallest proportion of small adipocytes (Figure 3-8), while OIGREU ($11.5 \pm 13.9\%$) had the largest proportion, and OHEU, YHSA and YHEU were intermediate ($p = 0.015$). OIGREU ($27.5 \pm 13.2\%$) had a smaller proportion of medium adipocytes than YHSA and OHEU (54.6 ± 20.4 and $54.4 \pm 15.0\%$), and YHEU ($72.9 \pm 10.2\%$) had more medium adipocytes than YHSA and OHEU. OETEU ($65.4 \pm 19.0\%$) was intermediate between YHSA and YHEU ($p < 0.0001$) (Figure 3-9). OIGREU ($58.7 \pm 14.8\%$) had a larger proportion of large adipocytes than YHSA and OHEU (37.3 ± 20.1 and $41.2 \pm 15.5\%$), and YHEU ($16.9 \pm 10.7\%$) had fewer large adipocytes than YHSA and OHEU, whereas OETEU ($31.1 \pm 20.1\%$) was intermediate between YHSA and YHEU ($p < 0.0001$) (Figure 3-10). There was an overall difference in very large adipocytes across the five groups ($p < 0.015$), but no significance was found in *post hoc* analysis (Figure 3-11, Table 3-4).
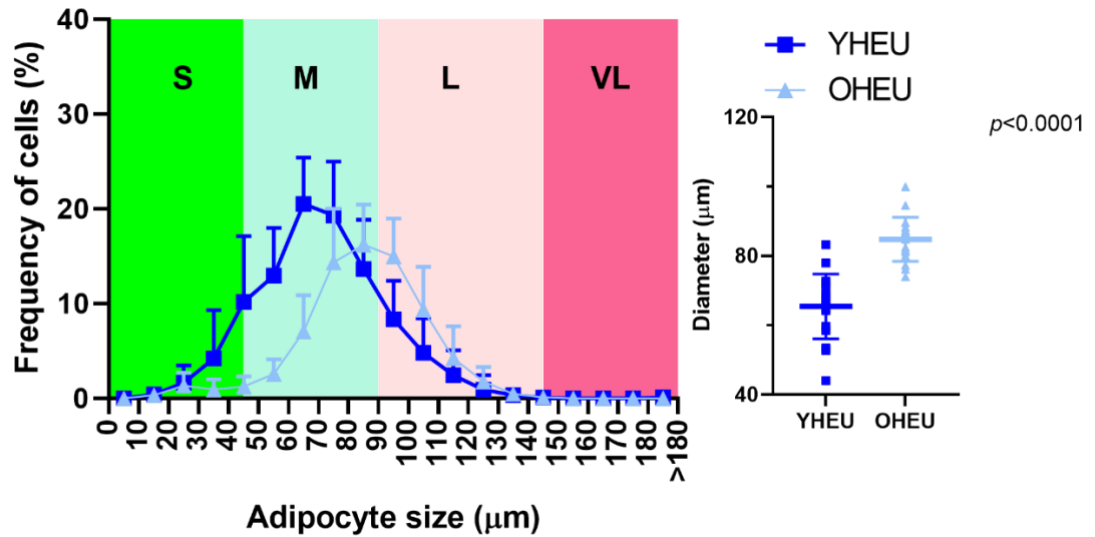
Figure 3-4 Adipocyte size distribution and adipocyte diameter between YHEU and OHEU.

Young Healthy European (YHEU) and Older Healthy European (OHEU) (n = 18 and 18). Results are shown as mean and standard deviation. Differences between two groups was by t test.
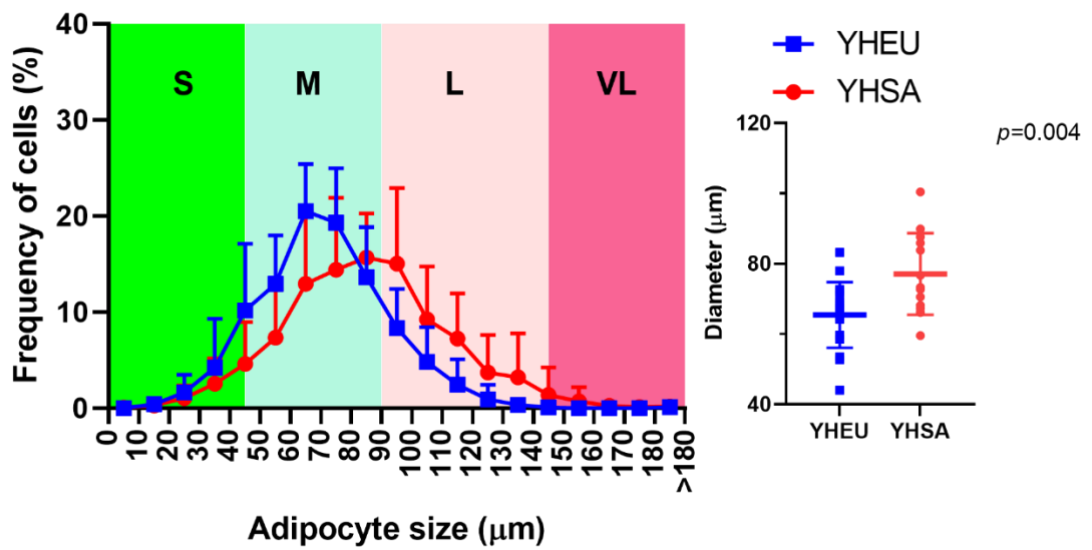
Figure 3-5 Adipocyte size distribution and adipocyte diameter between YHEU and YHSA.

Young Healthy European (YHEU) and Young Healthy South Asian (YHSA) (n = 18 and 13). Results are shown as mean and standard deviation. Differences between two groups was by t test.
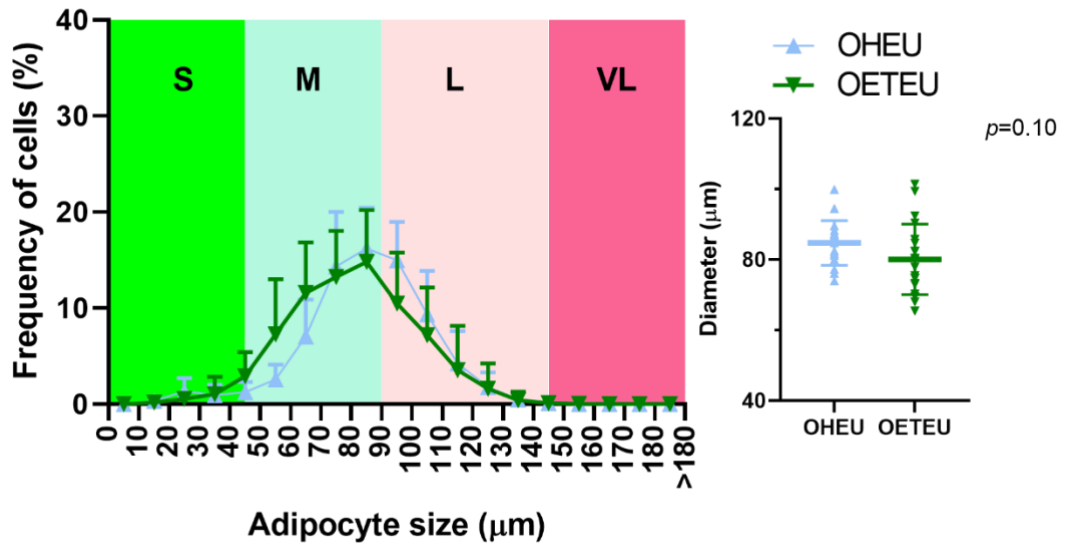
Figure 3-6 Adipocyte size distribution and adipocyte diameter between OHEU and OETEU.

Older Healthy European (OHEU) and Older Endurance trained European athletes (OETEU) (n = 18 and 20) with different fitness. Results are shown as mean and standard deviation. Differences between the two groups was by t test.
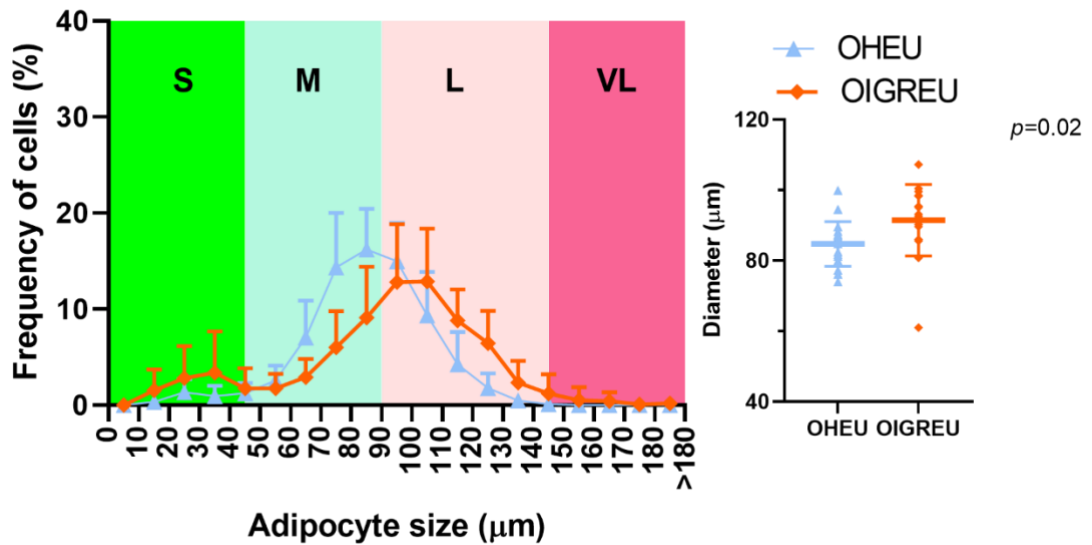
Figure 3-7 Adipocyte size distribution and adipocyte diameter between OHEU and OIRGEU.

Older Healthy European (OHEU) and Older Europeans with impaired glucose regulation (OIGREU) (n = 18 and 17) with different glycaemic status. Results are shown as mean and standard deviation. Differences between two groups was by t test.

	YHEU (n = 18) Percentage (n)	OHEU (n = 18) Percentage (n)	YHSA (n = 13) Percentage (n)	OETEU (n = 20) Percentage (n)	OIGREU (n = 17) Percentage (n)	ANOVA One-way	p value of chi square
Small adipocyte	10.0 ± 10^{AB} (181 ± 180)	4.4 ± 3.6^{AB} (79 ± 65)	6.2 ± 4.9^{AB} (80 ± 63)	3.4 ± 3.6^{A} (68 ± 72)	11.5 ± 13.9^{B} (196 ± 237)	0.015	
Medium adipocyte	72.9 ± 10.2^{A} $(1{,}312 \pm 184)$	54.4 ± 15.0^{B} (979 ± 268)	54.6 ± 20.4^{B} (710 ± 265)	65.4 ± 19.0^{AB} $(1{,}308 \pm 380.0)$	27.5 ± 13.2^{C} (468 ± 225)	< 0.0001	
Large adipocyte	16.9 ± 10.7^{A} (304 ± 193)	41.2 ± 15.5^{B} (741 ± 279)	37.3 ± 20.1^{B} (485 ± 261)	31.1 ± 20.1^{AB} (622 ± 40.2)	58.7 ± 14.8^{C} (997 ± 251)	< 0.0001	< 0.0001
Very large adipocyte	0.25 ± 0.58^{A} (5 ± 10)	0.04 ± 0.16^{A} (1 ± 3)	1.9 ± 3.6^{A} (25 ± 47)	0.1 ± 0.3^{A} (2 ± 6.5)	2.3 ± 4.5^{A} (39 ± 77)	0.015	

Table 3-4 Percentage of adipocytes categorized by size.

Participants: Young Healthy European (YHEU), Older Healthy European (OHEU), Young Healthy South Asian (YHSA), Older Endurance trained European athletes (OETEU), and Older Europeans with impaired glucose regulation (OIGREU). Results are shown as percentage (n). Differences in size distribution across 5 groups vs 4 categories were analysed using chi-squared analysis. Differences in each adipocyte size group across cohorts were analysed using one-way ANOVA. *Post hoc* analysis was examined using Tukey's test and means that do not share a letter (A, B or C) are significantly different.
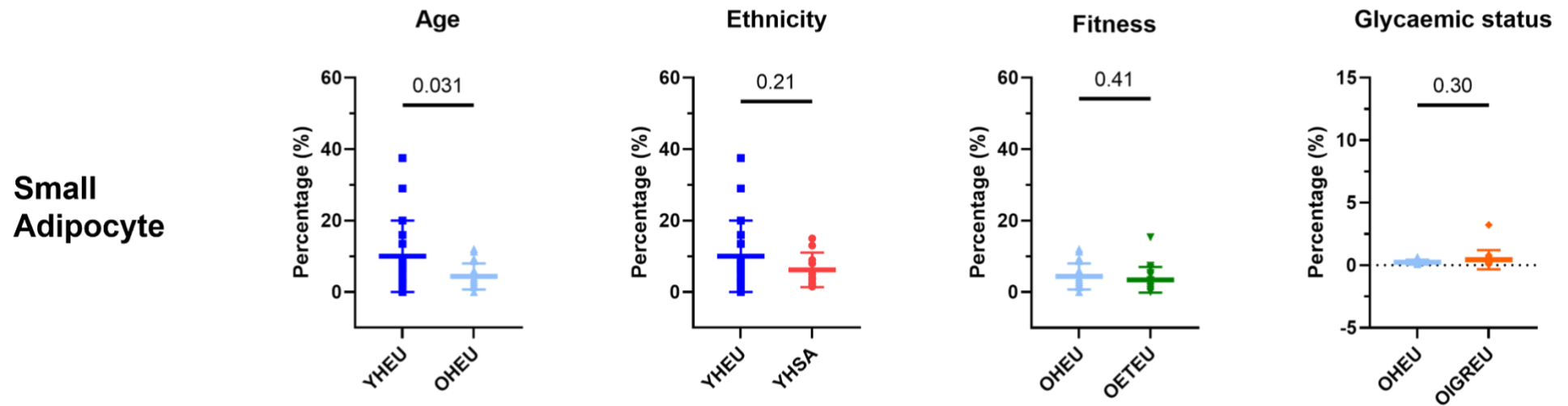
Figure 3-8 Percentage of small adipocytes across groups.

Participants: Young Healthy European (YHEU), older Healthy European (OHEU), Young Healthy South Asian (YHSA), Older Endurance trained European athletes (OETEU), and Older Europeans with impaired glucose regulation (OIGREU) (n = 18, 18, 13, 20 and 17, respectively) in groups with different age (YHEU vs OHEU), ethnicity (YHEU vs YHSA), fitness (OHEU vs OETEU), and glycaemic status (OHEU vs OIGREU). Results are shown as mean and standard deviation. Differences between two groups was by t test.
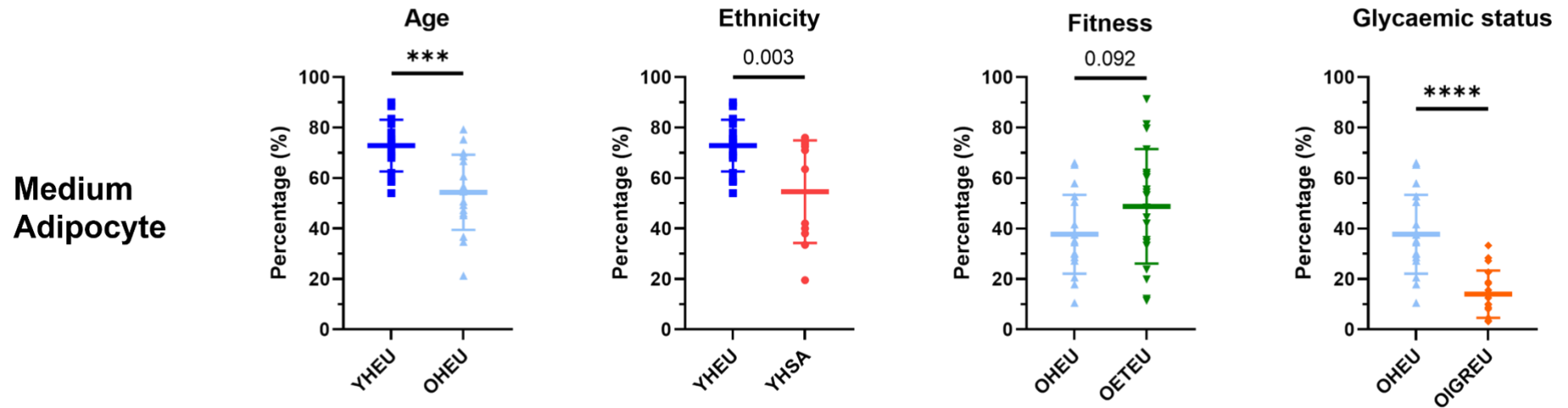
Figure 3-9 Percentage of medium adipocytes across groups.

Participants: Young Healthy European (YHEU), older Healthy European (OHEU), Young Healthy South Asian (YHSA), Older Endurance trained European athletes (OETEU), and Older Europeans with impaired glucose regulation (OIGREU) (n = 18, 18, 13, 20 and 17, respectively) in groups with different age (YHEU vs OHEU), ethnicity (YHEU vs YHSA), fitness (OHEU vs OETEU), and glycaemic status (OHEU vs OIGREU). Results are shown as mean and standard deviation. Differences between two groups was by t test. ***, $p < 0.001$; ****, $p < 0.0001$.
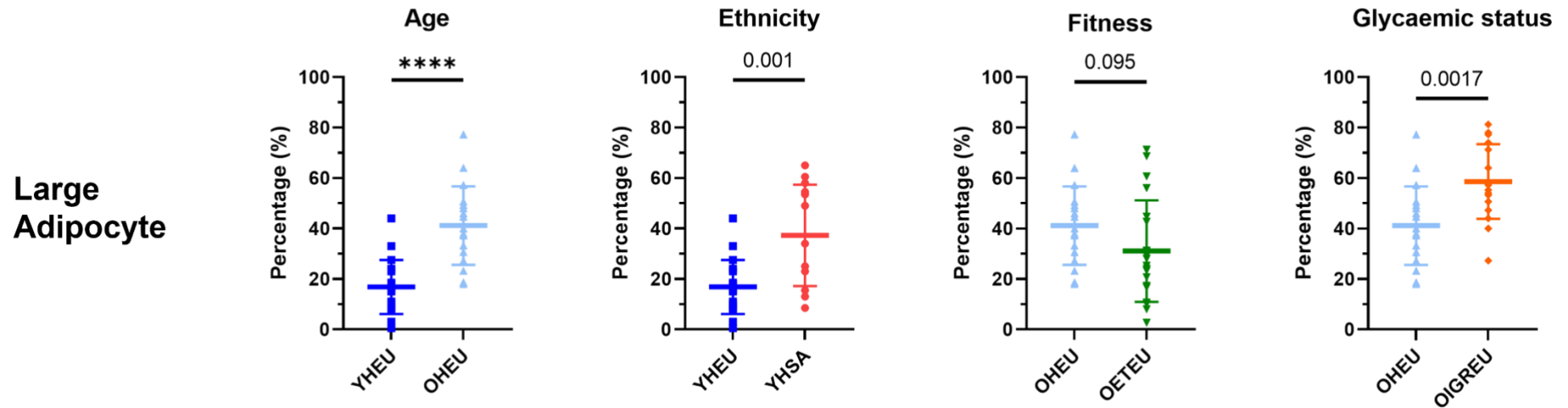
Figure 3-10 Percentage of large adipocytes across groups.

Participants: Young Healthy European (YHEU), older Healthy European (OHEU), Young Healthy South Asian (YHSA), Older Endurance trained European athletes (OETEU), and Older Europeans with impaired glucose regulation (OIGREU) (n = 18, 18, 13, 20 and 17, respectively) in groups with different age (YHEU vs OHEU), ethnicity (YHEU vs YHSA), fitness (OHEU vs OETEU), and glycaemic status (OHEU vs OIGREU). Results are shown as mean and standard deviation. Differences between two groups was by t test. ****, $p < 0.0001$.
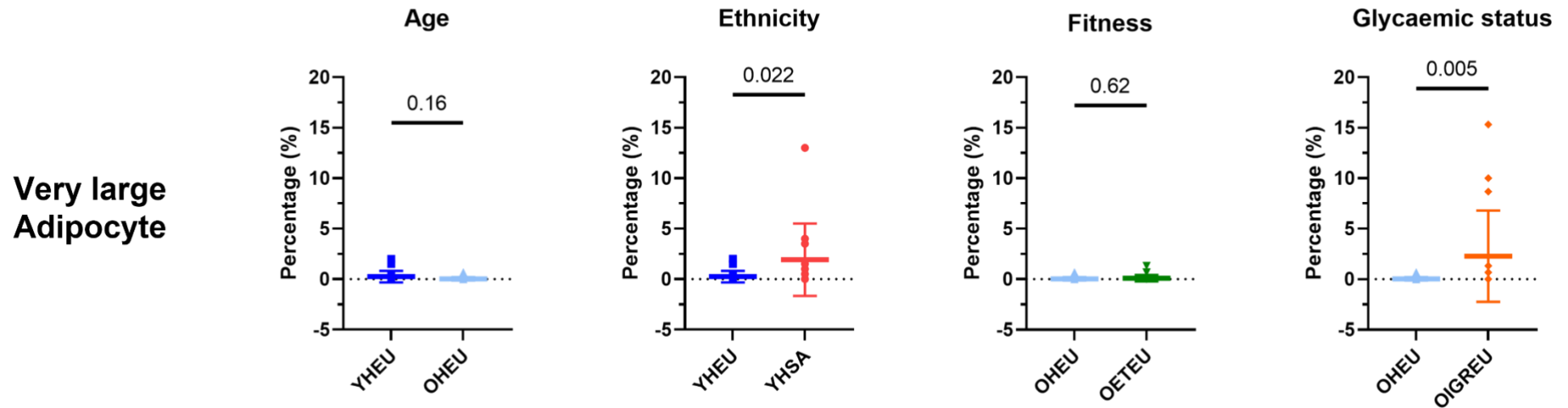
Figure 3-11 Percentage of very large adipocytes across groups.

Participants: Young Healthy European (YHEU), older Healthy European (OHEU), Young Healthy South Asian (YHSA), Older Endurance trained European athletes (OETEU), and Older Europeans with impaired glucose regulation (OIGREU) (n = 18, 18, 13, 20 and 17, respectively) in groups with different age (YHEU vs OHEU), ethnicity (YHEU vs YHSA), fitness (OHEU vs OETEU), and glycaemic status (OHEU vs OIGREU). Results are shown as mean and standard deviation. Differences between two groups was applied using Mann-Whitney test.

3.3.2.2 Adipocyte volume distribution in study cohorts

To demonstrate the quantity of fat stored in adipocytes of varying sizes, both the total adipocyte volume and diameter were evaluated. Total adipocyte volume distribution and percentage of total adipocyte volume distribution is shown in Figure 3-12, Figure 3-13, Figure 3-14 and Figure 3-15. The distribution was similar for total volume and percentage volume. All groups showed a single peak. OETEU and YHEU showed a single peak at 85 µm to the right of the medium adipocyte range, YHSA and OHEU showed peaks at 95 µm to the left of large adipocyte range, and OIGREU showed a single peak at 105 µm in the centre of the large adipocyte range.

The observed distribution was different from the expected distribution between the four adipocyte size range subgroups and five participant groups ($p < 0.0001$, Table 3-5). OETEU and OHEU (0.3 ± 0.5 and $0.2 \pm 0.2\%$) had the smallest volume of small adipocytes, while YHEU ($1.1 \pm 2.8\%$) had the largest volume of small adipocytes, and YHSA and OIGREU were intermediate ($p = 0.001$) (Figure 3-16). OIGREU ($12.3 \pm 9.4\%$) had a smaller volume of medium adipocytes than OHEU ($34.9 \pm 15.6\%$), and OETEU and YHEU (41.7 ± 22.7 and $53.7 \pm 18.1\%$) had a larger volume of medium adipocytes than OHEU, while YHSA ($26.8 \pm 19.5\%$) was intermediate between OETEU and OHEU ($p < 0.0001$) (Figure 3-17). OIGREU ($77.4 \pm 12.2\%$) had a larger volume of large adipocytes than OHEU ($64.7 \pm 15.6\%$), and OETEU and YHEU (57.4 ± 22.3 and $40.8 \pm 17.0\%$) had a smaller volume of larger adipocytes than OHEU, whereas YHSA ($62.0 \pm 20.3\%$) was intermediate between OETEU and OHEU ($p < 0.0001$) (Figure 3-18). OETEU and OHEU (0.6 ± 1.0 and $0.2 \pm 0.6\%$) had a smaller volume of very large adipocytes than YHSA and OIGREU (10.9 ± 11.8 and $9.9 \pm 13.9\%$), and YHEU ($4.4 \pm 7.0\%$) was intermediate ($p < 0.005$) (Figure 3-19).
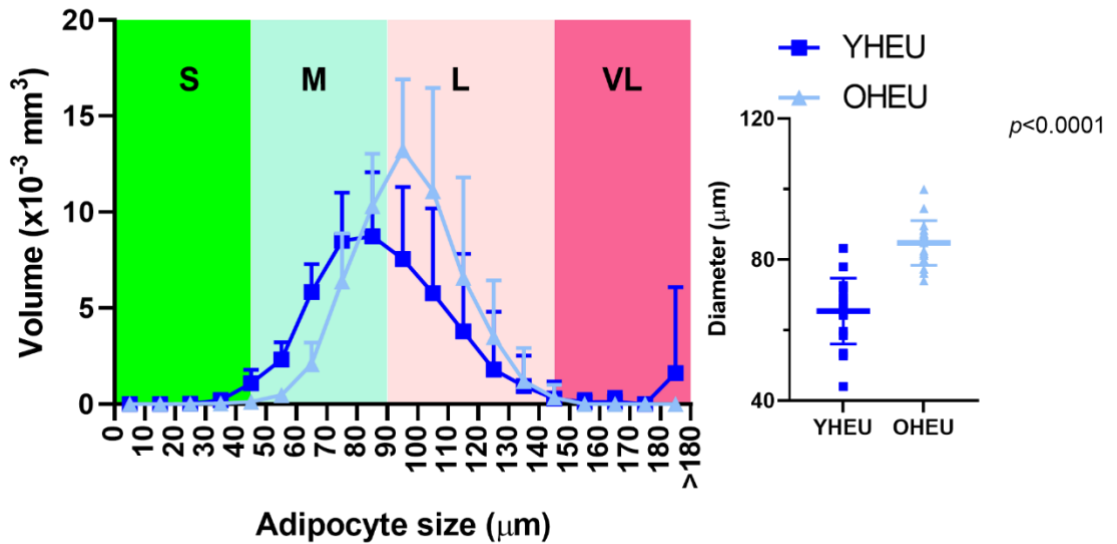
Figure 3-12 Adipocyte volume distribution by adipocyte diameter in YHEU and OHEU.

Young Healthy European (YHEU) and Older Healthy European (OHEU) (n = 18 and 18). Results are shown as mean and standard deviation. Differences between two groups was by t test. The total adipocyte volume is the cumulative sum of the volumes of all adipocytes within each size interval of 10 μm.
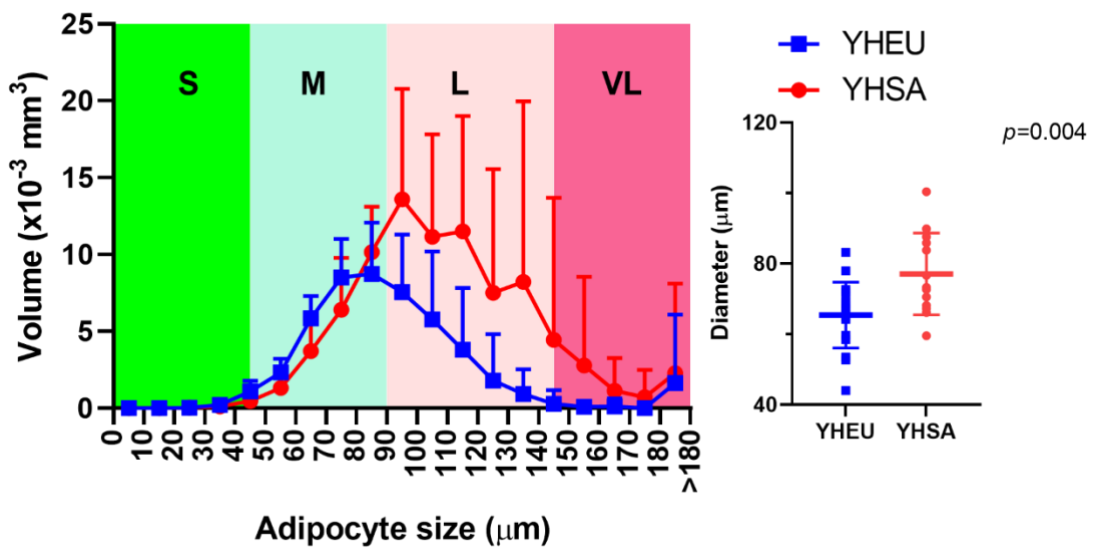
Figure 3-13 Adipocyte volume distribution by adipocyte diameter in YHEU and YHSA.

Young Healthy European (YHEU) and Young Healthy South Asian (YHSA) (n = 18 and 13). Results are shown as mean and standard deviation. Differences between two groups was by t test. The total adipocyte volume is the cumulative sum of the volumes of all adipocytes within each size interval of 10 μm.
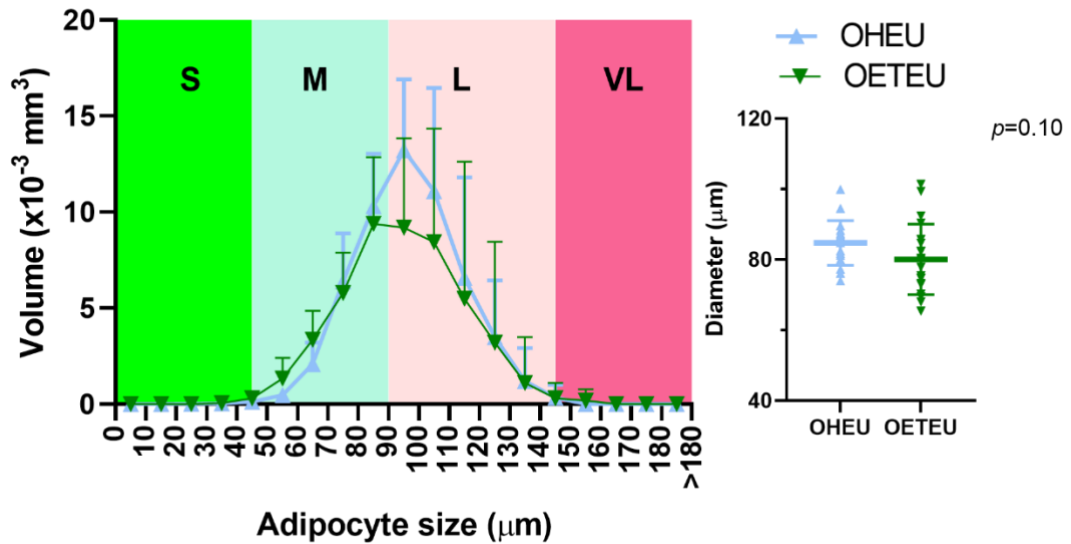
Figure 3-14 Adipocyte volume distribution by adipocyte diameter in OHEU and OETEU.

Older Healthy European (OHEU) and Older Endurance trained European athletes (OETEU) (n = 18 and 20) with different fitness. Results are shown as mean and standard deviation. Differences between two groups was by t test. The total adipocyte volume is the cumulative sum of the volumes of all adipocytes within each size interval of 10 μm.
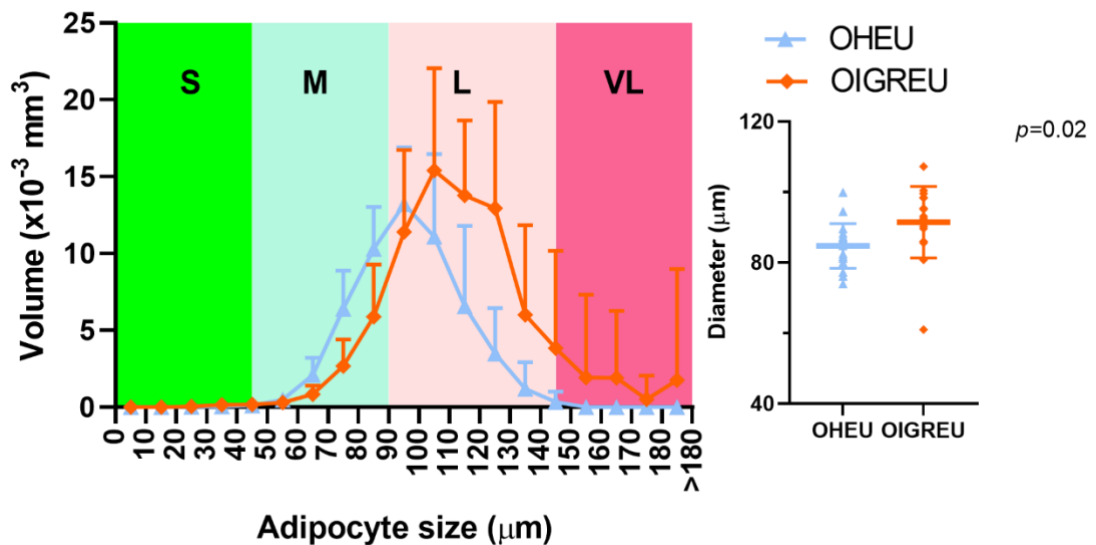
Figure 3-15 Adipocyte volume distribution by adipocyte diameter in OHEU and OIGREU.

Older Healthy European (OHEU) and Older Europeans with impaired glucose regulation (OIGREU) (n = 18 and 17) with different glycaemic status. Results are shown as mean and standard deviation. Differences between two groups was by t test. The total adipocyte volume is the cumulative sum of the volumes of all adipocytes within each size interval of 10 μm.

	YHEU (n = 18) Percentage (n)	OHEU (n = 18) Percentage (n)	YHSA (n = 13) Percentage (n)	OETEU (n = 20) Percentage (n)	OIGREU (n = 17) Percentage (n)	ANOVA One-way	*p* value of chi-square
Small adipocyte	1.1 ± 2.8^B (0.6 ± 0.6)	0.2 ± 0.2^A (0.1 ± 0.09)	0.4 ± 0.7^{AB} (0.3 ± 0.3)	0.3 ± 0.5^A (0.1 ± 0.2)	0.4 ± 0.8^{AB} (0.3 ± 0.4)	0.001	
Medium adipocyte	53.7 ± 18.1^B (26.2 ± 5.2)	34.9 ± 15.6^A (19.3 ± 4.8)	26.8 ± 19.5^{AB} (22.3 ± 7.0)	41.7 ± 22.7^A (20.1 ± 5.2)	12.3 ± 9.4^C (9.8 ± 5.2)	< 0.0001	< 0.0001
Large adipocyte	40.8 ± 17.0^B (19.9 ± 14.3)	64.7 ± 15.6^A (35.8 ± 15.9)	62.0 ± 20.3^{AB} (51.5 ± 33.2)	57.4 ± 22.3^A (27.7 ± 21.4)	77.4 ± 12.2^C (61.6 ± 16.3)	< 0.0001	
Very large adipocyte	4.4 ± 7.0^{AB} (2.1 ± 4.8)	0.2 ± 0.6^A (0.1 ± 0.4)	10.9 ± 11.8^B (9.0 ± 15.0)	0.6 ± 1.0^A (0.3 ± 0.9)	9.9 ± 13.9^B (7.9 ± 16.4)	0.005	

Table 3-5 Percentage of total adipocyte volume by adipocyte size across groups.
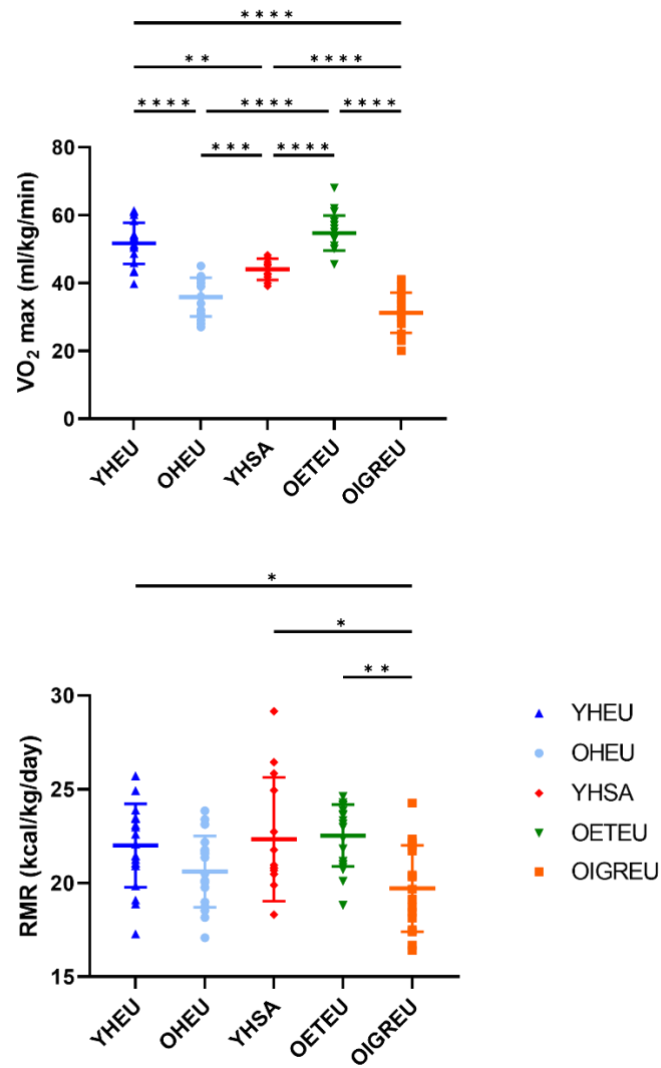
Participants: Young Healthy European (YHEU), older Healthy European (OHEU), Young Healthy South Asian (YHSA), Older Endurance trained European athletes (OETEU), and Older Europeans with impaired glucose regulation (OIGREU) (n = 18, 18, 13, 20 and 17, respectively). Results are shown as percentage (n). Differences in size distribution across 5 groups vs 4 categories were analysed using chi-squared analysis. Differences in each adipocyte size group across cohorts were analysed using one-way ANOVA. *Post hoc* analysis was examined using Tukey's test and means that do not share a letter (A, B or C) are significantly different. The total adipocyte volume is the cumulative sum of the volumes of all adipocytes within each size category.
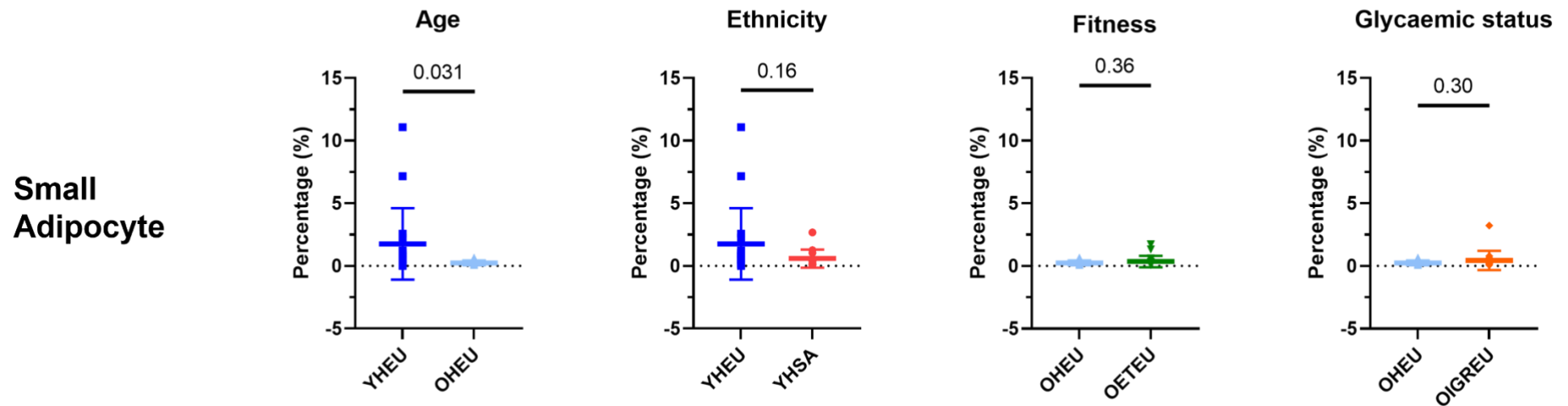
Figure 3-16 Percentage of total adipocyte volume taken by small adipocytes.

Young Healthy European (YHEU), older Healthy European (OHEU), Young Healthy South Asian (YHSA), Older Endurance trained European athletes (OETEU), and Older Europeans with impaired glucose regulation (OIGREU) (n = 18, 18, 13, 20 and 17, respectively) in groups with different age (YHEU vs OHEU), ethnicity (YHEU vs YHSA), fitness (OHEU vs OETEU), and glycaemic status (OHEU vs OIGREU). Results are shown as mean and standard deviation. Differences between two groups was by t test. The total adipocyte volume is the cumulative sum of the volumes of all adipocytes within each size category.
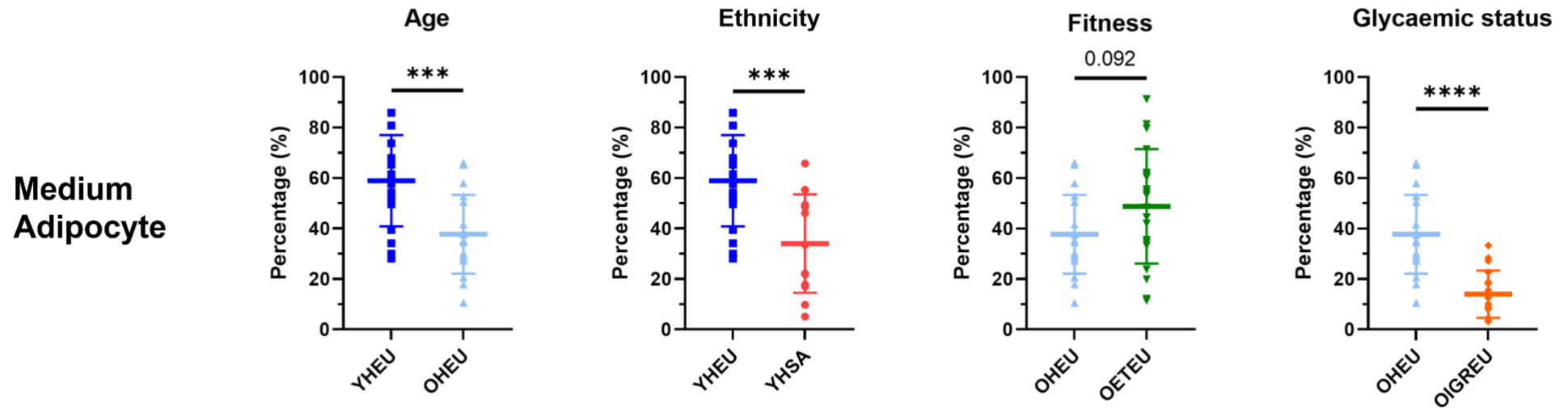
Figure 3-17 Percentage of total adipocyte volume taken by medium adipocytes.

Young Healthy European (YHEU), older Healthy European (OHEU), Young Healthy South Asian (YHSA), Older Endurance trained European athletes (OETEU), and Older Europeans with impaired glucose regulation (OIGREU) (n = 18, 18, 13, 20 and 17, respectively) in groups with different age (YHEU vs OHEU), ethnicity (YHEU vs YHSA), fitness (OHEU vs OETEU), and glycaemic status (OHEU vs OIGREU). Results are shown as mean and standard deviation. Differences between two groups was by t test. ***, $p < 0.001$; ****, $p < 0.0001$. The total adipocyte volume is the cumulative sum of the volumes of all adipocytes within each size category.
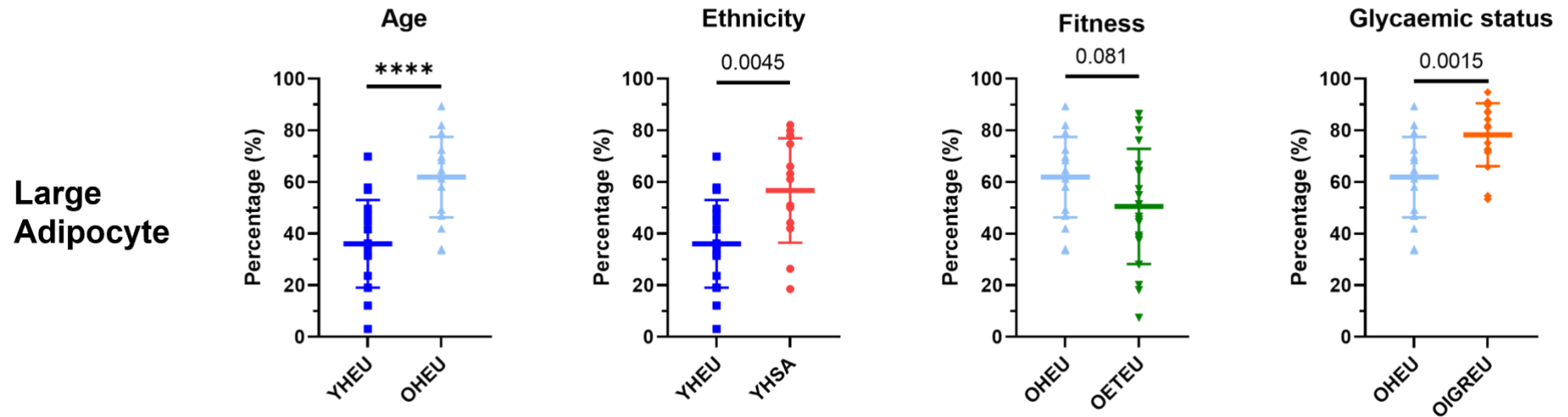
Figure 3-18 Percentage of total adipocyte volume taken by large adipocytes.

Young Healthy European (YHEU), older Healthy European (OHEU), Young Healthy South Asian (YHSA), Older Endurance trained European athletes (OETEU), and Older Europeans with impaired glucose regulation (OIGREU) (n = 18, 18, 13, 20 and 17, respectively) in groups with different age (YHEU vs OHEU), ethnicity (YHEU vs YHSA), fitness (OHEU vs OETEU), and glycaemic status (OHEU vs OIGREU). Results are shown as mean and standard deviation. Differences between two groups was applied by t test. ****, $p < 0.0001$. The total adipocyte volume is the cumulative sum of the volumes of all adipocytes within each size category.
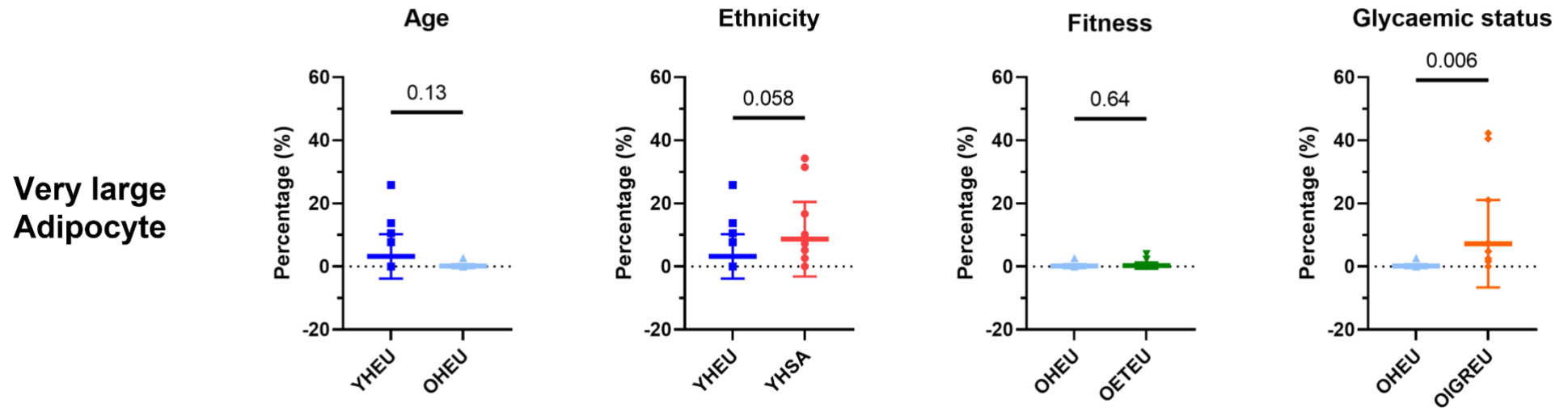
Figure 3-19 Percentage of total adipocyte volume taken by very large adipocytes.

Young Healthy European (YHEU), older Healthy European (OHEU), Young Healthy South Asian (YHSA), Older Endurance trained European athletes (OETEU), and Older Europeans with impaired glucose regulation (OIGREU) (n = 18, 18, 13, 20 and 17, respectively) in groups with different age (YHEU vs OHEU), ethnicity (YHEU vs YHSA), fitness (OHEU vs OETEU), and glycaemic status (OHEU vs OIGREU). Results are shown as mean and standard deviation. Differences between two groups was by Mann-Whitney test. The total adipocyte volume is the cumulative sum of the volumes of all adipocytes within each size category.

3.3.2.3 Association of anthropometric and metabolic parameters with mean adipocyte diameter

The correlations between mean adipocyte diameter and anthropometric and metabolic parameters including HOMA-IR, age, BMI, waist circumference, RMR, VO_2 max, fasting glucose and fasting TG, were analysed univariately (Figure 3-20, Figure 3-21 and Figure 3-22). Strong positive correlations were found between mean adipocyte diameter and HOMA-IR, age, BMI, waist, fasting glucose, fasting insulin and fasting TG (r = 0.50, 0.61, 0.54, 0.62, 0.45, 0.32 and 0.34, all $p \leq$ 0.004), and negative correlations were found between mean adipocyte diameter and VO_2 max and RMR (r = -0.55 and -0.33, $p < 0.001$ and = 0.002, respectively).

The relationship between mean adipocyte diameter and the proportions of small, medium, large, and very large adipocytes is presented in Figure 3-23. Notably, the proportions of small and medium-sized adipocytes were negatively correlated with mean adipocyte diameter (r = -0.41 and -0.75, $p < 0.0001$ and < 0.0001, respectively). Conversely, the proportions of large and very large adipocytes were positively correlated with mean adipocyte diameter (r = 0.90 and 0.34, $p < 0.0001$ and = 0.002, respectively).

Fasting insulin, proportion of S, M and large and group were significantly independently and positively associated with mean adipocyte diameter (Table 3-6).
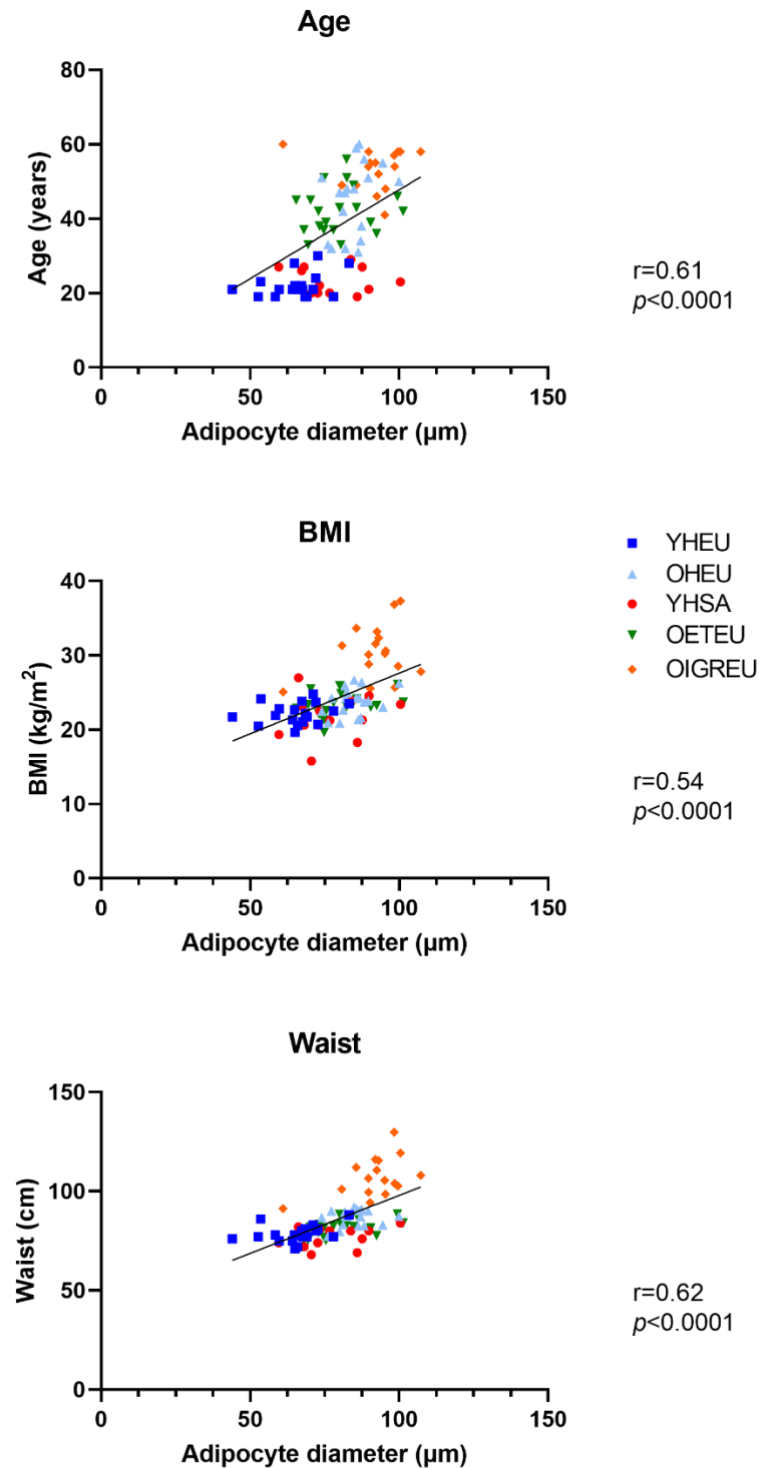
Figure 3-20 Univariate analysis: relationship between mean adipocyte diameter and anthropometric characteristics.

Participants: Young Healthy European (YHEU), older Healthy European (OHEU), Young Healthy South Asian (YHSA), Older Endurance trained European athletes (OETEU), and Older Europeans with impaired glucose regulation (OIGREU), n = 86.
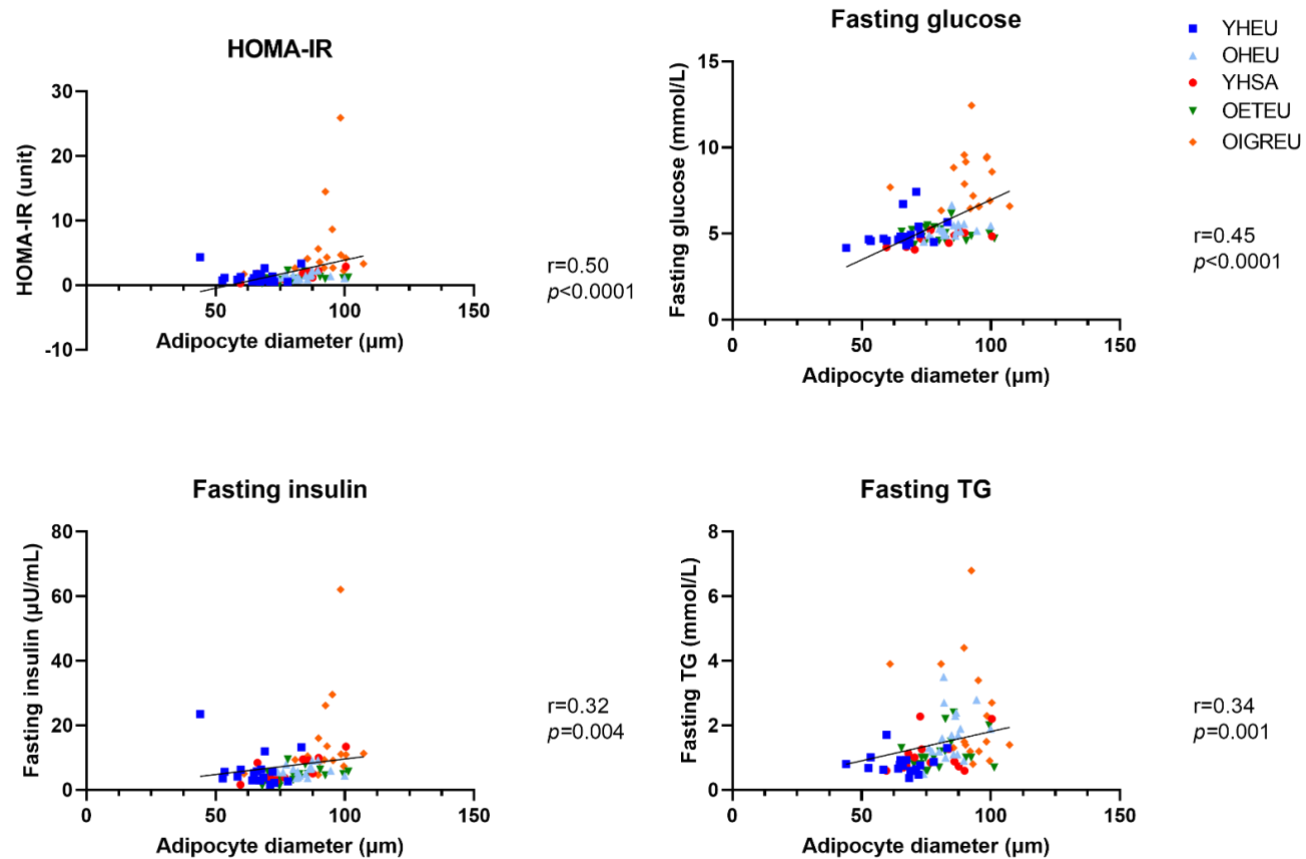
Figure 3-21 Univariate analysis: relationship between mean adipocyte diameter and blood metabolic parameters.

Participants: Young Healthy European (YHEU), older Healthy European (OHEU), Young Healthy South Asian (YHSA), Older Endurance trained European athletes (OETEU), and Older Europeans with impaired glucose regulation (OIGREU), n = 86.
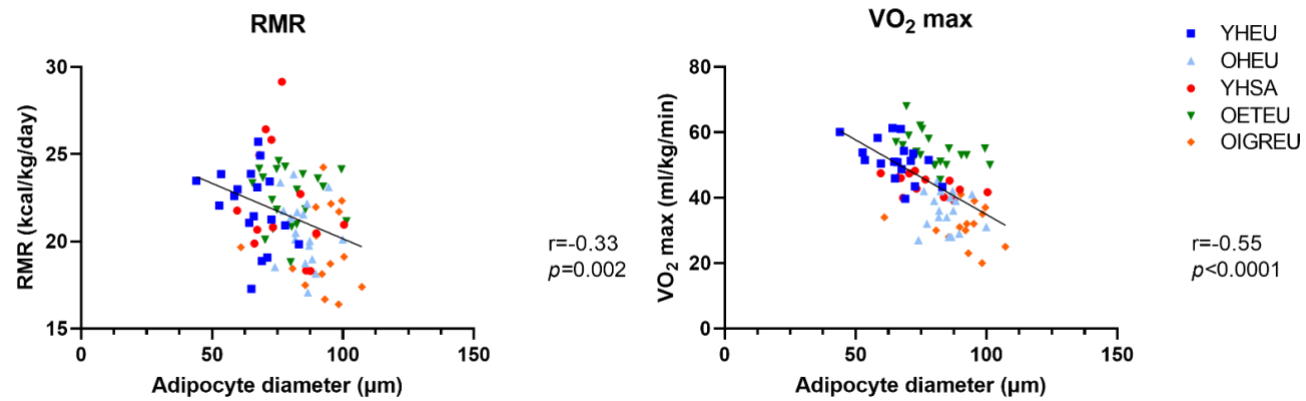
Figure 3-22 Univariate analysis: relationship between mean adipocyte diameter and fitness.

Participants: Young Healthy European (YHEU), older Healthy European (OHEU), Young Healthy South Asian (YHSA), Older Endurance trained European athletes (OETEU), and Older Europeans with impaired glucose regulation (OIGREU), n = 86.
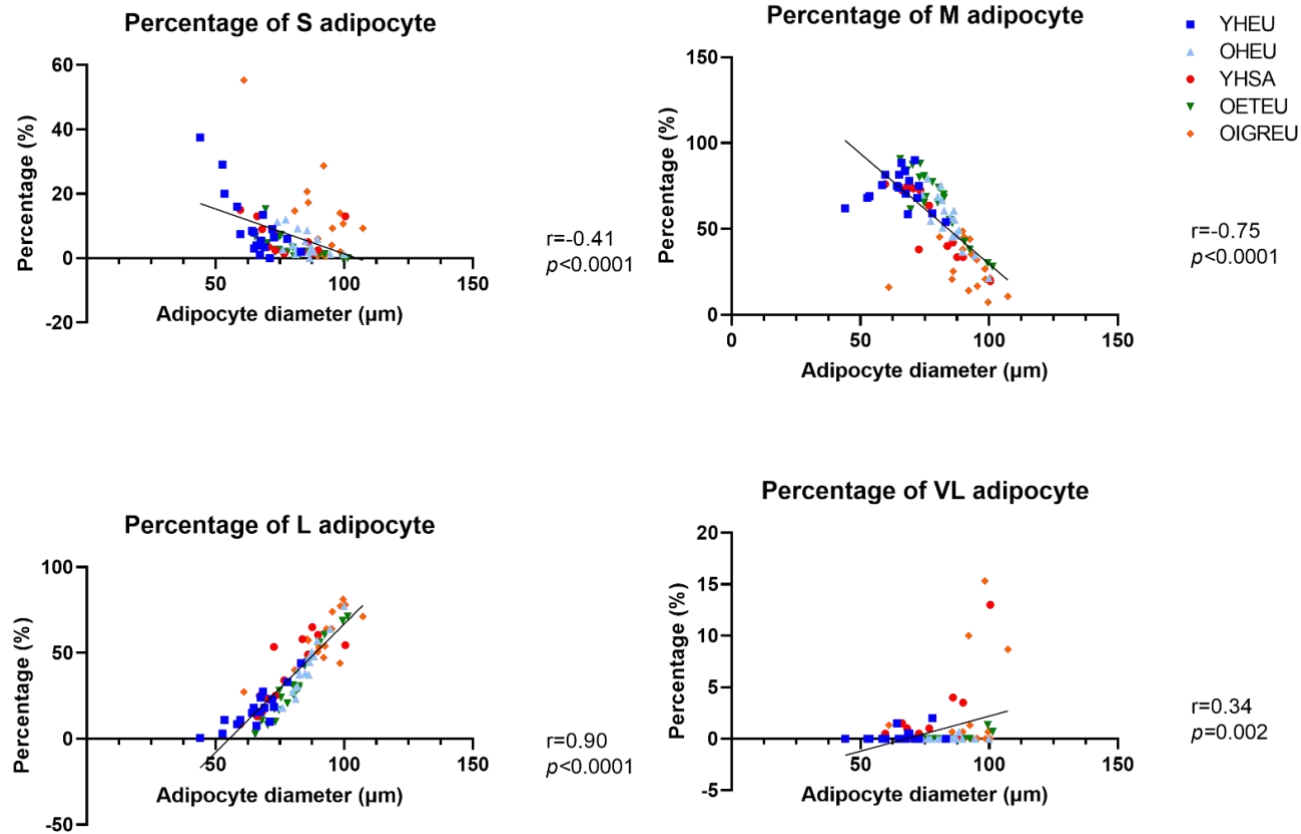
Figure 3-23 Univariate Analysis: Mean adipocyte diameter and proportional size distribution across groups.

Proportion of small (S), medium (M), large (L), and very large (VL) adipocyte in Young Healthy European (YHEU), older Healthy European (OHEU), Young Healthy South Asian (YHSA), Older Endurance trained European athletes (OETEU), and Older Europeans with impaired glucose regulation (OIGREU), n = 86.

Mean adipocyte diameter	B-coefficient	95% CI	*p*	R^2	R^2 of model
Fasting insulin	-0.12	(-0.20, -0.029)	0.010	10.0%	
VO₂ max	-0.091	(-0.19, -0.008)	0.072	21.0%	
% S adipocyte	-2.0	(-2.3, -1.7)	< 0.0001	20.5%	97.4%
% M adipocyte	-1.6	(-1.8, -1.3)	< 0.0001	38.3%	
% L adipocyte	-1.2	(-1.4, -0.9)	< 0.0001	1.8%	
Group			< 0.0001	5.9%	

Table 3-6 Regression analysis by fit regression model: mean adipocyte diameter versus factor and covariates.

Factor (group) and covariates (anthropometric characteristics, blood metabolic variables and fitness,).

3.3.3 Adipocyte expression of *PPARG*, a marker of adipocyte differentiation

The expression of *PPARG* was significantly different across OETEU, YHSA, YHEU, OHEU and OIGREU (Figure 3-24). *PPARG* was expressed at the highest level in OETEU. *PPARG* was expressed in adipocytes at a higher level in OHEU than YHEU and OIGREU. Expression of *PPARG* was similar in YHSA, YHEU and OIGREU.

Figure 3-24 *PPARG* expression relative to *PPIA* across groups.

Young Healthy European (YHEU), older Healthy European (OHEU), Young Healthy South Asian (YHSA), Older Endurance trained European athletes (OETEU), and Older Europeans with impaired glucose regulation (OIGREU) (n = 18, 18, 13, 20 and 17, respectively) in groups with different age (YHEU vs OHEU), ethnicity (YHEU vs YHSA), fitness (OHEU vs OETEU), and glycaemic status (OHEU vs OIGREU). Results are shown as mean and standard deviation. Differences between two groups was by t test.

3.3.3.1 Contribution of anthropometric and metabolic parameters and adipocyte diameter to adipocyte *PPARG* expression

The correlations between *PPARG* expression and HOMA-IR, age, BMI, waist, RMR, VO_2 max, fasting glucose, fasting insulin, fasting TG and adipocyte diameter were analysed in a univariate analysis (Figure 3-25, Figure 3-26, Figure 3-27 and Figure 3-28). Two positive correlations were found between *PPARG* expression and age and VO_2 max (R = 0.33 and 0.27, *p* = 0.002 and 0.020, respectively), and a negative correlation was found between *PPARG* expression and HOMA-IR (R = -0.28, *p* = 0.010).

Group was the only independent and significant predictor of *PPARG* expression (*p* < 0.0001, Table 3-7).

PPARG

Age

r=0.33
p=0.002

BMI

- ■ YHEU
- ▲ OHEU
- ● YHSA
- ▼ OETEU
- ◆ OIGREU

r=-0.090
p=0.42

Waist

r=-0.080
p=0.46

Figure 3-25 Univariate analysis: relationship between adipocyte *PPARG* expression and anthropometric characteristics.

Participants: Young Healthy European (YHEU), older Healthy European (OHEU), Young Healthy South Asian (YHSA), Older Endurance trained European athletes (OETEU), and Older Europeans with impaired glucose regulation (OIGREU), n = 86.

Figure 3-26 Univariate analysis: relationship between adipocyte *PPARG* expression and blood metabolism parameters.

Participants: Young Healthy European (YHEU), older Healthy European (OHEU), Young Healthy South Asian (YHSA), Older Endurance trained European athletes (OETEU), and Older Europeans with impaired glucose regulation (OIGREU), n = 86.
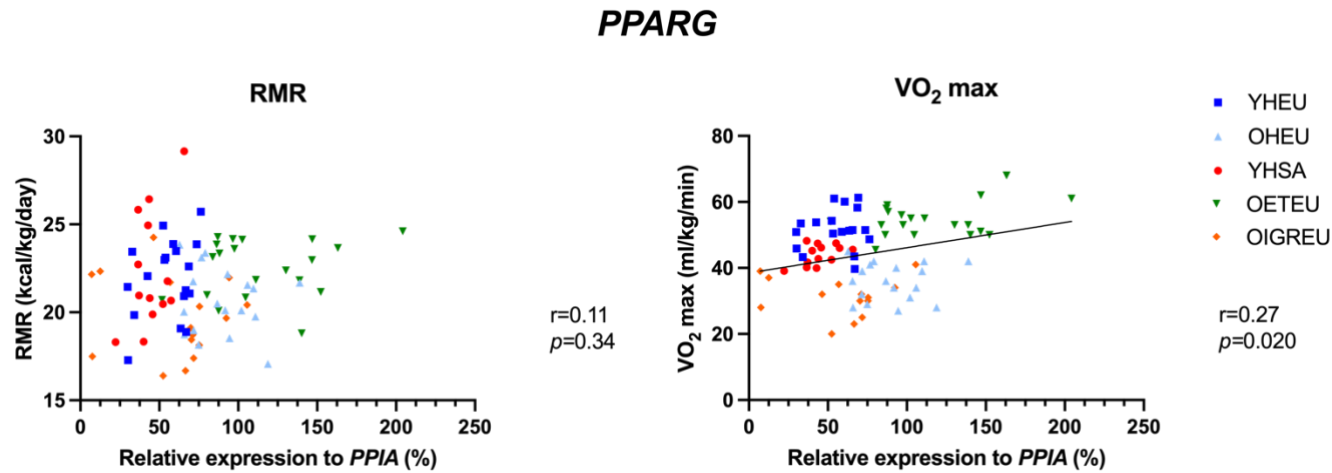
Figure 3-27 Univariate analysis: relationship between adipocyte *PPARG* expression and fitness.

Participants: Young Healthy European (YHEU), older Healthy European (OHEU), Young Healthy South Asian (YHSA), Older Endurance trained European athletes (OETEU), and Older Europeans with impaired glucose regulation (OIGREU), n = 86.
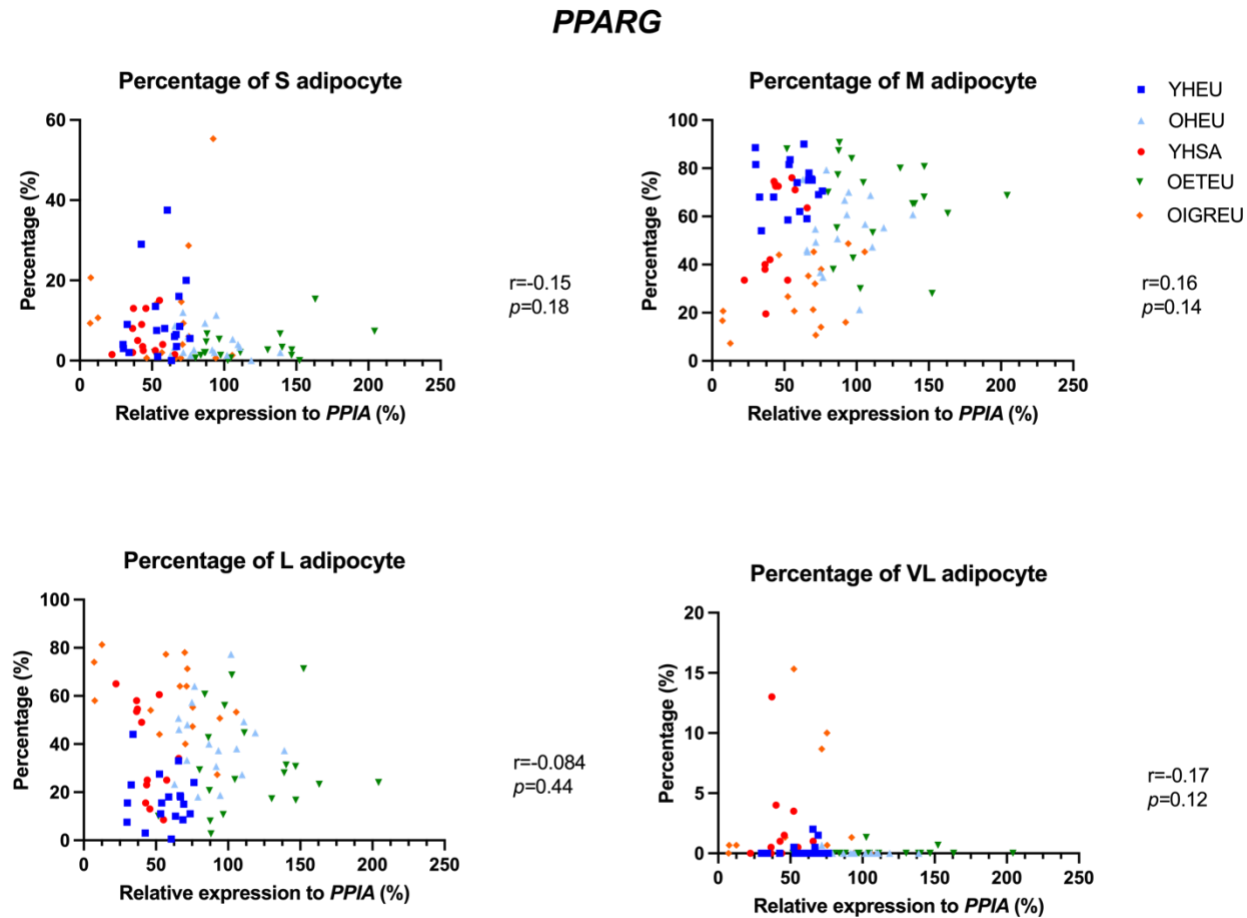
Figure 3-28 Univariate analysis: relationship between adipocyte *PPARG* expression and adipocyte size distribution.

Proportion of small (S), medium (M), large (L), and very large (VL) adipocyte in Young Healthy European (YHEU), older Healthy European (OHEU), Young Healthy South Asian (YHSA), Older Endurance trained European athletes (OETEU), and Older Europeans with impaired glucose regulation (OIGREU), n = 86.

PPARG	B-coefficient	95% CI	*p*	R^2	R^2 of model
HOMA-IR	-17.7	(-40.4, 5.0)	0.13	7.8%	
Group			< 0.0001	47.8%	55.6%

Table 3-7 Regression analysis by reverse stepwise: adipocyte *PPARG* expression versus factor and covariates.

Factor (group) and covariates (anthropometric characteristics, blood metabolic variables, fitness, and proportion of small, medium, large and very large adipocytes).

3.3.4 Adipocyte *TNF* expression, a marker of tissue stress response/ inflammation

The expression of *TNF* in adipocytes was significantly different across OETEU, YHSA, YHEU, OHEU and OIGREU (Figure 3-29). Adipocyte *TNF* was expressed at a higher level in OHEU, YHSA than YHEU, and higher in OHEU than OETEU.
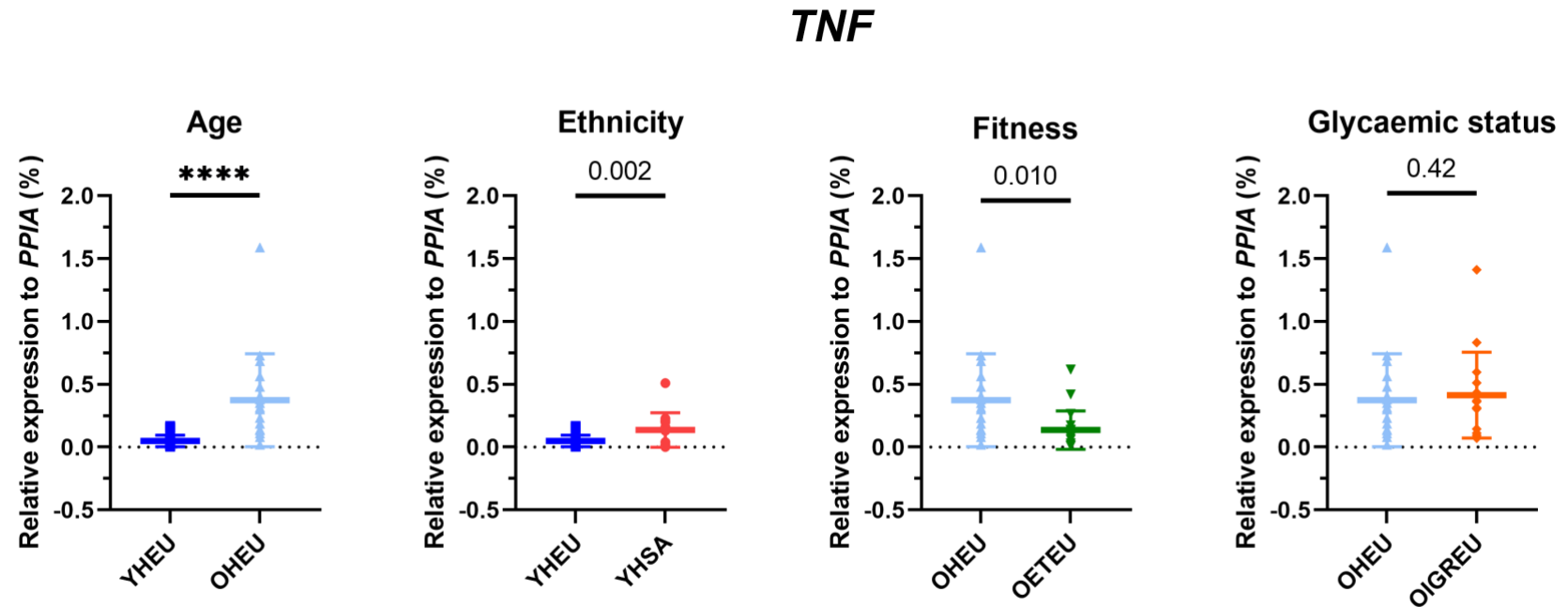
Figure 3-29 *TNF* **expression relative to** *PPIA* **across groups.**

Young Healthy European (YHEU), older Healthy European (OHEU), Young Healthy South Asian (YHSA), Older Endurance trained European athletes (OETEU), and Older Europeans with impaired glucose regulation (OIGREU) (n = 18, 18, 13, 20 and 17, respectively) in groups with different age (YHEU vs OHEU), ethnicity (YHEU vs YHSA), fitness (OHEU vs OETEU), and glycaemic status (OHEU vs OIGREU). Results are shown as mean and standard deviation. Differences between two groups was by t test.

3.3.4.1 Contribution of anthropometric and metabolic parameters and adipocyte diameter to adipocyte *TNF* expression

The correlations between *TNF* expression and HOMA-IR, age, BMI, waist, RMR, VO_2 max, fasting glucose, fasting insulin, fasting TG and adipocyte diameter, were analysed in a univariate analysis (Figure 3-30, Figure 3-31, Figure 3-32 and Figure 3-33). Six positive correlations were found between *TNF* expression and HOMA-IR, age, BMI, waist, fasting glucose, fasting TG and proportion of L adipocytes (R = 0.32, 0.48, 0.42, 0.49, 0.24, 0.34 and 0.41, *p* = 0.003, < 0.0001, < 0.0001, < 0.0001, 0.031, 0.002 and < 0.0001, respectively), and three negative correlations were found between *TNF* expression and RMR, VO_2 max and proportion of M adipocytes (R = -0.29, -0.54 and -0.45, *p* = 0.009, < 0.0001 and < 0.0001, respectively).

Fasting glucose was significantly independently and negatively associated with *TNF* expression (*p* = 0.038), and waist was significantly independently and positively associated with *TNF* expression (*p* = 0.007). Group significantly independently predicted the difference of TNF expression (*p* = 0.002) (Table 3-8).

Figure 3-30 Univariate analysis: relationship between adipocyte *TNF* expression and anthropometric characteristics.

Participants: Young Healthy European (YHEU), older Healthy European (OHEU), Young Healthy South Asian (YHSA), Older Endurance trained European athletes (OETEU), and Older Europeans with impaired glucose regulation (OIGREU), n = 86.

Figure 3-31 Univariate analysis: relationship between adipocyte *TNF* expression and blood metabolic parameters.

Participants: Young Healthy European (YHEU), older Healthy European (OHEU), Young Healthy South Asian (YHSA), Older Endurance trained European athletes (OETEU), and Older Europeans with impaired glucose regulation (OIGREU), n = 86.

TNF

Figure 3-32 Univariate analysis: relationship between adipocyte *TNF* expression and fitness.

Participants: Young Healthy European (YHEU), older Healthy European (OHEU), Young Healthy South Asian (YHSA), Older Endurance trained European athletes (OETEU), and Older Europeans with impaired glucose regulation (OIGREU), n = 86.

TNF

Figure 3-33 Univariate analysis: relationship between adipocyte *TNF* expression and adipocyte size distribution.

Proportion of small (S), medium (M), large (L), and very large (VL) adipocytes in Young Healthy European (YHEU), older Healthy European (OHEU), Young Healthy South Asian (YHSA), Older Endurance trained European athletes (OETEU), and Older Europeans with impaired glucose regulation (OIGREU), n = 86.

TNF	B-coefficient	95% CI	*P*	R^2	R^2 of model
Waist	0.026	(0.007, 0.044)	0.007	23.1%	
Fasting glucose	-0.13	(-0.25, -0.007)	0.038	5.1%	42.8%
Group			0.002	14.6%	

Table 3-8 Regression analysis by reverse stepwise: adipocyte *TNF* expression versus factor and covariates.

Factor (group) and covariates (anthropometric characteristics, blood metabolic variables, fitness, and proportion of small, medium, large and very large adipocytes).

3.3.5 Adipocyte *LPL* and *SREBF1* expression, markers of adipocyte lipid uptake and storage

The expression of *LPL* and *SREBF1* were significantly different across OETEU, YHSA, YHEU, OHEU and OIGREU (Figure 3-34 and Figure 3-35). Expression of *LPL* was higher in OETEU compared to OHEU. Expression of *SREBF1* was higher in OETEU compared to OHEH.
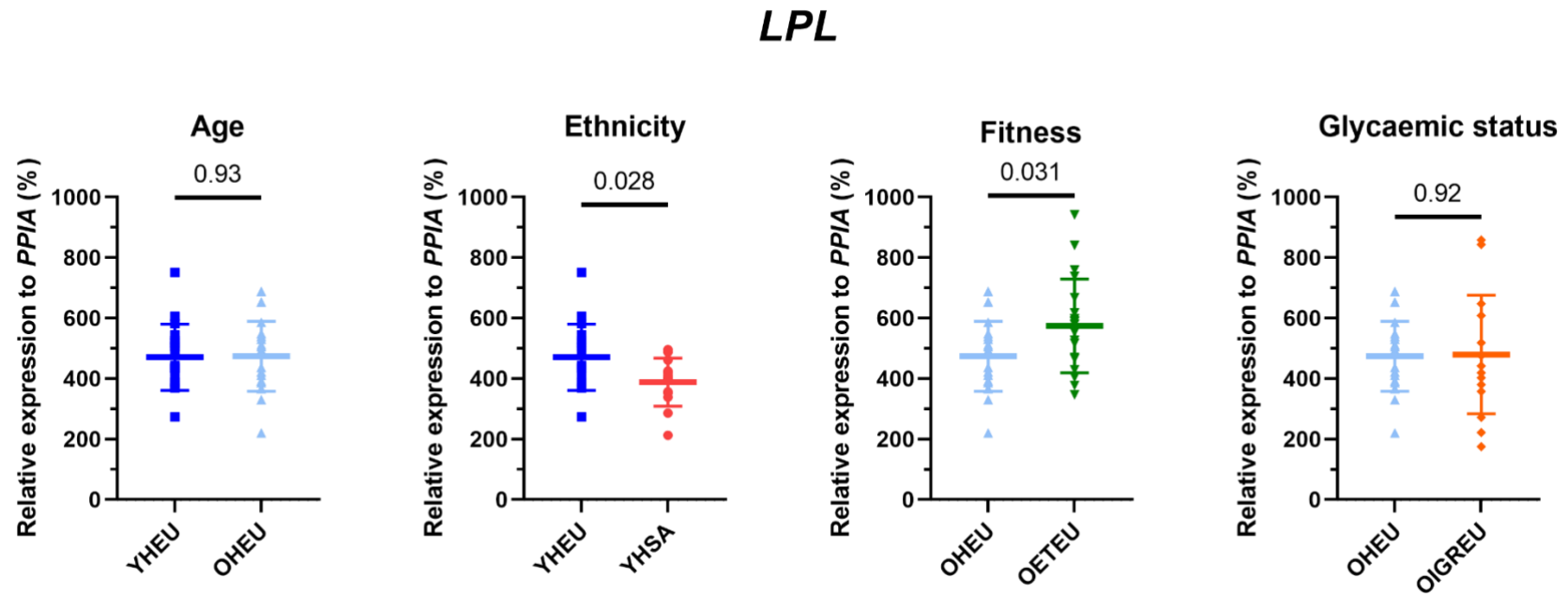
Figure 3-34 *LPL* expression relative to *PPIA* across groups.

Young Healthy European (YHEU), Older Healthy European (OHEU), Young Healthy South Asian (YHSA), Older Endurance trained European athletes (OETEU), and Older Europeans with impaired glucose regulation (OIGREU) (n = 18, 18, 13, 20 and 17, respectively) in groups with different age (YHEU vs OHEU), ethnicity (YHEU vs YHSA), fitness (OHEU vs OETEU), and glycaemic status (OHEU vs OIGREU). Results are shown as mean and standard deviation. Differences between two groups was applied using t test.
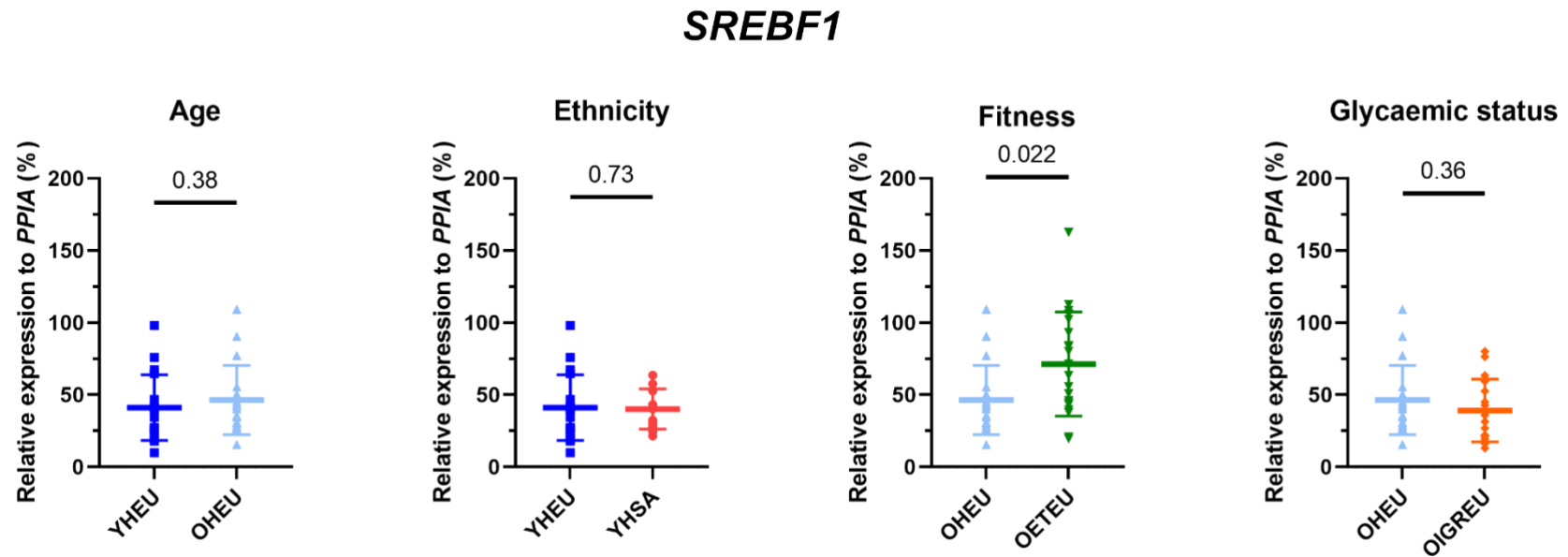
Figure 3-35 *SREBF1* expression relative to *PPIA* in across groups.

Young Healthy European (YHEU), Older Healthy European (OHEU), Young Healthy South Asian (YHSA), Older Endurance trained European athletes (OETEU), and Older Europeans with impaired glucose regulation (OIGREU) (n = 18, 18, 13, 20 and 17, respectively) in groups with different age (YHEU vs OHEU), ethnicity (YHEU vs YHSA), fitness (OHEU vs OETEU), and glycaemic status (OHEU vs OIGREU). Results are shown as mean and standard deviation. Differences between two groups was applied using t test.

3.3.5.1 Contribution of anthropometric and metabolic parameters and adipocyte diameter to adipocyte *LPL* expression

The correlations between *LPL* expression and HOMA-IR age, BMI, waist, RMR, VO_2 max, fasting glucose, fasting insulin, fasting TG and adipocyte diameter were analysed in a univariate analysis (Figure 3-36, Figure 3-37, Figure 3-38 and Figure 3-39). A positive correlation was found between *LPL* expression and VO_2 max (R = 0.27, *p* = 0.014) and negative correlations were found between *LPL* expression and fasting insulin and HOMA-IR (R = -0.27 and -0.22, *p* = 0.013 and 0.046, respectively).

BMI was independently negatively (*p* = 0.001) and group was independently and significantly associated with *LPL* expression (*p* < 0.0001, Table 3-9).

LPL

Age

r=0.21
p=0.051

BMI

- ■ YHEU
- ▲ OHEU
- ● YHSA
- ▼ OETEU
- ◆ OIGREU

r=-0.15
p=0.18

Waist

r=-0.11
p=0.33
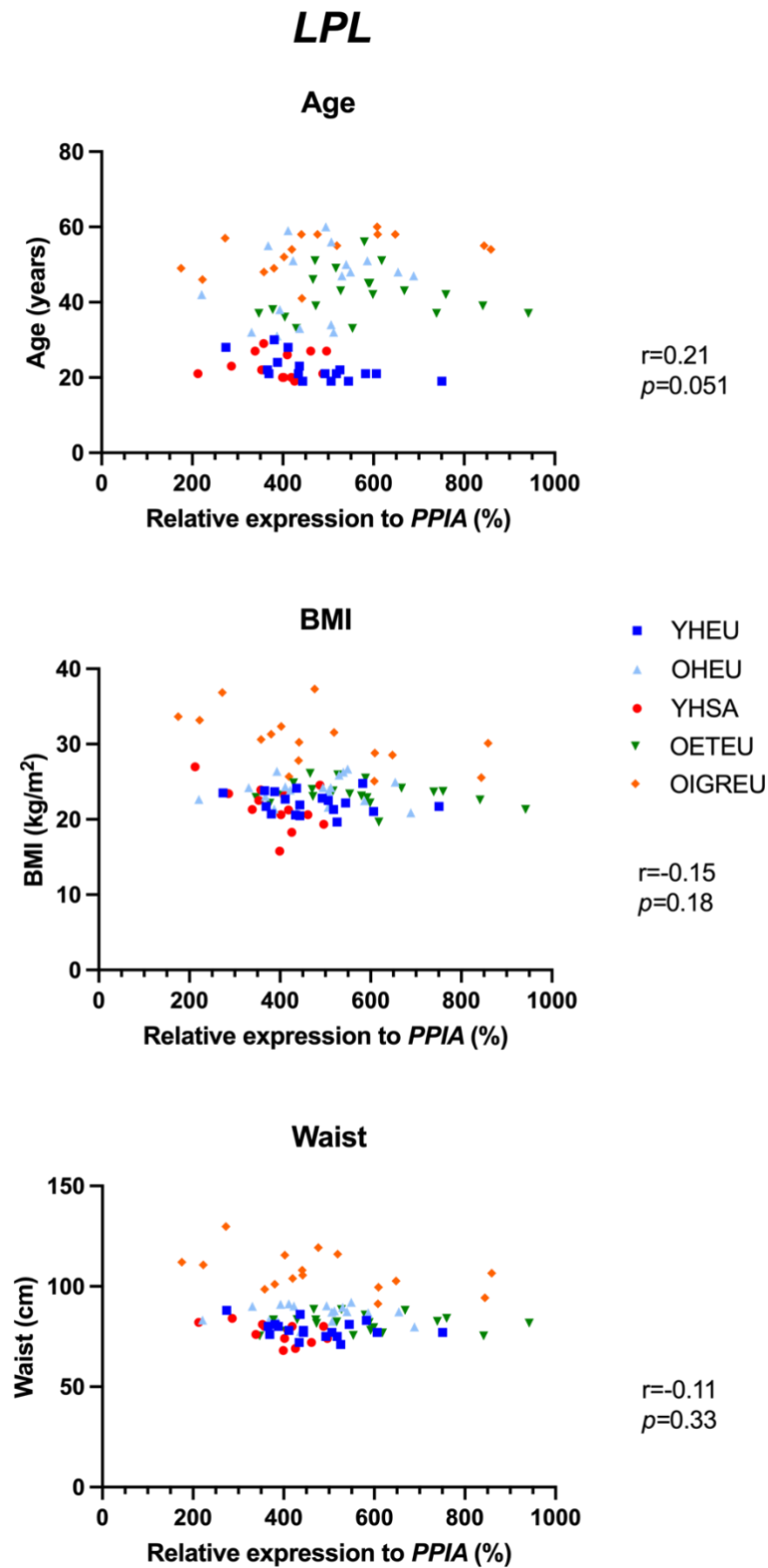
Figure 3-36 Univariate analysis: relationship between adipocyte *LPL* expression and anthropometric characteristics.

Participants: Young Healthy European (YHEU), older Healthy European (OHEU), Young Healthy South Asian (YHSA), Older Endurance trained European athletes (OETEU), and Older Europeans with impaired glucose regulation (OIGREU), n = 86.

LPL
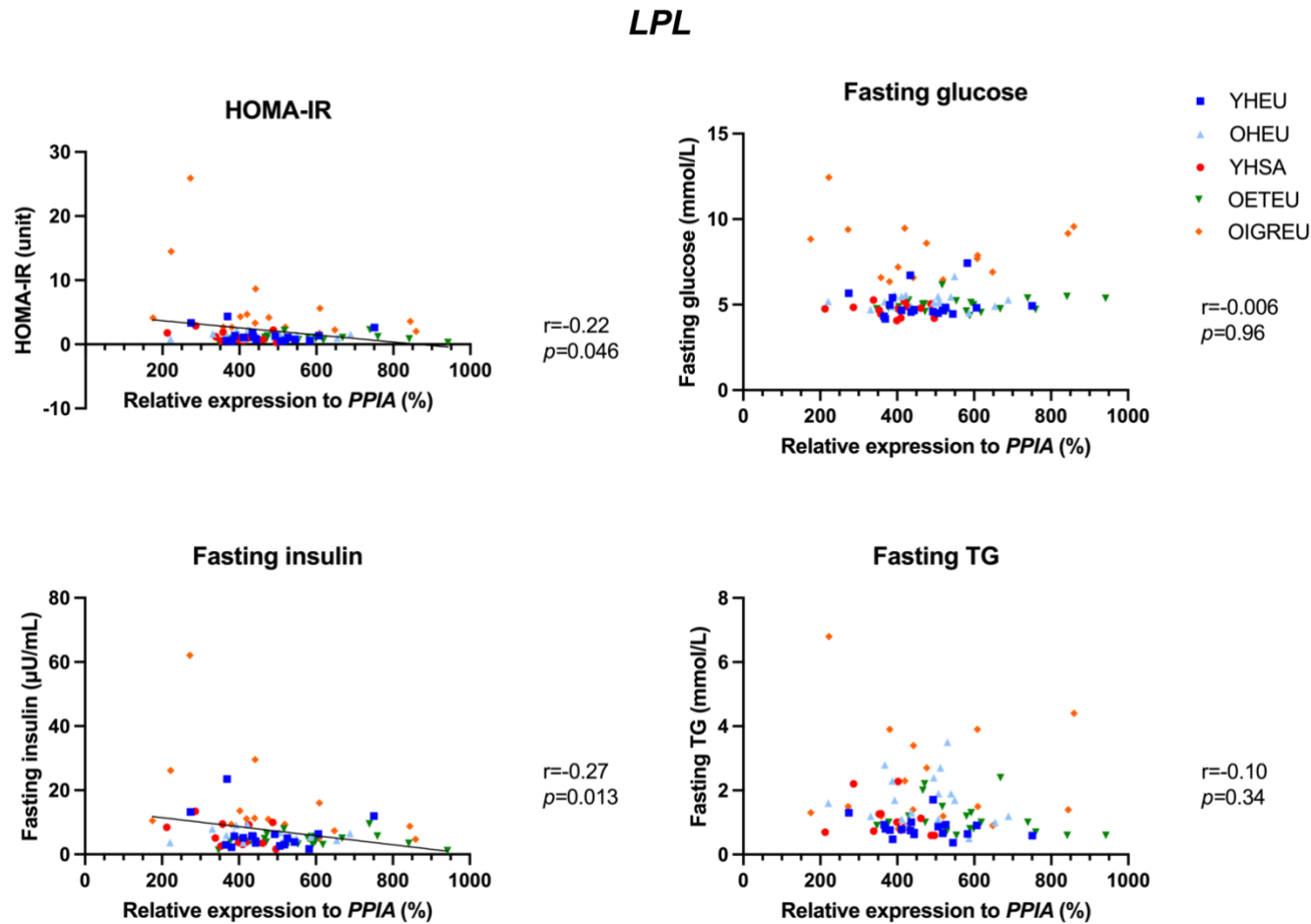
Figure 3-37 Univariate analysis: relationship between adipocyte *LPL* expression and blood metabolic parameters.

Participants: Young Healthy European (YHEU), older Healthy European (OHEU), Young Healthy South Asian (YHSA), Older Endurance trained European athletes (OETEU), and Older Europeans with impaired glucose regulation (OIGREU), n = 86.
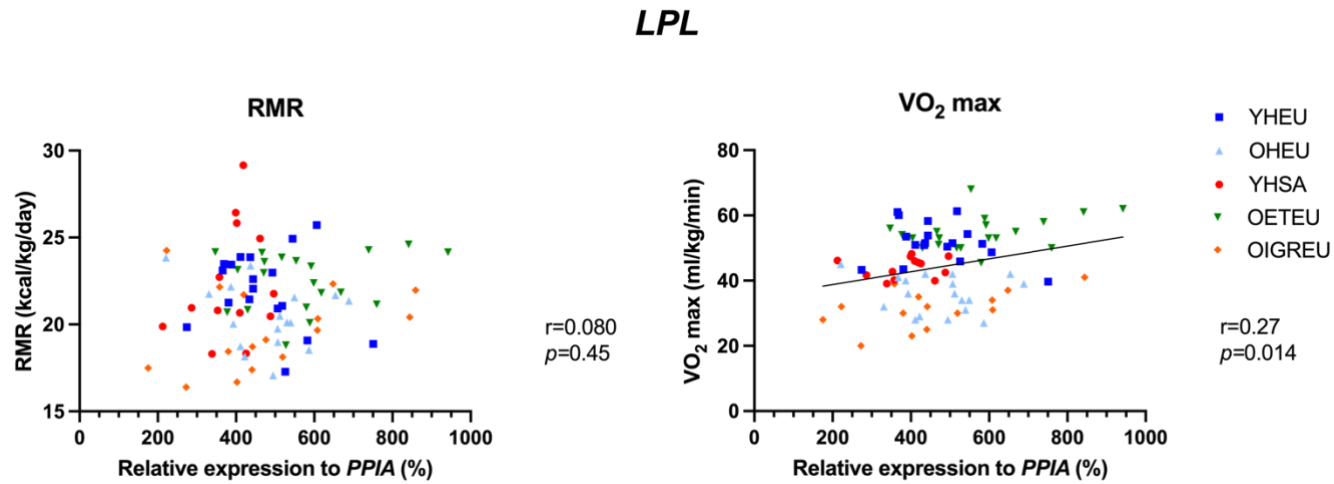
Figure 3-38 Univariate analysis: relationship between adipocyte *LPL* expression and fitness.

Participants: Young Healthy European (YHEU), older Healthy European (OHEU), Young Healthy South Asian (YHSA), Older Endurance trained European athletes (OETEU), and Older Europeans with impaired glucose regulation (OIGREU), n = 86.
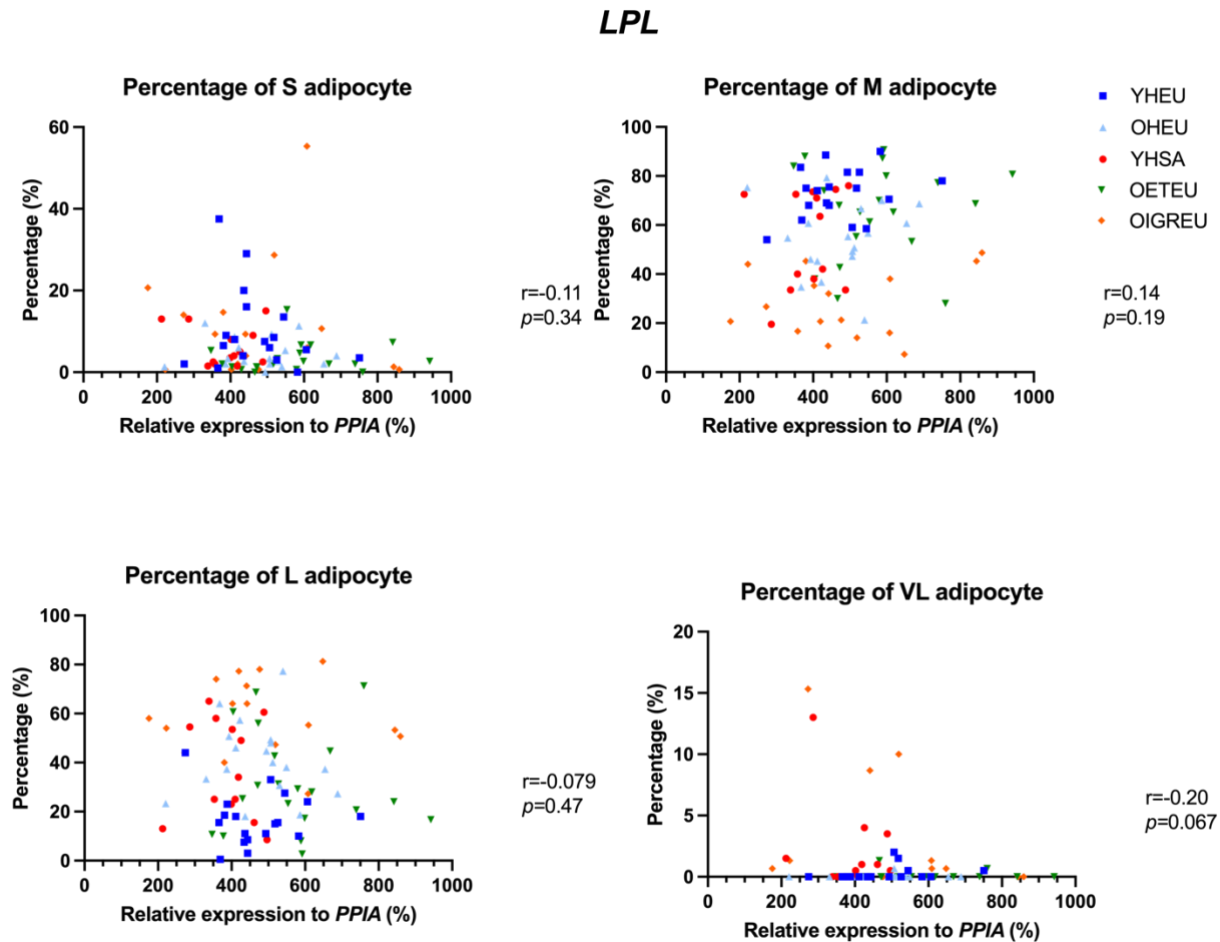
Figure 3-39 Univariate analysis: relationship between adipocyte *LPL* expression and adipocyte size distribution.

Proportion of small (S), medium (M), large (L), and very large (VL) adipocytes in Young Healthy European (YHEU), older Healthy European (OHEU), Young Healthy South Asian (YHSA), Older Endurance trained European athletes (OETEU), and Older Europeans with impaired glucose regulation (OIGREU), n = 86.

LPL	B-coefficient	95% CI	p	R^2	R^2 of model
BMI	-21.6	(-34.1, -9.2)	0.001	4.8%	32.8%
Fasting TG	-29.5	(-61.9, 2.9)	0.074	1.9%	
Group			< 0.0001	26.1%	

Table 3-9 Regression analysis by reverse stepwise: adipocyte *LPL* expression versus factor and covariates.

Factor (group) and covariates (anthropometric characteristics, blood metabolic variables, fitness, and proportion of small, medium, large and very large adipocytes).

3.3.5.2 Contribution of anthropometric and metabolic parameters and adipocyte diameter to adipocyte *SREBF1* expression

The correlations between *SREBF1* expression and HOMA-IR age, BMI, waist, RMR, VO_2 max, fasting glucose, fasting insulin, fasting TG and adipocyte diameter were analysed in a univariate analysis (Figure 3-40, Figure 3-41, Figure 3-42 and Figure 3-43). Two strong negative correlations were found between *SREBF1* expression and BMI and fasting glucose (R = -0.23 and -0.25, *p* = 0.033 and 0.021, respectively).

HOMA-IR was independently positively (*p* = 0.011), fasting glucose was independently negatively (*p* = 0.026), and group was independently and significantly associated with *SREBF1* expression (*p* = 0.001, Table 3-10).

SREBF1

Age

r=0.10
p=0.35

BMI

- ■ YHEU
- ▲ OHEU
- ● YHSA
- ▼ OETEU
- ◆ OIGREU

r=-0.23
p=0.033

Waist

r=-0.21
p=0.051
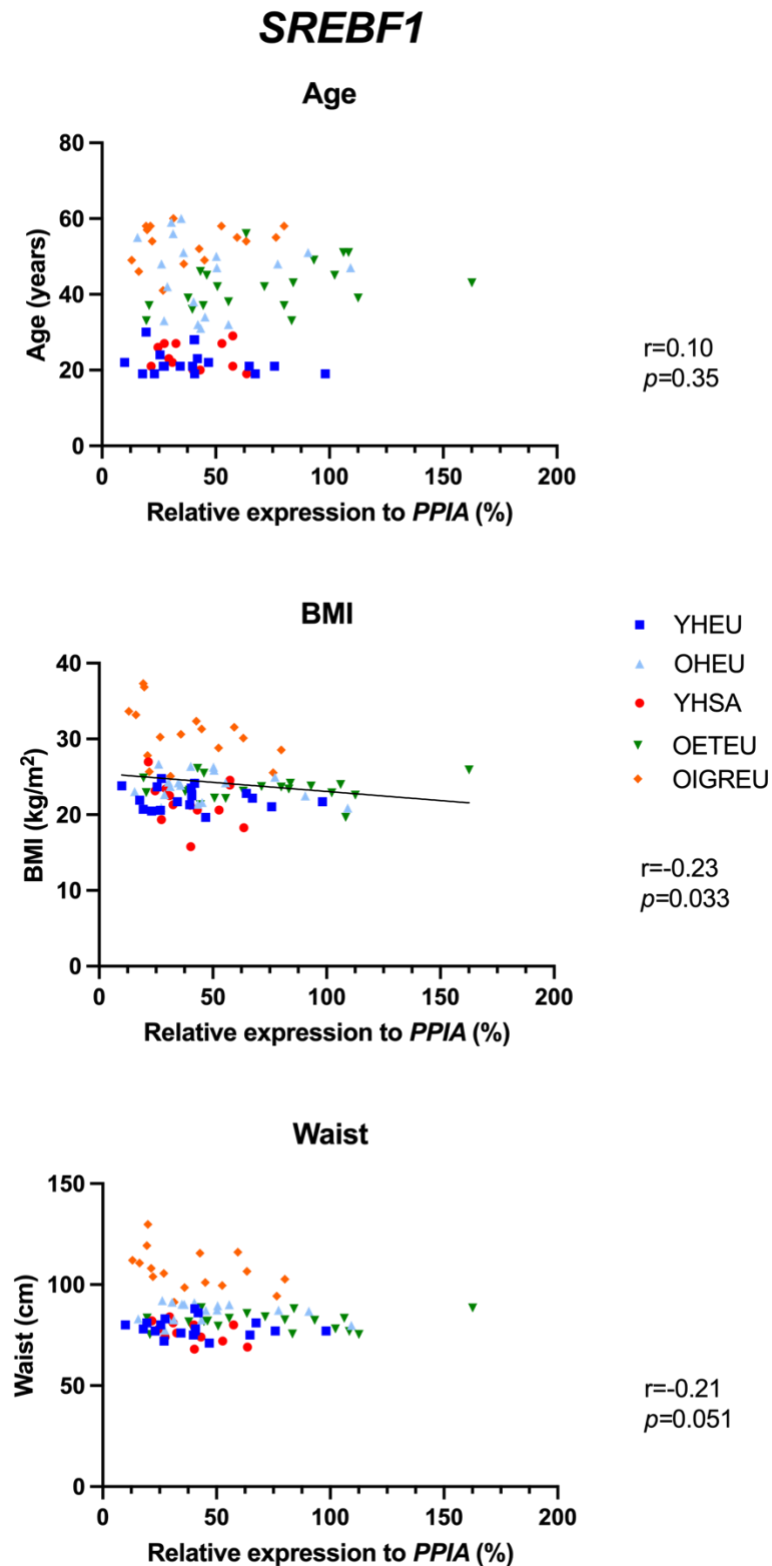
Figure 3-40 Univariate analysis: relationship between adipocyte *SREBF1* expression and anthropometric characteristics.

Participants: Young Healthy European (YHEU), older Healthy European (OHEU), Young Healthy South Asian (YHSA), Older Endurance trained European athletes (OETEU), and Older Europeans with impaired glucose regulation (OIGREU), n = 86.
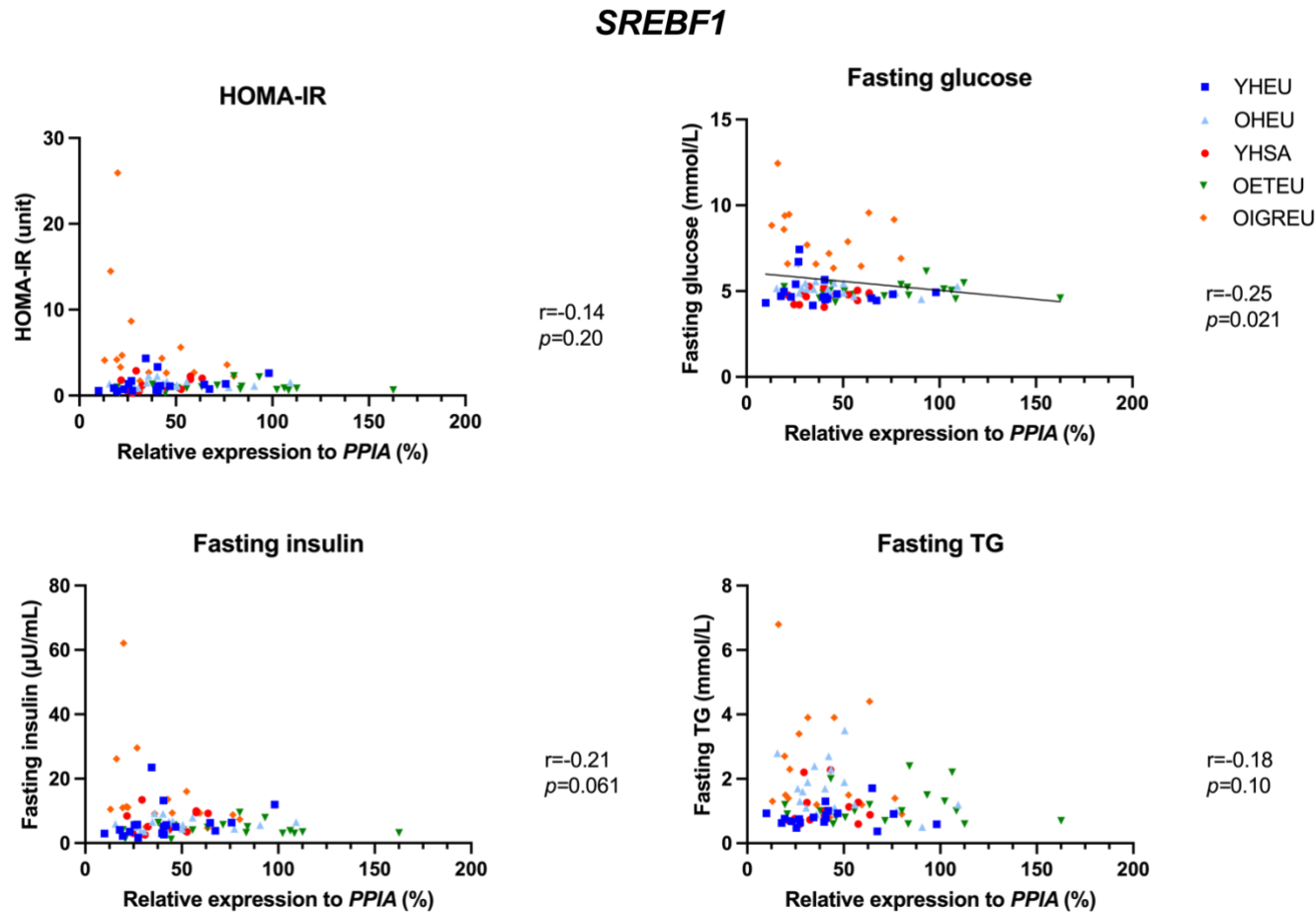
Figure 3-41 Univariate analysis: relationship between adipocyte *SREBF1* expression and blood metabolic parameters.

Participants: Young Healthy European (YHEU), older Healthy European (OHEU), Young Healthy South Asian (YHSA), Older Endurance trained European athletes (OETEU), and Older Europeans with impaired glucose regulation (OIGREU), n = 86.
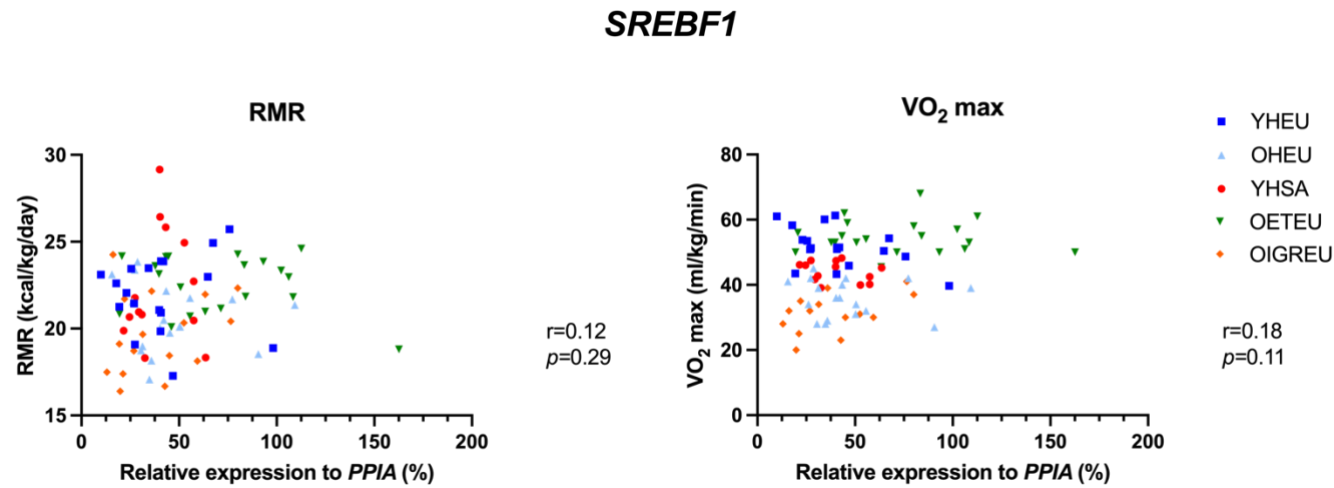
Figure 3-42 Univariate analysis: relationship between adipocyte *SREBF1* expression and fitness.

Participants: Young Healthy European (YHEU), older Healthy European (OHEU), Young Healthy South Asian (YHSA), Older Endurance trained European athletes (OETEU), and Older Europeans with impaired glucose regulation (OIGREU), n = 86.
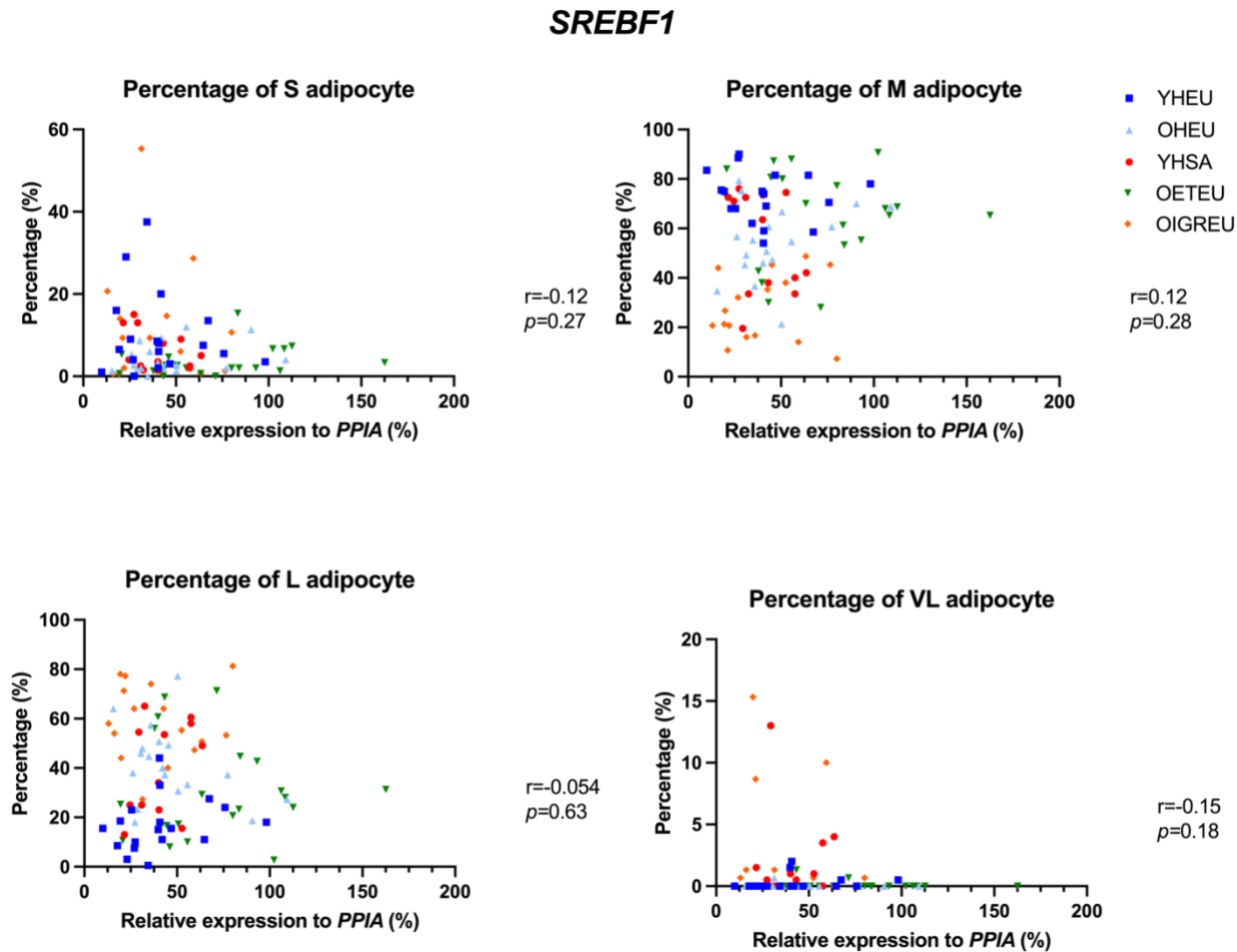
Figure 3-43 Univariate analysis: relationship between adipocyte *SREBF1* expression and adipocyte size distribution.

Proportion of small (S), medium (M), large (L), and very large (VL) adipocytes in Young Healthy European (YHEU), older Healthy European (OHEU), Young Healthy South Asian (YHSA), Older Endurance trained European athletes (OETEU), and Older Europeans with impaired glucose regulation (OIGREU), n = 86.

SREBF1	B-coefficient	95% CI	*p*	R^2	R^2 of model
BMI	-0.020	(-0.044, -0.003)	0.091	4.5%	
HOMA-IR	0.41	(0.10, 0.72)	0.011	0.06%	
Fasting glucose	-0.067	(-0.126, -0.008)	0.026	3.7%	30.4%
Fasting insulin	-0.009	(-0.021, -0.002)	0.11	3.3%	
Group			0.001	18.9%	

Table 3-10 Regression analysis by reverse stepwise: adipocyte *SREBF1* expression versus factor and covariates.

Factor (group) and covariates (anthropometric characteristics, blood metabolic variables, fitness, and proportion of small, medium, large and very large adipocytes).

3.3.6 Adipocyte expression of *ADIPOQ, INSR and LEP,* markers of insulin signalling and adipokine production

The expression of *ADIPOQ, INSR* and *LEP* were significantly different across OETEU, YHSA, YHEU, OHEU and OIGREU (Figure 3-44, Figure 3-45 and Figure 3-46). Expression of *ADIPOQ* was lower in YHSA compared to YHEU. Expression of *INSR* was lower in OIGREU compared to OHEU, and lower in YHSA than YHEU. Expression of *LEP* was higher in OHEU and YHSA compared to YHEU.
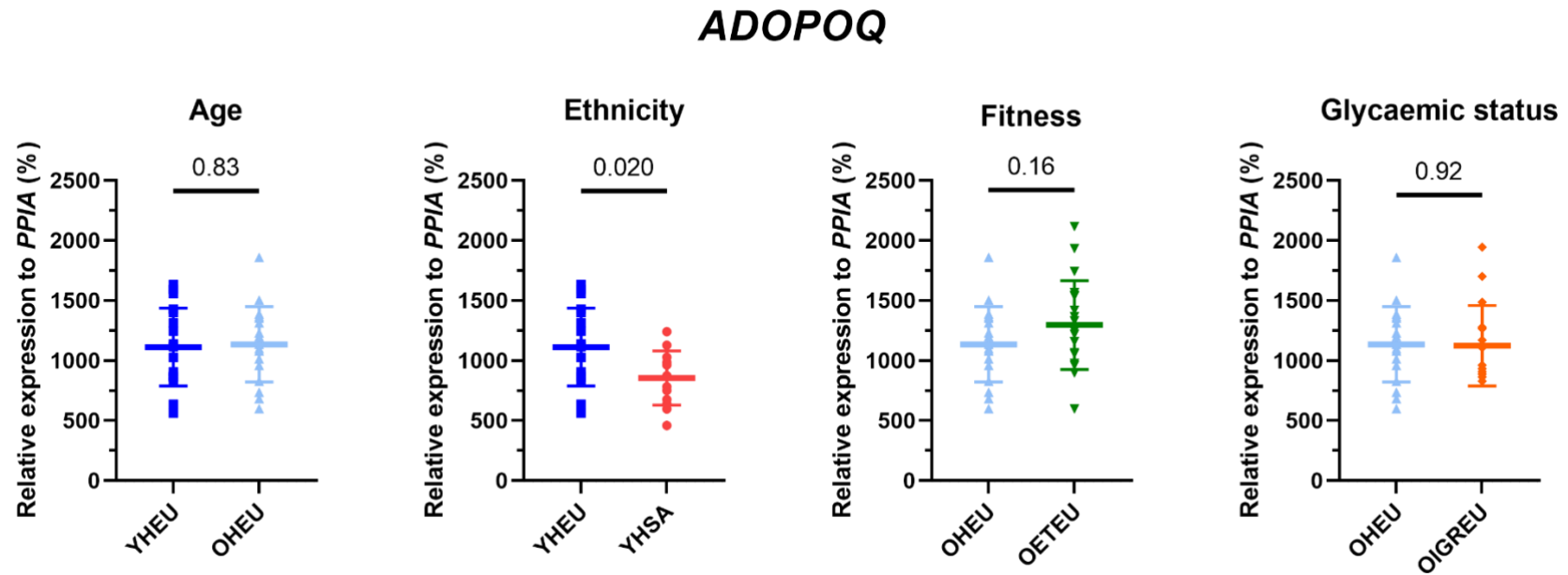
Figure 3-44 *ADIPOQ* expression relative to *PPIA* across groups.

Young Healthy European (YHEU), older Healthy European (OHEU), Young Healthy South Asian (YHSA), Older Endurance trained European athletes (OETEU), and Older Europeans with impaired glucose regulation (OIGREU) (n = 18, 18, 13, 20 and 17, respectively) in groups with different age (YHEU vs OHEU), ethnicity (YHEU vs YHSA), fitness (OHEU vs OETEU), and glycaemic status (OHEU vs OIGREU). Results are shown as mean and standard deviation. Differences between two groups was applied using t test.
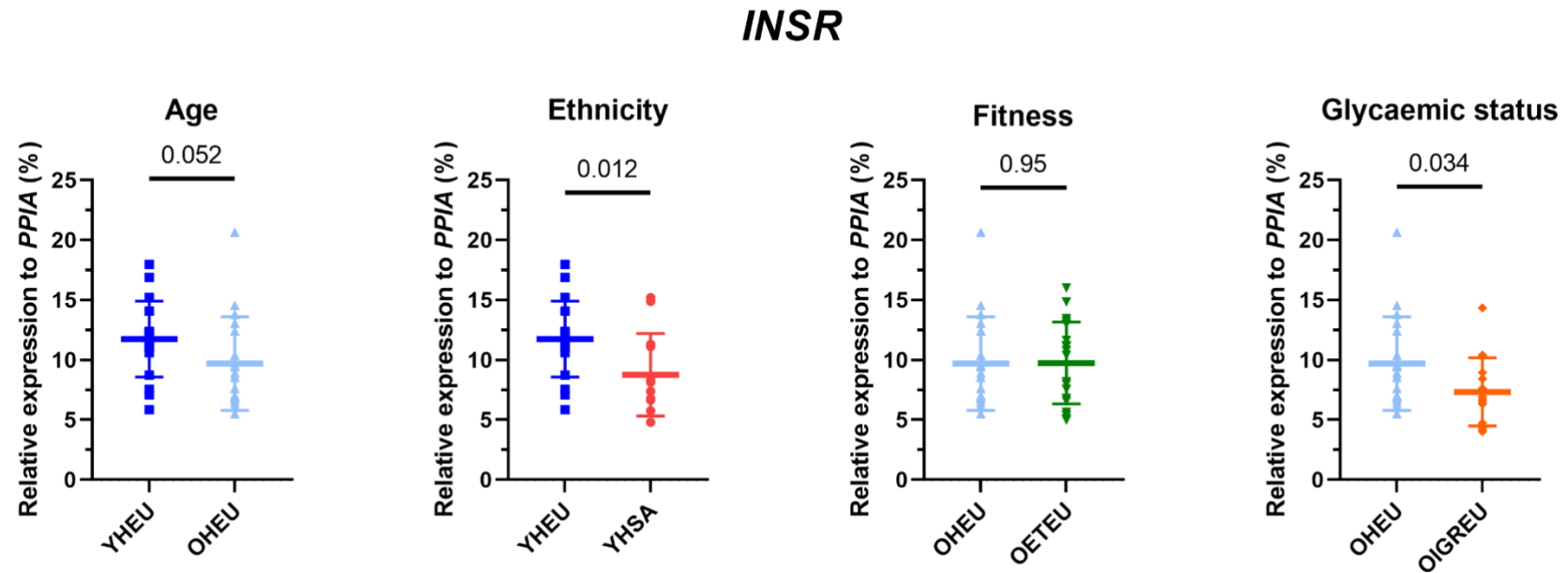
Figure 3-45 *INSR* expression relative to *PPIA* across groups.

Young Healthy European (YHEU), older Healthy European (OHEU), Young Healthy South Asian (YHSA), Older Endurance trained European athletes (OETEU), and Older Europeans with impaired glucose regulation (OIGREU) (n = 18, 18, 13, 20 and 17, respectively) in groups with different age (YHEU vs OHEU), ethnicity (YHEU vs YHSA), fitness (OHEU vs OETEU), and glycaemic status (OHEU vs OIGREU). Results are shown as mean and standard deviation. Differences between two groups was applied using t test.
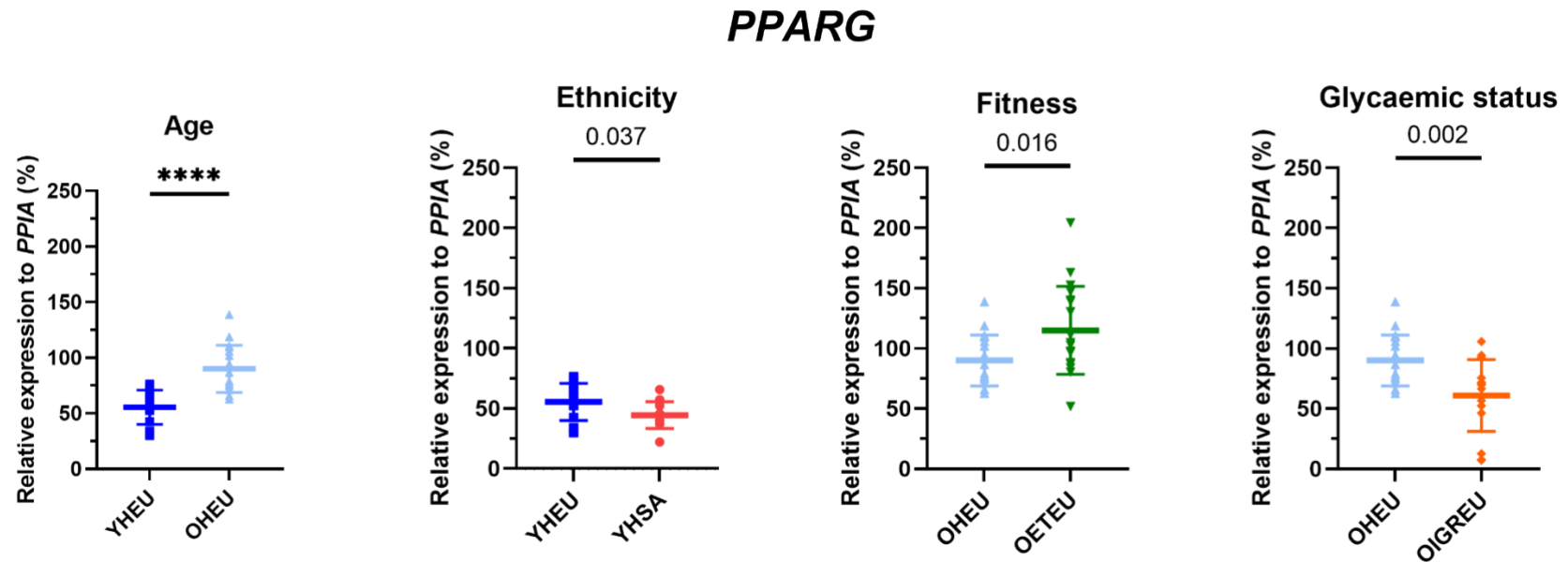
LEP
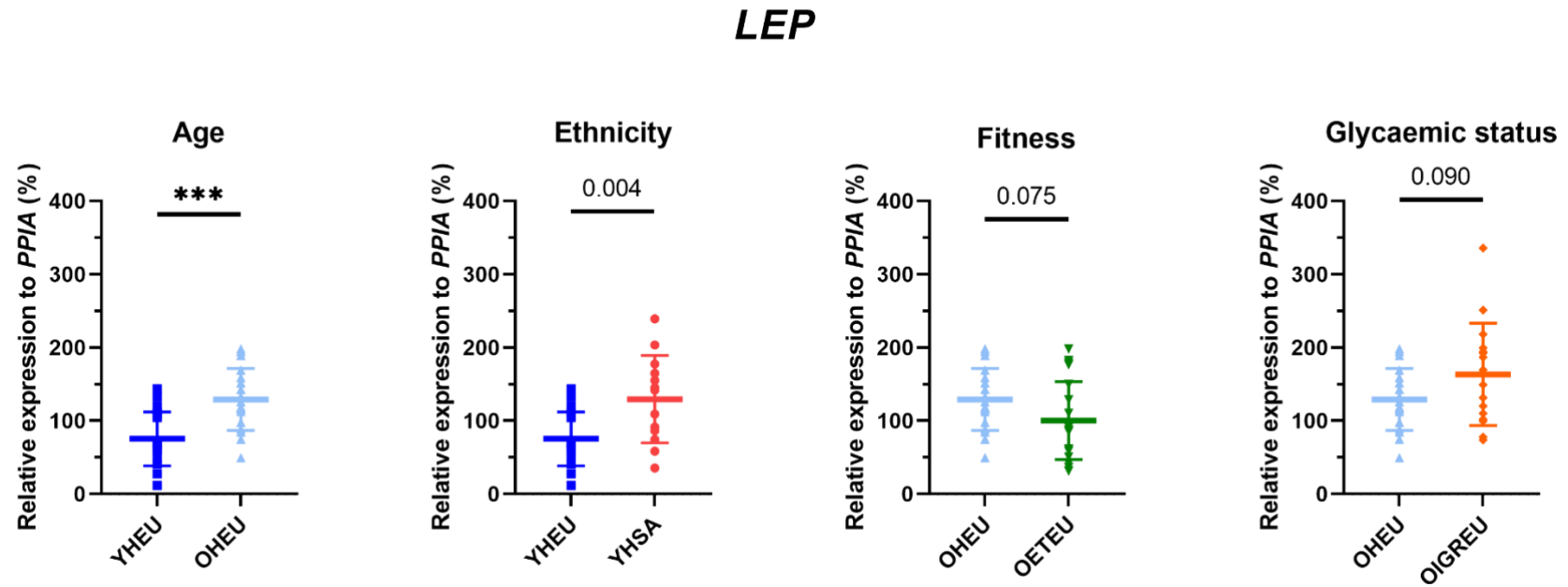
Figure 3-46 *LEP* expression relative to *PPIA* across groups.

Young Healthy European (YHEU), older Healthy European (OHEU), Young Healthy South Asian (YHSA), Older Endurance trained European athletes (OETEU), and Older Europeans with impaired glucose regulation (OIGREU) (n = 18, 18, 13, 20 and 17, respectively) in groups with different age (YHEU vs OHEU), ethnicity (YHEU vs YHSA), fitness (OHEU vs OETEU), and glycaemic status (OHEU vs OIGREU). Results are shown as mean and standard deviation. Differences between two groups was applied using t test.

3.3.6.1 Contribution of anthropometric and metabolic parameters and adipocyte diameter to adipocyte *ADIPOQ* expression

The correlations between *ADIPOQ* expression and HOMA-IR age, BMI, waist, RMR, VO_2 max, fasting glucose, fasting insulin, fasting TG and adipocyte diameter were analysed in a univariate analysis (Figure 3-47, Figure 3-48, Figure 3-49 and Figure 3-50). Two positive correlations were found between *ADIPOQ* expression and age and VO_2 max (R = 0.23 and 0.22, *p* = 0.036 and 0.043, respectively).

Fasting glucose was independently positively (*p* = 0.043), BMI was independently negatively (*p* = 0.033), and group was independently and significantly associated with *ADIPOQ* expression (*p* = 0.001, Table 3-11).
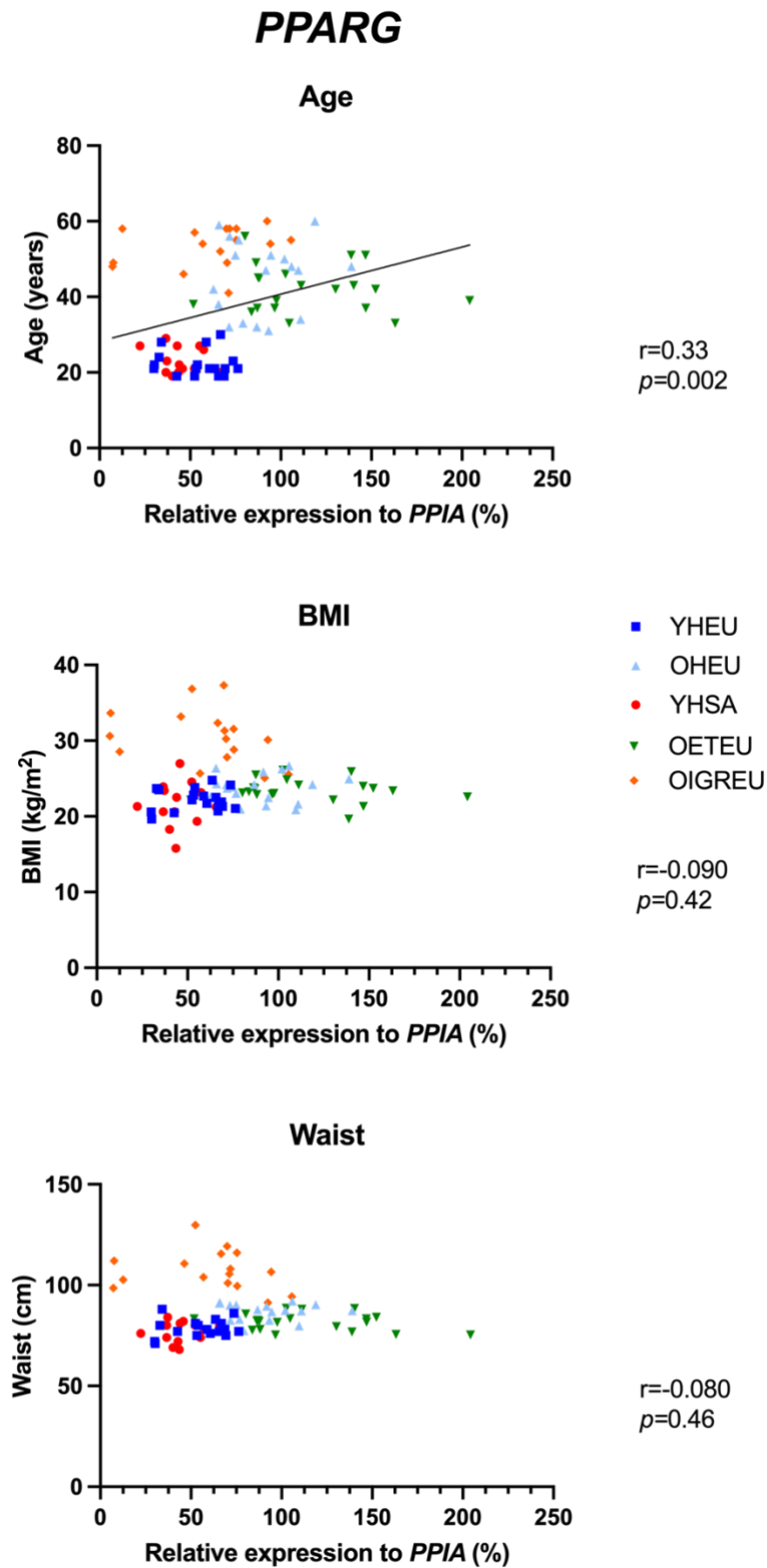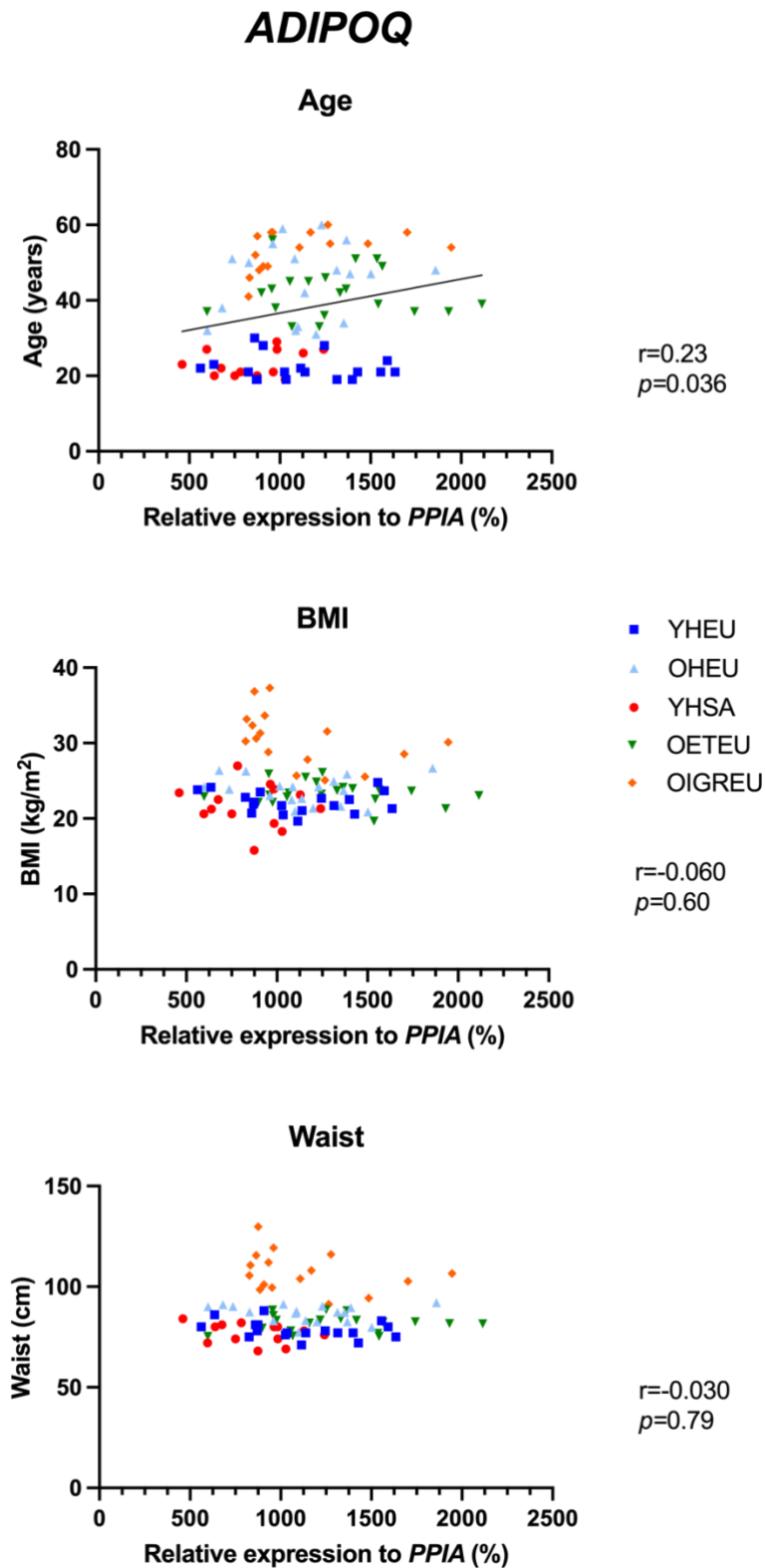
Figure 3-47 Univariate analysis: relationship between adipocyte *ADIPOQ* expression and anthropometric characteristics.

Participants: Young Healthy European (YHEU), older Healthy European (OHEU), Young Healthy South Asian (YHSA), Older Endurance trained European athletes (OETEU), and Older Europeans with impaired glucose regulation (OIGREU), n = 86.
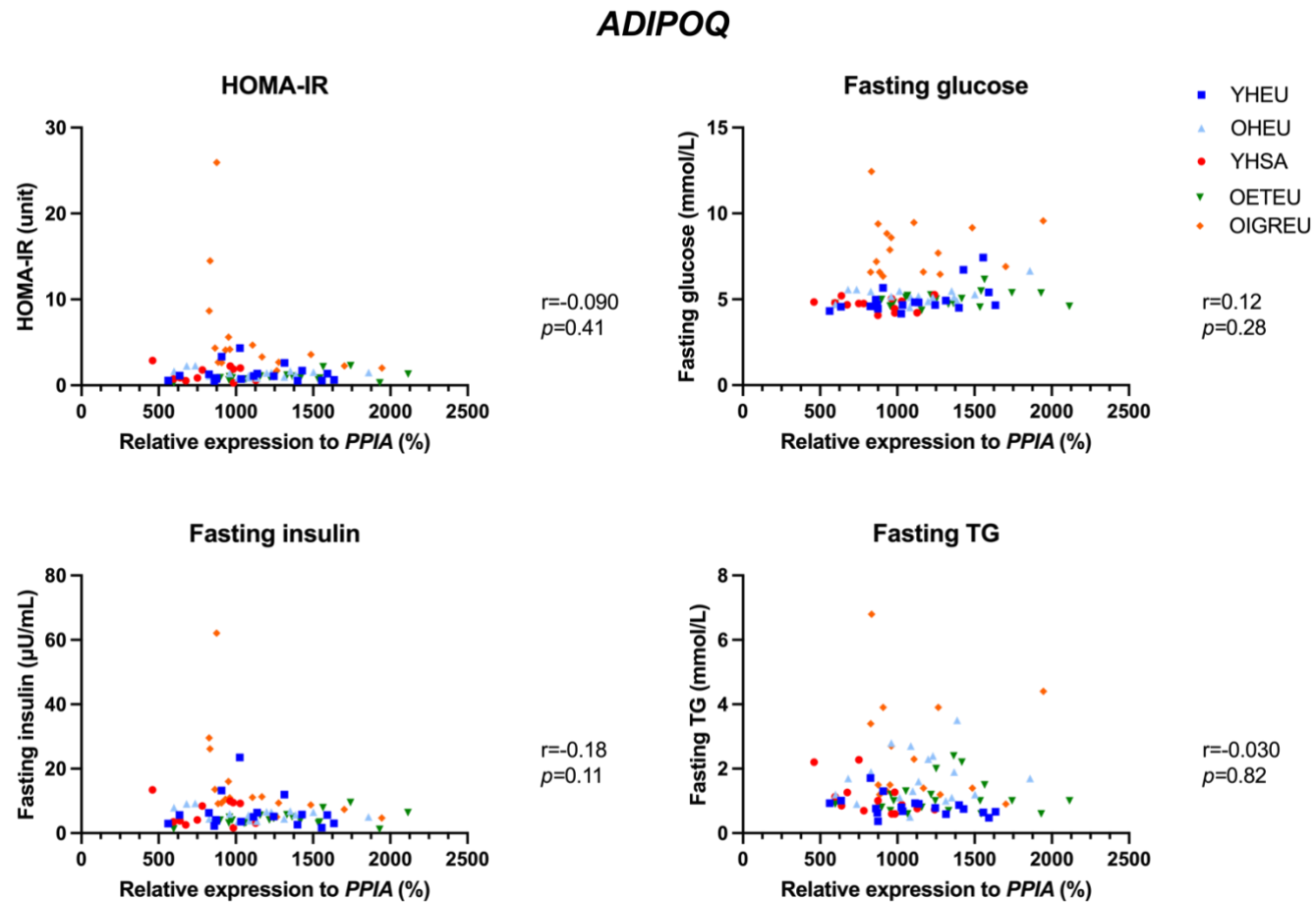
Figure 3-48 Univariate analysis: relationship between adipocyte *ADIPOQ* expression and blood metabolic parameters.

Participants: Young Healthy European (YHEU), older Healthy European (OHEU), Young Healthy South Asian (YHSA), Older Endurance trained European athletes (OETEU), and Older Europeans with impaired glucose regulation (OIGREU), n = 86.
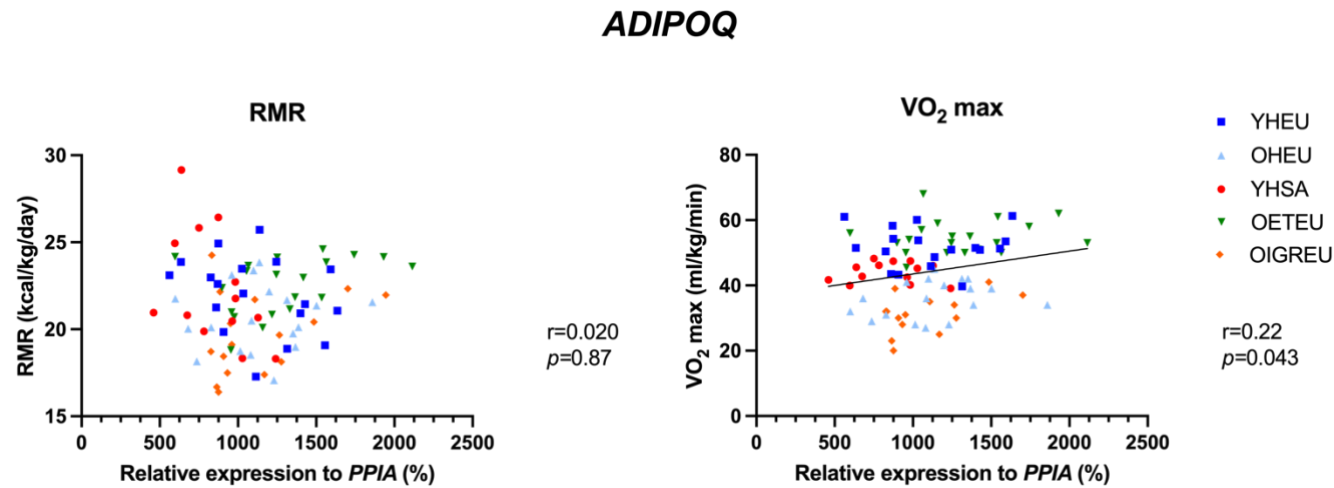
Figure 3-49 Univariate analysis: relationship between adipocyte *ADIPOQ* expression and fitness.

Participants: Young Healthy European (YHEU), older Healthy European (OHEU), Young Healthy South Asian (YHSA), Older Endurance trained European athletes (OETEU), and Older Europeans with impaired glucose regulation (OIGREU), n = 86.
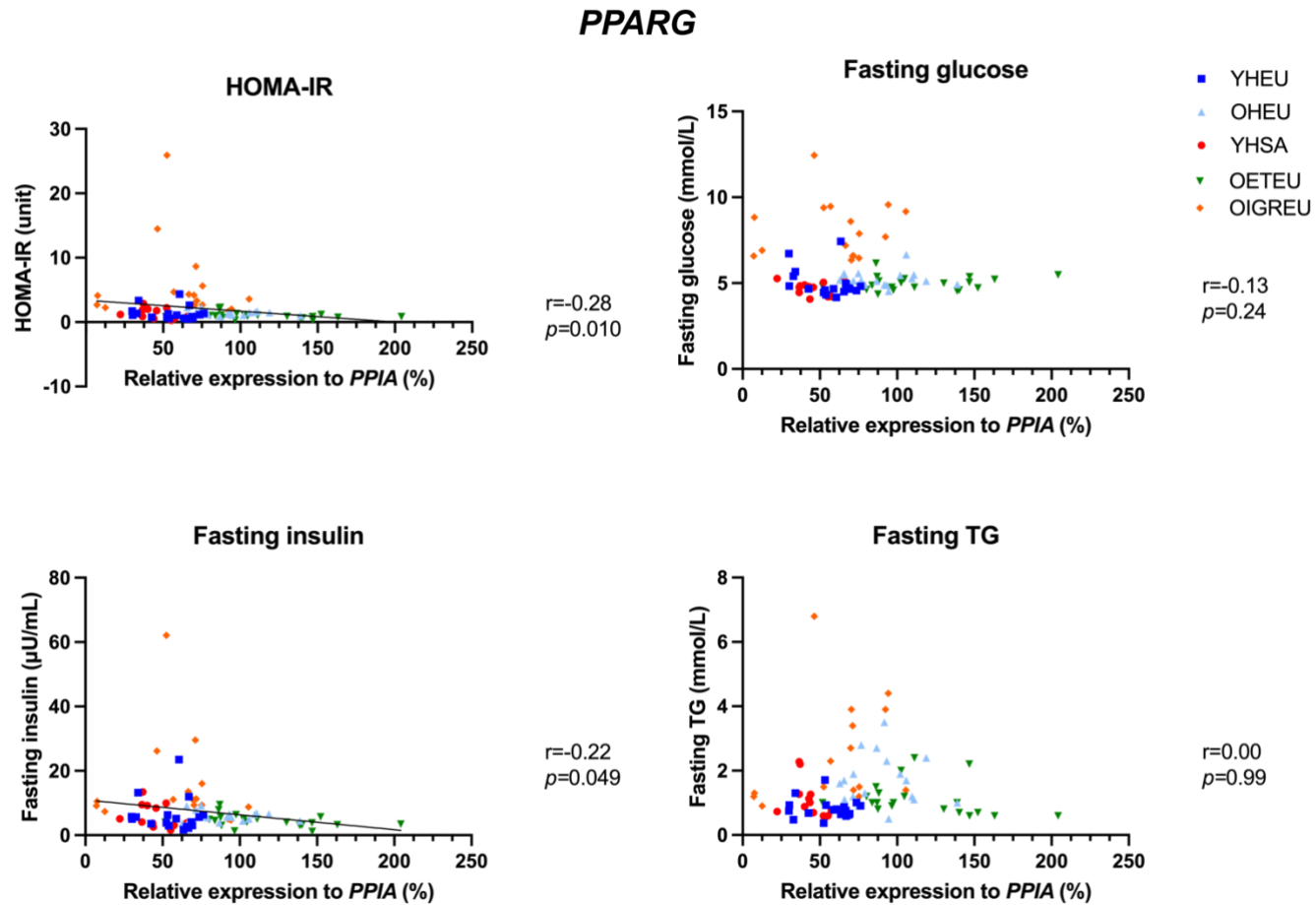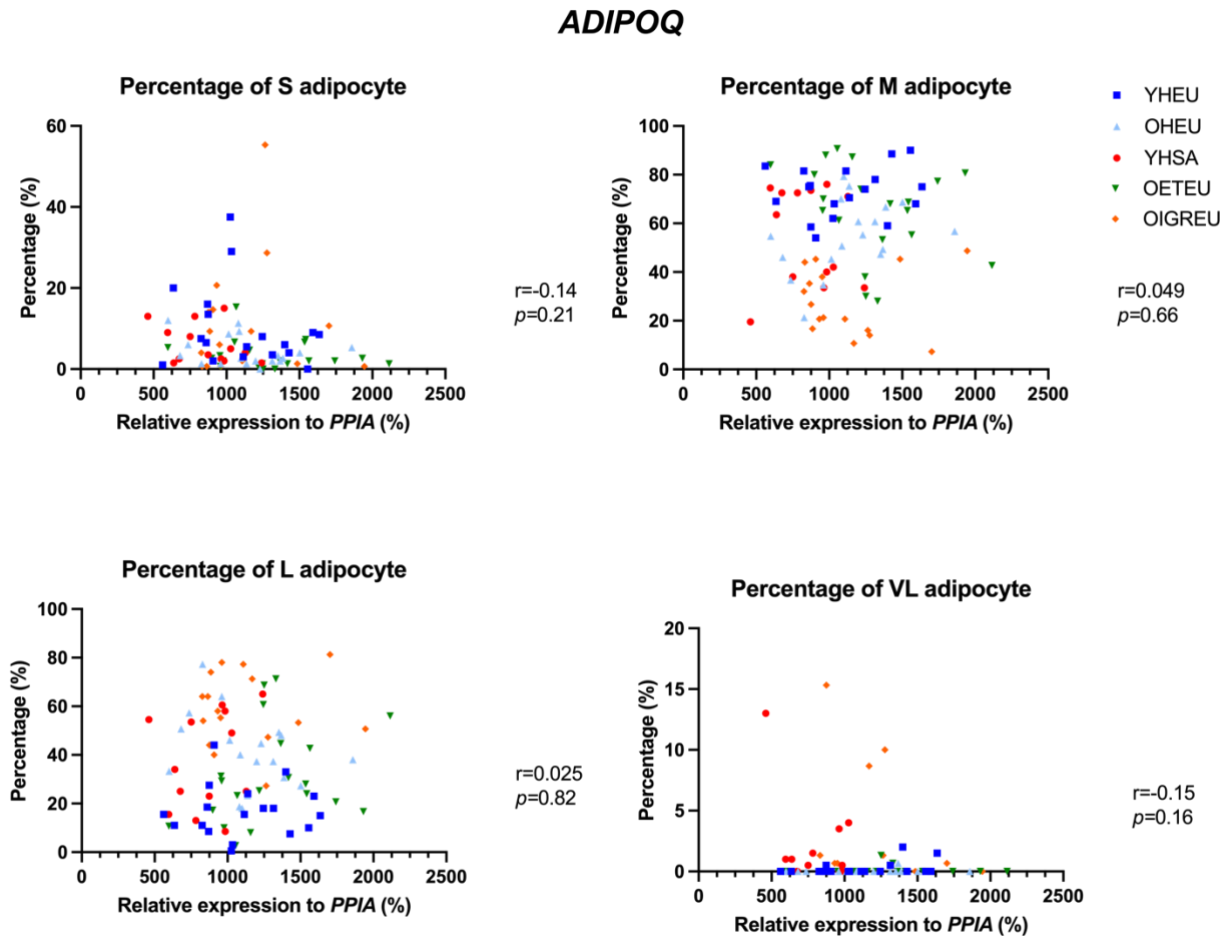
ADIPOQ

Figure 3-50 Univariate analysis: relationship between adipocyte *ADIPOQ* expression and adipocyte size distribution.

Proportion of small (S), medium (M), large (L), and very large (VL) adipocytes in Young Healthy European (YHEU), older Healthy European (OHEU), Young Healthy South Asian (YHSA), Older Endurance trained European athletes (OETEU), and Older Europeans with impaired glucose regulation (OIGREU), n = 86.

ADIPOQ	B-coefficient	95% CI	*p*	R^2	R^2 of model
BMI	-33.8	(-64.8, -2.9)	0.033	0.9%	
Fasting glucose	86.4	(2.9, 169.8)	0.043	3.1%	26.3%
Fasting TG	-68.3	(-152.0, 15.4)	0.11	2.5%	
Group			0.001	19.8%	

Table 3-11 Regression analysis by reverse stepwise: adipocyte *ADIPOQ* expression versus factor and covariates.

Factor (group) and covariates (anthropometric characteristics, blood metabolic variables, fitness, and proportion of small, medium, large and very large adipocytes).

3.3.6.2 Contribution of anthropometric and metabolic parameters and adipocyte diameter to adipocyte *INSR* expression

The correlations between *INSR* expression and HOMA-IR age, BMI, waist, RMR, VO_2 max, fasting glucose, fasting insulin, fasting TG and adipocyte diameter were analysed in univariate analysis (Figure 3-51, Figure 3-52, Figure 3-53 and Figure 3-54). Three positive correlations were found between *INSR* expression and RMR, VO_2 max and proportion of M adipocytes (R = 0.23, 0.38 and 0.28, *p* = 0.033, < 0.0001 and = 0.008, respectively), and seven negative correlations were found between *INSR* expression and HOMA-IR, BMI, waist, fasting glucose, fasting insulin, fasting TG and proportion of L adipocytes (R = -0.32, -0.21, -0.43, -0.39, -0.25, -0.30, -0.30 and -0.33, *p* = 0.003, < 0.0001, < 0.0001, 0.022, 0.006, 0.005 and 0.002, respectively).

BMI was significantly independently and negatively associated with *INSR* expression (*p* < 0.0001, Table 3-12).

INSR

Age

r=-0.21
p=0.052

BMI

- ■ YHEU
- ▲ OHEU
- ● YHSA
- ▼ OETEU
- ◆ OIGREU

r=-0.43
p<0.0001

Waist

r=-0.39
p<0.0001
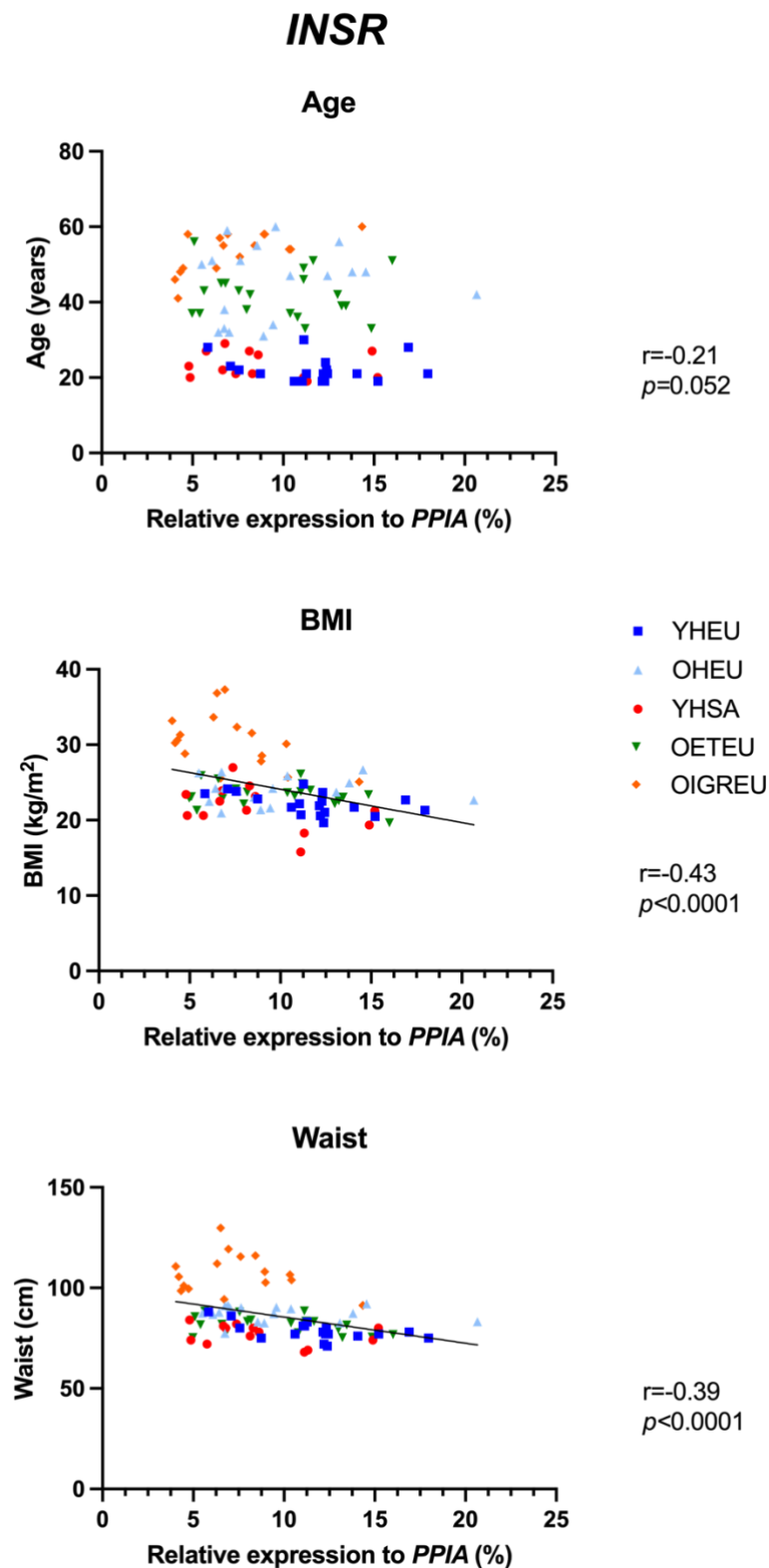
Figure 3-51 Univariate analysis: relationship between adipocyte *INSR* expression and anthropometric characteristics.

Participants: Young Healthy European (YHEU), older Healthy European (OHEU), Young Healthy South Asian (YHSA), Older Endurance trained European athletes (OETEU), and Older Europeans with impaired glucose regulation (OIGREU), n = 86.
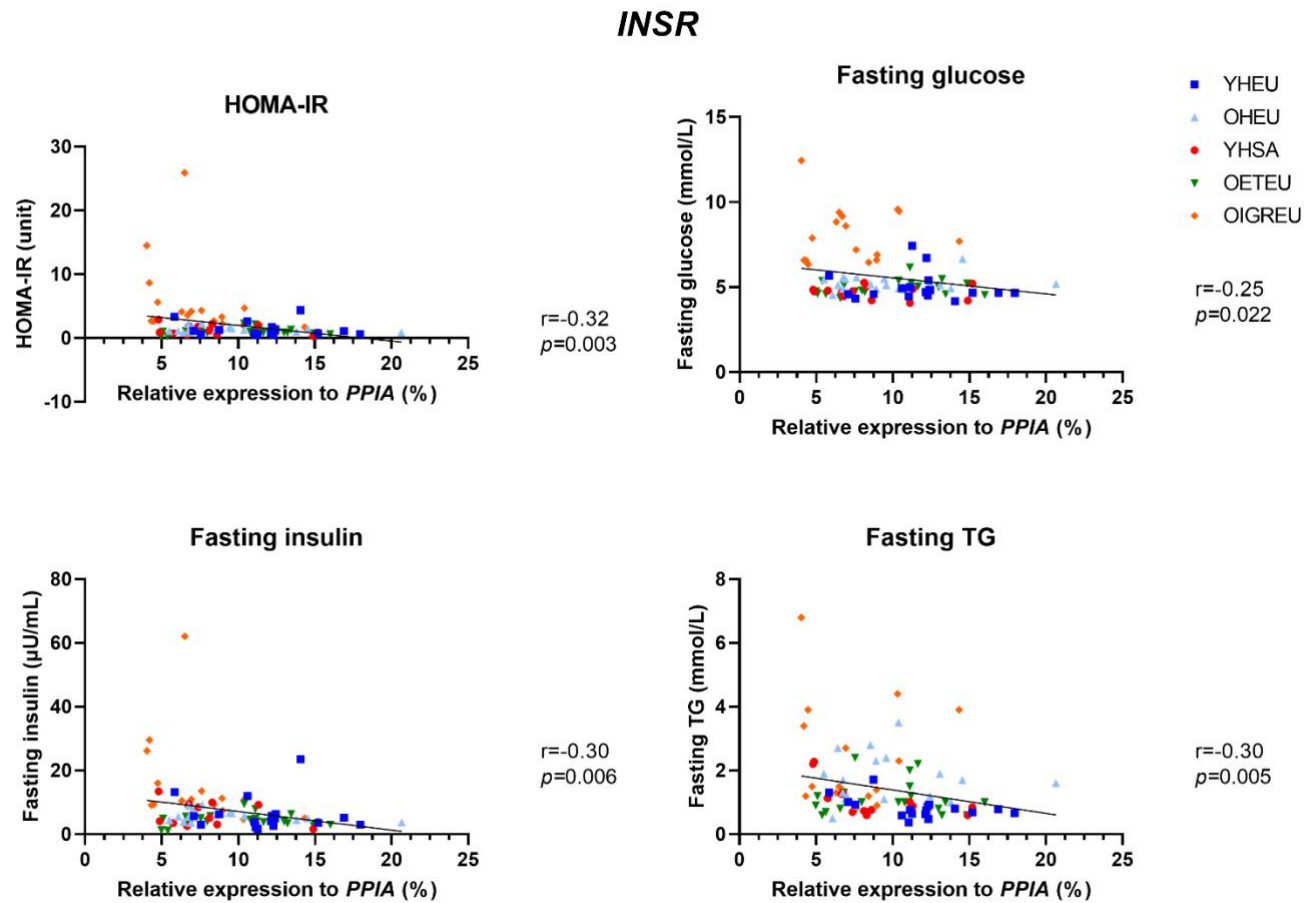
Figure 3-52 Univariate analysis: relationship between adipocyte *INSR* expression and blood metabolic parameters.

Participants: Young Healthy European (YHEU), older Healthy European (OHEU), Young Healthy South Asian (YHSA), Older Endurance trained European athletes (OETEU), and Older Europeans with impaired glucose regulation (OIGREU), n = 86.
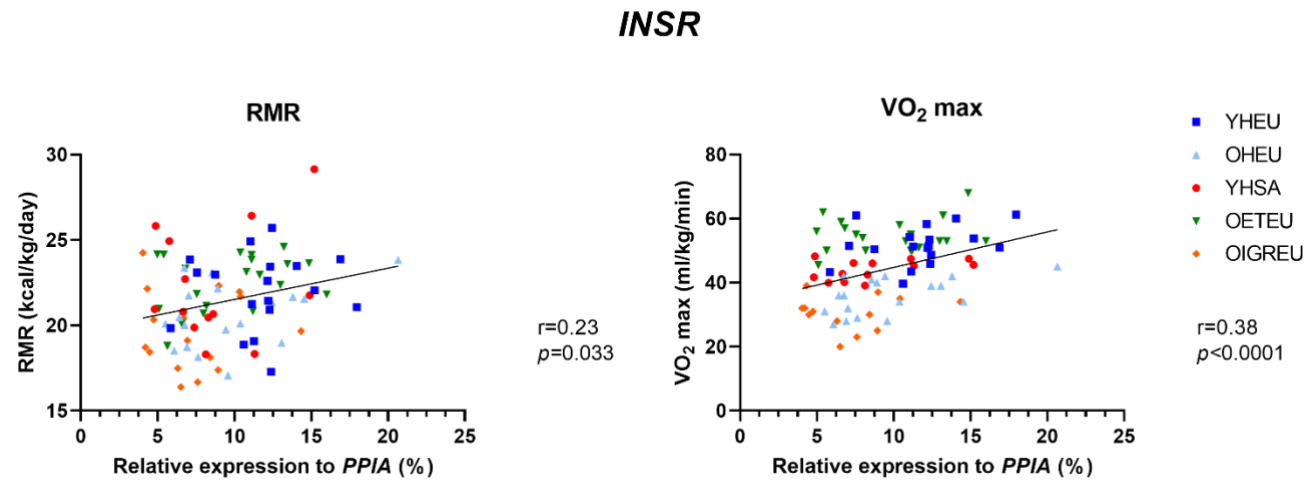
Figure 3-53 Univariate analysis: relationship between adipocyte *INSR* expression and fitness.

Participants: Young Healthy European (YHEU), older Healthy European (OHEU), Young Healthy South Asian (YHSA), Older Endurance trained European athletes (OETEU), and Older Europeans with impaired glucose regulation (OIGREU), n = 86.
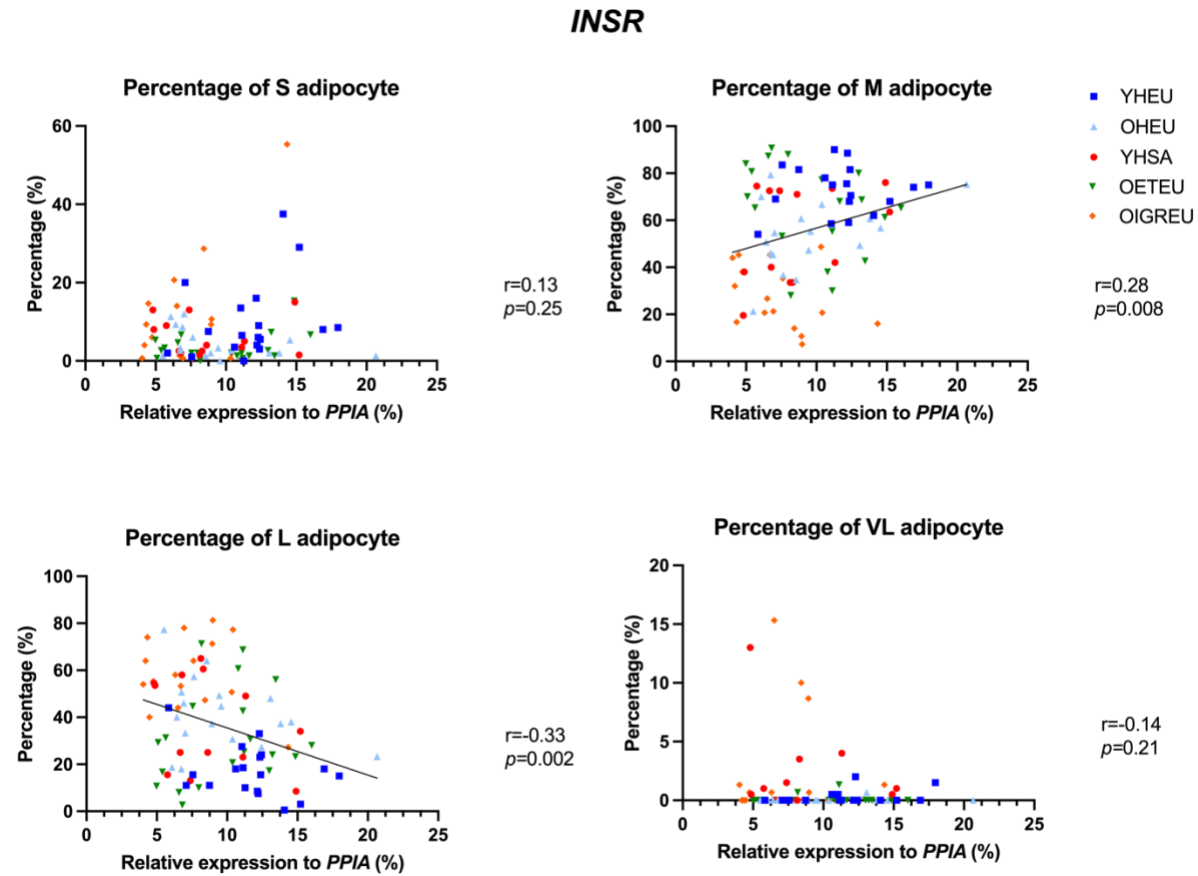
Figure 3-54 Univariate analysis: relationship between adipocyte *INSR* expression and adipocyte size distribution.

Proportion of small (S), medium (M), large (L), and very large (VL) adipocytes in Young Healthy European (YHEU), older Healthy European (OHEU), Young Healthy South Asian (YHSA), Older Endurance trained European athletes (OETEU), and Older Europeans with impaired glucose regulation (OIGREU), n = 86.

INSR	B-coefficient	95% CI	*p*	R^2	R^2 of model
BMI	-0.019	(-0.029, -0.009)	< 0.0001	20.6%	
Fasting TG	-0.031	(-0.068, 0.005)	0.091	2.7%	26.9%
% S adipocyte	0.004	(-0.00003, 0.007)	0.052	3.7%	

Table 3-12 Regression analysis by reverse stepwise: adipocyte *INSR* expression versus factor and covariates.

Factor (group) and covariates (anthropometric characteristics, blood metabolic variables, fitness, and proportion of small, medium, large and very large adipocytes).

3.3.6.3 Contribution of anthropometric and metabolic parameters and adipocyte diameter to adipocyte *LEP* expression

The correlations between *LEP* expression and covariates HOMA-IR age, BMI, waist, RMR, VO_2 max, fasting glucose, fasting insulin, fasting TG and adipocyte diameter were analysed in univariate analysis (Figure 3-55, Figure 3-56, Figure 3-57 and Figure 3-58). Eight positive correlations were found between *LEP* expression and HOMA-IR age, BMI, waist, fasting glucose, fasting TG and proportion of L and VL adipocytes (R = 0.38, 0.43, 0.40, 0.48, 0.26, 0.28, 0.63 and 0.37, *p* < 0.0001, < 0.0001, < 0.0001, < 0.0001, = 0.017, 0.009, < 0.0001 and = 0.001, respectively), and three negative correlations were found between *LEP* expression and RMR, VO_2 max and proportion of M adipocytes (R = -0.36, -0.54 and -0.61, *p* = 0.001, < 0.0001 and < 0.0001, respectively).

Fasting glucose and VO_2 max were independently and negatively, and proportion of L and VL adipocytes were independently positively associated with *LEP* expression (Table 3-13).
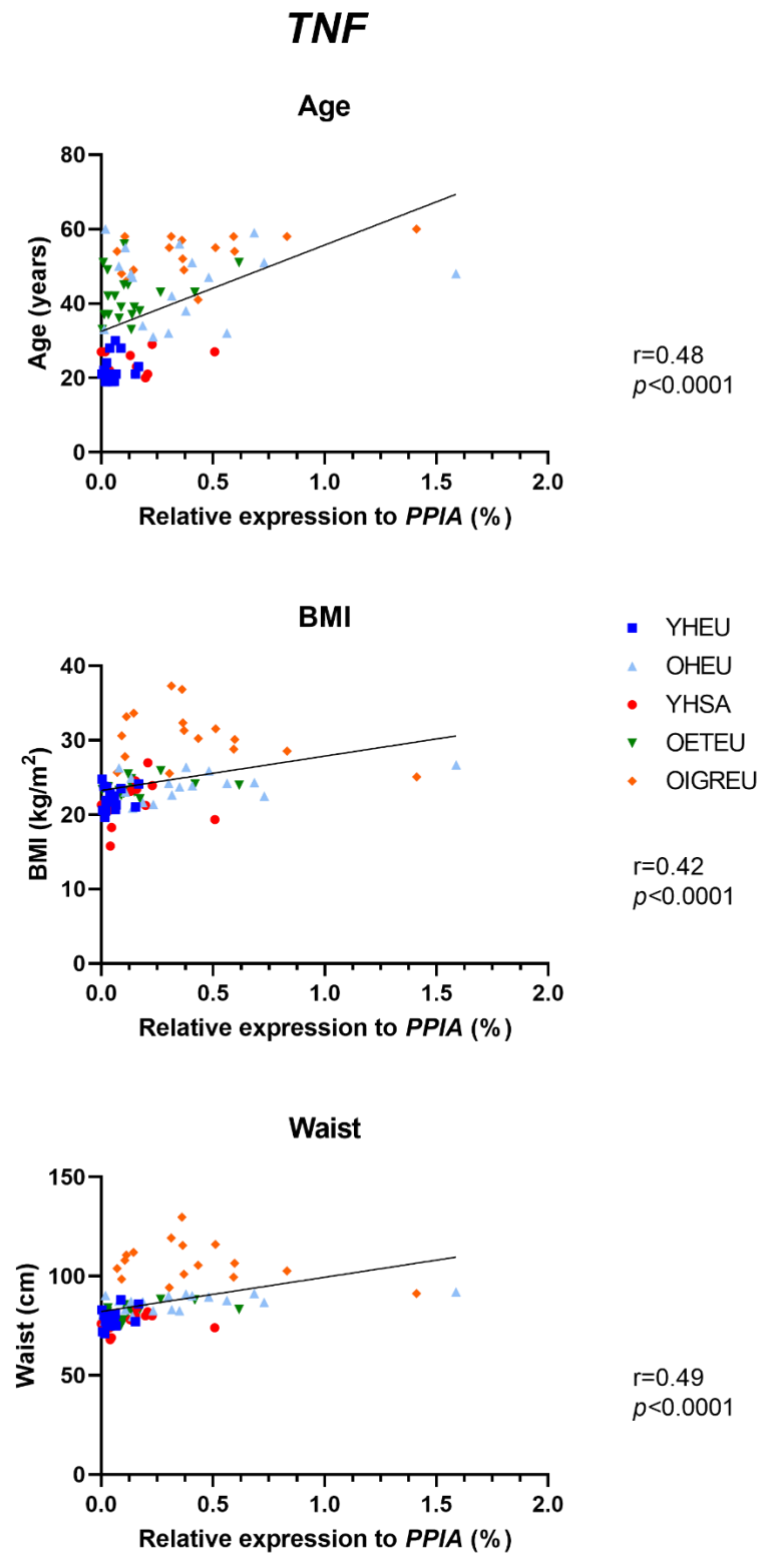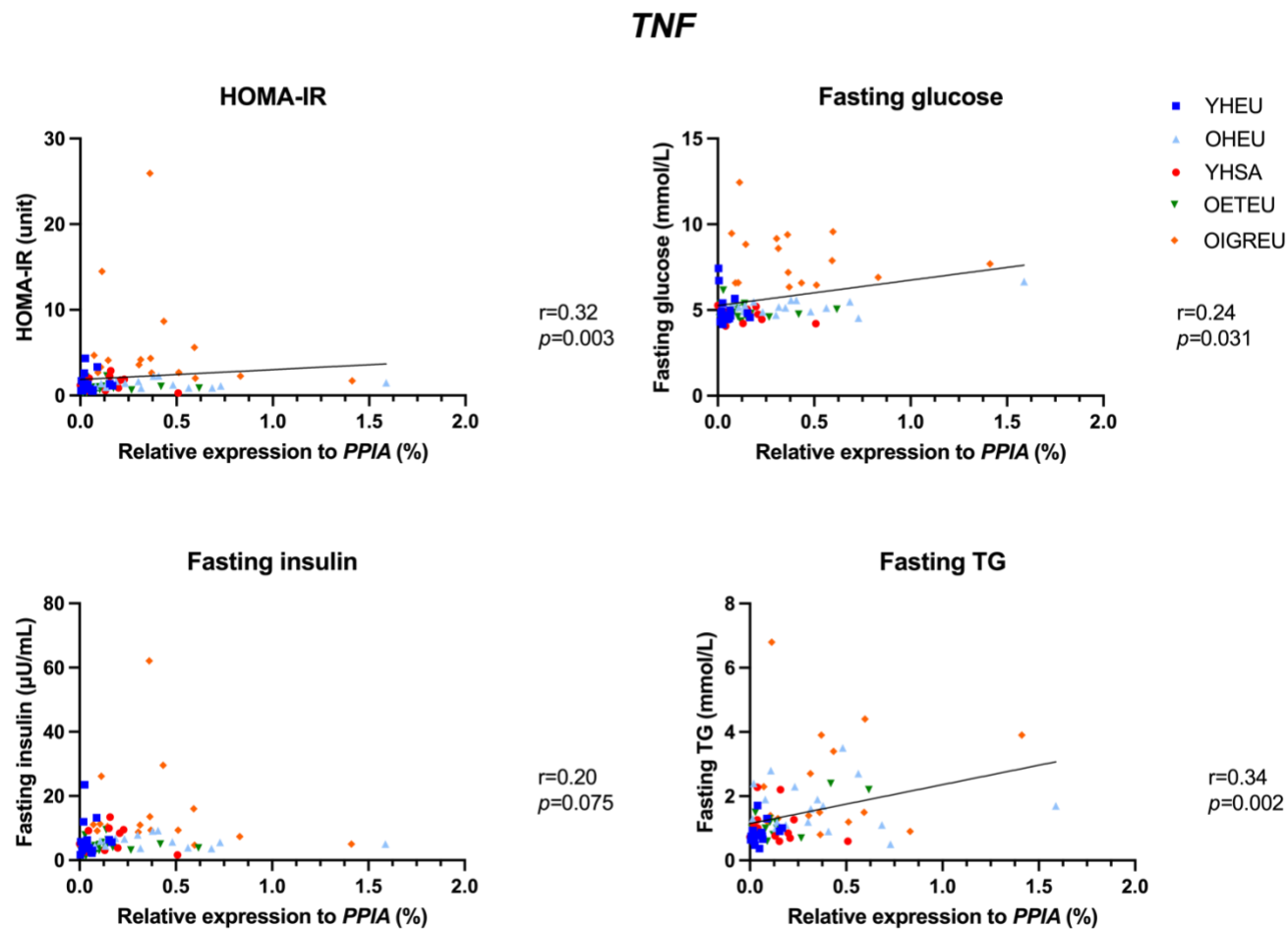
LEP

Age

BMI

Waist
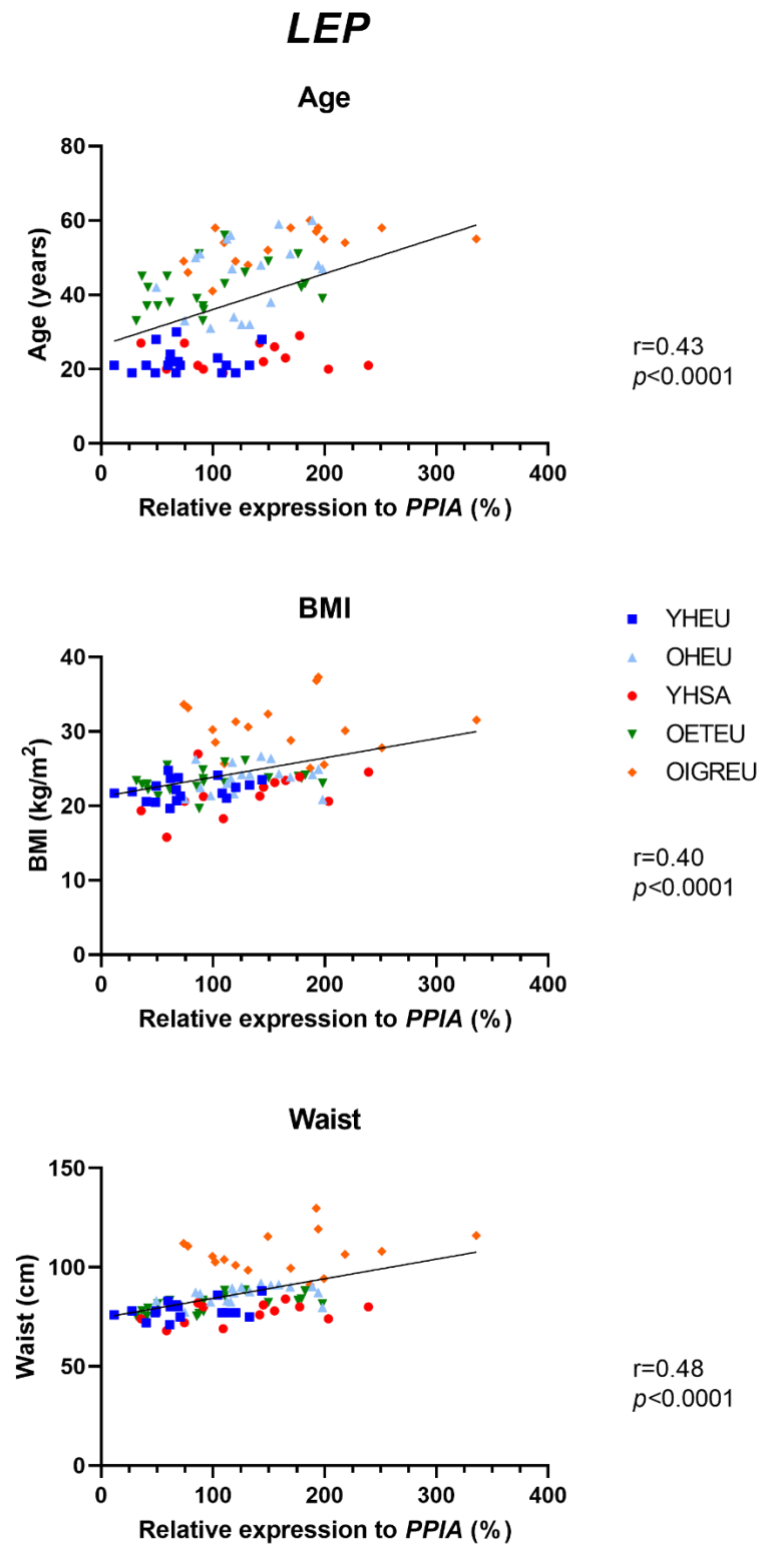
Figure 3-55 Univariate analysis: relationship between adipocyte *LEP* expression and anthropometric characteristics.

Participants: Young Healthy European (YHEU), older Healthy European (OHEU), Young Healthy South Asian (YHSA), Older Endurance trained European athletes (OETEU), and Older Europeans with impaired glucose regulation (OIGREU), n = 86.
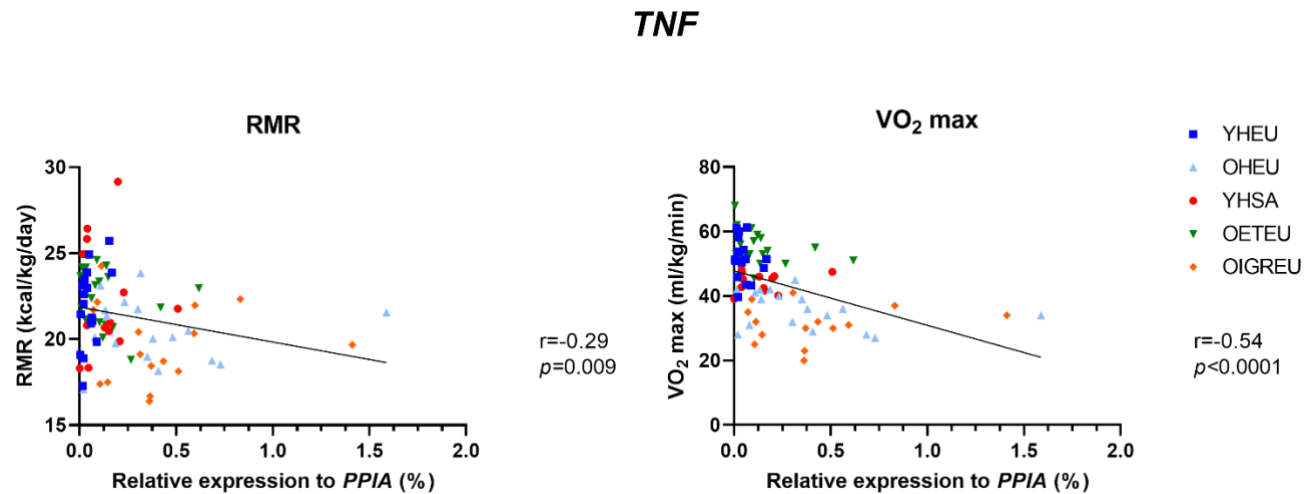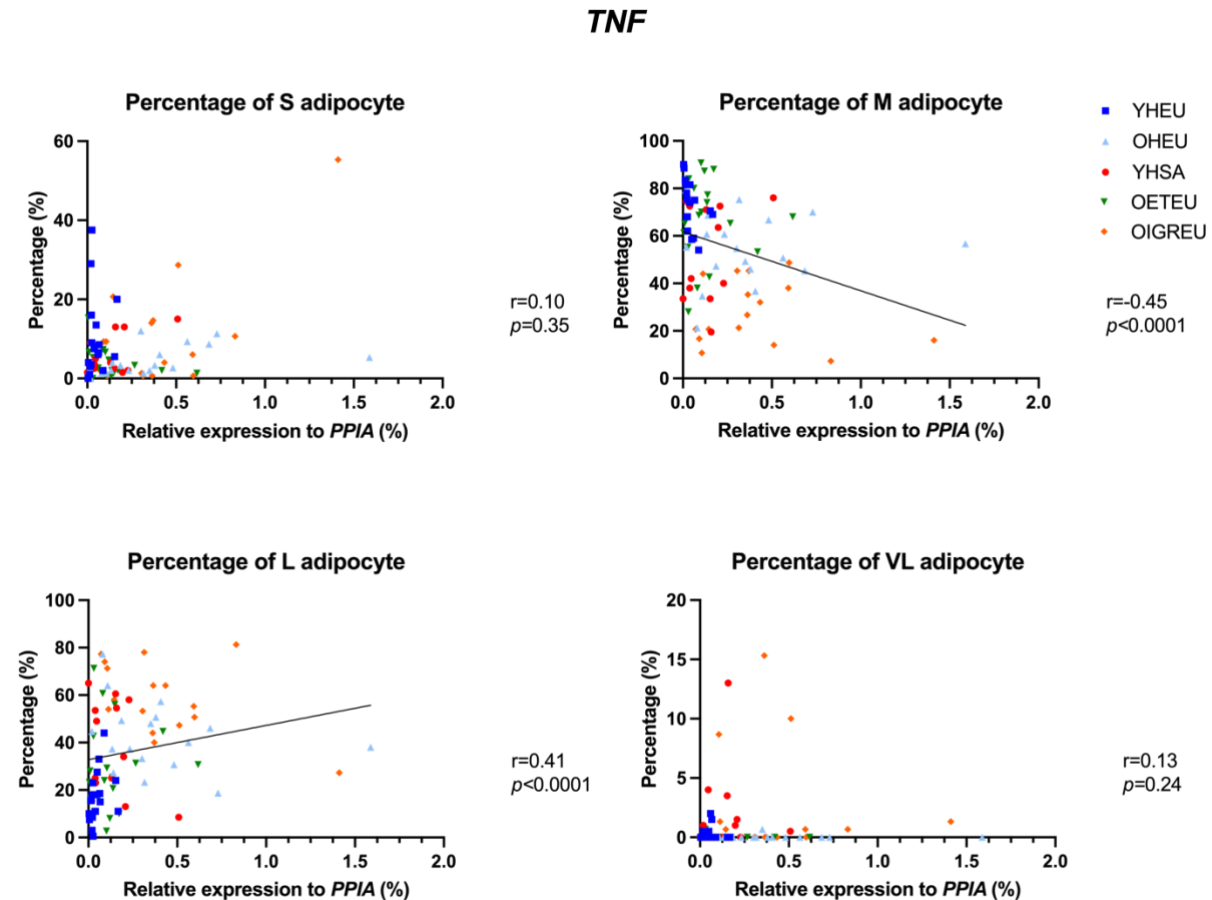
LEP
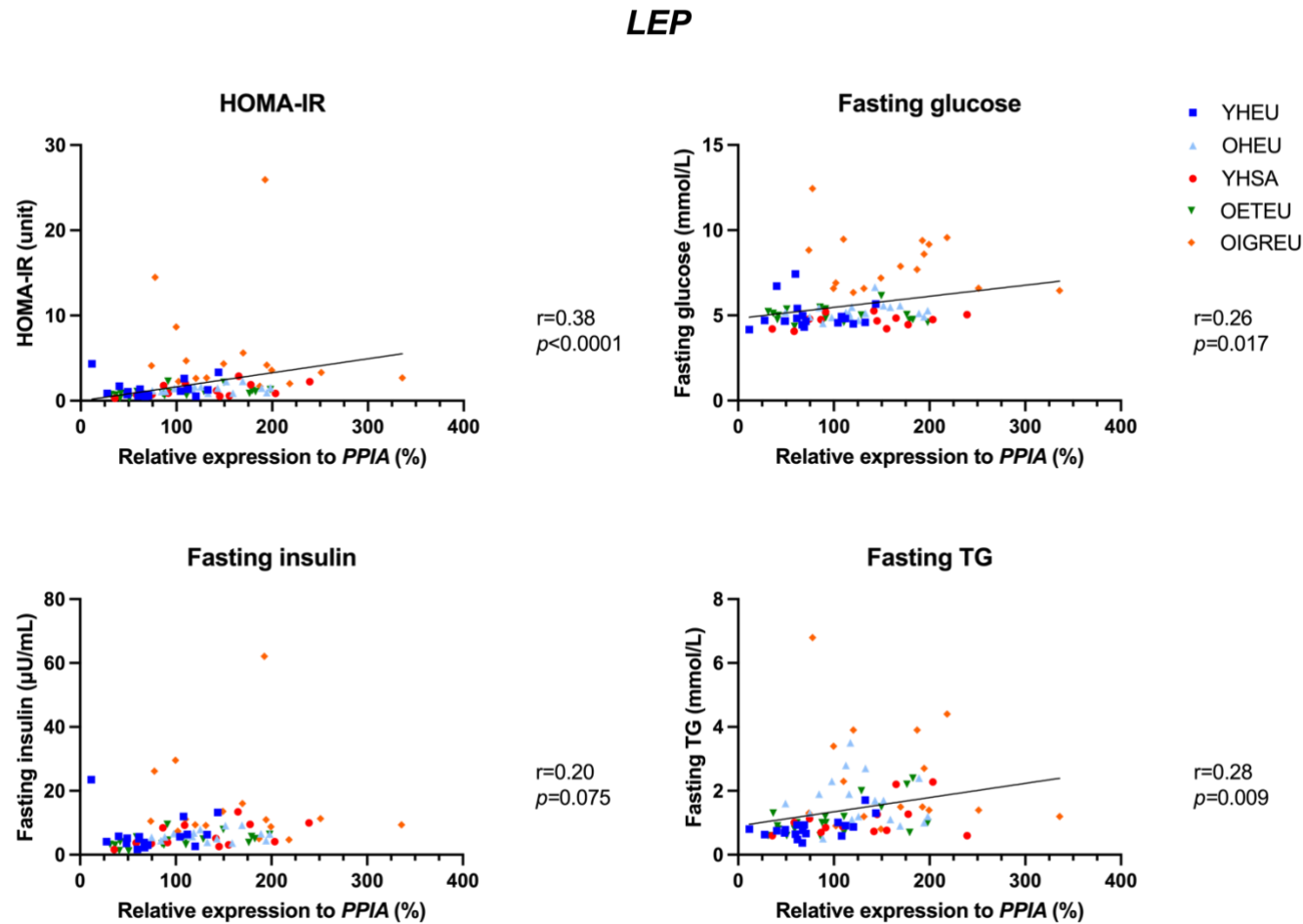
Figure 3-56 Univariate analysis: relationship between adipocyte *LEP* expression and blood metabolic parameters.

Participants: Young Healthy European (YHEU), older Healthy European (OHEU), Young Healthy South Asian (YHSA), Older Endurance trained European athletes (OETEU), and Older Europeans with impaired glucose regulation (OIGREU), n = 86.
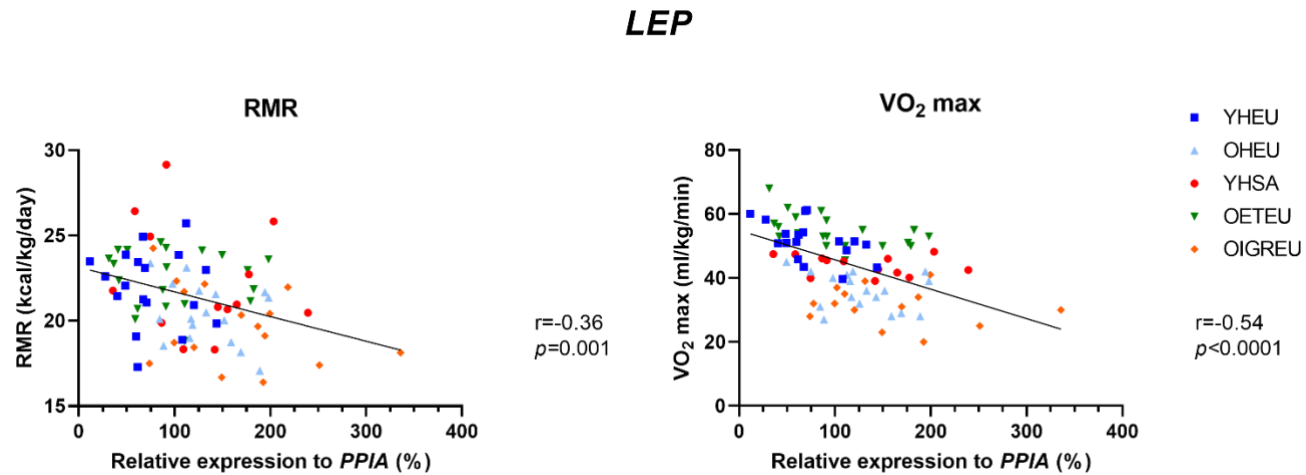
Figure 3-57 Univariate analysis: relationship between adipocyte *LEP* expression and fitness.

Participants: Young Healthy European (YHEU), older Healthy European (OHEU), Young Healthy South Asian (YHSA), Older Endurance trained European athletes (OETEU), and Older Europeans with impaired glucose regulation (OIGREU), n = 86.

LEP
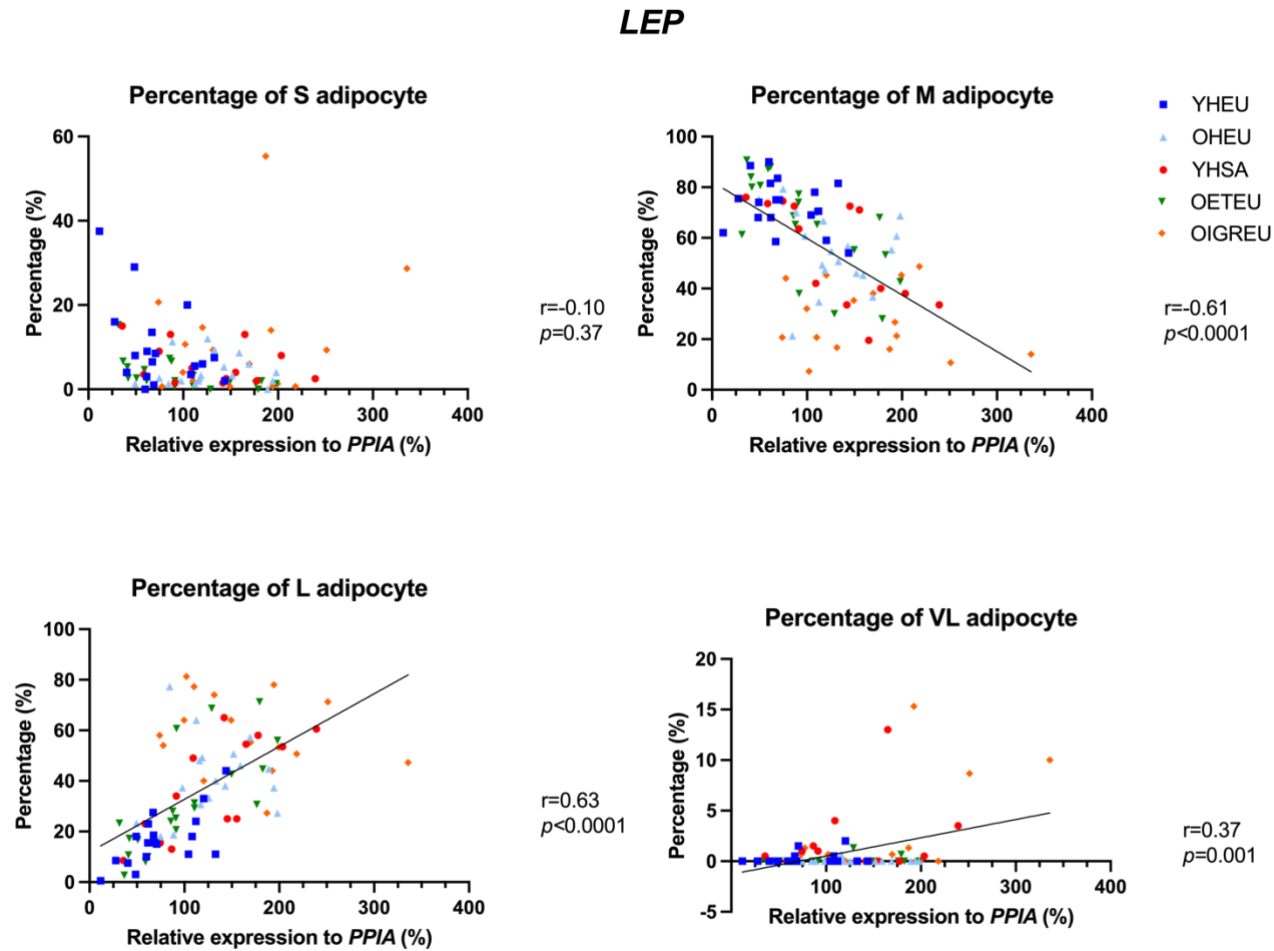
Figure 3-58 Univariate analysis: relationship between adipocyte *LEP* expression and adipocyte size distribution.

Proportion of small (S), medium (M), large (L), and very large (VL) adipocytes in Young Healthy European (YHEU), older Healthy European (OHEU), Young Healthy South Asian (YHSA), Older Endurance trained European athletes (OETEU), and Older Europeans with impaired glucose regulation (OIGREU), n = 86.

LEP	B-coefficient	95% CI	p	R^2	R^2 of model
Fasting insulin	-0.088	(-0.161, -0.016)	0.018	4.0%	
VO₂ max	-0.080	(-0.133, -0.027)	0.004	25.7%	51.7%
% L adipocyte	0.058	(0.033, 0.083)	< 0.0001	14.4%	
% VL adipocyte	0.36	(0.15, 0.56)	0.001	7.6%	

Table 3-13 Regression analysis by reverse stepwise: adipocyte *LEP* expression versus factor and covariates.

Factor (group) and covariates (anthropometric characteristics, blood metabolic variables, fitness, and proportion of small, medium, large and very large adipocytes).

3.4 Discussion

The observations of the current study were that size, size distribution and gene expression in subcutaneous adipocytes were significantly different across the OETEU, YHSA, YHEU, OHEU and OIGREU groups. As predicted, the size and function of adipocytes were independently associated with anthropometric and metabolic parameters.

The distributions of adipocyte size and volume were significantly different across the five groups. When all the parameters were included in a multivariate model to predict adipocyte diameter, age was the only significant independent predictor of adipocyte size without group, but not independent from group. Age predicted adipocyte diameters in YHEU, OHEU, OETEU and IGT, but not in YHSA. Adipocyte diameter in YHSA was similar to OETEU and OHEU. The distribution of adipocyte size was significantly different between young South Asians and Whites at similar age or adipocyte diameter. At a similar age, YHSA had fewer medium adipocytes and more large adipocytes than Whites (YHEU). At similar adipocyte size, YHSA stored more fat in very large adipocytes than Whites (OHEU and OETEU). YHSA stored a similar level of fat in very large adipocytes to Whites with impaired glucose tolerance i.e. than the OIGREU group. This agreed with other literature and the hypothesis that YHSA have similar adipocyte size to older Whites. It has been well recognised that adipocyte size is associated with insulin resistance, and reduced adipocyte diameter after weight loss improves insulin sensitivity (Andersson *et al.*, 2014, Andersson *et al.*, 2017, Ryden *et al.*, 2014, Eriksson-Hogling *et al.*, 2015). It has been highlighted that the distribution of adipocytes, in which increased very large (> 100 μm) or accumulation of small immature

adipocytes (< 55 µm), may contribute to insulin resistance and even inflammation (McLaughlin *et al.*, 2019, McLaughlin *et al.*, 2010a, McLaughlin *et al.*, 2007a). As obesity develops, the newly recruited small mature adipocytes may 'protect' the adipocytes from overload of excess energy and the development of hypertrophic adipocytes (Heilbronn *et al.*, 2004). However, patients with impaired maturation of small adipocytes into functional mature adipocytes undergo hypertrophic expansion into dysfunctional oversized mature adipocytes and are at higher risk of developing insulin resistance and T2DM (Fang *et al.*, 2015, Heilbronn *et al.*, 2004, DeFronzo, 2004, Yang *et al.*, 2004). Despite YHSA being of similar BMI and HOMA-IR to YHEU and OHEU and being younger, of lower BMI and fitter than OIGREU, YHSA stored a similar amount of fat in very large adipocytes to OIGREU. This suggests that YHSA have defects in adipocyte function relative to YHEU and OHEU that have not yet developed fully into the outright dysfunction of OIGREU. YHSA still maintain a healthy plasma fasting glucose and TG but may be at more risk of developing further adipocyte dysfunction in response to WG and age. However, the mechanism remains unclear.

In multivariate analysis, only *LEP* expression was strongly positively independently associated with adipocyte diameter and this was independent of group. Adipocyte diameter was an independent predictor of *LEP* expression between the groups. YHEU had the smallest adipocytes compared to other groups. All groups, apart from OETEU, had higher levels of *LEP* expression in adipocytes than YHEU. Adipocyte diameter predicted *LEP* expression in all groups except for OETEU. OETEU had larger adipocytes but lower expression of *LEP*. This may correlate with TG turnover in adipocytes, which was expected to be higher in OETEU, and in this situation *LEP* expression may be not increased with increased adipocyte size. By measuring the half-life of TG in adipocytes using the incorporation of atmospheric ^{14}C into adipocyte lipids, investigators found that TG turnover and lipolytic rate were decreased in overweight subjects (Rydén *et al.*, 2013). However, at similar BMI, highly trained athletes (Perseghin *et al.*, 2009) and marathon athletes (Leal-Cerro *et al.*, 1998) showed a significantly lower level of serum leptin than health controls. In addition, an *in vitro* study showed that norepinephrine-induced lipolysis rate, leptin secretion and *LEP* expression from human ASAT differentiated adipocytes increased to a similar extent, suggesting that leptin secretion, as well as *LEP* expression in adipocytes may represent the TG turnover rate (van Harmelen

et al., 2002). Interestingly, in the current study, expression of a lipogenesis gene (*SREBF1*) was markedly higher in OETEU compared to other groups, and a lipolysis marker (*LPL*) was higher in OETEU than YHSA, also suggesting that OETEU may have more active lipid metabolism in adipocytes compared to other groups. Growing evidence suggests that hypertrophy leads to adipocyte dysfunction and increased lipolysis, which results in overflow of fatty acids to visceral fat, liver and skeletal muscle (van Harmelen *et al.*, 2003, Arner *et al.*, 2010a, Sniderman *et al.*, 2007). However, the higher *LPL* expression in OETEU than YHSA did not result in a higher level of plasma TG in OETEU, which suggests that OETEU may have a higher capacity for fatty acid oxidation. This may protect the endurance trainers from damage resulting from overflow of FFA. Therefore, *LEP* expression in subcutaneous adipocytes predicts the size of adipocytes, however, endurance exercise may decrease *LEP* expression compared to controls with similar adipocyte size or/and BMI, and this may be mediated by increased TG turnover in adipocytes.

In univariate analysis, the current study found that adipocyte size was strongly associated with anthropometric and metabolic parameters, and expression of *TNF* and *INSR*. This indicates that adipocyte size is a strong predictor of whole body metabolism, fitness, and adipocyte function. The strong univariate correlations between adipocyte size and fasting glucose, fasting TG and HOMA-IR in the current study are similar to an earlier study showing that an increase in adipocyte size was associated with hypertriglyceridemia and hyperinsulinemia (Veilleux *et al.*, 2011, Misra and Khurana, 2011b, Indulekha *et al.*, 2011, Meena *et al.*, 2014a). Similarly, the univariate correlations between expression of *TNF*, *INSR* and *LEP* and adipocyte diameter were also found in previous human studies (Bambace *et al.*, 2011, Acosta *et al.*, 2016, Laviola *et al.*, 2006b).

VO_2 max independently predicted the expression of *PPARG*, *ADIPOQ* and *TNF* (negative association) in the current study. When group was added to the multivariate model, VO_2 max remained independently associated with *ADIPOQ* expression. Adiponectin, fasting and exercise are activators of AMP-activated protein kinase (AMPK) in adipocytes via changes in the AMP/ATP ratio. Once AMPK is activated, AMPK supresses fatty acid efflux from adipocytes and increases the local fatty acid oxidation in adipocytes. In young and lean healthy individuals, adiponectin suppressed both spontaneous and catecholamine-induced lipolysis, but this effect was decreased in obese subjects, and AMPK may be involved in this

mechanism (Wedellová *et al.*, 2011). In this way, metabolic fitness may improve insulin sensitivity by increasing adiponectin secretion from adipocytes and in return, suppressing the release of FFA into the circulation. Furthermore, cardiovascular fitness may increase the potential for adipocyte differentiation and hyperplastic expansion resulting in insulin sensitive adipocytes with enhanced efficiency for storage and oxidation of fatty acids. A study has shown similar results where plasma PPARγ was higher in participants with higher VO_2 max (Antunes *et al.*, 2020). This supports our finding that endurance exercise may increase the potential for adipocyte differentiation. In a study of 53 men, a strong correlation was found between VO_2 max and adiponectin/leptin ratio (r = -0.67, *p* < 0.01), the adiponectin/leptin ratio was lower in glucose intolerant patients than in trained men (0.27 ± 0.06 vs 4.75 ± 0.82, *p* < 0.0001), and fitness was the strongest independent predictor of insulin sensitivity (Huth *et al.*, 2016). This suggests that endurance exercise may increase insulin sensitivity independently by regulating the secretion of adipokines. There was a negative association between VO_2 max and adipocyte *TNF* expression in the current study which was independent of other metabolic predictors, but not of group. Cardiovascular fitness may decrease the inflammatory response in adipose tissue and may explain the higher adipocyte TNF expression in OHEU and OIGREU groups. A previous study has also shown a strong correlation between VO_2 max and serum TNF-α concentrations (r = -0.29, *p* < 0.01, n = 52) (Rosado-Perez and Mendoza-Nunez, 2018). The relatively high level of fat utilisation in cardiovascular exercise may lower plasma and ectopic fatty acid accumulation and subsequently lower the expression of *TNF* (Kelley, 2001). Interestingly, VO_2 max showed a trend towards a decrease with age in YHEU, OHEU and OIGREU, however, OETEU had higher fitness while YHSA had lower fitness than YHEU. This suggested that physical activity can improve fitness significantly, and South Asians have worse fitness compared to Whites at similar age, BMI and physical activities. The lower fitness of South Asians may in turn contribute to dysfunction of adipocytes via decreased adiponectin secretion, adipogenesis and increased TNF-α release from adipocytes.

Age was also an independent predictor of adipocyte expression of *PPARG* and *ADIPOQ*. When group was added to these models the association with age was lost suggesting that differences in age between the groups, at least in part, explained the group differences in adipocyte diameter, *PPARG* and *ADIPOQ* expression.

Mature adipocytes proliferate and differentiate from MSC in the adipose stromal fraction. The ability of adipose tissue to undergo hyperplastic expansion is determined by the replicative potential and differentiation capacity of MSC. In a previous study, isolated human ASC from subcutaneous adipose tissue of 12 female donors was classified into three age ranges: 25 - 30, 40 - 45, 55 - 60 years old. The results showed a decrease in both replicative potential and the differentiation capacity was primarily correlated with increasing age, where younger participants expressed PPAR-γ protein at a higher level than older participants (Schipper *et al.*, 2008). However, in the current study, expression of *PPARG* was higher in OHEU than in YHEU, and expression of *PPARG* was the highest in OETEU, but lower in YHSA, YHEU and OIGREU. The pattern of *PPARG* expression did not fit the pattern of age and did not agree with previous literature (Gustafson *et al.*, 2019a). This may suggest that *PPARG* expression in adipocytes may not be the same as in MSC. *PPARG* expression in adipocytes may not correlate with differentiation directly. In addition, there was an independent association with group which suggested age may not be the primary predictor of *PPARG* expression in adipocytes. To investigate the expression of *PPARG* in adipocytes and MSC related with other factors remains meaningful. There are few published data on age-related *ADIPOQ* expression in adipocytes, however, with increasing age after 75 years old, the decrease in white adipocyte depots and the appearance of dysfunctional adipocyte-like cells may contribute to a decreased secretion of adiponectin (Kirkland *et al.*, 2002).

Insulin resistance (HOMA-IR) was an independent predictor of *PPARG* expression (negative predictor), and fasting glucose, another index of insulin resistance, was an independent predictor of *TNF* and *LEP* expression. These associations were all lost when group was included in the model, and thus differences in insulin resistance may contribute to the significant differences in *PPARG*, *TNF* and *LEP* adipocyte expression observed between groups. A study of 42 T2DM and 25 non diabetic overweight patients of mixed sex but matched for age and BMI, showed that patients with T2DM had a significantly lower glucose disposal and lower expression of *PPARG* in the adipocytes than obese controls ($p < 0.001$, = 0.04 and = 0.02, respectively) (Dubois *et al.*, 2006). This suggests that impaired insulin sensitivity may lead to a decrease in adipogenesis and expression of genes that promote adipocyte differentiation. It is interesting that plasma glucose was

independently associated with adipocyte *TNF* and *LEP* expression in the current study. Elevated levels of plasma TNFα, primarily derived from immune cells within adipose tissue, are observed in dyslipidaemia and insulin resistance. This is due to the direct suppression of adiponectin production by TNFα in obesity-related T2DM (Cawthorn and Sethi, 2008). High adipose tissue and plasma TNFα concentrations are positively correlated with insulin resistance (Cawthorn and Sethi, 2008). A study has shown that deletion of *TNF* or its receptor (TNFR) can significantly reduce insulin resistance and increase insulin signalling in *ob/ob* mice and in diet-induced obese mice (Uysal *et al.*, 1997b) suggesting a direct link between TNFα and insulin resistance. Similarly, increased expression of *LEP* is associated with insulin resistance (Bidulescu *et al.*, 2020, Coimbra *et al.*, 2014, Frederich *et al.*, 1995). However, patterns of *TNF* and *LEP* expression in both YHSA and OETEU did not necessarily follow the insulin sensitivity and/or circulating glucose level. As previously detailed in OETEU, the enhancement of fitness, lipid metabolism, and local fatty acid oxidation could potentially moderate the inflammatory response and insulin resistance in adipocytes. YHSA, on the contrary, had a similar level of *TNF* and *LEP* expression with older Whites, suggesting that their higher risk of T2DM compared to Whites may involve the inflammatory response and adipokine secretion from adipocytes as well.

3.5 Strength and limitations

The endurance athletes in this study had a history of more than two years regular cardiovascular exercise, and many had been exercising for a significant proportion of their lives. Similarly, controls had been sedentary for a significant period. Due to this long period of consistent behaviour, it would be expected that the adipocyte measurements made in the current study will represent true metabolic differences and minimise the impact of acute changes in adipocyte function. YHSA and YHEU were well matched with each other in age and BMI, and the OHEU also had a similar BMI with YHEU. The patients in the OIGREU group were at an early stage of T2DM or "pre-diabetic" meaning that adipocyte function measures may reflect the pathological process of increasing insulin resistance and not the long-term effects of chronic insulin resistance which may include tissue necrosis. Therefore, the selection and rigour in recruitment criteria provide a reliable and comparable perspective to understand the role of adipocytes in the development of insulin resistance and T2DM.

However, there were limitations due to the combinations of the two studies. There was a difference between age, BMI and waist, which may contribute to the metabolic and physiological differences across the five groups rather than exercise and insulin resistance. However, age, RMR and VO$_2$ max were well spread, which allowed the current study to examine the changes continuously. Apart from OIGREU, BMI was well matched in the other four groups, especially between the YHEU and OHEU. The two studies were started at different times and biopsies were performed by different clinicians, however, there was a cross over in the period of recruitment. The biopsies in the two studies were the same and the outcome (tissue weight) was the same as well. The two studies examined percentage body fat using different methods, so it could not be used in the current study, which may limit the interpretation of the influence of adiposity on adipocyte function.

Recognising the progress in the field of insulin resistance evaluation, it is crucial to underscore the evolution of the HOMA-IR, notably the introduction of HOMA2-IR (Levy *et al.*, 1998). This refined model integrates further parameters, including variations in hepatic and peripheral glucose resistance, increases in the insulin secretion curve for plasma glucose concentration above 10 mmol/L, and the contribution of circulating proinsulin. This model also evaluates beta cell function (%B) and insulin sensitivity (%S) of 100% in healthy young adults. The improved sensitivity and specificity of HOMA2-IR facilitate a more detailed description of metabolic health (Demir *et al.*, 2020). A limitation of the current research is its reliance on the original HOMA-IR model, which does not consider these supplementary factors. The employment of HOMA2-IR might have provided a more accurate assessment of insulin resistance, thus enhancing the richness of the study's findings. Furthermore, it is pertinent to note that the original HOMA model recommends the use of the average of three fasting measurements to bolster the reliability of the evaluation. This study adhered to this guideline, thereby strengthening the robustness of our results. However, it also highlights the limitation that singular fasting measurements, commonly utilised in clinical practice, may not yield a comprehensive portrayal of insulin resistance.

In the present study, a systematic examination of the size of SAT and the expression of specific genes within the adipocytes was conducted across the study cohorts, alongside an analysis of anthropometric and metabolic parameters. This

approach facilitated a comprehensive understanding of the variations in adipocyte morphology and gene expression between cohorts with differing levels of insulin sensitivity. However, it is important to note the limitation that while gene expression was measured, this does not equate to a direct assessment of adipocyte function. Gene expression levels provide valuable insights, but they do not necessarily reflect the functional status of the encoded proteins. Factors such as post-translational modifications, protein stability, and interactions with other proteins can significantly influence the activity of an enzyme *in vivo*, e.g. lipoprotein lipase (LPL). Therefore, while gene expression data can suggest potential functional differences, direct functional assays would provide more definitive evidence. Moreover, it has been suggested that VAT may have a stronger association with insulin resistance than subcutaneous adipose tissue in certain populations, such as Indians (Indulekha *et al.*, 2011). The current study, due to the challenges associated with collecting visceral adipose tissue, did not examine adipocyte size or gene expression in VAT. This limitation restricted the ability to fully understand the distinct roles that VAT might play across the five cohorts. Future studies could benefit from incorporating functional assays and, where possible, an examination of VAT to provide a more comprehensive picture of adipose tissue's role in insulin sensitivity.

The current study contains no women. The aim of the current uni-sex study was to minimize the variables when systematically investigating adipocyte function, which is a strength of the study. However, previous studies have shown that significant correlations between adipocyte size and TG, TC and LDL-c were of a similar direction but stronger in females than males, which suggests that size of adipocytes may associate with metabolic parameters differently with sex (Meena *et al.*, 2014a). The absence of female participants limited the understanding of sex differences in adipocyte function, but the current study could be a reference for female (or mixed sex) studies in the future.

There was no RNA transcriptomics assay to examine the expression of all genes in adipocytes because of the budget. Therefore, only limited numbers of genes could be examined in adipocytes, so that the understanding of adipocytes at the gene expression level was not comprehensive in the current study. However, the selection of genes was based on literature review and covers the key pathways involved in the major metabolic function of adipocytes.

3.6 Conclusion

Endurance exercise improved metabolic fitness, which resulted in an increase in expression of genes associated with lipid metabolism and local fatty acid oxidation and decreased the inflammatory response and insulin resistance in adipocytes, without changing the size of adipocytes.

Aging positively correlated with adipocyte size, expression of genes associated with adipokine and adipocyte differentiation in adipocytes, but it was dependent on group. This may imply effects of age on adipokine secretion are attenuated by exercise. Severity of insulin resistance correlated with expression of genes associated with inflammatory response and adipokines in adipocytes, but was not independent from groups.

YHSA had a similar adipocyte size, and adipocyte expression of genes associated with adipogenesis, lipid metabolism, insulin signalling and adipokines to BMI matched older Whites. YHSA also stored similar amounts of fat in hypertrophic adipocytes to OIGREU Whites, but they showed normal insulin sensitivity. This suggests that YHSA still maintain a healthy plasma fasting glucose and TG but may be at more risk of developing further adipocyte dysfunction in response to WG and Age.

In order to understand the mechanisms in adipocytes underlying the higher risk of developing T2DM in YHSA at younger age and leaner weight, it would be useful to examine the difference in adipocyte morphology in Chapter 4, expression of genes associated with adipogenesis, insulin signalling, lipid metabolism, adipokine and inflammatory response in adipocytes in YHSA in response to WG compared to Whites with similar age and BMI in Chapter 5.

In order to understand the different roles of genes associated with adipogenesis in MSC and adipocytes, expression of these genes could be examined by *in vitro* stimulation of adipogenesis, using MSC isolated from different cohorts in Chapter 6.

Chapter 4   Change in subcutaneous adipocyte size in response to weight gain in young, lean European and South Asian men

4.1 Introduction

In normal healthy individuals, adipose tissue stores the majority of excess energy intake and regulates energy balance and glucose homeostasis (Rosen and Spiegelman, 2006). It stores excess free fatty acids (FFA) as triglycerides (TG) in a lipid droplet within each adipocyte (Ibrahim, 2010, Tandon *et al.*, 2018). Around 80% of body fat is stored in the SAT depot. Adipose tissue (AT) can expand its triglyceride storage capacity in response to excess energy intake by increasing the number of adipocytes (hyperplasia) and/or increasing the average volume of adipocytes (hypertrophy) (Salans *et al.*, 1973, Spalding *et al.*, 2008). Hypertrophic expansion is thought to have pathological consequences that are not associated with hyperplastic expansion. For example, adipocyte size predicted the degree of insulin resistance (IR) in 35 relatives of T2DM aged between 28 - 49 years (R^2 = 0.53, *p* < 0.001) (Yang *et al.*, 2012). Hypertrophy is also associated with hyperleptinemia (Després *et al.*, 2000) and dyslipidaemia (Veilleux *et al.*, 2011). When the capacity of SAT adipocytes to store fat is exceeded or the formation of new adipocytes via adipogenesis is reduced, the ability of adipocytes to store additional TG is diminished and spill-over of FFA from SAT adipocytes occurs and FFA are stored ectopically in visceral fat and other tissues in the form of triglyceride lipid droplets (Ibrahim, 2010). As mentioned in the introduction and discussed in result Chapter 3, with a similar BMI, SA have a higher chance of developing T2DM compared with EU, and the difference in the risk of T2DM between SA and EU increases significantly with increasing BMI. Therefore, it is of great importance to understand the differences in adipocyte function between SA and EU during the development of T2DM and obesity. This chapter will focus on the changes in adipocyte size, as a marker of hyperplastic or hypertrophic expansion, in response to WG in SA and EU.

There is no consensus as to what diameter constitutes a hypertrophic adipocyte. One commonly cited study has categorised adipocyte size by volume after osmium fixation into 4 sub-distributions: small (S; ~0.02 μL), medium (M; ~0.14 μL), large (L ~0.9 μL) and very large (VL; ~2.5 μL) (Smith *et al.*, 2006) but it should be noted

there is clearly a calculation error resulting in a1000X larger unit of volume in their paper. In this thesis, I have adjusted for this error and calculated the diameters of the four distributions of adipocytes and categorized adipocytes into four distribution groups by diameter as: small (S, mean ~34 μm, range 0-45 μm), medium (M; ~64 μm, 45 - 90 μm), large (L; ~120 μm, 90 – 145 μm) and very large (VL; ~168 μm, > 145 μm).

There are three commonly used methods of preparation of adipocytes for sizing that have been developed since the late 1960s. These are collagenase-digestion, histological fixation of whole adipose tissue and osmium tetroxide fixation of isolated adipocytes followed by automated cell sorter (Beckman Multisizer cell counter) analysis (Fried, 2017). Each method has its own advantages and disadvantages. Laforest *et al.* has shown that the median adipocyte diameter derived from all three methods were intercorrelated (r = 0.46 – 0.83, *p* < 0.001, n = 60) (Laforest *et al.*, 2017). In addition, the association between adipocyte diameter and donor adiposity was only slightly affected by the method used (Laforest *et al.*, 2017).

Of these three methods, collagenase-digestion is the most widely adopted method because of the low cost and short preparation time resulting in adipocyte preparations that are amenable to functional cell analysis and co-isolation of the adipose stromal vascular fraction (SVF) that contains mesenchymal stem cells (MSC)/ preadipocytes. Fixation of adipose tissue using histological fixation or osmium tetroxide fixation requires a large amount of tissue (50 – 100 mg) that cannot be used for further investigation, such as gene expression. Collagenase-digestion generates live adipocytes and SVF that allows functional cell assessment in addition to adipocyte sizing (Laforest *et al.*, 2017) and was therefore selected for the current analysis. Collagenase-digested isolated adipocytes are very fragile and are not suitable for automated sizing using a Multisizer cell counter, therefore adipocytes were sized using microscopic analysis.

The GlasVEGAs study aimed to understand the pathophysiology behind the higher risk of diabetes and IR in SA by studying the response of European Caucasians (EU) and South Asians (SA) to 7% (minimum 5%) weight gain (WG). As an adjunct to that study, this chapter isolated adipocytes from the adipose tissue biopsies collected from GlasVEGAs participants at baseline and after ~6.5% weight gain and

compared the effect of weight gain on the size of SAT adipocytes between EU and SA.

Based on the previous literature described in the introduction (Chapter 1), the hypotheses of this chapter were that:

1. The diameter and volume of SAT adipocytes are larger in SA than in EU at baseline (BL) and after WG;

2. SA store excess energy accumulated during weight gain by hypertrophic expansion, whereas EU store the excess energy by hyperplasic expansion i.e. SA adipocytes will increase in diameter in response to WG whereas EU adipocyte diameter will be unaffected;

3. SA have a higher percentage of large and very large adipocytes (i.e. hypertrophic adipocytes) than EU both before and after WG.

4.2 Methods

4.2.1 Subjects

GlasVEGAs was a longitudinal study to explore the relationship between adiposity and insulin resistance in South Asians. Participants (male, age 18 – 45 years and BMI < 27 kg/m^2, weight stable (± 2 kg) for more than six months) of white European origin (EU, n = 23, self-reported both parents of white European origin) or South Asian origin (SA, n = 18, self-reported both parents of Indian, Pakistani, Bangladeshi or Sri Lankan origin) were recruited from January 2015 to April 2017 by Dr James McLaren. Exclusion criteria included: diabetes (physician diagnosed or HbA1c ≥ 6.5% on screening), history of cardiovascular disease, regular participation in vigorous physical activity, current smoking, taking drugs or supplements thought to affect carbohydrate or lipid metabolism and other significant illness that would prevent full participation in the study.

Abdominal subcutaneous adipose tissue (ASAT) biopsies were collected from each participant by Dr James McLaren as described previously (3.2.4). Prior to each visit (BL and WG) participants were given a controlled three-day weight neutral diet to ensure weight and energy balance was stable prior to measurements. An

initial ASAT biopsy was taken at baseline (BL). Participants were then asked to regularly eat until they felt more full than usual and were provided with high energy snacks (premium ice cream, chocolate bars, potato chips, cheese, dried fruit and sugary drinks) in order to gain 7% (minimum of 5%) weight over approximately six weeks. An ASAT biopsy was collected again after the participant had achieved a minimum 5% weight gain (WG).

4.2.2 Abdominal SAT collection and adipocyte isolation

The methods for adipose tissue biopsy and adipocyte isolation have been described in more detail in the Chapter 2 and were based on a standard protocol from Prof Friedrik Karpe and his group (Marinou *et al.*, 2014). Briefly, a small amount of adipose tissue (0.31 ± 0.12 g, mean ± SD) was collected using a needle biopsy by Dr James McLaren. ASAT was cut into 25 - 30 mg pieces with autoclaved scissors and transferred into filtered digestion buffer (filtered through 0.2 µm filter to sterilise, used at 37°C, hyperlink of the table). The tissue was shaken in a water bath (Grant, OLS200) for 50 min at 37°C, 110 rotations/min, and then filtered through a Pierce nylon mesh 250 µm filter (Thermo Fisher Scientific, 87791) to remove undigested material.

The suspension was allowed to stand for 5 min, and the floating adipocyte layer (approx. 50 - 100 µL) was collected from the surface with a pipette using a wide bore tip resulting in an approximately 90% cytocrit suspension. An aliquot (5 µL) of adipocyte suspension was used for adipocyte sizing.

4.2.3 Assessment of adipocyte size

4.2.3.1 Assessment of adipocyte diameter

Adipocyte diameter was measured on freshly isolated adipocytes. Briefly, 2.5 µL adipocyte suspension was added to 5 µL Krebs Ringer HEPES (KRH) buffer (2.4.4) on a glass slide. Digital pictures (6 - 10 captures, Figure 2-3) were captured using a 10x lens on a BX50 microscope by Image-Pro Plus 4.0 (Isakson *et al.*, 2009). Then the diameters of adipocytes were measured both manually and using an automated digital analysis plug-in for ImageJ 1.52a (Wayne Rasband, NIH, USA).

Intracellular diameters of 100 cells were manually measured for each sample in Adobe Photoshop v7.0 in pixels. Diameter in pixels was converted to micrometres using the digital image of a stage micrometre at the same magnification. Pixels were converted into micrometres (μm) by the formula:

$$Micrometre \ = \ \frac{100}{78} \times Pixel$$

Adipocyte diameters (100) were ascertained by each of two independent observers for each sample.

Adipocyte diameters were also measured in an automated fashion using Image J 1.52a, which is a public domain software for processing and analysing scientific images. Briefly, a conversion factor between pixels and micrometres was measured by a granular ruler as 80.89 pixels = 100 μm[5]. Pictures were converted to default black and white images using an adjusted threshold. As the transparency of each sample was slightly different, the brightness of each sample varied, so the threshold of the brightness of each picture was adjusted to allow maximum numbers of adipocytes to be measured. Intracellular diameter was exported as Feret's diameter[6].

4.2.3.2 Adipocyte volume calculation

An adipocyte was assumed to be a sphere and the volume was calculated from the diameter using the formula:

$$Volume \ = \ \frac{4}{3}\pi(\frac{1}{2}diameter)^3$$

The total volume of adipocytes was determined by aggregating the volume of adipocytes in each category.

---

[5] This ratio was acquired by multiple measurement of a graticule. Images of a 100 μm graticule were taken under the same microscope settings as adipocyte images. For manual measurement, each observer measured the graticule ten times and the average was calculated. In automated measurement, this was performed by the Image J software. The precision level was higher using automated measurement.

[6] The longest distance between any two points along the selection boundary, also known as maximum calliper. Adipocytes are considered to be circular in KRH buffer, therefore, Feret's diameter was regarded as diameter in this thesis.

4.2.4 Statistics

Statistical analysis was performed using Minitab version 19 (Minitab Ltd) and figures were drawn using GraphPad Prism 8.3. Normal distribution of parameters was tested using the Ryan-Joiner test. Non-normally distributed data were log or square root transformed to achieve normal distribution as required. Results were displayed as mean ± standard deviation (SD) for parametric data, and as median and 95% confident interval (CI) for nonparametric data.

A Bland-Altman analysis was performed to describe agreement between two measurements (inter-observer measurement, manual vs automated measurement, and first 150 cells vs full data set). Two group comparisons of cross-sectional parameters were made using two-sample t-test for normally distributed data or Mann-Whitney U-test for non-parametric data. A paired t-test was utilised to compare the BL and WG within each ethnic group, either EU or SA. Correlations between two parametric data sets was made by Pearson's correlation, and Spearman's correlation was used for non-parametric data. Results of correlation were displayed with regression r squared and p value. Percentage of S, M, L and VL adipocytes were calculated for each sample and a two-way comparison was carried out (timepoint by participant group) using a mixed-effects ANOVA. Significance level was $p < 0.05$ for statistical comparisons, and < 0.10 for interactions.

4.3 Results

4.3.1 Study participants included in adipocyte size analysis

In total 23 EU and 18 SA were recruited to the GlasVEGAs study of which 20 EU and 13 SA completed both BL and WG appointments as shown in Figure 4-1. Adipocyte size was assessed where both WG and BL data were available (EU n = 17, SA n = 13).
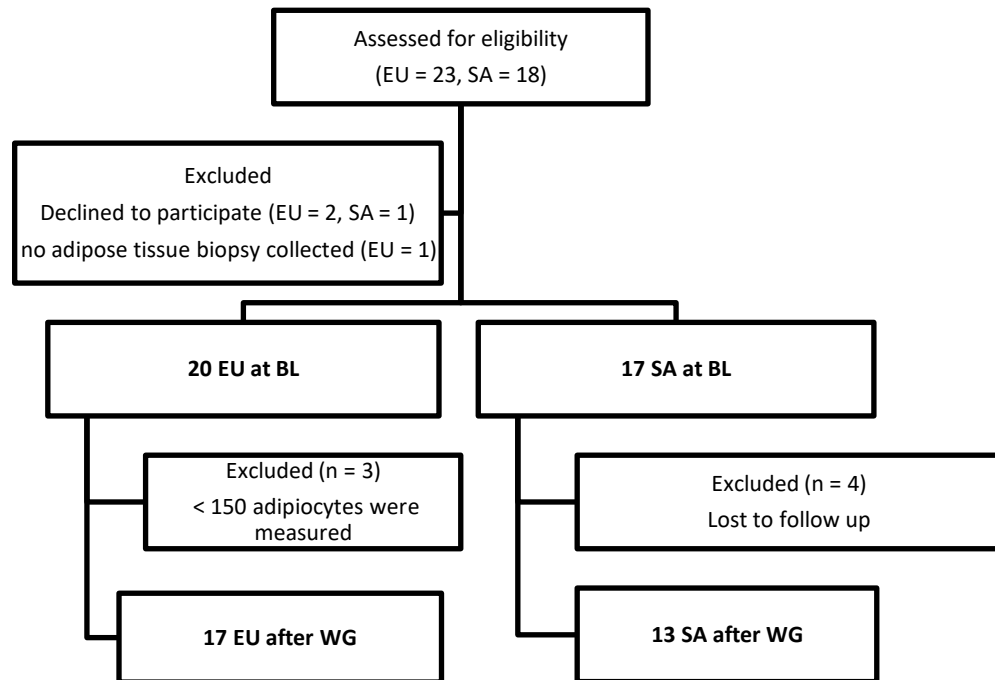
Figure 4-1 CONSORT flow diagram for the assessment of adipocyte sizing in GlasVEGAs study at BL and after WG.

4.3.2 Effect of weight gain on participant anthropometry

Anthropometry data are shown in Table 4-1. There were no significant differences between EU and SA in age, BMI, waist circumference and resting metabolic rate (RMR) at either BL or after 6.3 ± 1.3% WG. However, SA had more total adipose tissue compared to EU both at BL (18.7 ± 4.1 vs 14.2 ± 3.9 L, p = 0.005) and after WG (21.4 ± 4.0 vs 17.1 ± 4.9 L, p = 0.009).

Interestingly, the results indicated a significant rise in BMI, waist circumference, and total adipose tissue following WG in both EU and SA groups ($p \leqslant 0.0001$ in each group, Table 4-1). Despite these increases, the resting metabolic rate remained unchanged.

	Baseline			Weight gain			Delta BL vs WG	
	EU (n = 17)	SA (n = 13)	p value (EU vs. SA)	EU (n = 17)	SA (n = 13)	p value (EU vs. SA)	p value EU	p value SA
Age (years) $^{\$}$	22 ± 3	23 ± 3	0.45	22 ± 3	23 ± 3	0.45	N/A	N/A
BMI (kg/m^2)	22.2 ± 1.5	21.7 ± 2.9	0.55	23.5 ± 1.7	23.1 ± 3.1	0.58	< 0.0001	< 0.0001
Waist (cm)	78.5 ± 4.5	76.7 ± 4.9	0.32	82.2 ± 4.7	81.7 ± 6.0	0.78	< 0.0001	= 0.0001
Total adipose tissue (no arm) (L) $^{\$}$	14.2 ± 3.9	18.7 ± 4.1	0.005	17.1 ± 4.9$^{\$}$	21.4 ± 4.0	0.009	< 0.0001	< 0.0001
RMR (kcal/kg·day)	22.1 ± 2.3	22.3 ± 3.3	0.78	22.3 ± 2.4	23.5 ± 3.7	0.30	0.66	0.21

Table 4-1 Demographic data for European (EU) and South Asian (SA) participants in the GlasVEGAs study at baseline (BL) and after weight gain (WG).

This table showcases demographic information including body mass index (BMI) and resting metabolic rate (RMR) for both EU and SA participants at the initial stage and after experiencing weight gain. The changes between the baseline and weight gain are also indicated (Delta BL vs WG). Comparisons were made using a two-sample t-test. The symbol $ denotes statistical analysis performed on log-transformed data.

4.3.3 Agreement between manual and automated adipocyte sizing methods

Inter-observer agreement between the two independent observers for manual adipocyte sizing is shown in Figure 4-2a. There were no significant differences between the measurement between the two observers. The bias between two observers was 2.8 µm, which was 3.9% of the mean adipocyte diameter of all measurements. Only three outliers were found in over 88 measurements. The differences distributed similarly at each side of the bias and across mean diameter.

Similarly, there was no significant difference between manual and automated sizing methods with 8.7% bias (manual measurement was higher, Figure 1-3b). However, the results were strongly correlated with each other (R^2 = 0.93, $p <$ 0.0001) (Figure 1-3d). Moreover, adipocyte diameters from first 150 measurement showed no differences with diameters from all measured cells (bias: 0.34%) (Figure 1-3c). Therefore, later analysis has been performed using the first 150 adipocytes from automated measurement.
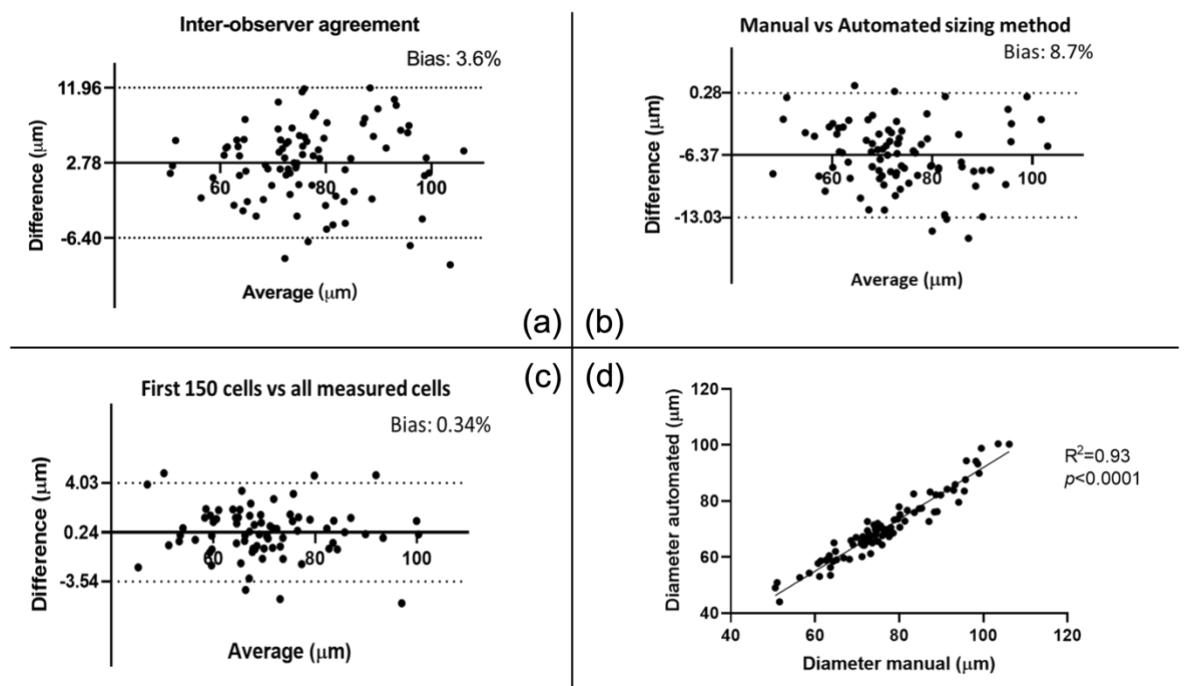
Figure 4-2 Agreement for adipocyte sizing methods

Bland Altman plots showing agreement a) between two observers (n = 88), b) between manual and automated (n = 87) and c) between the first 150 measured adipocytes and all the measured adipocytes (n = 76). Bias is shown as the solid line and ± 95% CI (confidence interval) is shown as a dotted line. d) Correlation between manually and automated measured adipocyte diameter (n = 87), Pearson's correlation, regression r squared and p were shown.

4.3.4 Changes in adipocyte size in EU and SA in response to WG

Adipocyte size was larger in SA than EU at BL and after WG (ethnicity $p = 0.015$), however, SA responded to WG in a similar way to EU regarding adipocyte diameter (interaction $p = 0.29$, Figure 4-3). Next, two-group comparison was made as post-hoc comparisons.
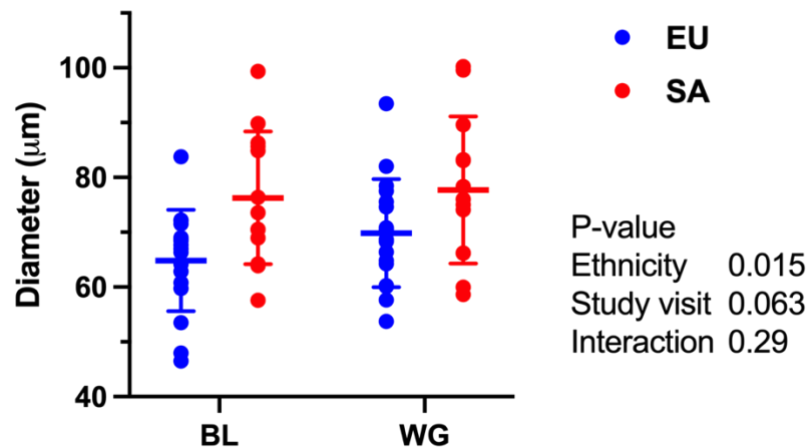
Figure 4-3 Changes in adipocytes in EU and SA in response to WG.

Two-way comparison was made by ANOVA mixed effects model.

4.3.5 Adipocyte size in EU and SA at BL and after WG

At BL, adipocyte diameter was larger in SA compared to EU (76.3 ± 11.6 vs 64.8 ± 9.1 μm respectively, $p < 0.01$, Figure 4-4). Adipocyte diameter was similar in SA and EU (77.3 ± 12.6 vs 69.8 ± 9.5 μm, Figure 4-4) after WG.
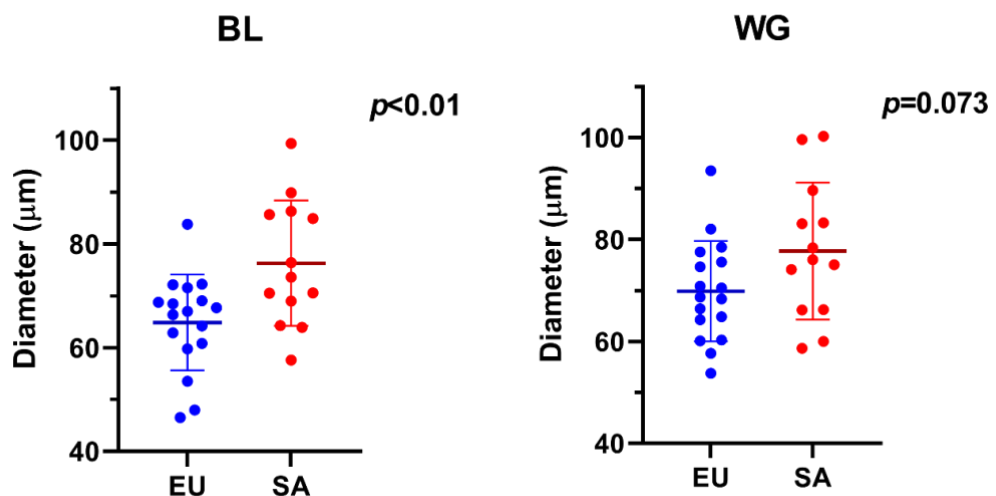
Figure 4-4 Adipocyte size in EU and SA at BL and after WG.

P value was obtained using paired t test, mean and SD are shown as bold line and error bar.

4.3.6 Effect of WG on mean adipocyte diameter in EU and SA

After 6.3 ± 1.3% WG, adipocyte diameter increased in the EU group (p = 0.027) but not in the SA group (Figure 4-5).
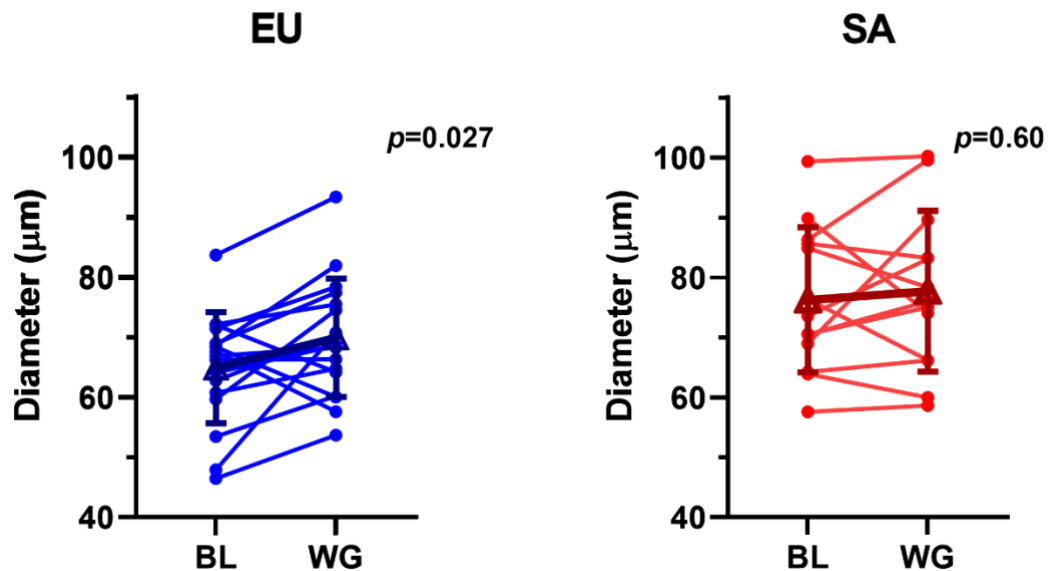
Figure 4-5 Individual changes in adipocyte size in response to WG in EU and SA.
P value was obtained using paired t test, mean and SD are shown as triangle and error bar.

4.3.7 Adipocyte diameter distribution in EU and SA at BL and after WG

After WG, both SA and EU lost a significant amount of S adipocytes (SA 9.3 ± 6.7 vs 8.1 ± 4.9%, EU 14.2 ± 14.5 vs 7.1 ± 7.2% respectively, p = 0.030) (Figure 4-6 and Table 4-2). SA have a higher percentage of L adipocytes compared to EU at BL and after WG (BL 25.0 ± 19.0 vs 9.0 ± 9.1%, WG 28.3 ± 23.6 vs 13.7 ± 14.7% respectively, p = 0.010) (Figure 4-6 and Table 4-2). However, after WG, SA have a lower percentage of M adipocytes compared to EU at BL and after WG (BL 64.5 ± 20.8 vs 76.7 ± 12.1%, WG 63.0 ± 23.0 vs 79.1 ± 12.2% respectively, p = 0.020) (Table 4-2, Figure 4-6).

However, SA respond to WG similarly to EU, as no interaction between diameter and time point was found (Table 4-2).
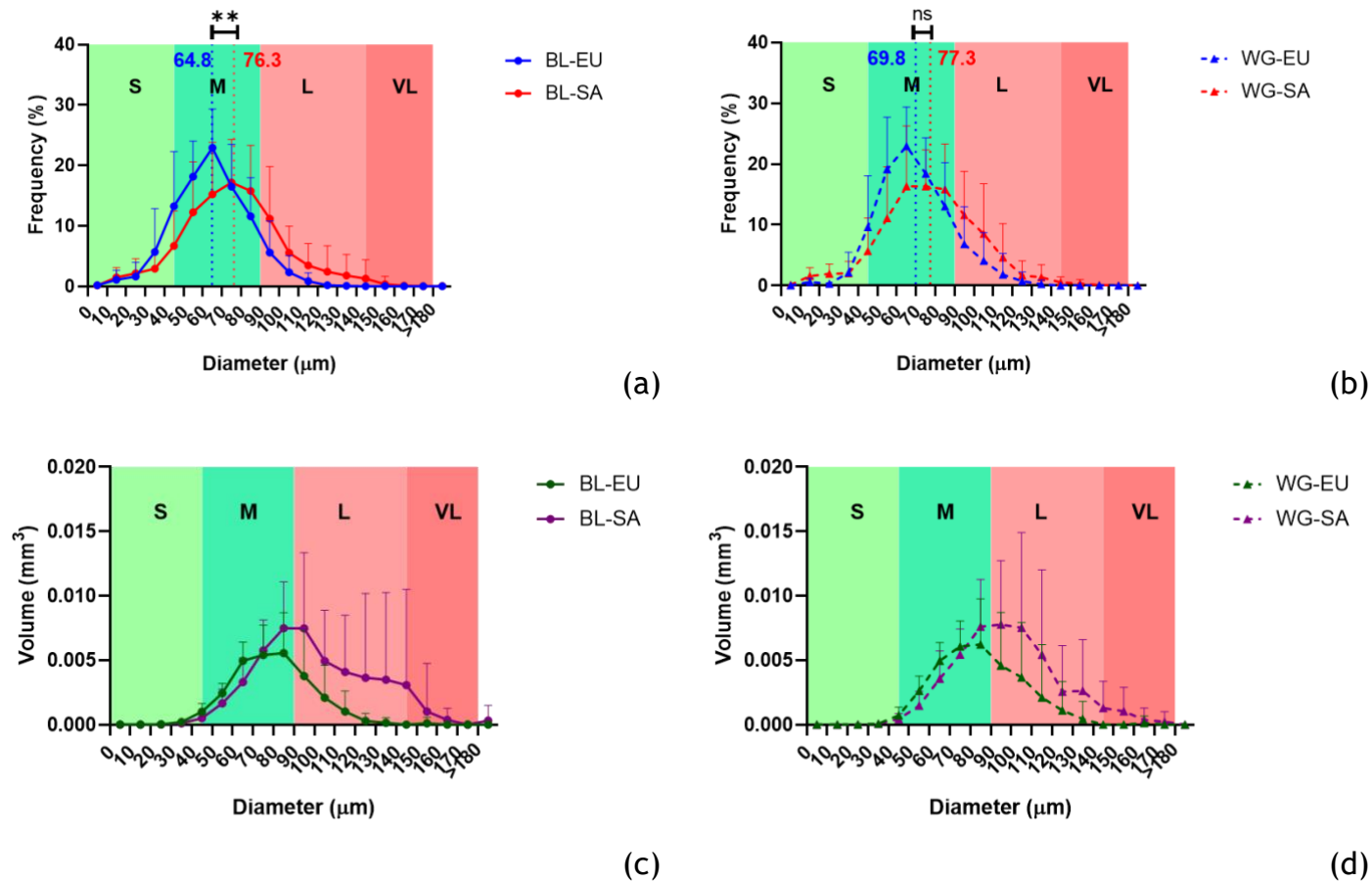
Figure 4-6 Adipocyte size distribution in diameter (a, b) and total adipocyte volume (c, d) in EU and SA at BL and after WG.

Mean adipocyte diameter of each ethnicity group is presented as a number next to a vertical dashed line indicator in figures (a) and (b). P value was obtained using two sample t test between EU and SA at BL and after WG. Error bar is presented as SD. ** $p < 0.01$. The total adipocyte volume was determined by aggregating the volume of all the adipocytes in each category.

	BL		WG		ANOVA mixed effect		
	EU	SA	EU	SA	Study visit	Ethnicity	Interaction
Small adipocyte (%)	14.2 ± 14.5	9.3 ± 6.7	7.1 ± 7.2	8.1 ± 4.9	0.030	0.21	0.12
Medium adipocyte (%)	76.7 ± 12.1	64.5 ± 20.8	79.1 ± 12.2	63.0 ± 23.0	0.88	0.020	0.48
Large adipocyte (%)	9.0 ± 9.1	25.0 ± 19.0	13.7 ± 14.7	28.3 ± 23.6	0.13	0.010	0.78
Very large adipocyte (%)	0.04 ± 0.16	1.1 ± 3.1	0.04 ± 0.16	0.7 ± 1.2	0.51	0.070	0.51

Table 4-2 Percentage of adipocytes categorized by size (mean ± SD).

An ANOVA mixed effects model was used to make a two-by-two comparison of study visit and ethnicity.

4.3.8 Total adipocyte volume distribution in EU and SA at BL and after WG

Total adipocyte volume distribution is shown in Figure 4-6 and Table 4-3. Briefly, both SA and EU lost significant volume of S adipocytes (p = 0.001, Table 4-3). SA stored less fat in M adipocyte (p = 0.034, Table 4-3) and more fat in L adipocytes (p = 0.001, Table 4-3) compared to EU at BL and after WG. Interestingly, SA stored a dramatically higher amount of fat in VL adipocytes compared to EU both at BL and after WG (BL 9.0 ± 15.0 vs 0.92 ± 2.0 x 10^{-3} mm^3, and WG 10.6 ± 14.7 vs 0.59 ± 1.3 x 10^{-3} mm^3, p = 0.002, Table 4-3).

However, SA respond to WG similarly to EU, as no interaction between diameter and time point was found (Table 4-3).

	BL		WG		ANOVA mixed effect		
	EU	SA	EU	SA	Study visit	Ethnicity	Interaction
Small adipocyte (x 10^{-3} mm^3)	0.64 ± 0.57	0.34 ± 0.26	0.30 ± 0.28	0.18 ± 0.13	0.001	0.088	0.23
Medium adipocyte (mm^3)	0.026 ± 0.006	0.022 ± 0.007	0.028 ± 0.005	0.023 ± 0.006	0.33	0.034	0.59
Large adipocyte (mm^3)	0.018 ± 0.014	0.051 ± 0.033	0.025 ± 0.026	0.055 ± 0.030	0.24	0.001	0.69
Very large adipocyte (x 10^{-3} mm^3)	0.9 ± 2.0	9.0 ± 15.0	0.6 ± 1.3	10.6 ± 14.7	0.80	0.002	0.71

Table 4-3 Total volume of adipocytes by size categorized (mean ± SD).

An ANOVA mixed effects model was used to make a two-by-two comparison of study visit and ethnicity. The total adipocyte volume was determined by aggregating the volume of all the adipocytes in each category.

4.3.9 Confounding effects of body weight, RMR and total adipose tissue on weight gain effects on adipocyte size

The correlations between adipocyte diameter and covariates, including body weight, BMI, waist, RMR and total adipose tissue, were analysed in a univariate analysis. A strong positive correlation was found between adipocyte diameter and total adipose tissue (R^2 = 0.40, p < 0.0001, Table 4-4), as well as HOMA-IR (R^2 = 0.29, p = 0.028, Table 4-4).

Then multivariate analysis was performed to examine the confounding effects of total adipose tissue on weight gain effects on adipocyte size. Total adipose tissue (no arm) (p = 0.003) was significantly independently associated with adipocyte size (Table 4-5).

Diameter versus:	DF	R^2	p
BMI (kg/m^2)	1	0.006	0.56
Body weight (kg)	1	0.009	0.47
Waist (cm)	1	0.033	0.16
RMR (kcal/kg·day)	1	0.0003	0.89
HOMA-IR	1	0.29	0.028
Total adipose tissue (no arm) (L)	1	0.40	< 0.0001

Table 4-4 Univariate analysis: correlation between adipocyte diameter versus covariates.

Covariates (BMI, bodyweight, waist, RMR and total adipose tissue). Linear correlation was obtained using Pearson correlation. RMR, resting metabolic rate. Total adipose tissue (no arm) was obtained using MRI by Dr James McLaren (McLaren, 2018). Samples used included SA and EU at BL and after WG, n = 60. Pearson's correlation, regression r squared and p were shown.

Term	DF	p	R^2 of model
Total adipose tissue (no arm) (L)	1	0.003	
HOMA-IR	1	0.68	
Study visit	1	0.67	83.29%
Ethnicity	1	0.14	
Study visit * Ethnicity	1	0.35	

Table 4-5 Mixed effects model: adipocyte diameter versus factors and covariates.

Random factor (patient), fixed factors (study visit, ethnicity and study visit*ethnicity) and covariates (total adipose tissue). Total adipose tissue (no arm) was obtained using MRI by Dr James McLaren (McLaren, 2018). Samples used included SA and EU at BL and after WG, n = 60.

4.4 Discussion

Mean adipocyte diameter was larger in SA than EU at BL which suggests that SA had more hypertrophic adipocytes compared to EU despite SA and EU having similar age, body weight, BMI and waist circumference. After WG, there was an increase in adipocyte diameter in EU only, resulting in EU and SA having a similar adipocyte diameter after weight gain. Overall, SA had a lower percentage of M and a higher percentage of L adipocytes than EU. WG caused a decrease in percentage of S adipocytes in both SA and EU. SA stored more fat in L and VL adipocytes and less fat in M adipocytes at BL and after WG than EU, supporting the presence of adipocyte hypertrophy. Adipose tissue mass was a predictor of adipocyte size independent of WG and ethnicity, suggesting that the additional 4L fat mass carried by SA is stored in these hypertrophic adipocytes.

These data provide evidence that SA have hypertrophic adipocytes relative to EU even in this group of low BMI (22 – 23 kg/m^2), young (22 - 23 years old) men. Hypertrophy of adipocytes is related to insulin resistance and other metabolic diseases/ syndromes (Krotkiewski *et al.*, 1983, Arner *et al.*, 2010b, Yang *et al.*, 2012). Hypertrophy has also been shown to be an independent predictor of T2DM (Weyer *et al.*, 2000, Lonn *et al.*, 2010). According to Lundgren *et al.*, 2007, adipocyte enlargement is associated with insulin resistance (R^2 = -0.32, *p* = 0.009, n = 83) in healthy individuals independent of BMI, but this association was not found in individuals with diabetes (n = 49) (Lundgren *et al.*, 2007). Moreover, in the current study, it was found that HOMA-IR was positively associated with adipocyte diameter. These data suggest that adipocyte diameter is associated with IR and is consistent with the SA being more insulin resistant than EU at baseline.

Although SA had larger diameter adipocytes than EU at BL, an increase in adipocyte diameter in response to WG was found in EU but not in SA. The correlation between adipocyte hypertrophy and metabolic disease (especially T2DM) is context-dependent: lean individuals with higher percentage of smaller adipocytes (< 0.4 nL, diameter < 91 μm, represented by S and M adipocytes in the current study) manifest a worse metabolic response to overfeeding (Johannsen *et al.*, 2014, Muir *et al.*, 2016) than obese individuals with lower levels of smaller adipocytes at baseline. This suggests that in the lean state, increased adipocyte

size may reflect nutrient buffering capacity. However, extreme adipocyte hypertrophy in obesity correlates with BMI and is associated with metabolic disease in both humans and mice (Arner *et al.*, 2010b, Cotillard *et al.*, 2014, Eriksson-Hogling *et al.*, 2015, Landgraf *et al.*, 2015, Ryden *et al.*, 2014), and the size of large adipocytes (mean diameter between 100 - 150 μm, represented by L and VL adipocytes in the current study) predicts the degree of insulin resistance in T2DM (Yang *et al.*, 2012). In the present study, SA stored fat in larger adipocytes compared to EU and this may result in decreased nutrient buffering capacity. This may cause overspill of fat in SAT or ectopic fat storage and increase the risk of SA getting T2DM compared to EU. At BL and after WG, SA always stored more fat in L and VL adipocytes and less fat in M adipocytes. The size of adipocytes was positively correlated with HOMA-IR. This suggests that adipocyte diameter predicts the degree of insulin resistance. SA tend to store more fat in adipocytes of larger size, which is associated with a higher degree of insulin resistance. This suggests that the higher proportion of larger adipocytes (> 90 μm) and lower proportion of smaller adipocytes in SA may underlie the higher risk of getting T2DM than EU.

The distribution of adipocyte diameters observed in the current study showed a significant difference between SA and EU. In both ethnic groups, the proportion of S adipocytes decreased in response to WG, and the difference in the proportion of S adipocytes between two ethnicity groups decreased. These S adipocytes may become larger and form M and L adipocytes in response to WG in both SA and EU. SA showed a trend for a lower ability of recruiting S adipocytes into larger adipocytes compared to EU. Others have observed a higher proportion of small subcutaneous adipocytes (< 50 μm) in patients with diabetes compared to those without (31.4 vs 14.9%, *p* = 0.006, n = 15 per group) (Fang *et al.*, 2015). The ability to efficiently recruit smaller sized adipocytes to store fat may lower the risk of type 2 diabetes. Impaired maturation of small adipocytes (< 50 μm) into fully functional adipocytes results in the deposition of lipid in ectopic sites and leads to insulin resistance (Björntorp, 1990, Heilbronn *et al.*, 2004, DeFronzo, 2004, Salans and Dougherty, 1971). Therefore, a lower efficiency of recruiting small adipocytes for maturation in SA than EU may be responsible for the higher risk of T2DM at lower BMI and younger age. This will be investigated later in the current study by the examination the expression of genes that are relevant to lipid storage

(*ADIPOQ, LEP*, and *APOE*) and by assessing differentiation potential (*PPARG*) in adipocytes and pre-adipocytes.

SA have a much higher risk of developing diabetes at lower BMI than EU. SA men with a BMI of 21.6 kg/m^2 (21.5 and 22.3 kg/m^2 for Pakistani and Indian men respectively) had a similar prevalence of diabetes to EU men at a BMI of 30 kg/m^2 (Ntuk *et al.*, 2014). A waist circumstance of 79 cm in SA men (78 vs 80 cm for Pakistani and Indian respectively) had an equivalent risk of diabetes to EU men with a waist circumference of 102 cm (Ntuk *et al.*, 2014). Even though at BL, SA had a 'healthy' waist circumference, after WG, the SA group in GlasVEGAs (BMI 23.2 ± 3.0 kg/m^2, waist 81.9 ± 5.8 cm), had a relatively high risk of diabetes while the EU men were at low risk according to Ntuk's criteria. In the current study, total adipose tissue was found to be an independent predictor of adipocyte size. This suggests that total adipose tissue might be a more accurate measurement of metabolic phenotype than body weight, waist and BMI, as has been suggested elsewhere (Goossens, 2017b). On the other hand, pharmacological treatment with thiazolidinediones (PPARγ agonists) improves insulin sensitivity, despite an significant increase in fat mass (Fonseca, 2003). This may be a beneficial effect as PPAR gamma agonists promote adipocyte differentiation and provide more storage capacity in adipose tissue and therefore less pathogenic spillover. However, total adipose tissue may not always be the predominant factor that explains the higher risk of T2DM. In the current study, the strong correlation between total body fat and adipocyte size suggests that total body fat may be a strong predictor of adipocyte size in healthy, young men at least.

4.4.1 Strengths and limitations

At BL and after WG, the SA participants had a similar phenotype to the EU, including age, BMI, waist circumference and RMR, which means the groups were well matched. Another strength is that it was a longitudinal study which observed the changes in adipocyte morphology in response to WG in SA and EU – known to be high and low risk ethnicities for T2DM.

However, one limitation was that only < 1 g adipose tissue was obtained from around < 100 cm^2 area from each individual at each study visit. Compared to the total amount of abdominal SAT, only a small proportion of fat was sampled. This

sampling method may provide biopsies that are less representative compared to tissue collection from surgery, however, it was more ethical and less time-consuming. Another limitation was that VAT was not accessed in the present study. SAT and VAT have different associations with insulin resistance. Although it has been widely reported that VAT is associated with an increased risk of IR, T2DM and overall mortality, SAT expansion improves insulin sensitivity and is associated with a decreased T2DM relative risk (Mittal, 2019, Costa and Duarte, 2006). VAT may just be a marker of the ability of SAT to expand. Therefore, after considering ethical reasons and time constraints, using the more insulin sensitive SAT depots was appropriate for the current study.

Lastly, regarding the sizing method, the current study used collagenase-digested adipose tissue, and this might be a limitation whereby a large proportion of small adipocytes may be lost during the tissue processing. As discussed in the introduction to this chapter, osmium tetroxide fixation followed by Multisizer counter analysis can generate a bimodal distribution of two populations of small and large adipocytes (Smith *et al.*, 2006, Etherton *et al.*, 1977). This may be better for the investigation of adipocyte size distribution. Moreover, osmium tetroxide fixation tends to provide a higher estimation of the proportion of small adipocytes (50 - 65%) compared with electron microscopy scanning (20 - 25%) and collagenase digestion (5 - 20%) (Laforest *et al.*, 2017, McLaughlin *et al.*, 2007b, Mersmann and MacNeil, 1986). The number of small adipocytes may have been underestimated by using collagenase digestion, due to small sized adipocytes failing to float and not being collected in the floating adipocyte layer. However, osmium fixation could interfere with the tissue to be used for the later study for adipocyte gene expression analysis and differentiation experiments, and it consumes more adipocytes for sizing than collagenase digestion. Different sizing techniques have systematic differences in adipocyte size, adipocyte size measured by osmium fixation was smaller than that by collagenase digestion (Laforest *et al.*, 2017). However, associations between adipocyte size and adiposity measurements, including anthropometrics, body fat composition, adipose tissue area, glucose homeostasis, plasma lipid profile and adipokines/ cytokines, were only slightly affected by different isolation methods (Laforest *et al.*, 2017). Thus, even though the current study may have a smaller proportion of small adipocytes than osmium fixation because of the limitation of the technique, attaining the aim of the study,

the comparison of adipocytes between different groups and the associations between adipocyte size and the parameters, may be only slightly affected.

Collagenase-digestion adipocyte images could be analysed either manually or using automated sizing using ImageJ 1.52a (NIH). One strength of the current study was that both methods were performed and the inter-method agreement was measured using a Bland-Altman analysis. This analysis showed that there was a good agreement between the manual and automated sizing methods using collagenase-digested adipocytes. This has not only improved the reliability of the current study, but also helped later researchers to measure adipocyte size more quickly when using the collagenase digestion method.

4.5 Summary

Adipocyte diameter was larger in SA than EU at BL, however, after WG, an increase in adipocyte diameter in EU but not in SA led to a similar size of adipocytes between SA and EU. However, at BL and after WG, SA stored more fat in L and VL adipocytes and less fat in M adipocytes compared to EU. These data may suggest that due to the greater amount of fat that can be stored in an adipocyte of higher diameter adipocyte diameter, a higher proportion of fat stored in larger and a lower proportion in smaller adipocytes, may explain the higher risk of T2DM in SA compared to EU. In healthy, lean and young individuals, total adipose tissue was a strong predictor of adipocyte size.

In addition, SA showed a trend towards a lower efficiency of recruiting S adipocytes for maturation, and this may be responsible for the greater degree of hypertrophy. Therefore, in the next chapter, genes associated with adipocyte differentiation and maturation were examined to explore whether or not there was a difference between SA and EU in the ability of adipocytes to undergo hypertrophic or hyperplasic expansion at the mRNA level of gene expression.

Chapter 5   Changes in subcutaneous adipocyte gene expression in response to weight gain in young, lean European and South Asian men

5.1 Introduction

Adipose tissue expansion is a key factor in the development of obesity (Kashyap *et al.*, 2010, Hossain *et al.*, 2007). SA develop metabolic complications associated with obesity (insulin resistance, dyslipidaemia and/or T2DM) at a lower BMI and younger age than EU (Ntuk *et al.*, 2014, Dudeja *et al.*, 2001, Deurenberg *et al.*, 2002). In response to the excess energy intake, adipose tissue stores fat by increasing the number of adipocytes (hyperplasia) and/or increasing the size of adipocytes (hypertrophy). However, when adipose tissue is overloaded with fatty acid delivery requiring storage as TG, the metabolism of adipocytes, including insulin regulation of lipid storage, lipolysis, cholesterol metabolism, secretion of cytokines and hormones and inflammatory/ tissue stress response may be altered (as shown in Figure 5-1). The data in Chapter 4 suggested that SA tend to store fat in larger adipocytes compared to EU which would suggest that the metabolism of adipocytes may be different between SA and EU, which may be reflected by differences in gene expression.

(a)

(b)
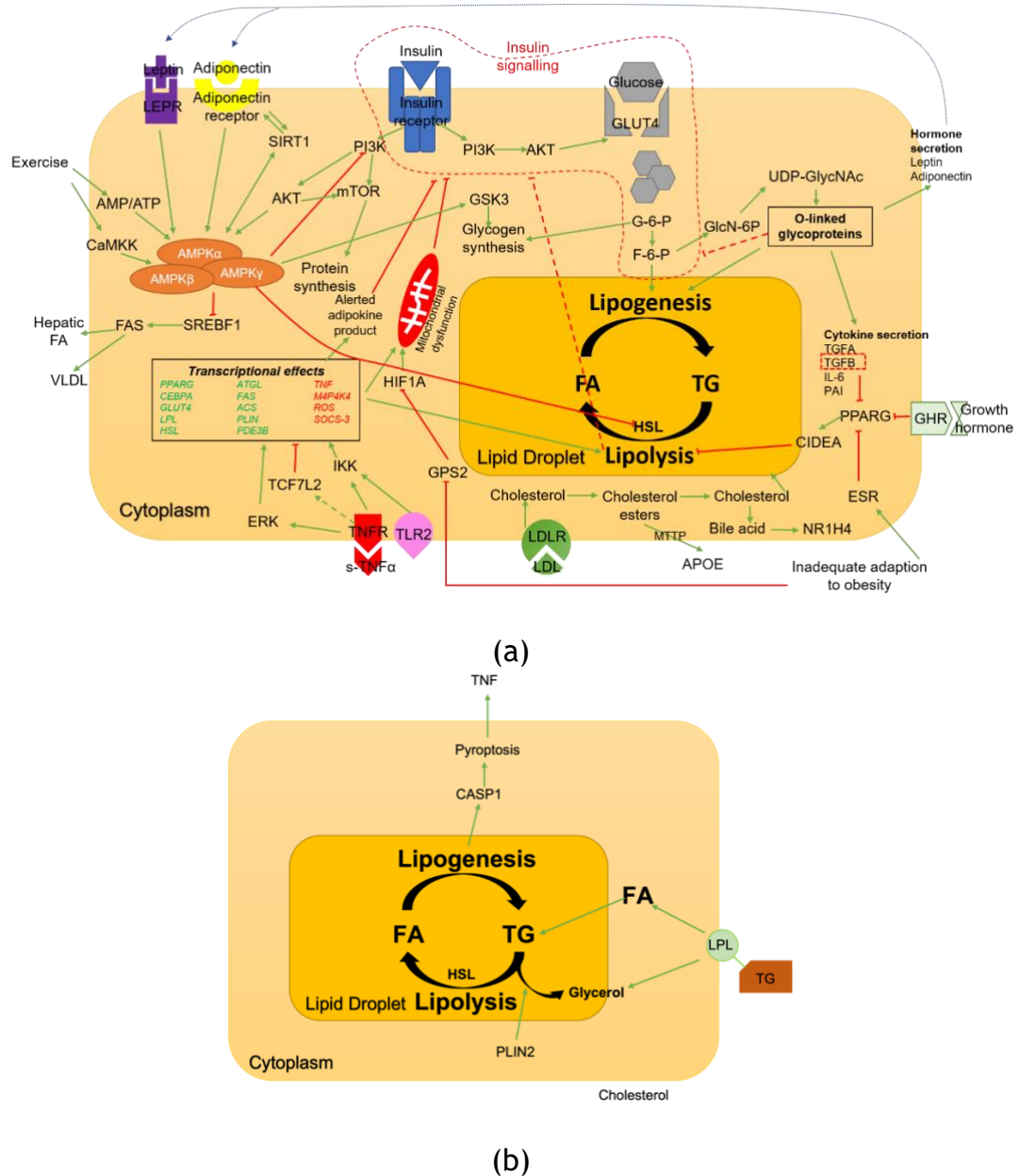
Figure 5-1 Pathways involved in (a) adipocyte metabolism with (b) lipid metabolism.

Insulin stimulates mature adipocyte excess energy storage as TG in lipid droplets either from glucose or FA (lipogenesis). These TG can be broken down to FA and glycerol by HSL when energy is required, and FA is released into the blood FFA (lipolysis). Adipokines, including adiponectin and leptin, can decrease the secretion of FFA by activating AMPK, and AMPK downregulates lipolysis by inhibiting HSL. As the body's largest free cholesterol reservoir, adipocytes store almost exclusively free cholesterol. Cholesterol is transported to adipocytes by LDL and high-density lipoprotein (HDL), and cholesteryl ester stimulates the secretion of apoprotein, a major protein in lipoprotein. Overaccumulation of TG in adipocytes can increase the secretion of TNFα in macrophages in adipose tissue by increasing CASP1 and pyroptosis. TNFα, along with other inflammatory factors, can heighten the inflammatory and tissue stress responses in adipocytes. This is achieved by stimulating the expression of membrane receptors such as TNFR and TLR2, thereby activating the downstream pathways of these receptors**.** Abbreviations: ACS, Acetyl-coenzyme A synthetase; AKT, protein kinase B; AMPK, 5' AMP-activated protein kinase; APOE, Apolipoprotein E; CASP1, Caspase 1; CaMKK, Calcium/calmodulin-dependent protein kinase kinase; CIDEA, cell death inducing DFFA Like effector A; ESR, estrogen receptor; FA, fatty acid; FAS, Fas cell surface death receptor; GPS2, G protein pathway suppressor 2; GSK3, glycogen synthase kinase 3; HSL, hormone sensitive lipase; IKK, IκB kinase; LPL, lipoprotein lipase; MTTP, microsomal triglyceride transfer protein; SIRT1, sirtuin 1; TG, triglyceride. (Otvos, 2019, Moro and Lafontan, 2013, Newell-Fugate, 2017, Becnel *et al.*, 2017, Slayton *et al.*, 2019, Qian *et al.*, 2020, Son *et al.*, 2014, Cawthorn and Sethi, 2008, Marshall, 2006, Sakamuri *et al.*, 2016, SinoBiological, 2020a, SinoBiological, 2020b, KEGG, 2020, Whirl-Carrillo *et al.*, 2012, Dra200 *et al.*, 2018)

One way of monitoring changes in the pathways of interest is to measure mRNA transcription of key genes in the pathway. As adipocytes contain predominantly lipid, the yield of RNA per gram of tissue is more than ten-fold less than the RNA yield from other tissues. In order to circumvent this limitation, pre-amplification of cDNA, reverse transcribed from RNA, was adopted in the current study. PCR-based pre-amplification of cDNA can be used to enrich the target gene cDNA content in a sample prior to qRT-PCR analysis. The enrichment of the sample with the targets of interest in a concentration-dependent manner provides sufficient signal for real time PCR experiments. Pre-amplification increases the concentration of each selected target gene by 1000-fold or more. The relative concentration of each target gene is maintained as long as the uniformity of pre-amplification is maintained. Uniformity of pre-amplification can be assessed by comparing amplification of a relevant uniformity control gene between samples with and without pre-amplification (Kibschull *et al.*, 2016).

In order to understand the potential nature and magnitude of the differences in gene expression in response to weight gain between EU and SA, an initial pilot study was performed to examine the expression of eight genes in adipocytes from SA and EU at BL and after WG, which were involved in lipid transport and storage (*ADOPOQ* and *LPL*), cholesterol metabolism (*SREBF1* and *LDLR*), regulation of insulin sensitivity (*INSR*), and inflammatory and endocrine factors (*HIF1A, TNF* and *LEP*). After this initial scan identified a number of significant changes in gene expression, the candidate gene list for testing was expanded using ingenuity pathway analysis (IPA) to suggest additional candidates. The list of genes examined are shown in Table 5-1.

	Gene symbol	Function of gene
Lipid storage pathway	*ADIPOQ*	Codes for adiponectin, an adipokine. End differentiation marker for adipose tissue. Adiponectin can also increase lipid oxidation and decrease the secretion of FFA by activating AMPK complex in adipocytes. Adiponectin can reduce plasma glucose and increase insulin sensitivity in whole body. (Diez and Iglesias, 2003)
	APOE	Codes for apolipoprotein E. Promote adipocyte triglyceride turnover involved in lipoprotein uptake. Apolipoprotein E is a major protein for cholesterol transporters including LDL, HDL and VLDL (Huang *et al.*, 2015).
	CYP19A1	Codes for aromatase, which converts a class of hormones called androgens. In males, aromatase is most active in adipocytes. Androgen regulates lipid and cholesterol metabolism by stimulating the activities of LPL and HSL (Zhao *et al.*, 2009).
	KLF14	Codes for Kruppel-like factor 14. Strongly associated with low HDL cholesterol levels, high TG levels, risk of type 2 diabetes mellitus (Ding *et al.*, 2014). It is a master regulator of gene expression in subcutaneous adipocytes and the mechanism is not exclusively understood.
	LDLR	Codes for the LDL receptor. Bind remnants of chylomicrons and LDL, mediates lipid transport (Hofmann *et al.*, 2007).
	LEP	Codes for leptin, an adipokine. It increases lipid oxidation and decrease the secretion of FFA by activating the AMPK complex in adipocytes. Negatively correlates with total body fat storage by inhibiting food intake and decreases adipocyte sensitivity to insulin thereby inhibiting lipid accumulation (Harris, 2014).
	LPL	Codes for lipoprotein lipase. It is an enzyme that hydrolyses circulating TG so that generates FA used in the synthesis of TG in lipid droplets. Essential for lipid uptake and storage (Gonzales and Orlando, 2007).
	SREBF1	Codes for Sterol Regulatory Element Binding Transcription Factor 1. Promotes lipid storage and oxidation by promoting LDLR gene expression and other genes involved in sterol biosynthesis (Crewe *et al.*, 2019).
Insulin signalling pathway	*CASP1*	Codes for Caspase 1. Lipolysis stimulates the expression of *CASP1*, secreting agents that promote pyroptosis, resulting in the release of the inflammatory factor TNFα.

		CASP1 is upregulated during adipogenesis and directs adipocytes into a more insulin resistant phenotype (Stienstra *et al.*, 2010).
	CIDEA	Codes for cell death-inducing DFFA-like effector A. Lipid droplet associated protein and positively correlated with insulin sensitivity (Abreu-Vieira *et al.*, 2015).
	ESR1	Codes for estrogen receptor 1. Estrogen activates (M2) macrophages to stimulate the secretion of catecholamines. This improves adipocytes metabolism and insulin sensitivity by facilitating FFA oxidation in SAT, and in VAT, by improving mitochondria β-oxidation (Zhou *et al.*, 2020b, Vieira-Potter *et al.*, 2015).
	GHR	Codes for growth hormone receptor. Activation of growth hormone receptor plays an insulin-like role in increasing glucose transport and FA oxidation, by activation of the PI3K/AKT pathway. Strong regulator of lipid and glucose metabolism and plays a key role the proliferation and differentiation of pre-adipocytes (Glad *et al.*, 2019, Ridderstrale, 2005).
	INSR	Codes for insulin receptor. A major endocrine hormone receptor involved in the regulation of energy and lipid metabolism.
	PIK3R1	Codes for phosphatidylinositol 3-kinase. A key kinase in the insulin pathway, downstream of the insulin receptor.
	PLIN2	Codes for Perilipin 2. Expression of *PLIN2* is insulin sensitive. Perilipin 2 is essential for the formation of lipid droplets in adipocytes to store fat (Li *et al.*, 2018)
	SIRT1	Codes for sirtuin 1. It is the most conserved mammalian NAD+ dependent histone deacetylase. Regulated by insulin, NAD^+-dependent protein that regulates natural aging and other stress-related conditions (Hui *et al.*, 2017, Salminen *et al.*, 2013).
Adipocyte differentiation	*BSCL2*	Codes for seipin, a multi-pass transmembrane protein. An essential, cell-autonomous regulator of adipogenesis by regulating the formation of lipid droplets through actin cytoskeleton remodelling (Payne *et al.*, 2008).
	EPAS1	Codes for endothelial PAS domain protein 1, a transcription factor. Promotes adipocyte differentiation, but the mechanism is unclear (Shimba *et al.*, 2004).
	PPARG	Codes for peroxisome proliferator-activated receptor. Key factor of terminal adipocyte differentiation. Initiates and maintains adipocyte differentiation and

maturation by a positive feedback loop with C/EBPα (Tontonoz and Spiegelman, 2008).

	TGFB1	Codes for transforming growth factor beta 1. In MSC, TGFß inhibits commitment to differentiation to pre-adipocytes by inhibiting expression of *PPARG* (Choy and Derynck, 2003). In mature adipocytes, TGFß stimulates TGFBR/SMAD pathways, which activate extracellular matrix to increase focal adhesion kinase (FAK)/AKT signalling, to stimulate lipogenesis pathways and lipid storage (Toyoda *et al.*, 2022).
Tissue stress response/ inflammation	*HIF1A*	Codes for hypoxia inducible fact 1 subunit alpha. Increases chronic inflammatory responses in adipocyte in patients with obesity (He *et al.*, 2011). An important paralog of *EPAS1*.
	TCF7L2	Codes for transcription factor 7 like 2, inflammatory factor. Regulates adipocyte size, endocrine function, and glucose metabolism by directly regulating genes involved in lipid metabolism (*ADIPOQ*) and insulin signalling pathways (*GLUT4* and *LEP*) (Geoghegan *et al.*, 2019, Nguyen-Tu *et al.*, 2021b).
	TNF	Codes for tumour necrosis factor alpha, an inflammatory factor. Promotes inflammatory response and decreases insulin sensitivity in adipocytes by activation of adipokine products (Sethi and Hotamisligil, 1999).
	TLR2	Codes for toll like receptor 2. Plays a fundamental role in pathogen recognition and activation of innate immunity and mediates inflammatory processes in obese adipose tissue. Decreases insulin sensitivity by decreasing the expression of *GLUT4*, and the translocation of GLUT4 (Poulain-Godefroy *et al.*, 2010, Ferrari *et al.*, 2019).

Table 5-1 Function of genes of interests in adipocytes in the current study.

IPA software programme is one of a suite of advanced bioinformatic tools, which can analyse gene expression patterns, visualize data in the form of interactive pathway diagrams and/or gene-gene biological interactions using a built-in scientific literature based database (Yu *et al.*, 2016, Cirillo *et al.*, 2017). Thus, IPA can be used to enhance the interpretation of scientific data, understand the conclusions drawn and discuss follow-up research questions, and it can also be used in a reverse manner to identify potential genes of interest using specific terms (Cirillo *et al.*, 2017). In the present study, IPA was used to select potential genes of interest that may differ in adipocyte hyperplasic and hypertrophic responses. The genes studied in this chapter were integral to a number of key pathways of adipocyte function as detailed below.

5.1.1 Insulin signalling pathway

Insulin is a major endocrine hormone involved in the regulation of energy and lipid metabolism via the activation of an intracellular signalling cascade involving the insulin receptor (INSR), insulin receptor substrate (IRS) proteins, phosphatidylinositol 3-kinase (PI3K) and protein kinase B (AKT) (Cignarelli *et al.*, 2019). Insulin also regulates adipocyte growth and differentiation, by enhancing the gene expression of various transcription factors, including *SREBP1C* and *PPARG* (Laviola *et al.*, 2006a). Young and lean healthy SA (n = 49, aged 28.7 ± 8.3 years, BMI, 22.4 ± 2.3 kg/m^2) had significantly higher HOMA-IR (2.75 [2.40, 3.15] vs 1.95 [1.84, 2.05] unit, *p* < 0.005) compared to EU (n = 292, aged 26.0 ± 7.0 years, BMI, 22.2 ± 2.1 kg/m^2) (Petersen *et al.*, 2006). This suggests that SA tend to show a lower whole body insulin sensitivity compared to EU, this may be reflected on the expression of genes associated with insulin signalling pathway in adipocytes.

Caspase-1 (CASP1) is an inflammatory factor that is expressed in mouse and human adipocytes. In *in vitro* adipocyte differentiation experiments using human primary pre-adipocytes, CASP1 protein expression was significantly higher in differentiated cells compared to undifferentiated cells (Stienstra *et al.*, 2010). In mice, caspase-1 regulates lipid metabolism via transcriptional mechanisms that are poorly understood, leading to an increase in circulating TG, increased insulin resistance and reduced adipocyte differentiation (Li *et al.*, 2017). CASP1-deficient adipocytes secreted higher levels of adiponectin compared to WT and showed an increased insulin sensitivity as visualised by increased phosphorylation of AKT

(Stienstra *et al.*, 2010). Thus, the expression of *CASP1* may promote adipocyte insulin resistance by altering lipid metabolism.

Cell death-inducing DNA fragmentation factor alpha-like effector A (CIDEA) is mainly expressed in WAT at a high-level (Abreu-Vieira *et al.*, 2015). In adipocytes, it is important for the formation of lipid droplets and adipose tissue expansion. In humans, low expression of CIDEA was linked to metabolic syndrome, and depletion of human adipocyte CIDEA using RNA interference increased lipolysis and TNFα secretion (Nordstrom *et al.*, 2005). In transgenic mice that express the human *CIDEA* gene, there was a significant increase in adipose tissue expansion, and these transgenic mice showed higher insulin sensitivity than WT (Abreu-Vieira *et al.*, 2015). Similarly, in obese patients, expression of CIDEA protein was negatively associated with HOMA-IR, thus positively associated with insulin sensitivity (Puri *et al.*, 2008a). In obese patients, expression of *CIDEA* mRNA level was positively correlated with insulin sensitivity (assessed by HOMA-IR index) independently of BMI (Montastier *et al.*, 2014). Thus, CIDEA expression in adipocytes is positively correlated with insulin sensitivity and healthy obesity.

Estrogen is a sex hormone and plays an important role in whole body metabolism regulation in both males and females (Stubbins *et al.*, 2012, Tchernof *et al.*, 2004). ESR1 is the major estrogen receptor in adipocytes. Estrogen plays different roles in body fat distribution between males and females, which leads to the differences in body fat distribution between male and female. Women have higher body fat percentage than men, but men tend to have more visceral fat than women (Sparks *et al.*, 2009, Palmer and Clegg, 2015). However, estrogen may supress lipid accumulation, reduce adipocyte size and reduce adipocyte inflammatory response in a similar way in adipocytes in both men and women. ESR KO male mice show a whole-body insulin resistance, and lower energy expenditure and inflammation than WT mice, and feeding a high fat diet made it more severe (Ribas *et al.*, 2010). In males, estrogen is produced from testosterone mainly. In hypogonadal men, whose ability to produce sex hormones is decreased, testosterone treatment increased circulating estrogen, and helped participants reduce truncal fat. Participants who had the highest *ESR1* mRNA expressed in subcutaneous adipocytes, lost the most truncal fat after six months treatment (Colleluori *et al.*, 2018). Similarly, estrogen treatment in postmenopausal women resulted in increased insulin-mediated glucose disposal (skeletal muscle insulin

sensitivity) and insulin-mediated suppression of lipolysis (adipocyte insulin sensitivity) (Pereira *et al.,* 2015, Van Pelt *et al.,* 2003). Thus, estrogen improves whole body and adipocyte insulin sensitivity in both sexes.

Growth hormone (GH) is key regulator of lipid and glucose metabolism and plays a key role the proliferation and differentiation of pre-adipocytes to stimulate adipogenesis (Glad *et al.,* 2019, Lewitt, 2017). The effects of GH are thought to be mediated by the growth hormone receptor (GHR), which is highly expressed within human adipocytes (Franco *et al.,* 2006). In mature adipocytes, the GHR stimulates glucose transportation and FA oxidation in an insulin-like way by activating PI3K/ AKT pathways (Ridderstrale, 2005). The structure and amount of adipose tissue in adipose depots are influenced by GH-induced lipolysis, which is regulated by the abundance of GHR on the adipocyte membrane (Mekala and Tritos, 2009).

Perilipin 2 (PLIN2) is a member of the family of perilipin lipid droplet coating proteins and is widely expressed. PLIN2 is essential for the formation of lipid droplets both in adipocytes (Li *et al.,* 2018) and skeletal muscle *(*Bosma *et al.,* 2012). Overexpression of PLIN2 improves the insulin sensitivity of skeletal muscle *in vitro* and *in vivo* in mice (Bosma *et al.,* 2012).

Sirtuin 1 (SIRT1) is the first discovered member of the SIRTuin family, a group of NAD^+-dependent proteins that regulate natural aging and other stress-related conditions (Hui *et al.,* 2017). AMPK increases SIRT1 activity by increasing intracellular NAD+ levels, and AMPK activity is strongly associated with exercise and insulin signalling. It has been shown that adipocyte-selective ablation of SIRT1 resulted in exacerbated insulin resistance of the adipocyte (Chalkiadaki and Guarente, 2012). A study has shown that adipocyte-specific deletion of *SIRT1* introduced glucose intolerance, hyperinsulinemia and insulin resistance in HFD mice (Hui *et al.,* 2017). In mature adipocytes, SIRT1 promotes fat mobilization through suppression of *PPARG* (Hossain *et al.,* 2007).

5.1.2 Lipid storage

Lipid storage starts with free fatty acids (FFA) entering the adipocyte. Plasma TG, transported in triglyceride-rich lipoproteins (TRL) such as very-low density

lipoprotein (VLDL) and chylomicrons, are lipolyzed by lipoprotein lipase (LPL) to FFA, which are then taken up by adipocytes (Clemente-Postigo *et al.*, 2011). Additionally, in adipocytes, APOE on circulating lipoproteins interacts with the VLDL receptor to facilitate TG hydrolysis by LPL (Huang *et al.*, 2009b). Intracellular lipids are stored in a lipid droplet in adipocytes (mainly in white adipocytes), and utilized by neutral hydrolases in cytoplasm to supply lipids (Liu and Czaja, 2013). During fasting, FFA is released into plasma mainly by subcutaneous adipocytes, and accumulate in non-adipose tissue as TG, which is degraded by β-oxidation in mitochondria and produces energy for homeostasis of cells and tissues (Saponaro *et al.*, 2015a). Over-accumulation of lipids in adipose tissue and/ or peripheral organs (where it is called ectopic fat), may lead to lipotoxicity, cell dysfunction and alteration in metabolic pathways (Saponaro *et al.*, 2015a). Adipose tissue is also the major depot for the storage of cholesterol in humans, in which most of (> 93%) cholesterol is stored in unesterified form (free cholesterol) (Krause and Hartman, 1984, Schreibman and Dell, 1975). In adipocytes, the majority of (> 88%) free cholesterol is located on the surface of lipid droplets (Schreibman and Dell, 1975, Prattes *et al.*, 2000). In normal conditions, cholesterol is transported in and out of adipocytes by lipoproteins with TG, mainly HDL. Therefore, lipoprotein uptake is not only for the transportation of cholesterol, but also involved in TG turnover (Nazir *et al.*, 2020). In the current study, a total of seven genes involved in the regulation of lipid and cholesterol metabolism have been selected and their function is described in Table 5-1. Briefly, LPL is essential for lipid uptake and storage, and adiponectin stimulates lipid oxidation and suppresses FFA release. APOE, LDLR, SREBF1 and CYP19A1 increase cholesterol metabolism and lipid turnover. In addition, KLF14 predicts the risk of T2DM, including high TG levels and low HDL levels. Leptin is primarily produced by WAT and the circulating concentration of leptin negatively correlates with total body fat storage by inhibiting food intake and decreasing adipocyte sensitivity to insulin thereby inhibiting lipid accumulation (Harris, 2014). Leptin has also been shown to directly inhibit lipid synthesis in adipocytes. Adipocytes exposed to physiological concentrations of leptin (20 ng/ml) showed a time-dependent suppression of fatty acid synthase expression such that there was a 90% inhibition after 24 hours (Wang *et al.*, 1999). This suggests that the expression of *LEP* may negatively correlate with adipocyte size and lipid accumulation.

Abnormal lipid metabolism results in the elevation of plasma FFA, which in turn results in whole body insulin resistance and T2DM. Elevated FFA release from adipocytes may contribute to the higher risk of T2DM in SA. Compared to EU, SA had higher circulating TG concentrations and lower levels of HDL-C at the same age and BMI, both in healthy participants and in patients with metabolic syndrome (Ajjan *et al.*, 2007). Young and lean SAs had significantly higher liver TG and lower levels of circulating adiponectin compared to EU (Petersen *et al.*, 2006). Similarly, young and lean SAs had lower circulating HDL-C but higher total circulating cholesterol compared to EU (Ehtisham *et al.*, 2005). These metabolic differences may be linked to the differences of expression of genes in adipocytes between SA and EU. Furthermore, weight gain and obesity increase the chance of adipocyte dysfunction in all ethnicities, and this may be worse in SA than EU. In patients with impaired glucose tolerance, SA had twice as much as liver TG than EU (Misra and Khurana, 2011a). In obese patients with abnormal insulin sensitivity, SA (n = 906, BMI, 25.8 ± 6.8 kg/m^2, age not given) had only half the level of circulating adiponectin (12.8 ± 13.6 vs 23.5 ± 20.4 ng/mL, *p* < 0.0001), and similar levels of HDL-C and circulating TG compared with EU of 2 BMI unit higher (n = 2,622, BMI, 27.8 ± 5.1 kg/m^2, age not given) (Shah *et al.*, 2016b). Thus, expression of genes associated with lipid metabolism in adipocytes in SA may be different compared with EU, and WG may worsen this situation.

5.1.3 Tissue stress response/ inflammation

In obesity-related inflammation that enhances systemic inflammation and metabolic disorders, insulin secretion and signalling is suppressed. WAT is the most relevant inflamed tissue in obesity-related inflammation (Skeldon *et al.*, 2014). As obesity-related inflammation in WAT is highly linked to insulin resistance this may be an important mechanism that underlies the increased risk of T2DM in WG and in SA.

Tumour necrosis factor alpha (TNFα) is a multi-functional cytokine that can regulate a variety of cellular and biological processes including immune function, cell differentiation, proliferation, apoptosis and energy metabolism. The expression of *TNF* in adipose tissue was increased under both catabolic and lipodystrophic conditions (for example cancer and sepsis) and in the pathological state of nutrition overload (for example obesity) leading to systemic insulin

resistance (Cawthorn and Sethi, 2008). Studies have shown that in rodent obese models, impairment of TNF processing improves systemic insulin sensitivity and that an absence of TNF-α (either TNF-α or its receptor) results in a significant improvement in insulin sensitivity. (Togashi *et al.*, 2002, Serino *et al.*, 2007, Uysal *et al.*, 1997a, Uysal *et al.*, 1998). Therefore, TNF alpha is involved in insulin resistance. The current study selected other two genes of inflammatory factors (*HIF1A* and *TCF7L2*), and a gene of inflammatory factor receptor (*TLR2*) to explore.

5.1.4 Adipocyte differentiation

White adipocytes differentiate from mesenchymal stem cells (MSC) in two phases (Gregoire *et al.*, 1998). MSC firstly commit to become pre-adipocytes in the commitment phase. There are two main pathways associated with preadipocyte commitment: the Wingless-INT (WNT) signalling pathway and the transforming growth factor-beta (TGFB) superfamily signalling pathway. Both pathways can influence adipogenesis. Canonical WNT signalling inhibits adipogenesis, even though it is essential for the survival of adipocyte precursors whereas canonical TGFß signalling is positively related to adipogenesis and obesity in human and animal models (Cristancho and Lazar, 2011).

The second phase of adipogenesis is terminal differentiation in which the mature white adipocyte is formed from the preadipocyte, resulting in the characteristic appearance of the mature adipocytes. This phase starts after activation of *PPARG* and/or *CEBPA* by various of transcriptional factors such as additional sex combs like 2 (ASXL2), nocturnin, nuclear receptor subfamily 1 group D member 1 (NR1D1), and transducing-like enhancer 3 (TLE3) (Cristancho and Lazar, 2011). PPARG and CEBPA are initially in a positive feedback loop and subsequently induce each other's expression and accumulation. Consequently, both transcription factors stimulate the expression of a large number of downstream genes, including those involved in the formation of lipid droplets (*BSCL2* and *PLIN2*) and those coding for proteins expressed by mature adipocytes (*ADIPOQ* and *FABP4*) (Gregoire *et al.*, 1998). These downstream genes enable the mature adipocyte to acquire its functional abilities. In this phase, TGFß1 may suppress adipocyte differentiation by signalling through small mothers against decapentaplegic

homolog 3 (SMAD3) interacting with CEBPA, and the transactivation function of CEBPA is repressed as well (Choy and Derynck, 2003).

5.1.5 Hypotheses

1. Adipocytes from SA express lower levels of genes involved in adipocyte insulin sensitivity (*ESR1, GHR, INSR, PIK3R1, PLN2* and *SIRT1*) and higher levels of genes involved in adipocyte insulin resistance (*CASP1*) than EU. After WG there is decreased expression of genes involved in promoting insulin sensitivity and an increase in expression of genes involved in insulin resistance.

2. Adipocytes from SA express lower levels of genes involved in promoting adipocyte differentiation (*BSCL2*, *EPAS1* and *PPARG*) and higher levels of genes involved in suppressing adipocyte differentiation (*TGFB*) than EU. After WG there is a decrease in expression of genes involved in promoting differentiation and an increase in genes involved in suppressing differentiation.

3. Inflammatory gene (*HIF1A*, *TCF7L2*, *TNF* and *TLR*) expression in adipocytes is higher in SA than EU and increased after WG.

4. SA adipocytes express higher levels of genes involved in lipolysis (*KLF14*) and lower levels of genes involved in lipogenesis (*LPL*), lipid oxidation (*ADIPOQ*), lipid accumulation (*LEP*) and lipid turnover (*APOE, LDLR, SREBF1* and *CYP19A1*) than EU. After WG, there is a decrease in genes involved in lipolysis and an increase in genes involved in lipogenesis, lipid oxidation, lipid accumulation and lipid turnover.

5. SA and EU respond to WG differently with respect to adipocyte gene expression.

5.2 Methods

5.2.1 RNA extraction and purification

Total RNA was extracted from abdominal subcutaneous adipocytes isolated from 0.31 ± 0.12 g (mean ± SD) ASAT (4.2.2) using the RNeasy Lipid Tissue Mini Kit (QIAGEN, 74804) according to the manufacturer's instructions. The RNA was dissolved in 30 µL nuclease-free water (QIAGEN, 129115).

5.2.1.1 Quantifying RNA yield

The integrity and purification of isolated RNA was confirmed using a NanoDrop 1000 (Thermo Fisher Scientific). The optical density 260/280 nm ratio (1.8 - 2.0 acceptable purity) and concentration of RNA were recorded.

5.2.1.2 Removal of DNA contamination

DNase treatment was applied to 21.5 µL RNA samples (19.6 ± 15.4 ng/µL) to remove any DNA contamination in the samples. A DNA-free kit (Thermo Fisher Scientific, AM1906) was used according to the manufacturer's instructions. The purified RNA was stored at -80°C for future use.

5.2.2 Synthesis of complementary DNA

Single stranded complimentary DNA (cDNA) used for qPCR was reverse transcribed from purified RNA (Pincu *et al.*, 2016) using a high-capacity cDNA reverse transcription kit (Thermo Fisher Scientific, 4368813) according to the manufacturer's instructions. The cDNA was stored at -20°C.

5.2.3 Pre-amplification of cDNA

The quantity of specific cDNA targets was pre-amplified using TaqMan® PreAmp master mix (2x) (Thermo Fisher Scientific, 4384266). Briefly, Tris-EDTA (TE), pH 8.0 buffer (10 mM Tris, 1 mM EDTA, Thermo Fisher Scientific, AM9849) was mixed 1:1 with the TaqMan® Gene Expression assay for the selected target genes (each target TaqMan® Gene Expression Assay mix contributed equal amount) to make a pooled assay mix. The target Taqman® Gene Expression Assays were purchased from ThermoFisher Scientific as listed in Table 5-2. Pre-amplification Reaction Mix

was made up as described in Table 2-5, sufficient quantity to allow amplification of the number of cDNA samples being pre-amplified (Pincu *et al.*, 2016). Pre-amplification (10 cycles) was carried out in a StepOnePlus Real-Time PCR system (Thermo Fisher Scientific) using the following cycling programme: 95°C for 10 min, then 10 x of 95°C for 15 secs and 60°C for 4 min. After pre-amplification, each sample was 1:5 diluted in TE, pH 8.0 buffer and stored at -20°C.

Gene symbol	Assay ID	Reporter
ADIPOQ	Hs00605917_m1	FAM-NFQ
APOE	Hs00171168_m1	FAM-NFQ
BSCL2	Hs00949220_m1	FAM-NFQ
CASP1	Hs00354836_m1	FAM-NFQ
CDKN1B	Hs00153277_m1	FAM-NFQ
CIDEA	Hs00154455_m1	FAM-NFQ
CYP19A1	Hs00903411_m1	FAM-NFQ
EPAS1	Hs01026149_m1	FAM-NFQ
ESR1	Hs01046816_m1	FAM-NFQ
FABP4	Hs01086177_m1	FAM-NFQ
GHR	Hs00174872_m1	FAM-NFQ
HIF1A	Hs00153153_m1	FAM-NFQ
HOXC13	Hs00600868_m1	FAM-NFQ
INSR	Hs00961554_m1	FAM-NFQ
KLF14	Hs00370951_s1	FAM-NFQ
LDLR	Hs00181192_m1	FAM-NFQ
LEP	Hs00174877_m1	FAM-NFQ
LPL	Hs00173425_m1	FAM-NFQ
NR1H4	Hs01026590_m1	FAM-NFQ
PIK3R1	Hs00933163_m1	FAM-NFQ
PLIN2	Hs00605340_m1	FAM-NFQ
PPARG	Hs01115513_m1	FAM-NFQ
PPIA	Hs99999904_m1	FAM-NFQ
SIRT1	Hs01009006_m1	FAM-NFQ
SREBF1	Hs01088691_m1	FAM-NFQ
TCF7L2	Hs01009044_m1	FAM-NFQ
TGFB1	Hs00998133_m1	FAM-NFQ
TLR2	Hs00610101_m1	FAM-NFQ
TNF	Hs00174128_m1	FAM-NFQ

Table 5-2 TaqMan® Gene Expression Assays used for RT-qPCR.

Reference genes and genes of interest. Hs – *Homo sapiens*; '_m' indicates an essay whose probe spans an exon junction and will not detect genomic DNA; '_s' indicates an assay whose probes are designed within a single exon, and will, by definition, detect genomic DNA. The '_s' probe was only selected when there was no '_m' available by the time when experiments were carried.

5.2.3.1 Uniformity of pre-amplification

The bias of amplification was assessed by comparing the qPCR results (C_T value) with and without pre-amplification. *CDKN1B* was used as endogenous control for

pre-amplification efficiency as per the manufacturer's instructions. Briefly, RT-qPCR was carried for samples after pre-amplification as described below (5.2.4). Pre-amplified samples were serially diluted to 1/10, 1/20 and 1/200. ΔC_T was calculated between gene of interest (GOI) and *CDKN1B* (C_{TGOI} – $C_{TCDKN1B}$) for the diluted pre-amplified sample with the nearest C_T to the non-amplified sample. Then, $\Delta\Delta C_T$ was calculated as the difference of ΔC_T between these two groups ($\Delta C_{Tpre\text{-}amplified}$ - $\Delta C_{Tnon\text{-}amplified}$). Less than ± 1.5 difference in $\Delta\Delta C_T$ between the diluted pre-amplified sample and the non-amplified sample was acceptable (as recommended by the manufacturer).

5.2.4 RT-qPCR

The pre-amplified cDNA for specific target genes was quantitated using Taqman® real time PCR on a StepOnePlus Real-Time PCR system. Briefly, a RT-PCR reaction mix was made up for each target gene: 1.25 µL target Taqman® Gene Expression Assay, 12.5 µL TaqMan universal PCR master mix (Thermo Fisher Scientific, 4304437), and 5 µL nuclease-free water. Diluted pre-amplified cDNA, 6.25 µL, (2.6.4) was mixed with each PCR reaction mix in duplicate in a MicroAmp fast optical 96-well reaction plate (ThermoFisher Scientific), and underwent PCR according to the following programme: 50°C for 2 min, 95°C for 10 min, then 40 x of 95°C for 15 secs and 60°C for 1 min.

The fluorescence threshold for the FAM-NFQ reporter in each target assay was optimised as 0.2 ΔRn following the manufacturer's recommendation. No fluorescent signals were analysed for gene expression earlier than C_T = 15, as signals between cycle 3 and cycle 15 were considered to be background fluorescence according to the manufacturer's recommendation. Cycle threshold (Ct) value was determined by the StepOnePlus v2.3 software. *PPIA* was used as endogenous control for delta Ct and delta delta Ct analysis (Neville *et al.*, 2011).

5.2.5 Ingenuity pathway analysis

A pilot study of eight GOI (*ADIPOQ, LPL, SREBF1, LDLR, HIF1A, INSR, TNF* and *LEP*) were examined first to establish whether quantitative differences in gene expression could be detected, and the results were analysed. After it was confirmed that differences in expression were detectable, IPA was used to identify

potential genes that may respond to WG differently between SA and EU using the terms 'insulin resistance', 'weight gain', 'weight loss', 'size of adipocytes' and 'adipocyte differentiation' from the IPA database (Kramer *et al.*, 2014). The lists of genes were then analysed using a Venn diagram (Heberle *et al.*, 2015).

Between two and six hundred genes for each term inputted were identified by IPA. The output genes for each term were combined and analysed using a Venn diagram. A Venn diagram is used to compare sets of data such as genes, proteins, organisms as well as other entities (Heberle *et al.*, 2015). In this study, five sets of data from five inputted terms were combined to identify overlaps, and at least one gene was chosen from areas where four or five terms overlapped.

5.2.6 Statistics

Statistics were performed using Minitab version 19 (Minitab Ltd) and figures were drawn using GraphPad Prism 8.3. Normal distribution for all the parameters was checked using the Ryan-Joiner test. Non-normally distributed data were log or square root transformed to achieve normal distribution as required. Where a normal distribution was not achieved, non-parametric analysis was used. Results were displayed as mean ± standard deviation (SD) for parametric data and median [95% confident intervals] for non-parametric data.

Two group comparisons of cross-sectional parameters were made using two-sample t-test for normally distributed data or Mann-Whitney U-test for non-parametric data. A paired t-test was utilised to compare the BL and WG within each ethnic group, either EU or SA. Two-way comparisons (by ethnicity and time point) were carried out using a mixed-effect ANOVA. Univariate analysis was carried out using Pearson's correlation for parametric and Spearman's correlation for non-parametric data. Multivariate analysis was carried out within the mixed effect model ANOVA. Significance level was $p < 0.05$, and for interactions $p < 0.10$ was adopted.

5.3 Results

5.3.1 Study participants included in adipocyte gene expression analysis

In total 23 EU and 18 SA were recruited to the GlasVEGAs study of which 20 EU and 13 SA completed both BL and WG appointments as shown in Figure 5-2. Adipocyte gene expression was assessed where both WG and BL data were available (EU n = 20, SA n = 13).
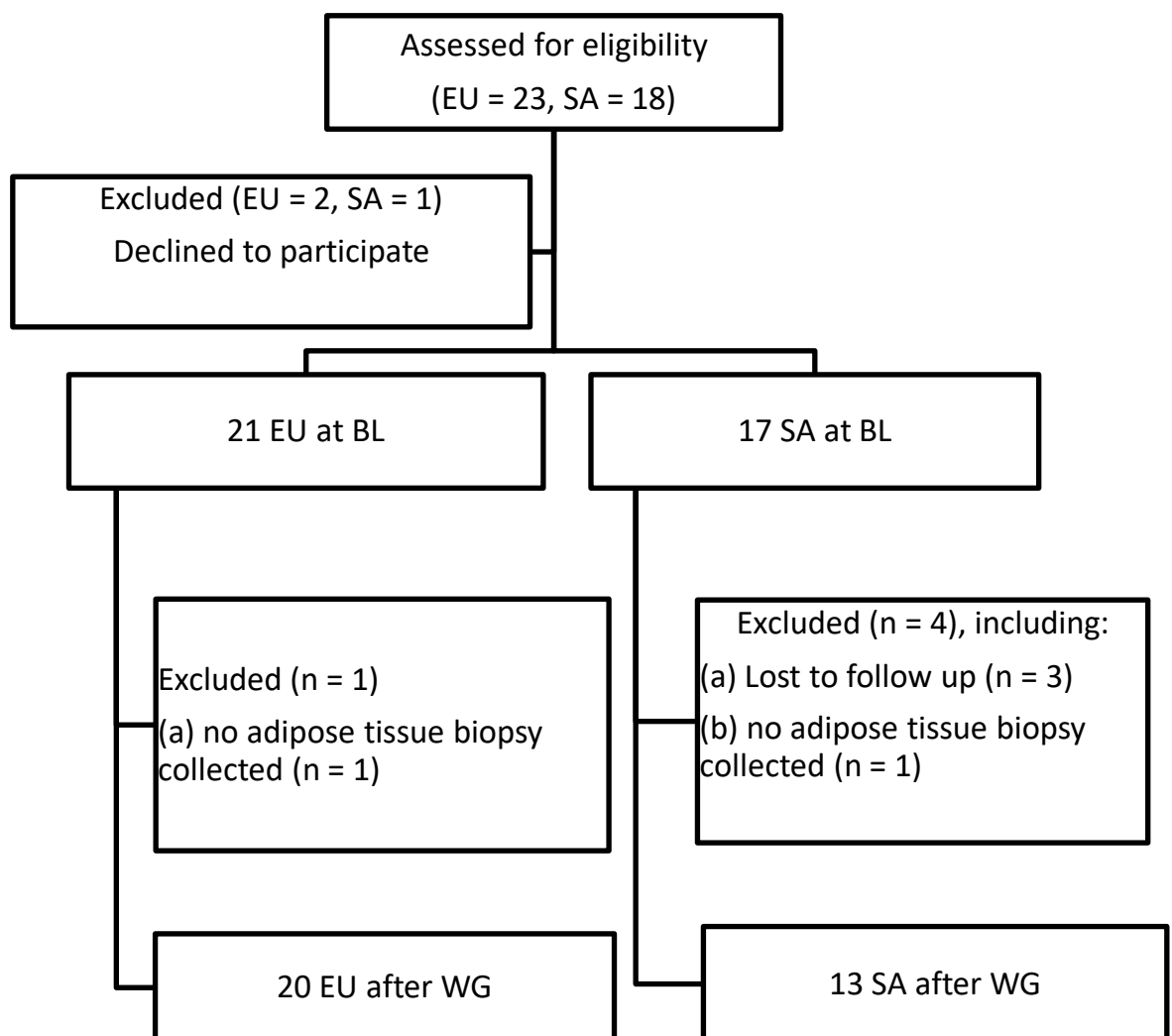
Figure 5-2 The CONSORT flow diagram for adipocyte size and gene expression assessment in GlasVEGAs study at BL and after WG.

5.3.2 Effect of weight gain on participant anthropometry

Anthropometry data are shown in Table 5-3. There were no significant differences between EU and SA in age, BMI, waist circumference and resting metabolic rate (RMR) at either BL or after WG. However, SA had a lower body weight and VO_2 max and higher total adipose tissue (no arm) than EU at BL and after WG.

The results showed a significant elevation in BMI, waist circumference, weight and total adipose tissue due to WG in both the EU and SA groups ($p \leqslant 0.0001$ in each group, Table 5-3). Despite these increases, the resting metabolic rate remained constant. Interestingly, a decrease in VO_2 max was observed exclusively in the EU group ($p = 0.044$), with no significant reduction noted in the SA group ($p = 0.120$).

	Baseline			Weight gain			Delta BL vs WG	
	EU (n = 20)	SA (n = 13)	*p* value (EU vs. SA)	EU (n = 20)	SA (n = 13)	p value (EU vs. SA)	*p* value EU	*p* value SA
Age (years) $	22 ± 3	23 ± 3	0.34	22 ± 3	23 ± 3	0.34	N/A	N/A
BMI (kg.m^{-2})	22.3 ± 1.5	21.7 ± 2.8	0.45	23.7 ± 1.7	23.2 ± 3.0	0.49	< 0.0001	< 0.0001
Waist (cm)	78.2 ± 4.2	76.7 ± 4.9	0.33	82.1 ± 4.3	81.9 ± 5.8	0.93	< 0.0001	< 0.0001
Weight (kg)	74.7 ± 8.1	67.9 ± 7.4	0.019	79.4 ± 9.0	72.3 ± 7.9	0.023	< 0.0001	< 0.0001
VO$_2$ max (ml/kg/min)	52.3 ± 5.0	44.0 ± 3.0	< 0.0001	48.3 ± 5.0	41.6 ± 4.7	0.0008	0.044	0.120
Total adipose tissue (no arm) (L)	14.2 ± 3.6	18.3 ± 4.1	0.006	17.2 ± 4.6	21.3 ± 3.9	0.015	< 0.0001	< 0.0001
RMR (kcal/kg/day)	22.0 ± 2.3	22.2 ± 3.2	0.82	22.1 ± 2.2	23.3 ± 3.6	0.25	0.98	0.19

Table 5-3 Demographic data for European (EU) and South Asian (SA) participants in the GlasVEGAs study at baseline (BL) and after weight gain (WG).

This table showcases demographic information including body mass index (BMI) and resting metabolic rate (RMR) for both EU and SA participants at the initial stage and after experiencing weight gain. The changes between the baseline and weight gain are also indicated (Delta BL vs WG). Comparisons were made using a two-sample t-test. The symbol $ denotes statistical analysis performed on log-transformed data.

5.3.3 Candidate Gene Selection

Five terms, 'insulin resistance', 'weight gain', 'weight loss', 'size of adipocytes' and 'adipocyte differentiation', were searched in the IPA database, based on the results of a pilot study of eight GOI (*ADIPOQ, LPL, SREBF1, LDLR, HIF1A, INSR, TNF* and *LEP*). A list of 656 genes were found relevant to 'insulin resistance', 577 genes for 'weight gain', 448 genes for 'weight loss', 164 genes for 'size of adipocytes' and 492 genes for 'adipocyte differentiation'.

All the genes were combined in a Venn diagram according to the search terms (Figure 5-3). Eight GOI (*BSCL2, CASP1, NR1H4, PIK3R1, PPARG, SIRT, TLR2* and *TGFB1*) were selected where at least four search terms overlapped.

After this initial analysis, based on the pilot study and results of initial analysis, another ten GOI (*APOE, CIDEA, CYP19A1, ESR, EPAS1, GHR, HOXC13, KLF14, PLIN2 and TCF7L2*) was added by literature review. Therefore, in total of 26 GOI had been selected and examined in the current study.
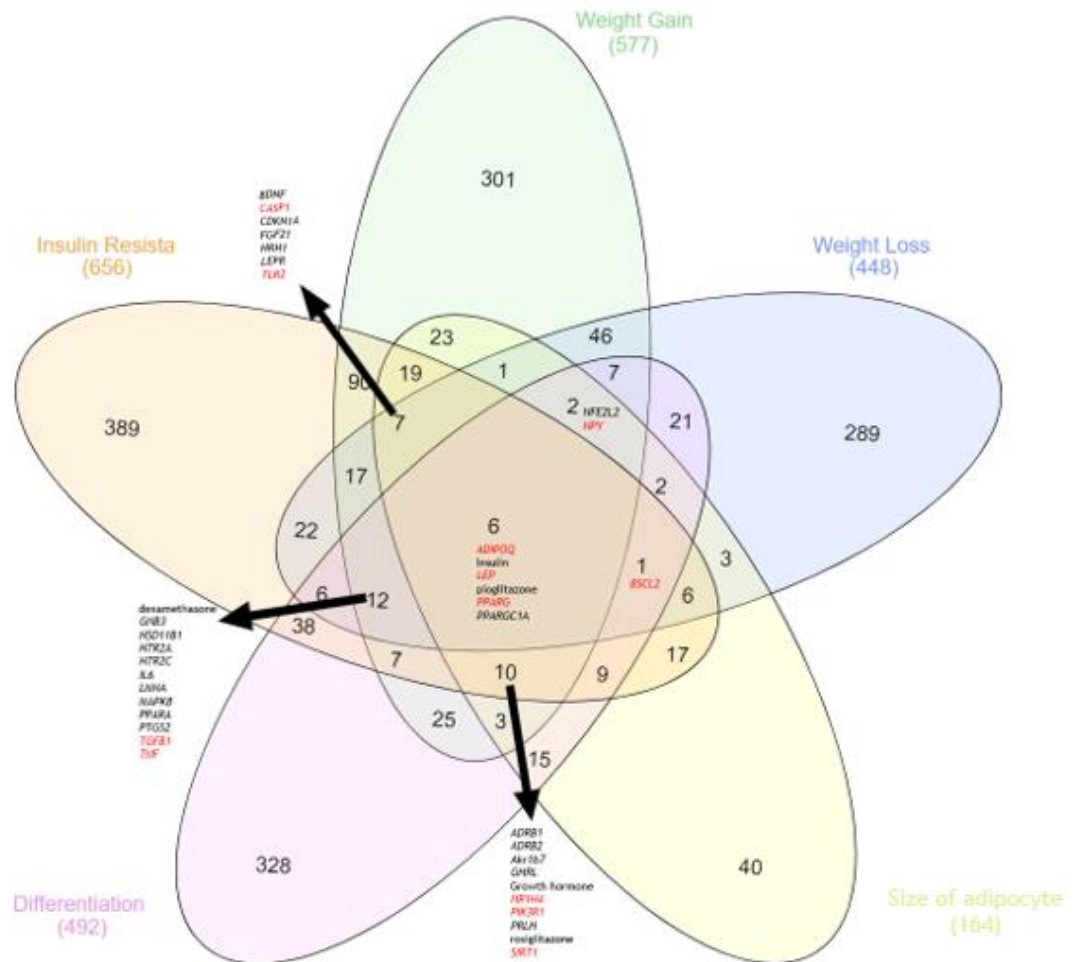
Figure 5-3 Venn diagram: overlap of key genes in adipocyte function and insulin resistance

This Venn diagram illustrates the interplay of genes associated with 'insulin resistance', 'weight gain', 'weight loss', 'adipocyte size', and 'adipocyte differentiation' as identified through Ingenuity Pathway Analysis. Genes particularly pertinent to this study are emphasised in red.

5.3.4 Uniformity of pre-amplification

Uniformity of pre-amplification for the 27 (26 genes of interest and *PPIA*) analysed in this chapter is shown in Figure 5-4. All the probes showed pre-amplification uniformity as the $\Delta\Delta C_T$ values fell within ± 1.5 range. Because of the low expression of *HOXC13* and *NR1H4* in the adipocytes tested, these genes were removed from further analysis.
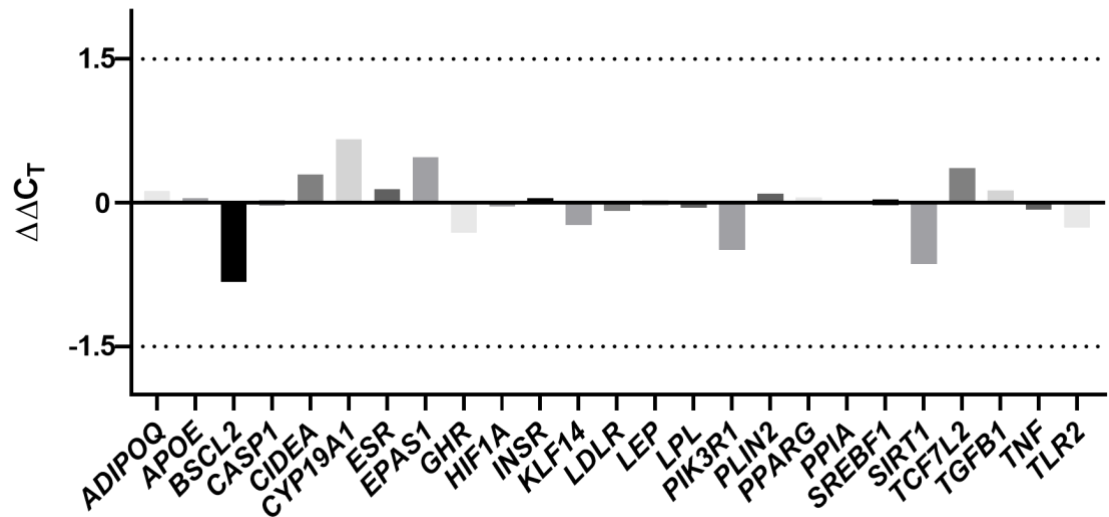
Figure 5-4 Uniformity of 26 genes of interest and the endogenous control gene (*PPIA*) in adipocytes from the GlasVEGAs study.

Because of the low expression of *HOXC13* and *NR1H4* in the adipocytes tested, they were not able to be analysed.

5.3.5 Adipocyte gene expression in SA and EU at BL and after WG

Gene expression in adipocytes from EU and SA GlasVEGAs participants at baseline and after weight gain was determined. The data from the n = 8 genes assessed in the pilot study and then n = 18 genes identified by Ingenuity Pathway Analysis and literature review are shown together. Percentage gene expression relative to *PPIA* was plotted for ethnicity group and study visit. A two-way analysis using the mixed effects model was carried out to assess the independent effects of WG and ethnicity and their interaction (study visit*ethnicity) on gene expression. Gene expression was found to be significantly different between SA and EU and/or between BL and WG in thirteen out of 24 GOI (Figure 5-5).

Figure 5-5 Differential expression of key adipocyte genes: a comparative analysis between EU and SA

This figure presents the significant variances in the expression of adipocyte genes involved in (a) insulin signalling, (b) tissue stress response/inflammation, and (c) & (d) lipid storage pathways, between European (EU) and South Asian (SA) subjects, both at baseline (BL) and post weight gain (WG). The expression levels are shown as a percentage relative to PPIA. A mixed effects model ANOVA was used for two-way comparisons between ethnicity and study visit. Key genes include: *INSR*: insulin receptor; CIDEA, cell death inducing DFFA like effector A; ESR1, estrogen receptor 1; *SIRT1*: sirtuin 1; *PLIN2*: perilipin 2; *GHR*: growth hormone receptor; *TCF7L2*, transcription factor 7 like 2; *TNF*: tumour necrosis factor; *TLR2*, toll like receptor 1; *ADIPOQ*, adiponectin; *SREBF1*: sterol regulatory element binding transcription factor 1; *LEP*: leptin; *APOE*: apolipoprotein E. Error bars are shown as standard deviation.

5.3.5.1 Significant differences in genes involved in insulin sensitivity

Expression of genes involved in the regulation of insulin sensitivity, including *INSR, CIDEA, SIRT1, PLIN2* and *GHR*, were lower in SA than EU and decreased after WG, whereas *ESR1* also had lower expression in SA compared to EU but was unaffected by WG (Figure 5-5(a)). No interactions between ethnicity and WG were found.

5.3.5.2 Significant differences in genes involved in tissue stress response/ inflammation

SA had higher *TNF* expression than EU at BL and after WG (Figure 5-5 (b)). In response to WG the expression of *TCF7L2* and *TLR2* decreased significantly in both SA and EU compared to BL, however, no interaction between ethnicity and WG was found (Figure 5-5 (b)).

5.3.5.3 Significant differences in genes involved in lipid storage

LEP and *SREBF1*, were higher in SA than EU and increased after WG, whereas *ADIPOQ* expression was lower in SA than EU (Figure 5-5 (c)). *APOE* expression was lower in SA than in EU and decreased after WG. *APOE* expression decreased to a lesser degree in SA compared to EU in response to WG (interaction term $p = 0.060$, Figure 5-5 (d)).

5.3.5.4 Genes with no significant differences between ethnicity or in response to WG

Eleven genes showed no significant differences in expression according to ethnicity or in response to weight gain and are shown in Figure 5-6.

(a)
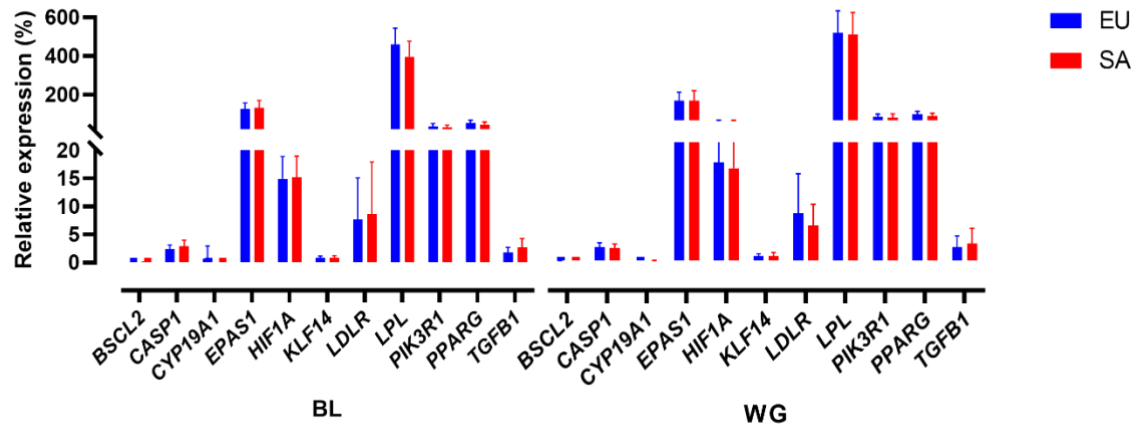
(b)

Genes	Study visit (*p*)	Ethnicity (*p*)
BSCL2	0.11	0.55
CASP1	0.14	0.28
CYP19A1	0.20	0.37
EPAS1	0.15	0.79
HIF1A	0.23	0.80
KLF14	0.98	0.92
LDLR	0.55	0.82
LPL	0.56	0.24
PIK3R1	0.41	0.26
PPARG	0.21	0.060
TGFB1	0.22	0.16

Figure 5-6 Unaltered adipocyte gene expression in EU and SA: at BL and after WG

(a) Represents the constant adipocyte gene expression in European (EU) and South Asian (SA) participants at baseline (BL) and following weight gain (WG). (b) Displays the *p*-value for the study visit and ethnicity. A mixed effects model ANOVA was used for two-way comparisons between ethnicity and study visit. Key genes include: *BSCL2*, lipid droplet biogenesis associated seipin; *CASP1*, caspase 1; *CYP19A1*, cytochrome P450 family 19 subfamily A member 1; *EPAS1*, endothelial PAS domain protein 1; *HIF1A*, hypoxia inducible factor 1 subunit alpha; *KLF14*, kruppel like factor 14; *LDLR*, low density lipoprotein receptor; *LPL*, lipoprotein lipase; *PIK3R1*, phosphatidylinositol 3-kinase regulatory subunit 1; *PPARG*, peroxisome proliferator activated receptor gamma; *TGFB1*, transforming growth factor beta 1.

5.3.6 Confounding effects of patient anthropometry on weight gain effects on adipocyte gene expression

Genes where there were significant differences in expression (study visit and/or ethnicity) were tested for whether the differences in gene expression could be explained by differences in body composition or fitness using multi-variate analysis by ANOVA mixed effect models. Univariate analysis of correlation with gene expression was first carried out for each covariate (weight, BMI, RMR, waist, VO$_2$ max, total adipose tissue (no arm) and adipocyte diameter). Covariates that

showed significant correlation with gene expression were included in an ANOVA mixed effects model with study visit and ethnicity to identify their contribution to variation in gene expression as determined by R^2 and p value.

5.3.6.1 INSR

The correlations between *INSR* expression and covariates, including weight, BMI, waist, adipocyte diameter, RMR, VO_2 max and total adipose tissue, were analysed in a univariate analysis. A strong positive correlation was found between *INSR* expression and VO_2 max (r = 0.34, p = 0.010, Table 5-4), and three negative correlations were found between *INSR* expression and waist, adipocyte diameter and total adipose tissue (r = -0.32, -0.38 and -0.52, p = 0.013, 0.003 and < 0.0001, respectively, Table 5-4).

Then multivariate analysis was performed to examine the confounding effects of waist, adipocyte diameter, VO_2 max and total adipose tissue on weight gain effects on *INSR* expression between SA and EU. However, when adipocyte diameter and VO_2 max were added, the significance of study visit and ethnicity dropped out, and the proportion of variance explained by the model decreased (r^2 = 52.6%). A better model of higher r^2 was generated when these variables were removed. In this optimised model, ethnicity independently explained the differences in *INSR* expression (p = 0.017) independent of waist, total adipose tissue and study visit (Table 5-5).

Terms	r	p value
Weight	-0.010	0.94
BMI	-0.25	0.052
Waist	-0.32	0.013
Adipocyte diameter	-0.38	0.003
RMR	-0.17	0.19
VO_2 max	0.34	0.010
Total adipose tissue (no arm)	-0.52	< 0.0001

Table 5-4 Correlation between *INSR* expression and patient anthropometry using Pearson's correlation.

Terms	p value	r^2 of model
Waist	0.35	
Total adipose tissue (no arm)	0.45	58.5 %
Study visit	0.57	
Ethnicity	0.017	

Table 5-5 ANOVA mixed effect model: *INSR* expression versus factor and covariates.

Factor (ethnicity and study visit) and covariates (waist, adipocyte diameter, VO_2 max and total adipose tissue).

5.3.6.2 CIDEA

The correlations between *CIDEA* expression and covariates, including weight, BMI, waist, adipocyte diameter, RMR, VO_2 max and total adipose tissue, were analysed in a univariate analysis. A strong positive correlation was found between *CIDEA* expression and VO_2 max (r = 0.44, p = 0.001,Table 5-6), and two negative correlations were found between *CIDEA* expression and adipocyte diameter and total adipose tissue (r = -0.40 and -0.63, p = 0.001, and < 0.0001, respectively, Table 5-6).

Then multivariate analysis was performed to examine the confounding effects of adipocyte diameter, VO_2 max and total adipose tissue on weight gain and ethnicity effects on *CIDEA* expression. Total adipose tissue, study visit, and ethnicity were significantly independently associated with *CIDEA* expression (p = 0.015, 0.048 and 0.042, respectively) (Table 5-7).

Terms	r	p value
Weight	0.23	0.080
BMI	-0.070	0.59
Waist	-0.17	0.19
Adipocyte diameter	-0.40	0.001
RMR	-0.17	0.20
VO_2 max	0.44	0.001
Total adipose tissue (no arm)	-0.63	< 0.0001

Table 5-6 Correlation between *CIDEA* expression and patient anthropometry using Pearson correlation.

Terms	p value	r^2 of model
Adipocyte diameter	0.77	
VO$_2$ max	0.70	
Total adipose tissue (no arm)	0.015	58.1 %
Study visit	0.048	
Ethnicity	0.042	

Table 5-7 ANOVA mixed effect model: *CIDEA* expression versus factors and covariates.

Factors (study visit and ethnicity) and covariates (adipocyte diameter, VO$_2$ max and total adipose tissue).

5.3.6.3 ESR1

The correlations between *ESR1* expression and covariates, including weight, BMI, waist, adipocyte diameter, RMR, VO$_2$ max and total adipose tissue, were analysed in a univariate analysis. A positive correlation was found between *ESR1* expression and VO$_2$ max (r = 0.32, p = 0.016, Table 5-8). Three negative correlations were found between *ESR1* expression and adipocyte diameter, RMR and total adipose tissue (r = -0.38, -0.30 and -0.39, p = 0.003, 0.022 and 0.003, respectively, Table 5-8).

Then multivariate analysis was performed to examine the confounding effects of adipocyte diameter, RMR, VO$_2$ max and total adipose tissue on ethnicity effects on *ESR1* expression. Ethnicity was significantly independently associated with *ESR1* expression (p = 0.015) (Table 5-9).

Terms	r	p value
Weight	0.080	0.55
BMI	-0.029	0.83
Waist	-0.18	0.17
Adipocyte diameter	-0.38	0.003
RMR	-0.30	0.022
VO$_2$ max	0.32	0.016
Total adipose tissue (no arm)	-0.39	0.003

Table 5-8 Correlation between *ESR1* expression and patient anthropometry using Pearson correlation.

Terms	*p* value	r² of model
Adipocyte diameter	0.75	
RMR	0.14	
VO₂ max	0.46	53.07 %
Total adipose tissue (no arm)	0.16	
Study visit	0.080	
Ethnicity	0.015	

Table 5-9 ANOVA mixed effect model: *ESR1* expression versus factors and covariates.

Factors (study visit and ethnicity) and covariates (adipocyte diameter, RMR, VO₂ max and total adipose tissue).

5.3.6.4 GHR

The correlations between *GHR* expression and covariates, including weight, BMI, waist, adipocyte diameter, RMR, VO₂ max and total adipose tissue, were analysed in a univariate analysis. Two positive correlations were found between *GHR* expression and weight and VO₂ max (r = 0.28 and 0.33, *p* = 0.032 and 0.012, respectively, Table 5-10). Three negative correlations were found between *GHR* expression and adipocyte diameter, RMR and total adipose tissue (r = -0.30, -0.37 and -0.48, *p* = 0.021, 0.003 and < 0.0001, respectively, Table 5-10).

Then multivariate analysis was performed to examine the confounding effects of weight, adipocyte diameter, RMR, VO₂ max and total adipose tissue on weight gain effects on *GHR* expression between SA and EU. However, when adipocyte diameter was added, significance of study visits and ethnicity dropped out, and less variance was explained by the model (r² = 52.8%). A better model with higher r² was generated when these variables were removed. In this model, ethnicity, study visit and total adipose tissue independently explained the differences in expression of *GHR* (Table 5-11).

Terms	r	*p* value
Weight	0.28	0.032
BMI	0.028	0.83
Waist	-0.060	0.68
Adipocyte diameter	-0.30	0.021
RMR	-0.37	0.003
VO₂ max	0.33	0.012
Total adipose tissue (no arm)	-0.48	< 0.0001

Table 5-10 Correlation between *GHR* expression and patient anthropometry using Pearson correlation.

Terms	*p* value	r^2 of model
Weight	0.32	
RMR	0.085	
VO$_2$ max	0.48	55.1 %
Total adipose tissue (no arm)	0.038	
Study visit	0.033	
Ethnicity	0.005	

Table 5-11 ANOVA mixed effect model: *GHR* expression versus factors and covariates.

Factors (study visit and ethnicity) and covariates (weight, RMR, VO$_2$ max and total adipose tissue).

5.3.6.5 SIRT1

The correlations between *SIRT1* expression and covariates, including weight, BMI, waist, adipocyte diameter, RMR, VO$_2$ max and total adipose tissue, were analysed in a univariate analysis. A positive correlation was found between *SIRT1* expression and VO$_2$ max (r = 0.31, *p* = 0.019,Table 5-12). Two negative correlations were found between *SIRT1* expression and adipocyte diameter and total adipose tissue (r = -0.34 and -0.41, *p* = 0.008 and 0.002, respectively, Table 5-12).

Then multivariate analysis was performed to examine the confounding effects of adipocyte diameter, VO$_2$ max and total adipose tissue on weight gain and ethnicity effects on *SIRT1* expression. Ethnicity was significantly independently associated with *SIRT1* expression (*p* = 0.008) (Table 5-13).

Terms	r	*p* value
Weight	0.068	0.61
BMI	-0.24	0.065
Waist	-0.24	0.062
Adipocyte diameter	-0.34	0.008
RMR	-0.15	0.26
VO$_2$ max	0.31	0.019
Total adipose tissue (no arm)	-0.41	0.0020

Table 5-12 Correlation between *SIRT1* expression and patient anthropometry using Pearson correlation.

Terms	p value	r^2 of model
Adipocyte diameter	0.73	
VO$_2$ max	0.62	
Total adipose tissue (no arm)	0.37	48.9 %
Ethnicity	0.008	
Study visit	0.083	

Table 5-13 ANOVA mixed effect model: *SIRT1* expression versus factors and covariates.

Factors (study visit and ethnicity) and covariates (adipocyte diameter, VO$_2$ max and total adipose tissue).

5.3.6.6 PLIN2

The correlations between *PLIN2* expression and covariates, including weight, BMI, waist, adipocyte diameter, RMR, VO$_2$ max and total adipose tissue, were analysed in a univariate analysis. A positive correlation was found between *PLIN2* expression and VO$_2$ max (r = 0.29, *p* = 0.029, Table 5-14). Two negative correlations were found between *PLIN2* expression and adipocyte diameter and total adipose tissue (r = -0.28 and -0.37, *p* = 0.031 and 0.005, respectively, Table 5-14).

Then multivariate analysis was performed to examine the confounding effects of adipocyte diameter, VO$_2$ max and total adipose tissue on weight gain effects on *PLIN2* expression. Study visit, but not ethnicity, was significantly independently associated with *PLIN2* expression (*p* = 0.018) (Table 5-15).

Terms	r	p value
Weight	0.20	0.14
BMI	-0.14	0.27
Waist	-0.13	0.32
Adipocyte diameter	-0.28	0.031
RMR	-024	0.062
VO$_2$ max	0.29	0.029
Total adipose tissue (no arm)	-0.37	0.005

Table 5-14 Correlation between *PLIN2* expression and patient anthropometry using Pearson correlation.

Terms	p value	r^2 of model
Adipocyte diameter	0.99	
VO$_2$ max	0.92	
Total adipose tissue (no arm)	0.45	52.2 %
Study visit	0.018	
Ethnicity	0.069	

Table 5-15 ANOVA mixed effect model: *PLIN2* expression versus factors and covariates.

Factors (study visit and ethnicity) and covariates (adipocyte diameter, VO₂ max and total adipose tissue).

5.3.6.7 TCF7L2

The correlations between *TCF7L2* expression and covariates, including weight, BMI, waist, adipocyte diameter, RMR, VO₂ max and total adipose tissue, were analysed in a univariate analysis. However, no significant correlation was found (Table 5-16).

Study visit and ethnicity explained 60.2% of the variance in *TCF7L2* expression (Table 5-17).

Terms	r	p value
Weight	0.0090	0.95
BMI	-0.12	0.36
Waist	-0.19	0.14
Adipocyte diameter	-0.12	0.38
RMR	-0.074	0.57
VO$_2$ max	0.062	0.65
Total adipose tissue (no arm)	-0.220	0.10

Table 5-16 Correlation between *TCF7L2* expression and patient anthropometry using Pearson correlation.

Terms	p value	r^2 of model
Study visit	0.007	60.2 %
Ethnicity	0.052	

Table 5-17 ANOVA mixed effect model: *TCF7L2* expression versus factors.

Factors (study visit and ethnicity).

5.3.6.8 TNF

The correlations between *TNF* expression and covariates, including weight, BMI, waist, adipocyte diameter, RMR, VO₂ max and total adipose tissue, were analysed in a univariate analysis. Two positive correlations were found between *TNF* expression and adipocyte diameter and total adipose tissue (r = 0.30 and 0.47, *p*

= 0.020 and < 0.0001, respectively, Table 5-18). One negative correlation was found between *TNF* expression and VO_2 max (r = -0.36, *p* = 0.007, Table 5-18).

Then multivariate analysis was performed to examine the confounding effects of adipocyte diameter, VO_2 max and total adipose tissue on weight gain effects on *TNF* expression between SA and EU. Total adipose tissue and ethnicity were significantly independently associated with *TNF* expression (*p* = 0.021 and 0.031, respectively) (Table 5-19).

Terms	r	*p* value
Weight	-0.005	0.97
BMI	0.12	0.37
Waist	0.25	0.060
Adipocyte diameter	0.30	0.020
RMR	-0.11	0.39
VO_2 max	-0.36	0.007
Total adipose tissue (no arm)	0.47	< 0.0001

Table 5-18 Correlation between *TNF* expression and patient anthropometry using Pearson correlation.

Terms	*p* value	r^2 of model
Adipocyte diameter	0.83	
VO_2 max	0.37	
Total adipose tissue (no arm)	0.021	74.1 %
Study visit	0.054	
Ethnicity	0.031	

Table 5-19 ANOVA mixed effect model: *TNF* expression versus factors and covariates.

Factors (study visit and ethnicity) and covariates (adipocyte diameter, total adipose tissue (no arm) and VO_2 max).

5.3.6.9 TLR2

The correlations between *TLR2* expression and covariates, including weight, BMI, waist, adipocyte diameter, RMR, VO_2 max and total adipose tissue, were analysed in a univariate analysis. Two positive correlations were found between *TLR2* expression and VO_2 max and total adipose tissue (r = 0.30 and 0.27, *p* = 0.025 and 0.042, respectively, Table 5-20).

Then multivariate analysis was performed to examine the confounding effects of VO_2 max and total adipose tissue on weight gain effects on *TLR2* expression

between SA and EU. Interestingly, in this model ethnicity was now significantly independently associated with *TLR2* expression (p = 0.010) (Table 5-21).

Terms	r	p value
Weight	0.10	0.43
BMI	-0.04	0.74
Waist	-0.11	0.39
Adipocyte diameter	-0.18	0.16
RMR	0.17	0.21
VO$_2$ max	0.30	0.025
Total adipose tissue (no arm)	0.27	0.042

Table 5-20 Correlation between *TLR2* expression and patient anthropometry using Pearson correlation.

Terms	p value	r^2 of model
VO$_2$ max	0.39	
Total adipose tissue (no arm)	0.88	40.1 %
Ethnicity	0.010	
Study visit	0.71	

Table 5-21 ANOVA mixed effect model: *TLR2* expression versus factors and covariates.

Factors (study visit and ethnicity) and covariates (VO$_2$ max and total adipose tissue).

5.3.6.10 *SREBF1*

The correlations between *SREBF1* expression and covariates, including weight, BMI, waist, adipocyte diameter, RMR, VO$_2$ max and total adipose tissue, were analysed in a univariate analysis. A negative correlation was found between *SREBF1* expression and VO$_2$ max (r = -0.30, p = 0.024, Table 5-22).

Then multivariate analysis was performed to examine the confounding effects of VO$_2$ max on weight gain and ethnicity effects on *SREBF1* expression. Study visit and ethnicity were significantly independently associated with *SREBF1* expression (p = 0.032 and 0.036, respectively) (Table 5-23).

Terms	r	p value
Weight	0.023	0.86
BMI	-0.003	0.98
Waist	0.030	0.82
Adipocyte diameter	0.12	0.36
RMR	0.19	0.15
VO$_2$ max	-0.30	0.024
Total adipose tissue (no arm)	0.24	0.073

Table 5-22 Correlation between *SREBF1* expression and patient anthropometry using Pearson correlation.

Terms	p value	r^2 of model
VO$_2$ max	0.57	
Ethnicity	0.036	43.4 %
Study visit	0.032	

Table 5-23 ANOVA mixed effect model: *SREBF1* expression versus factors and covariate.

Factors (study visit and ethnicity) and covariate (VO$_2$ max).

5.3.6.11   *ADIPOQ*

The correlations between *ADIPOQ* expression and covariates, including weight, BMI, waist, adipocyte diameter, RMR, VO$_2$ max and total adipose tissue, were analysed in a univariate analysis. A negative correlation was found between *ADIPOQ* expression and total adipose tissue (r = -0.28, p = 0.037, Table 5-24).

Then multivariate analysis was performed to examine the confounding effects of total adipose tissue on ethnicity effects on *ADIPOQ* expression. Total adipose tissue was significantly independently associated with *ADIPOQ* expression (p = 0.003) and ethnicity was now no longer a significant predictor (Table 5-25).

Terms	R	p value
Weight	0.080	0.54
BMI	0.002	0.99
Waist	-0.17	0.20
Adipocyte diameter	-0.13	0.32
RMR	-0.14	0.30
VO$_2$ max	0.15	0.28
Total adipose tissue (no arm)	-0.28	0.037

Table 5-24 Correlation between *ADIPOQ* expression and patient anthropometry using Pearson correlation.

Terms	*p* value	R^2 of model
Total adipose tissue (no arm)	0.003	
Study visit	0.96	41.4 %
Ethnicity	0.19	

Table 5-25 ANOVA mixed effect model: *ADIPOQ* expression versus factors and covariate.

Factors (ethnicity and study visit) and covariate (total adipose tissue).

5.3.6.12   LEP

The correlations between *LEP* expression and covariates, including weight, BMI, waist, adipocyte diameter, RMR, VO$_2$ max and total adipose tissue, were analysed in a univariate analysis. Four positive correlations were found between *LEP* expression and BMI, waist, adipocyte diameter and total adipose tissue (r = 0.31, 0.28, 0.59 and 0.67, *p* = 0.017, 0.028, < 0.0001 and < 0.0001, respectively, Table 5-26). A negative correlation was found between LEP expression and VO2 max (r = -0.67, P < 0.0001, Table 5-26).

Then multivariate analysis was performed to examine the confounding effects of BMI, waist, adipocyte diameter, VO$_2$ max and total adipose tissue on weight gain and ethnicity effects on *LEP* expression. Ethnicity and total adipose tissue independently explained the variance in expression of *LEP* (*p* = 0.009 and 0.026, ethnicity and total adipose tissue, respectively) (Table 5-27).

Terms	r	*p* value
Weight	0.060	0.64
BMI	0.31	0.017
Waist	0.28	0.028
Adipocyte diameter	0.59	< 0.0001
RMR	-0.070	0.61
VO$_2$ max	-0.67	< 0.0001
Total adipose tissue (no arm)	0.67	< 0.0001

Table 5-26 Correlation between *LEP* expression and patient anthropometry using Pearson correlation.

Terms	p value	r^2 of model
BMI	0.19	
Waist	0.36	
Adipocyte diameter	0.17	91.1 %
VO$_2$ max	0.79	
Total adipose tissue (no arm)	0.026	
Study visit	0.38	
Ethnicity	0.009	

Table 5-27 ANOVA mixed effect model: *LEP* expression versus factors and covariates.

Factors (ethnicity and study visit) and covariates (BMI, waist, adipocyte diameter, VO$_2$ max and total adipose tissue).

5.3.6.13 APOE

The correlations between *APOE* expression and covariates, including weight, BMI, waist, adipocyte diameter, RMR, VO$_2$ max and total adipose tissue, were analysed in a univariate analysis. Two positive correlations were found between *APOE* expression and weight and VO$_2$ max (r = 0.28 and 0.32, *p* = 0.030 and 0.016, respectively, Table 5-28). Two negative correlations were found between APOE expression and adipocyte diameter and total adipose tissue (r = -0.42 and -0.43, *P* = 0.001 and 0.001, respectively, Table 5-28)

Then multivariate analysis was performed to examine the confounding effects of weight, adipocyte diameter, VO$_2$ max and total adipose tissue on weight gain, ethnicity and interactive effects on *APOE* expression. Study visit was significantly independently associated with *APOE* expression (*p* < 0.001). Furthermore, *APOE* expression decreased to a lesser degree in SA compared to EU in response to WG (independent interaction term (*p* = 0.062) (Table 5-29).

Terms	r	p value
Weight	0.28	0.030
BMI	0.034	0.80
Waist	-0.090	0.51
Adipocyte diameter	-0.42	0.001
RMR	-0.17	0.20
VO$_2$ max	0.32	0.016
Total adipose tissue (no arm)	-0.43	0.0010

Table 5-28 Correlation between *APOE* expression and patient anthropometry using Pearson correlation.

Terms	p value	r^2 of model
Weight	0.053	
Adipocyte diameter	0.23	
VO$_2$ max	0.60	
Total adipose tissue (no arm)	0.29	85.4 %
Ethnicity	0.43	
Study visit	< 0.001	
Interaction	0.062	

Table 5-29 ANOVA mixed effect model: *APOE* expression versus factors and covariates.

Factors (ethnicity, study visit) and covariates (weight, adipocyte diameter, VO$_2$ max and total adipose tissue).

5.4 Discussion

The main findings of this study indicate that adipocyte gene expression is different between SA and EU at BL and changes in response to 6% WG in body mass. Six genes that are involved in the insulin signalling pathway were expressed at lower levels in SA than EU and/or decreased in response to WG. SA showed an overall higher level of adipocyte inflammation than EU, however, after WG, expression of *TLR2* and *TCF7L2* decreased, suggesting a decrease in inflammation in both SA and EU. Three genes in lipid storage pathways expressed differently between SA and EU, BL and/or after WG. *ADIPOQ* expression was lower in SA than EU which confirms the hypothesis that SA express lower levels of genes associated with FA oxidation and lipid storage. However, both *LEP* and *SREBF1* genes were expressed at higher levels in SA arguing against the hypothesis and will be discussed later. There was no difference in the expression of genes associated with adipocyte differentiation between SA and EU, BL and after WG. This suggested that in mature adipocytes, expression of genes associated with adipogenesis may be similar and the differences may be found in pre-adipocytes during adipogenesis.

Genes involved in the regulation of insulin sensitivity showed an overall lower expression level in SA than EU and decreased after WG, which is consistent with the observations that SA develop insulin resistance at younger age and lower BMI than EU, and this propensity for insulin resistance is exacerbated by an increase in body weight) (Petersen *et al.*, 2006). SA men with a BMI of 21.6 kg/m^2 (21.5 and 22.3 kg/m^2 for Pakistani and Indian men respectively) had a similar prevalence of diabetes to EU men at a BMI of 30 kg/m^2 (Ntuk *et al.*, 2014). These six genes covered different aspects of adipocyte regulation of whole body insulin sensitivity

as shown in 5.1.1, including hormone response (*ESR1* and *GHR*), lipid droplet formation (*CIDEA* and *PLIN2*), and insulin regulation and insulin-like mechanism (*INSR* and *SIRT1*). This may suggest that the higher risk in SA of getting T2DM compared to EU may involve mechanisms in different aspects of adipose tissue and whole-body mechanism. INSR and SIRT1 expression are associated with insulin sensitivity. A lower level of *INSR* and *SIRT1* expression in adipocytes in SA than EU suggests lower adipocyte insulin sensitivity in SA. In mouse white adipocytes, ESR1 controlled oxidative metabolism by restraining the targeted elimination of mitochondria via the E3 ubiquitin ligase parkin in an insulin-like manner (Zhou *et al.*, 2020a). Lower *ESR1* expression in SA suggests lower oxidative metabolism in adipocytes than EU. Ectopic adiposity is defined as an accumulation of fat not associated with adipose tissue storage and may contribute to inflammation and insulin resistance (Hens *et al.*, 2017). Loss of lean mass, especially in relative muscle mass, is negatively associated with development of T2DM (Hong *et al.*, 2017). Thus, this may contribute to the higher risk of diabetes in SA. A study indicated that the absence of *PLIN2* prevents HFD-induced obesity in mice (McManaman *et al.*, 2013), but because of the crucial role of *PLIN2* during the development of formation of intracellular lipid droplets (Itabe *et al.*, 2017), the lower expression of *PLIN2* in SA may be associated with decreased adipogenesis because of the difficulty of maturing adipocytes when lipid droplet formation is impaired.

In line with our hypothesis, SA showed a consistently higher *TNF* expression than EU at BL and after WG, which may indicate that SA develop abnormal regulation of inflammatory responses in their adipocytes. TNFα may also impair IR-proximal signalling through the activation of IRS serine kinases and the production of toxic lipids (Cawthorn and Sethi, 2008). This may worsen the local inflammation in WAT. However, after WG, expression of *TCF7L2* and *TLR2*, decreased, and does not agree with the observation that in SA and EU, decreases in genes associated with inflammation had been found. In adipocyte specific TCF7L2 knockout mice, HFD introduced more severe weight gain, glucose resistance and lipolysis than WT (Geoghegan *et al.*, 2019, Nguyen-Tu *et al.*, 2021a). TCF7L2 in adipocytes also plays an important role in maintaining body weight and insulin sensitivity, and during the progress of WG expression of TCF7L2 may be suppressed and this happened similarly in both SA and EU.

ADIPOQ expression was lower in SA than EU and decreased after WG, and this agreed with the hypothesis. Increased adiponectin (*ADIPOQ*) mRNA expression leads to enhanced adiponectin release, and this promotes ß-oxidation and energy dissipation by inducing acyl-CoA oxidase and uncoupling protein-2 expression activity (Yamauchi *et al.*, 2001). Circulating adiponectin also increases insulin sensitivity by inhibiting FFA release from adipocytes (Diez and Iglesias, 2003). Thus, low *ADIPOQ* expression in adipocytes may contribute to the higher insulin resistance in SA than EU. However, expression of *LEP* and *SREBF1* was higher in SA and increased after WG, this agreed with our hypothesis as SREBF promotes lipid storage and LEP is a marker of lipid storage. Thus, SA may develop leptin resistance in response to WG even at a relatively low BMI, as higher level of *LEP* expression was found in SA than EU at a similar BMI. In healthy humans it has been shown that an increase in *LEP* expression is positively correlated to an increase of *CAV1* (caveolin-1) expression which may in turn impair leptin signalling and attenuate leptin-dependent lowering of intra-cellular lipid accumulation (Singh *et al.*, 2012). Therefore, with a higher level of *LEP* expression, SA may have more difficulty storing fat via leptin-dependent lipid accumulation, which may in turn result in a decrease in lipogenesis in adipocytes and/or increased FFA, resulting in ectopic fat storage and thus, increased risk of T2DM (Ragheb and M. Medhat, 2011). Expression of *SREBF1* was higher in SA than EU and increased after WG. However, this is different to the London Life Sciences Prospective Population (LOLIPOP) study. The LOLIPOP study showed that the DNA methylation score of *SREBF1* was significantly higher in SA compared to EU, which suggests the expression of *SREBF1* is lower in SA compared to EU (Chambers *et al.*, 2015). Previous studies have shown that *SREBF1* (p = 0.006) had significantly lower expression in subjects with obesity and higher VAT/(VAT+SAT) ratio (n = 38) compared to obese subjects with low VAT/(VAT+SAT) ratio (n = 38) (Kursawe *et al.*, 2010). The higher expression of *SREBF1* in SA than EU and increased after WG may be caused by the higher VAT/(VAT+SAT) ratio in SA than EU, and this ratio increased after WG.

Regarding the multi-variate analysis, an interesting finding in the current study was that total body adipose tissue independently explained the expression of genes, including *ADIPOQ, CIDEA, GHR, LEP*, and *TNF*. In the current study, SA had more total body fat than EU at BL and after WG, with same BMI and age. This is

consistent with many other studies that show that SA tend to have more fat mass and less lean mass than EU with BMI and age (Chandalia *et al.*, 2007, Kalra *et al.*, 2013, Rao *et al.*, 2009). It is well acknowledged that fat mass contributes to the high risk of metabolism syndrome, T2DM and mortality (Rao *et al.*, 2009). The current study suggested that higher total fat in SA independently causes the differences in adipocytes function at mRNA level, at least. As mentioned previously, adiponectin, as an adipokine that promotes insulin sensitivity and lipid oxidation, helps the whole body to maintain low fat content, especially ectopic fat in liver and muscle. *CIDEA* expression in WAT of obese human subjects was found to correlate positively with whole-body insulin sensitivity independent of gender or BMI (Slayton *et al.*, 2019). Diet-induced weight loss shows a positive correlation with CIDEA expression and metabolic health, and changes in adipose tissue *CIDEA* expression correlated with insulin sensitivity independent of BMI (Montastier *et al.*, 2014). As mentioned before, CIDEA is positively correlated with insulin sensitivity, especially in 'healthy obese' patients. Thus, as the SA in the current study had more total body fat but less *CIDEA* expression in adipocytes, this may also contribute to the higher risk of T2DM in SA than EU. A study has suggested that stimulation of *GHR* expression is a protective mechanism against obesity which reduces lipolysis via mitogen-activated protein kinase kinase/extracellular signal-regulated kinase (MEK/ERK) activation, and reduces FFA release. This prevented ectopic adiposity by suppressing PPARγ transcriptional activity and leads to an increase in lean mass (Mekala and Tritos, 2009). GHR reduces the accumulation of ectopic fat. In adipocytes, as previously noted, activation of GHR enhances the process by which insulin promotes FA oxidation. Hence, the lower level of GHR expression in SA may result in relatively higher ectopic fat accumulation and a diminished capacity for fat utilisation in adipocytes compared to EU, leading to increased overall body fat accumulation. This is similar to the mechanism of LEP as discussed previously. Expression of TNF is significantly independently associated with ethnicity and total adipose tissue, which suggests that the higher total body adipose tissue in SA may also contribute to a higher level of *TNF* expression and may lead to the higher risk of T2DM in SA. In patients with obesity, increased levels of plasma TNFα expression may contribute to the elevated levels of basal lipolysis, and subsequently circulating FFAs, which is a characteristic of obese subjects (Ramsay, 1996). In adipose tissue, increased TNFα will upregulate the expression of genes that encode proteins involved in responses

to ER stress and oxidative stress (Ruan *et al.*, 2002), in return this positive feedback loop may contribute to long-term inflammatory responses. Additionally, an increase in TNFα in abdominal adipose tissue was found to be an early event in abdominal fat accumulation (Olszanecka-Glinianowicz *et al.*, 2011). This may suggest abdominal fat accumulation, rather than BMI, may be a stronger predictor of *TNF* expression, especially in the early stage of abdominal fat accumulation. Overall, SA adipocytes expressed lower levels of genes that associated with lipid oxidation and insulin sensitivity than EU, and this may lead SA to accumulate more body fat than EU in adipose tissue or ectopic depots. As a consequence, the higher body fat in SA causes an inflammatory response in adipocytes which may worsen this scenario, and this may contribute to the higher risk of SA in getting T2DM compared with EU.

Our study has shown that SA expressed lower levels of *APOE* than EU, and that levels decreased to a higher degree in response to WG. SA showed more sensitivity to WG in the change of *APOE* expression compared to EU, as an interaction was found between SA and EU in response to WG. Additionally, the change in APOE expression was independently correlated with WG. Studies have shown that apoE synthesized by adipocytes is negatively associated with adipocyte hypertrophy both *in vivo* and *in vitro* (Huang *et al.*, 2009b, Huang *et al.*, 2006). Thus, the lower level of *APOE* expression suggested SA had more adipocyte hypertrophy. Adipocyte-synthesized APOE may influence adipocyte utilisation of fatty acid by increasing FFA uptake (Huang *et al.*, 2006). A higher sensitivity of *APOE* to WG in SA, and an inherently lower level of *APOE* expression in SA, may interfere with the utilization of fatty acids in adipocytes and lead to adipocyte hypertrophy and thus, a higher risk of diabetes.

5.5 Strengths and limitations

The phenotype of South Asian and European participants, including age, BMI, waist circumference, and Resting Metabolic Rate (RMR), were well matched at baseline, and this is one of the study's strengths. The risk factors associated with anthropometry were effectively controlled due to the high similarity in anthropometric measurements. At each time point, fitness, adipose tissue metabolism, MRI, as well as blood biology were examined, which is a significant

strength of the study. These data provide a comprehensive picture to investigate why South Asians have a higher risk of T2DM.

Another strength is that the present study is a longitudinal study looking at changes in adipocyte gene expression in response to WG in SA and EU – known to be diabetes high and low risk ethnicities respectively. This design allowed the current study to detect changes in adipocyte gene expression in response to WG of SA and EU at individual level and is more powerful than a cross-sectional study.

This study examined samples from the subcutaneous adipose depot, which is three to four times the volume of the visceral depot, and there may be anatomical differences between the two depots (Gustafson *et al.*, 2007). For practical reasons, VAT could not be obtained from these young, healthy subjects. This limits the ability to examine adipocyte gene expression from different WAT depots.

The current study did not check the expression of a larger number of genes in adipocytes by mRNA array because of cost. Therefore, this limited the current study to exclusively examine genes that adipocytes expressed. Instead, it examined candidate genes involved in insulin signalling, lipid storage, differentiation and inflammation pathways, which covered key aspects of adipocyte metabolism. Based on a pilot study, the use of IPA combined with literature review helped select a list of GOI that are well researched but may not be immediately obvious candidates. Approximately half of the candidate genes studied showed significant differences in expression, and this suggested that a) the current study has selected GOI in an efficient way by which genes that expressed differently between SA and EU are selected; b) gene expression in adipocytes may be vastly different between SA and EU at BL and after WG.

Measuring gene expression is only indicative of protein expression and adipocyte function. Future studies might confirm protein expression using western blots or activity assays.

5.6 Conclusion

Overall, SA expressed lower levels of genes associated with insulin sensitivity, lipid turnover and lipid oxidation than EU which decreased after WG. SA expressed

higher levels of genes associated with lipid accumulation and inflammatory response than EU which increased after WG. This may contribute to the higher risk of T2DM in SA than EU and in response to WG.

An interaction was found in the expression of APOE, where SA was lower at BL and decreased to a higher extent than EU after WG. This may contribute to adipocyte hypertrophy and suppressed lipid oxidation and turnover in SA, and lead to insulin resistance.

The current study failed to find differences in genes associated with adipogenesis in mature adipocytes between SA and EU. Thus, it would be interesting to examine them in pre-adipocytes and to assess *in vitro* adipogenesis.

Chapter 6 *In vitro* preadipocyte proliferation and differentiation in response to weight gain in young, lean European and South Asian men – a pilot study

6.1 Introduction

Mesenchymal stem cells (MSC) differentiate into various cell types including white adipocytes, brown adipocytes, chondrocytes, osteoblasts, and myocytes. The process of differentiation into adipocytes is specifically known as adipogenesis. (Cristancho and Lazar, 2011). In adults, the number of mature white adipocytes is constant in mammals, after an increase in number through puberty (Cristancho and Lazar, 2011, Hirsch and Han, 1969, Spalding *et al.*, 2008). However, in adult WAT, there is approximately 10% adipocyte turnover, which requires adipogenesis to replace (Spalding *et al.*, 2008). In response to over-nutrition, adipocyte hypertrophy (cell size increase) occurs primarily followed by adipocyte hyperplasia (cell number increase) if excess energy intake is continuous (Kim *et al.*, 2014). Tchoukalova *et al.* showed that in the short-term a high-fat diet can result in an increased number of adipocytes in lower body SAT ($p < 0.01$, n = 28) but that hypertrophic expansion occurred in abdominal SAT (Tchoukalova *et al.*, 2010). These data indicate that both hypertrophic and hyperplastic adipogenesis exists in adult WAT in response to weight gain or adipocyte turnover. Hypertrophy appears in the early stages of weight gain, after which WAT hyperplasia is initiated to meet the increased requirement for energy storage capacity in obesity (Jo *et al.*, 2009). Additionally, hypertrophy is shown to be associated with disturbed metabolism such as hyperleptinemia (Lemieux *et al.*, 2000) and dyslipidemia (Veilleux *et al.*, 2011).

The multipotent MSC is first committed to white preadipocytes, which are morphologically indistinguishable from other MSC differentiating fibroblast-like cells (Figure 6-1) (Cristancho and Lazar, 2011). There are two pathways associated with the regulation of preadipocyte commitment: the Wingless-INT (WNT)

signalling pathway [7] (Takada *et al.*, 2007, Takada *et al.*, 2009) and the transforming growth factor-beta (TGFß) superfamily[8] (Li and Wu, 2020) signalling pathway both of which influence adipogenesis. The WNT pathway is essential for the survival of adipocyte precursors. WNT 10b stimulates the proliferation of 3T3-L1 cells (Ross *et al.*, 2000) and WNT1 protects preadipocytes from serum starvation induced apoptosis by increasing expression of insulin-like growth factor (IGF) 1 and 2 (Longo *et al.*, 2002). The role of WNT signalling pathways in pre-adipocyte commitment is controversial. On one hand, canonical WNT signalling has been proved to inhibit adipogenesis (Takada *et al.*, 2009, Kawai *et al.*, 2007, Longo *et al.*, 2004). On the other hand, the non-canonical WNT ligand WNT5B, promotes adipogenesis by inhibiting the canonical WNT pathway and preventing nuclear translocation of ß-catenin to stimulate preadipocyte commitment (Kanazawa *et al.*, 2005). Canonical TGFß signalling starts with the TGFß superfamily ligands binding to the TGFß superfamily receptors type I and type II, thus activating both the mothers against decapentaplegic homolog (SMAD) dependent pathway (TGFß-SMAD signalling pathway) and SMAD independent pathways (Derynck and Zhang, 2003). The TGFß-SMAD signalling pathway plays an opposing role during preadipocyte commitment, whereby BMP-SMAD signalling promotes commitment and TGFß-SMAD signalling inhibits commitment (Li and Wu, 2020, Zamani and Brown, 2011). BMP4 induces commitment of MSC as preadipocytes via the SMAD4 complex. This has been validated mainly in C3H10T1/2 cells, a mouse MSC cell line isolated from 14 - to 17 - day old C3H mice embryos (Ahrens *et al.*, 1993, Tang *et al.*, 2004). Similarly, BMP2 signalling stimulates the commitment of MSC as preadipocytes in C3H10T1/2 cells, but the mechanism remains unclear (Ahrens *et al.*, 1993, Tang *et al.*, 2004, Huang *et al.*, 2009a, Wang *et al.*, 1993). In contrast, TGFß signalling inhibits MSC commitment as preadipocytes via the SMAD3 complex in human bone marrow derived MSCs (Ng *et al.*, 2008). Knock-out of the TGFß gene in mouse MSC resulted in a significant expansion of adipocytes in bone marrow and significantly increased mRNA expression of *PPARG* and fatty acid binding protein 4 (*FABP4*, a marker of mature

---

[7] The WNT signalling pathways includes canonical WNT signalling and non-canonical signalling. Canonical WNT signalling is activated by WNT ligands binding to low density lipoprotein receptor-related protein (LRP) 5 and 6. This stimulates a β-catenin-dependent co-activator complex and downstream gene transcription. In non-canonical signalling, WNT ligands stimulate β-catenin-independent cell surface receptors activating different intracellular pathways.

[8] TGFβ superfamily ligands include TGFβ, activin, inhibin, bone morphogenetic proteins (BMPs), growth differentiation factors (GDFs), Lefty, and Nodal.

adipocytes) (Abou-Ezzi *et al.*, 2019). In addition, physical stimuli such as low extracellular matrix (ECM) stiffness, confluency and round shape, and other unknown factors can stimulate MSCs to start transforming to committed white preadipocytes (Cristancho and Lazar, 2011). (Figure 6-1).
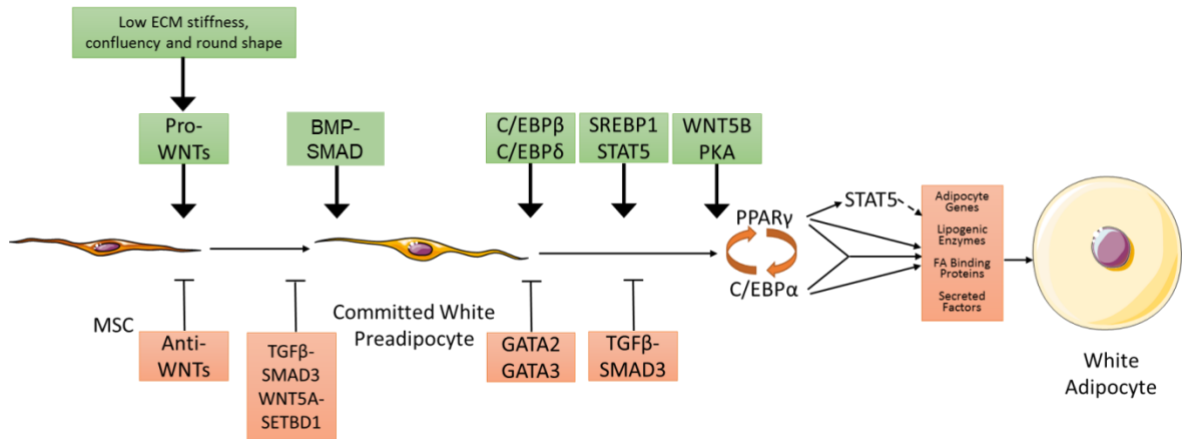
Figure 6-1 WAT adipogenesis and the influencing factors, based on Cristancho and Lazar, 2011.

WNT signalling and the TGFβ superfamily signalling pathways regulate the commitment of white adipocytes to differentiation. PPARγ and C/EBPα are key genes triggering terminal differentiation and formation of mature adipocytes. Abbreviations: BMP, bone morphogenetic protein; C/EBP, CCAAT-enhancer binding proteins; GATA, GATA binding protein; ECM, extracellular matrix; PKA, protein kinase A; SMAD3, mothers against decapentaplegic homolog 3; SETBD1, suvar3-9 enhancer-of-zeste and trithorax domain bifurcated histone lysine methyltransferase 1; SREBP1, Sterol regulatory element-binding protein 1; STAT5, Signal transducer and activator of transcription 5; TGFβ, transforming growth factor beta; WNTs, wingless-related integration site proteins.

Once MSC lose their multipotency to differentiate to other types of cells and are restricted to differentiating as adipocytes, they become preadipocytes. These preadipocytes are restricted to differentiating into adipocytes, but they cannot enter terminal differentiation spontaneously without exogenous stimuli for adipogenesis. *In vivo*, the preadipocyte is morphologically indistinguishable from the MSC and other MSC differentiated precursor cells. However, gene expression in MSC and preadipocytes is different, which makes them distinguishable using surface markers and products of gene expression. The common markers to distinguish preadipocytes from MSC include surface markers Lin, CD11b, CD14, CD41, CD45, CD105, CD117 and CD140a, and products of preadipocyte specific genes PPARγ, delta like non-canonical notch ligand 1 (DLK1, as known as preadipocyte factor 1, Pref1), lipoprotein lipase (LPL), WNT10b and WNT6 (Cawthorn *et al.*, 2012b, Hepler *et al.*, 2017). In human adults, preadipocytes reside in the adipose stromal vascular fraction (SVF) of adipose tissue depots. The abilities of preadipocytes isolated from the SVF of different adipose tissue depots

are different. The ability to proliferate and differentiate of preadipocytes isolated from adult human SVF was higher in SAT-SVF than VAT-SVF (Hauner *et al.*, 1988, Maslowska *et al.*, 1993, Niesler *et al.*, 1998). Interestingly, another study showed by adipocyte cell count a greater ability for hyperplastic expansion in abdominal SAT compared to VAT. In middle-aged overweight adults (age: 47 ± 5 years; BMI 27.9 ± 5.3 kg/m^2), there was a relatively steeper slope in the relationship between adipose tissue fat accumulation and total fat mass in SAT compared to VAT whereas there was a similar slope between adipocyte size and total fat mass in SAT and VAT (Drolet *et al.*, 2008). These data suggest that when the relative adipocyte size is the same in SAT and VAT, there is more fat stored in SAT and therefore the rate of adipocyte hyperplastic expansion in SAT must be higher (Drolet *et al.*, 2008). The ability of preadipocytes to proliferate and differentiate to mature adipocytes may directly influence the number of adipocytes, and this may subsequently correlate to the size of adipocytes. This may contribute to the differences in insulin sensitivity between different individuals. Thus, the preadipocytes residing in human adipose tissue SVF play a key role in the hyperplastic expansion of adipose tissue via their ability to proliferate and to differentiate into mature adipocytes. This may explain the differences in size of adipocyte between SA and EU at BL and after WG as mentioned in previous chapters.

Terminal differentiation is the formation of mature white adipocytes from preadipocytes resulting in the characteristic appearance of the mature adipocyte (Figure 6-1). The WAT adipocyte acquires the ability to take up lipid, form lipid droplets, undertake lipogenesis and lipolysis and respond to insulin (Moreno-Navarrete and Fernández-Real, 2017). Terminal differentiation involves the transcriptional regulation of a series of pathways. Transcription factors, such as CCAAT-enhancer binding protein ß (C/EBP-ß) and C/EBP-δ, are activated in the preadipocyte, and stimulate the preadipocyte to re-enter the cell cycle under the stimulation of different exogenous stimuli (Moreno-Navarrete and Fernández-Real, 2017). Both C/EBPß and C/EBPδ can directly stimulate the expression of the key transcriptional regulators of terminal differentiation PPARγ and C/EBPα (Tang *et al.*, 2004). PPARγ and C/EBPα initially positively feedback on each other and amplify their expression and action. This results in the stimulation of the expression of downstream genes including genes associated with lipid droplet

formation, lipid accumulation and insulin signalling (Rosen *et al.*, 2002, Cristancho and Lazar, 2011, Li and Wu, 2020). The expression of these downstream genes enables the mature adipocyte to acquire its functional abilities. Studies have shown that PPARγ is critical for adipocyte differentiation and a lack of PPARγ expression significantly reduces the expression of C/EBPα in preadipocytes and other cell types (Rosen *et al.*, 1999, Kubota *et al.*, 1999, Rosen *et al.*, 2002). Interestingly, C/EBPα$^{-/-}$ mice embryo fibroblasts (mainly MSC) exhibited a significantly reduced ability for adipogenesis and expression of PPARγ compared with WT (Wu *et al.*, 1999). Introduction of PPARγ using a retroviral vector restored the ability of adipogenesis (Wu *et al.*, 1999). These data suggest that activation of the PPARγ and C/EBPα loop is the marker of the activation of terminal differentiation in preadipocytes and that PPARγ plays a critical role. DLK1, also known as preadipocyte marker Pref1, is a transmembrane protein and a gatekeeper of adipogenesis. In preadipocytes, DLK1 inhibits adipogenesis by activating the extracellular signal regulated kinase/ mitogen activated protein kinase (ERK/MAPK) pathway to upregulate expression of SRY-box transcription factor 9 (SOX9), and interaction with fibronectin (Hudak and Sul, 2013). This suppresses the expression of C/EBPß and C/EBPδ, and the downstream gene PPARγ. Similarly, TGFß signalling inhibits terminal differentiation by phosphorylation of PPARγ (Kim *et al.*, 2009, Walenda *et al.*, 2013). The mechanism of ending differentiation is unclear, but accumulated C/EBPα protein is phosphorylated by cyclin D3, which may be associated with ending adipogenesis (Wang *et al.*, 2014).

The pre-adipocyte differentiation protocol used in this chapter followed a standard protocol used by Prof. Ulf Smith and his team in Gothenburg, Sweden (Gustafson and Smith, 2012, Isakson *et al.*, 2009). The design of the experiment is shown in Figure 6-2. The adipose tissue stromal vascular fraction (ASVF) was initially cultured in a two-passage culture starting in a 25 cm^2 (T25) flask followed by culture in a 75 cm^2 (T75) flask. Most of stromal cells including blood cells and immune cells were washed away after 24 hours of incubation, as they do not attach to the flask. Only fibroblast-like cells (mainly preadipocytes) remain attached to the flask. As contaminating fibroblasts and non-preadipocyte fibroblast-like cells have little influence on adipogenesis and do not participate, preadipocytes were assumed to be the predominant cell type in the flask. When

undertaking preadipocyte proliferation experiments, it was apparent that the total number of days that it took for preadipocytes to grow to confluence varied considerably between donors. As described in the introduction to this chapter, the ability of preadipocyte to proliferate and differentiate to adipocytes is a measure of the hyperplastic expansion ability of adipose tissue. Total days of growth, as well as pre-adipocyte cell count at harvest for freezing were routinely noted to assess the behaviour of the pre-adipocytes prior to differentiation. These properties were considered as a potential influencer of the ability of pre-adipocytes to undergo hyperplastic expansion. The differences between two culture protocols were considered and the results presented in this chapter. In addition, the association of anthropometric measures (including weight, BMI, waist, resting metabolism rate [RMR], VO_2 max and total body fat), adipocyte diameter, expression of genes in adipocytes that were significantly different between SA and EU (in Chapter 5) and tissue weight (at biopsy) will be considered as well.
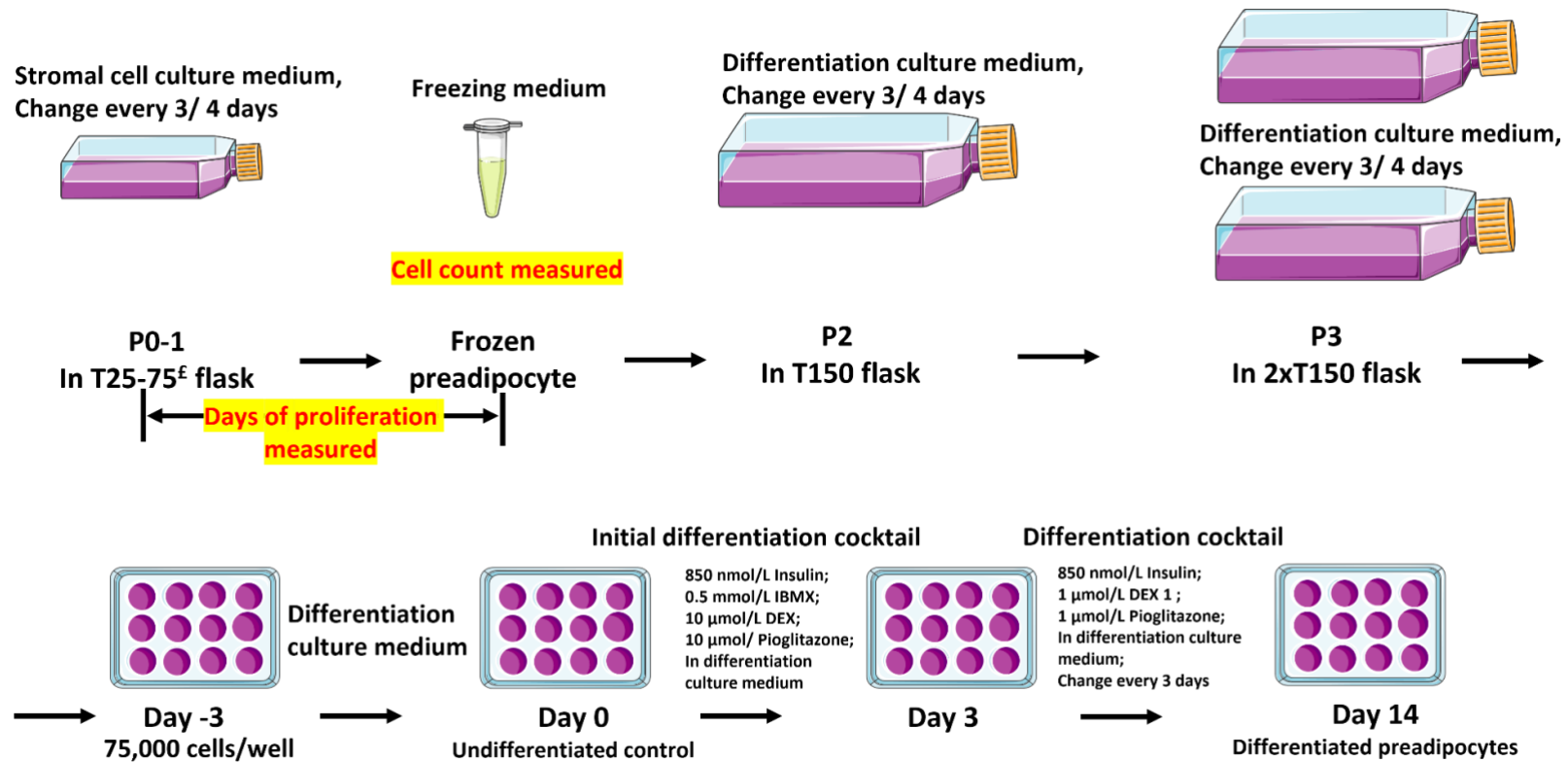
Figure 6-2 Process of preadipocyte proliferation and differentiation.

The adipose tissue stromal vascular fraction (mainly preadipocytes) was first cultured in 25cm^2 (T25) or 75cm^2 (T75) flasks and cultured using stromal cell culture medium (6.2.1) until cell reached 80-90% confluence. Cells were then frozen. The duration, in days, of proliferation and cell count at freezing were measured. For differentiation experiments, frozen cells (predominantly preadipocytes) were defrosted and cultured using differentiation culture medium (6.2.3) in 150cm^2 (T150) flasks until confluent. For differentiation, cells were transferred into a 12-well plate and left to adhere for three days. Then cells were stimulated to differentiate using an initial differentiation cocktail (6.2.3) for three days followed by maintenance in differentiation cocktail (6.2.3) for 14 days in total. All cells were incubated in a 37°C 5% CO$_2$ incubator. £: Some stromal cells underwent a two-passage transfer from T25 to T75 flasks. Most blood and immune cells were washed away after 24 hours incubation leaving predominantly preadipocytes. The figure was partly generated using Servier Medical Art, provided by Servier, licensed under a Creative Commons Attribution 3.0 unported license.

In the current study, preadipocytes were stimulated to differentiate into adipocytes using insulin, isobutylmethylxanthine (IBMX), dexamethasone and pioglitazone (Figure 6-1) (Gustafson and Smith, 2012, Isakson *et al.*, 2009). Insulin is an essential hormone that stimulates adipogenesis and adipocyte maturation by switching on a variety of transcription factors involved in adipocyte differentiation, such as SREBP1c (Gustafson and Smith, 2012, Bowers *et al.*, 2006, Cignarelli *et al.*, 2019). IBMX, combined with dexamethasone induces the expression of PPARγ which stimulates adipogenesis (Gurriaran-Rodriguez *et al.*, 2011). IBMX is a nonselective phosphodiesterase inhibitor that increases intracellular cAMP and PKA, which is necessary for adipogenesis (Kim *et al.*, 2010). Both IBMX and dexamethasone stimulate the expression of C/EBPß and C/EBPδ which induce the differentiation of adipocytes (Cao *et al.*, 1991). Pioglitazone is a drug that increases insulin sensitivity and induces adipogenesis *in vitro* by activation of PPAR gamma (Hallakou *et al.*, 1997, Sandouk *et al.*, 1993). Oil red O, a lipid-specific stain, was used to visualize and quantify adipocyte lipid accumulation and acted as a measure of the degree of differentiation. Lipid droplets are markers of end differentiation and are found only in adipocytes and not in preadipocytes. RT-qPCR was used to quantitate mRNA expression of key adipogenic regulatory genes in preadipocytes and differentiated adipocytes. Actin B (*ACTB*) was used as endogenous control because it is stably expressed in preadipocytes and in *in vitro* differentiated adipocytes (Dessels and Pepper, 2019). Adiponectin is a adipocyte specific hormone, and the expression of *ADIPOQ* was examined as a gene expression marker of mature adipocytes (Sarjeant and Stephens, 2012). *DLK1* (*Pref1*) was used as a biomarker for preadipocytes (Hepler *et al.*, 2017). Expression of *PPARG* was determined as an indicator of the activation of differentiation at the mRNA level (Moreno-Navarrete and Fernández-Real, 2017), and *TGFB* was determined as a suppressor of adipocyte differentiation (Choy and Derynck, 2003). Together, these markers allowed this pilot study to explore the difference in the ability of preadipocytes to differentiate in SA and EU at BL and after WG.

6.1.1 Hypotheses

(a) Preadipocyte count per gram of tissue is lower in SA than EU and lower after WG relative to BL. Preadipocytes, seeded at equivalent cell

concentration, proliferate more slowly in SA than EU and after WG relative to BL.

(b) Preadipocytes isolated from SA have a lower ability to differentiate *in vitro* than EU at BL and after WG. Specifically, lipid accumulation over 14 days differentiation, assessed by Oil red O staining, will be lower in SA than EU at BL and after WG; cellular expression of genes promoting adipogenesis (*PPARG*) and representing end differentiation of adipocytes (*ADIPOQ*) will be lower and expression of genes that inhibit adipogenesis (*TGFB*) and are a biomarker of preadipocytes (*DLK1*) will be higher in SA than EU at BL and after WG.

(c) WG decreases the ability of preadipocyte to differentiate into adipocytes to a greater degree in SA compared to EU, as assessed by lipid accumulation and gene expression described in (b) above.

6.2 Methods

6.2.1 Preadipocyte proliferation

ASAT was collected using a needle biopsy from participants in GlasVEGAs as described in Chapter 2. The weight of tissue was measured. The adipose tissue stromal vascular fraction (ASVF) was isolated and transferred into a T25 flask. Non-adherent cells were removed after 24 hours of incubation and the remaining cells were regarded as preadipocytes. Pre-adipocytes were then cultured as described below (shown in Figure 6-2) (Gustafson and Smith, 2012, Isakson *et al.*, 2009).

Preadipocytes were cultured in T25 flasks (passage 0), in a 37°C 5% CO_2 incubator in 5 mL stromal cell culture medium (Dulbecco's modified eagle medium [DMEM, Sigma-Aldrich, D5671], 10% FBS, 100 U/mL penicillin-streptomycin, and 2 mM L-glutamine) which was changed every 3 to 4 days until the cells were 80% confluent. Once confluence was reached, the culture medium was removed and the cells washed twice with 1x Dulbecco's phosphate-buffered saline (DPBS, Thermo Fisher

Scientific, 14190094) at 37°C, before adding 2.5 mL 37°C 0.25% trypsin[9] (2.5% Sigma-Aldrich T4049) and incubating in a 37°C 5% CO_2 incubator for four minutes. The flask was then tapped gently to detach the cells, and a volume of stromal cell culture medium twice that of trypsin solution used was added and mixed. The cell suspension was then centrifuged at 200 x g for 5 min at room temperature. The supernatant was removed, and the preadipocyte pellet was resuspended and transferred into T75 flasks (passage 1) and cultured until 80% confluent as described above.

Once the preadipocytes became 80% confluent in the T75 flask, they were detached from the flask with 4 mL trypsin as described above. The stromal cells were resuspended in freezing medium (DMEM [Sigma-Aldrich, D5671], 20% FBS, 10% dimethyl sulfoxide [DMSO, DLM-10RG-PK], 100 U/mL penicillin-streptomycin, and 2 mM L-glutamine) at a maximum cell concentration of 500,000 cells/mL. Cells were added in 1mL aliquots to cryo-vials (Greiner bio-one) and immediately transferred into a Mr Frosty Cryo 1°C freezing container (Thermo Fisher Scientific) overnight at -80°C, and then transferred to liquid nitrogen for longer term storage.

6.2.1.1 Total days of proliferation and cell count after proliferation

Total days of proliferation was counted from day of initial seeding of ASVF at the start of passage 0 (day 0) to the day on which preadipocytes were frozen at the end of passage 0 or 1.

Concentrations of the preadipocytes were counted manually using a haemocytometer (Camlab UK) according to the manufacturer's protocol just before they were frozen at passage 0 or 1. Cell count after proliferation was then calculated by concentration x volume of the preadipocyte preparation.

6.2.2 Preadipocyte defrosting and expansion

Preadipocytes that had been frozen in liquid nitrogen (or a -80°C freezer) (6.2.1) were used for differentiation experiments, as shown in Figure 6-2. The cells were

---

[9] For a T25 flask, 2.5 ml of trypsin was used, for a T75 flask, 4 ml of trypsin was used and for a 150 cm^2 (T150) flask, 6 ml of trypsin was used.

defrosted in a 37°C water bath for 2 min before adding to 5 mL of differentiation culture medium (Table 2-3), and then centrifuged at 350 x g for 3 min at room temperature. The supernatant was removed, and the cell pellet was resuspended in 18 mL differentiation culture medium and transferred into a 150 cm^2 (T150) flask (passage 2) and incubated in a 37°C 5% CO_2 incubator, until 90% confluent. They were then split into two T150 flasks (passage 3) as described previously (6.2.1) and cultured until 90% confluent.

Reagent	Final Concentration
DMEM (Sigma-Aldrich, D6249)	1x
Fetal bovine serum (Gibco, 10270)	10%
P/S (Sigma-Aldrich, P0781)	100U/mL
L-Glutamine (Sigma-Aldrich, G7513)	2mM

Table 6-1 Differentiation culture medium.

6.2.3 Preadipocyte differentiation *in vitro*

Once the preadipocytes reached 90% confluence at passage 3, they were harvested and 1mL of 75,000 cells/mL in differentiation culture medium was added to each of 12 wells of a 12-well plate. Plates were incubated for three days at 37°C 5% CO_2 incubator until cells adhered.

Preadipocytes from six wells were harvested immediately after three days incubation to act as undifferentiated controls on day 0 of the experiment. Two of these wells were used for oil red O (ORO) staining of cellular lipid accumulation (2.5.3), two wells were used for RNA isolation (2.5.4) and mRNA expression quantitation, and two wells were used for cell lysis (2.5.4) for future measurement of protein expression by western blotting. In the current study, these preadipocytes were called undifferentiated control preadipocytes, or day 0 cells.

The remaining six wells were induced to differentiate and harvested after 14 days of differentiation. On day 0 of the differentiation experiment, preadipocytes were induced to differentiate by incubation for three days with 1 mL/well initial differentiation cocktail (DMEM [Sigma-Aldrich, D6249], 3% FBS [Gibco, 10270], 850 nM insulin [Sigma-Aldrich, I9278], 0.5 mM IBMX, [Sigma-Aldrich, I7018], 10 μM dexamethasone [Sigma-Aldrich, D4902], 10 μM pioglitazone [Cayman Chemical, 71745], 2 mM L-glutamine and 100 U/mL P/S). On day 3, the medium was changed

to 1 mL/well differentiation cocktail (DMEM [Sigma-Aldrich, D6249], 10% FBS [Gibco, 10270], 850 nM insulin, 1 μM dexamethasone, 1 μM pioglitazone, 2 mM L-glutamine, and 100 U/mL P/S), in order to maintain the differentiation. The differentiation cocktail was changed every three days until day 14. The total time taken for differentiation (including induction and maintenance) was 14 days. The differentiated cells were then harvested for assessment of cellular lipid accumulation, mRNA expression and protein expression as described for undifferentiated controls (Gustafson and Smith, 2006). In the current study, these preadipocytes were called differentiated preadipocytes, or day 14 cells.

6.2.3.1 Quantitation of cellular lipid accumulation by Oil red O staining

Medium was removed and cells were washed twice with 1x DPBS. The cells were fixed directly in the tissue culture well with 800 μL 4% formaldehyde for 20 min at room temperature, and then washed once with 1x DPBS, followed by two washes with distilled water. The water was then removed, without allowing the cells to dry out completely, and the tissue culture plate was sealed in a plastic bag and kept at -20°C until stained.

On the day of staining, the plate was defrosted and allowed to completely dry out. Freshly prepared ORO solution (1mL, 6:4 Oil Red O [Sigma-Aldrich, O1391]: Millli Q water) was added to each well, and incubated for 60 min at room temperature, and then washed gently with water and drained. Isopropanol (1 mL) was then added to each well and incubated for 6 min at room temperature to solubilise the intracellular ORO. Two aliquots per well of 200 μL isopropanol containing the solubilised ORO was transferred to a flat 96-well plate (Corning, 9018), and the absorbance at λ510 nm was read and recorded. The difference between ORO absorbance of differentiated (day 14) minus the undifferentiated control (day 0) cells was calculated as absolute change i.e., OD_{14} - OD_0. An example of ORO staining of day 0 undifferentiated control cells and day 14 differentiated preadipocytes is shown in Figure 6-3.
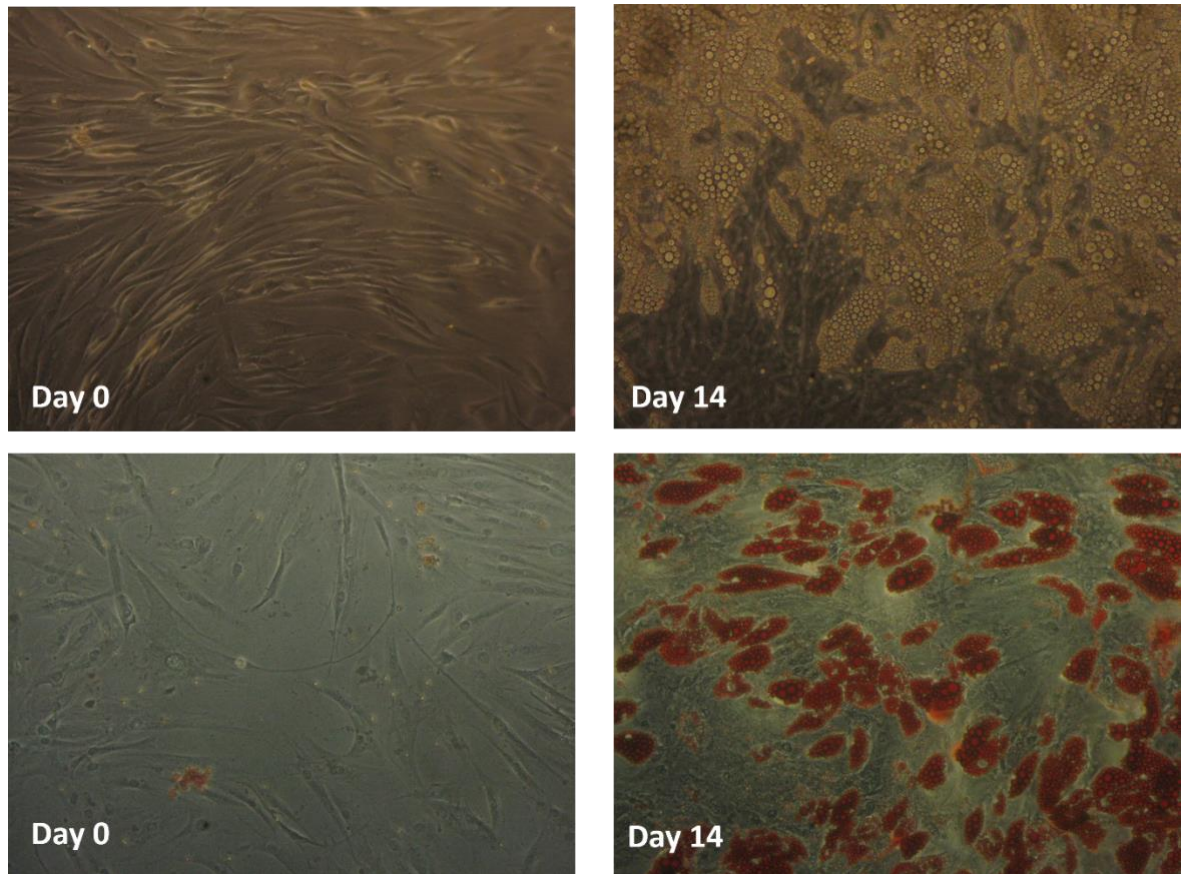
Figure 6-3 Lipid accumulation in day 0 undifferentiated control preadipocytes and day 14 differentiated preadipocytes.

Images were taken at 10x magnification on a BX50 microscope using a Canon digital camera. Top row: live cells without ORO staining; bottom row: cells stained with ORO. The scale bar could not be implemented as the camera settings varied during the capture of these images. The intention of these photographs is solely to demonstrate the successful differentiation and ORO staining.

6.2.3.2 RNA extraction from the preadipocyte differentiation experiment

Total RNA was extracted from undifferentiated control (day 0) and differentiated (day 14) preadipocytes (2.5.2) using Trizol reagent (Thermo Fisher Scientific, 15596026) according to the manufacturer's instructions. Trizol (1 mL) was added to each well (of a 12-well plate) and the isolated RNA was dissolved in 20 µL nuclease-free water (QIAGEN, 129115).

6.2.3.3 Cell lysis from the preadipocyte differentiation experiments for protein quantitation

Total protein was extracted from undifferentiated control (day 0) and differentiated (day 14) preadipocytes (2.5.2) using lysis buffer (Table 6-2) (Gustafson and Smith, 2006). Briefly, the cells were washed twice with ice cold 1x DPBS and then allowed to air dry. Lysis buffer (50 µL; Table 6-2) was added to

each well and incubated for 15 secs. The well was then scraped to solubilise cellular material and the resulting suspension collected. The suspension was then centrifuged at 20,000 x g for 10 min at 4°C to remove cellular debris, and the supernatant was stored at -80°C for future use.

Reagent	Final Concentration
Tris-HCl (pH 7.4)	25 mM
NaCl	25 mM
IGEPAL CA-630 (Sigma-Aldrich, I8896)	1%
NaF	10 mM
Protease inhibitor solution (1 tablet in 10 ml water, SIGMAFAST Protease Inhibitor tablets, S8820)	10%

Table 6-2 Cell lysis buffer for preadipocyte differentiation.

IGEPAL CA-630: nonionic, non-denaturing detergent suitable for solubilization, isolation and purification of membrane protein complexes.

6.2.4 RT-qPCR

RNA from cultured primary preadipocytes was purified using a DNA-free kit (Thermo Fisher Scientific, AM1906) according to the manufacturer's instructions. A high-capacity cDNA reverse transcription kit (Thermo Fisher Scientific, 4368813) was used for synthesis of cDNA according to the manufacturer's instructions. The synthesised cDNA was used for RT-qPCR for quantifying gene expression. Briefly, a RT-PCR reaction mix was made up for each target gene: 1.25 µL target Taqman® Gene Expression Assay (Table 6-3), 12.5 µL TaqMan universal PCR master mix (Thermo Fisher Scientific, 4304437), and 10.25 µL nuclease-free water. cDNA, 1 µL was mixed with each PCR reaction mix in duplicate in a MicroAmp fast optical 96-well reaction plate (ThermoFisher Scientific), and underwent PCR according to the following programme: 50°C for 2 min, 95°C for 10 min, then 40 x of 95°C for 15 sec and 60°C for 1 min.

Gene symbol	Assay ID	Reporter
ACTB	Hs00605340_m1	Vic-Tamra
ADIPOQ	Hs00605917_m1	FAM-NFQ
DLK1	Hs00171584_m1	FAM-NFQ
PPARG	Hs01115513_m1	FAM-NFQ
TGFB	Hs00998133_m1	FAM-NFQ

Table 6-3 TaqMan® Gene Expression Assays used for RT-qPCR in preadipocyte differentiation.

Reference genes and genes of interest. Hs – *Homo sapiens*; '_m' indicates an essay whose probe spans an exon junction and will not detect genomic DNA.

The fluorescence threshold for the FAM-NFQ reporter in each target assay was optimised as 0.2 ΔRn following the manufacturer's recommendation. For the Vic-Tamra reporter, the threshold was optimised individually, in this case, it was 0.12 ΔRn for *ACTB*. No fluorescent signals were analysed for gene expression earlier than Ct = 15, as signals between cycle 3 and cycle 15 were considered to be background fluorescence according to the manufacturer's recommendation. Cycle threshold (Ct) value was determined by the StepOnePlus v2.3 software. *ACTB* was used as endogenous control for delta Ct and delta delta Ct analysis (Dessels and Pepper, 2019).

Relative expression to *ACTB* was used to describe the relative expression level of each gene of interest (GOI) according to the delta Ct between target gene and *ACTB*. The formula for relative expression was:

$$Relative\ expression\ (\%)\ =\ 2^{-(Ct\ GOI - Ct\ ACTB)} \times 100\%$$

However, as there was no expression of *ADIPOQ* in undifferentiated controls and low expression of *DLK1*, for the undetectable samples, relative expression was given a decimal by a Ct value of 45 in those samples. Absolute differences between day 14 and day 0 cells was calculated by relative expression (day14) – relative expression (day 0) of each sample.

In the current study, expression relative to *TGFB* was also calculated for biological purposes to understand the relative changes of pro-differentiation genes relative

to the differentiation inhibitor gene (*TGFB*) in preadipocytes. The formula for relative expression to *TGFB* expression was:

$$Relative\ expression\ to\ TGFB\ (\%)\ =\ 2^{-(Ct\ GOI - Ct\ TGFB)} \times 100\%$$

6.2.5 Statistics

Statistics were performed using Minitab version 19 (Minitab Ltd) and figures were drawn using GraphPad Prism 8.3. Normal distribution for all the parameters was tested using the Ryan-Joiner test. Non-normally distributed data were log transformed to achieve normal distribution as required. Results were displayed as mean ± standard deviation (SD) for parametric data and median [95% confidence interval (CI)] for non-parametric data.

Two group comparisons of cross-sectional parameters were made using two-sample t-test for normally distributed data. A paired t-test was utilised to compare the BL and WG within each ethnic group, either EU or SA. Gene expressions were calculated for each sample and two-way comparison was carried out using a mixed-effects ANOVA. Pearson correlation analysis was carried out between two parametric datasets and Spearman correlation was carried out when one or both datasets were non-parametric. Significance level was $p < 0.05$, and for interactions $p < 0.10$ was adopted.

Post hoc power calculations for sample size were calculated using a two-level factorial design. The effect size was acquired from the actual differences between two groups (ethnicity or study visit). Power value was set as 0.95 in the current study.

6.3 Results

6.3.1 Study participants included in preadipocyte differentiation analysis

In total 23 EU and 18 SA were recruited to the GlasVEGAs study.

During the proliferation of preadipocytes, 11 samples were contaminated, including 3 EU and 2 SA samples at BL, and 2 EU and 4 SA samples after WG. Two

SA samples at BL were discarded because of failure to proliferate. Therefore, a total of 57 samples were included in the preadipocyte proliferation analysis, including 17 EU and 13 SA at BL, and 18 EU and 9 SA after WG (Figure 6-4).

During the re-establishment of pre-adipocyte cultures after freezing, a total of 6 samples were discarded because of failure to reach confluence, including 1 EU and 1 SA samples at BL, and 2 EU and 2 SA samples after WG. For differentiation experiments, a paired design was chosen thereby excluding n = 6 EU and n = 7 SA at BL, and n = 6 EU and n = 2 SA after WG. Therefore, preadipocyte differentiation was assessed where both WG and BL data were available in the sample person (EU n = 10, SA n = 5) as shown in Figure 6-4.
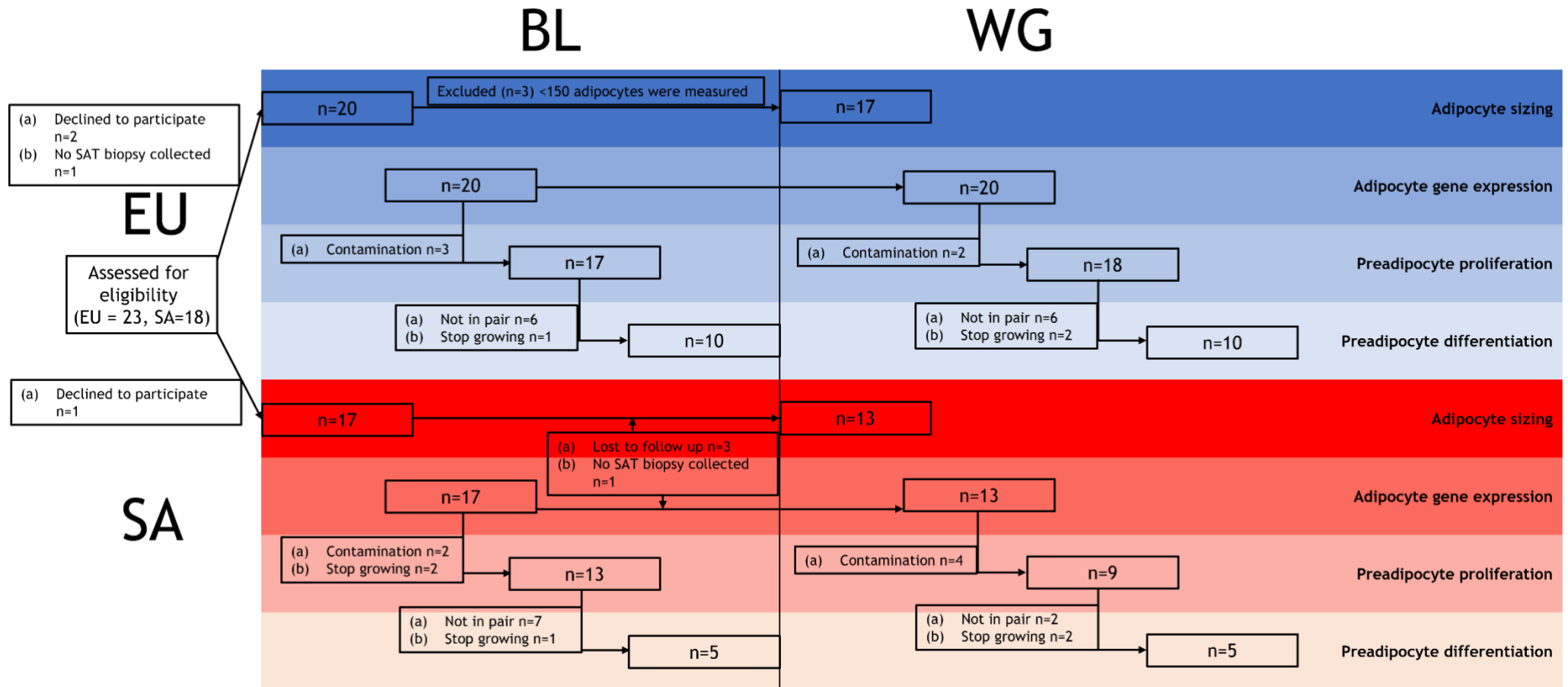
Figure 6-4 CONSORT flow diagram for the assessment of adipocyte sizing in GlasVEGAs study at BL and after WG.

Preadipocyte differentiation was only carried out and analysed in participants with both BL and WG samples forming a paired analysis.

6.3.2 Characterisation of pre-adipocyte donors for proliferation experiments

Anthropometric and metabolic data for the participants who donated pre-adipocytes for the proliferation experiments are shown in Table 6-4. There were no significant differences between EU and SA in age, BMI, waist circumference and resting metabolic rate (RMR) at either BL or after WG. However, SA had a lower body weight and VO_2 max and higher total adipose tissue (no arm) than EU at BL and after WG.

The results demonstrated a significant increase in BMI, waist circumference, weight, and total adipose tissue in response to WG in both the EU and SA groups ($p \leqslant 0.0001$ in each group, Table 6-4). Despite these enhancements, both the resting metabolic rate and VO_2 max remained unaltered.

	Baseline			Weight gain			Delta BL vs WG	
	EU (n = 17)	SA (n = 13)	*p* value (EU vs. SA)	EU (n = 18)	SA (n = 9)	*p* value (EU vs. SA)	*p* value EU	*p* value SA
Age (years) [$]	22 ± 3	23 ± 3	0.51	22 ± 3	23 ± 3	0.51	N/A	N/A
BMI (kg.m^{-2})	22.3 ± 1.6	21.7 ± 2.9	0.48	23.7 ± 1.7	23.1 ± 3.1	0.52	< 0.0001	< 0.0001
Waist (cm)	78.8 ± 4.5	76.7 ± 5.1	0.27	82.4 ± 4.7	81.7 ± 6.0	0.72	< 0.0001	= 0.0001
Weight (kg)	75.7 ± 8.0	67.8 ± 7.7	0.014	80.0 ± 8.5	72.1 ± 8.2	0.016	< 0.0001	< 0.0001
VO$_2$ max (ml/kg/min)	52.3 ± 5.5	44.0 ± 3.1	< 0.0001	48.7 ± 5.3	41.9 ± 4.8	0.002	0.087	0.151
Total adipose tissue (no arm) (L)	14.2 ± 3.9	18.7 ± 4.1	0.007	17.1 ± 4.9	21.4 ± 4.0	0.016	< 0.0001	< 0.0001
RMR (kcal/kg/day)	22.1 ± 2.2	22.3 ± 3.3	0.87	22.2 ± 2.5	23.5 ± 3.7	0.29	0.96	0.21

Table 6-4 Demographic data for European (EU) and South Asian (SA) participants in the GlasVEGAs study at baseline (BL) and after weight gain (WG).

This table showcases demographic information including body mass index (BMI) and resting metabolic rate (RMR) for both EU and SA participants at the initial stage and after experiencing weight gain. The changes between the baseline and weight gain are also indicated (Delta BL vs WG). Comparisons were made using a two-sample t-test. The symbol $ denotes statistical analysis performed on log-transformed data.

6.3.3 The effect of date of biopsy collection on preadipocyte proliferation

It took on average 47 ± 12 days (n = 57) for the preadipocytes to proliferate, and an average of 46.1 ± 23.7 x10^4 cells (n = 57) were harvested after proliferation.

The total number of days taken for preadipocytes to proliferate to confluence prior to freezing increased significantly across the course of the study (R = 0.51, p < 0.0001, Figure 6-5 (a)). Additionally, cell count yield at time of freezing decreased significantly across the course of the study (R = -0.45, p < 0.0001, Figure 6-5 (b)).
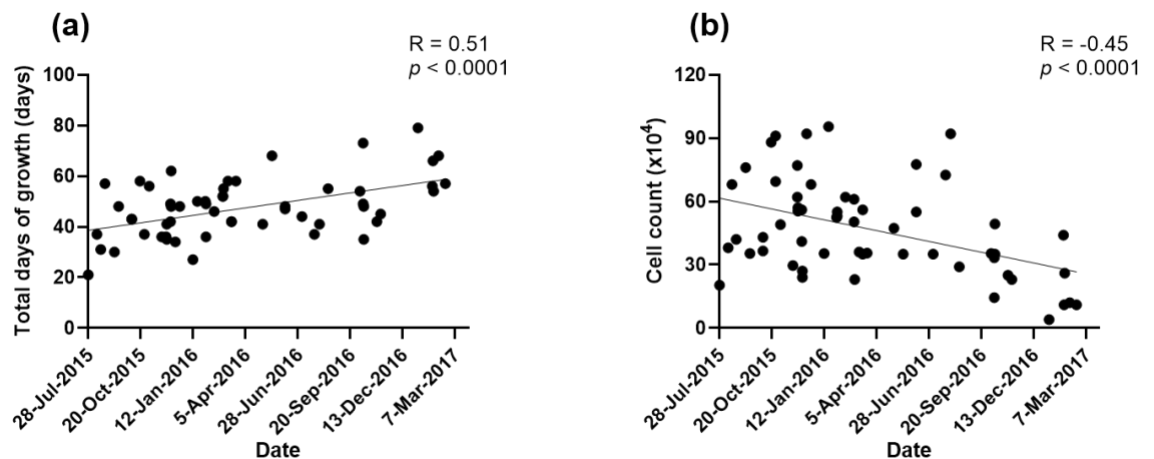
Figure 6-5 Correlation between biopsy collection date and proliferation metrics.

This figure illustrates the correlation between the date of biopsy collection and two key proliferation metrics: (a) the total number of days of proliferation, and (b) the cell counts after proliferation. Pearson correlation coefficient was used to determine the linear correlation, (n = 57).

6.3.4 Adipose tissue biopsy weights collected over the study

On average, 0.31 ± 0.12 g (n = 57) SAT was collected by biopsy from each participant in the GlasVEGAs study. The tissue weight of the SAT needle biopsies decreased over the duration of the study (R = -0.06, p = 0.038, Figure 6-6).
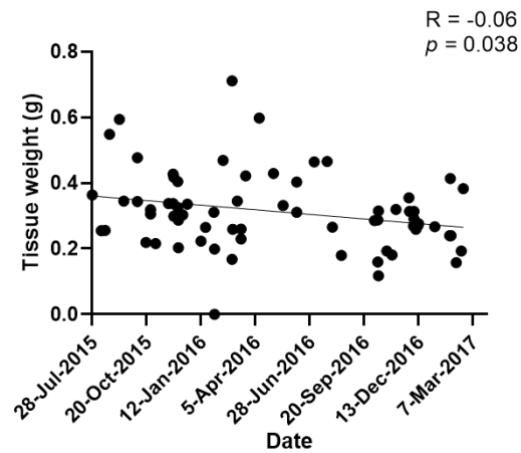
Figure 6-6 Correlation between date of biopsy collection and weight of ASAT biopsy collected.

Pearson correlation coefficient was used to analyse the linear correlation, (n = 57).

6.3.5 Relationships between preadipocyte proliferation, cell count and tissue weight

There was a strong negative correlation between total days of proliferation and cell counts yields after proliferation (R = -0.45, p < 0.0001, Figure 6-7 (a)). Tissue weight of the ASAT biopsy was negatively associated with the total days of proliferation (R = -0.31, p = 0.019, Figure 6-7 (b)). There was no relationship between cell count after proliferation and tissue weight (R = 0.12, p = 0.40, Figure 6-7 (c)).
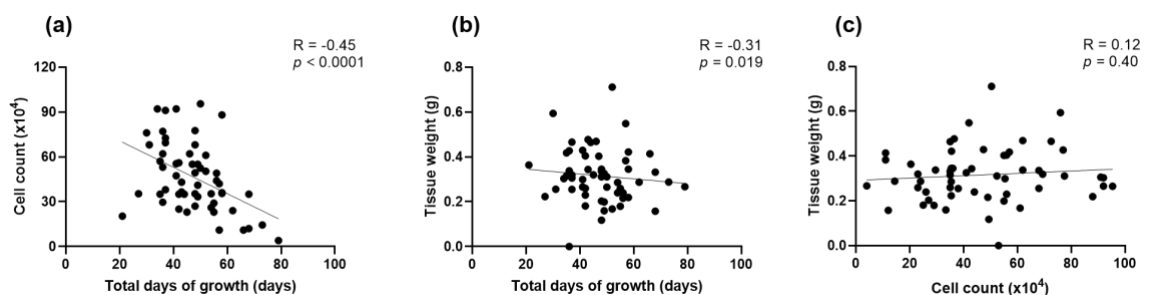
Figure 6-7 Correlations among preadipocyte proliferation, tissue weight of ASAT biopsy, and cell counts.

This figure illustrates the correlations between (a) the total days for preadipocyte proliferation and subsequent cell counts; (b) the total days of proliferation and the tissue weight of the abdominal subcutaneous adipose tissue (ASAT) biopsy; and (c) cell counts post-proliferation and the tissue weight of the ASAT biopsy. The Pearson correlation coefficient was used to determine the linear correlation amongst these variables, (n = 57).

6.3.6 The effects of ethnicity and weight gain on preadipocyte proliferation

Preadipocytes took a similar number of days to reach confluence when collected from biopsies from SA and EU and at BL and after WG. The length of time preadipocytes took to proliferate to confluence was the same in SA and EU at BL (SA vs EU: 48 ± 12 vs 46 ± 10 days) and after WG (SA vs EU: 47 ± 11 vs 49 ± 15 days) (Figure 6-8 (a)). Similarly, the yield of the preadipocytes was the same in SA and EU at BL (SA vs EU: 40.7 ± 22.8 vs 53.6 ± 26.7 x10^4 cells) and after WG (SA vs EU: 46.5 ± 22.2 vs 43.5 ± 22.9 x10^4 cells) (Figure 6-8 (B)).
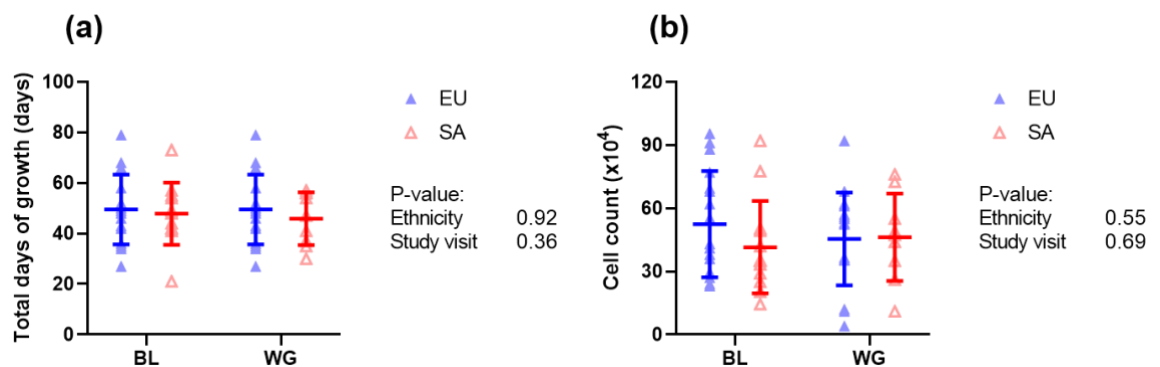
Figure 6-8 Comparison of cell proliferation in SA and EU.

(a) Displays total days of proliferation. (b) Shows cell count post-proliferation in South Asians (SA) and Europeans (EU) at baseline (BL) (SA n = 13; EU n = 17) and after weight gain (WG) (SA n = 9; EU n = 18). A two-way comparison was performed using an ANOVA mixed effects model to analyse differences between ethnicity (SA vs EU) and study visit (BL vs WG).

6.3.7 The effects of ethnicity and weight gain on cell count after proliferation per tissue weight of biopsy

Cell count after proliferation per tissue weight of biopsy was calculated and no difference was found between SA and EU at BL and after WG. The yield of preadipocytes per gram tissue weight of biopsy was the same in SA and EU at BL (SA vs EU: 155.7 ± 126.0 vs 191.5 ± 98.5 x10^4 cells/g) and after WG (SA vs EU: 143.6 ± 106.6 vs 152.3 ± 103.0 x10^4 cells/g).
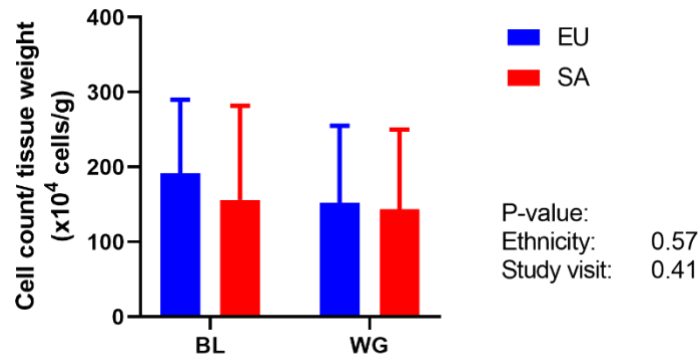
Figure 6-9 Cell proliferation per gram of biopsy tissue in SA and EU

This figure displays the cell count after proliferation per gram of biopsy tissue in South Asian (SA) and European (EU) participants, both at baseline (BL; SA n = 13; EU n = 17) and after weight gain (WG; SA n = 9; EU n = 18). A two-way comparison was conducted using an ANOVA mixed effects model to analyse differences between ethnicities (SA vs EU) and study visits (BL vs WG)

6.3.8 Association between patient anthropometry and adipocyte size on preadipocyte proliferation

The correlations between preadipocyte proliferation and participant anthropometry and adipocyte diameter were first assessed using univariate analysis.

The correlations between preadipocyte proliferation and covariates, including weight, BMI, waist, adipocyte diameter, RMR, VO$_2$ max and total adipose tissue, were analysed in a univariate analysis. No significant correlation was found between either total days of proliferation or cell counts after proliferation and anthropometric parameters and adipocyte diameter (Table 6-5 and Table 6-6).

Terms	r	*p* value
Weight	0.16	0.24
BMI	0.23	0.090
Waist	0.08	0.56
Adipocyte diameter	-0.10	0.48
RMR	-0.12	0.38
VO$_2$ max	-0.10	0.49
Total adipose tissue (no arm)	0.05	0.71

Table 6-5 Correlation between total days of proliferation and patient anthropometry and adipocyte diameter.

Pearson correlation coefficient was adopted to analyse the linear correlation, (n = 57).

Terms	r	*p* value
Weight	-0.16	0.24
BMI	-0.17	0.22
Waist	-0.02	0.91
Adipocyte diameter	0.004	0.98
RMR	-0.13	0.34
VO$_2$ max	0.11	0.41
Total adipose tissue (no arm)	-0.12	0.41

Table 6-6 Correlation between cell count after proliferation and patient anthropometry and adipocyte diameter.

Pearson correlation coefficient was adopted to analyse the linear correlation, (n = 57).

6.3.9 Relationship between *in vivo* adipocyte gene expression and preadipocyte proliferation

Expression of genes in adipocytes *in vivo* that differed in SA and EU at BL and after WG, including genes involved in the insulin signalling pathway (*CIDEA*, *ESR1*, *GHR*, *INSR*, *PLIN2* and *SIRT1*), tissue stress and inflammation (*TCF7L2*, *TLR2* and *TNF*) and the lipid storage pathway (*ADIPOQ*, *APOE*, *LEP* and *SREBF1*)[10] (were correlated with pre-adipocyte proliferation time and cell yield. Initially univariate correlation between expression of these genes in adipocytes and preadipocyte proliferation (total days of proliferation and cell counts after proliferation) was explored, after which multivariate analysis was performed to examine independent effects.

6.3.9.1 Univariate correlation between adipocyte gene expression and preadipocyte proliferation measures

The correlations between preadipocyte proliferation (including total days of proliferation and cell count after proliferation) and adipocyte gene expression were analysed in a univariate analysis. A strong negative correlation was found between the expression of *SREBF1* in adipocyte and cell count of proliferation (R = -0.39, *p* = 0.003, Table 6-7 and Table 6-8).

---

[10] *ADIPOQ*, adiponectin; *APOE*: apolipoprotein E; *CIDEA*, cell death inducing DFFA like effector A; *ESR1*, estrogen receptor 1; *GHR*: growth hormone receptor; *INSR*: insulin receptor; *LEP*: leptin; *PLIN2*: perilipin 2; *SIRT1*: sirtuin 1; *SREBF1*: sterol regulatory element binding transcription factor 1; *TCF7L2*, transcription factor 7 like 2; *TLR2*, toll like receptor 1; *TNF*: tumour necrosis factor.

Terms	r	*p* value
ADIPOQ	0.18	0.19
APOE	-0.01	0.95
CIDEA	0.01	0.97
ESR	0.10	0.45
GHR	0.06	0.65
INSR	< 0.0001	1.00
LEP	0.23	0.09
PLIN2	-0.04	0.77
SIRT1	-0.08	0.55
SREBF1	0.22	0.11
TCF7L2	0.07	0.59
TLR2	0.21	0.12
TNF	0.13	0.32

Table 6-7 Correlation between total days of proliferation and adipocyte gene expression.

Pearson correlation coefficient was adopted to analyse the linear correlation, (n = 57).

Terms	r	*p* value
ADIPOQ	-0.09	0.50
APOE	-0.02	0.91
CIDEA	0.08	0.53
ESR	0.02	0.90
GHR	0.10	0.47
INSR	0.09	0.52
LEP	-0.21	0.11
PLIN2	0.05	0.69
SIRT1	0.12	0.37
SREBF1	-0.39	0.003
TCF7L2	-0.08	0.54
TLR2	-0.07	0.61
TNF	0.04	0.77

Table 6-8 Correlation between cell count after proliferation and adipocyte gene expression.

Pearson correlation coefficient was adopted to analyse the linear correlation, (n = 57).

6.3.9.2 Multivariate analysis of predictors of preadipocyte proliferation

Multivariate analysis was performed to examine the effects on preadipocyte proliferation. Tissue weight was negatively significantly independently associated with total days of growth of preadipocyte proliferation (p = 0.03, Table 6-9). In addition, the expression of *SREBF1* in adipocytes, negatively independently predicted cell count after proliferation (p = 0.017, Table 6-10).

Terms	p value	r² of model
Tissue weight	0.030	
Ethnicity	0.96	54.3 %
Study visit	0.51	

Table 6-9 ANOVA mixed effect model: total days of growth of preadipocyte proliferation versus factors and covariate.

Factors (study visit and ethnicity) and covariate (tissue weight) (n = 57).

Terms	p value	r² of model
Tissue weight	0.35	
SREBF1	0.017	
Study visit	0.96	44.0 %
Ethnicity	0.95	

Table 6-10 ANOVA mixed effect model: cell count of preadipocyte proliferation versus factors and covariates.

Factors (study visit and ethnicity) and covariate (tissue weight and expression of *SREBF1* in adipocytes) (n = 57).

6.3.10 Anthropometry of participants involved in preadipocyte differentiation pilot study

Anthropometry data for the subjects included in the pilot study are shown in Table 6-11. There were no significant differences between EU and SA in age, BMI, waist circumference, body weight and resting metabolic rate (RMR) at either BL or after WG. However, SA had a lower VO_2 max than EU at BL (SA vs EU, 43.8 ± 3.3 vs 51.0 ± 6.9 ml/kg/min, p = 0.018). After WG, SA had more adipose tissue than EU (SA vs EU, 22.8 ± 3.9 vs 15.8 ± 11.5 L, p = 0.031).

	Baseline			Weight gain		
	Europeans (n = 10)	South Asians (n = 5)	*p* value (EU vs. SA)	Europeans (n = 10)	South Asians (n = 5)	*p* value (EU vs. SA)
Age (years) [$]	22 ± 4	22 ± 3	0.86	22 ± 4	22 ± 3	0.86
BMI (kg.m^{-2})	21.8 ± 1.6	20.0 ± 3.0	0.26	23.1 ± 1.8	21.4 ± 3.3	0.32
Waist (cm)	77.1 ± 3.8	75.4 ± 6.9	0.63	79.9 ± 3.4	79.4 ± 7.7	0.90
Weight (kg)	72.1 ± 8.6	64.4 ± 11.0	0.23	76.4 ± 9.5	69.1 ± 11.7	0.27
VO$_2$ max (ml/kg/min)	51.0 ± 6.9	43.8 ± 3.3	0.018	42.2 ± 15.3	33.2 ± 19.1	0.39
Total adipose tissue (no arm) (L)	13.0 ± 2.5	19.4 ± 4.3	0.070	15.8 ± 11.5	22.8 ± 3.9	0.031
RMR (kcal/kg/day)	20.9 ± 2.0	22.6 ± 4.9	0.49	21.3 ± 2.5	23.8 ± 4.7	0.32

Table 6-11 Demographic data for EU and SA GlasVEGAs study participants involved in preadipocyte differentiation at BL and after WG.

BMI, body mass index; RMR, resting metabolic rate. Comparison was made using two sample t test. $: Statistical analysis on log transformed data.

6.3.11 Quantitation of cellular lipid accumulation by Oil red O staining before and after preadipocyte differentiation

After differentiation (1.33 ± 0.48 OD, Day 14), lipid accumulation had significantly increased compared to undifferentiated preadipocytes (0.98 ± 0.41 OD, Day 0) (n = 24, $p < 0.0001$, Figure 6-10), suggesting that preadipocytes had differentiated to mature adipocytes. There was one outlier.
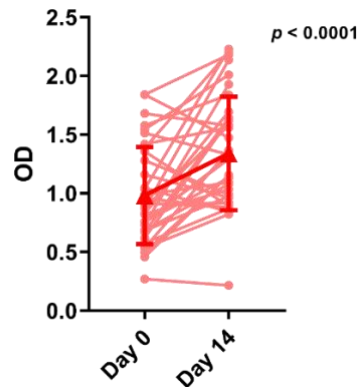
Figure 6-10 Oil red O absorbance increased between undifferentiated (Day 0) and differentiated (Day 14) preadipocytes.

OD, optical density read at λ510. Paired t test was used for the comparison between Day 0 and Day 14. Mean and standard deviation is shown in red, individual data is shown in pink (n = 24[£]). £: Result from ORO staining was missing for n = 3 EU as there was insufficient pre-adipocytes to carry out this experiment.

6.3.11.1 Cellular lipid content after pre-adipocyte differentiation in SA and EU at BL and after WG

The increase in cellular lipid content between preadipocyte and differentiated adipocytes was similar in SA and EU at BL and after WG (BL: SA 0.51 ± 0.65, EU 0.47 ± 0.34 OD; WG: SA 0.21 ± 0.59, EU 0.25 ± 0.40 OD, $p = 0.995$, Figure 6-11). After WG, there was no difference in cellular lipid content compared to baseline in both ethnicity groups ($p = 0.086$, Figure 6-11). No significant ethnicity x study visit interaction was found.
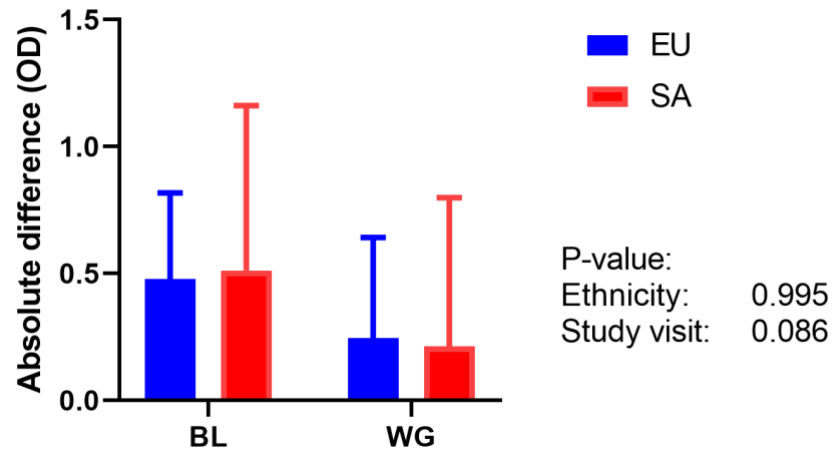
Figure 6-11 Cellular lipid content in SA (n = 5) and EU (n = 7[£]) at BL and after WG.

Cellular lipid content was assessed using oil red O staining (absorbance optical density [OD] read at λ510) and calculated as the difference of OD differentiated (Day 14) minus undifferentiated (Day 0) preadipocytes. A two-way comparison between ethnicity and study visit was made using an ANOVA mixed effect model. £: Result from ORO staining was missing from n = 3 EU as there were insufficient cells to carry out the experiment.

6.3.12 Gene expression in differentiated and undifferentiated control preadipocytes in SA and EU at BL and after WG – a pilot study

After differentiation, the expression of *ADIPOQ,* a marker of adipocyte end differentiation, was significantly increased after 14 days differentiation in EU at BL and after WG ($p < 0.01$ at both time points, Figure 6-12 (a)). While expression was increased in SA also at both time points, this did not reach significance.

The expression of *DLK1*, a marker of preadipocytes, did not change in response to differentiation in SA and EU at BL or after WG (Figure 6-12 (b)).

On the contrary, significant increases were observed in the expression of *PPARG*, a key factor of adipogenesis, in response to differentiation in SA and EU at BL and after WG (Figure 6-12 (c)).

After differentiation, there was a decrease in the expression of *TGFB*, an inhibitor of adipogenesis, in SA at BL ($p < 0.05$) but not after WG, whereas the expression of *TGFB* decreased in EU at BL and after WG ($p < 0.01$ and $p < 0.05$ respectively, Figure 6-12 (d)).

However, there was no significant difference found between ethnicities or study visits using multi-variate analysis.
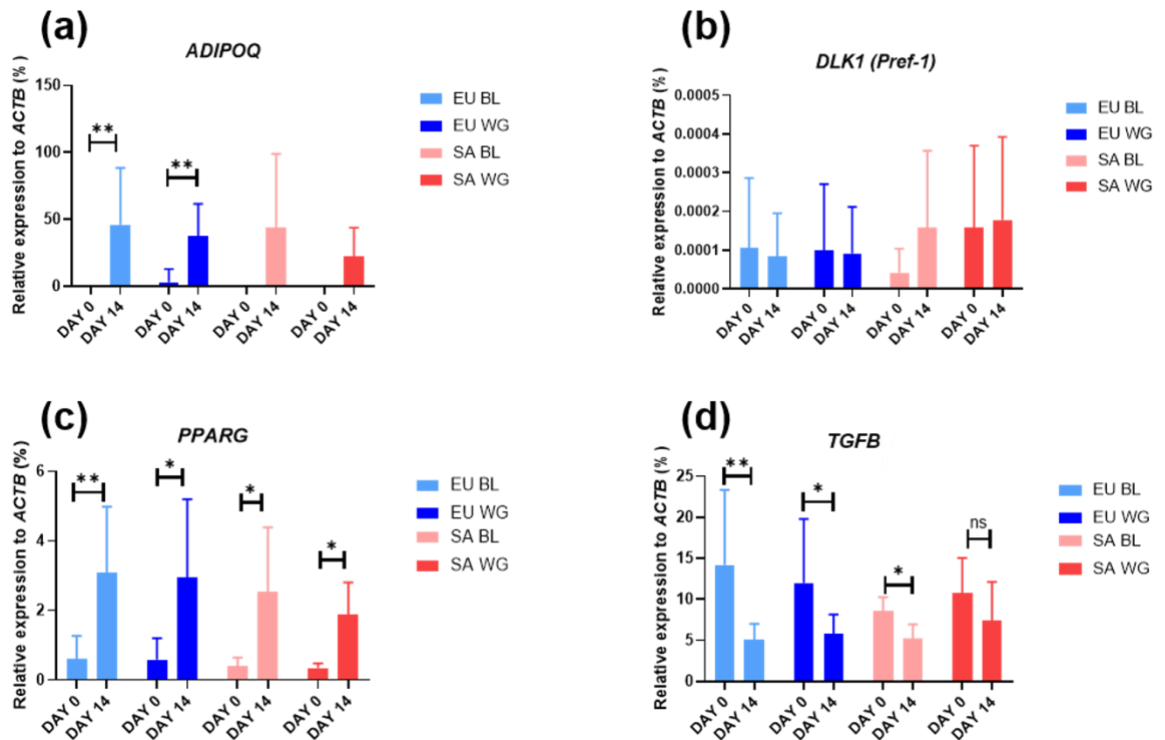
Figure 6-12 Preadipocyte gene expression before and after differentiation in SA and EU at BL and after WG.

(a) *ADIPOQ*, (b) *DLK1*, (c) *PPARG* and (d) *TGFB*. Day 0: undifferentiated preadipocyte; Day 14: differentiated preadipocytes. *, $p < 0.05$; ** $p < 0.01$, EU: n = 10; SA: n = 5.

6.3.12.1 Gene expression in response to differentiation in SA and EU at BL and after WG

The difference in gene expression of the adipocyte differentiation function markers between differentiated and undifferentiated preadipocytes was compared between SA and EU at BL and after WG. There was no significant difference found between ethnicities or study visits using ANOVA mixed effect analysis (Figure 6-13).
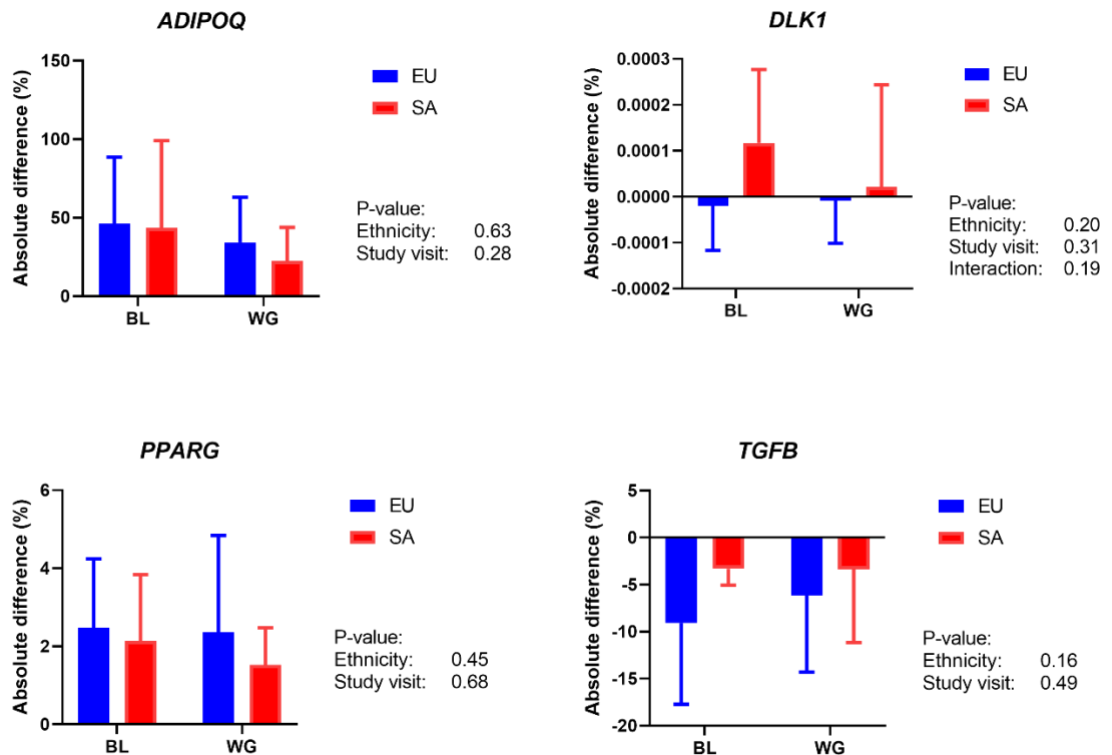
Figure 6-13 Changes of preadipocyte gene expression before and after differentiation in SA and EU at BL and after WG in absolute difference.

Arranged from left to right and top to bottom, the four genes are *ADIPOQ*, *DLK1*, *PPARG* and *TGFB*. Absolute difference was calculated by relative expression (day 14) – relative expression (day 0). Two-way comparison was analysed using ANOVA mixed effect between ethnicity and study visit. EU n = 10, SA n = 5.

6.3.12.2   Biological perspective of gene expression and the changes of gene expression in preadipocyte differentiation in SA and EU at BL and after WG

Relative expression to *TGFB* of *ADIPOQ*, *DLK1* and *PPARG* is shown in Figure 6-14. After differentiation, a significant increase was found in *PPARG* expression relative to *TGFB* in in SA after WG ($p < 0.05$), however, in EU, relative expression to *TGFB* of both adipocyte marker *ADIPOQ* and expression driver *PPARG* were significantly increased after differentiation both at BL and WG ($p < 0.01$). There was no significant change found in relative expression to *TGFB* in preadipocyte marker *DLK1* after differentiation in SA and EU at BL and after WG.
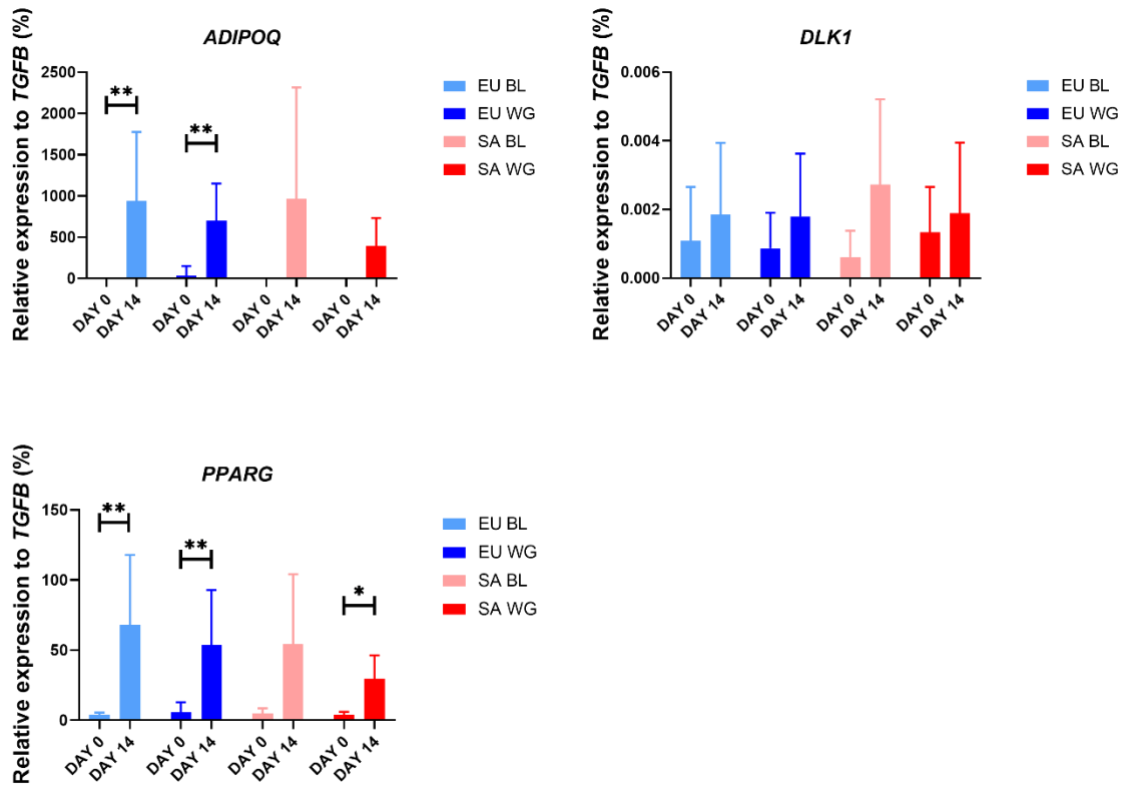
Figure 6-14 Relative expression to *TGFB* before and after differentiation in preadipocytes in SA and EU at BL and after WG.

Arranged from left to right and top to bottom, the three genes are *ADIPOQ*, *DLK1* and *PPARG*. Day 0: undifferentiated preadipocyte; Day 14: differentiated preadipocytes. *, $p < 0.05$; ** $p < 0.01$, EU: n = 10; SA: n = 5.

Absolute difference in relative expression to TGFB between differentiated and undifferentiated preadipocytes was measured and analysed as shown in Figure 6-15. However, there was no significant difference found between ethnicities or study visits using ANOVA mixed effect analysis.
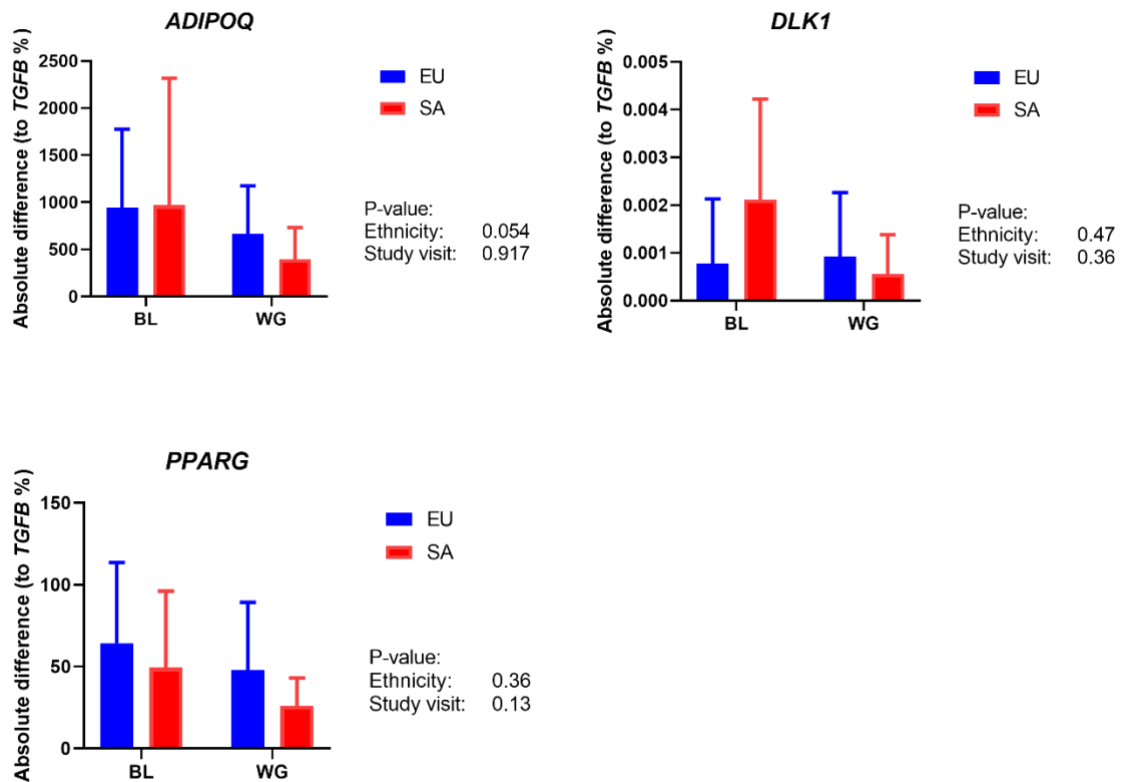
Figure 6-15 Changes of preadipocyte gene expression before and after differentiation in SA and EU at BL and after WG in absolute difference between relative expression to *TGFB*.

Arranged from left to right and top to bottom, the three genes are *ADIPOQ, DLK1* and *PPARG*. Absolute difference was calculated by relative expression to *TGFB* (day 14) – relative expression to *TGFB* (day 0). Two-way comparison was analysed using ANOVA mixed effect between ethnicity and study visit. EU n = 10, SA n = 5.

6.4 Discussion

Preadipocytes were successfully cultured from the SVF of adipose tissue. The current study demonstrated successful stimulation of preadipocytes to differentiate into adipocytes *in vitro* in SA and EU and at BL and WG, as there were significant increases in lipid content accumulation and expression of preadipocyte expression driver gene (*PPARG*). Experiments looking at differentiation of preadipocytes into adipocytes suggested that lipid accumulation after differentiation tended to be lower after weight gain in both SA and EU. The pattern also showed a tendency towards a sharper decrease in preadipocyte differentiation ability (expression of *ADIPOQ* and *PPARG*) in SA than EU in response to WG. Similarly, expression of preadipocyte inhibitors tended to be higher after differentiation in SA than EU at BL and after WG.

Expression of *SREBF1* in mature adipocytes *in vivo* was independently negatively associated with the yield of preadipocytes. Interestingly, expression of adipocyte

marker (*ADIPOQ*) was significantly increased only in EU and no decreased expression of differentiation inhibitor (*TGFB*) in SA after WG. There was no statistical significance in differentiation potential found in this pilot study between ethnicity and weight gain, however, the non-significant pattern suggested that the sample size was small, and it was under powered. A *post hoc* power calculation was carried out to calculate sample sizes that would be required to detect such differences and the sample size for each gene in order to get 95 power value in ethnicity and/or study visit was listed as follows: lipid accumulation (n = 65), *ADIPOQ* (n = 78), *DLK1* (n = 35), *PPARG* (n = 126) and *TGFB* (n = 41).

The adipose biopsy collection was conducted over a span of three years. As the study progressed, a minor reduction in the volume of SAT collected was observed, potentially due to diminishing technician performance over the extended duration. Additionally, the recruitment of SA participants occurred later in the study, which may have contributed to lower adipose tissue quantities, as their adipose tissue may be more difficult to collect. Lower tissue weight was independently associated with increased time for preadipocytes to proliferate to confluence, as fewer preadipocytes were isolated from lower amounts of tissue. However, tissue weight had no effect on the yield of preadipocytes. In addition, duration of proliferation, yield of preadipocytes, and cells yield of preadipocytes per tissue weight was similar between SA and EU and at both time points, BL and WG. These data suggest that the impact tissue weight collected has on adipocyte proliferation had a minor influence on the current study.

SREBF1a, a protein coded by *SREBF1* gene, plays a key role in fatty acid metabolism (*de novo* lipogenesis) in adipocytes and promotes adipocyte differentiation *in vitro* (Kim and Spiegelman, 1996, Price *et al.*, 2016). The current study found that the expression of *SREBF1* in adipocytes *in vivo* was independently negatively associated with the yield of preadipocytes after proliferation *in vitro*. This is different from other *in vitro* and *in vivo* studies. Decreasing *SREBF1* expression using knockdown with short hairpin RNA (shRNA) in a human Simpson-Golabi Behmel Syndrome (SGBS) preadipocyte cell line significantly decreased

preadipocyte proliferation without inducing senescence[11] (Alvarez *et al.*, 2014). *In vivo* studies consistently show that *SREBF1* expression is not critical for adipose tissue development and/or expansion (Sarjeant and Stephens, 2012). However, the current study may suggest that *in vivo* expression of *SREBF1* in adipocytes suppresses preadipocyte proliferation, which is different from the function of *in vitro* expression of *SREBF1* in preadipocytes. The role of SREBF1a in lipogenesis may contribute more to adipocyte hypertrophy and maturing of adipocytes than adipocyte hyperplasia and thus preadipocyte proliferation. The regulation of *SREBF1* expression in adipocytes and preadipocyte proliferation is unclear, this may be relevant to the expression of WNT pathway. In mature adipocytes, the expression of canonical WNT signalling is critical for the expression of *SREBF1*, and the *de novo* lipogenesis function of SREBF1a (Bagchi *et al.*, 2020). Canonical WNT genes, including WNT1 and WNT3a, which are adipogenesis inhibitors, are expressed constitutively in preadipocytes and adipocytes (Bagchi and MacDougald, 2021). Expression of *SREBF1* in mature adipocytes, in turn, may reflect the level of these adipogenesis inhibitors and thus, reflect a lower level of preadipocyte proliferation. The expression level of *SREBF1* was higher in SA than EU at BL and after WG, and this may suggest a lower ability of hyperplastic expansion on SAT of SA compared to EU (Chapter 5). This is interesting for future work to investigate the mechanism by which *in vivo* expression of *SREBF1* in adipocytes inhibits proliferation of preadipocytes.

The current study successfully stimulated preadipocytes to differentiate to adipocyte *in vitro*. There was a trend of lower lipid accumulation in differentiated adipocytes in SA and EU after WG compared to BL, which suggested that after WG, the ability of preadipocytes to differentiate into fully mature adipocytes has decreased. The loss of lipid accumulation in differentiated adipocytes may be a result of counter regulation in order to protect against excessive weight gain and to maintain body weight. Studies have shown that impaired insulin sensitivity and obesity inhibit adipogenesis (Ioannidou *et al.*, 2022, Gustafson *et al.*, 2019b, Gustafson *et al.*, 2015, Hammarstedt *et al.*, 2018). However, that $6.2 \pm 1.1\%$ (1.32 ± 0.28 kg/m^2) weight gain resulted in a decreased ability of preadipocyte

---

[11] The degree of senescence was estimated by the percentage of β-galactosidase-positive cells of total cell number, after culture the cells in SA-β-galactosidase (pH 6.0) for three days.

differentiation in young and lean participants was observed for the first time in the current study.

Interestingly, even though expression of adipogenesis driver *PPARG* increased significantly in preadipocytes after differentiation in SA and EU at BL and WG, *ADIPOQ* was only increased in EU after differentiation but not in SA. This suggests that there were fewer adipocytes that fully differentiated in SA than in EU at both time points. A study has shown that silencing of *ADIPOQ* in porcine preadipocyte differentiation *in vitro*, not only decreased lipid accumulation, assessed both as total fat accumulated and as number of lipid droplets ($p < 0.01$), but also decreased the expression of *PPARG, LPL and FABP4* ($p < 0.01$) (Gao *et al.*, 2013). Similarly, the current study also found a strong positive correlation between absolute difference in expression of *ADIPOQ* and *PPARG* (r = 0.85, $p < 0.0001$, EU n = 10, SA n = 5), and a trend of positive correlation between absolute difference in ORO and expression of *ADIPOQ* (r = 0.40, $p = 0.052$, EU n = 7, SA n = 5). Lower levels of *ADIPOQ* expression in SA than EU after differentiation suggests that a relatively lower number of preadipocytes from differentiate to mature adipocytes with a consequent lower ability to store lipid in SA than EU. *TGFB* expression decreased in differentiated preadipocyte in EU and SA at baseline as expected, however after WG, expression was decreased in EU but not in SA. This suggests that after WG, SA have a decreased ability to differentiate preadipocytes into mature adipocytes compared to BL. There were no changes in the expression of *DLK1,* an inhibitor of preadipocyte differentiation, in SA and EU at BL and after WG in response to differentiation. A study has shown that *DLK1* is highly expressed in human adipose-derived progenitor cells (Mitterberger *et al.*, 2012), which may suggest that there was still a certain number of uncommitted preadipocytes remaining after differentiation.

It is less understood how adipogenesis affects adipocyte function and whole-body glucose intolerance in SA[12]. The current study showed non-significant patterns of expression of a group of genes associated with adipogenesis in differentiated and undifferentiated preadipocytes which suggested there might be inherent differences existed between SA and EU in the progress of adipogenesis. Lipid

---

[12] No relevant reference can be found in PubMed using ((adipogenesis) OR (adipocyte differentiation)) AND (South Asian).

accumulation, increased expression of *ADIPOQ* and *PPARG* seemed to be lower in SA than EU and even lower after WG in SA than EU. This suggests that WG may be associated with a decreased ability of preadipocytes to differentiate into mature adipocytes. Differentiation potential may also be lower in SA than EU and lower after WG in SA than EU. This could contribute to the hypertrophic expansion and larger adipocyte size observed in SA compared to EU. After differentiation, expression of *DLK1* tended to be higher in SA at both time points but lower in EU at BL. After WG, expression of DLK tended to be increased to a smaller extent in SA but decreased similarly in EU. This may suggest that at BL, preadipocytes in SA had reduced differentiation potential compared to EU which worsened after WG. Similarly, after differentiation, expression of *TGFB* decreased to a smaller degree in SA than EU. Combined, these results may indicate that preadipocytes in young, lean SA have a lower ability to differentiate than EU. After WG, this ability decreased further in SA.

To sum up, even though there was no statistical significance found in the changes of lipid accumulation and expression of genes associated with adipogenesis in SA and EU due to the small sample size, the current pilot study for the first time indicated a picture that how SA and EU respond to WG at the preadipocyte differentiation level. It would be interesting for future work to investigate this topic in a larger group size and more target genes included in other signalling pathways, for example targets of *SREBF1* could be investigated as well.

6.5 Strengths and limitations

This study was a well-designed longitudinal study with two well matched (age, BMI and inactive) ethnicity groups, that allowed the current study to investigate the biological changes of adipose tissue in response to WG in a relatively more comparable way, which was a strength. However, a major limitation of this study was that there were a smaller number of samples available to be processed for differentiation due to a large number of failures in cell culture. Even though only some samples were contaminated (n = 11) or failed to reach confluency (n = 8), most participants were not included (SA n = 12, EU n = 10) due to lack of pairing in the differentiation experiment. This limited the power of the current pilot study to detect statistically significant findings, however the non-significant results

were insightful and provided a clear direction for future studies and a basis on which to determine future sample size.

The current study has exclusively examined the size of adipocytes *in vivo*, gene expression of adipocytes *in vivo*, preadipocyte proliferation *in vitro* and the ability of differentiation of preadipocytes *in vitro* from the same ASAT. This strength allowed the current study to explore the relationships between adipocyte morphology, function and development in SA and EU at BL and after WG. Another strength was that the differentiation experiment followed a robust protocol from Prof. Ulf Smith and his group, that has been tested using preadipocytes from sources, including animal, animal cell lines, human and human cell lines (Gustafson and Smith, 2006). The current study successfully stimulated human primary preadipocytes to differentiate to adipocytes *in vitro* as assessed by lipid accumulation and gene expression changes. The establishment of this technique allows future investigation of this topic in the future.

Because of the limitations of cost, the current pilot study did not carry out mRNA sequencing or expression arrays to examine expression of many genes in differentiated and undifferentiated cells. However, the genes that were examined in the current pilot study allowed an understanding of the process of adipogenesis in the GlasVEGAs study, and the non-significant patterns of these genes provided clear guidance for future work. Although the current study recorded the duration of proliferation and the final yield of cells at the end of proliferation, there was no cell count at isolation or at the end of passage 0, therefore the growth rate could not be calculated.

6.6 Conclusion and future work

The ability of preadipocyte to proliferation *in vitro* was negatively correlated with expression of *SREBF1* in adipocytes *in vivo* independent of ethnicity and weight gain in young and lean men.

Preadipocytes were successfully stimulated to differentiate *in vitro*. However, no significant differences were found in any measure. The pattern of gene expression in differentiated and undifferentiated adipocytes suggested that SA may have an

overall lower ability of adipogenesis than EU at BL and after WG yet lacked statistical significance.

This pilot study strongly suggests that adipogenesis should be taken into account in future research examining the relationship between adipose tissue function and T2DM in South Asians and Europeans, as well as possibly other populations. Investigation of the mechanism how *in vivo* expression of *SREBF1* in adipocytes inhibits proliferation of preadipocytes may help future studies understand adipocyte turnover better.

Chapter 7   The influence of a mixed meal on the concentration, size and miRNA content of plasma extracellular vesicles (EV) – A pilot study

7.1 Introduction

Expansion of adipocytes and adipose tissue function in obesity plays an important role in the development of insulin resistance and T2DM. As mentioned in previous chapters, this may be affected by anthropometric characteristics of participants, adipogenesis potential and adipocyte expression of genes involved in insulin signalling pathways, lipid metabolism, adiponectin secretion and the inflammatory response. EVs are nanosized spherical vesicles which are membrane-bound and are released from almost all living cells. EVs transport cargos of nucleic acids and proteins from donor cells to other cells, for intercellular communication (Zaborowski *et al.*, 2015). In recent studies, an important role for circulating EV in regulating whole body metabolic status, including T2DM, NAFLD and other metabolic syndromes, has been increasingly recognised (1.3.2). For example, the concentration of circulating EV was around 10-fold higher in obese individuals than in individuals of heathy weight, and the concentration of EV can be reduced by weight loss, both in humans and in rodents (Pardo *et al.*, 2018). However, it is unclear to what extent adipose tissue derived EVs are involved. Moreover, a positive correlation between the concentration of plasma EV and fasting plasma insulin levels and HOMA-IR level has been reported in a group of 20 obese patients before and after weight loss (Campello *et al.*, 2016). This suggests that circulating EV may directly be involved in the whole-body insulin metabolism, and this may also be influenced by adipose tissue directly or indirectly.

Adipose tissue plays important and contrasting roles during fasting and after feeding, under the regulation of insulin, for example lipogenesis and lipolysis. Therefore, it would be of great interest to understand the changes in circulating EV concentration, size and content between fasting and fed status. However, there are no studies showing the acute effects of fasted and fed status on EV concentration. As mentioned above, it could be predicted that concentration of circulating EV may be evaluated post-prandially along with the increased insulin level (Campello *et al.*, 2016). Differences in EV concentration and size between the sexes are few and the studies mainly focus on the influence of exercise rather

than nutritional status. In an exercise intervention study, the concentrations of circulating EV were the same in male and female at baseline within different size ranges (Lansford *et al.*, 2016, Durrer *et al.*, 2015, Rigamonti *et al.*, 2020). After a bout of acute exercise on a cycle ergometer or a treadmill, EV size between males and female became significantly different. Briefly, EV size reduced in obese males but not females (Durrer *et al.*, 2015). EV was lower and higher in females than males within different size ranges (30 - 130 nm and 130 - 700 nm) (Rigamonti *et al.*, 2020). However, no data illustrates the relationship between circulating EV size and activity of donor cells. Thus, there is a lack of direct evidence showing the relationship between circulating EV size and adipocyte function in response to fast and fed status.

In order to understand the role of circulating EV in regulating whole-body metabolic status, it is of great importance to find EV specific markers so that particles can be confirmed as EV and so that the origin of the EV might be determined. As described in the introduction chapter (1.1.7), the tetraspanin family of proteins, including CD63, CD9 and CD81, are commonly found in EV and are often enriched in EVs compared to cell lysates (Witwer *et al.*, 2013, Sinha *et al.*, 2014). Tetraspanin proteins were also found at 100-fold higher concentrations in EVs than in cell lysates (Escola *et al.*, 1998). Therefore, tetraspanin proteins are commonly used as protein markers for EV in current research. However, as explained in the introduction, there is a lack of tissue specific markers for adipose tissue derived EV. Currently a combination of EV size, cell source (usually in cell culture), and protein content (tetraspanin and tissue specific protein, such as adiponectin) are suggested to be used for the identification of EV from adipose tissue (Kranendonk *et al.*, 2014c). However, even though adiponectin is uniquely expressed in adipocytes, only a minor proportion of EVs secreted from 3T3-L1 adipocytes contain adiponectin (DeClercq *et al.*, 2015) and therefore it is not a reliable marker of plasma adipocyte derived EVs. Similarly, perilipin A, an important regulator of lipid storage essential for the mobilization of fat in adipose tissue, is another potential adipocyte specific marker for EV. Plasma EVs that were positive for perilipin A from *ob/ob* mice, activated monocytes in blood and adipose tissue of WT mice (Eguchi *et al.*, 2015). EVs containing perilipin A were higher in mice with HFD-induced obesity and in humans with metabolic disorders than their respective controls (Eguchi *et al.*, 2016). However, in healthy individuals,

extensive proteomic characterization of circulating EV was unable to detect the presence of perilipin A (Muller *et al.*, 2009, Ostergaard *et al.*, 2012). Fatty acid binding protein is expressed uniquely in adipocytes and is involved in fatty acid uptake, transport and metabolism. In some research, FABP4 positive EV have been regarded as adipocyte-derived EV (Hubal *et al.*, 2017). However, FABP4 and PPARγ were also found in EV derived from cultured adipose-derived stem cells, so FABP4 may be a marker of adipogenesis rather than adipocytes *per se* (Gugerell *et al.*, 2014). There are few published data on FABP4 as a biomarker of adipocyte-derived EV. Only three adipocyte-specific protein EV markers – adiponectin, perilipin A and FABP4 - have been suggested and all are unreliable. Therefore, additional adipocyte-specific EV markers are being sought.

miRNA are small non-coding RNAs that can fine tune mRNA expression by binding to complementary sequences mainly in the 3' untranslated region of target mRNA (Bartel, 2004). miRNA can decrease protein translation of target mRNA through this mechanism (Ameres *et al.*, 2007). As a major RNA component of EVs, miRNA in adipose tissue-derived EV also may be involved in the regulation of whole-body metabolic status. In mouse liver-associated fat, aerobically trained obese mice showed reduced adipocyte hypertrophy and expression of adipogenesis markers (Fabp4, Pparg and Cebpa) (de Mendonca *et al.*, 2020). miRNA-22 in circulating EVs was negatively correlated with the expression of these adipogenesis markers (de Mendonca *et al.*, 2020). However, no stable and reliable miRNA marker of adipocyte EV has been found so far. One year after gastric bypass surgery, FABP4 positive EVs were isolated from the plasma of the patients and miRNA profiling was performed (Hubal *et al.*, 2017). The miRNA profile in FABP EV changed after gastric bypass surgery. Changes in miRNA profile were shown *in silico* to be associated with the regulation of insulin signalling pathways by Ingenuity Pathway Analysis (IPA). The degree of miRNA change was correlated with HOMA-IR and plasma concentrations of branched-chain amino acids.

There is a lack of research regarding how EV miRNA is affected by feeding and fasting and a lack of miRNA profiling of circulating EV derived from adipocytes in the literature. However, the functions of adipocytes are strongly affected by fasting and feeding, and evidence shows that miRNA content in circulating EV was associated with adipocyte metabolism, for example, response to insulin. Therefore, a preliminary step in understanding changes in miRNA content in EV

from the fasting to the post-prandial state is required to begin to understand the role of EV in adipose tissue function.

7.1.1 Aim and objectives

This chapter aimed to evaluate the changes in plasma EV concentration, size and miRNA profile in response to a mixed meal and to assess the association of EV concentration and size with anthropometric parameters in healthy individuals.

The objectives were

1. To collect blood samples from fourteen participants when fasting and at different time points after a standard mixed meal (7 males and 7 females).

2. To isolate EVs from the blood samples and measure their size and concentration by NTA.

3. To isolate total RNA from the EV and to collect miRNA profiles using next generation miRNA sequencing and compare between fasting and fed states.

7.2 Methods

7.2.1 Study design

The current study recruited fourteen healthy individuals (male, n = 7, female, n = 7), who ingested a mixed meal, and their blood was collected at fasting and at several time points post-prandially. EVs were isolated from plasma using size exclusion chromatography (SEC), after which the size and concentration of EVs were measured using nanoparticle tracking analysis (NTA). miRNA profiles were identified in a subset of male participants at two time points i.e., fasting (time - 0 hours) and at peak EV concentration (time – 2 hours) due to resource constraints. The miRNA profile of plasma EV was identified using 'next-generation sequencing' and was carried out by the Glasgow Polyomics Facility.

Next-generation sequencing for miRNA profiling has been used to detect known and novel miRNA and the specific sequences of miRNA from different tissues, including plasma EV (Pritchard *et al.*, 2012).The general approach begins with

total RNA extraction and purification. Then a small RNA cDNA library is prepared from the isolated total RNA. Briefly, the RNA is firstly ligated with adapters[13] at both ends, and then it is reverse transcribed and amplified. This is followed by a "massively parallel" sequencing of millions of individual cDNA molecules in the small RNA cDNA library in a single run (Pritchard *et al*., 2012). A short sequence database is generated from all the identified miRNA in the sample. The results (sequence of miRNA and counts for each sequence) are validated by a series of QC analytics.

7.2.2 Subjects

Staff and postgraduate students at the University of Glasgow (n = 14) were recruited by email, advertisement poster and word of mouth for this study. Exclusion criteria included metabolic disease (such as type 2 diabetes, cardiovascular disease, thyroid disease) and age < 18 years. This study was approved by the University of Glasgow Ethics committee (project number University of Glasgow Ethical Approval 200170080). All participants gave informed consent, and all studies were carried out according to the Declaration of Helsinki.

Blood (~10 mL, after at least 10 hours fasting) was collected from each participant (2.7.1) using a cannula inserted into the antecubital fossa by Dr Anne Sillars. Participants were then provided with a standard mixed test meal (~800 Kcal, 30% fat, 47% carbohydrate and 17% protein), reflecting the typical west coast of Scotland diet (Burton *et al*., 2008). Further 10mL samples were collected via the intravenous cannula at 0.5, 1, 2, 4, and 6 hours as shown in Figure 7-1.

---

[13] Adapters are anti-sense to the primers to allow amplification of all the RNAs in the sample.
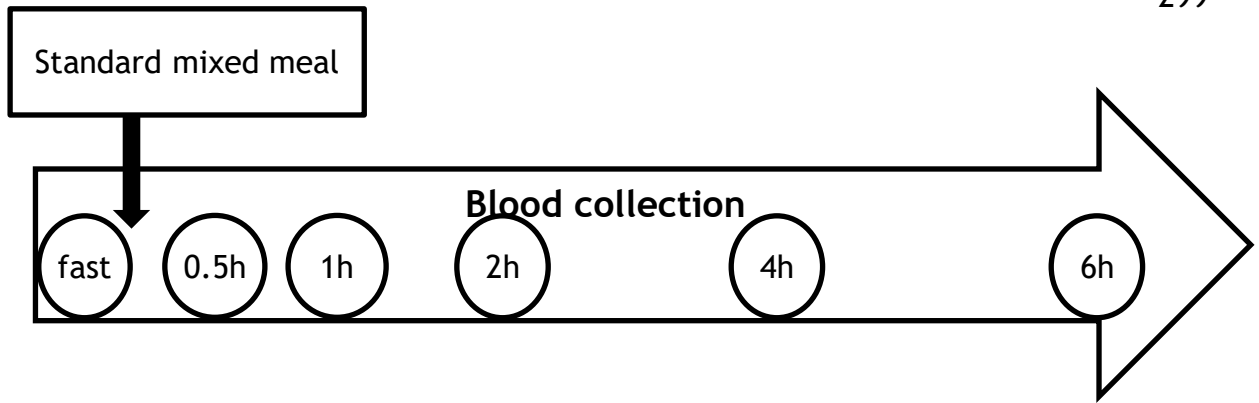
Figure 7-1 Blood collection in the mixed meal EV study.

Blood from each participant was collected after at least 10 hours fast using a cannula inserted into the antecubital fossa, and then the participant was provided with a standard mixed test meal. After this, further blood samples were collected via the intravenous cannula at 0.5, 1, 2, 4, and 6 hours.

7.2.3 Blood collection and plasma isolation

Around 10 mL of blood was collected into sodium fluoride/potassium oxalate (2mL) (Greiner Bio-one, 454061), sodium citrate 3.8% 4.5 mL (Greiner Bio-one, 454389), and K_2EDTA blood tubes (4 ml) (Greiner Bio-one, 454209). Plasma was collected by centrifugation (2,000 x g for 15 min at 4°C [oxalate tube] or room temperature [K_2EDTA tube]) within 30 min and stored at -80°C in 1 mL aliquots. Platelet-free plasma was collected from citrate tubes centrifuged at 2,000 x g for 15 min at room temperature followed by two centrifugations of the plasma and collection of the supernatant each at 2,500 x g for 15 min at room temperature.

7.2.4 Measurement of plasma insulin and glucose

Plasma glucose and insulin determination was performed by Elaine Butler and Josephine Cooney, Institute of Cardiovascular and Medical Sciences, University of Glasgow. Plasma glucose and insulin level were analysed in one batch at the end of the study on the Roche/Hitachi Cobus systems (Roche Diagnostics GmbH, Mannheim, Germany). Glucose was analysed on the Cobus c311 system using an enzyme colourimetric assay with a hexokinase reference. Insulin concentration was analysed by electrochemiluminescence immunoassay (ECLIA) on the Cobus e411 system. HOMA-IR was calculated as fasting glucose concentration multiplied by fasting insulin concentration divided by 22.5 using fasting values (Matthews *et al.*, 1985).

7.2.5 Isolation of EV

Plasma (2.7.1) collected using EDTA as an anti-coagulant was defrosted and a 500 µL aliquot of each sample was centrifuged at 2,000 x g for 30 min at 4°C to remove erythrocytes and most of the leukocytes and platelets. The supernatant was collected and centrifuged at 12,000 x g for 45 min at 4°C to remove all platelets and leukocytes. The supernatant was used for size exclusion chromatography (SEC).

7.2.5.1 Size Exclusion Chromatography

Disposable 10 mL polypropylene columns (Thermo Fisher Scientific, 29924) were prepared according to the manufacturer's instructions. Sepharose CL-2B slurry [bead diameter 60 - 200 µm] (14 mL; Sigma-Aldrich CL2B300) was transferred into a prepared 10 mL column (with a porous disc at the bottom) and left at 4°C for 48 hours to pack. A second porous disc was positioned on top of the sepharose and pushed down to just above the gel (~10 mL). The stock liquid was flushed through, and the gel was washed with 10 mL 1x DPBS (Dulbecco's phosphate buffered saline) to make it ready to use.

Prepared plasma (~500 µL, 2.7.1) was loaded onto the topmost porous disc, and after all the plasma had passed through the disc, 3 - 5 mL of 1x DPBS was loaded onto the column to keep it flowing. Eluate was collected in 25 x 500 µL sequential fractions once the plasma was loaded. All fractions were assessed to determine nanoparticle concentration using nanoparticle tracking analysis (2.7.3) and protein content using a Bradford assay (Bio-Rad DC). Desired fractions enriched with nanoparticles were concentrated (2.7.4) for further study.

Each column was used twice for one participant. First, the blood sample was processed, and second, the citrated sample was processed. Columns were washed three times with 10 mL 1x DPBS between each sample run, followed by 10 - 14 mL 0.5 M NaOH until the pH of the eluate reached 14. The column was then reset to pH 7.0 by flushing with 10 - 15 mL 1x DPBS until the pH of the eluate reached 7.0.

7.2.6 Nanoparticle tracking analysis (NTA)

NTA was used to analyse particle size and concentration in SEC fractions. The author analysed SEC fractions from EDTA plasma using a Nanosight NS 500 (Nanosight Ltd, Amesbury, UK) equipped with an autosampler and Nanosight NTA v3 software in the Exosome Biology Laboratory (EBL, University of Queensland, Australia). NTA was carried out according to the manufacturer's instructions. Samples were diluted to 50 - 100 particles in each frame (Salomon *et al.*, 2014a, Salomon *et al.*, 2014b). SEC fractions enriched in EV (2.7.4) were used to represent plasma EV.

7.2.7 The concentration of pooled EV preparations

Pooled plasma EV samples were concentrated using an Amicon ultra-15 centrifugal filter unit (ultracel-100K, Sigma-Aldrich, UFC910096). Briefly, the EV pool produced in 1.1.5 was loaded into the filter unit and centrifuged at 4,000 x g for 5 min at 4°C. The eluate (~250 µL) was collected from the receptacle (column) using a glass Pasteur pipette. The volume was then made up of the original volume of plasma loaded onto the SEC column. EV samples were stored at -80°C.

Each filter unit was used twice for each participant's EDTA and citrate plasma samples. The filter units were washed between each sample using three centrifugations at 4,000 x g for 15 min at 4°C with 15 mL 1x DPBS, 15 mL 0.1 M NaOH, and 15 mL 1x DPBS, respectively.

7.2.8 Micro RNA sequencing

RNA was extracted from 200 µL concentrated EV samples (2.7.4) using exoRNeasy Plasma Kits (Qiagen 217004, UK). In collaboration with Glasgow Polyomics, Julie Galbraith undertook miRNA sequencing on the NextSeq platform. miRNA libraries were prepared using a small RNAseq QIAgen kit, and quality control was assessed on the Agilent Bioanalyzer. Samples were examined using a single end, 75 bp read length achieving at least 10 million reads per sample on the NextSeq platform. miRNA sequencing analysis was performed only for the male participants (n = 7) using the samples collected at baseline and 120 mins postprandially. The miRNA sequencing experiment was supervised by Dr Martin McBride.

7.2.8.1 Quality control assessment of miRNA sequencing

A MultiQC report (generated by MultiQC, version v1.11, https://multiqc.info/) for the quality of miRNA sequencing was generated by Graham Hamilton from Glasgow Polyomics. The Multi QC website scored the sequencing quality for each stage of the miRNA sequencing. The QC analysis of each aspect of the miRNA sequencing was graded as 'entirely normal', 'slightly abnormal', or 'very unusual'. The aspects of miRNA sequencing quality graded were as follows:

1. Basic statistics tested if the miRNA sequencing was valid in terms of the overall composition of each sample in the report. Statistics included a count of the total number of sequences processed, the distribution of each sequence length, and the overall %GC composition.

2. The quality of the read was assessed by a quality score ranging between 0-33 (normal > 27, very unusual < 20). The score reflects the quality of each size subset sequence within the total read. A larger score means there was a lower percentage of failure in the sequencing read. A quality score of 27 indicates that 0.2% of all the reads failed, and a quality score of 20 indicates a 1% failure rate.

3. Per sequence/tile quality refers to the average per-read quality value of each subset of sequences.

4. Per base sequence content plots out the proportion of each base position in a file for each of the four normal nucleotides (G, A, T or C). This quality control analytic warns 'very unusual' when at any position of the sequence read there is a greater than 20% difference between A and T, or G and C.

5. Per sequence GC content assesses the GC content across the whole length of each sequence in a file and compares it to a modelled normal distribution of GC content.

6. Per base N content refers to the base where the sequencer software could not make a base call, and an N rather than a conventional base call was reported. An extremely low level of N content (< 5% at each position) is expected in a sequence.

7. Sequence length distribution examines the distribution of fragment sizes. Some high throughput sequencers generate sequence fragments of uniform length, but others might contain reads of varying lengths. Even within uniform-length libraries, some post-sequencing analysis pipelines will trim sequences to remove poor-quality base calls from the end of longer sequences.

8. The duplicate sequences model measures each sequence's duplication degree in a library. A low level of sequence duplication may indicate a high coverage of the targets. In contrast, a high level of sequence duplication more likely indicates enrichment bias (such as technical and biological duplicates).

9. Usually, a normal high-throughput library contains a diverse set of sequences, with each sequence making up a tiny fraction of the whole. A high number of reads of overrepresented sequences suggests that the sequence set may either be highly biologically duplicated (highly expressed) or have been contaminated or is not as diverse as expected.

10. An adapter sequence is a short DNA sequencing that provides a primer annealing site in unknown cDNA to facilitate miRNA sequencing. This quality control check is normal if no adapter sequence is present at more than 5% of all reads.

7.2.9 Statistics

Statistics were performed using Minitab version 19 (Minitab Ltd) and figures were drawn using GraphPad Prism 8.3. Normal distribution for all the parameters was tested using the Ryan-Joiner test. Non-normally distributed data were log or square root transformed to achieve normal distribution as required. Results were displayed as mean ± standard deviation (SD) for parametric data and displayed as median [95% confident interval (CI)] for non-parametric data.

Two group comparisons of cross-sectional parameters were made using a two-sample t-test for normally distributed data or Mann-Whitney U-test for non-parametric data that could not be transformed to achieve normality.

One-way ANOVA analysis with repeated measures was adopted using a general linear model to compare the different time plots, followed by *post-hoc* analysis using paired t-test.

A uni-variate correlation was assessed using Pearson's correlation, and the results were shown as coefficient value (r) and p-value. Multi-variate analysis was performed using a mixed effects model (two-way). The contribution of the confounders to predict the response was shown as R^2 of the coefficient. The significance level was $p < 0.05$.

Mr Simon Fisher performed a variety of downstream analyses under the supervision of Dr Martin McBride. A DeSeq2 Wald test was used to regress experimental and control means to determine if explanatory variables contribute significantly to the model. Afterwards, Padplot was generated using PadPlot_Web (https://github.com/SimonF92/PadPlot) to detect the best statistical analysis method for the datasets. The p-values were not corrected for multiple testing.

7.3 Results

7.3.1 Metabolic and demographic parameters of study participants

There was no significant difference between female and male participants in HOMA-IR, age, and BMI (Table 7-1).

	Female (n = 7)	Male (n = 7)	p value
Age$^\$$ (years)	31 [22, 42]	27 [24, 37]	0.85
BMI (kg/m^2)	22.1 ± 1.6	23.7 ± 2.5	0.18
HOMA-IR	1.2 ± 1.1	1.4 ± 0.9	0.77

Table 7-1 Anthropometric characteristics of the female and male participants.

Results are shown as mean ± SD for parametric data and median [95% CI] for non-parametric data$. Differences between groups were analysed using t-test. $, statistical analysis was applied using log-transformed data. HOMA-IR, homeostatic model assessment of insulin resistance.

7.3.2 Changes in plasma concentrations of glucose and insulin level after a mixed meal

Plasma glucose concentrations of the participants changed significantly after the mixed meal ($p < 0.0001$, Figure 7-2 (a)). There was a peak of glucose 0.5 hours

after food intake after which plasma glucose concentration dropped to fasting levels by one hour. The concentration of plasma glucose in female and male participants was the same (Table 7-2).

Similarly, the plasma insulin concentrations of the participants changed significantly after a mixed meal ($p < 0.0001$, Figure 7-2 (b)). There was a peak of insulin at 0.5 h after food intake after which the insulin level declined until reaching the fasting level after six hours. The plasma insulin concentration in female and male participants was the same (Table 7-3).
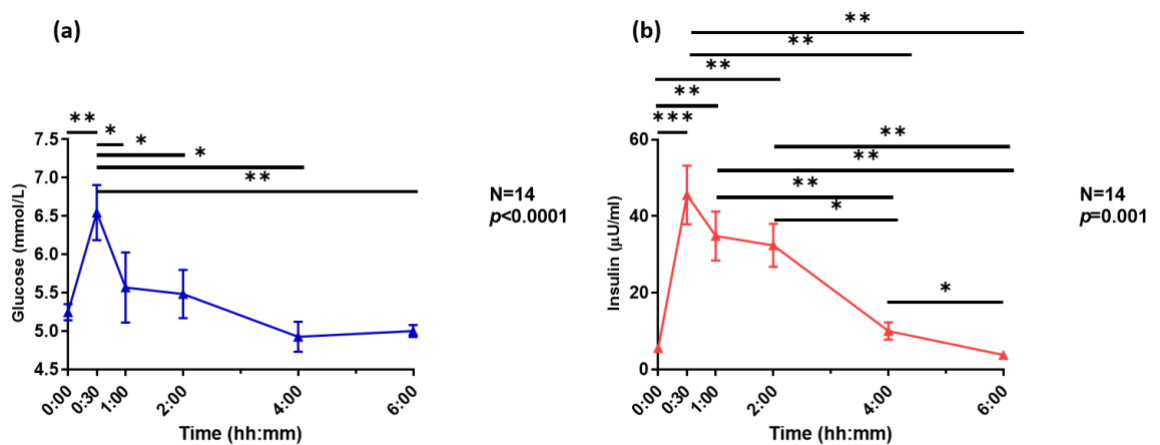
Figure 7-2 Changes in plasma (a) glucose and (b) insulin concentration at each sampling point.

Results are shown as mean and SD at each time point. Group difference across six-time plots was analysed using one-way repeated measures ANOVA analysis, and *post hoc* analysis was performed by Tukey's test. *, $p < 0.05$; **, $p < 0.01$, ***, $p < 0.001$, n = 14.

Glucose	p value	R^2 of model
Sex	0.76	
Sampling point	< 0.0001	50.2%
Interaction (sex*sampling point)	0.54	

Table 7-2 Two-way repeated measures ANOVA model: glucose concentration and factors.

Factors (Sex and sampling point).

Insulin	*p* value	R² of model
Sex	0.44	
Sampling point	< 0.0001	63.2%
Interaction (sex*sampling point)	0.48	

Table 7-3 Two-way repeated measures ANOVA model: insulin concentration and factors.

Factors (Sex and sampling point).

7.3.3 Plasma EV concentration after a mixed meal

Plasma EV concentrations of the participants changed significantly after a mixed meal ($p < 0.0001$, Figure 7-3). EV concentrations increased to a peak 2 hours after food intake and thereafter EV concentration declined to a concentration lower than baseline 6 hours after feeding. The plasma concentration of EV between female and male participants was the same (Table 7-4).
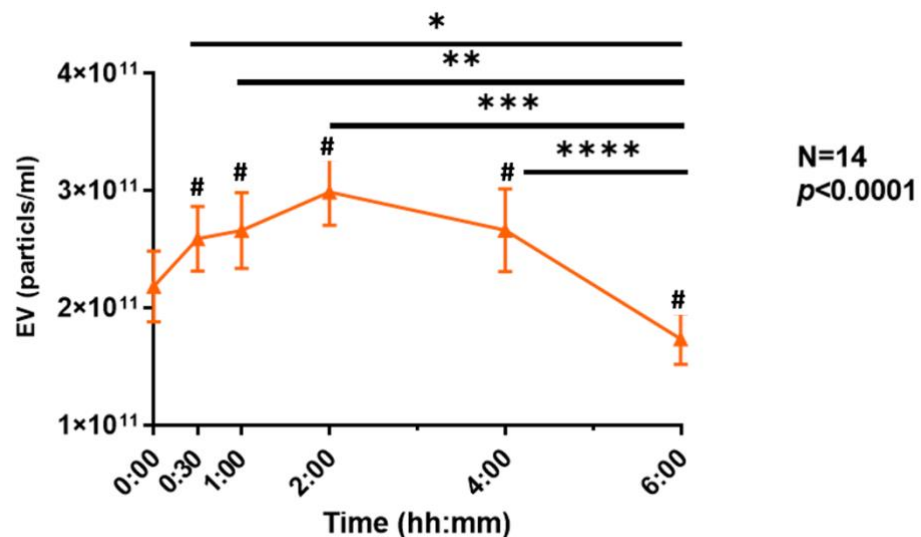
Figure 7-3 Plasma EV concentration against time of all the participants.

Results was shown as mean and SD at each time point. Group differences across six time points were analysed using one-way repeated measures ANOVA analysis, and *post hoc* analysis was performed by Tukey's analysis and is shown as symbols *, $p < 0.05$; **, $p < 0.01$, ***, $p < 0.001$, ****$p < 0.0001$, n = 14. Symbols # on each time point set showed the comparison vs starting time (T0), and symbols * with bars showed a comparison between the two time-points to the ends of the bar.

EV concentration vs.	*p* value	R² of model
Sex	0.90	
Sampling point	< 0.0001	76.9%
Interaction (sex*sampling point)	0.70	

Table 7-4 Two-way repeated measures ANOVA model: EV concentration and factors.

Factors (Sex and sampling point).

7.3.3.1 Associations of demographic and metabolic parameters with EV concentration

The correlations between EV concentration and HOMA-IR age, and BMI were analysed in a univariate analysis. However, no significant associations were found (Table 7-5).

EV concentration vs.	R	*p* value
Age (years)	0.22	0.051
BMI (kg/m^2)	-0.10	0.43
HOMA-IR	0.14	0.22

Table 7-5 Univariate analysis: correlation between EV concentration versus covariates.

Covariates (HOMA-IR, age, and BMI). Linear correlation was obtained using Pearson correlation, (n = 14). Age was analysed using log transformed data.

7.3.4 Plasma EV size after a mixed meal

EV size in the participants changed significantly after the mixed meal ($p = 0.014$, Figure 7-3). The size of EV showed a trend towards a decrease half an hour after food intake, after which there was a trend of increasing EV size until size reached a peak two hours after food intake. EV size declined thereafter up to the six-hour post food intake. The mean EV size measured at 6 hours post food intake was significantly lower than the peak mean EV size observed at 2 hours and also the mean EV size at 4 hours post food intake. However, it should be noted that measurements were not taken beyond this 6-hour period, and as such, further reductions in mean EV size could potentially occur. The size of EV in female and male participants was the same (Table 7-6).

Interestingly, the changes in EV size were almost coincident with the change in plasma EV concentration. Plasma EV concentration started to change immediately

after the mixed meal prior to the change in EV size which commenced after 30 minutes. EV size and concentration go in opposite directions for the first 30 mins and then in the same direction for the rest of the time.
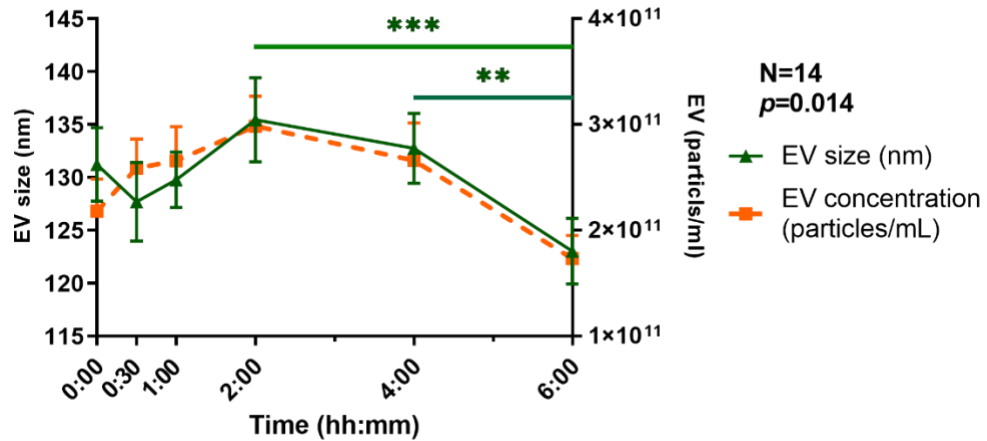
Figure 7-4 EV size over time for all the participants.

Results are shown as mean and SD at each time point. Group differences across the six time points were analysed using one-way repeated measures ANOVA using a mixed effect analysis, and *post hoc* analysis was performed by Tukey's test. **, $p < 0.01$, ***, $p < 0.001$, n = 14. Symbols on each time point set showed the comparison vs starting time (T0), symbols with bars showed comparison between the two time points to the ends of the bar. EV concentration was displayed without error bars, which are previously shown in Figure **7-3**.

EV size vs.	*p* value	R^2 of model
Sex	0.33	
Sampling point	0.002	66.3%
Interaction (sex*sampling point)	0.22	

Table 7-6 Two-way repeated measures ANOVA model: EV size and factors.

Factors (Sex and sampling point).

7.3.4.1 Association of participant demographic and metabolic parameters to plasma EV size

Correlations between EV size and concentration versus age, BMI and HOMA-IR were analysed in a univariate analysis. EV size was strongly correlated with age and EV concentration (R = 0.45 and 0.51, *p* < 0.0001 and < 0.0001, respectively, Table 7-7).

These positive associations remained independent on a multivariate analysis (Table 7-8).

EV size vs.	R	*p* value
Age (years)	0.45	< 0.0001
BMI (kg/m^2)	0.039	0.72
HOMA-IR	-0.005	0.97
EV concentration (particles/ml)	0.51	< 0.0001

Table 7-7 Univariate analysis: correlation between EV size versus covariates.

Covariates (HOMA-IR, age, BMI, and EV concentration). Linear correlation was obtained using Pearson correlation, (n = 14). Age was analysed using log transformed data.

EV size	*p* value	R^2 of model
Age (years)	0.041	62.3%
EV concentration (particles/ml)	< 0.0001	

Table 7-8 ANOVA mixed effect model: EV size and covariates.

Covariates (Age and EV concentration). Age was analysed using log transformed data, (n = 14).

7.3.5 miRNA sequencing quality control analysis

The quality of FastQC miRNA sequencing of the fourteen samples (baseline and two hours after a mixed meal) from seven male participants is shown in Figure 7-5. Overall, the quality report for the miRNA sequencing in the current study was acceptable.

Per sequence quality, per sequence GC content (cont), per base N content and adapter content passed the quality control analysis.

There were three sections shown as 'slightly abnormal', which were sequence length distribution (dist), sequence duplication and overrepresented sequence (sequ).
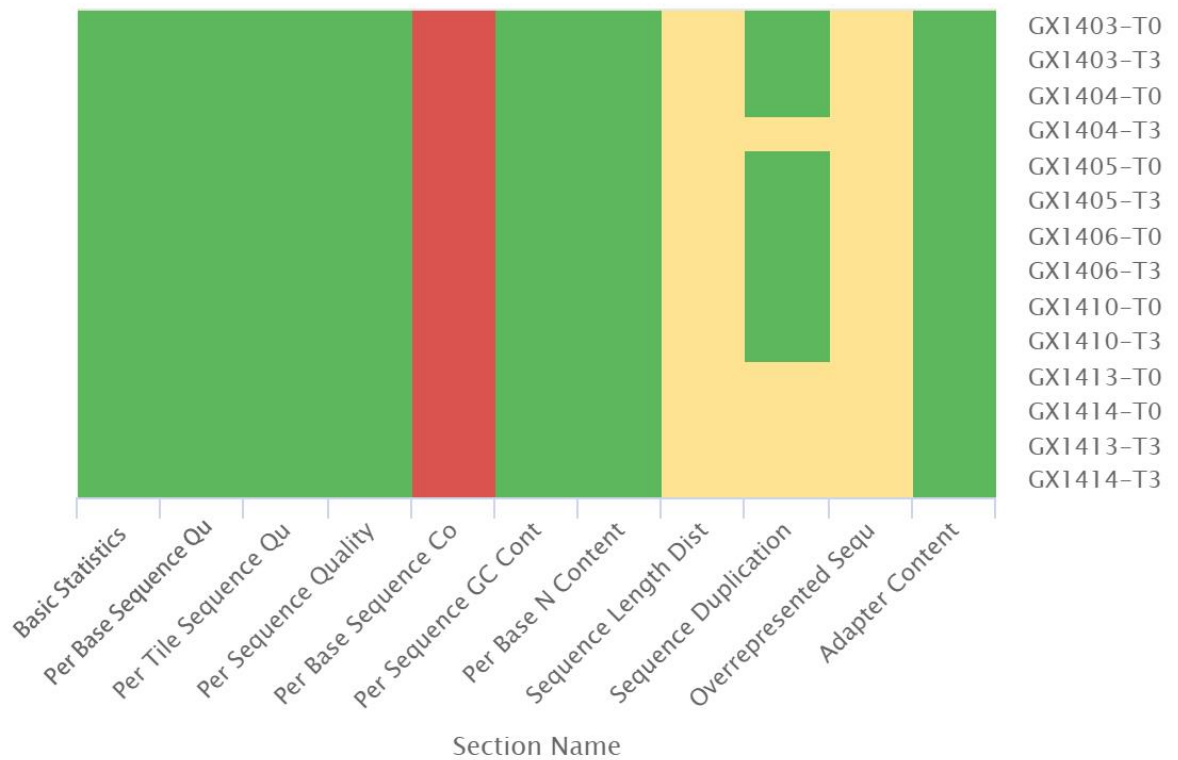
Figure 7-5 Heat map of status check for FastQC miRNA sequencing analysis.

Status for each FastQC section showing whether results seem entirely normal (green), slightly abnormal (orange) or very unusual (red). GX1403-GX1414, coded participant number. T0, sampling point 0 at 0 min, T3, sampling point 4 at two hours, when there was the peak of EV concentration and size. The figure was generated by Graham Hamilton.

The slightly abnormal sequence length distribution (dist) suggested that some high throughput sequencer generated sequence fragments were of uniform length, but others contained reads with varying lengths. However, for miRNA sequencing it is usual to have different read lengths so warnings here can be ignored.

'Slightly abnormal' is flagged in sequence duplication if non-unique sequences make up 20%-50% of the total and this was highlighted for five out of fourteen samples in the current study. This happened in some samples, where there was a tendency to over-sequence parts of the samples and therefore generate duplications. In this case, because of the low expression of miRNA in EV samples, random extension by non-specific binding of the adapters or primers may occur, and these sequences may be duplicated. Thus, in a sample of low miRNA complexity, this 'slightly abnormal' may be disregarded in this case.

'Slightly abnormal' for overrepresented sequences (sequ) was flagged in the current study and is highlighted when a sequence is found to represent more than 0.1% of the total. However, this does not suggest a problem in the current analysis as this is widely reported abnormal when small RNA libraries are analysed. In such scenarios sequences are not subjected to random fragmentation, and therefore some sequences may naturally represent a significantly higher proportion of the library.

The 'abnormal' rating of the above three sections in the MultiQC report represents characteristic anomalies that are quite frequently observed in miRNA sequencing analyses and these quality control flags can be ignored for the current analysis.

The only section that was labelled as 'very unusual' was the per base sequence content. In the current study, a high percentage of adenine (A, >30%) was observed in base pair 17 and beyond across all the samples. This may be caused by a composition bias at the end of the reads (poly-A tail) that may have been introduced, i.e., an artefact.

7.3.6 miRNA content of EV from male participants at baseline and at peak EV concentration and size (2 hours post food intake)

There was a total of 548 different miRNA identified, of which five miRNAs (MIRLET7B, MIRLET7A1, MIRLET7A3, MIRLET7C and MIR125B2) had more than 10,000 repeat reads as shown in Table 7-9. Of these five genes, four belonged to the MIRLET7 family.

Gene ID	Gene symbol	GX 1403 T0	GX 1404 T0	GX 1405 T0	GX 1406 T0	GX 1410 T0	GX 1413 T0	GX 1414 T0	GX 1403 T3	GX 1404 T3	GX 1405 T3	GX 1406 T3	GX 1410 T3	GX 1413 T3	GX 1414 T3	Total number of read
ENSG00000207875	MIRLET7B	375	1,971	10,081	1,459	8,311	4,181	8,879	18,96	2,006	2,187	9,633	2,982	14,401	930	69,292
ENSG00000199165	MIRLET7A1	163	665	2,833	461	2,179	765	1,615	511	602	544	2,046	452	3,778	318	16,932
ENSG00000198986	MIRLET7A3	171	627	2,837	464	2,103	718	1,537	497	570	548	1,990	442	3,886	304	16,694
ENSG00000199030	MIRLET7C	57	268	1,029	268	1,397	573	1,221	301	327	258	1,763	343	2,550	259	10,614
ENSG00000207863	MIR125B2	54	809	1,247	168	1,374	478	1,050	530	456	361	1,149	685	1,832	64	10,257
ENSG00000199072	MIRLET7F1	185	400	1,967	241	1,173	330	717	278	392	423	879	245	1,867	88	9,185
ENSG00000199179	MIRLET7I	91	234	1,480	238	980	299	608	208	161	258	779	261	1,477	107	7,181
ENSG00000199161	MIR126	484	548	695	208	896	267	627	310	328	316	681	302	1,162	241	7,065
ENSG00000208008	MIR125A	45	703	795	106	1,008	307	634	348	321	197	689	439	1,277	49	6,918
ENSG00000198987	MIR16-2	308	377	2,323	160	416	186	432	252	346	333	611	146	788	152	6,830
ENSG00000280859	*	7	558	354	46	535	96	466	385	376	329	567	197	654	31	4,601
ENSG00000198975	MIRLET7A2	32	165	531	121	626	209	444	135	145	128	596	162	1,149	91	4,534
ENSG00000208035	MIR143	13	190	278	74	686	173	221	162	123	89	516	186	681	26	3,418
ENSG00000277048	*	601	179	221	33	299	117	256	178	167	120	158	224	300	154	3,007
ENSG00000274705	MIR486-1	121	259	1,047	28	220	98	196	119	144	171	215	154	165	31	2,968
ENSG00000207971	MIR125B1	11	171	250	26	324	106	223	117	88	65	232	170	385	24	2,192
ENSG00000198972	MIRLET7E	11	72	229	32	285	81	281	81	84	53	342	68	523	5	2,147
ENSG00000199071	*	38	214	411	31	211	117	190	74	108	130	164	132	159	37	2,016
ENSG00000274735	*	310	121	103	27	203	68	154	96	95	66	87	64	149	124	1,667
ENSG00000275530	*	285	105	122	24	182	50	126	70	86	64	108	69	147	112	1,550
ENSG00000277105	*	318	84	94	12	171	49	120	86	70	67	71	91	137	113	1,483
ENSG00000199150	MIRLET7G	26	68	315	31	164	40	149	42	58	51	113	45	330	25	1,457
ENSG00000276736	*	332	82	104	21	158	66	112	68	79	48	79	88	126	81	1,444
ENSG00000280494	*	45	91	158	15	167	65	95	137	136	65	98	91	149	20	1,332
ENSG00000199075	MIR26A1	54	138	127	21	159	53	108	55	57	40	172	62	249	24	1,319
ENSG00000280646	RNA5SP196	46	58	159	11	143	65	102	103	123	61	111	87	162	24	1,255
ENSG00000280102	RN7SL2	14	80	122	24	81	68	140	76	104	95	122	51	242	30	1,249
ENSG00000208012	MIRLET7F2	28	52	195	35	189	45	88	50	52	35	125	46	290	13	1,243

ENSG00000273667	*	124	103	238	41	82	62	69	76	99	60	83	72	96	30	1,235
ENSG00000208037	MIR320	12	121	121	6	155	65	149	67	65	37	83	154	121	5	1,161
ENSG00000265764	*	75	92	91	60	67	87	133	51	52	49	77	71	78	140	1,123
ENSG00000274804	*	101	80	92	16	136	63	118	54	85	47	64	106	112	42	1,116
ENSG00000276924	*	117	86	93	15	132	48	101	56	91	63	73	98	100	34	1,107
ENSG00000199121	MIR26B	67	98	168	32	129	35	76	39	52	41	110	50	195	12	1,104
ENSG00000277765	*	116	74	76	16	144	61	104	54	77	50	75	102	86	38	1,073
ENSG00000278047	*	95	72	96	16	127	54	111	60	74	43	69	98	113	26	1,054
ENSG00000277145	*	97	76	94	18	153	52	96	61	65	43	58	88	112	38	1,051
ENSG00000278436	*	96	71	78	19	130	58	108	63	84	30	57	93	105	34	1,026
ENSG00000207782	MIR150	107	126	112	23	98	48	66	56	66	46	86	60	94	15	1,003

Table 7-9 Gene ID and symbols of miRNA with more than 1,000 total number of reads in mixed meal EV study.

GX1403-GX1414, coded participant number. T0, sampling point 0 at 0 min, T3, sampling point 4 at two hours, when there was the peak of EV concentration and size. *, gene ID was novel in gene bank.

7.3.6.1 Normalisation and differential expression analysis pipeline for miRNA sequencing data

Because of the difficulties with the analysis due to the low concentration and complexity of the data, raw data (gene counts) were unable to be analysed directly.

DeSeq2 Wald regression test of cellular miRNA and EV RNA data sequencing data sets from Dr Simon Fisher show the correlation of gene expression between control (x-axis) and experimental samples (Figure 7-6 (a) and (b)). Points that lie on the line show no difference in expression between control and experimental samples. Points furthest from the line show greatest difference in expression between control and experimental samples. The 95% confidence interval when plotted on the same scale (c and d respectively) was much wider in EV RNA sequencing due to fewer data points (Figure 7-6 (c) and (d)). The increased variance associated with fewer data points undermines the usual RNA sequencing analysis pipeline for cellular miRNA software which cannot therefore be applied to this dataset. Unfortunately, no formal analysis of differential expression could be undertaken for EV RNA sequencing and therefore alternative approaches were explored.
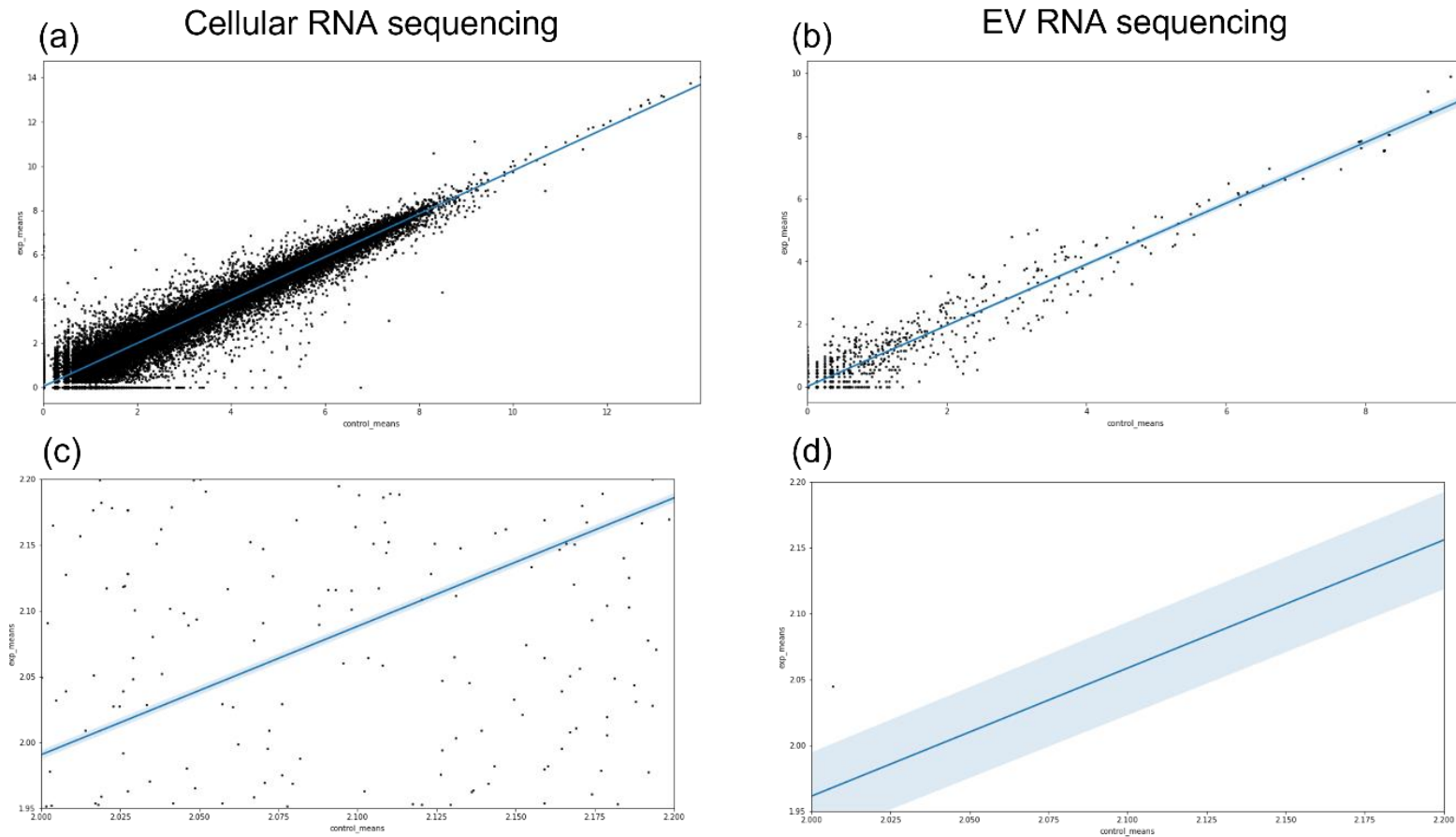
Figure 7-6 DeSeq2 Wald test: experimental (y-axis) versus control (x-axis) mean count per gene (logged) using RNA sequencing.

(a) Cellular RNA samples and (b) EV RNA samples, plotted to include all values. (c) and (d) the same best fit lines for (c) cellular and (d) EV RNA plotted at the same scale. Regression line is shown in dark blue line 95% confident interval was shown in light blue shadows in each figure. The figure was produced by Dr Simon Fisher, utilising data from his personal database.

Transformation of the data to a normal distribution could not directly use logarithmic corrections as the dataset contains a large number of zero values. The current study sought an alternative way of normalising the data so that differences between different time points could be analysed. Therefore, a statistical transformation using the formula log (gene+1)/ log (total read counts for sample) was used to transform data with total read counts of number '0' (n = 108), and a normal distribution of data was achieved (p>0.010, Figure 7-7).
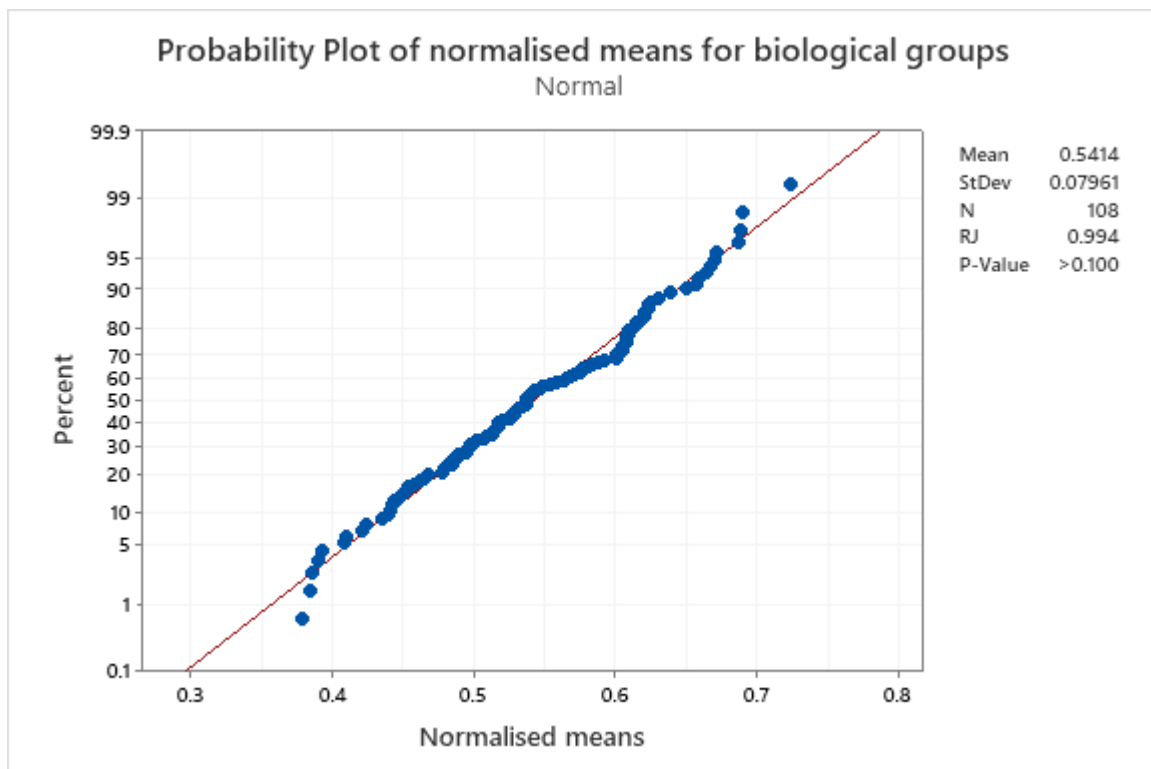
Figure 7-7 Normal distribution of transformed miRNA sequence read numbers.

This figure represents the Ryan-Joiner analysis of the normal distribution of transformed mean miRNA sequence read numbers across biological groups (n=108). Read numbers were transformed using the formula: log (gene+1)/ log (total read counts for sample).

7.3.6.2 Feasibility of using a t-test with Welch correlation examined by PadPlot

A volcano distribution plot was created in PadPlot, showing the relationship between differences in gene expression (T0 vs T3) and the p-value of the test (Figure 7-8). Two statistical tests were tried (a) the Welch correlation t-test and (b) Wald statistic. The plot (a) appears as a typical Volcano plot i.e., showed a decreased p-value with increased group difference, whereas (b) does not. This suggested that the Welch correlation t-test could be used to interpret the group difference in miRNA

expression from EV samples in the current study. Five genes with a significant p-value ($p < 0.01$) in the plot were identified. Four genes were expressed at a higher level in T3 than in T0, whereas MIR23A showed an expression that was lower in T3 than in T0 (Figure 7-8).
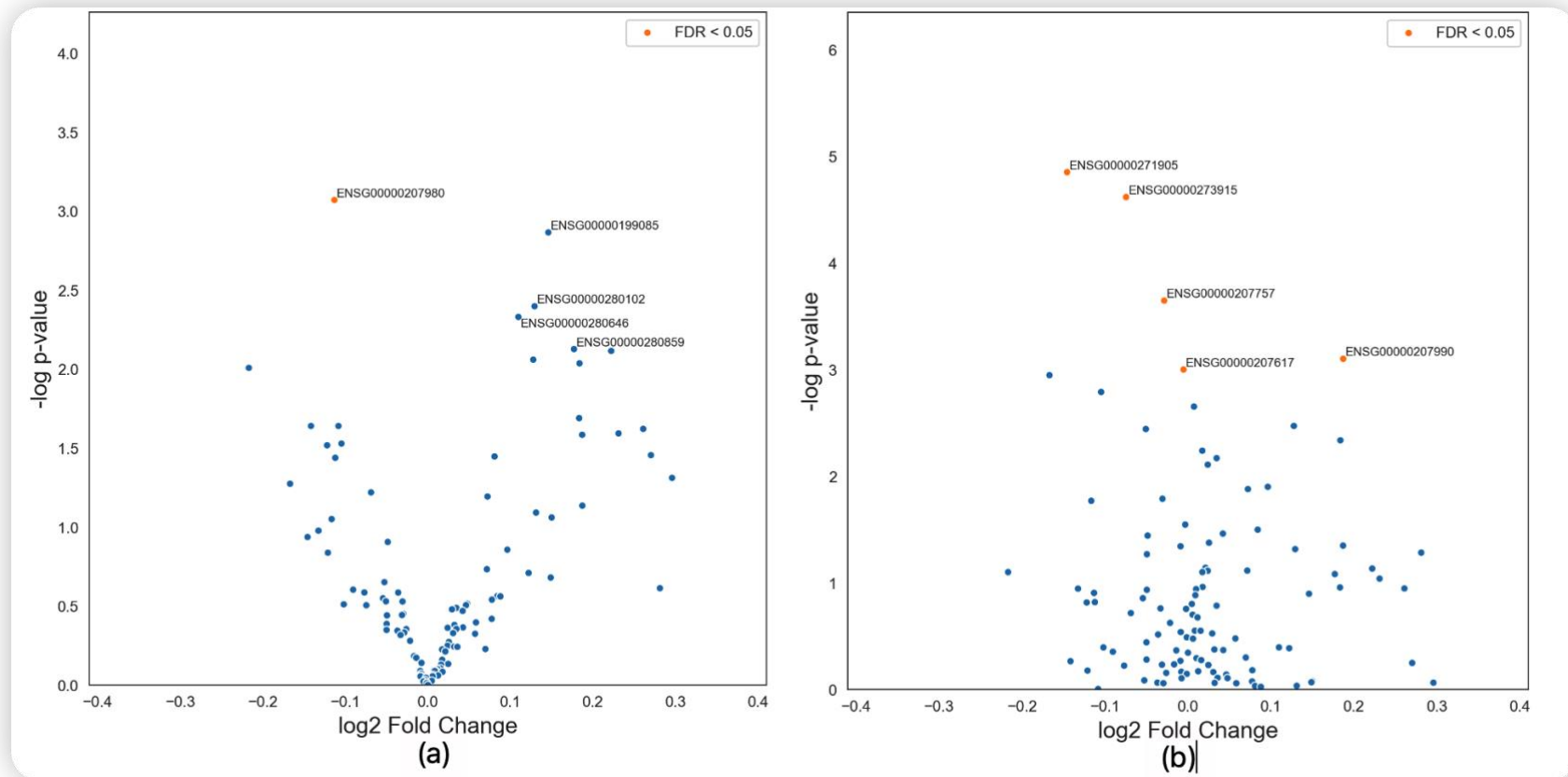
Figure 7-8 Volcano plat: Relationship between gene expression group differences (T0 vs T3) and p-value.

This figure illustrates the relationship between group differences in gene expression (T0 vs T3) and the corresponding p-value, using (a) the Welch correlation t-test and (b) the Wald statistic. The x-axis represents the log fold change between peak EV concentration and size time (T3) and baseline (T0), while the y-axis represents the -log p-value. Samples with a significant p-value are highlighted in orange. The figure was created by Dr Simon Fisher. Key: FDR - False Discovery Rate; ENSG00000207980 - MIR23A.

7.3.6.3 miRNA content of EV from male participants at baseline and at peak EV concentration and size (2 hours post food intake)

Transformed data were compared using a paired t-test to visualise the miRNA count between T3 and T0 for genes that previously showed statistical differences in the volcano plot (7.3.6.2). The results of the t-test are shown in Figure 1.10. There were no differences in miRNA content, which showed the highest -log p-value for difference on the Volcano plot between male participants at baseline and peak EV concentration and size (2 hours post food intake), as shown in Figure 7-9.
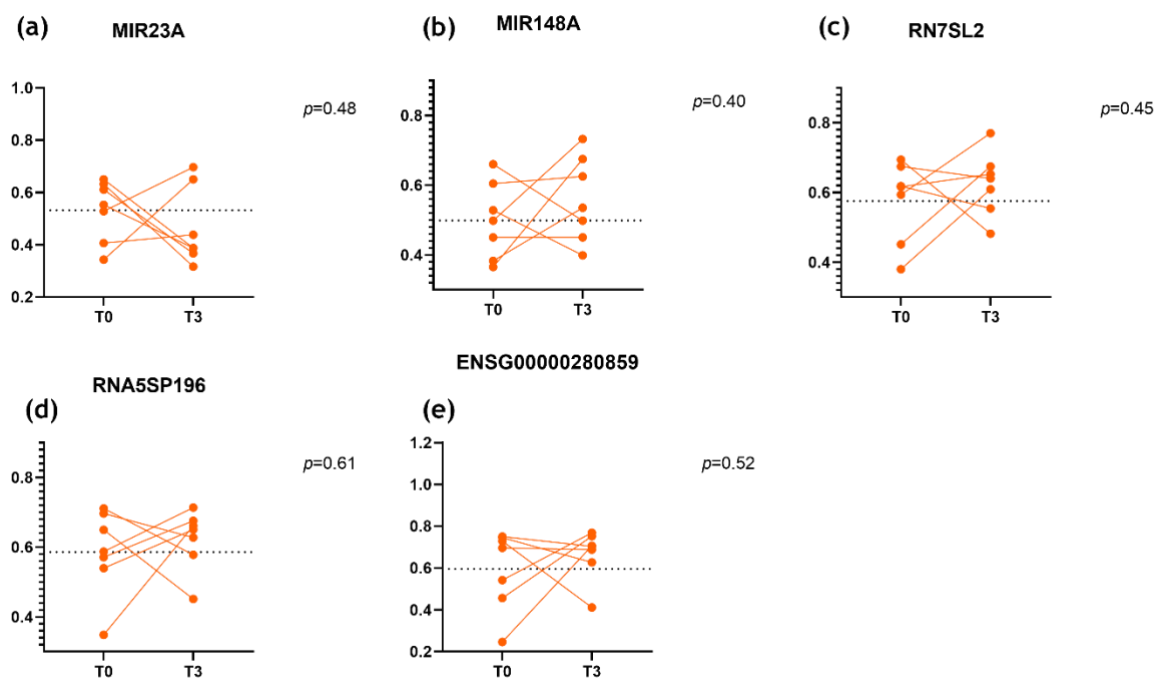
Figure 7-9 Paired t-test on miRNA content of EV.

The miRNA content of EV was extracted from seven male participants at baseline (T0) and at peak EV concentration and size (T3, 2 hours post food intake) on genes with statistical differences in the volcano plot (7.3.6.2). Y-axis shows normalised read number using the formular log(gene+1)/log (total read counts for sample).

There were no differences in the miRNA content, of the five most expressed genes (>10,000 of total counts), between male participants at baseline and at peak EV concentration and size (2 hours post food intake) as shown in Figure 7-10.
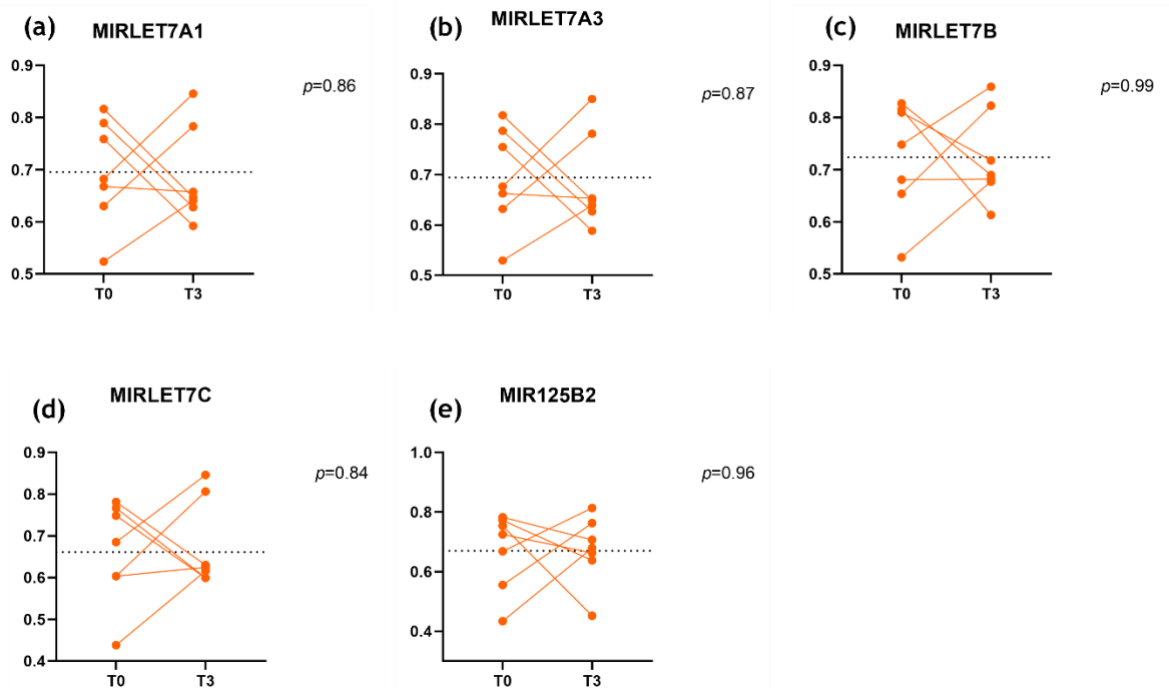
Figure 7-10 Paired t-test on most expressed miRNA content.

The miRNA content of EV was extracted from seven male participants at baseline (T0) and at peak EV concentration and size (T3, 2 hours post food intake). Y-axis normalised read number using the formula log(gene+1)/log (total read counts for sample).

7.4 Discussion

The current study examined changes in circulating EV concentration, size and miRNA profile in normal weight and insulin-sensitive male and female participants in response to a mixed meal. The concentration of circulating EV increased after a mixed meal and reached a peak concentration around two hours after feeding, decreasing to the baseline level by 6 hours. Interestingly, the changes in circulating EV concentration followed a similar pattern to those in plasma insulin and glucose concentrations but peaked much later than glucose and insulin. Plasma insulin and glucose increased rapidly in response to feeding, and changes in EV concentration followed the event. Plasma EV concentration increased and remained relatively high until two hours later, whereas plasma insulin and glucose dropped sharply to baseline level half an hour after the peak. Plasma EV concentration dropped to baseline level six hours later. This is to the best of the author's knowledge, the first time EV size and concentration have been shown to be affected by feeding status.

A previous study showed that circulating EV levels were positively correlated with fasting plasma insulin level and HOMA-IR in middle-aged (43 ± 12 years) obese

patients (BMI > 40 kg/m^2, n = 20) with T2DM (Campello *et al.*, 2016). However, the current study failed to find the correlation. This suggested that fasting circulating EV concentration changes may reflect whole-body insulin and glucose mechanism changes. In addition, patients with obesity (Pardo *et al.*, 2018) and T2DM (Freeman *et al.*, 2018) had higher circulating EV levels than normal-weight healthy individuals. It was suggested that insulin signalling and energy homeostasis may play an important role in regulating circulating EV concentrations. This could result from impaired adipocyte function in T2DM patients leading to an increase in EV shedding. Alternatively, abnormally high circulating insulin levels may stimulate cells to release more EV into the blood. However, in the current study, there was no correlation between circulating fasting insulin and EV concentrations suggesting there was no direct action of insulin on the secretion of EVs.

Similarly, plasma EV size was correlated to EV concentration at all time points except in the first half an hour. The decrease in EV size in the first 0.5 h may be related to EV function, suggesting different EVs with different functions. EV size was positively independently correlated with age in the current study. This was in contrast to a study in mice where EV size was assessed using transmission electron microscopy, where older mice (18 - 21 months old) had smaller EV than younger mice (3 months old), with more than a 2-fold higher proportion of small EV (~50 nm) and 50% lower proportion of large EV (125 - 150 nm) than young mice (Alibhai *et al.*, 2020). EV size and function in older mice could be shifted towards that of younger mice by senolytic treatment (dasatinib and quercetin (D + Q) or vehicle, biweekly for 2 months) (Alibhai *et al.*, 2020). This may suggest that changes in EV size change during ageing, and the direction of changes need to be further investigated. Also, it would be interesting to investigate the relationship between EV size and function.

There was no difference in circulating EV concentration and size between males and females at any time point in the present study. This is to the best of the author's knowledge, the first time illustrating no difference in EV concentration and size between the sexes at fasting and after feeding. This may suggest that circulating EV may play a similar role in males and females in response to feeding and that there may be a common role for circulating EV in signalling insulin, glucose and/or lipid storage status. Thus, it may be interesting to investigate further the function of circulating EV on adipocytes after feeding.

Both the concentration and size of EV increased after feeding. Six hours after feeding, size of EV went back to fasting level, whereas concentration of EV was significantly lower than the fasting level. These data indicate that fasting samples may be a good control for future EV studies, as feeding may be a potential stimulator of EV secretion into the blood and may change the size and/or contents of EV. It would be interesting to investigate where these EV came from and the function of them. Whether these EV signal from or to adipocytes, or both, may be further investigated.

Due to the low miRNA count in EV, the current study failed to generate stable and consistent miRNA sequencing findings and I was unable to determine whether there were differences in miRNA abundance at each time point. However, an interesting observation was that the MIR125B2 and the MIRLET7 family were the most highly expressed miRNA in circulating EV at baseline and after feeding in normal weight, healthy men. MIR125B2 may be involved in regulating normal lipid storage. A study indicated that MIR125B2 knockout (KO) mice showed higher liver, epididymal white fat and inguinal white fat weights compared to WT (n = 8) (Wei *et al.*, 2020). Moreover, fat tissue accumulation was increased in MIR125B2 KO mice with high fat diet-induced obesity compared to normal-weight WT mice, whereas there was no difference in other tissues. Expression of genes associated with adipogenesis, including PPARγ and C/EBPα, were increased in MIR125B2 KO mice (Wei *et al.*, 2020). Thus, MIR125B2 may contribute to limited adiposity, which may decrease adipogenesis. The participants in the current study were healthy with normal body weight. Thus, the relatively high MIR125B2 expression in circulating EV might be expected. However, again, this needs to be further investigated.

The intracellular expression of the MIRLET7 family is widely involved in regulating the cell cycle, cell signalling and the maintenance of differentiation, as previously reviewed (Chirshev *et al.*, 2019). Expression of MIRLET7 during embryogenesis initially increased during brain development. Later, increased expression of the MIRLET7 family has been reported in other organs, including adipose tissue (Boyerinas *et al.*, 2010). However, due to the redundant roles of the MIRLET7 family, it has been biologically impossible to knock out the MIRLET7 family in the same animal. Thus, the direct function of the MIRLET7 family during development

and adipogenesis remains unclear. There is no evidence identifying MIRLET7 as cargo in circulating EV.

7.5 Strengths and limitations

The current study involved male and female participants of known age, BMI and insulin sensitivity. Participants in the current study were all self-reported healthy. This allowed the current study to understand how a mixed meal affected the concentration, size and content of circulating EV. In each sex group, age was spread from young to mid-aged participants, which was another strength. This enabled the current study to understand how circulating EV was affected by an increase in age in adults.

The current study administered a mixed meal tolerance test and collected blood up to six hours post-prandially, another strength of the study. Compared to an oral glucose tolerance test, a mixed meal is more similar to a standard meal for participants, as it contains not only carbohydrate but also fat and protein. This helped the current study understand more about how a meal acutely affects the concentration, size and content of circulating EV. The collection of blood samples up to six hours post-prandially was long enough in the current study to show EV size back to normal, and concentration was lower than fasting. However, as it was not a full fasting fed cycle of eight hours, this may limit the current study to get a full picture of circulating EV in response to feeding.

The current study adhered to mature and standard protocols for EV isolation, purification, and concentration and size examination using Nanoparticle Tracking Analysis (NTA) (Salomon *et al.*, 2014a, Salomon *et al.*, 2014b). This approach enhances the reliability of the results pertaining to EV concentration and size. The standard protocol also enabled the isolation of RNA from circulating EV in this study, paving the way for future investigations into EV content. In collaboration with Dr Carlos Salomon, we will isolate proteins from EV and conduct proteomics in Australia. This will bolster our understanding of the protein cargo in circulating EV post-prandially.

However, a limitation was observed during the isolation of EV from serum, where we employed the standard protocol by Dr Salomon using size exclusion

chromatography (SEC). As illustrated in Figure 7-11, the EV size overlapped with chylomicrons in the SEC size range of 75 - 150 nm, suggesting the potential presence of chylomicrons in the isolated EV samples. Moreover, the similar density of high-density lipoprotein (HDL) and EV implies that an iodixanol-PBS gradient and ultra-centrifugation isolation method may not entirely remove HDL. Therefore, a combination of SEC and gradient ultra-centrifugation would be optimal for isolating EV from serum, despite the potential for greater EV loss during the process, a notion supported by other literature (Brennan *et al.*, 2020). As such, changes in particle concentration and size in response to a meal may not be solely attributed to EV, but also chylomicrons, necessitating further investigation. Nevertheless, as the study's main focus was on the microRNA content of EV, which is absent in chylomicrons, this did not significantly impact the current study.
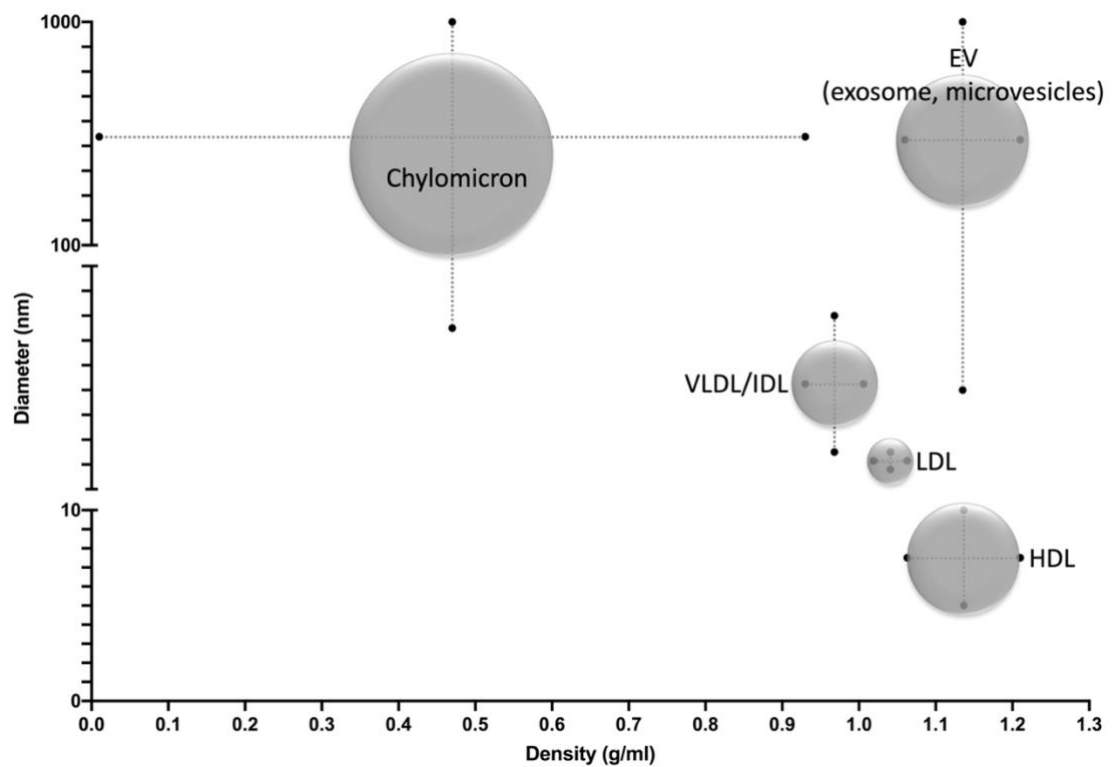
Figure 7-11 Particle size and density distribution in human serum.

This figure depicts the spectrum of particle sizes and densities present in human serum, which includes extracellular vesicles (EV), high-density lipoprotein (HDL), low-density lipoprotein (LDL), very low-density/ intermediate-density lipoprotein (VLDL/IDL), and chylomicrons. The figure's layout and structure were influenced by Dr Patamat Patanapirunhakit, while the data for diameter and density were derived from (Brennan *et al.*, 2020).

The current study used Next-generation RNA sequencing for miRNA profiling, another strength. This allowed the examination of the EV miRNA profile

systematically using only a small amount of RNA. However, due to only a small number of genes being detected and the low read counts measured compared to cellular RNA sequencing, the current study could not normalise and formally statistically analyse the RNA sequencing results. The lack of validation by Rt-PCR due to time limitations is a weakness of the study as there was no direct assessment of miRNA expression to confirm, the RNA sequencing data. Due to cost limitations, the current study only chose seven male samples at two time-points for RNA sequencing. Therefore, only having seven males and two timepoints limited the current study to chasing for statistical significance, and the results are underpowered.

7.6 Conclusion and future work

The current study is the first study showing changes of concentration and size in circulating EV in response to acute feeding. Both EV concentration and size reached a peak at two hours after feeding. Six hours after feeding, EV size went back to fasting state, and concentration was lower than fasting status. The EV size and concentration changes were similar in healthy males and females. This suggested that fasting samples might be a control for circulating EV studies in healthy humans. In addition, circulating EV size was positively correlated with age in males and females, similarly in humans aged 20 - 60 years. This suggests that adjusting for age in future circulating EV studies is important as it might affect circulating EV size.

Observation of the miRNA profile suggested that the MIRLET7 family and MIR125B2 were the highest copy number of miRNA in circulating EV in healthy men both in the fasting and fed states. However, the current study could not statistically analyse these data due to routine data normalisation procedures unsuitable for the low number of genes detected and low read counts.

The current study was at an early stage of development. So far, the current study has successfully generated a protocol that collected and isolated EV from blood, measured EV concentration and size and extracted RNA from circulating EV in Glasgow. Dr Carlos Salomon and his team will carry out the proteomics of the EV samples in Australia. This will expand the picture of EV composition in the current study. Taqman RT-qPCR should be carried out to validate the expression of miRNA

found in the current study in the future to help the current study solidify the initial findings.

Chapter 8   General Discussion

8.1 Experimental chapter summaries

The aim of this thesis was to explore the role of adipocytes in insulin resistance and T2DM by examining adipocyte size, gene expression, and differentiation, as well as their relationships with anthropometric and physiological data, ethnicity, and other factors. This study contributes to the development of a systemic understanding of T2DM. In simple terms the data presented suggest that, in European Caucasian males, ageing leads to hypertrophic changes in adipocytes, resulting in reduced gene expression associated with adipocyte function and adipokines. Interestingly, exercise appears to mitigate the effects of age on adipocyte morphology and gene expression. South Asians exhibit adipocyte size and gene expression patterns similar to older and higher BMI European Caucasians. This may explain the earlier onset of insulin resistance and T2DM in South Asians from the perspective of adipocyte morphology and function. Additionally, this study successfully induced *in vitro* adipocyte differentiation and isolated extracellular vesicles (EV) from serum, measuring EV size, and concentration in response to a meal.

Chapter 3 of this thesis employed a cross-sectional approach to compare adipocyte morphology and gene expression in individuals of different ethnicities, ages, exercise status, and insulin sensitivity. It was found that increased age was positively correlated with adipocyte size and negatively associated with metabolic fitness. Age was also associated with reduced adipocyte adipokine expression and differentiation gene expression. Long-term endurance exercise was associated with improved adipocyte metabolic fitness without altering adipocyte size. As individuals age, adipocyte differentiation capacity declines, causing adipose tissue to rely more on hypertrophy than hyperplasia for storing excess energy, consistent with previous findings. Adipocyte differentiation depends on mesenchymal stem cells (MSCs) within adipose tissue. With increasing age, MSCs isolated from adipose tissue display significantly reduced capacity for cell division and differentiation *in vitro* (Schipper *et al.*, 2008). Moreover, adipocyte activity, such as the secretion of adiponectin (ADIPOQ), declines with age (Kirkland *et al.*, 2002). Interestingly, as demonstrated in Figure 8-1, long-term exercise may significantly reduce the impact of ageing on adipocyte metabolic fitness.

Numerous studies have established the beneficial effects of long-term exercise on skeletal muscle and the cardiovascular system. This thesis confirms that long term endurance exercise can delay adipocyte volume enlargement and functional decline possibly by promoting adipocyte proliferation, thus maintaining a more youthful state and delaying the onset of insulin resistance and diabetes caused by adipocyte dysfunction. This study fills the gap in our understanding of the role of adipocytes in the anti-ageing effects of exercise.
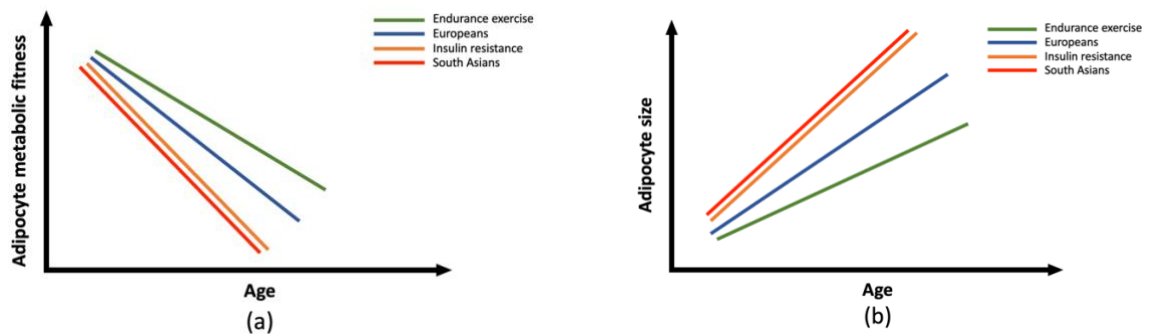
Figure 8-1 Comparative changes in adipocyte fitness and size with age.

This illustrative figure demonstrates the putative changes in (a) metabolic fitness and (b) size of adipocytes as individuals age. Different colours represent different groups: blue for healthy European Caucasians, green for physically active European Caucasians, orange for insulin-resistant European Caucasians, and red for South Asians. Note that this is a trend line representation, not based on actual data.

Another interesting finding was that, despite having a similar adipocyte size to healthy individuals and those who engage in long-term exercise, European Caucasians with insulin resistance exhibit differences in the distribution of adipocyte size and metabolic fitness. A notable difference is that insulin-resistant European Caucasians, when compared to healthy individuals of the same age and BMI with similar adipocyte size, have a significantly higher proportion of very large adipocytes. Traditional views suggest that adipocyte size differences are substantial, with large and very large adipocytes often associated with impaired insulin response, increased free fatty acid (FFA) secretion, and decreased adipokine secretion, leading to an imbalance in energy metabolism and making fat tissue more prone to inflammatory reactions that further exacerbate insulin resistance (Stenkula and Erlanson-Albertsson, 2018). However, this thesis found that it may not be average adipocyte size that affects insulin sensitivity, but the presence of very large adipocytes themselves. These giant adipocytes, which accumulate excessive fat, impair normal adipocyte function, resulting in

potentially significant differences in adipocyte function even when average adipocyte size is similar. Therefore, focusing on the distribution of adipocyte size, especially the proportion of very large adipocytes, may provide better insight into adipocyte function.

Chapter 3 also discovered that young and thinner South Asians have similar adipocyte size and gene expression to older and heavier European Caucasians. As shown in Figure 8-1, South Asians, like insulin-resistant European Caucasians, may have older and metabolically unfit adipocytes. Moreover, both South Asians and insulin-resistant European Caucasians store excess energy in very large adipocytes. This adipocyte volume distribution suggests that South Asians may be more susceptible to diabetes, likely due to a direct effect of their adipocytes. Furthermore, like many other studies, Chapter 3 also found that insulin resistance (HOMA-IR) can predict adipocyte differentiation (negatively) and inflammatory response.

In order to further investigate the ethnic differences between South Asians and Caucasians, Chapters 4, 5, and 6 utilized a longitudinal overfeeding study to explore the role of adipocytes in South Asian diabetes risk. These three chapters analysed adipocyte morphology, gene expression and differentiation, and the impact of weight gain.

Chapter 4 initially revealed that, both at baseline and after weight gain, South Asians store more fat in large and very large adipocytes. Compared to Caucasians, South Asians possess more large and very large adipocytes and fewer medium and small adipocytes. These additional medium and small adipocytes may provide Caucasians with greater potential to cope with the stress of weight gain. They can store excess energy brought about by weight gain by recruiting more small and medium adipocytes to become larger ones over a short period of time. This prevents the formation of very large adipocytes, avoiding the production of metabolically unhealthy adipocytes, as mentioned earlier. Moreover, the ability to efficiently recruit smaller-sized adipocytes for fat storage may lower the risk of type 2 diabetes. Impaired maturation of small adipocytes (<50 µm) into fully functional adipocytes results in the deposition of lipids in ectopic sites and leads to insulin resistance (Björntorp, 1990, Heilbronn *et al.*, 2004, DeFronzo, 2004, Salans and Dougherty, 1971). South Asians, on the other hand, store more fat in

large and very large adipocytes due to their reduced ability to mobilize small adipocytes. Consequently, they produce more very large adipocytes, which, as previously mentioned, may cause T2DM and insulin resistance. However, whether this morphological difference in adipocytes is indeed related to their functionality requires further substantiation, which is the focus of Chapter 5.

Chapter 5 investigated the differences in adipocyte gene expression between South Asians and Caucasians at baseline and after weight gain. The study first identified significant differences in overall gene expression between South Asian and Caucasian adipocytes. Furthermore, this overall difference indicated that South Asian adipocytes are more metabolically unhealthy compared to those of Caucasians. In both baseline and post-weight gain conditions, South Asian adipocytes exhibit lower levels of genes related to insulin sensitivity, fat oxidation, and lipid turnover than Caucasians. Weight gain further reduced the expression of these genes, suggesting that South Asian adipocytes may be less insulin sensitive and less efficient at fat utilization than those of Caucasians. At the same time, South Asian adipocytes express more genes related to lipid storage and inflammatory response. This may contribute to the development of larger adipocytes and earlier onset of inflammation and insulin resistance in South Asians compared to Caucasians. The study also discovered an interaction in the expression of APOE, where South Asians exhibit lower levels at baseline and a more significant decrease than Caucasians after weight gain. Furthermore, South Asians have larger adipocyte but lower APOE which decline on WG - that would suggest a negative relationship between APOE and adipocyte size. The distinct variations in APOE expression between South Asian and Caucasian adipocytes upon weight gain may explain the predisposition of South Asians to adipocyte hypertrophy and suppressed lipid oxidation and turnover. This may account for the increased susceptibility of South Asians to insulin resistance and T2DM compared to Caucasians (Huang *et al.*, 2009b, Huang *et al.*, 2006). In addition, this chapter identified a positive correlation between the expression of certain genes (*TNF* and *LEP*) in adipocytes and adipocyte size. However, whether this positive correlation an inherent difference, and whether it is related to adipocyte differentiation and maturation, still requires validation. No significant differences were found in the expression of genes related to cell differentiation in mature adipocytes, which does not answer the earlier question of why South Asians have

fewer small adipocytes. This difference may be related to the differentiation of MSCs into adipocytes and the maturation of adipocytes. Therefore, Chapter 6 further explored the differences in adipocyte differentiation between South Asians and Caucasians.

This study successfully stimulated the *in vitro* differentiation of adipocytes, i.e., the pathway from MSCs to mature adipocytes. The success of adipocyte differentiation is confirmed from three aspects: adipocyte morphology, lipid accumulation, and gene expression. The differentiation of adipocytes was successfully introduced to our group and the institution (ICAMS) from Prof. Ulf Smith's laboratory. Chapter 6 first analysed the proliferation of MSCs *in vitro*. It revealed a connection between the expression of *SREBF1* in adipocytes and the proliferation capacity of MSCs. That is, when mature adipocytes undergo hypertrophic growth by expressing lipid storage genes, they no longer need to store excess energy through proliferation. However, due to the limited sample size, this study did not identify any significant ethnic differences in the *in vitro* differentiation of MSCs to adipocytes. Although analysis of adipocyte markers and the expression of differentiation-promoting and inhibiting genes suggest that South Asian adipocyte differentiation capacity is weaker than that of Caucasians, no statistically significant results were obtained due to a lack of power. Nevertheless, this study still recommends that future research can consider *in vitro* adipocyte differentiation as a direction for investigating adipocytes in diabetes research. To a large extent, it may influence, or even determine, whether adipocytes store excess energy through hypertrophy or hyperplasia, thereby affecting the risk of insulin resistance and T2DM.

After investigating the functions of adipocytes, in the final experimental chapter, this study attempted to understand how adipose tissue communicates with other tissues through EVs. In collaboration with Dr. Carlos Salomon from Brisbane, this study successfully extracted EVs from serum and measured their size and concentration. Through a mixed meal experiment, for the first time, it was discovered that both the concentration and size of EVs increased postprandially, reaching a peak at two hours and subsequently declining. Six hours later, the size of EVs returned to that of the fasting state, while the concentration decreased to a slightly lower level than in the fasting state. The changes in EV concentration and size in response to food intake were similar in both men and women. This

study is the first to suggest that fasting may be required for standardisation of plasma EV measurement in EV research. This finding fills a gap in EV research regarding whether fasting or post prandial collection should be used in studies. Subsequently, this study successfully extracted RNA from EVs and carried out miRNA sequencing. However, due to the low content and limited variety of miRNAs, as well as the experiment involving only two time points from seven individuals, no effective analysis could be conducted even after attempting to apply standard processing to the results. Nonetheless, despite the inability to successfully analyse the miRNA contents of EVs with statistical significance, this study provides valuable insights into the field and lays the groundwork for future research in understanding the role of EVs in inter-tissue communication.

8.2 Implications for future studies

In this study, various measurements and experiments were conducted on mature cells and MSCs isolated from subcutaneous adipose tissue (SAT), including cell size, gene expression, and *in vitro* stimulation of adipocyte differentiation, to explore the role of adipose tissue in the development of diabetes and insulin resistance. While the study found that age and ethnicity may influence adipocyte size and metabolic fitness, long-term exercise can mitigate these changes. The distribution of adipocytes, particularly the increase in large adipocytes and the decrease in small to medium-sized adipocytes may be a reflection of adipocyte hypertrophy. This hypertrophy could potentially lead to insulin resistance and T2DM. However, the study did not successfully explain the reason for this difference through adipocyte differentiation experiments. The relationship between MSC proliferation and ethnicity, and the nature of this relationship, warrants future investigation.

In future research, further exploration of MSC proliferation and differentiation in adipose tissue, as well as the maturation of small and medium-sized adipocytes, will be an interesting area of study. These data will help expand our understanding of adipose tissue function, especially the causes of adipocyte hypertrophy and hyperplasia. Moreover, the role of large adipocytes in diabetes development also deserves further investigation. The emergence of large adipocytes is directly related to the metabolic unhealthiness of adipocytes. However, the reasons for their emergence, as well as the differences in gene expression between large

adipocytes and healthy large adipocytes, could potentially be investigated through size exclusion in the future. Interestingly, the presence of large adipocytes in adipose tissue of healthy lean South Asians also warrants further exploration. This could be one of the main reasons why South Asians develop diabetes earlier and at a lower BMI compared to Caucasians.

Exercise has a positive effect on adipocyte function, not just limited to muscle and the cardiovascular system. However, how exercise improves adipocyte function and gene expression still warrants further investigation. In particular, the crosstalk between skeletal muscle and adipose tissue will be an interesting area of study. How exercise affects adipose tissue through skeletal muscle activity, the medium through which this occurs, and whether EVs are involved, are questions that need to be addressed. These studies will fill gaps in the field of exercise science.

Furthermore, although this study did not provide significant results confirming the impact of food intake on EV function, it is worth considering that changes in EV size and concentration may be related to function. Whether changes in EV size and concentration after eating are related to EV function and content remains to be determined. The origin of these EVs, the reason for the decrease in EV concentration six hours after eating, and the relationship between EV size, concentration, and function are all important questions for future research. The source of blood EVs, particularly postprandial EVs, could be helpful for diabetes and cardiovascular-related research and may expand our understanding of these fields.

List of References

ABDUL-WAHED, A., GAUTIER-STEIN, A., CASTERAS, S., SOTY, M., ROUSSEL, D., *et al.* 2014. A link between hepatic glucose production and peripheral energy metabolism via hepatokines. *Molecular metabolism,* 3**,** 531-543.

ABDULLAHI, A., CHEN, P., STANOJCIC, M., SADRI, A. R., COBURN, N., *et al.* 2017. IL-6 Signal From the Bone Marrow is Required for the Browning of White Adipose Tissue Post Burn Injury. *Shock,* 47**,** 33-39.

ABOU-EZZI, G., SUPAKORNDEJ, T., ZHANG, J., ANTHONY, B., KRAMBS, J., *et al.* 2019. TGF-β Signaling Plays an Essential Role in the Lineage Specification of Mesenchymal Stem/Progenitor Cells in Fetal Bone Marrow. *Stem Cell Reports,* 13**,** 48-60.

ABREU-VIEIRA, G., FISCHER, A. W., MATTSSON, C., DE JONG, J. M., SHABALINA, I. G., *et al.* 2015. Cidea improves the metabolic profile through expansion of adipose tissue. *Nat Commun,* 6**,** 7433.

ACOSTA, J. R., DOUAGI, I., ANDERSSON, D. P., BÄCKDAHL, J., RYDÉN, M., *et al.* 2016. Increased fat cell size: a major phenotype of subcutaneous white adipose tissue in non-obese individuals with type 2 diabetes. *Diabetologia,* 59**,** 560-570.

AFRISHAM, R., SADEGH-NEJADI, S., MESHKANI, R., EMAMGHOLIPOUR, S. & PAKNEJAD, M. 2020. Effect of circulating exosomes derived from normal-weight and obese women on gluconeogenesis, glycogenesis, lipogenesis and secretion of FGF21 and fetuin A in HepG2 cells. *Diabetology & Metabolic Syndrome,* 12**,** 32.

AHRENS, M., ANKENBAUER, T., SCHRÖDER, D., HOLLNAGEL, A., MAYER, H., *et al.* 1993. Expression of human bone morphogenetic proteins-2 or -4 in murine mesenchymal progenitor C3H10T1/2 cells induces differentiation into distinct mesenchymal cell lineages. *DNA Cell Biol,* 12**,** 871-80.

AHUJA, V., KADOWAKI, T., EVANS, R. W., KADOTA, A., OKAMURA, T., *et al.* 2015. Comparison of HOMA-IR, HOMA-β% and disposition index between US white men and Japanese men in Japan: the ERA JUMP study. *Diabetologia,* 58**,** 265-71.

AJJAN, R., CARTER, A. M., SOMANI, R., KAIN, K. & GRANT, P. J. 2007. Ethnic differences in cardiovascular risk factors in healthy Caucasian and South Asian individuals with the metabolic syndrome. *J Thromb Haemost,* 5**,** 754-60.

ALIBHAI, F. J., LIM, F., YEGANEH, A., DISTEFANO, P. V., BINESH-MARVASTI, T., *et al.* 2020. Cellular senescence contributes to age-dependent changes in circulating extracellular vesicle cargo and function. *Aging cell,* 19**,** e13103-e13103.

ALVAREZ, M. S., FERNANDEZ-ALVAREZ, A., CUCARELLA, C. & CASADO, M. 2014. Stable SREBP-1a knockdown decreases the cell proliferation rate in human preadipocyte cells without inducing senescence. *Biochem Biophys Res Commun,* 447**,** 51-6.

AMERES, S. L., MARTINEZ, J. & SCHROEDER, R. 2007. Molecular Basis for Target RNA Recognition and Cleavage by Human RISC. *Cell,* 130**,** 101-112.

AMERICAN THORACIC SOCIETY 2003. ATS/ACCP Statement on cardiopulmonary exercise testing. *Am J Respir Crit Care Med,* 167**,** 211-77.

AMOSSE, J., DURCIN, M., MALLOCI, M., VERGORI, L., FLEURY, A., *et al.* 2018. Phenotyping of circulating extracellular vesicles (EVs) in obesity identifies large EVs as functional conveyors of Macrophage Migration Inhibitory Factor. *Molecular Metabolism,* 18**,** 134-142.

ANAND, S. S., TARNOPOLSKY, M. A., RASHID, S., SCHULZE, K. M., DESAI, D., *et al.* 2011. Adipocyte hypertrophy, fatty liver and metabolic risk factors in South Asians: the Molecular Study of Health and Risk in Ethnic Groups (mol-SHARE). *PLoS One,* 6**,** e22112.

ANDERSSON, D. P., ARNER, E., HOGLING, D. E., RYDÉN, M. & ARNER, P. 2017. Abdominal subcutaneous adipose tissue cellularity in men and women. *Int J Obes (Lond),* 41**,** 1564-1569.

ANDERSSON, D. P., ERIKSSON HOGLING, D., THORELL, A., TOFT, E., QVISTH, V., *et al.* 2014. Changes in subcutaneous fat cell volume and insulin sensitivity after weight loss. *Diabetes Care,* 37**,** 1831-6.

ANSTEY, K. J., CHERBUIN, N., BUDGE, M. & YOUNG, J. 2011. Body mass index in midlife and late-life as a risk factor for dementia: a meta-analysis of prospective studies. *Obes Rev,* 12**,** e426-37.

ANTUNES, B. M., ROSA-NETO, J. C., BATATINHA, H. A. P., FRANCHINI, E., TEIXEIRA, A. M., *et al.* 2020. Physical fitness status modulates the inflammatory proteins in peripheral blood and circulating monocytes: role of PPAR-gamma. *Sci Rep,* 10**,** 14094.

ARFAI, K., PITUKCHEEWANONT, P. D., GORAN, M. I., TAVARE, C. J., HELLER, L., *et al.* 2002. Bone, muscle, and fat: sex-related differences in prepubertal children. *Radiology,* 224**,** 338-44.

ARNER, E., RYDÉN, M. & ARNER, P. 2010a. Tumor Necrosis Factor α and Regulation of Adipose Tissue. *New England Journal of Medicine,* 362**,** 1151-1153.

ARNER, E., WESTERMARK, P. O., SPALDING, K. L., BRITTON, T., RYDÉN, M., *et al.* 2010b. Adipocyte turnover: relevance to human adipose tissue morphology. *Diabetes,* 59**,** 105-9.

ARNER, E., WESTERMARK, P. O., SPALDING, K. L., BRITTON, T., RYDÉN, M., *et al.* 2010c. Adipocyte Turnover: Relevance to Human Adipose Tissue Morphology. *Diabetes,* 59**,** 105.

ARNER, P., MARCUS, C., KARPE, B., SONNENFELD, T. & BLOME, P. 1987. Role of alpha-adrenoceptors for adipocyte size in man. *Eur J Clin Invest,* 17**,** 58-62.

ARNER, P. & SPALDING, K. L. 2010. Fat cell turnover in humans. *Biochem Biophys Res Commun,* 396**,** 101-4.

ASTRUP, A., BÜLOW, J., CHRISTENSEN, N. J. & MADSEN, J. 1984. Ephedrine-Induced Thermogenesis in Man: No Role for Interscapular Brown Adipose Tissue. *Clinical Science,* 66**,** 179-186.

BABST, M., KATZMANN, D. J., ESTEPA-SABAL, E. J., MEERLOO, T. & EMR, S. D. 2002. Escrt-III: an endosome-associated heterooligomeric protein complex required for mvb sorting. *Dev Cell,* 3**,** 271-82.

BAGCHI, D. P. & MACDOUGALD, O. A. 2021. Wnt Signaling: From Mesenchymal Cell Fate to Lipogenesis and Other Mature Adipocyte Functions. *Diabetes,* 70**,** 1419-1430.

BAGCHI, D. P., NISHII, A., LI, Z., DELPROPOSTO, J. B., CORSA, C. A., *et al.* 2020. Wnt/β-catenin signaling regulates adipose tissue lipogenesis and adipocyte-specific loss is rigorously defended by neighboring stromal-vascular cells. *Mol Metab,* 42**,** 101078.

BALAJ, L., LESSARD, R., DAI, L., CHO, Y.-J., POMEROY, S. L., *et al.* 2011. Tumour microvesicles contain retrotransposon elements and amplified oncogene sequences. *Nature Communications,* 2**,** 180.

BALAKRISHNAN, P., GRUNDY, S. M., ISLAM, A., DUNN, F. & VEGA, G. L. 2012. Influence of upper and lower body adipose tissue on insulin sensitivity in South Asian men. *J Investig Med,* 60**,** 999-1004.

BAMBACE, C., TELESCA, M., ZOICO, E., SEPE, A., OLIOSO, D., *et al.* 2011. Adiponectin gene expression and adipocyte diameter: a comparison between epicardial and subcutaneous adipose tissue in men. *Cardiovasc Pathol,* 20**,** e153-6.

BARTEL, D. P. 2004. MicroRNAs: Genomics, Biogenesis, Mechanism, and Function. *Cell,* 116**,** 281-297.

BARWELL, N. D., MALKOVA, D., LEGGATE, M. & GILL, J. M. 2009. Individual responsiveness to exercise-induced fat loss is associated with change in resting substrate utilization. *Metabolism,* 58**,** 1320-8.

BECNEL, L. B., OCHSNER, S. A., DARLINGTON, Y. F., MCOWITI, A., KANKANAMGE, W. H., *et al.* 2017. Discovering relationships between nuclear receptor signaling pathways, genes, and tissues in Transcriptomine. *Science Signaling,* 10**,** eaah6275.

BEDOGNI, G., GASTALDELLI, A., MANCO, M., DE COL, A., AGOSTI, F., *et al.* 2012. Relationship between fatty liver and glucose metabolism: a cross-sectional study in 571 obese children. *Nutr Metab Cardiovasc Dis,* 22**,** 120-6.

BELLINGHAM, S. A., COLEMAN, B. M. & HILL, A. F. 2012. Small RNA deep sequencing reveals a distinct miRNA signature released in exosomes from prion-infected neuronal cells. *Nucleic Acids Res,* 40**,** 10937-49.

BELLOU, V., BELBASIS, L., TZOULAKI, I. & EVANGELOU, E. 2018. Risk factors for type 2 diabetes mellitus: An exposure-wide umbrella review of meta-analyses. *PLoS One,* 13**,** e0194127.

BERG, J., TYMOCZKO, J. & STRYER, L. 2002. Glycogen Breakdown and Synthesis Are Reciprocally Regulated. *Biochemistry.* New York: W H Freeman.

BERMAN, D. M., NICKLAS, B. J., RYAN, A. S., ROGUS, E. M., DENNIS, K. E., *et al.* 2004. Regulation of lipolysis and lipoprotein lipase after weight loss in obese, postmenopausal women. *Obes Res,* 12**,** 32-9.

BIDULESCU, A., DINH, P. C., SARWARY, S., FORSYTH, E., LUETKE, M. C., *et al.* 2020. Associations of leptin and adiponectin with incident type 2 diabetes and interactions among African Americans: the Jackson heart study. *BMC Endocrine Disorders,* 20**,** 31.

BJÖRNTORP, P. 1990. "Portal" adipose tissue as a generator of risk factors for cardiovascular disease and diabetes. *Arteriosclerosis,* 10**,** 493-6.

BJÖRNTORP, P., KARLSSON, M., PERTOFT, H., PETTERSSON, P., SJÖSTRÖM, L., *et al.* 1978. Isolation and characterization of cells from rat adipose tissue developing into adipocytes. *Journal of Lipid Research,* 19**,** 316-324.

BLAIR, S. N., KAMPERT, J. B., KOHL, H. W., III, BARLOW, C. E., MACERA, C. A., *et al.* 1996. Influences of Cardiorespiratory Fitness and Other Precursors on Cardiovascular Disease and All-Cause Mortality in Men and Women. *JAMA,* 276**,** 205-210.

BLÜHER, M., BULLEN, J. W., JR., LEE, J. H., KRALISCH, S., FASSHAUER, M., *et al.* 2006. Circulating Adiponectin and Expression of Adiponectin Receptors in Human Skeletal Muscle:

Associations with Metabolic Parameters and Insulin Resistance and Regulation by Physical Training. *The Journal of Clinical Endocrinology & Metabolism,* 91**,** 2310-2316.

BLÜHER, M., MICHAEL, M. D., PERONI, O. D., UEKI, K., CARTER, N., *et al.* 2002. Adipose Tissue Selective Insulin Receptor Knockout Protects against Obesity and Obesity-Related Glucose Intolerance. *Developmental Cell,* 3**,** 25-38.

BODEN, G., CHEN, X., RUIZ, J., WHITE, J. V. & ROSSETTI, L. 1994. Mechanisms of fatty acid-induced inhibition of glucose uptake. *J Clin Invest,* 93**,** 2438-46.

BODEN, G., LEBED, B., SCHATZ, M., HOMKO, C. & LEMIEUX, S. 2001. Effects of Acute Changes of Plasma Free Fatty Acids on Intramyocellular Fat Content and Insulin Resistance in Healthy Subjects. *Diabetes,* 50**,** 1612-1617.

BODICOAT, D. H., GRAY, L. J., HENSON, J., WEBB, D., GURU, A., *et al.* 2014. Body mass index and waist circumference cut-points in multi-ethnic populations from the UK and India: the ADDITION-Leicester, Jaipur heart watch and New Delhi cross-sectional studies. *PLoS One,* 9**,** e90813.

BOLAND, B. B., RHODES, C. J. & GRIMSBY, J. S. 2017. The dynamic plasticity of insulin production in β-cells. *Molecular metabolism,* 6**,** 958-973.

BONAFEDE, R., SCAMBI, I., PERONI, D., POTRICH, V., BOSCHI, F., *et al.* 2016. Exosome derived from murine adipose-derived stromal cells: Neuroprotective effect on in vitro model of amyotrophic lateral sclerosis. *Exp Cell Res,* 340**,** 150-8.

BORGES, F. T., REIS, L. A. & SCHOR, N. 2013. Extracellular vesicles: structure, function, and potential clinical uses in renal diseases. *Braz J Med Biol Res,* 46**,** 824-30.

BOSMA, M., HESSELINK, M. K., SPARKS, L. M., TIMMERS, S., FERRAZ, M. J., *et al.* 2012. Perilipin 2 improves insulin sensitivity in skeletal muscle despite elevated intramuscular lipid levels. *Diabetes,* 61**,** 2679-90.

BOSTRÖM, P., WU, J., JEDRYCHOWSKI, M. P., KORDE, A., YE, L., *et al.* 2012. A PGC1-α-dependent myokine that drives brown-fat-like development of white fat and thermogenesis. *Nature,* 481**,** 463-468.

BOWERS, R. R., KIM, J. W., OTTO, T. C. & LANE, M. D. 2006. Stable stem cell commitment to the adipocyte lineage by inhibition of DNA methylation: role of the BMP-4 gene. *Proc Natl Acad Sci U S A,* 103**,** 13022-7.

BOYERINAS, B., PARK, S.-M., HAU, A., MURMANN, A. E. & PETER, M. E. 2010. The role of let-7 in cell differentiation and cancer. *Endocrine-Related Cancer,* 17**,** F19-F36.

BREDELLA, M. A., KARASTERGIOU, K., BOS, S. A., GERWECK, A. V., TORRIANI, M., *et al.* 2017. GH administration decreases subcutaneous abdominal adipocyte size in men with abdominal obesity. *Growth Horm IGF Res,* 35**,** 17-20.

BREHM, A., KRSSAK, M., SCHMID, A. I., NOWOTNY, P., WALDHÄUSL, W., *et al.* 2006. Increased Lipid Availability Impairs Insulin-Stimulated ATP Synthesis in Human Skeletal Muscle. *Diabetes,* 55**,** 136-140.

BRENNAN, K., MARTIN, K., FITZGERALD, S. P., O'SULLIVAN, J., WU, Y., *et al.* 2020. A comparison of methods for the isolation and separation of extracellular vesicles from protein and lipid particles in human serum. *Scientific Reports,* 10**,** 1039.

BROWN, L. M. & CLEGG, D. J. 2010. Central effects of estradiol in the regulation of food intake, body weight, and adiposity. *The Journal of steroid biochemistry and molecular biology,* 122**,** 65-73.

BUNGAU, S., BEHL, T., TIT, D. M., BANICA, F., BRATU, O. G., *et al.* 2020. Interactions between leptin and insulin resistance in patients with prediabetes, with and without NAFLD. *Exp Ther Med,* 20**,** 197.

BUNNEY, P. E., ZINK, A. N., HOLM, A. A., BILLINGTON, C. J. & KOTZ, C. M. 2017. Orexin activation counteracts decreases in nonexercise activity thermogenesis (NEAT) caused by high-fat diet. *Physiology & behavior,* 176**,** 139-148.

BURDI, A. R., POISSONNET, C. M., GARN, S. M., LAVELLE, M., SABET, M. D., *et al.* 1985. Adipose tissue growth patterns during human gestation: a histometric comparison of buccal and gluteal fat depots. *Int J Obes,* 9**,** 247-56.

BURKS, D. J. & WHITE, M. F. 2001. IRS proteins and beta-cell function. *Diabetes,* 50 Suppl 1**,** S140-5.

BURTON, F. L., MALKOVA, D., CASLAKE, M. J. & GILL, J. M. 2008. Energy replacement attenuates the effects of prior moderate exercise on postprandial metabolism in overweight/obese men. *Int J Obes (Lond),* 32**,** 481-9.

BUSCHOW, S. I., VAN BALKOM, B. W., AALBERTS, M., HECK, A. J., WAUBEN, M., *et al.* 2010. MHC class II-associated proteins in B-cell exosomes and potential functional implications for exosome biogenesis. *Immunol Cell Biol,* 88**,** 851-6.

CAMHI, S. M., BRAY, G. A., BOUCHARD, C., GREENWAY, F. L., JOHNSON, W. D., *et al.* 2011. The relationship of waist circumference and BMI to visceral, subcutaneous, and total body fat: sex and race differences. *Obesity (Silver Spring),* 19**,** 402-8.

CAMPELLO, E., ZABEO, E., RADU, C. M., SPIEZIA, L., FOLETTO, M., *et al.* 2016. Dynamics of circulating microparticles in obesity after weight loss. *Intern Emerg Med,* 11**,** 695-702.

CANNON, B. & NEDERGAARD, J. 2004. Brown Adipose Tissue: Function and Physiological Significance. *Physiological Reviews,* 84**,** 277-359.

CAO, Z., UMEK, R. M. & MCKNIGHT, S. L. 1991. Regulated expression of three C/EBP isoforms during adipose conversion of 3T3-L1 cells. *Genes Dev,* 5**,** 1538-52.

CAPLAN, A. I. 1991. Mesenchymal stem cells. *J Orthop Res,* 9**,** 641-50.

CARMELLI, D., MCELROY, M. R. & ROSENMAN, R. H. 1991. Longitudinal changes in fat distribution in the Western Collaborative Group Study: a 23-year follow-up. *Int J Obes,* 15**,** 67-74.

CARMICHAEL, R. E., WILKINSON, K. A. & CRAIG, T. J. 2019. Insulin-dependent GLUT4 trafficking is not regulated by protein SUMOylation in L6 myocytes. *Scientific Reports,* 9**,** 6477.

CARROLL, J. F., CHIAPA, A. L., RODRIQUEZ, M., PHELPS, D. R., CARDARELLI, K. M., *et al.* 2008. Visceral Fat, Waist Circumference, and BMI: Impact of Race/ethnicity. *Obesity,* 16**,** 600-607.

CASO, G., MCNURLAN, M. A., MILEVA, I., ZEMLYAK, A., MYNARCIK, D. C., *et al.* 2013. Peripheral fat loss and decline in adipogenesis in older humans. *Metabolism,* 62**,** 337-340.

CAWTHORN, W. P., BREE, A. J., YAO, Y., DU, B., HEMATI, N., *et al.* 2012a. Wnt6, Wnt10a and Wnt10b inhibit adipogenesis and stimulate osteoblastogenesis through a β-catenin-dependent mechanism. *Bone,* 50**,** 477-489.

CAWTHORN, W. P., SCHELLER, E. L. & MACDOUGALD, O. A. 2012b. Adipose tissue stem cells meet preadipocyte commitment: going back to the future. *J Lipid Res,* 53**,** 227-46.

CAWTHORN, W. P. & SETHI, J. K. 2008. TNF-alpha and adipocyte biology. *FEBS Lett,* 582**,** 117-31.

CELIS-MORALES, C. A., LYALL, D. M., ANDERSON, J., ILIODROMITI, S., FAN, Y., *et al.* 2017. The association between physical activity and risk of mortality is modulated by grip strength and cardiorespiratory fitness: evidence from 498 135 UK-Biobank participants. *Eur Heart J,* 38**,** 116-122.

CENTERS FOR DISEASE CONTROL AND PREVENTION 2011. National diabetes fact sheet: national estimates and general information on diabetes and prediabetes in the United States, 2011.

CERF, M. E. 2013. Beta cell dysfunction and insulin resistance. *Frontiers in endocrinology,* 4**,** 37-37.

CHALKIADAKI, A. & GUARENTE, L. 2012. High-fat diet triggers inflammation-induced cleavage of SIRT1 in adipose tissue to promote metabolic dysfunction. *Cell Metab,* 16**,** 180-8.

CHAMBERS, J. C., LOH, M., LEHNE, B., DRONG, A., KRIEBEL, J., *et al.* 2015. Epigenome-wide association of DNA methylation markers in peripheral blood from Indian Asians and Europeans with incident type 2 diabetes: a nested case-control study. *The Lancet Diabetes & Endocrinology,* 3**,** 526-534.

CHANDALIA, M., LIN, P., SEENIVASAN, T., LIVINGSTON, E. H., SNELL, P. G., *et al.* 2007. Insulin resistance and body fat distribution in South Asian men compared to Caucasian men. *PLoS One,* 2**,** e812.

CHEN, L. K., LIN, M. H., CHEN, Z. J., HWANG, S. J. & CHIOU, S. T. 2006. Association of insulin resistance and hematologic parameters: study of a middle-aged and elderly Chinese population in Taiwan. *J Chin Med Assoc,* 69**,** 248-53.

CHEN, Y., HE, D., YANG, T., ZHOU, H., XIANG, S., *et al.* 2020. Relationship between body composition indicators and risk of type 2 diabetes mellitus in Chinese adults. *BMC Public Health,* 20**,** 452.

CHETTIMADA, S., LORENZ, D. R., MISRA, V., WOLINSKY, S. M. & GABUZDA, D. 2020. Small RNA sequencing of extracellular vesicles identifies circulating miRNAs related to inflammation and oxidative stress in HIV patients. *BMC Immunology,* 21**,** 57.

CHIRSHEV, E., OBERG, K. C., IOFFE, Y. J. & UNTERNAEHRER, J. J. 2019. Let-7 as biomarker, prognostic indicator, and therapy for precision medicine in cancer. *Clin Transl Med,* 8**,** 24.

CHOY, L. & DERYNCK, R. 2003. Transforming growth factor-beta inhibits adipocyte differentiation by Smad3 interacting with CCAAT/enhancer-binding protein (C/EBP) and repressing C/EBP transactivation function. *J Biol Chem,* 278**,** 9609-19.

CHRISTIANSON, H. C., SVENSSON, K. J., VAN KUPPEVELT, T. H., LI, J.-P. & BELTING, M. 2013. Cancer cell exosomes depend on cell-surface heparan sulfate proteoglycans for their internalization and functional activity. *Proceedings of the National Academy of Sciences,* 110**,** 17380-17385.

CIGNARELLI, A., GENCHI, V. A., PERRINI, S., NATALICCHIO, A., LAVIOLA, L., *et al.* 2019. Insulin and Insulin Receptors in Adipose Tissue Development. *Int J Mol Sci,* 20.

CIRILLO, E., PARNELL, L. D. & EVELO, C. T. 2017. A Review of Pathway-Based Analysis Tools That Visualize Genetic Variants. *Front Genet,* 8**,** 174.

CLEMENTE-POSTIGO, M., QUEIPO-ORTUNO, M. I., FERNANDEZ-GARCIA, D., GOMEZ-HUELGAS, R., TINAHONES, F. J., *et al.* 2011. Adipose tissue gene expression of factors related to lipid processing in obesity. *PLoS One,* 6, e24783.

CLEVERS, H. 2006. Wnt/beta-catenin signaling in development and disease. *Cell,* 127, 469-80.

COELHO, M., OLIVEIRA, T. & FERNANDES, R. 2013. Biochemistry of adipose tissue: an endocrine organ. *Archives of medical science: AMS,* 9, 191-200.

COIMBRA, S., BRANDÃO PROENÇA, J., SANTOS-SILVA, A. & NEUPARTH, M. J. 2014. Adiponectin, leptin, and chemerin in elderly patients with type 2 diabetes mellitus: a close linkage with obesity and length of the disease. *Biomed Res Int,* 2014, 701915.

COLLELUORI, G., AGUIRRE, L. E., QUALLS, C., CHEN, R., NAPOLI, N., *et al.* 2018. Adipocytes ESR1 Expression, Body Fat and Response to Testosterone Therapy in Hypogonadal Men Vary According to Estradiol Levels. *Nutrients,* 10.

CONSIDINE, R. V., SINHA, M. K., HEIMAN, M. L., KRIAUCIUNAS, A., STEPHENS, T. W., *et al.* 1996. Serum immunoreactive-leptin concentrations in normal-weight and obese humans. *N Engl J Med,* 334, 292-5.

CORNELIUS, P., MACDOUGALD, O. A. & LANE, M. D. 1994. Regulation of Adipocyte Development. *Annual Review of Nutrition,* 14, 99-129.

COSTA, J. V. & DUARTE, J. S. 2006. [Adipose tissue and adipokines]. *Acta Med Port,* 19, 251-6.

COTILLARD, A., POITOU, C., TORCIVIA, A., BOUILLOT, J. L., DIETRICH, A., *et al.* 2014. Adipocyte size threshold matters: link with risk of type 2 diabetes and improved insulin resistance after gastric bypass. *J Clin Endocrinol Metab,* 99, E1466-70.

COUSIN, B., CINTI, S., MORRONI, M., RAIMBAULT, S., RICQUIER, D., *et al.* 1992. Occurrence of brown adipocytes in rat white adipose tissue: molecular and morphological characterization. *J Cell Sci,* 103 (Pt 4), 931-42.

CRAIG, R. & MINDELL, J. 2008. Health survey for England 2006. cardiovascular disease and risk factors in adults.

CRANDALL, D. L., BUSLER, D. E., NOVAK, T. J., WEBER, R. V. & KRAL, J. G. 1998. Identification of estrogen receptor beta RNA in human breast and abdominal subcutaneous adipose tissue. *Biochem Biophys Res Commun,* 248, 523-6.

CREWE, C., ZHU, Y., PASCHOAL, V. A., JOFFIN, N., GHABEN, A. L., *et al.* 2019. SREBP-regulated adipocyte lipogenesis is dependent on substrate availability and redox modulation of mTORC1. *JCI Insight,* 5.

CRISTANCHO, A. G. & LAZAR, M. A. 2011. Forming functional fat: a growing understanding of adipocyte differentiation. *Nat Rev Mol Cell Biol,* 12, 722-34.

CUI, X. B., LUAN, J. N., YE, J. & CHEN, S. Y. 2015. RGC32 deficiency protects against high-fat diet-induced obesity and insulin resistance in mice. *J Endocrinol,* 224, 127-37.

CUTHBERTSON, D. J., STEELE, T., WILDING, J. P., HALFORD, J. C., HARROLD, J. A., *et al.* 2017. What have human experimental overfeeding studies taught us about adipose tissue expansion and susceptibility to obesity and metabolic complications? *Int J Obes (Lond),* 41, 853-865.

DA LUZ, G., FREDERICO, M. J. S., DA SILVA, S., VITTO, M. F., CESCONETTO, P. A., *et al.* 2011. Endurance exercise training ameliorates insulin resistance and reticulum stress in adipose and hepatic tissue in obese rats. *European Journal of Applied Physiology,* 111, 2015-2023.

DE LUCIA ROLFE, E., ONG, K. K., SLEIGH, A., DUNGER, D. B. & NORRIS, S. A. 2015. Abdominal fat depots associated with insulin resistance and metabolic syndrome risk factors in black African young adults. *BMC Public Health,* 15, 1013.

DE MENDONCA, M., ROCHA, K. C., DE SOUSA, É., PEREIRA, B. M. V., OYAMA, L. M., *et al.* 2020. Aerobic exercise training regulates serum extracellular vesicle miRNAs linked to obesity to promote their beneficial effects in mice. *Am J Physiol Endocrinol Metab,* 319, E579-e591.

DECLERCQ, V., D'EON, B. & MCLEOD, R. S. 2015. Fatty acids increase adiponectin secretion through both classical and exosome pathways. *Biochimica et Biophysica Acta (BBA) - Molecular and Cell Biology of Lipids,* 1851, 1123-1133.

DEFRONZO, R. A. 2004. Dysfunctional fat cells, lipotoxicity and type 2 diabetes. *Int J Clin Pract Suppl,* 9-21.

DEMIR, A. K., ŞAHIN, Ş., KAYA, S. U., BÜTÜN, İ., ÇITIL, R., *et al.* 2020. Prevalence of insulin resistance and identifying HOMA1-IR and HOMA2-IR indexes in the Middle Black Sea region of Turkey. *Afr Health Sci,* 20, 277-286.

DENG, Z. B., POLIAKOV, A., HARDY, R. W., CLEMENTS, R., LIU, C., *et al.* 2009. Adipose tissue exosome-like vesicles mediate activation of macrophage-induced insulin resistance. *Diabetes,* 58, 2498-505.

DERYNCK, R. & ZHANG, Y. E. 2003. Smad-dependent and Smad-independent pathways in TGF-β family signalling. *Nature,* 425, 577-584.

DESPRÉS, J.-P., COUILLARD, C., GAGNON, J., BERGERON, J., LEON ARTHUR, S., *et al.* 2000. Race, Visceral Adipose Tissue, Plasma Lipids, and Lipoprotein Lipase Activity in Men and Women. *Arteriosclerosis, Thrombosis, and Vascular Biology,* 20**,** 1932-1938.

DESSELS, C. & PEPPER, M. S. 2019. Reference Gene Expression in Adipose-Derived Stromal Cells Undergoing Adipogenic Differentiation. *Tissue Eng Part C Methods,* 25**,** 353-366.

DEURENBERG, P., DEURENBERG-YAP, M. & GURICCI, S. 2002. Asians are different from Caucasians and from each other in their body mass index/body fat per cent relationship. *Obesity Reviews,* 3**,** 141-146.

DIABETESUK. 2017. *Diabetes Prevalence 2017 (Npvember 2017)* [Online]. Diabetes UK. Available: https://www.diabetes.org.uk/professionals/position-statements-reports/statistics/diabetes-prevalence-2017 [Accessed 12/02 2019].

DIABETESUK 2019. Diabetes prevalence 2019.

DIABETESUK 2021. Diabetes statistics.

DIEZ, J. J. & IGLESIAS, P. 2003. The role of the novel adipocyte-derived hormone adiponectin in human disease. *European Journal of Endocrinology Eur J Endocrinol,* 148**,** 293-300.

DING, Q., GUPTA RAJAT, M., RAGHAVAN, A. & MUSUNURU, K. 2014. Abstract 70: KLF14 is a Novel Regulator of Human Metabolism. *Arteriosclerosis, Thrombosis, and Vascular Biology,* 34**,** A70-A70.

DING, Y.-S., GUO, S.-X., MA, R.-L., LI, S.-G., GUO, H., *et al.* 2015. Association of Metabolic Syndrome with the Adiponectin to Homeostasis Model Assessment of Insulin Resistance Ratio. *Mediators of Inflammation,* 2015**,** 607364.

DOYLE, L. M. & WANG, M. Z. 2019. Overview of Extracellular Vesicles, Their Origin, Composition, Purpose, and Methods for Exosome Isolation and Analysis. *Cells,* 8.

DRARENI, K., BALLAIRE, R., BARILLA, S., MATHEW, M. J., TOUBAL, A., *et al.* 2018. GPS2 Deficiency Triggers Maladaptive White Adipose Tissue Expansion in Obesity via HIF1A Activation. *Cell Rep,* 24**,** 2957-2971 e6.

DROLET, R., RICHARD, C., SNIDERMAN, A. D., MAILLOUX, J., FORTIER, M., *et al.* 2008. Hypertrophy and hyperplasia of abdominal adipose tissues in women. *Int J Obes (Lond),* 32**,** 283-91.

DUBOIS, S. G., HEILBRONN, L. K., SMITH, S. R., ALBU, J. B., KELLEY, D. E., *et al.* 2006. Decreased Expression of Adipogenic Genes in Obese Subjects with Type 2 Diabetes*. *Obesity,* 14**,** 1543-1552.

DUDEJA, V., MISRA, A., PANDEY, R. M., DEVINA, G., KUMAR, G., *et al.* 2001. BMI does not accurately predict overweight in Asian Indians in northern India. *Br J Nutr,* 86**,** 105-12.

DUNCAN, B. B., SCHMIDT, M. I., PANKOW, J. S., BALLANTYNE, C. M., COUPER, D., *et al.* 2003. Low-Grade Systemic Inflammation and the Development of Type 2 Diabetes. *The Atherosclerosis Risk in Communities Study,* 52**,** 1799-1805.

DURRER, C., ROBINSON, E., WAN, Z., MARTINEZ, N., HUMMEL, M. L., *et al.* 2015. Differential Impact of Acute High-Intensity Exercise on Circulating Endothelial Microparticles and Insulin Resistance between Overweight/Obese Males and Females. *PLOS ONE,* 10**,** e0115860.

EASTWOOD, S. V., TILLIN, T., WRIGHT, A., HEASMAN, J., WILLIS, J., *et al.* 2013. Estimation of CT-derived abdominal visceral and subcutaneous adipose tissue depots from anthropometry in Europeans, South Asians and African Caribbeans. *PLoS One,* 8**,** e75085.

ECKEL, N., LI, Y., KUXHAUS, O., STEFAN, N., HU, F. B., *et al.* 2018. Transition from metabolic healthy to unhealthy phenotypes and association with cardiovascular disease risk across BMI categories in 90 257 women (the Nurses' Health Study): 30 year follow-up from a prospective cohort study. *Lancet Diabetes Endocrinol,* 6**,** 714-724.

ECKEL, N., MEIDTNER, K., KALLE-UHLMANN, T., STEFAN, N. & SCHULZE, M. B. 2016. Metabolically healthy obesity and cardiovascular events: A systematic review and meta-analysis. *Eur J Prev Cardiol,* 23**,** 956-66.

EGUCHI, A., LAZIC, M., ARMANDO, A. M., PHILLIPS, S. A., KATEBIAN, R., *et al.* 2016. Circulating adipocyte-derived extracellular vesicles are novel markers of metabolic stress. *J Mol Med (Berl),* 94**,** 1241-1253.

EGUCHI, A., MULYA, A., LAZIC, M., RADHAKRISHNAN, D., BERK, M. P., *et al.* 2015. Microparticles release by adipocytes act as "find-me" signals to promote macrophage migration. *PloS one,* 10**,** e0123110-e0123110.

EHTISHAM, S., CRABTREE, N., CLARK, P., SHAW, N. & BARRETT, T. 2005. Ethnic differences in insulin resistance and body composition in United Kingdom adolescents. *J Clin Endocrinol Metab,* 90**,** 3963-9.

EIRIN, A., RIESTER, S. M., ZHU, X. Y., TANG, H., EVANS, J. M., *et al.* 2014. MicroRNA and mRNA cargo of extracellular vesicles from porcine adipose tissue-derived mesenchymal stem cells. *Gene,* 551**,** 55-64.

ERIKSSON-HOGLING, D., ANDERSSON, D. P., BACKDAHL, J., HOFFSTEDT, J., ROSSNER, S., *et al.* 2015. Adipose tissue morphology predicts improved insulin sensitivity following moderate or pronounced weight loss. *Int J Obes (Lond),* 39**,** 893-8.

ESCOLA, J. M., KLEIJMEER, M. J., STOORVOGEL, W., GRIFFITH, J. M., YOSHIE, O., *et al.* 1998. Selective enrichment of tetraspan proteins on the internal vesicles of multivesicular endosomes and on exosomes secreted by human B-lymphocytes. *J Biol Chem,* 273**,** 20121-7.

ETHERTON, T. D., THOMPSON, E. H. & ALLEN, C. E. 1977. Improved techniques for studies of adipocyte cellularity and metabolism. *Journal of Lipid Research,* 18**,** 552-7.

FANG, L., GUO, F., ZHOU, L., STAHL, R. & GRAMS, J. 2015. The cell size and distribution of adipocytes from subcutaneous and visceral fat is associated with type 2 diabetes mellitus in humans. *Adipocyte,* 4**,** 273-9.

FARINAZZO, A., TURANO, E., MARCONI, S., BISTAFFA, E., BAZZOLI, E., *et al.* 2015. Murine adipose-derived mesenchymal stromal cell vesicles: in vitro clues for neuroprotective and neuroregenerative approaches. *Cytotherapy,* 17**,** 571-8.

FARRELL, S. W., KAMPERT, J. B., KOHL, H. W., 3RD, BARLOW, C. E., MACERA, C. A., *et al.* 1998. Influences of cardiorespiratory fitness levels and other predictors on cardiovascular disease mortality in men. *Med Sci Sports Exerc,* 30**,** 899-905.

FERNANDEZ-TWINN, D. S., ALFARADHI, M. Z., MARTIN-GRONERT, M. S., DUQUE-GUIMARAES, D. E., PIEKARZ, A., *et al.* 2014. Downregulation of IRS-1 in adipose tissue of offspring of obese mice is programmed cell-autonomously through post-transcriptional mechanisms. *Molecular Metabolism,* 3**,** 325-333.

FERRARI, F., BOCK, P., MOTTA, M. & HELAL, L. 2019. Biochemical and Molecular Mechanisms of Glucose Uptake Stimulated by Physical Exercise in Insulin Resistance State: Role of Inflammation. *Arquivos Brasileiros de Cardiologia.*

FERRIS, W. F., NARAN, N. H., CROWTHER, N. J., RHEEDER, P., VAN DER MERWE, L., *et al.* 2005. The relationship between insulin sensitivity and serum adiponectin levels in three population groups. *Horm Metab Res,* 37**,** 695-701.

FINK, R. I., KOLTERMAN, O. G., GRIFFIN, J. & OLEFSKY, J. M. 1983. Mechanisms of Insulin Resistance in Aging. *The Journal of Clinical Investigation,* 71**,** 1523-1535.

FOMON, S. J., HASCHKE, F., ZIEGLER, E. E. & NELSON, S. E. 1982. Body composition of reference children from birth to age 10 years. *Am J Clin Nutr,* 35**,** 1169-75.

FONSECA, V. 2003. Effect of thiazolidinediones on body weight in patients with diabetes mellitus. *Am J Med,* 115 Suppl 8A, 42s-48s.

FRANCO, C., BENGTSSON, B.-A. & JOHANNSSON, G. 2006. The GH/IGF-1 Axis in Obesity: Physiological and Pathological Aspects. *Metabolic syndrome and related disorders,* 4**,** 51-56.

FREDERICH, R. C., HAMANN, A., ANDERSON, S., LÖLLMANN, B., LOWELL, B. B., *et al.* 1995. Leptin levels reflect body lipid content in mice: evidence for diet-induced resistance to leptin action. *Nat Med,* 1**,** 1311-4.

FREEMAN, D. W., NOREN HOOTEN, N., EITAN, E., GREEN, J., MODE, N. A., *et al.* 2018. Altered Extracellular Vesicle Concentration, Cargo, and Function in Diabetes. *Diabetes,* 67**,** 2377-2388.

FRIED, S. K. 2017. Adipocyte size redux. *Obesity (Silver Spring),* 25**,** 15.

FRIESEN, M., HUDAK, C. S., WARREN, C. R., XIA, F. & COWAN, C. A. 2016. Adipocyte insulin receptor activity maintains adipose tissue mass and lifespan. *Biochemical and Biophysical Research Communications,* 476**,** 487-492.

FRYSTYK, J., VESTBO, E., SKJÆRBAEK, C., MOGENSEN, C. E. & ØRSKOV, H. 1995. Free insulin-like growth factors in human obesity. *Metabolism,* 44**,** 37-44.

FU, Z., GILBERT, E. R. & LIU, D. 2013. Regulation of insulin synthesis and secretion and pancreatic Beta-cell dysfunction in diabetes. *Current diabetes reviews,* 9**,** 25-53.

GALICIA-GARCIA, U., BENITO-VICENTE, A., JEBARI, S., LARREA-SEBAL, A., SIDDIQI, H., *et al.* 2020. Pathophysiology of Type 2 Diabetes Mellitus. *International journal of molecular sciences,* 21**,** 6275.

GAO, Y., LI, F., ZHANG, Y., DAI, L., JIANG, H., *et al.* 2013. Silencing of ADIPOQ efficiently suppresses preadipocyte differentiation in porcine. *Cell Physiol Biochem,* 31**,** 452-61.

GAUTIER, A., BONNET, F., DUBOIS, S., MASSART, C., GROSHENY, C., *et al.* 2013. Associations between visceral adipose tissue, inflammation and sex steroid concentrations in men. *Clin Endocrinol (Oxf),* 78**,** 373-8.

GEOGHEGAN, G., SIMCOX, J., SELDIN, M. M., PARNELL, T. J., STUBBEN, C., *et al.* 2019. Targeted deletion of Tcf7l2 in adipocytes promotes adipocyte hypertrophy and impaired glucose metabolism. *Mol Metab,* 24**,** 44-63.

GLAD, C. A. M., SVENSSON, P. A., NYSTROM, F. H., JACOBSON, P., CARLSSON, L. M. S., *et al.* 2019. Expression of GHR and Downstream Signaling Genes in Human Adipose Tissue- Relation to Obesity and Weight Change. *J Clin Endocrinol Metab,* 104**,** 1459-1470.

GÓMEZ-AMBROSI, J., SILVA, C., GALOFRÉ, J. C., ESCALADA, J., SANTOS, S., *et al.* 2011. Body Adiposity and Type 2 Diabetes: Increased Risk With a High Body Fat Percentage Even Having a Normal BMI. *Obesity,* 19**,** 1439-1444.

GONZALES, A. M. & ORLANDO, R. A. 2007. Role of adipocyte-derived lipoprotein lipase in adipocyte hypertrophy. *Nutr Metab (Lond),* 4**,** 22.

GOODPASTER, B. H., HE, J., WATKINS, S. & KELLEY, D. E. 2001. Skeletal Muscle Lipid Content and Insulin Resistance: Evidence for a Paradox in Endurance-Trained Athletes. *The Journal of Clinical Endocrinology & Metabolism,* 86**,** 5755-5761.

GOODYEAR, L. J., GIORGINO, F., SHERMAN, L. A., CAREY, J., SMITH, R. J., *et al.* 1995. Insulin receptor phosphorylation, insulin receptor substrate-1 phosphorylation, and phosphatidylinositol 3-kinase activity are decreased in intact skeletal muscle strips from obese subjects. *J Clin Invest,* 95**,** 2195-204.

GOOSSENS, G. H. 2017a. The Metabolic Phenotype in Obesity: Fat Mass, Body Fat Distribution, and Adipose Tissue Function. *Obesity Facts,* 10**,** 207-215.

GOOSSENS, G. H. 2017b. The Metabolic Phenotype in Obesity: Fat Mass, Body Fat Distribution, and Adipose Tissue Function. *Obes Facts,* 10**,** 207-215.

GORAN, M., FIELDS, D. A., HUNTER, G. R., HERD, S. L. & WEINSIER, R. L. 2000. Total body fat does not influence maximal aerobic capacity. *International Journal of Obesity,* 24**,** 841-848.

GREEN, H. & MEUTH, M. 1974. An established pre-adipose cell line and its differentiation in culture. *Cell,* 3**,** 127-33.

GREGOIRE, F. M., SMAS, C. M. & SUL, H. S. 1998. Understanding Adipocyte Differentiation. *Physiological Reviews,* 78**,** 783-809.

GROOP, L. C., BONADONNA, R. C., DELPRATO, S., RATHEISER, K., ZYCK, K., *et al.* 1989. Glucose and free fatty acid metabolism in non-insulin-dependent diabetes mellitus. Evidence for multiple sites of insulin resistance. *The Journal of clinical investigation,* 84**,** 205-213.

GUESCINI, M., GENEDANI, S., STOCCHI, V. & AGNATI, L. F. 2009. Astrocytes and Glioblastoma cells release exosomes carrying mtDNA. *Journal of Neural Transmission,* 117**,** 1.

GUGERELL, A., KOBER, J., LAUBE, T., WALTER, T., NÜRNBERGER, S., *et al.* 2014. Electrospun poly(ester-Urethane)- and poly(ester-Urethane-Urea) fleeces as promising tissue engineering scaffolds for adipose-derived stem cells. *PLoS One,* 9**,** e90676.

GUILHERME, A., VIRBASIUS, J. V., PURI, V. & CZECH, M. P. 2008. Adipocyte dysfunctions linking obesity to insulin resistance and type 2 diabetes. *Nat Rev Mol Cell Biol,* 9**,** 367-77.

GUPTA, A., GUPTA, V., AGRAWAL, S., NATU, S. M., AGRAWAL, C. G., *et al.* 2010. Association between circulating leptin and insulin resistance, the lipid profile, and metabolic risk factors in North Indian adult women. *Biosci Trends,* 4**,** 325-32.

GURRIARAN-RODRIGUEZ, U., AL-MASSADI, O., ROCA-RIVADA, A., CRUJEIRAS, A. B., GALLEGO, R., *et al.* 2011. Obestatin as a regulator of adipocyte metabolism and adipogenesis. *J Cell Mol Med,* 15**,** 1927-40.

GUSTAFSON, B., HAMMARSTEDT, A., ANDERSSON, C. X. & SMITH, U. 2007. Inflamed adipose tissue: a culprit underlying the metabolic syndrome and atherosclerosis. *Arterioscler Thromb Vasc Biol,* 27**,** 2276-83.

GUSTAFSON, B., HEDJAZIFAR, S., GOGG, S., HAMMARSTEDT, A. & SMITH, U. 2015. Insulin resistance and impaired adipogenesis. *Trends Endocrinol Metab,* 26**,** 193-200.

GUSTAFSON, B., NERSTEDT, A. & SMITH, U. 2019a. Reduced subcutaneous adipogenesis in human hypertrophic obesity is linked to senescent precursor cells. *Nature Communications,* 10**,** 2757.

GUSTAFSON, B., NERSTEDT, A. & SMITH, U. 2019b. Reduced subcutaneous adipogenesis in human hypertrophic obesity is linked to senescent precursor cells. *Nat Commun,* 10**,** 2757.

GUSTAFSON, B. & SMITH, U. 2006. Cytokines promote Wnt signaling and inflammation and impair the normal differentiation and lipid accumulation in 3T3-L1 preadipocytes. *J Biol Chem,* 281**,** 9507-16.

GUSTAFSON, B. & SMITH, U. 2012. The WNT Inhibitor Dickkopf 1 and Bone Morphogenetic Protein 4 Rescue Adipogenesis in Hypertrophic Obesity in Humans. *Diabetes,* 61**,** 1217-1224.

HADA, M., OH, H., PFEIFFER, R. M., FALK, R. T., FAN, S., *et al.* 2019. Relationship of circulating insulin-like growth factor-I and binding proteins 1–7 with mammographic density among women undergoing image-guided diagnostic breast biopsy. *Breast Cancer Research,* 21**,** 81.

HAINES, L., WAN, K. C., LYNN, R., BARRETT, T. G. & SHIELD, J. P. 2007. Rising incidence of type 2 diabetes in children in the U.K. *Diabetes Care,* 30**,** 1097-101.

HALBAN, P. A. 1994. Proinsulin processing in the regulated and the constitutive secretory pathway. *Diabetologia,* 37 Suppl 2**,** S65-72.

HALL, L. M., MORAN, C. N., MILNE, G. R., WILSON, J., MACFARLANE, N. G., *et al.* 2010. Fat oxidation, fitness and skeletal muscle expression of oxidative/lipid metabolism genes in South Asians: implications for insulin resistance? *PLoS One,* 5, e14197.

HALLAKOU, S., DOARÉ, L., FOUFELLE, F., KERGOAT, M., GUERRE-MILLO, M., *et al.* 1997. Pioglitazone induces in vivo adipocyte differentiation in the obese Zucker fa/fa rat. *Diabetes,* 46, 1393-9.

HAMER, M., BELL, J. A., SABIA, S., BATTY, G. D. & KIVIMÄKI, M. 2015. Stability of metabolically healthy obesity over 8 years: the English Longitudinal Study of Ageing. *Eur J Endocrinol,* 173, 703-8.

HAMMARSTEDT, A., GOGG, S., HEDJAZIFAR, S., NERSTEDT, A. & SMITH, U. 2018. Impaired Adipogenesis and Dysfunctional Adipose Tissue in Human Hypertrophic Obesity. *Physiol Rev,* 98, 1911-1941.

HARRIS, R. B. 2014. Direct and indirect effects of leptin on adipocyte metabolism. *Biochim Biophys Acta,* 1842, 414-23.

HAUNER, H., WABITSCH, M. & PFEIFFER, E. F. 1988. Differentiation of adipocyte precursor cells from obese and nonobese adult women and from different adipose tissue sites. *Horm Metab Res Suppl,* 19, 35-9.

HE, Q., GAO, Z., YIN, J., ZHANG, J., YUN, Z., *et al.* 2011. Regulation of HIF-1{alpha} activity in adipose tissue by obesity-associated factors: adipogenesis, insulin, and hypoxia. *American journal of physiology. Endocrinology and metabolism,* 300, E877-E885.

HEBERLE, H., MEIRELLES, G. V., DA SILVA, F. R., TELLES, G. P. & MINGHIM, R. 2015. InteractiVenn: a web-based tool for the analysis of sets through Venn diagrams. *BMC Bioinformatics,* 16, 169.

HEILBRONN, L., SMITH, S. R. & RAVUSSIN, E. 2004. Failure of fat cell proliferation, mitochondrial function and fat oxidation results in ectopic fat storage, insulin resistance and type II diabetes mellitus. *Int J Obes Relat Metab Disord,* 28 Suppl 4, S12-21.

HEINE, P. A., TAYLOR, J. A., IWAMOTO, G. A., LUBAHN, D. B. & COOKE, P. S. 2000. Increased adipose tissue in male and female estrogen receptor-α knockout mice. *Proceedings of the National Academy of Sciences,* 97, 12729-12734.

HELLERSTEIN, M. K. 1999. De novo lipogenesis in humans: metabolic and regulatory aspects. *Eur J Clin Nutr,* 53 Suppl 1, S53-65.

HEMMINGSSON, E. 2021. The unparalleled rise of obesity in China: a call to action. *Int J Obes (Lond),* 45, 921-922.

HENS, W., VISSERS, D., HANSEN, D., PEETERS, S., GIELEN, J., *et al.* 2017. The effect of diet or exercise on ectopic adiposity in children and adolescents with obesity: a systematic review and meta-analysis. *Obesity Reviews,* 18, 1310-1322.

HEPLER, C., VISHVANATH, L. & GUPTA, R. K. 2017. Sorting out adipocyte precursors and their role in physiology and disease. *Genes & Development,* 31, 127-140.

HEYMSFIELD, S. B., GREENBERG, A. S., FUJIOKA, K., DIXON, R. M., KUSHNER, R., *et al.* 1999. Recombinant Leptin for Weight Loss in Obese and Lean AdultsA Randomized, Controlled, Dose-Escalation Trial. *JAMA,* 282, 1568-1575.

HIRSCH, J. & HAN, P. W. 1969. Cellularity of rat adipose tissue: effects of growth, starvation, and obesity. *J Lipid Res,* 10, 77-82.

HODDY, K. K., KROEGER, C. M., TREPANOWSKI, J. F., BARNOSKY, A., BHUTANI, S., *et al.* 2014. Meal timing during alternate day fasting: Impact on body weight and cardiovascular disease risk in obese adults. *Obesity (Silver Spring),* 22, 2524-31.

HOFMANN, S. M., ZHOU, L., PEREZ-TILVE, D., GREER, T., GRANT, E., *et al.* 2007. Adipocyte LDL receptor-related protein-1 expression modulates postprandial lipid transport and glucose homeostasis in mice. *J Clin Invest,* 117, 3271-82.

HØJBJERRE, L., SONNE, M. P., ALIBEGOVIC, A. C., NIELSEN, N. B., DELA, F., *et al.* 2011. Impact of physical inactivity on adipose tissue low-grade inflammation in first-degree relatives of type 2 diabetic patients. *Diabetes care,* 34, 2265-2272.

HONG, S., CHANG, Y., JUNG, H. S., YUN, K. E., SHIN, H., *et al.* 2017. Relative muscle mass and the risk of incident type 2 diabetes: A cohort study. *PLoS One,* 12, e0188650.

HORBER, F. F., ZÜRCHER, R. M., HERREN, H., CRIVELLI, M. A. C., ROBOTTI, G., *et al.* 1986. Altered body fat distribution in patients with glucocorticoid treatment and in patients on long-term dialysis. *The American Journal of Clinical Nutrition,* 43, 758-769.

HOSSAIN, P., KAWAR, B. & EL NAHAS, M. 2007. Obesity and Diabetes in the Developing World — A Growing Challenge. *New England Journal of Medicine,* 356, 213-215.

HOWLEY, E. T., BASSETT, D. R., JR. & WELCH, H. G. 1995. Criteria for maximal oxygen uptake: review and commentary. *Med Sci Sports Exerc,* 27, 1292-301.

HU, F. B., MANSON, J. E., STAMPFER, M. J., COLDITZ, G., LIU, S., *et al.* 2001. Diet, lifestyle, and the risk of type 2 diabetes mellitus in women. *N Engl J Med,* 345, 790-7.

HUANG, H., SONG, T. J., LI, X., HU, L., HE, Q., *et al.* 2009a. BMP signaling pathway is required for commitment of C3H10T1/2 pluripotent stem cells to the adipocyte lineage. *Proc Natl Acad Sci U S A,* 106**,** 12670-5.

HUANG, X., YUAN, T., TSCHANNEN, M., SUN, Z., JACOB, H., *et al.* 2013. Characterization of human plasma-derived exosomal RNAs by deep sequencing. *BMC Genomics,* 14**,** 319.

HUANG, Z. H., MINSHALL, R. D. & MAZZONE, T. 2009b. Mechanism for endogenously expressed ApoE modulation of adipocyte very low density lipoprotein metabolism: role in endocytic and lipase-mediated metabolic pathways. *J Biol Chem,* 284**,** 31512-22.

HUANG, Z. H., REARDON, C. A., GETZ, G. S., MAEDA, N. & MAZZONE, T. 2015. Selective suppression of adipose tissue apoE expression impacts systemic metabolic phenotype and adipose tissue inflammation. *J Lipid Res,* 56**,** 215-26.

HUANG, Z. H., REARDON, C. A. & MAZZONE, T. 2006. Endogenous ApoE expression modulates adipocyte triglyceride content and turnover. *Diabetes,* 55**,** 3394-402.

HUBAL, M. J., NADLER, E. P., FERRANTE, S. C., BARBERIO, M. D., SUH, J. H., *et al.* 2017. Circulating adipocyte-derived exosomal MicroRNAs associated with decreased insulin resistance after gastric bypass. *Obesity (Silver Spring),* 25**,** 102-110.

HUDAK, C. S. & SUL, H. S. 2013. Pref-1, a gatekeeper of adipogenesis. *Front Endocrinol (Lausanne),* 4**,** 79.

HUGHES, V. A., ROUBENOFF, R., WOOD, M., FRONTERA, W. R., EVANS, W. J., *et al.* 2004. Anthropometric assessment of 10-y changes in body composition in the elderly. *Am J Clin Nutr,* 80**,** 475-82.

HUI, X., ZHANG, M., GU, P., LI, K., GAO, Y., *et al.* 2017. Adipocyte SIRT1 controls systemic insulin sensitivity by modulating macrophages in adipose tissue. *EMBO Rep,* 18**,** 645-657.

HUNTER, S. J. & GARVEY, W. T. 1998. Insulin action and insulin resistance: diseases involving defects in insulin receptors, signal transduction, and the glucose transport effector system. *Am J Med,* 105**,** 331-45.

HUTH, C., PIGEON, É., RIOU, M., ST-ONGE, J., ARGUIN, H., *et al.* 2016. Fitness, adiposopathy, and adiposity are independent predictors of insulin sensitivity in middle-aged men without diabetes. *J Physiol Biochem,* 72**,** 435-44.

IBRAHIM, M. M. 2010. Subcutaneous and visceral adipose tissue: structural and functional differences. *Obes Rev,* 11**,** 11-8.

INDULEKHA, K., ANJANA, R. M., SURENDAR, J. & MOHAN, V. 2011. Association of visceral and subcutaneous fat with glucose intolerance, insulin resistance, adipocytokines and inflammatory markers in Asian Indians (CURES-113). *Clin Biochem,* 44**,** 281-7.

IOANNIDOU, A., ALATAR, S., SCHIPPER, R., BAGANHA, F., ÅHLANDER, M., *et al.* 2022. Hypertrophied human adipocyte spheroids as in vitro model of weight gain and adipose tissue dysfunction. *J Physiol,* 600**,** 869-883.

ISAKSON, P., HAMMARSTEDT, A., GUSTAFSON, B. & SMITH, U. 2009. Impaired preadipocyte differentiation in human abdominal obesity: role of Wnt, tumor necrosis factor-alpha, and inflammation. *Diabetes,* 58**,** 1550-7.

ITABE, H., YAMAGUCHI, T., NIMURA, S. & SASABE, N. 2017. Perilipins: a diversity of intracellular lipid droplet proteins. *Lipids Health Dis,* 16**,** 83.

ITO, H., OHSHIMA, A., OHTO, N., OGASAWARA, M., TSUZUKI, M., *et al.* 2001. Relation between body composition and age in healthy Japanese subjects. *European Journal of Clinical Nutrition,* 55**,** 462-470.

JACKSON, A. S., STANFORTH, P. R., GAGNON, J., RANKINEN, T., LEON, A. S., *et al.* 2002. The effect of sex, age and race on estimating percentage body fat from body mass index: The Heritage Family Study. *International Journal of Obesity,* 26**,** 789-796.

JENUM, A. K., BREKKE, I., MDALA, I., MUILWIJK, M., RAMACHANDRAN, A., *et al.* 2019. Effects of dietary and physical activity interventions on the risk of type 2 diabetes in South Asians: meta-analysis of individual participant data from randomised controlled trials. *Diabetologia,* 62**,** 1337-1348.

JO, J., GAVRILOVA, O., PACK, S., JOU, W., MULLEN, S., *et al.* 2009. Hypertrophy and/or Hyperplasia: Dynamics of Adipose Tissue Growth. *PLoS Comput Biol,* 5**,** e1000324.

JOHANNSEN, D. L., TCHOUKALOVA, Y., TAM, C. S., COVINGTON, J. D., XIE, W., *et al.* 2014. Effect of 8 weeks of overfeeding on ectopic fat deposition and insulin sensitivity: testing the "adipose tissue expandability" hypothesis. *Diabetes Care,* 37**,** 2789-97.

JOHNSTON, B. C., KANTERS, S., BANDAYREL, K., WU, P., NAJI, F., *et al.* 2014. Comparison of weight loss among named diet programs in overweight and obese adults: a meta-analysis. *JAMA,* 312**,** 923-33.

KAHLERT, C., MELO, S. A., PROTOPOPOV, A., TANG, J., SETH, S., *et al.* 2014. Identification of double-stranded genomic DNA spanning all chromosomes with mutated KRAS and p53 DNA in the serum exosomes of patients with pancreatic cancer. *J Biol Chem,* 289**,** 3869-75.

KAISANLAHTI, A. & GLUMOFF, T. 2019. Browning of white fat: agents and implications for beige adipose tissue to type 2 diabetes. *Journal of Physiology and Biochemistry,* 75**,** 1-10.

KALRA, S., MERCURI, M. & ANAND, S. S. 2013. Measures of body fat in South Asian adults. *Nutr Diabetes,* 3**,** e69.

KAMINSKY, L. A., ARENA, R. & MYERS, J. 2015. Reference Standards for Cardiorespiratory Fitness Measured With Cardiopulmonary Exercise Testing: Data From the Fitness Registry and the Importance of Exercise National Database. *Mayo Clin Proc,* 90**,** 1515-23.

KANAZAWA, A., TSUKADA, S., KAMIYAMA, M., YANAGIMOTO, T., NAKAJIMA, M., *et al.* 2005. Wnt5b partially inhibits canonical Wnt/beta-catenin signaling pathway and promotes adipogenesis in 3T3-L1 preadipocytes. *Biochem Biophys Res Commun,* 330**,** 505-10.

KANG, T., JONES, T. M., NADDELL, C., BACANAMWO, M., CALVERT, J. W., *et al.* 2016. Adipose-Derived Stem Cells Induce Angiogenesis via Microvesicle Transport of miRNA-31. *Stem Cells Transl Med,* 5**,** 440-50.

KARAM, J. 1997. Pancreatic Hormones and Diabetes Mellitus *In:* FS GREENSPAN, G. S. (ed.) *Basic and Clinical Endocrinology.* Appleton & Lange, Stamford CT USA.

KARPE, F., DICKMANN, J. R. & FRAYN, K. N. 2011. Fatty acids, obesity, and insulin resistance: time for a reevaluation. *Diabetes,* 60**,** 2441-9.

KARPE, F., OLIVECRONA, T., WALLDIUS, G. & HAMSTEN, A. 1992. Lipoprotein lipase in plasma after an oral fat load: relation to free fatty acids. *J Lipid Res,* 33**,** 975-84.

KARTER, A. J., SCHILLINGER, D., ADAMS, A. S., MOFFET, H. H., LIU, J., *et al.* 2013. Elevated rates of diabetes in Pacific Islanders and Asian subgroups: The Diabetes Study of Northern California (DISTANCE). *Diabetes Care,* 36**,** 574-9.

KASHYAP, S. R., GATMAITAN, P., BRETHAUER, S. & SCHAUER, P. 2010. Bariatric surgery for type 2 diabetes: weighing the impact for obese patients. *Cleve Clin J Med,* 77**,** 468-76.

KATSUDA, T., TSUCHIYA, R., KOSAKA, N., YOSHIOKA, Y., TAKAGAKI, K., *et al.* 2013. Human adipose tissue-derived mesenchymal stem cells secrete functional neprilysin-bound exosomes. *Scientific reports,* 3**,** 1197-1197.

KAWAI, M., MUSHIAKE, S., BESSHO, K., MURAKAMI, M., NAMBA, N., *et al.* 2007. Wnt/Lrp/beta-catenin signaling suppresses adipogenesis by inhibiting mutual activation of PPARgamma and C/EBPalpha. *Biochem Biophys Res Commun,* 363**,** 276-82.

KEATING, A. 2006. Mesenchymal stromal cells. *Current opinion in hematology,* 13**,** 419-425.

KEGG 2020. Regulation of lipolysis in adipocytes - Homo sapiens (human).

KELLEY, D. S. 2001. Modulation of human immune and inflammatory responses by dietary fatty acids. *Nutrition,* 17**,** 669-673.

KELLY, T., YANG, W., CHEN, C. S., REYNOLDS, K. & HE, J. 2008. Global burden of obesity in 2005 and projections to 2030. *Int J Obes (Lond),* 32**,** 1431-7.

KENNEDY, A., GETTYS, T. W., WATSON, P., WALLACE, P., GANAWAY, E., *et al.* 1997. The Metabolic Significance of Leptin in Humans: Gender-Based Differences in Relationship to Adiposity, Insulin Sensitivity, and Energy Expenditure*. *The Journal of Clinical Endocrinology & Metabolism,* 82**,** 1293-1300.

KERSHAW, E. E. & FLIER, J. S. 2004. Adipose Tissue as an Endocrine Organ. *The Journal of Clinical Endocrinology & Metabolism,* 89**,** 2548-2556.

KHAN, M. A. B., HASHIM, M. J., KING, J. K., GOVENDER, R. D., MUSTAFA, H., *et al.* 2020. Epidemiology of Type 2 Diabetes - Global Burden of Disease and Forecasted Trends. *Journal of epidemiology and global health,* 10**,** 107-111.

KHOO, C. M., LEOW, M. K., SADANANTHAN, S. A., LIM, R., VENKATARAMAN, K., *et al.* 2014. Body fat partitioning does not explain the interethnic variation in insulin sensitivity among Asian ethnicity: the Singapore adults metabolism study. *Diabetes,* 63**,** 1093-102.

KIBSCHULL, M., LYE, S. J., OKINO, S. T. & SARRAS, H. 2016. Quantitative large scale gene expression profiling from human stem cell culture micro samples using multiplex pre-amplification. *Syst Biol Reprod Med,* 62**,** 84-91.

KIDO, Y., NAKAE, J. & ACCILI, D. 2001. Clinical review 125: The insulin receptor and its cellular targets. *J Clin Endocrinol Metab,* 86**,** 972-9.

KIM, J. B. & SPIEGELMAN, B. M. 1996. ADD1/SREBP1 promotes adipocyte differentiation and gene expression linked to fatty acid metabolism. *Genes & Development,* 10**,** 1096-1107.

KIM, S. M., LUN, M., WANG, M., SENYO, S. E., GUILLERMIER, C., *et al.* 2014. Loss of white adipose hyperplastic potential is associated with enhanced susceptibility to insulin resistance. *Cell Metab,* 20**,** 1049-58.

KIM, S. P., HA, J. M., YUN, S. J., KIM, E. K., CHUNG, S. W., *et al.* 2010. Transcriptional activation of peroxisome proliferator-activated receptor-gamma requires activation of both protein kinase A and Akt during adipocyte differentiation. *Biochem Biophys Res Commun,* 399**,** 55-9.

KIM, Y. B., NIKOULINA, S. E., CIARALDI, T. P., HENRY, R. R. & KAHN, B. B. 1999. Normal insulin-dependent activation of Akt/protein kinase B, with diminished activation of phosphoinositide 3-kinase, in muscle in type 2 diabetes. *The Journal of clinical investigation,* 104**,** 733-741.

KIM, Y. J., HWANG, S. J., BAE, Y. C. & JUNG, J. S. 2009. MiR-21 regulates adipogenic differentiation through the modulation of TGF-beta signaling in mesenchymal stem cells derived from human adipose tissue. *Stem Cells,* 27**,** 3093-102.

KIRKLAND, J. L., TCHKONIA, T., PIRTSKHALAVA, T., HAN, J. & KARAGIANNIDES, I. 2002. Adipogenesis and aging: does aging make fat go MAD? *Exp Gerontol,* 37**,** 757-67.

KLEY, S., HOENIG, M., GLUSHKA, J., JIN, E. S., BURGESS, S. C., *et al.* 2009. The impact of obesity, sex, and diet on hepatic glucose production in cats. *Am J Physiol Regul Integr Comp Physiol,* 296**,** R936-43.

KOECK, E. S., IORDANSKAIA, T., SEVILLA, S., FERRANTE, S. C., HUBAL, M. J., *et al.* 2014. Adipocyte exosomes induce transforming growth factor beta pathway dysregulation in hepatocytes: a novel paradigm for obesity-related liver disease. *J Surg Res,* 192**,** 268-75.

KOTANI, K., TOKUNAGA, K., FUJIOKA, S., KOBATAKE, T., KENO, Y., *et al.* 1994. Sexual dimorphism of age-related changes in whole-body fat distribution in the obese. *Int J Obes Relat Metab Disord,* 18**,** 207-2.

KRAMER, A., GREEN, J., POLLARD, J., JR. & TUGENDREICH, S. 2014. Causal analysis approaches in Ingenuity Pathway Analysis. *Bioinformatics,* 30**,** 523-30.

KRAMER, C. K., ZINMAN, B. & RETNAKARAN, R. 2013. Are metabolically healthy overweight and obesity benign conditions?: A systematic review and meta-analysis. *Ann Intern Med,* 159**,** 758-69.

KRANENDONK, M. E., DE KLEIJN, D. P., KALKHOVEN, E., KANHAI, D. A., UITERWAAL, C. S., *et al.* 2014a. Extracellular vesicle markers in relation to obesity and metabolic complications in patients with manifest cardiovascular disease. *Cardiovasc Diabetol,* 13**,** 37.

KRANENDONK, M. E., VISSEREN, F. L., VAN BALKOM, B. W., NOLTE-'T HOEN, E. N., VAN HERWAARDEN, J. A., *et al.* 2014b. Human adipocyte extracellular vesicles in reciprocal signaling between adipocytes and macrophages. *Obesity (Silver Spring),* 22**,** 1296-308.

KRANENDONK, M. E., VISSEREN, F. L., VAN HERWAARDEN, J. A., NOLTE-'T HOEN, E. N., DE JAGER, W., *et al.* 2014c. Effect of extracellular vesicles of human adipose tissue on insulin signaling in liver and muscle cells. *Obesity (Silver Spring),* 22**,** 2216-23.

KRAUSE, B. R. & HARTMAN, A. D. 1984. Adipose tissue and cholesterol metabolism. *J Lipid Res,* 25**,** 97-110.

KREBS, N. J., NEVILLE, C. & VACANTI, J. P. 2007. 12 - Cellular Transplants for Liver Diseases. *In:* HALBERSTADT, C. & EMERICH, D. (eds.) *Cellular Transplantation.* Burlington: Academic Press.

KROTKIEWSKI, M., BJÖRNTORP, P., SJÖSTRÖM, L. & SMITH, U. 1983. Impact of obesity on metabolism in men and women. Importance of regional adipose tissue distribution. *J Clin Invest,* 72**,** 1150-62.

KUBOTA, N., TERAUCHI, Y., MIKI, H., TAMEMOTO, H., YAMAUCHI, T., *et al.* 1999. PPAR gamma mediates high-fat diet-induced adipocyte hypertrophy and insulin resistance. *Mol Cell,* 4**,** 597-609.

KUK, J. L., SAUNDERS, T. J., DAVIDSON, L. E. & ROSS, R. 2009. Age-related changes in total and regional fat distribution. *Ageing Res Rev,* 8**,** 339-48.

KURI-HARCUCH, W. & GREEN, H. 1978. Adipose conversion of 3T3 cells depends on a serum factor. *Proc Natl Acad Sci U S A,* 75**,** 6107-9.

KURSAWE, R., ESZLINGER, M., NARAYAN, D., LIU, T., BAZUINE, M., *et al.* 2010. Cellularity and adipogenic profile of the abdominal subcutaneous adipose tissue from obese adolescents: association with insulin resistance and hepatic steatosis. *Diabetes,* 59**,** 2288-96.

LABRIE, F., SIMARD, J., LUU-THE, V., TRUDEL, C., MARTEL, C., *et al.* 1991. Expression of 3 beta-hydroxysteroid dehydrogenase/delta 5-delta 4 isomerase (3 beta-HSD) and 17 beta-hydroxysteroid dehydrogenase (17 beta-HSD) in adipose tissue. *Int J Obes,* 15 Suppl 2**,** 91-9.

LACLAUSTRA, M., LOPEZ-GARCIA, E., CIVEIRA, F., GARCIA-ESQUINAS, E., GRACIANI, A., *et al.* 2018. LDL Cholesterol Rises With BMI Only in Lean Individuals: Cross-sectional U.S. and Spanish Representative Data. *Diabetes Care,* 41**,** 2195.

LAFOREST, S., MICHAUD, A., PARIS, G., PELLETIER, M., VIDAL, H., *et al.* 2017. Comparative analysis of three human adipocyte size measurement methods and their relevance for cardiometabolic risk. *Obesity (Silver Spring),* 25**,** 122-131.

LAINE, M. K., ERIKSSON, J. G., KUJALA, U. M., WASENIUS, N. S., KAPRIO, J., *et al.* 2014. A former career as a male elite athlete--does it protect against type 2 diabetes in later life? *Diabetologia,* 57**,** 270-4.

LANDGRAF, K., ROCKSTROH, D., WAGNER, I. V., WEISE, S., TAUSCHER, R., *et al.* 2015. Evidence of early alterations in adipose tissue biology and function and its association with obesity-related inflammation and insulin resistance in children. *Diabetes,* 64**,** 1249-61.

LANSFORD, K. A., SHILL, D. D., DICKS, A. B., MARSHBURN, M. P., SOUTHERN, W. M., *et al.* 2016. Effect of acute exercise on circulating angiogenic cell and microparticle populations. *Experimental Physiology,* 101**,** 155-167.

LAVIOLA, L., PERRINI, S., CIGNARELLI, A. & GIORGINO, F. 2006a. Insulin signalling in human adipose tissue. *Archives of Physiology and Biochemistry,* 112**,** 82-88.

LAVIOLA, L., PERRINI, S., CIGNARELLI, A., NATALICCHIO, A., LEONARDINI, A., *et al.* 2006b. Insulin Signaling in Human Visceral and Subcutaneous Adipose Tissue In Vivo. *Diabetes,* 55**,** 952-961.

LAZAR, I., CLEMENT, E., DAUVILLIER, S., MILHAS, D., DUCOUX-PETIT, M., *et al.* 2016. Adipocyte Exosomes Promote Melanoma Aggressiveness through Fatty Acid Oxidation: A Novel Mechanism Linking Obesity and Cancer. *Cancer Res,* 76**,** 4051-7.

LEAL-CERRO, A., GARCIA-LUNA, P. P., ASTORGA, R., PAREJO, J., PEINO, R., *et al.* 1998. Serum leptin levels in male marathon athletes before and after the marathon run. *J Clin Endocrinol Metab,* 83**,** 2376-9.

LEAN, M. E., JAMES, W. P., JENNINGS, G. & TRAYHURN, P. 1986. Brown adipose tissue uncoupling protein content in human infants, children and adults. *Clin Sci (Lond),* 71**,** 291-7.

LEAR, S. A., HUMPHRIES, K. H., KOHLI, S., CHOCKALINGAM, A., FROHLICH, J. J., *et al.* 2007. Visceral adipose tissue accumulation differs according to ethnic background: results of the Multicultural Community Health Assessment Trial (M-CHAT). *Am J Clin Nutr,* 86**,** 353-9.

LEE, C. D., JACKSON, A. S. & BLAIR, S. N. 1998. US weight guidelines: is it also important to consider cardiorespiratory fitness? *Int J Obes Relat Metab Disord,* 22 Suppl 2**,** S2-7.

LEE, P., GREENFIELD, J. R., HO, K. K. & FULHAM, M. J. 2010. A critical appraisal of the prevalence and metabolic significance of brown adipose tissue in adult humans. *Am J Physiol Endocrinol Metab,* 299**,** E601-6.

LEMIEUX, I., PASCOT, A., COUILLARD, C., LAMARCHE, B. T., TCHERNOF, A., *et al.* 2000. Hypertriglyceridemic Waist. *Circulation,* 102**,** 179-184.

LEVY, J. C., MATTHEWS, D. R. & HERMANS, M. P. 1998. Correct homeostasis model assessment (HOMA) evaluation uses the computer program. *Diabetes Care,* 21**,** 2191-2.

LEWITT, M. S. 2017. The Role of the Growth Hormone/Insulin-Like Growth Factor System in Visceral Adiposity. *Biochemistry Insights,* 10**,** 1178626417703995.

LEY, C. J., LEES, B. & STEVENSON, J. C. 1992. Sex- and menopause-associated changes in body-fat distribution. *The American Journal of Clinical Nutrition,* 55**,** 950-954.

LI, P., WANG, Y., ZHANG, L., NING, Y. & ZAN, L. 2018. The Expression Pattern of PLIN2 in Differentiated Adipocytes from Qinchuan Cattle Analysis of Its Protein Structure and Interaction with CGI-58. *Int J Mol Sci,* 19.

LI, S.-N. & WU, J.-F. 2020. TGF-β/SMAD signaling regulation of mesenchymal stem cells in adipocyte commitment. *Stem Cell Research & Therapy,* 11**,** 41.

LI, Y., NANAYAKKARA, G., SUN, Y., LI, X., WANG, L., *et al.* 2017. Analyses of caspase-1-regulated transcriptomes in various tissues lead to identification of novel IL-1β-, IL-18- and sirtuin-1-independent pathways. *Journal of Hematology & Oncology,* 10**,** 40.

LIANG, Y. J., XI, B., SONG, A. Q., LIU, J. X. & MI, J. 2012. Trends in general and abdominal obesity among Chinese children and adolescents 1993-2009. *Pediatr Obes,* 7**,** 355-64.

LIBBY, A. E., BALES, E., ORLICKY, D. J. & MCMANAMAN, J. L. 2016. Perilipin-2 Deletion Impairs Hepatic Lipid Accumulation by Interfering with Sterol Regulatory Element-binding Protein (SREBP) Activation and Altering the Hepatic Lipidome. *J Biol Chem,* 291**,** 24231-24246.

LITWACK, G. 2018. Chapter 8 - Glycolysis and Gluconeogenesis. *In:* LITWACK, G. (ed.) *Human Biochemistry.* Boston: Academic Press.

LIU, K. & CZAJA, M. J. 2013. Regulation of lipid stores and metabolism by lipophagy. *Cell Death Differ,* 20**,** 3-11.

LIU, L., FENG, J., ZHANG, G., YUAN, X., LI, F., *et al.* 2018. Visceral adipose tissue is more strongly associated with insulin resistance than subcutaneous adipose tissue in Chinese subjects with pre-diabetes. *Current Medical Research and Opinion,* 34**,** 123-129.

LIU, Z. & BARRETT, E. J. 2002. Human protein metabolism: its measurement and regulation. *American Journal of Physiology-Endocrinology and Metabolism,* 283**,** E1105-E1112.

LONGO, K. A., KENNELL, J. A., OCHOCINSKA, M. J., ROSS, S. E., WRIGHT, W. S., *et al.* 2002. Wnt signaling protects 3T3-L1 preadipocytes from apoptosis through induction of insulin-like growth factors. *J Biol Chem,* 277**,** 38239-44.

LONGO, K. A., WRIGHT, W. S., KANG, S., GERIN, I., CHIANG, S. H., *et al.* 2004. Wnt10b inhibits development of white and brown adipose tissues. *J Biol Chem,* 279**,** 35503-9.

LONN, M., MEHLIG, K., BENGTSSON, C. & LISSNER, L. 2010. Adipocyte size predicts incidence of type 2 diabetes in women. *FASEB J,* 24**,** 326-31.

LONNQVIST, F., NYBERG, B., WAHRENBERG, H. & ARNER, P. 1990. Catecholamine-induced lipolysis in adipose tissue of the elderly. *The Journal of clinical investigation,* 85, 1614-1621.

LONNROTH, P. & SMITH, U. 1986. Aging enhances the insulin resistance in obesity through both receptor and postreceptor alterations. *J Clin Endocrinol Metab,* 62, 433-7.

LOOZE, C., YUI, D., LEUNG, L., INGHAM, M., KALER, M., *et al.* 2009. Proteomic profiling of human plasma exosomes identifies PPARgamma as an exosome-associated protein. *Biochemical and biophysical research communications,* 378, 433-438.

LOPATINA, T., BRUNO, S., TETTA, C., KALININA, N., PORTA, M., *et al.* 2014. Platelet-derived growth factor regulates the secretion of extracellular vesicles by adipose mesenchymal stem cells and enhances their angiogenic potential. *Cell communication and signaling: CCS,* 12, 26-26.

LOZANO, R., NAGHAVI, M., FOREMAN, K., LIM, S., SHIBUYA, K., *et al.* 2012. Global and regional mortality from 235 causes of death for 20 age groups in 1990 and 2010: a systematic analysis for the Global Burden of Disease Study 2010. *The Lancet,* 380, 2095-2128.

LU, H., DUANMU, Z., HOUCK, C., JEN, K. L., BUISON, A., *et al.* 1998. Obesity due to high fat diet decreases the sympathetic nervous and cardiovascular responses to intracerebroventricular leptin in rats. *Brain Res Bull,* 47, 331-5.

LUHAR, S., TIMÆUS, I. M., JONES, R., CUNNINGHAM, S., PATEL, S. A., *et al.* 2020. Forecasting the prevalence of overweight and obesity in India to 2040. *PloS one,* 15, e0229438-e0229438.

LUNDGREN, M., SVENSSON, M., LINDMARK, S., RENSTROM, F., RUGE, T., *et al.* 2007. Fat cell enlargement is an independent marker of insulin resistance and 'hyperleptinaemia'. *Diabetologia,* 50, 625-33.

MANSOUR, M. F., CHAN, C.-W. J., LAFOREST, S., VEILLEUX, A. & TCHERNOF, A. 2017. Sex Differences in Body Fat Distribution. *In:* SYMONDS, M. E. (ed.) *Adipose Tissue Biology.* Cham: Springer International Publishing.

MARCHAND, G. B., CARREAU, A.-M., WEISNAGEL, S. J., BERGERON, J., LABRIE, F., *et al.* 2018. Increased body fat mass explains the positive association between circulating estradiol and insulin resistance in postmenopausal women. *American Journal of Physiology-Endocrinology and Metabolism,* 314, E448-E456.

MARINOU, K., HODSON, L., VASAN, S. K., FIELDING, B. A., BANERJEE, R., *et al.* 2014. Structural and functional properties of deep abdominal subcutaneous adipose tissue explain its association with insulin resistance and cardiovascular risk in men. *Diabetes Care,* 37, 821-9.

MARSHALL, S. 2006. Role of Insulin, Adipocyte Hormones, and Nutrient-Sensing Pathways in Regulating Fuel Metabolism and Energy Homeostasis: A Nutritional Perspective of Diabetes, Obesity, and Cancer. *Science's STKE,* 2006, re7.

MARTIN, M., PALANIAPPAN, L. P., KWAN, A. C., REAVEN, G. M. & REAVEN, P. D. 2008. Ethnic differences in the relationship between adiponectin and insulin sensitivity in South Asian and Caucasian women. *Diabetes Care,* 31, 798-801.

MASLOWSKA, M. H., SNIDERMAN, A. D., MACLEAN, L. D. & CIANFLONE, K. 1993. Regional differences in triacylglycerol synthesis in adipose tissue and in cultured preadipocytes. *J Lipid Res,* 34, 219-28.

MATSUZAWA, Y. 2006. The metabolic syndrome and adipocytokines. *FEBS Lett,* 580, 2917-21.

MATTHEWS, D. R., HOSKER, J. P., RUDENSKI, A. S., NAYLOR, B. A., TREACHER, D. F., *et al.* 1985. Homeostasis model assessment: insulin resistance and beta-cell function from fasting plasma glucose and insulin concentrations in man. *Diabetologia,* 28, 412-9.

MAURIÈGE, P., PRUD'HOMME, D., MARCOTTE, M., YOSHIOKA, M., TREMBLAY, A., *et al.* 1997. Regional differences in adipose tissue metabolism between sedentary and endurance-trained women. *American Journal of Physiology-Endocrinology and Metabolism,* 273, E497.

MAZUR, I. I., DROZDOVSKA, S., ANDRIEIEVA, O., VINNICHUK, Y., POLISHCHUK, A., *et al.* 2020. PPARGC1A gene polymorphism is associated with exercise-induced fat loss. *Molecular Biology Reports,* 47, 7451-7457.

MCKEIGUE, P. M., SHAH, B. & MARMOT, M. G. 1991. Relation of central obesity and insulin resistance with high diabetes prevalence and cardiovascular risk in South Asians. *Lancet,* 337, 382-6.

MCLAREN, J. 2018. *Adiposity and diabetes risk mechanisms in South Asians.* Ph.D., University of Glasgow.

MCLAUGHLIN, T., ABBASI, F., LAMENDOLA, C., YEE, G., CARTER, S., *et al.* 2019. Dietary weight loss in insulin-resistant non-obese humans: Metabolic benefits and relationship to adipose cell size. *Nutr Metab Cardiovasc Dis,* 29, 62-68.

MCLAUGHLIN, T., DENG, A., YEE, G., LAMENDOLA, C., REAVEN, G., *et al.* 2010a. Inflammation in subcutaneous adipose tissue: relationship to adipose cell size. *Diabetologia,* 53, 369-77.

MCLAUGHLIN, T., DENG, A., YEE, G., LAMENDOLA, C., REAVEN, G., *et al.* 2010b. Inflammation in subcutaneous adipose tissue: relationship to adipose cell size. *Diabetologia,* 53**,** 369-377.

MCLAUGHLIN, T., SHERMAN, A., TSAO, P., GONZALEZ, O., YEE, G., *et al.* 2007a. Enhanced proportion of small adipose cells in insulin-resistant vs insulin-sensitive obese individuals implicates impaired adipogenesis. *Diabetologia,* 50**,** 1707-15.

MCLAUGHLIN, T., SHERMAN, A., TSAO, P., GONZALEZ, O., YEE, G., *et al.* 2007b. Enhanced proportion of small adipose cells in insulin-resistant vs insulin-sensitive obese individuals implicates impaired adipogenesis. *Diabetologia,* 50**,** 1707-1715.

MCMANAMAN, J. L., BALES, E. S., ORLICKY, D. J., JACKMAN, M., MACLEAN, P. S., *et al.* 2013. Perilipin-2-null mice are protected against diet-induced obesity, adipose inflammation, and fatty liver disease. *J Lipid Res,* 54**,** 1346-59.

MEENA, V. P., SEENU, V., SHARMA, M. C., MALLICK, S. R., BHALLA, A. S., *et al.* 2014a. Relationship of adipocyte size with adiposity and metabolic risk factors in Asian Indians. *PLoS One,* 9**,** e108421.

MEENA, V. P., SEENU, V., SHARMA, M. C., MALLICK, S. R., BHALLA, A. S., *et al.* 2014b. Relationship of adipocyte size with adiposity and metabolic risk factors in Asian Indians. *PloS one,* 9**,** e108421-e108421.

MEIJSSEN, S., CABEZAS, M. C., BALLIEUX, C. G. M., DERKSEN, R. J., BILECEN, S., *et al.* 2001. Insulin Mediated Inhibition of Hormone Sensitive Lipase Activity in Vivo in Relation to Endogenous Catecholamines in Healthy Subjects. *The Journal of Clinical Endocrinology & Metabolism,* 86**,** 4193-4197.

MEILLEUR, K. G., DOUMATEY, A., HUANG, H., CHARLES, B., CHEN, G., *et al.* 2010. Circulating adiponectin is associated with obesity and serum lipids in West Africans. *The Journal of clinical endocrinology and metabolism,* 95**,** 3517-3521.

MEISINGER, C., DÖRING, A., THORAND, B., HEIER, M. & LÖWEL, H. 2006. Body fat distribution and risk of type 2 diabetes in the general population: are there differences between men and women? The MONICA/KORA Augsburg Cohort Study. *The American Journal of Clinical Nutrition,* 84**,** 483-489.

MEKALA, K. C. & TRITOS, N. A. 2009. Effects of recombinant human growth hormone therapy in obesity in adults: a meta analysis. *J Clin Endocrinol Metab,* 94**,** 130-7.

MENTE, A., RAZAK, F., BLANKENBERG, S., VUKSAN, V., DAVIS, A. D., *et al.* 2010. Ethnic variation in adiponectin and leptin levels and their association with adiposity and insulin resistance. *Diabetes Care,* 33**,** 1629-34.

MERSMANN, H. J. & MACNEIL, M. D. 1986. Variables in estimation of adipocyte size and number with a particle counter. *J Anim Sci,* 62**,** 980-91.

MICHAILIDOU, Z., JENSEN, M. D., DUMESIC, D. A., CHAPMAN, K. E., SECKL, J. R., *et al.* 2007. Omental 11beta-hydroxysteroid dehydrogenase 1 correlates with fat cell size independently of obesity. *Obesity (Silver Spring),* 15**,** 1155-63.

MIKI, H., YAMAUCHI, T., SUZUKI, R., KOMEDA, K., TSUCHIDA, A., *et al.* 2001. Essential role of insulin receptor substrate 1 (IRS-1) and IRS-2 in adipocyte differentiation. *Mol Cell Biol,* 21**,** 2521-32.

MILLER, K. N., BURHANS, M. S., CLARK, J. P., HOWELL, P. R., POLEWSKI, M. A., *et al.* 2017. Aging and caloric restriction impact adipose tissue, adiponectin, and circulating lipids. *Aging cell,* 16**,** 497-507.

MISRA, A. & KHURANA, L. 2011a. Obesity-related non-communicable diseases: South Asians vs White Caucasians. *Int J Obes (Lond),* 35**,** 167-87.

MISRA, A. & KHURANA, L. 2011b. Obesity-related non-communicable diseases: South Asians vs White Caucasians. *International journal of obesity (2005),* 35**,** 167-87.

MITTAL, B. 2019. Subcutaneous adipose tissue & visceral adipose tissue. *The Indian journal of medical research,* 149**,** 571-573.

MITTERBERGER, M. C., LECHNER, S., MATTESICH, M., KAISER, A., PROBST, D., *et al.* 2012. DLK1(PREF1) is a negative regulator of adipogenesis in CD105+/CD90+/CD34+/CD31−/FABP4− adipose-derived stromal cells from subcutaneous abdominal fat pats of adult women. *Stem Cell Research,* 9**,** 35-48.

MOHAMED-ALI, V., PINKNEY, J. H. & COPPACK, S. W. 1998. Adipose tissue as an endocrine and paracrine organ. *Int J Obes Relat Metab Disord,* 22**,** 1145-58.

MOKDAD, A. H., MARKS, J. S., STROUP, D. F. & GERBERDING, J. L. 2004. Actual Causes of Death in the United States, 2000. *JAMA,* 291**,** 1238-1245.

MONTASTIER, E., DEJEAN, S., LE GALL, C., SARIS, W. H., LANGIN, D., *et al.* 2014. Adipose tissue CIDEA is associated, independently of weight variation, to change in insulin resistance during a longitudinal weight control dietary program in obese individuals. *PLoS One,* 9**,** e98707.

MORA, S., LEE, I.-M., BURING, J. E. & RIDKER, P. M. 2006. Association of Physical Activity and Body Mass Index With Novel and Traditional Cardiovascular Biomarkers in Women. *JAMA*, 295**,** 1412-1419.

MORENO-NAVARRETE, J. M. & FERNÁNDEZ-REAL, J. M. Chapter 2 Adipocyte Differentiation. 2017.

MORIN, C. L., PAGLIASSOTTI, M. J., WINDMILLER, D. & ECKEL, R. H. 1997. Adipose tissue-derived tumor necrosis factor-alpha activity is elevated in older rats. *J Gerontol A Biol Sci Med Sci,* 52**,** B190-5.

MORO, C. & LAFONTAN, M. 2013. Natriuretic peptides and cGMP signaling control of energy homeostasis. *Am J Physiol Heart Circ Physiol,* 304**,** H358-68.

MUIR, L. A., NEELEY, C. K., MEYER, K. A., BAKER, N. A., BROSIUS, A. M., *et al.* 2016. Adipose tissue fibrosis, hypertrophy, and hyperplasia: Correlations with diabetes in human obesity. *Obesity (Silver Spring),* 24**,** 597-605.

MULLER, G., JUNG, C., STRAUB, J., WIED, S. & KRAMER, W. 2009. Induced release of membrane vesicles from rat adipocytes containing glycosylphosphatidylinositol-anchored microdomain and lipid droplet signalling proteins. *Cellular Signalling,* 21**,** 324-338.

NAKANO, T. & ITO, H. 2007. Epidemiology of diabetes mellitus in old age in Japan. *Diabetes Res Clin Pract,* 77 Suppl 1**,** S76-81.

NATCENSOCIALRESEARCH&UCL 2014. Health Survey for England Conbined data 2010-12.

NATIONALDIABETESAUDIT 2010. National Diabetes Auddit 2009-10.

NATIONALTASKFORCE 2000. Overweight, obesity, and health risk. *Archives of Internal Medicine,* 160**,** 898-904.

NAZIR, S., JANKOWSKI, V., BENDER, G., ZEWINGER, S., RYE, K. A., *et al.* 2020. Interaction between high-density lipoproteins and inflammation: Function matters more than concentration! *Adv Drug Deliv Rev,* 159**,** 94-119.

NCHS 2018. National Health and Nutrition Examination Survey.

NEDERGAARD, J., BENGTSSON, T. & CANNON, B. 2007. Unexpected evidence for active brown adipose tissue in adult humans. *Am J Physiol Endocrinol Metab,* 293**,** E444-52.

NEVILLE, M. J., COLLINS, J. M., GLOYN, A. L., MCCARTHY, M. I. & KARPE, F. 2011. Comprehensive human adipose tissue mRNA and microRNA endogenous control selection for quantitative real-time-PCR normalization. *Obesity (Silver Spring),* 19**,** 888-92.

NEWELL-FUGATE, A. E. 2017. The role of sex steroids in white adipose tissue adipocyte function. 153**,** R133.

NG, F., BOUCHER, S., KOH, S., SASTRY, K. S., CHASE, L., *et al.* 2008. PDGF, TGF-beta, and FGF signaling is important for differentiation and growth of mesenchymal stem cells (MSCs): transcriptional profiling can identify markers and signaling pathways important in differentiation of MSCs into adipogenic, chondrogenic, and osteogenic lineages. *Blood,* 112**,** 295-307.

NG, M., FLEMING, T., ROBINSON, M., THOMSON, B., GRAETZ, N., *et al.* 2014. Global, regional, and national prevalence of overweight and obesity in children and adults during 1980–2013: a systematic analysis for the Global Burden of Disease Study 2013. *The Lancet,* 384**,** 766-781.

NGUYEN, K. D., QIU, Y., CUI, X., GOH, Y. P. S., MWANGI, J., *et al.* 2011. Alternatively activated macrophages produce catecholamines to sustain adaptive thermogenesis. *Nature,* 480**,** 104-108.

NGUYEN-TU, M.-S., MARTINEZ-SANCHEZ, A., LECLERC, I., RUTTER, G. A. & DA SILVA XAVIER, G. 2021a. Adipocyte-specific deletion of Tcf7l2 induces dysregulated lipid metabolism and impairs glucose tolerance in mice. *Diabetologia,* 64**,** 129-141.

NGUYEN-TU, M. S., MARTINEZ-SANCHEZ, A., LECLERC, I., RUTTER, G. A. & DA SILVA XAVIER, G. 2021b. Adipocyte-specific deletion of Tcf7l2 induces dysregulated lipid metabolism and impairs glucose tolerance in mice. *Diabetologia,* 64**,** 129-141.

NHS. 2012. *Diabetes: cases and costs predicte to rise* [Online]. nhs.uk. Available: https://www.nhs.uk/news/diabetes/diabetes-cases-and-costs-predicted-to-rise/ [Accessed 12/02 2019].

NICHOLLS, D. G. & LOCKE, R. M. 1984. Thermogenic mechanisms in brown fat. *Physiological Reviews,* 64**,** 1-64.

NIESLER, C. U., SIDDLE, K. & PRINS, J. B. 1998. Human preadipocytes display a depot-specific susceptibility to apoptosis. *Diabetes,* 47**,** 1365-8.

NOPPA, H., ANDERSSON, M., BENGTSSON, C., BRUCE, A. & ISAKSSON, B. 1980. Longitudinal studies of anthropometric data and body composition. The population study of women in Götenberg, Sweden. *Am J Clin Nutr,* 33**,** 155-62.

NORDSTROM, E. A., RYDEEN, M., BACKLUND, E. C., DAHLMAN, I., KAAMAN, M., *et al.* 2005. A Human-Specific Role of Cell Death-Inducing DFFA (DNA Fragmentation Factor-α)-Like Effector A (CIDEA) in Adipocyte Lipolysis and Obesity. *Diabetes,* 54**,** 1726-1734.

NTAMBI, J. M. & YOUNG-CHEUL, K. 2000. Adipocyte Differentiation and Gene Expression. *The Journal of Nutrition,* 130**,** 3122S-3126S.

NTUK, U. E., GILL, J. M., MACKAY, D. F., SATTAR, N. & PELL, J. P. 2014. Ethnic-specific obesity cutoffs for diabetes risk: cross-sectional study of 490,288 UK biobank participants. *Diabetes Care,* 37**,** 2500-7.

NTZOUVANI, A., FRAGOPOULOU, E., PANAGIOTAKOS, D., PITSAVOS, C. & ANTONOPOULOU, S. 2016. Reduced circulating adiponectin levels are associated with the metabolic syndrome independently of obesity, lipid indices and serum insulin levels: a cross-sectional study. *Lipids in Health and Disease,* 15**,** 140.

OECD 2019. The heavy burden of obesity: the economics of prevention.

OGDEN, C. L., CARROLL, M. D., KIT, B. K. & FLEGAL, K. M. 2014. Prevalence of Childhood and Adult Obesity in the United States, 2011-2012. *JAMA,* 311**,** 806-814.

OHSAKI, Y., CHENG, J., SUZUKI, M., SHINOHARA, Y., FUJITA, A., *et al.* 2009. Biogenesis of cytoplasmic lipid droplets: From the lipid ester globule in the membrane to the visible structure. *Biochimica et Biophysica Acta (BBA) - Molecular and Cell Biology of Lipids,* 1791**,** 399-407.

OLSZANECKA-GLINIANOWICZ, M., CHUDEK, J., KOCEŁAK, P., SZROMEK, A. & ZAHORSKA-MARKIEWICZ, B. 2011. Body fat changes and activity of tumor necrosis factor α system--a 5-year follow-up study. *Metabolism,* 60**,** 531-6.

OSEGBE, I., OKPARA, H. & AZINGE, E. 2016. Relationship between serum leptin and insulin resistance among obese Nigerian women. *Annals of African medicine,* 15**,** 14-19.

OSTERGAARD, O., NIELSEN, C. T., IVERSEN, L. V., JACOBSEN, S., TANASSI, J. T., *et al.* 2012. Quantitative proteome profiling of normal human circulating microparticles. *J Proteome Res,* 11**,** 2154-63.

OTVOS, L., JR. 2019. Potential Adiponectin Receptor Response Modifier Therapeutics. *Front Endocrinol (Lausanne),* 10**,** 539.

OUCHI, N., PARKER, J. L., LUGUS, J. J. & WALSH, K. 2011. Adipokines in inflammation and metabolic disease. *Nat Rev Immunol,* 11**,** 85-97.

PALMER, B. F. & CLEGG, D. J. 2015. The sexual dimorphism of obesity. *Mol Cell Endocrinol,* 402**,** 113-9.

PARDO, F., VILLALOBOS-LABRA, R., SOBREVIA, B., TOLEDO, F. & SOBREVIA, L. 2018. Extracellular vesicles in obesity and diabetes mellitus. *Molecular Aspects of Medicine,* 60**,** 81-91.

PARK, Y.-M., MYERS, M. & VIEIRA-POTTER, V. J. 2014. Adipose tissue inflammation and metabolic dysfunction: role of exercise. *Missouri medicine,* 111**,** 65-72.

PATEL, J. V., SOSIN, M., LIM, H. S., CHUNG, I., PANJA, N., *et al.* 2007. Raised leptin concentrations among South Asian patients with chronic heart failure. *Int J Cardiol,* 122**,** 34-40.

PAUL, S. K., OWUSU ADJAH, E. S., SAMANTA, M., PATEL, K., BELLARY, S., *et al.* 2017. Comparison of body mass index at diagnosis of diabetes in a multi-ethnic population: A case-control study with matched non-diabetic controls. *Diabetes, Obesity and Metabolism,* 19**,** 1014-1023.

PAYNE, V. A., GRIMSEY, N., TUTHILL, A., VIRTUE, S., GRAY, S. L., *et al.* 2008. The human lipodystrophy gene BSCL2/seipin may be essential for normal adipocyte differentiation. *Diabetes,* 57**,** 2055-60.

PEREIRA, R. I., CASEY, B. A., SWIBAS, T. A., ERICKSON, C. B., WOLFE, P., *et al.* 2015. Timing of Estradiol Treatment After Menopause May Determine Benefit or Harm to Insulin Action. *J Clin Endocrinol Metab,* 100**,** 4456-62.

PERSEGHIN, G., LATTUADA, G., RAGOGNA, F., ALBERTI, G., LA TORRE, A., *et al.* 2009. Free leptin index and thyroid function in male highly trained athletes. *Eur J Endocrinol,* 161**,** 871-6.

PETERSEN, K. F., DUFOUR, S., FENG, J., BEFROY, D., DZIURA, J., *et al.* 2006. Increased prevalence of insulin resistance and nonalcoholic fatty liver disease in Asian-Indian men. *Proc Natl Acad Sci U S A,* 103**,** 18273-7.

PETRICK, H. L., FOLEY, K. P., ZLITNI, S., BRUNETTA, H. S., PAGLIALUNGA, S., *et al.* 2020. Adipose Tissue Inflammation Is Directly Linked to Obesity-Induced Insulin Resistance, while Gut Dysbiosis and Mitochondrial Dysfunction Are Not Required. *Function,* 1.

PETROVIC, N., WALDEN, T. B., SHABALINA, I. G., TIMMONS, J. A., CANNON, B., *et al.* 2010. Chronic peroxisome proliferator-activated receptor gamma (PPARgamma) activation of epididymally derived white adipocyte cultures reveals a population of thermogenically competent, UCP1-containing adipocytes molecularly distinct from classic brown adipocytes. *J Biol Chem,* 285**,** 7153-64.

PINCU, Y., HUNTSMAN, H. D., ZOU, K., DE LISIO, M., MAHMASSANI, Z. S., *et al.* 2016. Diet-induced obesity regulates adipose-resident stromal cell quantity and extracellular matrix gene expression. *Stem Cell Res,* 17**,** 181-90.

POLEDNAK, A. P. 2008. Estimating the number of U.S. incident cancers attributable to obesity and the impact on temporal trends in incidence rates for obesity-related cancers. *Cancer Detect Prev,* 32**,** 190-9.

POU KARLA, M., MASSARO JOSEPH, M., HOFFMANN, U., VASAN RAMACHANDRAN, S., MAUROVICH-HORVAT, P., *et al.* 2007. Visceral and Subcutaneous Adipose Tissue Volumes Are Cross-Sectionally Related to Markers of Inflammation and Oxidative Stress. *Circulation,* 116**,** 1234-1241.

POULAIN-GODEFROY, O., LE BACQUER, O., PLANCQ, P., LECOEUR, C., PATTOU, F., *et al.* 2010. Inflammatory role of Toll-like receptors in human and murine adipose tissue. *Mediators Inflamm,* 2010**,** 823486.

PRATTES, S., HÖRL, G., HAMMER, A., BLASCHITZ, A., GRAIER, W. F., *et al.* 2000. Intracellular distribution and mobilization of unesterified cholesterol in adipocytes: triglyceride droplets are surrounded by cholesterol-rich ER-like surface layer structures. *J Cell Sci,* 113 (Pt 17)**,** 2977-89.

PREIS, S. R., MASSARO, J. M., ROBINS, S. J., HOFFMANN, U., VASAN, R. S., *et al.* 2010. Abdominal subcutaneous and visceral adipose tissue and insulin resistance in the Framingham heart study. *Obesity (Silver Spring, Md.),* 18**,** 2191-2198.

PRESTWICH, T. C. & MACDOUGALD, O. A. 2007. Wnt/β-catenin signaling in adipogenesis and metabolism. *Current Opinion in Cell Biology,* 19**,** 612-617.

PREVIS, S. F., WITHERS, D. J., REN, J.-M., WHITE, M. F. & SHULMAN, G. I. 2000. Contrasting Effects of IRS-1 Versus IRS-2 Gene Disruption on Carbohydrate and Lipid Metabolism in Vivo. *Journal of Biological Chemistry,* 275**,** 38990-38994.

PRICE, N. L., HOLTRUP, B., KWEI, S. L., WABITSCH, M., RODEHEFFER, M., *et al.* 2016. SREBP-1c/MicroRNA 33b Genomic Loci Control Adipocyte Differentiation. *Mol Cell Biol,* 36**,** 1180-93.

PRITCHARD, C. C., CHENG, H. H. & TEWARI, M. 2012. MicroRNA profiling: approaches and considerations. *Nature reviews. Genetics,* 13**,** 358-369.

PURI, V., KONDA, S., RANJIT, S., AOUADI, M., CHAWLA, A., *et al.* 2007. Fat-specific protein 27, a novel lipid droplet protein that enhances triglyceride storage. *J Biol Chem,* 282**,** 34213-8.

PURI, V., RANJIT, S., KONDA, S., NICOLORO, S. M., STRAUBHAAR, J., *et al.* 2008a. Cidea is associated with lipid droplets and insulin sensitivity in humans. *Proc Natl Acad Sci U S A,* 105**,** 7833-8.

PURI, V., RANJIT, S., KONDA, S., NICOLORO, S. M. C., STRAUBHAAR, J., *et al.* 2008b. Cidea is associated with lipid droplets and insulin sensitivity in humans. *Proceedings of the National Academy of Sciences,* 105**,** 7833-7838.

PUTIGNANO, P., PECORI GIRALDI, F. & CAVAGNINI, F. 2004. Tissue-specific dysregulation of 11beta-hydroxysteroid dehydrogenase type 1 and pathogenesis of the metabolic syndrome. *J Endocrinol Invest,* 27**,** 969-74.

QIAN, S., PAN, J., SU, Y., TANG, Y., WANG, Y., *et al.* 2020. BMPR2 promotes fatty acid oxidation and protects white adipocytes from cell death in mice. *Commun Biol,* 3**,** 200.

RADER, D. J. 2008. Lipoprotein Metabolism. *In:* OFFERMANNS, S. & ROSENTHAL, W. (eds.) *Encyclopedia of Molecular Pharmacology.* Berlin, Heidelberg: Springer Berlin Heidelberg.

RAGHEB, R. & M. MEDHAT, A. 2011. Mechanisms of Fatty Acid-Induced Insulin Resistance in Muscle and Liver. *Journal of Diabetes & Metabolism,* 02.

RAJI, C. A., HO, A. J., PARIKSHAK, N. N., BECKER, J. T., LOPEZ, O. L., *et al.* 2010. Brain structure and obesity. *Hum Brain Mapp,* 31**,** 353-64.

RAMSAY, T. G. 1996. FAT CELLS. *Endocrinology and Metabolism Clinics of North America,* 25**,** 847-870.

RANDERIA, S. N., THOMSON, G. J. A., NELL, T. A., ROBERTS, T. & PRETORIUS, E. 2019. Inflammatory cytokines in type 2 diabetes mellitus as facilitators of hypercoagulation and abnormal clot formation. *Cardiovascular Diabetology,* 18**,** 72.

RAO, N., JOHRI, N., HARVEY, D., ROBERTSON, L., THOMAS, M., *et al.* 2009. BODY FAT DISTRIBUTION IN MEN AND WOMEN OF SOUTH ASIAN ORIGIN: AN OBSERVATIONAL STUDY. *Atherosclerosis,* 207**,** 309.

REARDON, M. A. & WEBER, G. 1983. Action of insulin on liver carbamoyl-phosphate synthetase II (glutamine-hydrolyzing) activity. *Biochem Biophys Res Commun,* 114**,** 255-60.

REAVEN, G. M., HOLLENBECK, C., JENG, C.-Y., WU, M. S. & CHEN, Y.-D. I. 1988. Measurement of Plasma Glucose, Free Fatty Acid, Lactate, and Insulin for 24 h in Patients With NIDDM. *Diabetes,* 37**,** 1020-1024.

REES, S. D., ISLAM, M., HYDRIE, M. Z., CHAUDHARY, B., BELLARY, S., *et al.* 2011. An FTO variant is associated with Type 2 diabetes in South Asian populations after accounting for body mass index and waist circumference. *Diabet Med,* 28**,** 673-80.

RIBAS, V., NGUYEN, M. T., HENSTRIDGE, D. C., NGUYEN, A. K., BEAVEN, S. W., *et al.* 2010. Impaired oxidative metabolism and inflammation are associated with insulin resistance in ERalpha-deficient mice. *Am J Physiol Endocrinol Metab,* 298**,** E304-19.

RIDDERSTRALE, M. 2005. Signaling Mechanism for the Insulin-like Effects of Growth Hormone - Another Example of a Classical Hormonal Negative Feedback Loop. *Current drug targets. Immune, endocrine and metabolic disorders,* 5**,** 79-92.

RIGAMONTI, A. E., BOLLATI, V., PERGOLI, L., IODICE, S., DE COL, A., *et al.* 2020. Effects of an acute bout of exercise on circulating extracellular vesicles: tissue-, sex-, and BMI-related differences. *International Journal of Obesity,* 44**,** 1108-1118.

RONDINONE, C. M., WANG, L. M., LONNROTH, P., WESSLAU, C., PIERCE, J. H., *et al.* 1997. Insulin receptor substrate (IRS) 1 is reduced and IRS-2 is the main docking protein for phosphatidylinositol 3-kinase in adipocytes from subjects with non-insulin-dependent diabetes mellitus. *Proceedings of the National Academy of Sciences of the United States of America,* 94**,** 4171-4175.

RORSMAN, P. & ASHCROFT, F. M. 2018. Pancreatic β-Cell Electrical Activity and Insulin Secretion: Of Mice and Men. *Physiological reviews,* 98**,** 117-214.

ROSADO-PEREZ, J. & MENDOZA-NUNEZ, V. M. 2018. Relationship Between Aerobic Capacity With Oxidative Stress and Inflammation Biomarkers in the Blood of Older Mexican Urban-Dwelling Population. *Dose Response,* 16**,** 1559325818773000.

ROSEN, E. D., HSU, C. H., WANG, X., SAKAI, S., FREEMAN, M. W., *et al.* 2002. C/EBPalpha induces adipogenesis through PPARgamma: a unified pathway. *Genes Dev,* 16**,** 22-6.

ROSEN, E. D., SARRAF, P., TROY, A. E., BRADWIN, G., MOORE, K., *et al.* 1999. PPAR gamma is required for the differentiation of adipose tissue in vivo and in vitro. *Mol Cell,* 4**,** 611-7.

ROSEN, E. D. & SPIEGELMAN, B. M. 2000. Molecular Regulation of Adipogenesis. *Annual Review of Cell and Developmental Biology,* 16**,** 145-171.

ROSEN, E. D. & SPIEGELMAN, B. M. 2006. Adipocytes as regulators of energy balance and glucose homeostasis. *Nature,* 444**,** 847-853.

ROSS, S. E., HEMATI, N., LONGO, K. A., BENNETT, C. N., LUCAS, P. C., *et al.* 2000. Inhibition of Adipogenesis by Wnt Signaling. *Science,* 289**,** 950-953.

RUAN, H., MILES, P. D. G., LADD, C. M., ROSS, K., GOLUB, T. R., *et al.* 2002. Profiling Gene Transcription In Vivo Reveals Adipose Tissue as an Immediate Target of Tumor Necrosis Factor-α. *Diabetes,* 51**,** 3176.

RYDEN, M., ANDERSSON, D. P., BERGSTROM, I. B. & ARNER, P. 2014. Adipose tissue and metabolic alterations: regional differences in fat cell size and number matter, but differently: a cross-sectional study. *J Clin Endocrinol Metab,* 99**,** E1870-6.

RYDÉN, M., ANDERSSON, D. P., BERNARD, S., SPALDING, K. & ARNER, P. 2013. Adipocyte triglyceride turnover and lipolysis in lean and overweight subjects. *Journal of lipid research,* 54**,** 2909-2913.

SAKAMURI, S. S., PUTCHA, U. K., VEETTIL, G. N. & AYYALASOMAYAJULA, V. 2016. Transcriptome profiling of visceral adipose tissue in a novel obese rat model, WNIN/Ob & its comparison with other animal models. *Indian J Med Res,* 144**,** 409-423.

SALANS, L. B., CUSHMAN, S. W. & WEISMANN, R. E. 1973. Studies of human adipose tissue. Adipose cell size and number in nonobese and obese patients. *J Clin Invest,* 52**,** 929-41.

SALANS, L. B. & DOUGHERTY, J. W. 1971. The effect of insulin upon glucose metabolism by adipose cells of different size. Influence of cell lipid and protein content, age, and nutritional state. *J Clin Invest,* 50**,** 1399-410.

SALMINEN, A., KAARNIRANTA, K. & KAUPPINEN, A. 2013. Crosstalk between Oxidative Stress and SIRT1: Impact on the Aging Process. *Int J Mol Sci,* 14**,** 3834-59.

SALOMON, C., TORRES, M. J., KOBAYASHI, M., SCHOLZ-ROMERO, K., SOBREVIA, L., *et al.* 2014a. A gestational profile of placental exosomes in maternal plasma and their effects on endothelial cell migration. *PLoS One,* 9**,** e98667.

SALOMON, C., YEE, S., SCHOLZ-ROMERO, K., KOBAYASHI, M., VASWANI, K., *et al.* 2014b. Extravillous trophoblast cells-derived exosomes promote vascular smooth muscle cell migration. *Front Pharmacol,* 5**,** 175.

SANDOUK, T., REDA, D. & HOFMANN, C. 1993. Antidiabetic agent pioglitazone enhances adipocyte differentiation of 3T3-F442A cells. *Am J Physiol,* 264**,** C1600-8.

SANTOMAURO, A. T., BODEN, G., SILVA, M. E., ROCHA, D. M., SANTOS, R. F., *et al.* 1999. Overnight lowering of free fatty acids with Acipimox improves insulin resistance and glucose tolerance in obese diabetic and nondiabetic subjects. *Diabetes,* 48**,** 1836-41.

SAPONARO, C., GAGGINI, M., CARLI, F. & GASTALDELLI, A. 2015a. The Subtle Balance between Lipolysis and Lipogenesis: A Critical Point in Metabolic Homeostasis. *Nutrients,* 7**,** 9453-74.

SAPONARO, C., GAGGINI, M., CARLI, F. & GASTALDELLI, A. 2015b. The Subtle Balance between Lipolysis and Lipogenesis: A Critical Point in Metabolic Homeostasis. *Nutrients,* 7**,** 9453-9474.

SARJEANT, K. & STEPHENS, J. M. 2012. Adipogenesis. *Cold Spring Harbor perspectives in biology,* 4**,** a008417-a008417.

SATTAR, N. & GILL, J. M. 2015. Type 2 diabetes in migrant south Asians: mechanisms, mitigation, and management. *Lancet Diabetes Endocrinol,* 3**,** 1004-16.

SBARBATI, A., ACCORSI, D., BENATI, D., MARCHETTI, L., ORSINI, G., *et al.* 2010. Subcutaneous adipose tissue classification. *European Journal of Histochemistry,* 54**,** e48.

SCHELLENBERG, E. S., DRYDEN, D. M., VANDERMEER, B., HA, C. & KOROWNYK, C. 2013. Lifestyle interventions for patients with and at risk for type 2 diabetes: a systematic review and meta-analysis. *Ann Intern Med,* 159**,** 543-51.

SCHERER, P. E. 2006. Adipose Tissue. *From Lipid Storage Compartment to Endocrine Organ,* 55**,** 1537-1545.

SCHIPPER, B. M., MARRA, K. G., ZHANG, W., DONNENBERG, A. D. & RUBIN, J. P. 2008. Regional anatomic and age effects on cell function of human adipose-derived stem cells. *Ann Plast Surg,* 60**,** 538-44.

SCHREIBMAN, P. H. & DELL, R. B. 1975. Human adipocyte cholesterol. Concentration, localization, synthesis, and turnover. *J Clin Invest,* 55**,** 986-93.

SEINO, S., SHIBASAKI, T. & MINAMI, K. 2011. Dynamics of insulin secretion and the clinical implications for obesity and diabetes. *J Clin Invest,* 121**,** 2118-25.

SELL, H., DESHAIES, Y. & RICHARD, D. 2004. The brown adipocyte: update on its metabolic role. *Int J Biochem Cell Biol,* 36**,** 2098-104.

SERINO, M., MENGHINI, R., FIORENTINO, L., AMORUSO, R., MAURIELLO, A., *et al.* 2007. Mice Heterozygous for Tumor Necrosis Factor-α Converting Enzyme Are Protected From Obesity-Induced Insulin Resistance and Diabetes. *Diabetes,* 56**,** 2541.

SETHI, J. K. & HOTAMISLIGIL, G. S. 1999. The role of TNF alpha in adipocyte metabolism. *Semin Cell Dev Biol,* 10**,** 19-29.

SHAH, A. D., KANDULA, N. R., LIN, F., ALLISON, M. A., CARR, J., *et al.* 2016a. Less favorable body composition and adipokines in South Asians compared with other US ethnic groups: results from the MASALA and MESA studies. *International journal of obesity (2005),* 40**,** 639-645.

SHAH, A. D., KANDULA, N. R., LIN, F., ALLISON, M. A., CARR, J., *et al.* 2016b. Less favorable body composition and adipokines in South Asians compared with other US ethnic groups: results from the MASALA and MESA studies. *Int J Obes (Lond),* 40**,** 639-45.

SHEPHERD, P. R. & KAHN, B. B. 1999. Glucose transporters and insulin action--implications for insulin resistance and diabetes mellitus. *N Engl J Med,* 341**,** 248-57.

SHIMBA, S., WADA, T., HARA, S. & TEZUKA, M. 2004. EPAS1 promotes adipose differentiation in 3T3-L1 cells. *J Biol Chem,* 279**,** 40946-53.

SHIMOKATA, H., ANDRES, R., COON, P. J., ELAHI, D., MULLER, D. C., *et al.* 1989a. Studies in the distribution of body fat. II. Longitudinal effects of change in weight. *Int J Obes,* 13**,** 455-64.

SHIMOKATA, H., TOBIN, J. D., MULLER, D. C., ELAHI, D., COON, P. J., *et al.* 1989b. Studies in the distribution of body fat: I. Effects of age, sex, and obesity. *J Gerontol,* 44**,** M66-73.

SIAL, S., COGGAN, A. R., CARROLL, R., GOODWIN, J. & KLEIN, S. 1996. Fat and carbohydrate metabolism during exercise in elderly and young subjects. *Am J Physiol,* 271**,** E983-9.

SIDDIQUI, K., SCARIA JOY, S. & GEORGE, T. P. 2020. Circulating resistin levels in relation with insulin resistance, inflammatory and endothelial dysfunction markers in patients with type 2 diabetes and impaired fasting glucose. *Endocrine and Metabolic Science,* 1**,** 100059.

SIMERLY, R. B., CHANG, C., MURAMATSU, M. & SWANSON, L. W. 1990. Distribution of androgen and estrogen receptor mRNA-containing cells in the rat brain: an in situ hybridization study. *J Comp Neurol,* 294**,** 76-95.

SINGH, P., PETERSON, T. E., SERT-KUNIYOSHI, F. H., GLENN, J. A., DAVISON, D. E., *et al.* 2012. Leptin signaling in adipose tissue: role in lipid accumulation and weight gain. *Circ Res,* 111**,** 599-603.

SINHA, A., IGNATCHENKO, V., IGNATCHENKO, A., MEJIA-GUERRERO, S. & KISLINGER, T. 2014. In-depth proteomic analyses of ovarian cancer cell line exosomes reveals differential enrichment of functional categories compared to the NCI 60 proteome. *Biochem Biophys Res Commun,* 445**,** 694-701.

SINOBIOLOGICAL 2020a. AMPK Signaling Pathway.

SINOBIOLOGICAL 2020b. p53 Pathway.

SKELDON, A. M., FARAJ, M. & SALEH, M. 2014. Caspases and inflammasomes in metabolic inflammation. *Immunol Cell Biol,* 92**,** 304-13.

SKURK, T., ALBERTI-HUBER, C., HERDER, C. & HAUNER, H. 2007. Relationship between Adipocyte Size and Adipokine Expression and Secretion. *The Journal of Clinical Endocrinology & Metabolism,* 92**,** 1023-1033.

SLAYTON, M., GUPTA, A., BALAKRISHNAN, B. & PURI, V. 2019. CIDE Proteins in Human Health and Disease. *Cells,* 8.

SMITH, S. R., XIE, H., BAGHIAN, S., NEEDHAM, A., MCNEIL, M., *et al.* 2006. Pioglitazone changes the distribution of adipocyte size in type 2 diabetes. *Adipocytes,* 2**,** 11-22.

SMITH, U. 2002. Impaired ('diabetic') insulin signaling and action occur in fat cells long before glucose intolerance--is insulin resistance initiated in the adipose tissue? *Int J Obes Relat Metab Disord,* 26**,** 897-904.

SNIDERMAN, A. D., BHOPAL, R., PRABHAKARAN, D., SARRAFZADEGAN, N. & TCHERNOF, A. 2007. Why might South Asians be so susceptible to central obesity and its atherogenic consequences? The adipose tissue overflow hypothesis. *International Journal of Epidemiology,* 36**,** 220-225.

SON, Y. H., KA, S., KIM, A. Y. & KIM, J. B. 2014. Regulation of Adipocyte Differentiation via MicroRNAs. *Endocrinol Metab (Seoul),* 29**,** 122-35.

SPALDING, K. L., ARNER, E., WESTERMARK, P. O., BERNARD, S., BUCHHOLZ, B. A., *et al.* 2008. Dynamics of fat cell turnover in humans. *Nature,* 453**,** 783-7.

SPARKS, L. M., PASARICA, M., SEREDA, O., DEJONGE, L., THOMAS, S., *et al.* 2009. Effect of adipose tissue on the sexual dimorphism in metabolic flexibility. *Metabolism,* 58**,** 1564-71.

SPRANGER, J., KROKE, A., MÖHLIG, M., HOFFMANN, K., BERGMANN, M. M., *et al.* 2003. Inflammatory Cytokines and the Risk to Develop Type 2 Diabetes. *Results of the Prospective Population-Based European Prospective Investigation into Cancer and Nutrition (EPIC)-Potsdam Study,* 52**,** 812-817.

STAIANO, A. E. & KATZMARZYK, P. T. 2012. Ethnic and sex differences in body fat and visceral and subcutaneous adiposity in children and adolescents. *International journal of obesity (2005),* 36**,** 1261-1269.

STARR, M. E., EVERS, B. M. & SAITO, H. 2009. Age-associated increase in cytokine production during systemic inflammation: adipose tissue as a major source of IL-6. *J Gerontol A Biol Sci Med Sci,* 64**,** 723-30.

STENKULA, K. G. & ERLANSON-ALBERTSSON, C. 2018. Adipose cell size: importance in health and disease. *Am J Physiol Regul Integr Comp Physiol,* 315**,** R284-r295.

STIENSTRA, R., JOOSTEN, L. A., KOENEN, T., VAN TITS, B., VAN DIEPEN, J. A., *et al.* 2010. The inflammasome-mediated caspase-1 activation controls adipocyte differentiation and insulin sensitivity. *Cell Metab,* 12**,** 593-605.

STINKENS, R., BROUWERS, B., JOCKEN, J. W., BLAAK, E. E., TEUNISSEN-BEEKMAN, K. F., *et al.* 2018. Exercise training-induced effects on the abdominal subcutaneous adipose tissue phenotype in humans with obesity. *Journal of Applied Physiology,* 125**,** 1585-1593.

STUBBINS, R. E., HOLCOMB, V. B., HONG, J. & NÚÑEZ, N. P. 2012. Estrogen modulates abdominal adiposity and protects female mice from obesity and impaired glucose tolerance. *Eur J Nutr,* 51**,** 861-70.

STUFFERS, S., SEM WEGNER, C., STENMARK, H. & BRECH, A. 2009. Multivesicular endosome biogenesis in the absence of ESCRTs. *Traffic,* 10**,** 925-37.

STULTS-KOLEHMAINEN, M. A., STANFORTH, P. R., BARTHOLOMEW, J. B., LU, T., ABOLT, C. J., *et al.* 2013. DXA estimates of fat in abdominal, trunk and hip regions varies by ethnicity in men. *Nutrition & Diabetes,* 3**,** e64-e64.

SU, K.-Z., LI, Y.-R., ZHANG, D., YUAN, J.-H., ZHANG, C.-S., *et al.* 2019. Relation of Circulating Resistin to Insulin Resistance in Type 2 Diabetes and Obesity: A Systematic Review and Meta-Analysis. *Frontiers in physiology,* 10**,** 1399-1399.

SUBRAMANIAN, S. & CHAIT, A. 2012. Hypertriglyceridemia secondary to obesity and diabetes. *Biochim Biophys Acta,* 1821**,** 819-25.

SULISTYONINGRUM, D. C., GASEVIC, D., LEAR, S. A., HO, J., MENTE, A., *et al.* 2013. Total and high molecular weight adiponectin and ethnic-specific differences in adiposity and insulin resistance: a cross-sectional study. *Cardiovasc Diabetol,* 12**,** 170.

TAKADA, I., KOUZMENKO, A. P. & KATO, S. 2009. Wnt and PPARgamma signaling in osteoblastogenesis and adipogenesis. *Nat Rev Rheumatol,* 5**,** 442-7.

TAKADA, I., MIHARA, M., SUZAWA, M., OHTAKE, F., KOBAYASHI, S., *et al.* 2007. A histone lysine methyltransferase activated by non-canonical Wnt signalling suppresses PPAR-gamma transactivation. *Nat Cell Biol,* 9**,** 1273-85.

TAKAHASHI, Y., SHINODA, A., KAMADA, H., SHIMIZU, M., INOUE, J., *et al.* 2016. Perilipin2 plays a positive role in adipocytes during lipolysis by escaping proteasomal degradation. *Scientific Reports,* 6**,** 20975.

TANDON, P., WAFER, R. & MINCHIN, J. E. N. 2018. Adipose morphology and metabolic disease. *J Exp Biol,* 221.

TANG, Q.-Q., OTTO, T. C. & LANE, M. D. 2004. Commitment of C3H10T1/2 pluripotent stem cells to the adipocyte lineage. *Proceedings of the National Academy of Sciences of the United States of America,* 101**,** 9607-9611.

TARNOPOLSKY, M. A., RENNIE, C. D., ROBERTSHAW, H. A., FEDAK-TARNOPOLSKY, S. N., DEVRIES, M. C., et al. 2007. Influence of endurance exercise training and sex on intramyocellular lipid and mitochondrial ultrastructure, substrate use, and mitochondrial enzyme activity. *American Journal of Physiology-Regulatory, Integrative and Comparative Physiology,* 292, R1271-R1278.

TAURO, B. J., GREENING, D. W., MATHIAS, R. A., MATHIVANAN, S., JI, H., et al. 2013. Two distinct populations of exosomes are released from LIM1863 colon carcinoma cell-derived organoids. *Mol Cell Proteomics,* 12, 587-98.

TCHERNOF, A., DESMEULES, A., RICHARD, C., LABERGE, P., DARIS, M., et al. 2004. Ovarian hormone status and abdominal visceral adipose tissue metabolism. *J Clin Endocrinol Metab,* 89, 3425-30.

TCHOUKALOVA, Y. D., VOTRUBA, S. B., TCHKONIA, T., GIORGADZE, N., KIRKLAND, J. L., et al. 2010. Regional differences in cellular mechanisms of adipose tissue gain with overfeeding. *Proc Natl Acad Sci U S A,* 107, 18226-31.

TEBOUL, L., GAILLARD, D., STACCINI, L., INADERA, H., AMRI, E.-Z., et al. 1995. Thiazolidinediones and Fatty Acids Convert Myogenic Cells into Adipose-like Cells(*). *Journal of Biological Chemistry,* 270, 28183-28187.

TEH, B. H., PAN, W. H. & CHEN, C. J. 1996. The reallocation of body fat toward the abdomen persists to very old age, while body mass index declines after middle age in Chinese. *Int J Obes Relat Metab Disord,* 20, 683-7.

TITCHENELL, P. M., LAZAR, M. A. & BIRNBAUM, M. J. 2017. Unraveling the Regulation of Hepatic Metabolism by Insulin. *Trends Endocrinol Metab,* 28, 497-505.

TOGASHI, N., URA, N., HIGASHIURA, K., MURAKAMI, H. & SHIMAMOTO, K. 2002. Effect of TNF-α–Converting Enzyme Inhibitor on Insulin Resistance in Fructose-Fed Rats. *Hypertension,* 39, 578-580.

TOGLIATTO, G., DENTELLI, P., GILI, M., GALLO, S., DEREGIBUS, C., et al. 2016. Obesity reduces the pro-angiogenic potential of adipose tissue stem cell-derived extracellular vesicles (EVs) by impairing miR-126 content: impact on clinical applications. *International Journal of Obesity,* 40, 102-111.

TONTONOZ, P. & SPIEGELMAN, B. M. 2008. Fat and beyond: the diverse biology of PPARgamma. *Annu Rev Biochem,* 77, 289-312.

TOYODA, S., SHIN, J., FUKUHARA, A., OTSUKI, M. & SHIMOMURA, I. 2022. Transforming growth factor beta1 signaling links extracellular matrix remodeling to intracellular lipogenesis upon physiological feeding events. *J Biol Chem,* 298, 101748.

UGUR-ALTUN, B. & ALTUN, A. 2007. Circulating leptin and osteoprotegerin levels affect insulin resistance in healthy premenopausal obese women. *Arch Med Res,* 38, 891-6.

UYSAL, K. T., WIESBROCK, S. M. & HOTAMISLIGIL, G. S. 1998. Functional analysis of tumor necrosis factor (TNF) receptors in TNF-alpha-mediated insulin resistance in genetic obesity. *Endocrinology,* 139, 4832-8.

UYSAL, K. T., WIESBROCK, S. M., MARINO, M. W. & HOTAMISLIGIL, G. S. 1997a. Protection from obesity-induced insulin resistance in mice lacking TNF-alpha function. *Nature,* 389, 610-4.

UYSAL, K. T., WIESBROCK, S. M., MARINO, M. W. & HOTAMISLIGIL, G. S. 1997b. Protection from obesity-induced insulin resistance in mice lacking TNF-α function. *Nature,* 389, 610-614.

VAN DER SLUIS, I. M., DE RIDDER, M. A. J., BOOT, A. M., KRENNING, E. P. & DE MUINCK KEIZER-SCHRAMA, S. M. P. F. 2002. Reference data for bone density and body composition measured with dual energy x ray absorptiometry in white children and young adults. *Archives of disease in childhood,* 87, 341-347.

VAN HARMELEN, V., DICKER, A., RYDÉN, M., HAUNER, H., LÖNNQVIST, F., et al. 2002. Increased lipolysis and decreased leptin production by human omental as compared with subcutaneous preadipocytes. *Diabetes,* 51, 2029-36.

VAN HARMELEN, V., SKURK, T., RÖHRIG, K., LEE, Y. M., HALBLEIB, M., et al. 2003. Effect of BMI and age on adipose tissue cellularity and differentiation capacity in women. *Int J Obes Relat Metab Disord,* 27, 889-95.

VAN LOON, L. J. & GOODPASTER, B. H. 2006. Increased intramuscular lipid storage in the insulin-resistant and endurance-trained state. *Pflugers Arch,* 451, 606-16.

VAN PELT, D. W., GUTH, L. M. & HOROWITZ, J. F. 2017. Aerobic exercise elevates markers of angiogenesis and macrophage IL-6 gene expression in the subcutaneous adipose tissue of overweight-to-obese adults. *J Appl Physiol (1985),* 123, 1150-1159.

VAN PELT, R. E., GOZANSKY, W. S., SCHWARTZ, R. S. & KOHRT, W. M. 2003. Intravenous estrogens increase insulin clearance and action in postmenopausal women. *Am J Physiol Endocrinol Metab,* 285, E311-7.

VARGAS E, P. V., CARRILLO SEPULVEDA MA. 2020. *Physiology, Glucose Transporter Type 4,* StatPearls Treasure Island (FL): StatPearls Publishing.

VEILLEUX, A., CARON-JOBIN, M., NOEL, S., LABERGE, P. Y. & TCHERNOF, A. 2011. Visceral adipocyte hypertrophy is associated with dyslipidemia independent of body composition and fat distribution in women. *Diabetes,* 60**,** 1504-11.

VIEIRA-POTTER, V. J., ZIDON, T. M. & PADILLA, J. 2015. Exercise and Estrogen Make Fat Cells "Fit". *Exercise and sport sciences reviews,* 43**,** 172-178.

VON RUESTEN, A., STEFFEN, A., FLOEGEL, A., VAN DER, A. D., MASALA, G., *et al.* 2011. Trend in obesity prevalence in European adult cohort populations during follow-up since 1996 and their predictions to 2015. *PLoS One,* 6**,** e27455.

WALENDA, G., ABNAOF, K., JOUSSEN, S., MEURER, S., SMEETS, H., *et al.* 2013. TGF-beta1 does not induce senescence of multipotent mesenchymal stromal cells and has similar effects in early and late passages. *PLoS One,* 8**,** e77656.

WALKER, G. E., MARZULLO, P., VERTI, B., GUZZALONI, G., MAESTRINI, S., *et al.* 2008. Subcutaneous abdominal adipose tissue subcompartments: potential role in rosiglitazone effects. *Obesity (Silver Spring),* 16**,** 1983-91.

WANG, E. A., ISRAEL, D. I., KELLY, S. & LUXENBERG, D. P. 1993. Bone morphogenetic protein-2 causes commitment and differentiation in C3H10T1/2 and 3T3 cells. *Growth Factors,* 9**,** 57-71.

WANG, M. Y., LEE, Y. & UNGER, R. H. 1999. Novel form of lipolysis induced by leptin. *J Biol Chem,* 274**,** 17541-4.

WANG, Q. A., SCHERER, P. E. & GUPTA, R. K. 2014. Improved methodologies for the study of adipose biology: insights gained and opportunities ahead. *J Lipid Res,* 55**,** 605-24.

WANG, X. & HAI, C. 2015. Redox modulation of adipocyte differentiation: hypothesis of "Redox Chain" and novel insights into intervention of adipogenesis and obesity. *Free Radic Biol Med,* 89**,** 99-125.

WEDELLOVÁ, Z., DIETRICH, J., SIKLOVÁ-VÍTKOVÁ, M., KOLOŠTOVÁ, K., KOVÁČIKOVÁ, M., *et al.* 2011. Adiponectin inhibits spontaneous and catecholamine-induced lipolysis in human adipocytes of non-obese subjects through AMPK-dependent mechanisms. *Physiol Res,* 60**,** 139-48.

WEI, J. J., CHEN, Y. F., XUE, C. L., MA, B. T., SHEN, Y. M., *et al.* 2016. Protection of Nerve Injury with Exosome Extracted from Mesenchymal Stem Cell. *Zhongguo Yi Xue Ke Xue Yuan Xue Bao,* 38**,** 33-6.

WEI, L.-M., SUN, R.-P., DONG, T., LIU, J., CHEN, T., *et al.* 2020. MiR-125b-2 knockout increases high-fat diet-induced fat accumulation and insulin resistance. *Scientific Reports,* 10**,** 21969.

WEISBERG, S. P., MCCANN, D., DESAI, M., ROSENBAUM, M., LEIBEL, R. L., *et al.* 2003. Obesity is associated with macrophage accumulation in adipose tissue. *The Journal of clinical investigation,* 112**,** 1796-1808.

WELLEN, K. E. & HOTAMISLIGIL, G. S. 2003. Obesity-induced inflammatory changes in adipose tissue. *The Journal of clinical investigation,* 112**,** 1785-1788.

WELLS, J. C. K. 2007. Sexual dimorphism of body composition. *Best Practice & Research Clinical Endocrinology & Metabolism,* 21**,** 415-430.

WEST, J., LAWLOR, D. A., FAIRLEY, L., BHOPAL, R., CAMERON, N., *et al.* 2013. UK-born Pakistani-origin infants are relatively more adipose than white British infants: findings from 8704 mother-offspring pairs in the Born-in-Bradford prospective birth cohort. *J Epidemiol Community Health,* 67**,** 544-51.

WEYER, C., FOLEY, J. E., BOGARDUS, C., TATARANNI, P. A. & PRATLEY, R. E. 2000. Enlarged subcutaneous abdominal adipocyte size, but not obesity itself, predicts type II diabetes independent of insulin resistance. *Diabetologia,* 43**,** 1498-506.

WHIRL-CARRILLO, M., MCDONAGH, E. M., HEBERT, J. M., GONG, L., SANGKUHL, K., *et al.* 2012. Statin Pathway, Pharmacodynamics. Clinical pharmacology and therapeutics. 2012: Pharmacogenomics knowledge for personalized medicine.

WHO 2000. Obesity: preventing and managing the global epidemic. Report of a WHO consultation. *World Health Organ Tech Rep Ser,* 894**,** i-xii, 1-253.

WHO 2016. Global report on Diabetes.

WHO. 2017. *Obesity and overweight* [Online]. Available: http://www.who.int/en/news-room/fact-sheets/detail/obesity-and-overweight [Accessed 05 July 2018].

WHO 2018. Health situation in the European region 2.

WHO 2019. Life expectancy and causes of death.

WICKMAN, G., JULIAN, L. & OLSON, M. F. 2012. How apoptotic cells aid in the removal of their own cold dead bodies. *Cell Death Differ,* 19**,** 735-42.

WILCOX, G. 2005. Insulin and insulin resistance. *The Clinical biochemist. Reviews,* 26**,** 19-39.

WILKINSON, H. A., DAHLLUND, J., LIU, H., YUDKOVITZ, J., CAI, S. J., *et al.* 2002. Identification and characterization of a functionally distinct form of human estrogen receptor beta. *Endocrinology,* 143**,** 1558-61.

WITHERS, D. J., GUTIERREZ, J. S., TOWERY, H., BURKS, D. J., REN, J.-M., *et al.* 1998. Disruption of IRS-2 causes type 2 diabetes in mice. *Nature,* 391**,** 900-904.

WITHERS, D. J. & WHITE, M. 2000. Perspective: The insulin signaling system--a common link in the pathogenesis of type 2 diabetes. *Endocrinology,* 141**,** 1917-21.

WITTERS, L. A., WATTS, T. D., DANIELS, D. L. & EVANS, J. L. 1988. Insulin stimulates the dephosphorylation and activation of acetyl-CoA carboxylase. *Proceedings of the National Academy of Sciences of the United States of America,* 85**,** 5473-5477.

WITWER, K. W., BUZAS, E. I., BEMIS, L. T., BORA, A., LASSER, C., *et al.* 2013. Standardization of sample collection, isolation and analysis methods in extracellular vesicle research. *J Extracell Vesicles,* 2.

WOLINS, N. E., BRASAEMLE, D. L. & BICKEL, P. E. 2006. A proposed model of fat packaging by exchangeable lipid droplet proteins. *FEBS Letters,* 580**,** 5484-5491.

WOLLERT, T. & HURLEY, J. H. 2010. Molecular mechanism of multivesicular body biogenesis by ESCRT complexes. *Nature,* 464**,** 864-9.

WRONSKA, A. & KMIEC, Z. 2012. Structural and biochemical characteristics of various white adipose tissue depots. *Acta Physiologica,* 205**,** 194-208.

WU, H. & BALLANTYNE, C. M. 2020. Metabolic Inflammation and Insulin Resistance in Obesity. *Circulation Research,* 126**,** 1549-1564.

WU, L., ZHANG, L., LI, B., JIANG, H., DUAN, Y., *et al.* 2018. AMP-Activated Protein Kinase (AMPK) Regulates Energy Metabolism through Modulating Thermogenesis in Adipose Tissue. *Frontiers in physiology,* 9**,** 122-122.

WU, Z., ROSEN, E. D., BRUN, R., HAUSER, S., ADELMANT, G., *et al.* 1999. Cross-Regulation of C/EBPα and PPARγ Controls the Transcriptional Pathway of Adipogenesis and Insulin Sensitivity. *Molecular Cell,* 3**,** 151-158.

YAMAMOTO, S., MATSUSHITA, Y., NAKAGAWA, T., HAYASHI, T., NODA, M., *et al.* 2014. Circulating adiponectin levels and risk of type 2 diabetes in the Japanese. *Nutr Diabetes,* 4**,** e130.

YANG, J., ELIASSON, B., SMITH, U., CUSHMAN, S. W. & SHERMAN, A. S. 2012. The size of large adipose cells is a predictor of insulin resistance in first-degree relatives of type 2 diabetic patients. *Obesity (Silver Spring),* 20**,** 932-8.

YANG, X., JANSSON, P. A., NAGAEV, I., JACK, M. M., CARVALHO, E., *et al.* 2004. Evidence of impaired adipogenesis in insulin resistance. *Biochem Biophys Res Commun,* 317**,** 1045-51.

YARAK, S. & OKAMOTO, O. K. 2010. Human adipose‐derived stem cells: current challenges and clinical perspectives. *An Bras Dermatol,* 85**,** 647-656.

YATAGAI, T., NISHIDA, Y., NAGASAKA, S., NAKAMURA, T., TOKUYAMA, K., *et al.* 2003. Relationship between exercise training-induced increase in insulin sensitivity and adiponectinemia in healthy men. *Endocr J,* 50**,** 233-8.

YI, W., KIM, K., IM, M., RYANG, S., KIM, E. H., *et al.* 2022. Association between visceral adipose tissue volume, measured using computed tomography, and cardio-metabolic risk factors. *Scientific Reports,* 12**,** 387.

YIM, J. E., HESHKA, S., ALBU, J. B., HEYMSFIELD, S. & GALLAGHER, D. 2008. Femoral-gluteal subcutaneous and intermuscular adipose tissues have independent and opposing relationships with CVD risk. *J Appl Physiol (1985),* 104**,** 700-7.

YU, J., GU, X. & YI, S. 2016. Ingenuity Pathway Analysis of Gene Expression Profiles in Distal Nerve Stump following Nerve Injury: Insights into Wallerian Degeneration. *Front Cell Neurosci,* 10**,** 274.

ZABOROWSKI, M. P., BALAJ, L., BREAKEFIELD, X. O. & LAI, C. P. 2015. Extracellular Vesicles: Composition, Biological Relevance, and Methods of Study. *BioScience,* 65**,** 783-797.

ZAMANI, N. & BROWN, C. W. 2011. Emerging roles for the transforming growth factor-{beta} superfamily in regulating adiposity and energy expenditure. *Endocr Rev,* 32**,** 387-403.

ZAMBONI, M., ZOICO, E., SCARTEZZINI, T., MAZZALI, G., TOSONI, P., *et al.* 2003. Body composition changes in stable-weight elderly subjects: The effect of sex. *Aging Clinical and Experimental Research,* 15, 321-327.

ZHANG, H. H., HALBLEIB, M., AHMAD, F., MANGANIELLO, V. C. & GREENBERG, A. S. 2002. Tumor necrosis factor-alpha stimulates lipolysis in differentiated human adipocytes through activation of extracellular signal-related kinase and elevation of intracellular cAMP. *Diabetes,* 51**,** 2929-35.

ZHAO, H., INNES, J., BROOKS, D. C., REIERSTAD, S., YILMAZ, M. B., *et al.* 2009. A novel promoter controls Cyp19a1 gene expression in mouse adipose tissue. *Reprod Biol Endocrinol,* 7**,** 37.

ZHOU, Z., MOORE, T. M., DREW, B. G., RIBAS, V., WANAGAT, J., *et al.* 2020a. Estrogen receptor α controls metabolism in white and brown adipocytes by regulating *Polg1* and mitochondrial remodeling. *Science Translational Medicine,* 12**,** eaax8096.

ZHOU, Z., MOORE, T. M., DREW, B. G., RIBAS, V., WANAGAT, J., *et al.* 2020b. Estrogen receptor α controls metabolism in white and brown adipocytes by regulating Polg1 and mitochondrial remodeling. *Science Translational Medicine,* 12**,** eaax8096.

ZHU, B., GUO, X., XU, H., JIANG, B., LI, H., *et al.* 2021. Adipose tissue inflammation and systemic insulin resistance in mice with diet-induced obesity is possibly associated with disruption of PFKFB3 in hematopoietic cells. *Laboratory Investigation,* 101**,** 328-340.